The role of SHP-1 in *in vivo* $CD8^+$ T cell responses to antigenic stimulation

By Garry Dolton

Cardiff University

School of Medicine

Department of Medical Biochemistry and Immunology

A thesis submitted in candidature for the degree of Doctor of Philosophy

September 2008

UMI Number: U584321

All rights reserved

INFORMATION TO ALL USERS
The quality of this reproduction is dependent upon the quality of the copy submitted.

In the unlikely event that the author did not send a complete manuscript
and there are missing pages, these will be noted. Also, if material had to be removed,
a note will indicate the deletion.



UMI U584321
Published by ProQuest LLC 2013. Copyright in the Dissertation held by the Author.
Microform Edition © ProQuest LLC.
All rights reserved. This work is protected against
unauthorized copying under Title 17, United States Code.



ProQuest LLC
789 East Eisenhower Parkway
P.O. Box 1346
Ann Arbor, MI 48106-1346

Dedicated to the memory of my late Grandparents, Ken and Joan.

Acknowledgements

Firstly, I would like to thank my supervisor, James Matthews, for his support throughout my PhD. I am thankful to Jean Sathish and Frances LeRoy for sharing their expertise with me.

I would also like to thank the following people for their technical support, Awen Gallimore, Simone Cuff, Richard Darley, Jason Twohig, Gareth Betts, Ann-Catherine Raby and Sian Llewellyn-Lacey.

I am grateful to Tenovus for providing the funding that allowed this research.

Finally, I would like to thank my family and Robin for their friendship and support over the past four years.

Summary

The immune system has immense clinical potential for combating pathogens and tumourigenesis. More specifically, $CD8^+$ T cells have the ability to eradicate infected and malignant cells. In light of this, the factors that may influence the speed at which antigen is detected, the magnitude of the response and the efficiency of pathogen/tumour clearance require ongoing investigation.

The src homology 2 (SH2) domain containing protein tyrosine phosphatase - 1 (SHP-1) is a negative regulator of T cell signalling pathways. Prior to this study, in vitro data had demonstrated that SHP-1 deficient $CD8^+$ T cells possess a hyper-responsive phenotype when stimulated with cognate peptide. Therefore, the remit of this study was to establish whether this in vitro observation has an *in vivo* relevance.

In order to explore the role of SHP-1 in an *in vivo* setting, $CD8^+$ T cells from the spontaneous mouse mutant, motheaten, which lacks SHP-1 expression were utilised. Specifically, $CD8^+$ T cells were purified from motheaten (SHP-1 deficient) and control (SHP-1 sufficient) mice and adoptively transferred to recipient mice where they could be studied.

This study demonstrates that following adoptive transfer, naive SHP-1 deficient $CD8^+$ T cells exhibit an enhanced *in vivo* expansion upon antigenic stimulation, which notably results in the killing of more peptide labelled target cells. Furthermore, SHP-1 deficient $CD8^+$ T cells also exhibit an enhanced memory response upon antigenic challenge. These findings suggest that modulation of SHP-1 expression may improve the efficacy of tumour immunotherapy strategies, which use antigen specific $CD8^+$ T cells to eradicate malignant cells in tumour-bearing patients.

In further support of potentially targetting SHP-1 expression in $CD8^+$ T cells used in immunotherapy strategies, it has been importantly shown in this study that mice receiving SHP-1 deficient $CD8^+$ T cells exhibit an enhanced protection against pulmonary tumour formation when compared to mice receiving SHP-1 sufficient $CD8^+$ T cells.

Abbreviations

β2M	Beta2-microglobulin
μ	micro
2-ME	2-Mercaptoethanol
ACT	Adoptive cell transfer
AP-1	Activator protein-1
APC	Antigen presenting cell
BALT	Bronchus associated lymphoid tissue
Bcl-10	B cell lymphoma 10
BCR	B cell receptor
BSA	Bovine serum albumin
BSU	Biological service unit
C	Carboxyl
C	Celsius
CARMA-1	Caspase recruitment domain containing membrane associated guanylate kinase protein-1
Cbl	Casitas B cell lymphoma
CCR	Chemokine (C-C motif) receptor
CD	Cluster of differentiation
cDNA	Complementary deoxyribonucleic acid
CDR	Complementarity determining regions
CEA	Carcinoembryonic antigen
CEACAM-1	Carcinoembryonic antigen related cell adhesion molecule-1
CFSE	Carboxy fluorescein Succinimidyl ester
cGy	Centi-Grey
CLA	Cutaneous lymphocyte antigen
CMV	Cytlomegalovirus
cSMAC	Central supramolecular activation cluster
CTLA-4	Cytotoxic T lymphocyte antigen-4
CTL	Cytotoxic T lymphocyte
D	Diversity
DAG	Diacyl glycerol
DC	Dendritic cell
DDAO-SE	7-hydroxy-9H(1,3-dichloro-9,9,-dimethyacridin-2-one)-succinimydyl ester
DMEM	Dulbecco modified eagle's minimal essential media
DMSO	Dimethyl sulphoxide
DNA	Deoxyribonucleic acid
EBV	Epstein Barr virus
ECL	Enahnced chemiluminescene
Elk-1	ETS domain containing protein
ER	Endoplasmic reticulum
Erk	Extracellular signal-related kinase
FACS	Fluorescence activated cell sorting
FCS	Foetal calf serum
FITC	Fluorescein isothiocyante
GADS	Grb-2 related protein
GALT	Gut associated lymphoid tissue

G-CSF	Granulocyte colony stimulating factor
GDP	Guanosine diphosphate
GEF	Guanosine nucleotide exchange factor
GFP	Green fluorescent protein
GlyCAM-1	Glycosylation-dependent cell adhesion molecule-1
GM-CSF	Granulocyte-macrophage colony stimulating factor
Grb-2	Growth factor receptor binding protein 2
GTP	Guanosine trisphosphate
GTPase	Guanosine trisphosphatase
HBSS	Hank's balanced salt solution
HEC	High endothelial cell
HEK	Human embryonic kidney
Hem	Hemizygous
HER-2	Human epidermal growth factor-2
HEV	High endothelial venule
HIV	Human immunodeficiency virus
HLA	Human leukocyte antigen
Hom	Homozygous
HRP	Horse radish peroxidise
HSP	Heat shock protein
IκB	Inhibitor of NFκB
ICAM-1	Intercellular adhesion molecule-1
ICOS	Inducible costimulatory
IDO	Indoleamine 2, 3-dioxygenase
IFN	Interferon
IKK	Inhibitor of NFκB kinase
IL	Interleukin
ILT2	Ig-like transcript-2
IP_3	Inositol 1, 4, 5-triphosphate
IRS	Inhibitory-receptor superfamily
IRES	Internal ribosome entry site
IS	Immunological synapse
ITAM	Immunoreceptor tyrosine-based activation motif
ITIM	Immunoreceptor tyrosine-based inhibition motif
Itk	Inducible T cell kinase
IU	International units
J	Joining
JNK	c-Jun N-terminal kinase
KIR	Killer cell Ig-like receptor
L	Liter
LAIR-1	Leukocyte-associated immunoglobulin-like receptor-1
LAMP-1	Lysosomal associated membrane protein-1
LAT	Linker for activation of T cells
LB	Lysogeny broth
Lck	Leukocyte-specific protein tyrosine kinase
Lef-1	Lymphoid enhancer-binding factor-1
LFA-1	Leukocyte functional antigen-1
Luc	Luciferase
m	Milli
M	Molar

MIIC	MHC class II compartments
mAb	Monoclonal antibody
MadCAM-1	Mucosal vascular addressin cell adhesion molecule-1
MAGE	Melanoma antigen genes
MALT	Mucosal associated lymphoid tissue
MALT-1	Mucosal associated lymphoid tissue gene-1
MAPK	Mitogen activated protein kinase
MART-1	Melanoma antigen recognised by T cells
MCA	Methylcholanthrene
me	Motheaten
Mek	Mitogen-activated or extracellular signal-regulated protein kinase
me^v	Motheaten viable
MHC	Major histocompatability complex
MIC	MHC-class-I polypeptide related sequence
mRNA	Messenger ribonucleic acid
MTOC	Microtubule organising centre
n	Nano
N	Amino
N	Non-germline
NALT	Nasal associated lymphoid tissue
NFAT	Nuclear factor of activated T cells
NFκB	Nuclear factor-kappa B
NK	Natural killer
NKG2D	Natural-killer group 2, member D
NP	Nucleoprotein
NP-40	Nonidet P-40
P	Palindromic
PBMC	Peripheral blood mononuclear cells
PBS	Phosphate buffered saline
PD-1	Programmed death-1
PE	Phycoerythrin
PH	Pleckstrin homology
PI	Propidium iodide
PI3-K	Phosphatidylinositol3-kinase
PIP	Phosphatidylinositol 4-phopshate
PIP_2	Phosphatidylinositol 4, 5-bisphosphate
PIP_3	Phosphatidylinositol 3, 4, 5-trisphosphate
PKC	Protein kinase C
PLC-γ1	Phospholipase C gamma 1
PMA	Phorbol 12-myristate 13 acetate
PNAd	Peripheral node addressin
Pol	Polymerase
PP	Peyer's Patches
PSGL-1	P-selectin glycoprotein ligand-1
pSMAC	Peripheral supramolecular activation complex
PTK	Protein tyrosine kinase
PTP	Protien tyrosine phosphatase
PY	Phosphotyrosine
r	Recombinant
RAG	Recombinase-activating gene

RasGRP	Ras Guanine Nucleotide releasing protein
RECIST	Response evaluation criteria in solid tumours
RISC	RNA-induced silencing complex
RNA	Ribonucleic acid
RNAi	RNA interference
rpm	Revolutions per minute
RPMI	Roswell Park Memorial Institute medium
RSS	recombination signal sequences
S1P	Sphingosine-1-phosphate
SDS	Sodium dodecyl sulphate
SDS-PAGE	Sodium dodecyl sulphate-Polyacrylamide gel electrophoresis
SFFV	Spleen focus-forming virus
SH2	Src homology 2
SH3	Src homology 3
SHIP	SH2 domain containing insositolphosphate 5-phosphatase
SHP-1	SH2 domain containing phosphatase -1
SHP-2	SH2 domain containing phosphatase -2
shRNA	Short hairpin RNA
siRNA	Short interfering RNA
SLC	Secondary lymphoid tissue chemokine
SLP-76	SH2 domain containing leukocyte protein of 75kD
SLAP-130	SLP-76 associated phosphoprotein of 130kD
SMAC	Supramolecular activation complex
Sos	Son of sevenless
SR/CR	Spontaneous regression/complete remission
STAT	Signal transducers and activators of trnascription
TAA	Tumour associated antigen
TAP	Transporter associated with antigen processing
T_{CM}	Central memory T
TCR	T cell receptor
T_{EFF}	Effector T
T_{EM}	Effector memory T
TGF	Tumour growth factor
Th	T helper
TIL	Tumour infiltrating lymphocytes
TRA	Tumour rejection antigen
TRAIL	TNF related apoptosis inducing ligand
Treg	Regulatory T cell
TSA	Tumour specific antigen
V	Variable
V	Volts
VCAM-1	Vascular cell adhesion molecule-1
VLA-4	Very late activation antigen-4
WASP	Wiskott-Aldrich syndrome protein
YFP	Yellow fluorescent protein

Contents

Chapter 1

Introduction

1.1 The Immune system **1**

1.1.1 Innate immunity 2

1.1.2 Adaptive immunity 3

1.2 Antigen recognition by T cells **6**

1.2.1 MHC molecules and peptide presentation 6

1.2.2 αβ T cell receptors 8

1.2.3 T cell coreceptors 10

Figure 1.1 The T cell receptor 12

Figure 1.2 The CD8 coreceptor 13

1.3 Antigenic $CD8^+$ T cell responses **14**

1.3.1 TCR signalling 15

1.3.2 Costimulatory signalling 19

1.3.3 Inhibitory signalling 21

Figure 1.3 TCR and costimulatory signalling pathways 23

1.4 T cell maturation **24**

1.5 T cell immunosurveillance **26**

1.5.1 Naive $CD8^+$ T cell surveillance of lymphoid tissue 26

1.5.2 Antigen presentation to naive $CD8^+$ T cells 29

1.5.3 Activated $CD8^+$ T cell surveillance of peripheral tissue 31

1.5.4 $CD8^+$ T cell effector function 33

Figure 1.4 Naive T cell surveillance 36

Figure 1.5 Activated T cell surveillance 37

1.6 $CD8^+$ T cell memory **38**

Figure 1.6 $CD8^+$ T cell surveillance 43

1.7 Tumour Immunology **44**

1.7.1 Tumour antigens 45

1.7.2 The role of the immune system in tumourigenesis 47

1.7.3 Cancer immunoediting 51

Figure 1.7 Cancer immunoediting 55

1.8 Conventional tumour therapies 56

1.9 Tumour immunotherapy 58

1.9.1 General approaches 58

1.9.2 Therapeutic vaccination involving $CD8^+$ T cells 60

1.9.3 Genetic modification of $CD8^+$ T cell for use in ACT immunotherapy 67

Figure 1.8 Tumour immunotherapy approaches 72

1.10 RNA interference 73

Figure 1.9 Basis of RNA interference 75

1.11 Protein tyrosine phosphatases 76

1.11.1 SHP-1 77

Figure 1.10 Overall structure of SHP-1 87

Figure 1.11 Activation of SHP-1 88

Figure 1.12 Motheaten and motheaten viable transcripts 89

Figure 1.13 Motheaten and littermate mice 90

1.12 Aims of the study 91

Chapter 2

Materials and methods

2.1 Reagents and consumables 92

2.1.1 Antibiotics 92

2.1.2 Antibodies 92

2.1.3 Cell media and associated reagents 93

2.1.4 Chemicals 93

2.1.5 Distilled water 94

2.1.6 Foetal calf serum 94

2.1.7 Interleukin-2 (IL-2) 94

2.1.8 Intracellular dyes 94

2.1.9 NP68 peptide 95

2.1.10 Plasmid DNA 95

2.1.11 Retinoic acid 95

2.1.12 Tissue culture plastic 96

2.1.13 Viruses 96

2.2 Cell based analytical techniques 96

2.2.1 Counting cells by trypan blue exclusion 96

2.2.2 Flow cytometry 96

2.2.2a Labelling cells with fluorescent conjugated antibodies 97

2.2.2b Labelling cells with intracellular dyes 97

2.2.3 Protein analyses 98

2.2.3a Detergent lysis of cells 98

2.2.3b SDS-PAGE 99

2.2.3c Immunoblotting 99

2.2.3d Immuno-detection 100

2.3 *Escherichia Coli* 100

2.3.1 Culture media 100

2.3.2 Clonal selection 100

2.3.3 Clonal expansion 100

2.3.4 Storage conditions 100

2.4 Tissue culture and cell lines 100

2.4.1 Culture conditions 100

2.4.2 Human transformed cell lines 102

2.4.2a Production of Hela cell expressing mouse SHP-1 102

2.4.2b Production of Hela cell expressing human SHP-1 103

2.4.2c Mouse GM-CSF production 103

2.4.3 Viral packaging cell line 103

2.4.3a Phoenix cells 104

2.4.3b Retrovirus production 104

2.4.4 Transformed mouse cell lines 105

2.4.5 Production of B16 melanoma cell expressing the NP68 epitope and luciferase 106
2.4.5a Infection of B16 melanoma cells 106
2.4.5b Luciferse assay 106
2.4.5c Cloning of B16 cells 106
2.4.5d Assessing GFP expression of transfected B16 cells 108
2.4.6 Primary mouse cell lines 108
2.4.6a Generation of dendritic cells 108
2.4.6b Production of mouse $CD8^+$ F5 T cell blasts 109
2.4.7 Cryopreservation of cells 110
2.5 Animals **110**
2.5.1 Husbandry 110
2.5.2 Breeding of motheaten F5 mice 110
2.5.3 Genotyping motheaten mice 111
2.5.4 Genetic backgrounds 112
2.6 *In vivo* methods **112**
2.6.1 Harvesting and preparation of mouse tissue 112
2.6.1a Lymph nodes 113
2.6.1b Mesenteric lymph nodes 113
2.6.1c Peyer's patches 113
2.6.1d Spleens 114
2.6.1e Lungs 114
2.6.1f Blood 115
2.6.1g Bone marrow 115
2.6.1h Ovaries 116
2.6.1i Gut tissue 116
2.6.2 Immunomagnetic separation of $CD8^+$ T cells 116
2.6.3 Adoptive cell transfers 117
2.6.3a Donor mice 117
2.6.3b Recipient mice 117

2.6.3c Intravenous route 118

2.6.3d Peritoneal route 118

2.6.3e Subcutaneous route 118

2.6.4 *In vivo* antigenic stimulation of $CD8^+$ F5 T cells 119

2.6.4a Dendritic cells 119

2.6.4b Incomplete Freund's adjuvant 119

2.6.4c Influenza A virus 120

2.6.5 The provision of target cells 120

2.6.5a Splenocytes 120

2.6.5b B16 melanoma cells 121

2.7 *In vivo* assays **121**

2.7.1 T cell expansion 122

2.7.2 Cytotoxicity 122

2.7.2a Primary T cell response 122

2.7.2b Memory T cell response 123

2.7.2c Effector memory T cell response 124

2.7.3 Anti-tumour T cell response 124

2.7.3a Detecting B16 cells by flow cytometry 124

2.7.3b Tumour protection assay 125

2.7.3c Tumour regression assay 125

2.7.3d Tumour protection versus enhancement 125

2.7.4 T cell migration studies 126

2.7.4a Peyer's patches 126

2.7.4b Vaccinia infected ovaries 127

2.7.5 T cell infiltration into the bowel 127

2.7.5a Histological analysis of gut tissue 127

2.7.5b Haematoxylin and eosin staining of tissue sections 128

2.8 *In vitro* assays **128**

2.10.1 CD107a assay 128

2.10.2 Regulatory T cell assay 129

2.10.3 Cytotoxicity assay 130

2.9 Silencing SHP-1 expression using shRNA technology 132

2.11.1 Candidate siRNA sequences for SHP-1 132

2.11.2a Synthesis and annealing 132

Figure 2.1 shRNA sequences 133

2.11.2b Cloning 134

2.11.2c Sequencing 134

2.11.2d Functional testing 134

2.11.2 *MISSION*^{TM} shRNA 135

Figure 2.2 *MISSION*^{TM} shRNA sequences 136

2.11.2a Functional testing 136

Chapter 3

Exploring the role of SHP-1 in T cells during *in vivo* antigenic stimulation

3.1 Introduction 138

3.2 Mouse bone marrow cells cultured with GM-CSF are enriched for CD11c+ cells and up-regulate CD86 following maturation with LPS 140

3.3 *In vitro* generated dendritic cells present NP68 peptide to naive $CD8^+$ F5 T cells 140

3.4 Mice receiving naive $CD8^+$ F5 T cells and *in vitro* generated dendritic cells pulsed with NP68 peptide are capable of killing NP68 loaded target cells 141

3.5 Mice receiving naive $CD8^+$ F5 T cells and the influenza A virus are able to kill NP68 labelled target cells 142

3.6 Mice receiving naive $CD8^+$ F5 T cells and NP68 in IFA are able to kill NP68 labelled target cells 143

3.7 Mice receiving naive motheaten $CD8^+$ F5 T cells kill more target cells during a primary T cell response than those mice receiving naive control $CD8^+$ F5 T cells 144

3.8 Enhanced accumulation of motheaten $CD8^+$ T cells in the spleens of recipient mice compared to the spleens of mice receiving control $CD8^+$ T cells 145

3.9 Mice receiving activated motheaten $CD8^+$ F5 T cells kill more target cells than mice receiving activated control $CD8^+$ F5 T cells 146

3.10 Altered ratios of motheaten $CD8^+$ F5 T cells in the blood and Peyer's patches of recipient mice 147

3.11 *In vitro* activated T cells labelled with intracellular dyes are evident in the ovaries of Vaccinia virus infected and non-infected mice following adoptive transfer 150

3.12 Motheaten $CD8^+$ F5 T cells exhibit a greater resistance to regulatory T cell induced inhibition on T cell proliferation than control $CD8^+$ F5 T cells 151

3.13 Summary of results 153

Figure 3.1 Bone marrow cells cultured with GM-CSF are enriched for $CD11c^+$ cells 155

Figure 3.2 Mouse bone marrow cells cultured with supernatant containing GM-CSF or commercially available GM-CSF for 10 days have a similar proportion of $CD11^+CD86^+$ cells after maturation with LPS 156

Figure 3.3 Mouse bone marrow cells cultured with supernatant containing GM-CSF or commercially available GM-CSF present NP68 peptide to $CD8^+$ F5 T cells 157

Figure 3.4 Adoptively transferred naive $CD8^+$ F5 T cells proliferate in mice receiving NP68 loaded dendritic cells 158

Figure 3.5 Mouse bone marrow cells cultured with supernatant containing GM-CSF or commercially available GM-CSF are able to present NP68 peptide to F5 T cells in an *in vivo* context 159

Figure 3.6 Mice receiving naive $CD8^+$ F5 T cells and the influenza A virus were able to mount a T cell response 160

Figure 3.7 A mouse receiving naive control $CD8^+$ F5 T cells and NP68 subcutaneously in IFA was able to kill NP68 loaded target cells 161

Figure 3.8 A mouse receiving naive motheaten $CD8^+$ F5 T cells kills more target cells during a primary T cell response than a mouse receiving naive control $CD8^+$ F5 T cells 162

Figure 3.9 A mouse receiving naive motheaten $CD8^+$ F5 T cells kills more target cells during a primary T cell response than a mouse receiving naive control $CD8^+$ F5 T cells 163

Figure 3.10 Mice receiving naive motheaten $CD8^+$ F5 T cells have more $CD8^+$ cells in their spleens than mice receiving control $CD8^+$ F5 T cells 164

Figure 3.11 A mouse receiving naive motheaten $CD8^+$ F5 T have a greater proportion of $CD8^+$ cells in their spleen after seven days, when compared to a mouse receiving naive control $CD8^+$ F5 T cells 165

Figure 3.12 Mice receiving *in vitro* activated control or motheaten $CD8^+$ F5 T cells were able to kill target cells 166

Figure 3.13 Mice receiving activated motheaten $CD8^+$ F5 T cells kill more target cells than mice receiving activated control $CD8^+$ F5 T cells 167

Figure 3.14 Mice receiving activated motheaten $CD8^+$ F5 T cells kill more target cells than mice receiving activated control $CD8^+$ F5 T cells 168

Figure 3.15 $CD8^+$ F5 T cells activated and expanded *in vitro* in the presence of retinoic acid are found in the Peyer's patches of a recipient mouse 169

Figure 3.16 $CD8^+$ F5 T cells activated *in vitro* in the absence of retinoic acid are found in the blood, spleen and lungs but not the Peyer's patches of recipient mice 170

Figure 3.17 Altered ratios of motheaten $CD8^+$ F5 T cells in the blood and Peyer's patches of recipient mice 171

Figure 3.18 Altered ratios of motheaten $CD8^+$ F5 T cells in the blood and Peyer's patches of recipient mice 172

Figure 3.19 Activated $CD8^+$ F5 T cells labelled with DDAO or CFSE are detected in the ovaries of recipient mice 173

Figure 3.20 Optimal naive $CD8^+$ F5 T cells proliferation seen in anti-$CD3^{Bio}$ coated U-bottomed plates when co-cultured with splenocytes 174

Figure 3.21 Regulatory T cells inhibited both naive control and motheaten $CD8^+$ F5 T cells proliferation 175

Figure 3.22 Greater regulatory T cell induced inhibition on naive control $CD8^+$ F5 T cell proliferation than on naive motheaten $CD8^+$ F5 T cell proliferation 176

Chapter 4

The role of SHP-1 in *in vivo* $CD8^+$ memory T cell responses

4.1 Introduction 177

4.2 Mice receiving naive control $CD8^+$ F5 T cells killed more target cells during a memory T cell response than mice receiving naive motheaten $CD8^+$ F5 T cells, when the memory T cells are recalled by priming with NP68 peptide in IFA 178

4.3 The mode of priming memory control and motheaten $CD8^+$ F5 T cells impacts upon the memory $CD8^+$ F5 T cell response 179

4.4 Mice receiving naive motheaten $CD8^+$ T cells killed more target cells during a memory T cell response than mice receiving naive control $CD8^+$ T cells, when memory T cells are recalled by priming with NP68 peptide-pulsed DCs 180

4.5 Mice receiving naive motheaten $CD8^+$ T cells killed more target cells during a memory T cell response than mice receiving naive control $CD8^+$ T cells, when both naive and memory T cells are primed with NP68 peptide pulsed DCs 181

4.6 Mice receiving *in vitro* activated control $CD8^+$ T cells kill target cells during a memory response seven weeks post transfer 182

4.7 A mouse kills target cells during a memory T cell response without being primed for a second time 183

4.8 Mice receiving naive motheaten $CD8^+$ F5 T cells kill more target cells during a memory T cell response than mice receiving naive control $CD8^+$ F5 T cells 184

4.9 Rag-1$^{-/-}$ mice receiving naive CD8$^+$ F5 T cells develop colitis 185

4.10 Mice receiving naive CD8$^+$ F5 T cells exhibit splenomegaly, lymphomegaly and a cellular infiltrate into their large intestine 186

4.11 Summary of results 188

Figure 4.1 A mouse receiving control CD8$^+$ F5 T cells kills more target cells during a memory T cell response than a mouse receiving motheaten CD8$^+$ F5 T cells, when memory T cells were primed with NP68 in IFA 190

Figure 4.2 A mouse receiving control CD8$^+$ F5 T cells kills more target cells during a memory T cell response than a mouse receiving motheaten CD8$^+$ F5 T cells, when memory T cells are primed with NP68 in IFA 191

Figure 4.3 The mode of priming memory control and motheaten CD8$^+$ F5 T cells influences the magnitude of the memory T cell response 192

Figure 4.4 A mouse receiving naive motheaten CD8$^+$ F5 T cells killed more target cells during a memory T cell response than a mouse receiving naive control CD8$^+$ F5 T cells, when memory T cells were primed with NP68 loaded dendritic cells 193

Figure 4.5 A mouse receiving naive motheaten CD8$^+$ F5 T cells kills more target cells during a memory T cell response than mice receiving naive control CD8$^+$ F5 T cells, when memory T cells are primed with NP68 loaded dendritic cells 194

Figure 4.6 Mice receiving naive motheaten CD8$^+$ F5 T cells kill more target cells during a memory T cell response than mice receiving naive control CD8$^+$ F5 T cells, when naive and memory T cells are primed with NP68 loaded dendritic cells 195

Figure 4.7 Mice receiving *in vitro* activated and expanded CD8$^+$ F5 T cells mount a memory T cell response 196

Figure 4.8 A mouse kills target cells during a memory response without being primed for a second time 197

Figure 4.9 Mice receiving naive motheaten CD8$^+$ F5 T cells kill more target cells when compared to mice receiving naive control CD8$^+$ F5 T cells 198

Figure 4.10 Mice receiving naive motheaten CD8$^+$ T cells kill more target cells when compared to mice receiving control T cells 199

Figure 4.11 Mice receiving CD8$^+$ F5 T cells lose body weight 200

Figure 4.12 Mice receiving NP68 and naive CD8$^+$ F5 T cells have a greater number of cells in their spleens and mesenteric lymph nodes than mice receiving no T cells 201

Figure 4.13 Cell infiltrate in the large intestine of mice receiving CD8$^+$ F5 T cells 202

Figure 4.14 Cryptitis in mice receiving CD8$^+$ F5 T cells 203

Chapter 5

The role of SHP-1 in anti-tumour $CD8^+$ T cell responses

5.1 Introduction 204

5.2 *In vitro* activated control $CD8^+$ F5 T cells kill NP68 peptide pulsed B16 melanoma cells in an *in vitro* setting 205

5.3 Sub-lethally irradiated mice have fewer lung tumour nodules compared to non-irradiated mice fourteen days post intravenous transfer of wild-type B16 cells 206

5.4 B16 cells labelled with intracellular dyes are detected in the lungs of mice twenty-four hours following intravenous transfer 207

5.5 A similar number of B16 nodules are present in mice receiving $CD8^+$ F5 T cells and either B16 cells pulsed with NP68 peptide or unpulsed B16 cells 209

5.6 Successful infection of B16 cells with a retrovirus encoding the NP68 epitope as a fusion protein with GFP 210

5.7 B16 cells infected with a retrovirus encoding the NP68 epitope are killed *in vitro* by $CD8^+$ F5 T cells 210

5.8 Mice receiving $3x10^6$ naive control $CD8^+$ F5 T cells and $1.5x10^5$ B16 cells expressing the NP68 epitope are clear of lung tumours 211

5.9 Complete protection from tumour development in the lungs of mice receiving either naive control or motheaten $CD8^+$ F5 T cells 212

5.10 Similar tumour nodule formation in mice receiving either $1x10^4$ control or motheaten $CD8^+$ F5 T cells or no T cells 213

5.11 Reduced tumour nodule formation in mice receiving $2x10^4$ naive motheaten $CD8^+$ F5 T cells compared to mice that receiving no T cells 214

5.12 Reduced tumour nodules formation in the lungs of mice receiving $3.2x10^4$ motheaten naive $CD8^+$ F5 T cells, when compared to mice receiving $3.2x10^4$ control naive $CD8^+$ F5 T cells 214

5.13 Significantly enhanced protection against lung tumour formation in mice receiving $3.2x10^4$ naive motheaten versus control $CD8^+$ F5 T cells 215

5.14 Activated motheaten $CD8^+$ F5 T cells exhibit an enhanced effector function on a per cell basis when compared to activated control $CD8^+$ F5 T cells 216

5.14a A greater proportion of activated motheaten $CD8^+$ F5 T cells upregulate CD107a upon encounter with B16 cells expressing the NP68 epitope in comparison to activated control $CD8^+$ F5 T cells 217

5.14b Activated motheaten versus control $CD8^+$ F5 T cells kill a greater proportion of NP68 peptide-pulsed B16 cells 218

5.15 Development of *in vivo* assays to examine other aspects associated with the enhance tumour protection seen with motheaten $CD8^+$ F5 T cells 219

5.15a A greater proportion of CD8$^+$ T cells are present in the blood of irradiated mice receiving naive control CD8$^+$ F5 T cells when compared to irradiated mice receiving no T cells 220

5.15b A greater proportion of CD8$^+$ cells were present in the lungs of mice receiving control naive CD8$^+$ F5 T cells when compared to mice receiving no T cells 221

5.15c Mice receiving B16 cells lost weight over the duration of the tumour protection assay, regardless of T cell transfer, whereas those that did not receive any B16 cells gained weight 221

5.16 Partial regression and delayed growth of a subcutaneous B16 melanoma in a mouse receiving motheaten naive CD8$^+$ F5 T cells 222

5.17 Successful co-infection of B16 cells with a retrovirus encoding the Luciferase gene and a retrovirus encoding the NP68 epitope 223

5.18 Significantly enhanced tumour formation in the lungs of irradiated mice receiving control CD8$^+$ F5 T cells, when compared to irradiated mice receiving no T cells 226

5.19 A tumour specific CD8$^+$ T cell response protects against lung tumour development, whereas a non-specific CD8$^+$ T cell response promotes lung tumour formation 227

5.20 Tumour specific CD8$^+$ T cells protect from tumour developments, whereas non-specific CD8+ T cells promote tumour growth 228

5.21 Partial downregulation of SHP-1 expression in Jurkat cells using siRNA sequences identified by online algorithms 229

5.22 Successful production of Hela cells expressing mouse and human SHP-1 231

5.23 Successful reduction of human SHP-1 expression in Hela cells receiving *MISSION*^{TM} shRNA sequences 231

5.24 Summary of results 232

Figure 5.1 Activated CD8$^+$ F5 T cells kill NP68 peptide pulsed B16 cells 234

Figure 5.2 Sub-lethally irradiated mice have fewer lung tumour nodules than non-irradiated mice 235

Figure 5.3 CFSE labelled B16 melanoma cells are present in the lungs of mice twenty-four hours post intravenous transfer 236

Figure 5.4 Detection of B16 cells labelled with either CFSE or DDAO are detected in the lungs of a mouse twenty-four hours post intravenous transfer 237

Figure 5.5 Detection of B16 melanoma cells labelled with different concentrations of CFSE cells in the lungs of a recipient mouse 238

Figure 5.6 A similar number of B16 lung tumour nodules are present in mice receiving CD8$^+$ F5 T cells and either B16 cells pulsed with NP68 peptide or unpulsed B16 cells 239

Figure 5.7	Successful infection of B16 cells with a retrovirus encoding the NP68 epitope as a fusion protein with GFP	240
Figure 5.8	Successful cloning of B16 melanoma cell expressing the NP epitope as a fusion protein with GFP	241
Figure 5.9	B16 cells infected with a retrovirus encoding the NP68 epitope are successfully killed by activated $CD8^+$ F5 T cells	242
Figure 5.10	Mice receiving $3x10^6$ $CD8^+$ F5 T cells and $1.5x10^5$ B16 cells expressing the NP68 epitope are clear of lung tumour nodule	243
Figure 5.11	Complete protection from B16 tumour formation in the lungs of mice receiving naive control or motheaten $CD8^+$ F5 T cells	244
Figure 5.12	Similar lung tumour formation in mice receiving no $CD8^+$ F5 T cells and mice receiving either $1x10^4$ naive control or motheaten $CD8^+$ F5 T cells	245
Figure 5.13	Statistically significant reduced lung tumour formation in mice receiving $2x10^4$ naive motheaten $CD8^+$ F5 T cells in comparison to mice that did not receive any T cells	246
Figure 5.14	A reduced tumour load in the lungs of a mouse receiving naive motheaten $CD8^+$ F5 T cells	247
Figure 5.15	A reduced number of tumour nodules in the lungs of mice receiving naive motheaten $CD8^+$ F5 T cells, when compared to those mice receiving naive control $CD8^+$ F5 T cells	248
Figure 5.16	A reduced tumour load in the lungs of mice receiving naive motheaten $CD8^+$ F5 T cells	249
Figure 5.17	Statistically significant reduced lung tumour nodule formation in the lungs of mice receiving naïve motheaten $CD8^+$ F5 T cells	250
Figure 5.18	Statistically significant reduced lung tumour nodule formation in mice receiving naïve motheaten $CD8^+$ F5 T cells in comparison to mice receiving naïve control $CD8^+$ F5 T cells	251
Figure 5.19	Activated control and motheaten $CD8^+$ F5 T cells upregulate CD107a upon encounter with NP68 peptide-pulsed B16 cells	252
Figure 5.20	A greater proportion of activated motheaten $CD8^+$ F5 T cells upregulate CD107a upon encounter with cognate peptide pulsed B16 cells in comparison to activated control $CD8^+$ F5 T cells	253
Figure 5.21	A greater proportion of activated control and motheaten $CD8^+$ F5 T cells upregulate CD107a upon encounter with NP68 peptide-pulsed B16 cells	254
Figure 5.22	A greater proportion of activated motheaten $CD8^+$ F5 T cells upregulate CD107a upon encounter with NP68 peptide-pulsed B16 cells than activated control $CD8^+$ F5 T cells	255
Figure 5.23	Activated motheaten $CD8^+$ F5 T cells kill more B16 cells expressing the NP68 epitope than activated control $CD8^+$ F5 T cells	256

Figure 5.24 Activated motheaten $CD8^+$ F5 T cells kill more B16 cells expressing the NP68 epitope in comparison to activated control $CD8^+$ F5 T cells 257

Figure 5.25 Significantly reduced tumour nodule formation in the lungs of mice receiving naive control $CD8^+$ F5 T cells 258

Figure 5.26 Adoptively transferred $CD8^+$ F5 T cells are detected in the blood of mice 259

Figure 5.27 Adoptively transferred $CD8^+$ F5 T cells are detected in the lungs of mice 260

Figure 5.28 Mice receiving B16/NP cells lost weight over the duration of a tumour protection experiment 261

Figure 5.29 Subcutaneous B16 tumour growth over 14 days 262

Figure 5.30 Partial regression and delayed growth of a subcutaneous B16 melanoma in a mouse receiving naïve motheaten $CD8^+$ F5 T cells 263

Figure 5.31 Production of monoclonal B16 cell lines expressing the luciferase gene 264

Figure 5.32 Infection of B16 luciferase/YFP cells with a retrovirus encoding the NP68 epitope as a fusion protein with GFP ' 265

Figure 5.33 Differential GFP expression by B16 luciferase/YFP cells infected with a retrovirus encoding the NP68 epitope as a fusion protein with GFP 266

Figure 5.34 GFP expression and luciferase activity of B16 luciferase/YFP cells infected with a retrovirus encoding GFP and NP68 267

Figure 5.35 B16 luciferase/YFP cells infected with a retrovirus encoding the NP68 epitope as a fusion protein with GFP are killed by activated $CD8^+$ F5 T cells 268

Figure 5.36 $CD8^+$ T cells enhance tumour nodule formation in the lungs of mice 269

Figure 5.37 A tumour-specific $CD8^+$ T cell response protects mice from tumour formation, whereas a non-specific $CD8^+$ T cell response promotes tumour formation 270

Figure 5.38 Mice primed with NP68 peptide in IFA have significantly more lung tumour nodules than mice that are not primed 271

Figure 5.39 Algorithm-identified candidate sequences within the SHP-1 transcript for siRNA targeting 272

Figure 5.40 SHP-1 protein detection in Jurkat cells by immunoblot analysis 273

Figure 5.41 Reduced SHP-1 expression in Jurkat cells receiving shRNA expression plasmids 274

Figure 5.42 Successful introduction of mouse and human SHP-1 genes to Hela cells 275

Figure 5.43 Reduced SHP-1 expression in Hela cells receiving *MISSION*™ shRNA plasmids 276

Chapter 6

Discussion

6.1 Aims and challenges of the study 277

6.2 Priming $CD8^+$ F5 T cells *in vivo* 278

6.3 The role SHP-1 in primary $CD8^+$ T cell responses 279

6.4 The role of SHP-1 in memory $CD8^+$ T cell responses 286

6.5 The role of $CD8^+$ T cells in irritable bowel disease (IBD) 291

6.6 *In vivo* tumour studies 294

6.7 siRNA studies 298

6.8 Pro-tumoural role of $CD8^+$ T cells in a lung tumour model 300

6.9 Overall summary and conclusions 302

References 304

Appendix

Sathish, J.G., Dolton, G., Leroy, F.G., and Matthews, R.J. (2007). Loss of Src homology region 2 domain-containing protein tyrosine phosphatase-1 increases CD8+ T cell-APC conjugate formation and is associated with enhanced *in vivo* CTL function. J Immunol *178*, 330-337. 341

Chapter 1

Introduction

1.1 The Immune System

The immune system is fundamental for the existence of multicellular animals. It offers host protection against invading pathogenic microorganisms, such as virus, bacteria, fungi and parasites. In addition to providing protection against these extrinsic threats, the immune system also plays a role in protecting against intrinsically generated hazards, such as malignant cells.

However, the immune system has a dual responsibility. In addition to protecting the host from infectious organisms and malignancies, the immune system has to be self-tolerant in order to prevent host cells from being harmed by the effector mechanisms it can deploy. In light of these demands, the immune system is regulated in such a way as to maintain homeostatic harmony. Nevertheless, in a dysregulated state the immune system is responsible for autoimmune diseases, such as type I diabetes and multiple sclerosis. The immune system may also react inappropriately as demonstrated by the occurrence of allergies. Moreover, the power of the immune system is demonstrated in a clinical setting, when transplant recipients reject organs, and immunodeficient individuals exhibit an increased susceptibility to infection and tumour development.

The cells of the immune system are generated in the bone marrow from pluripotent haematopoietic stem cells. Once mature, they are found throughout the body in anticipation of pathogen invasion or tumour development. The detection of a pathogen or tumour is enhanced by the presence of the lymphatic system, which consists of lymphoid channels and tissues that drain extracellular fluid from tissues.

The cellular components of the immune system have classically been divided into innate immunity, which provides primary protection against an assault, and adaptive immunity, which provides more effective defence against an infection or developing tumour.

1.1.1 Innate Immunity

Innate immunity has two modes that aim to provide protection to the host against an assault. A component of the first mode involves non-specific mechanisms of preventing pathogen entry to the host. These are attributed to the presence of preformed chemical, microbiological and mechanical barriers, such as the tight junctions between epithelial cells of the skin and gut. The first mode also involves broadly-specific innate immune cells such as macrophages and neutrophils. They are resident in peripheral tissues and are capable of recognising pathogens, via the expression of pattern recognition receptors (PRRs) that recognise common molecular patterns on the surface of a wide range of pathogens. Some of these receptors assist with the binding and subsequent phagocytosis of the pathogen, which is then destroyed within the cell. Innate-like lymphocytes, such as γδ T cells and NKT cells (Chan *et al.*, 2003) can also act as sentinels at peripheral sites, and provide an immediate response upon recognition of antigen.

If an assault is successful at breaching this first line of innate defence, an inducible and broadly-specific innate immune response occurs, which involves cellular elements and possibly the complement system. The release of inflammatory mediators from innate cells during initial detection of a pathogen mediates this phase of an innate response. It involves the active recruitment of innate cells, such as monocytes, neutrophils and natural killer (NK) cells from the blood to the site of pathogen invasion or tumourigenesis.

Pathogens and tumours have developed sophisticated mechanisms of evading an innate immune response and in order to prevent long-term damage from occurring to the host,

adaptive immune cells unite with innate cells in combating the assault. Innate antigen presenting cells (APCs), such as dendritic cells (DCs), process and present peptide antigens that are able to activate adaptive immune cells. In addition, cytokines produced by innate cells under inflammatory conditions act to ensure efficient priming of adaptive immune cells.

1.1.2 Adaptive Immunity

Adaptive immunity is an induced and highly specific response to pathogenic microorganisms or tumourigenesis. It is comprised of humoral immunity, involving B cells, and a cell-mediated immunity, involving T cells. The initiation of an adaptive response does not coincide with the subsidence of the innate response. Moreover, components of the innate and adaptive immune responses act concertedly to combat an assault. B and T cells are primed within secondary lymphoid organs, such as the spleen, peripheral lymph nodes and mucosal associated lymphoid tissue (MALT).

Mature conventional B cells leave the bone marrow and circulate between the cardiovascular and lymphatic systems. The antigen receptor on B cells, termed the B cell receptor (BCR) is a cell surface immunoglobulin. Once activated, B cells differentiate into plasma cells that secrete antibody molecules of the same specificity as the BCR. Antibodies are able to directly bind and neutralise pathogens and their components, or mark them for lysis or phagocytosis.

Immature T cells leave the bone marrow and undergo further development in the thymus before entering the cardiovascular and lymphatic systems as naive T cells. From here they survey lymphoid tissue for cognate antigen. Upon recognition of cognate antigen, T cells undergo clonal expansion and acquire effector function in order to provide protection from pathogen invasion or tumourigenesis. T cells possess an antigen receptor, termed the T cell receptor (TCR), composed of an α and β chain (Garcia *et al.*, 1999; Garcia *et al.*, 1996). TCRs

recognise antigenic peptides that are displayed at the surface of cells by glycoproteins, termed major histocompatability complex (MHC) molecules (Davis and Bjorkman, 1988). The peptides displayed by MHC molecules of a cell are generated by the intracellular degradation of proteins. Overall, the process of antigen binding by T cells is a tri-molecular process involving the TCR, a peptide and a MHC molecule. There are two types of αβ T cells, which are marked by the expression of the surface proteins, CD4 and CD8. The expression of these proteins also marks the effector capabilities of the T cell subsets.

Those T cells expressing the CD4 protein ($CD4^+$) recognise peptide fragments from the intravesicular degradation of proteins, which are subsequently presented by MHC class II molecules on APCs. They provide help to other cells during an immune response by releasing specific cytokines and by engaging with other cells via receptor ligand interactions. The differentiation of activated $CD4^+$ T cells into various subsets, which have distinct roles, is mediated by the release of cytokines from APCs. $CD4^+$ T helper 1(Th1) cells control intravesicular bacteria and extracellular pathogens by activating macrophages and B cells respectively. $CD4^+$ Th2 cells can also activate B cells and are involved in antibody class switching of B cells in order to control parasitic infections. A third subset of helper T cells, called Th17 cells, act early in the adaptive immune response and elicit a neutrophil response to combat bacterial infections. More recently, T follicular helper cells have been shown to play an important role in the formation of germinal centres and in antibody isotype switching of B cells (Vogelzang *et al.*, 2008) and therefore constitute a fourth subset of helper T cells. $CD4^+$ T cells can also have a regulatory role by suppressing T cell responses to both foreign and auto-antigens. Natural regulatory T cells (Tregs) develop in the thymus whereas adaptive Tregs gain their suppressive function in the periphery. Tregs exert their suppressive actions by either releasing inhibitory cytokines or conditioning APCs so they are less effective at priming T cells.

Those T cells expressing the CD8 protein ($CD8^+$) recognise peptides derived from the cytosolic degradation of proteins that are presented by MHC class I molecules. Most somatic cells including APCs express MHC class I molecules at their surface. The role of a $CD8^+$ T cell is to detect and directly eradicate cells displaying cognate antigen and are therefore called cytotoxic T lymphocytes (CTLs). The antigenic peptide can be derived from viruses, cytosolic bacteria and proteins associated with malignant conversion. $CD4^+$ T cells provide help to $CD8^+$ T cells during their priming and differentiation and are required for the optimal formation and maintenance of a $CD8^+$ memory T cell pool. Indeed, it is a hallmark of adaptive immune cells to persist as long-lived memory cells following antigen induced activation. This provides a host with a more sensitive and vigorous response upon re-encounter with an antigen.

1.2 Antigen recognition by T cells

1.2.1 MHC molecules and peptide presentation

MHC class I molecules consist of two non-covalently linked polypeptide chains. The polymorphic α chain is encoded in the MHC locus of chromosome six, and in the assembled molecule spans the cell membrane. The second chain is the non-polymorphic β_2-microglobulin, which does not have a transmembrane region. The assembled molecule contains four domains; three are contributed by the α chain (α1, α2 and α3) and one by β_2-microglobulin (Bjorkman *et al.*, 1987). Domains α1 and α2, are furthest away from the membrane, and fold in such a way to form a single structure termed the peptide-binding cleft. The peptide-binding cleft of the MHC class I molecules consists of two separated α helices on a bed of antiparallel β sheets (figure 1.1).

MHC class I molecules bind short peptides, which are stabilised by the formation of hydrogen bonds and ionic interactions between atoms at the free amino and carboxyl terminals of the peptide, and invariant sites at each end of the MHC molecule binding cleft. The peptide binds in an extended fashion with other residues aside from those at the amino and carboxyl terminus making additional interactions with the MHC molecule. These residues are termed anchor residues, and a given MHC variant will preferentially bind peptides with the same or similar residues at defined positions along the length of the peptide. Typically, peptides of 8-10 amino bind to MHC class I molecules (Madden *et al.*, 1993), although longer peptides can be accommodated by kinking of the peptide backbone or by post-binding cleavage of the peptide by exopeptidases.

MHC class I molecules acquire their peptide cargo during their biosynthesis and assembly inside the endoplasmic reticulum (ER). Endogenously and exogenously sourced proteins present within a nucleated cell are processed in the cytoplasm to yield peptides.

Endogenous peptides may be derived from normally expressed cytosolic, membrane and secreted proteins, but also from proteins associated with malignant transformation. Exogenous proteins can be derived from the direct infection of cells, as with virus and cytosolic bacteria. Furthermore, exogenous proteins and peptides can be cross presented on MHC class I molecules by specialist APCs (Heath and Carbone, 1999). APCs can phagocytose necrotic cells (Albert *et al.*, 1998a; Albert *et al.*, 1998b; Subklewe *et al.*, 2001) or engulf extracellular fluid (macropinocytosis) (Sallusto *et al.*, 1995) into their vesicular system. From here the proteins and peptides are transferred to the cytosol by a mechanism called retrotranslocation, where they are processed ready for presentation (Rodriguez *et al.*, 1999). Proteins destined for processing are labelled covalently with the peptide, ubiquitin, which signals for their subsequent degradation by a protease complex called the proteasome (Rock *et al.*, 2002). The standard proteasome degrades proteins under normal physiological conditions, whereas the immunoproteasome is activated in response to IFNγ and does not require proteins to be ubiquinated for degradation (Van den Eynde and Morel, 2001). Peptide fragments are moved from the cytoplasm, by the chaperone activities of heat shock proteins (HSPs) (Li *et al.*, 2002), to the ER via a heterodimeric transport molecule called, transporter associated with antigen processing (TAP), which is present in the ER membrane (Lankat-Buttgereit and Tampe, 2002). Once in the lumen of the ER, the peptides are transferred to newly synthesised MHC class I molecules, which are associated with TAP, via the TAP associated protein, tapasin. The assembled and stabilised peptide:MHC class I complex is then transported to the outer cell membrane.

Other pathways also exist that allow for the cross-presentation of peptides by MHC class I molecules. The first mechanism is both TAP and proteasome independent, and involves the putative release of peptides from endosomes at the cell surface (Pfeifer *et al.*, 1993). The resulting high concentration of peptides at the cell surface can then force an exchange with

a lower stability peptide that is already bound to an MHC class I molecule. Similarly, peptides generated by the extracellular action of enzymes, or those that are released from lysed or apoptotic cells, may act in the same manner (Smith *et al.*, 1992). In a research situation, the exogenous administration of a peptide to cells leads to the presentation of the peptide by MHC class I molecules. The second mechanism involves internalisation of peptide:MHC class I complexes from the surface of cells, which are subsequently transported, via vesicles, to acidified endosomal compartments termed, MHC class II compartments (MIIC). The acidic nature of the MIIC mediates the release of the peptide from the binding groove, allowing other peptides to bind. The new peptide:MHC class I complex is then transported back to the surface of the cell (Schirmbeck *et al.*, 1995).

MHC class II molecules are composed of heterodimers of membrane-anchored α and β chains, which together contain four extracellular domains. MHC class II molecules bind peptides that are variable in length, with anchor residues present at central residues of the peptides (Stern *et al.*, 1994). MHC class II molecules acquire their peptide cargo in MIIC, post synthesis, whilst en route to the plasma membrane (Hiltbold and Roche, 2002).

1.2.2 αβ T cell receptors

An αβ T cell may express approximately 30,000 TCR at its surface. Each is comprised of an α and β transmembrane chain, which create one antigen binding site (Chothia *et al.*, 1988). When assembled, the TCR chains have an extracellular portion consisting of a variable and constant region, and a stalk segment. Each chain has a hydrophobic transmembrane region containing positively charged amino acid residues. Each chain also contains a short cytoplasmic tail. Cysteine residues present in each chain lead to the formation of intramolecular and interchain disulphide bonds, with the latter forming between the stalk

segments of each chain. In addition, carbohydrate residues present in the constant and variable regions mediate interchain interactions, via the formation of hydrogen bonds.

The T cell repertoire of an individual is capable of recognising a wide range of peptidic antigens. This diversity is achieved by variations in the amino acid sequence at the antigen binding site. Bone marrow progenitor and immature T cells contain TCR genes in their inherited configuration. Somatic recombination of the gene segments at the TCR α and β loci enables a diverse number of antigen receptors to be generated. The human TCR α chain loci contains 1 constant, 37 functional variable (V) and >50 joining (J) region gene segments. The human TCR β chain loci contains 2 constant, 47 functional variable and 12-13 joining gene segments, and unlike the TCR α loci, 2 diversity (D) gene segments (Davis and Bjorkman, 1988). Somatic recombination of the V, (D) and J gene segments is mediated by a group of enzymes called the VDJ recombinases (Agrawal and Schatz, 1997). Recombinase-activating gene (RAG) -1 and -2 proteins recognise DNA sequences called recombination signal sequences (RSSs) that flank each TCR gene segment (Grawunder *et al.*, 1998). The enzymes act by bringing the V, D and J segments together and cleaving the DNA at specific sites, forming DNA hairpins. The DNA is subsequently ligated to yield a full length recombined VJ (TCRα) or VDJ (TCRβ) variable domain exon without intervening DNA segments, which then joins a constant gene region.

Diversity of TCR is achieved by the recombination of different V, (D) and J gene segments of the α and β gene loci (Arstila *et al.*, 1999). In addition to this combinatorial diversity, junctional diversity can lead to an even greater TCR diversity due to its imprecise nature (Gauss and Lieber, 1996). Junctional diversity can involve three types of sequence change, which are not mutually exclusive and may occur simultaneously during a single gene rearrangement. During the last stages of V(D)J recombination and in preparation for DNA ligation, the hairpin itself or neighbouring DNA is cut in a single-stranded manner.

Exonuclease activity may remove templated nucleotides from the gene segments junctions, and as long as this does not create a stop or nonsense codon, new sequences are produced. Nucleotides may also be added at this stage and depending upon their mode of introduction are termed P- or N-nucleotides. If the cutting of DNA takes place within the coding sequence at the junction site, the hairpin will open, creating a single stranded tail. DNA repair enzymes then introduce complementary P-nucleotides to form double stranded DNA, thus creating short palindromic sequences. If the hairpins are nicked in the non-coding intervening DNA of the RSSs, the lymphocyte specific enzyme called terminal deoxyribonucleotidyl transferase adds random, non-germline encoded nucleotides, termed N nucleotides, to sites of recombination.

In the assembled TCR, the V(D)J encoded regions determine the antigen binding specificity of the TCR (figure 1.1). The V regions of both chains contain complementary-determining regions (CDRs) 1 and 2. The CDR3 loop encompasses the highly variable junctions of either the VJ (TCRα) or VDJ (TCRβ) gene encoded segments; therefore TCR diversity is concentrated in this area. X-ray crystallographic studies of TCRs engaged with peptide:MHC class I molecules have shown that the TCR orientates diagonally across the occupied peptide binding cleft when viewed from above the MHC (Garcia *et al.*, 1996). The CDR3 regions of the TCR α and β chains bind to the middle of the peptide, whereas the CDR1 and CDR2 regions bind to the end of the bound peptide and also the MHC molecule (Garboczi *et al.*, 1996).

1.2.3 T cell coreceptors

In conjunction with the binding of TCRs to peptide:MHC molecules, other cell surface proteins, called CD8 and CD4, also interact with MHC molecules (Konig, 2002). They are required for the generation of effective T cell responses and are therefore termed T cell

coreceptors. They bind to membrane proximal domains of the MHC molecule that are distinct from the peptide binding domains (Tanabe *et al.*, 1992). The CD8 molecule, which is expressed by CTLs, consists of an α and β chain linked by a disulphide bridge. The CD8 coreceptor can also exist as a homodimer of two α chains. The immunoglobulin-like domains of CD8, which are found furthest from the membrane, bind to an invariant site on the α3 domain and the base of the α1 and α2 domains of the MHC class I molecule (figure 1.2). The cytoplasmic domains of the α CD8 chain are capable of interacting with intracellular proteins involved in TCR signalling pathways (Shaw *et al.*, 1990). The CD4 coreceptor, expressed by helper and regulatory T cells, is distantly related to CD8. It is composed of a single chain consisting of four immunoglobulin-like domains, with the membrane proximal domain (D1) making contact with MHC class II molecules.

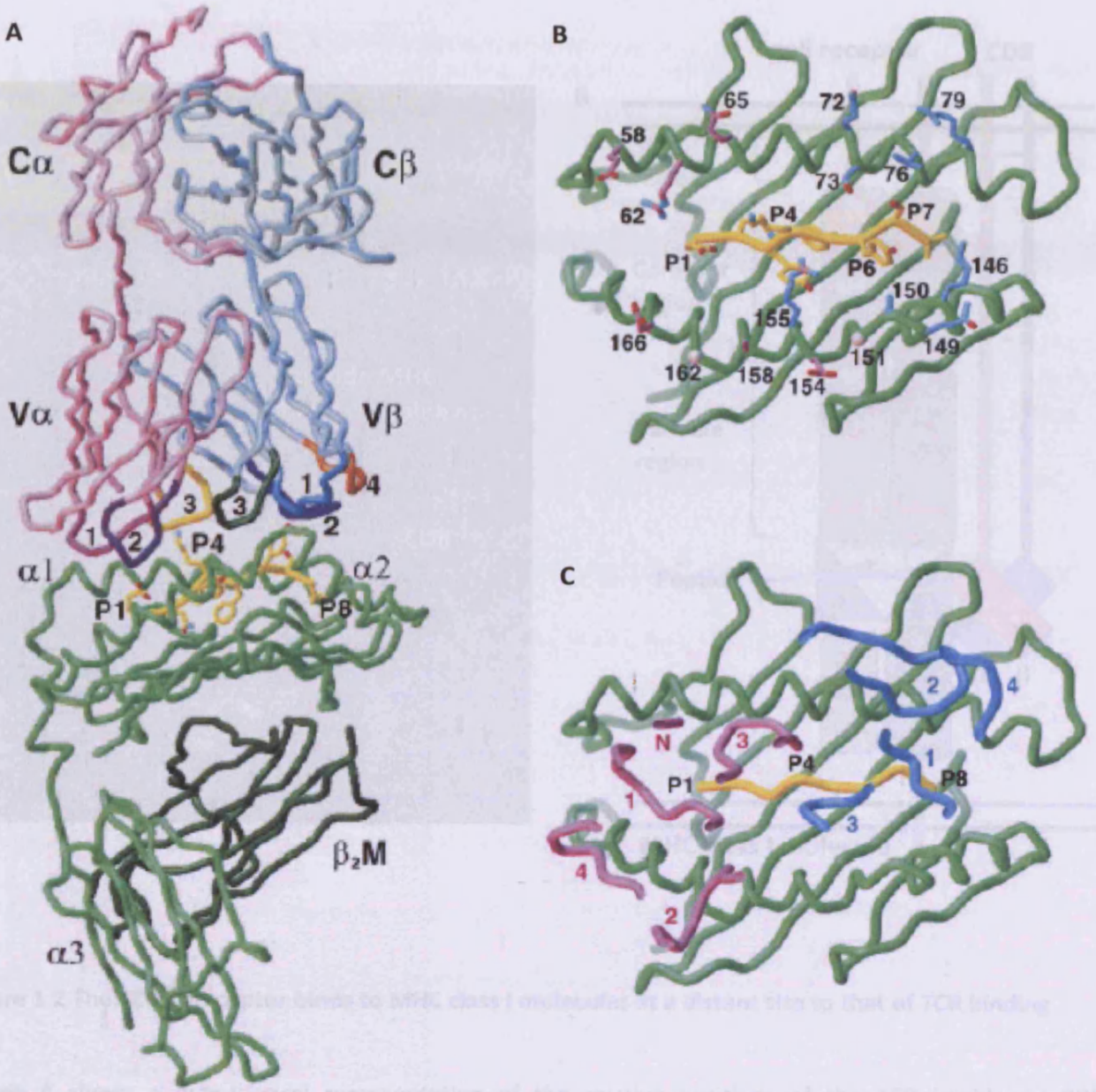


Figure 1.1: T cell receptor binding to a peptide:MHC complex.

In A, the α (pink) and β (blue) chains of the alloreactive mouse T cell receptor (2C) are shown above a peptide (dVE8) MHC class I (green) complex (H_2-K^b). The CDR regions of the TCR are shown in colour and numbered accordingly. B and C view the peptide MHC complex from above showing the peptide binding cleft, which consists of two separated α helices on a bed of antiparallel β sheets. In B, all peptide MHC complex residues involved in contact are labelled. C shows the CDRs of the TCR superimposed onto the peptide MHC complex; dark pink for those from the α TCR chain and blue for those from the β TCR chain. Figures adapted from Garcia *et al.*, 1998.

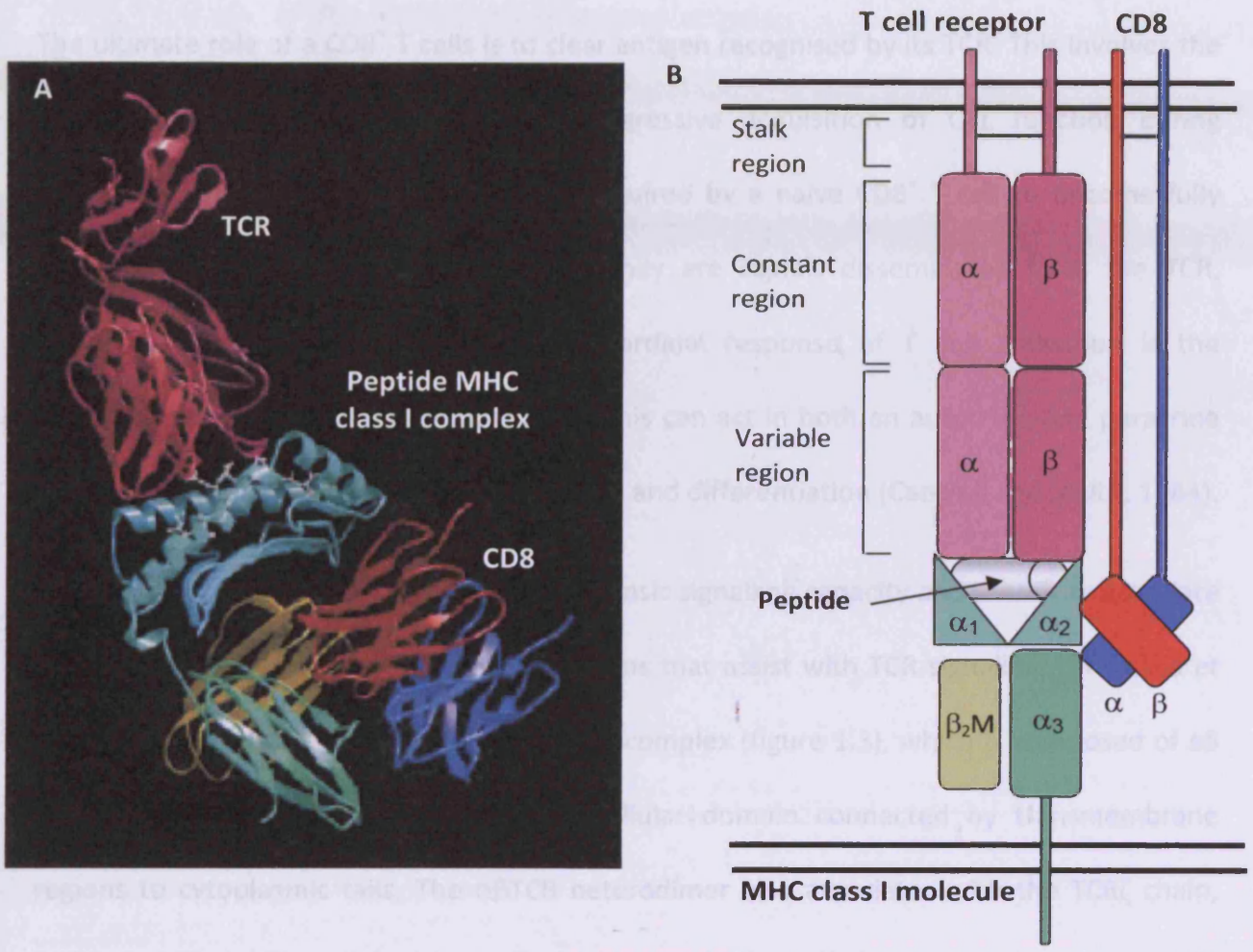


Figure 1.2 The CD8 coreceptor binds to MHC class I molecules at a distant site to that of TCR binding

Figure A shows a hypothetical representation of the relative positions of the TCR (pink) and CD8 coreceptor (red and blue) bound to the same MHC class I molecule (yellow and green). Figure B is a schematic representation of figure A and shows the binding of the CD8 coreceptor to the α_2 and α_3 of the peptide MHC class I complex. Figure A taken from Gao *et al.*, 1997.

1.3 Antigenic $CD8^+$ T cell responses

The ultimate role of a $CD8^+$ T cells is to clear antigen recognised by its TCR. This involves the activation of naive T cells and their progressive acquisition of CTL function during differentiation. Three distinct signals are required by a naive $CD8^+$ T cell to become fully activated and undergo clonal expansion. They are signals disseminated from the TCR, costimulatory and cytokine receptors. A cardinal response of T cell activation is the production of the mitogenic cytokine, IL-2. This can act in both an autocrine and paracrine manner to further facilitate T cell proliferation and differentiation (Cantrell and Smith, 1984).

The α and β chains of the TCR possess no intrinsic signalling capacity and therefore associate electrostatically with invariant accessory chains that assist with TCR signalling (Manolios *et al.*, 1994). The invariant chains form the CD3 complex (figure 1.3), which is composed of εδ and εγ heterodimers. Each has an extracellular domain connected by transmembrane regions to cytoplasmic tails. The αβTCR heterodimer also associates with the TCRζ chain, which is a homodimer linked by a disulphide bond. The ζ chains have a cytoplasmic tail, transmembrane domain and a short extracellular domain.

T cell signalling pathways involve the coordinated actions of transmembrane, membrane-associated and intracellular proteins, which may be enzymes or act as adaptors. The proteins can have a positive or negative influence on T cell signalling pathways. This ensures that T cells respond appropriately to antigenic stimulation. One of the proximal steps in TCR signalling is the phosphorylation of tyrosine (Y) residues belonging to key proteins (Hsi *et al.*, 1989). This is a post translational modification that can either alter the activity of a protein or create docking sites to allow proteins to interact (Pawson and Scott, 1997). Phosphates (p) are added to tyrosine residues by protein tyrosine kinases (PTKs), whilst the reverse reaction is performed by protein tyrosine phosphatases (PTPs) (Chan *et al.*, 1994). Therefore,

the tyrosyl-phosphorylated state of a T cell at any given time is a balance between the catalytic activities of PTKs and PTPs (Neel and Tonks, 1997).

1.3.1 TCR signalling (summarised in figure 1.3)

The mechanism by which TCR engagement with peptide:MHC leads to T cell stimulus is not fully understood. A proposed mechanism that involves oligomerisation of TCRs is supported by the *in vitro* observation that cross-linking TCR with anti-CD3 antibodies induces T cell activation. It seems that the close proximity of several TCR complexes and their associated proteins is required for the initiation of intracellular signalling. Indeed, the structure of the TCR is compatible with the formation of dimers (Fields *et al.*, 1995; Reich *et al.*, 1997) and it has been shown *in vitro* that TCRs bound to peptide MHC complexes tend to form dimers (Garboczi *et al.*, 1996). *In vivo*, the oligomerisation of antigen specific TCRs may be precluded by the low concentration of MHC molecules displaying antigenic peptide on a given APC. Alternatively, oligomerisation of TCRs may be achieved when they interact with both a cognate peptide:MHC molecule and a MHC molecule displaying a self peptide.

Although oligomerisation of TCRs may allow early signalling events, further events are required for sustained signalling to be achieved. The serial triggering model of TCR signalling suggests that numerous TCRs belonging to a given T cell engage with a relatively lower number of peptide MHC complexes on an APC. As a result this allows for sufficient triggering of an individual TCR and therefore signal transduction.

The TCR signalling cascade involves a series of events involving protein-protein and protein-lipid interactions (Norian and Koretzky, 2000; Zhang and Samelson, 2000). The presence of protein domains containing conserved amino acid motifs facilitates such interactions. Src Homology 2 (SH2) domains are approximately 100 amino acids in length and bind to context-specific phosphorylated (p) Y residues (Pawson, 1995). PY residues are present within

immunoreceptor tyrosine-based activation motifs (ITAMs) of TCR associated CD3 chains and have a consensus amino acid sequence of YXX[L/I]X6-12pYXX[L/I] (where X is any amino acid) (Cambier, 1995). SH3 domains are between 50-75 amino acids in length and contain the consensus motif XPpXP (where P is a preference for proline), which binds to polyproline sequence motifs. Phospho-tyrosine-binding (PTB) domains bind pY motifs, but differ from SH2 domains in structure and sequence preference. They bind to pY of the consensus sequence, NPXpY, which are preceded by amino acids in a β turn (Kavanaugh *et al.*, 1995). Finally, the Pleckstrin Homology (PH) domain mediates binding of proteins to anionic phospholipids (Pawson and Scott, 1997).

Upon initial T cell stimulus, the formation of a three dimensional molecular structure at the junction between the T cell and APC (Dustin and Chan, 2000), termed the immunological synapse (IS) further facilitates TCR signalling. Components necessary for TCR signalling congregate at the IS and form a supramolecular activation complex (SMAC) (Monks *et al.*, 1998). With regards to the T cell, the initial cluster comprises adhesion molecules surrounded by engaged TCRs. The initial SMAC then undergoes changes leading to the formation of a SMAC that is comprised of a concentric triple ring structure. The inner and outer peripheral SMAC (pSMAC) contains adhesive molecules such as CD2 and LFA-1. This ensures that the APC and T cell remain together for a sufficient duration to allow signal transduction. The central SMAC (cSMAC) contains the necessary proteins for TCR signal transduction. These include engaged TCRs, the CD3 complex, CD45 (transmembrane protein tyrosine phosphatase), protein kinase C-θ (PTK-θ), CD28 and CD8 its associated intracellular PTK, Lck (Monks *et al.*, 1998). Intracellularly, the PTKs, Lck and Fyn locate within the cSMAC and the actin binding protein, talin, is found in the pSMAC (Dustin and Cooper, 2000). Alterations in the geometry of the IS may assist in initiating TCR signalling pathways. Moreover, molecular components of the TCR signalling pathway may be selectively involved

during the formation of the IS, based upon the size of their extracellular domains (Wild *et al.*, 1999).

Phosphorylation of the ITAM motifs of the TCR complex invariant chains is one of the early events in TCR induced signalling. This is carried out by the coordinated activity of members of the Src family kinases, Lck and Fyn. These PTKs are associated with the inner leaflet of the plasma membrane by amino terminal myristylation and palmitoylation. Lck also interacts non-covalently with the CD8 or CD4 coreceptor (Koegl *et al.*, 1994; Turner *et al.*, 1990), which brings it in close proximity with its substrates. The event that leads to the activation of the PTKs is not known, but the removal of an inhibitory phosphate by CD45, and engagement of either their SH2 or SH3 domains induces their activation (Ashwell and D'Oro, 1999). Fully phosphorylated ITAMs allows zeta-chain associated protein of 70KDa (ZAP-70) to be recruited to the TCR via binding of its tandem SH2 domains to ITAMs (Chu *et al.*, 1998). ZAP-70 is then activated by Lck mediated tyrosine phosphorylation (Chan *et al.*, 1995; Neumeister *et al.*, 1995). Once activated, ZAP-70, which belongs to the Syk family of PTKs, phosphorylates the scaffold protein, linker of activated T cells (LAT), which allows Grb2 related adaptor proteins downstream of Shc (GADS) to bind to LAT's cytoplasmic domain (Zhang *et al.*, 2000). GADS is constitutively associated, via a SH3 domain, with SH2 containing leukocyte phosphoprotein of 76KDa (SLP-76) (Asada *et al.*, 1999), which is subsequently phosphorylated by ZAP-70.

This leads to the recruitment and activation of phospholipase Cγ1 (PLCγ1). PLCγ1 binds via its SH2 domain to phosphorylated motifs present in LAT and SLP-76 (Paz *et al.*, 2001). ZAP-70 phosphorylates PLCγ1 leading to its initial activation (Williams *et al.*, 1999), but additional phosphorylation is required for full activation of PLCγ1. A member of the Tec family of tyrosine kinases, inducible T cell kinase (Itk), is responsible for the sustained activation of PLCγ1. Itk is recruited to the plasma membrane by binding of its PH domain to

phosphoinositol trisphosphate (PIP_3), a product of PI3-Kinase (PI3K), which is activated during TCR signalling. Itk also binds via its SH3 and SH2 domains to SLP-76 (Bunnell *et al.*, 2000) and is therefore placed in close proximity to PLCγ1, which is then fully activated. PLCγ1 catalyses the generation of diacylglyceride (DAG) and Inositol 1,4,5 trisphosphate (IP_3) by the metabolism of phosphatidylinositol bisphosphate (PIP_2).

IP_3 diffuses into the cytosol and binds to the IP_3 receptors on the ER, which triggers the release of calcium (Ca^{2+}) into the cytosol from the endoplasmic reticulum (Berridge, 1993). The depletion of intracellular Ca^{2+} stores leads to capacitative Ca^{2+} entry from the extracellular surroundings by the activation of calcium release-activated calcium channels in the plasma membrane (Putney and Bird, 1993). Sustained levels of cytosolic Ca^{2+} leads to the indirect activation of the transcription factor, nuclear factor of activated T cells (NFAT) (Crabtree and Clipstone, 1994). The binding of Ca^{2+} to the protein calmodulin allows it to associate with the serine/theronine phosphatase, calcineurin. Calcineurin removes phosphorylated residues on constitutively expressed NFAT, thereby allowing translocation to the nucleus.

DAG diffuses in the plasma membrane and activates the guanosine exchange factor (GEF), Ras guanine nucleotide releasing protein (RasGRP), and also PKC-θ. RasGRP activates the small G protein Ras, by exchanging Ras-bound guanosine–diphosphate (GDP) with guanosine–triphosphate (GTP) (Ebinu *et al.*, 1998). Ras can also be activated by another GEF, called son of sevenless (SOS), which is recruited to the LAT and SLP-76 scaffold, via Growth Factor Receptor Binding Protein 2 (Grb2). Activated Ras then initiates a mitogen-activated kinase (MAPK) cascade involving the sequential phosphorylation of Raf, Mitogen-activated or extracellular signal-regulated protein kinase (Mek) (Kyriakis *et al.*, 1992) and extracellular signal-related kinase (Erk). Activated Erk gains entry to the nucleus where it phosphorylates the transcription factor Elk-1. This binds to the serum response element in the promoter of

the gene for the transcription factor c-Fos, which leads to an increase of its gene transcription. Dimers form between c-Fos and c-Jun, with the latter being constitutively expressed in T cells, and phosphorylated by the MAP kinase, JNK, in order to facilitate its translocation to the nucleus. Together, c-Fos and c-Jun form the transcriptional regulator AP-1 (Whitmarsh and Davis, 1996).

The association of PKC-θ with DAG at the plasma membrane allows it to phosphorylate the scaffold protein, caspase recruitment domain-containing membrane-associated guanylate kinase protein-1 (CARMA-1), which then forms a membrane-associated complex involving the proteins, Mucosa associated lymphoid tissue lymphoma translocation gene-1 (MALT-1) and B cell lymphoma 10 (Bcl10). Subsequently, a complex of serine kinases, which are collectively termed, IκB kinase (IKK) (Karin and Ben-Neriah, 2000), associate with the complex and mediate the activation of the transcription factor, NFκB. In un-stimulated cells this transcription factor exists in an inhibited state by its association with, IκB (inhibitor of NFκB). Activated IKK phosphorylates IκB, which induces its ubiquitination and degradation. This releases NFκB from inhibition allowing it to translocate to the nucleus and to stimulate the transcription of its target genes (May and Ghosh, 1998).

The multiple signalling pathways stemming from TCR engagement with cognate peptide:MHC complexes converge on the promoter of the IL-2 gene. Moreover, AP-1, NFAT, NFκB and constitutively expressed transcription factors bind to regulatory elements of the IL-2 gene promoter and induce expression of IL-2 (Fraser *et al.*, 1993), which in turn drives T cell proliferation and differentiation.

1.3.2 Costimulatory signalling

In conjunction with signalling through the TCR, signals from accessory molecules, termed costimulatory receptors, are required for T cell activation and clonal expansion. The

costimulatory molecule, CD28, is a homodimeric disulphide linked membrane protein constitutively expressed by T cells (Chambers, 2001). It binds to the costimulatory ligands, B7.1 and B7.2, which are expressed by activated APCs (Lenschow *et al.*, 1996). When engaged by its ligands, CD28 can enhance IL-2 production (Fraser *et al.*, 1993), by firstly inducing transcription factors that bind to the promoter of the IL-2 gene and secondly by stabilising IL-2 mRNA (figure 1.3).

CD28 is found in the pSMAC of the IS and upon engagement with its ligand becomes tyrosine phosphorylated on the motif, YXXM. This allows CD28 to recruit PI3K to the TCR signalling complex (Stein *et al.*, 1994), which can activate Akt, and as a result promote IL-2 production through activation of MAP kinases (Kane *et al.*, 2001). Furthermore, PI3K may promote T cell survival by inducing the synthesis of anti-apoptotic proteins (Boise *et al.*, 1995). Phosphorylation of CD28 on another motif, YXN, leads to the recruitment of Grb2 and thus the associated GEF, SOS. This acts to enhance TCR signalling directly by facilitating activation of the MAP kinase Erk, leading to enhanced IL-2 production due to the formation of the AP1 transcription factor. In addition, CD28 can also release the PTKs, Lck and Itk from inhibition by engaging with their SH3 domains, and therefore assisting with the downstream production of IL-2.

CD28 is also involved in the reorganisation of the cortical cytoskeleton (Wulfing and Davis, 1998) and redistribution of lipid rafts (Bi and Altman, 2001), which are both important in the formation of the IS and therefore TCR signalling. Actin polymerisation and accumulation of filamentous actin at the site of CD28 engagement leads to the polarisation of molecules to the IS. Changes in the actin cytoskeleton are attributed to the activity of a Rho family G protein, Rac (Martin *et al.*, 1995). Rac is activated by the GEF, Vav (Han *et al.*, 1997), which is further activated upon ligation of CD28. In turn, a change in the cytoskeleton drives the redistribution of lipid rafts, which allows for the optimal recruitment of PKC-θ (Coudronniere

et al., 2000). Therefore, the cooperative actions of Vav and PKC-θ lead to the activation of NFκB, which can assist with the production of IL-2 (Dienz *et al.*, 2000).

In addition to CD28, other costimulatory molecules, which are expressed by T cells once they are activated, provide additional signals that favour T cell activation and proliferation. ICOS (Inducuible costimulator), CD27, CD40 ligand (CD40L) and 4-1BB expressed by activated T cells bind counter-molecules expressed on activated antigen presenting cells. The binding of CD40L and 4-1BB to CD40 and 4-IBBL respectively, provide bi-directional stimulation, with both the T cell and APC being stimulated to further enhance T cell activation.

1.3.3 Inhibitory signalling

As well as expressing receptors that have a costimulatory function, T cells also express inhibitory receptors that help regulate the immune response. The inhibitory signalling pathways are mediated by immunoreceptor tyrosine-based inhibitory motifs (ITIMs), present in the cytoplasmic tail of inhibitory receptors. The sequence contains a large hydrophobic residue such as isoleucine or valine two residues upstream of a tyrosine residue, [S/I/V/L]XYXX[I/V/L] (Burshtyn *et al.*, 1999). When phosphorylated, the motif can recruit PTPs and inositol phosphatases, via their SH2 domains. Inositol phosphatases remove the phosphate from PIP_3 to give PIP_2, which abrogates the recruitment of proteins such as Tec kinases and Akt to the cell membrane and therefore interrupts the signalling pathways these proteins are involved in.

Expression of the CD28-related receptor, CTLA-4 is induced upon T cell activation and binds to the same ligands (B7.1 and B7.2) as CD28 present on APCs (Chen, 2004). CTLA4 binds the B7 ligands with approximately 20 times more avidity than CD28 and delivers an inhibitory signal (Scalapino and Daikh, 2008). It is thought that signalling from CTLA-4 is mediated via the recruitment of phosphatases to the phosphorylated ITIMs. The role of PTPs is discussed

in more detail in following sections. CTLA-4 limits the proliferative response of a T cell by limiting IL-2 production by the T cell. PD1 is another inhibitory receptor and contains two cytoplasmic ITIMs, and is expressed transiently by activated T cells (Keir *et al.*, 2008). PD1 can bind two ligands: PD1L, which is constitutively expressed by a range of cells, and PDL2, which is expressed by APCs during an inflammatory response. The coordinated expression of PD1 on T cells and its ligand on antigen presenting and tissue cells plays an important role in maintaining peripheral tolerance (Okazaki *et al.*, 2006).

In addition to the role intracellular signalling pathways disseminated from the TCR play in antigenic T cell responses, they are also involved in the maturation of T cells in the thymus.

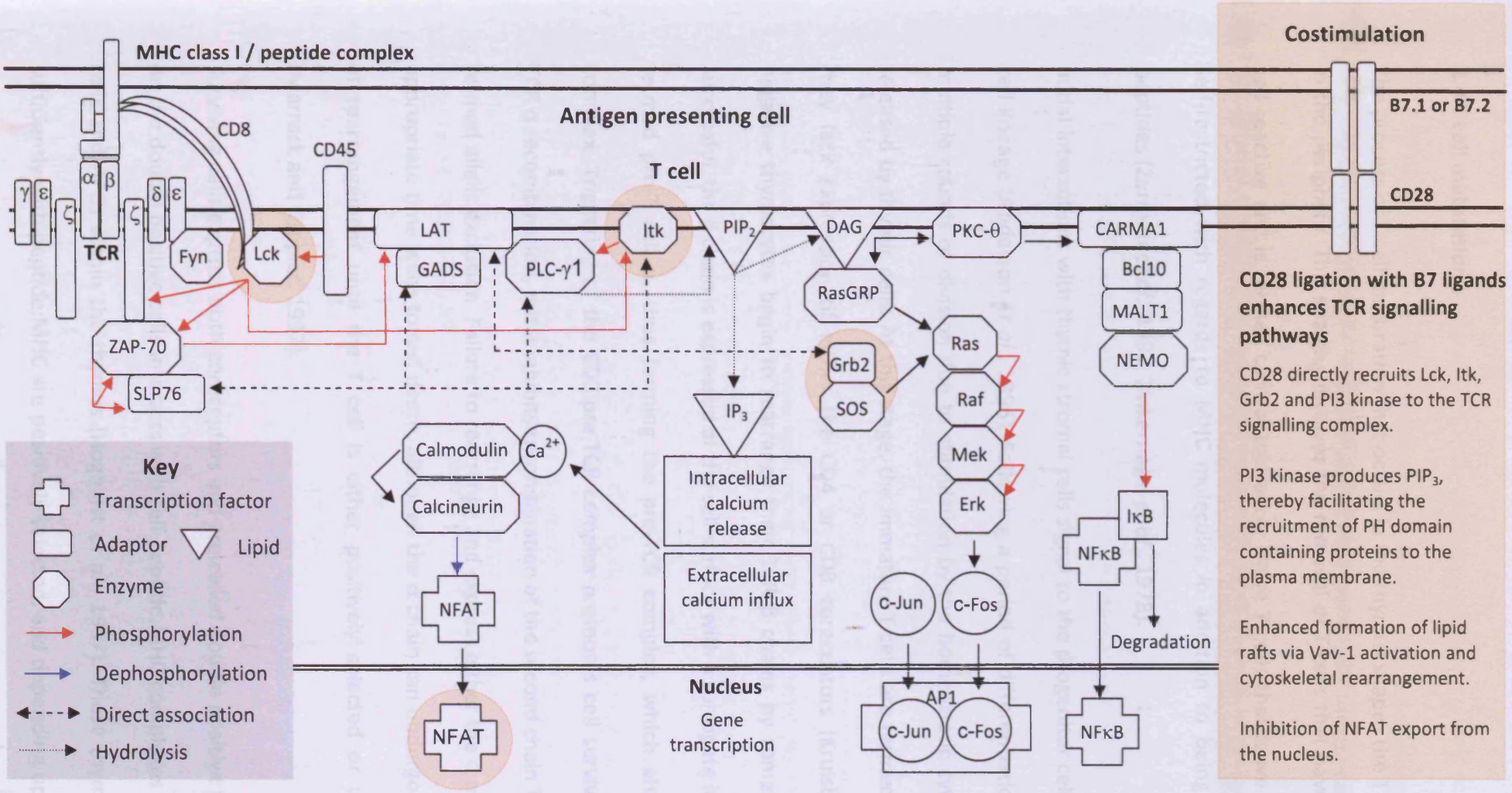


Figure 1.3: TCR engagement with peptide MHC class I complexes results in the transcription of genes necessary for T cell activation and proliferation. This process is coordinated by the action of enzymes, adaptor proteins and transcription factors (see key). For IL-2 production, the transcription factors NFAT, AP1 and NFκB are all required. Signals from the costimulatory receptor, CD28, are also required for the activation of T cells. Following ligation of CD28 with B7 ligands, which are expressed by APCs, CD28 is capable of directly recruiting many proteins involved in TCR signalling pathways (shaded areas). CD28 can also aid the TCR signalling cascade by promoting the coalescence of lipid rafts, which contain key proteins involved in TCR signalling. See the main text for abbreviations and full description.

1.4 T cell maturation

The process of T cell maturation that occurs in the thymus shapes the T cell repertoire found in the periphery. This shaping involves the removal of T cells that have the potential to be self-reactive and is termed central tolerance. Naive T cells that leave the thymus are also self-restricted with regards to MHC molecules in addition to being nonreactive to self peptides (Zerrahn *et al.*, 1997; Zinkernagel *et al.*, 1978).

Initial interactions with thymic stromal cells signal to the progenitor cells to commit to the T cell lineage (Anderson *et al.*, 1996). Following a period of differentiation, the cells undergo multiple rounds of division due to stimulation by the homeostatic cytokine, IL-7, which is released by thymic cells. At this stage, the immature T cells are termed double negative, as they lack expression of either the CD4 or CD8 coreceptors (Kruisbeek, 1993). Double negative thymocytes begin to rearrange their TCR β chains by somatic recombination. If successful, the β chain is expressed at the cell surface with a surrogate invariant TCR α chain, termed pre-T cell α, thus forming the pre-TCR complex, which also includes the CD3 complex. Triggering of the CD3:pre-TCR complex promotes cell survival, proliferation and TCR α recombination, but it inhibits recombination of the second chain TCRβ locus; a process termed allelic exclusion. Failure to rearrange and express either the α or β TCR chains at the appropriate time leads to cell death, although the α chain can undergo successive attempts at rearrangement until the T cell is either positively selected or undergoes apoptosis (Marrack and Kappler, 1997).

Surviving cells express both coreceptors and are called double positive thymocytes. The TCR on the double positive cells interacts with self peptide:MHC complexes expressed by thymic cells and APCs within the thymus (Hogquist *et al.*, 1997). Those thymocytes that interact sufficiently with peptide:MHC are positively selected, and depending upon the class of MHC

molecule the TCR is interacting with, the expression of the opposing coreceptor ceases, and a T cell positive for either CD4 or CD8 is produced. An alternative model suggests that commitment to the CD4 or CD8 lineage is independent of TCR specificity and occurs prior to selection (Itano *et al.*, 1994). The functional potential of the T cell is also defined at the same stage as surface phenotype, but the mechanism is not fully understood. Cells that are unable to recognise peptide:MHC complexes fail positive selection and undergo apoptosis. In conjunction with positive selection, double positive thymocytes are also subject to negative selection (Kishimoto and Sprent, 1997). This involves those T cells that react too avidly with self peptides:MHC complexes undergoing apoptosis, which therefore prevents them from entering the peripheral T cell pool where they could potentially elicit an autoimmune response.

Mice that are transgenic for rearranged α and β TCR chain genes, predominately express the transgenic TCR at the surface of their T cells. As the transgene does not require any further rearrangement, it is expressed earlier than the endogenous TCRβ chains. As a result, rearrangement of the endogenous β TCR chain is completely inhibited due to allelic exclusion (Uematsu *et al.*, 1988). Rearrangement of the endogenous TCR α chain is partially inhibited, although there is a preference for the transgenic α and β TCR chains to form a pair.

1.5 T cell immunosurveillance

1.5.1 Naive CD8$^+$ T cell surveillance of lymphoid tissue

Upon leaving the thymus a naive CD8$^+$ T cell enters the cardiovascular system and goes on a journey of surveillance for cognate antigen. This involves naive T cell homing to secondary lymphoid organs, including peripheral lymph nodes, the spleen and MALT. It is here that naive T cells interact with APCs in search of cognate antigen (Wiedle *et al.*, 2001).

Peripheral lymph nodes are organised lymphoid structures that occur at the point of convergence between blood and lymphatic vessels. They are serviced by specialised post capillary venules, termed high endothelial venules (HEVs) (Girard and Springer, 1995) and also afferent lymphatic vessels, which deliver lymph from the periphery. Lymph is created by the continual filtration of blood in peripheral tissue and can contain soluble antigens and APCs, such as dendritic cells. Overall, lymph nodes provide a specific site where naive CD8$^+$ T cells can survey for antigens that may be present in peripheral tissue. In order for a naive CD8$^+$ T cell to achieve this scanning it must leave the cardiovascular system and enter the parenchyma of a lymph node.

The binding of chemokines and adhesion molecules expressed by high endothelial cells (HECs) to counter-receptors expressed by naive CD8$^+$ T cells, mediates the recruitment of naive CD8$^+$ T cells to lymph nodes. The entry of naive CD8$^+$ T cells to lymph nodes is a non-antigen specific process, initiated by the light attachment of the T cell to the HEVs. This primary step is mediated by the action of the selectin, L-selectin (CD62L), which binds to mucin-like molecules collectively known as vascular addressins (Arbones *et al.*, 1994). L-selectin binds to sulphated siayl-lewis^x carbohydrate moieties of either CD34 or glycosylation-dependent cell adhesion molecule-1(GlyCAM-1). This tethering mediates the rolling of the T cell along the surface of the HEVs (figure 1.4). Chemokines that are released

by HECs, and also from stromal cells of the lymph nodes, bind to the proteoglycan matrix on the lumen side of the HEVs. The close physical proximity of a tethered T cell to the HECs, allows the extracellular matrix-bound chemokines to bind to T cell expressed chemokine receptors (del Pozo *et al.*, 1995). The secondary lymphoid tissue chemokine (SLC), CCL21 (Gunn *et al.*, 1998), binds to the chemokine receptor, CCR7, which is expressed by naive $CD8^+$ T cells. This binding constitutes the second step in T cell homing to lymph nodes as it leads to the activation of the integrin, leukocyte functional antigen-1 (LFA-1, $\alpha_L\beta_2$) (Stein *et al.*, 2000), which is expressed by naive $CD8^+$ T cells (figure 1.4). The activation of LFA-1 is associated with an increase in its affinity for the ligands, intercellular adhesion molecule-1 (ICAM-1, CD54) and ICAM-2 (CD102). In addition, there is an increase in the lateral movement of LFA-1 within the cell membrane, leading to an enhanced avidity of binding (Kucik *et al.*, 1996), and therefore firm adhesion of the naive $CD8^+$ T cell to the HEVs. Consequently, the naive $CD8^+$ T cell is able to make the final step in the process of homing to secondary lymphoid organs, which is the crossing of the HEC barrier, a process termed diapedesis (Cinamon *et al.*, 2001a; Cinamon *et al.*, 2001b) (figure 1.4). To achieve this, the naive $CD8^+$ T cell produces matrix metalloproteinases that enables it to break through the basement membrane on the apical surface of the HEV (Leppert *et al.*, 1995).

Once the naive T cell has fully extravasated and entered the lymph node, CCR7 on the T cell mediates chemotaxis from the paracortex to discrete areas known as T zones. CCR7 binds the chemoattractant CCL19, which is produced by lymph node stromal and DCs and also CCL18, which is produced by DCs (Luther *et al.*, 2002) (figure 1.4). The T cell continues its surveillance within the T zones by sampling dendritic cells for cognate antigen. If cognate antigen is not detected the naive T cell will pass from the T zone to medullary sinuses and then exit the lymph node in the efferent lymph, and re-enter the cardiovascular system via the draining of lymph into the thoracic duct (Gowans and Knight, 1964). This process is

mediated by the lipid, sphingosine-1 phosphate (S1P), which exists as a concentration gradient between lymphoid tissue and the cardiovascular system. The T cell expressed sphingosine-1 phosphate receptor mediates the chemotaxis of the T cell towards a higher concentration of S1P that is present in the blood (Matloubian *et al.*, 2004).

Mucosal surfaces represent a major entry point for pathogens, and are therefore serviced extensively by the immune system, which includes gut- (G), nasal- (N) and bronchus- (B) associated lymphoid tissues (ALTs). GALT includes the tonsils, intraepithelial lymphocytes, isolated lymphoid follicles and Peyer's patches (PPs). PPs are aggregations of lymphoid follicles that are found in the ileum of the small intestines. PPs appear as dome-like lymphoid clusters located in the lamina propria layer of the mucosa that extend into the sub-mucosa. They contain a large number of B cell follicles, below which are T cell zones. Amongst the enterocytes that overlay the PP are specialised epithelial cells, called microfold cells. The microfold cells are able to sample antigen from the intestinal lumen, which they pass to APCs within the PPs (Gebert *et al.*, 2000). The process of naive $CD8^+$ T cell homing to Peyer's patches follows the same pattern as for peripheral lymph nodes, although L-selectin binds to mucosal vascular addressin cellular adhesion molecule-1 (MAdCAM-1) (Berlin *et al.*, 1993), which is expressed by HEVs of PPs and other mucosal endothelial cells (figure 1.4). T cells leave the PPs via efferent lymph vessels and pass through the mesenteric lymph nodes before re-rentering the cardiovascular system via the thoracic duct.

The spleen collects antigen from the blood and is therefore involved in the control of blood-borne pathogens. $CD8^+$ T cells enter the spleen in the trabecular artery, which branches into a central arteriole. This in turn leads to smaller blood vessels that terminate in a specialised zone called the perifollicular zone. T cells leave the blood and enter the white pulp of the spleen through open blood-filled spaces of the perifollicular zone (Pabst, 1988). Once T cells have extravasated and entered the spleen, they reside within the periarteriole lymphoid

sheath, which is a component of the white pulp. Unlike lymph nodes and PPs the spleen is not in direct contact with the lymphatic system, instead T cells leave the spleen via the trabecular vein.

The interaction of naive T cells with non-cognate peptide:MHC class I complexes displayed by APCs is important for naive T cell survival. In addition, the binding of the homeostatic cytokine, IL-7, to its respective receptor on naive $CD8^+$ T cells is also important for their survival (Schluns *et al.*, 2000). If a naive T cell encounters its cognate antigen, the process of trafficking through lymphoid tissue ceases (Dustin *et al.*, 1997). The T cell then remains in the lymphoid tissue and continues to interact with the APC displaying cognate peptide.

1.5.2 Antigen presentation to naive $CD8^+$ T cells

Antigen, in the form of peptide bound to MHC class I complexes can potentially be presented to naive $CD8^+$ T cells by a number of different cells. By far the most efficient, and physiologically relevant APC with regards to $CD8^+$ T cells are conventional DCs, which are distinguishable by expression of the integrin, $\alpha_x\beta_2$ (CD11c:CD18). DCs may acquire antigenic proteins by direct infection with virus, or by the processes of phagocytosis and macropinocytosis (discussed earlier). In addition, DCs resident in lymph nodes may acquire antigen indirectly, via delivery from Langerhan cells that have migrated from the periphery (Carbone *et al.*, 2004). In order for DCs to fulfil their role as an APC, the antigenic peptides that they have acquired need to be presented in the correct context to initiate a $CD8^+$ T cell response. Signalling pathways ensuing from the engagement of PRRs, inflammatory cytokine receptors, and also from the detection of damaged tissue can lead to the activation and differentiation of immature DCs. Firstly, DC activation is associated with the expression of chemokine receptors, which allow the DCs to migrate to lymph nodes from peripheral sites (Lin *et al.*, 1998). Matured DCs arriving from the periphery, and those already present within

a lymphoid organ, will position themselves in T cell zones to maximise their interactions with T cells. Matured DCs will also undergo changes that lead to the enhanced efficiency of antigen processing, and therefore optimal presentation of antigenic peptides. The matured DCs will also express cytokines and costimulatory molecules that ensure the correct stimulus is delivered to T cells for their efficient activation. In effect, the activation and differentiation of DCs in response to infection and inflammation licenses them to prime naive $CD8^+$ T cells.

Interestingly, antigen recognition in the absence of co-stimulation, in situations that may involve the direct priming of T cells by tissue cells, tumour cells or immature DCs (Lutz *et al.*, 2000; Probst *et al.*, 2005), can render $CD8^+$ T cells anergic or signal for them to undergo programmed cell death. This process, known as peripheral tolerance (Teague *et al.*, 2008), maintains self-tolerance and therefore may abrogate autoimmune responses from being generated in the periphery (Miller *et al.*, 1998). An anergic T cell is unable to produce IL-2 and therefore cannot promote its own proliferation and differentiation upon encounter with antigenic peptide.

As naive T cells survey the DCs present in a secondary lymphoid organ they transiently bind with the DCs via pairings between cell adhesion molecules expressed on the T and DCs. These include LFA-1 binding with ICAM-1 (Scholer *et al.*, 2008) and -2, CD2 with CD58, and ICAM-3 (CD50) with DC-SIGN (CD209), with the latter being exclusive to the interaction between naive T cells and DCs. As already discussed, three distinct signals provided by APCs are required for the efficient priming of naive $CD8^+$ T cells. These signals are those delivered through the TCR, costimulatory receptors and cytokine receptors of the naive T cell. As a naive T cell crawls over the surface of the DC presenting cognate peptide, its receptors engage with their corresponding ligands, which can potentially lead to T cell activation and clonal expansion.

In addition to the signals provided by DCs to $CD8^+$ T cells, those from $CD4^+$ Th1 cells can also be important for the activity of $CD8^+$ T cells. $CD4^+$ Th1 cells can enhance a $CD8^+$ T cell response by increasing the costimulatory potential of DCs. CD40L expressed by $CD4^+$ Th1 cells binds to CD40 on DCs, and as a result enhance the expression of costimulatory molecule ligands by the DCs (Hernandez *et al.*, 2007). $CD4^+$ T cells may also contribute to $CD8^+$ T cell activation and proliferation, by the production of IL-2. The help provided by $CD4^+$ Th1 cell may be particularly important when antigen recognised by $CD8^+$ T cells is derived from a pathogen or tumour that does not elicit an inflammatory response. In this situation, the $CD4^+$ T cells ensure the DCs are activated appropriately in order to prime $CD8^+$ T cells. In light of this, when a pathogen causes inflammation sufficient to activate DCs, primary $CD8^+$ T cells responses may occur in the absence of $CD4^+$ T cell help: $CD8^+$ T cells can also be activated by DCs indirectly in a "bystander effect" (Raue *et al.*, 2004). Activated DCs release IL-12 and IL-18, which bind to the respective receptors on $CD8^+$ T cells. Rather than the $CD8^+$ T cells becoming CTLs they are activated to release IFNγ, which acts in a non-specific manner to clear a pathogen or tumour.

During the activation of T cells the surface expression of S1P receptors is downregulated, which sequesters the T cells in lymphoid tissue during clonal expansion. After several days of clonal expansion, the T cells upregulate the S1P receptor and exit the lymphoid tissue and re-enter the cardiovascular system. From here the activated $CD8^+$ T cells migrate to sites of infection and inflammation were they can exert their effector function, which is to kill cells displaying cognate peptide bound to MHC class I molecules.

1.5.3 Activated $CD8^+$ T cell surveillance of peripheral tissue

Upon activation, the role of a $CD8^+$ T cell changes from one of lymphoid tissue surveillance to that of peripheral surveillance, with the ultimate aim being to clear cognate antigen derived

from a pathogen or tumour. Firstly, the T cell is required to detect sites of infection and inflamed tissue, and then to enter the tissue in order to screen for cognate antigen on tissue cells. The physical process of tethering, rolling and firm adhesion, which was described for naive $CD8^+$ T cell homing to lymphoid tissues, also allows activated T cells to adhere to and cross endothelium at sites of infection or inflammation (figure 1.5). Activated T cells downregulate L-selectin, and are therefore unable to re-enter lymphoid tissue. Instead, activated T cells are able to bind P-selectin, by expression of P-selectin glycoprotein ligand-1 (PSGL-1). P-selectin is constitutively expressed by endothelia at peripheral sites and allows activated T cells to migrate to non-inflamed tissues that may harbour target cells. As with naive T cell trafficking, the firm adhesion of a T cell on the blood vessel wall is mediated by the binding of integrins to ligands on endothelial cells. Increased expression of LFA-1 by activated T cells, is mirrored by the increased expression of its ligand, ICAM-1, by activated endothelial cells. A second integrin, very late activation antigen-4 (VLA-4), is exclusively expressed by activated T cells and binds the ligand, vascular cell adhesion molecules-1 (VCAM-1) (van Dinther-Janssen *et al.*, 1991), which is expressed by activated endothelial cells. The entry of only a limited number of antigen specific $CD8^+$ T cells to an infected tissue can induce, and augment an inflammatory response, by the release of TNFα and IFNγ. These inflammatory mediators operate locally to activate endothelial cells. Consequently, the endothelial cells exhibit enhanced expression of VCAM-1 (Wang *et al.*, 2007b) and ICAM-1, which in turn enhances T cell recruitment to the area. The activated endothelium also undergoes conformational changes that allow easier access to the tissue for innate and adaptive immune cells.

Tissue-specific tropisms that are conferred to T cells during their initial priming by DCs come into operation during peripheral surveillance. The tropisms ensure that the activated clone of T cells homes to the tissue from which the antigen was derived. Activated $CD8^+$ T cells

preferentially migrate to the lamina propria of the gut when primed in the PPs (Mora *et al.*, 2003). This tropism is mediated by DCs in the PPs under the action of a vitamin A derivative. The DCs in PPs express retinal dehydrogenase, which metabolises vitamin A to the reactive metabolite, retinoic acid. The DCs of PPs are able to induce the expression of the integrin, $\alpha_4\beta_7$ (Stagg *et al.*, 2002), and the chemokine receptor, CCR9 (Zabel *et al.*, 1999), on the naive $CD8^+$ T cells (figure 1.5). These bind MAdCAM-1 and TECK (CCL25) respectively, which are expressed by endothelial cells of the small intestine. Similarly, T cells expressing CCR10 preferentially home to the colon and salivary glands, which express the ligand, CCL28 (Hieshima *et al.*, 2003). Once in the epithelial layer of the gut, the T cells may stop expressing $\alpha_4\beta_7$, and instead express $\alpha_E\beta_7$, which binds E-cadherin on epithelial cells, and may act to sequester the T cells at the specific site. Activated T cells that preferentially home to the skin express a glycosylated form of PSGL-1, called cutaneous lymphocyte antigen (CLA), which binds to E-selectin expressed by cutaneous endothelium. The cutaneous endothelium also expresses the chemokine, TARC (CCL17). This binds to the chemokine receptor CCR4 (Campbell *et al.*, 1999), which is co-expressed with CLA by T cells (figure 1.5). Skin-homing T cells maybe further directed to the epidermis by expression of CCL27 by keratinocytes, which binds to CCR10 on T cells (Homey *et al.*, 2002). Vitamin D metabolites produced in the skin by the action of UVB irradiation can confer skin-homing capabilities to T cells primed in the skin, by resident DCs (Sigmundsdottir *et al.*, 2007).

1.5.4 $CD8^+$ T cell effector function

Once an activated $CD8^+$ T cell has extravasated it screens tissue cells through transient, antigen non-specific interactions. This is mediated through binding of CD2 and LFA-1, which are expressed at higher concentrations by activated versus naive T cells, to their respective ligands on tissue cells. In addition to the increased expression of adhesion molecules, activated T cells also express an alternative form of CD45, due to the alternate splicing of the

RNA transcript. CD45RO associates with the CD8 coreceptor (Dornan *et al.*, 2002) and allows for more sensitive detection of peptide:MHC class I complexes. Unlike the priming of naive T cells, activated T cells do not require costimulation in order to recognise and kill target cells. Upon recognition of cognate peptide:MHC class I complexes, the adhesive interactions between T cell and target cell are enhanced by an increase in the affinity of LFA-1 for ICAM-1. In order for the T cell to effectively kill a target cell, without damaging surrounding cells, the T cell undergoes a process of polarisation, which involves reorganisation of the cytoskeleton (Ryser *et al.*, 1982) microtubule organisation centre and golgi apparatus (Stinchcombe *et al.*, 2001). This ensures that the non-specific effector molecules are released from the T cell at the site of contact in a focused and targeted manner. The primary mode of killing by $CD8^+$ T cells is attributed to production and release of cytotoxic granules from modified lysosomes containing the cytotoxic effector proteins: perforin, granulysin and serine proteases called granzymes (Raja *et al.*, 2002). Perforin's main role is to act as a translocator of mulitmeric complexes containing the structural proteoglycan, serglycin, and granzymes (Metkar *et al.*, 2002). Once in the cytoplasm of a target cell, granzymes trigger a caspase mediated proteolytic cascade, by cleavage induced activation of caspase-3. Activated caspases then activate caspase activated deoxyribonuclease (CAD), by cleavage of an associated inhibitory protein, which can then degrade genomic DNA. In addition, granzymes and activated caspase-3 also activate BH3-interacting domain death agonist protein (BID), which can then disrupt the mitochondrial outer membrane, leading to the release of cytocrome C from the inter-membrane space. The release of cytochrome C reinforces the caspase cascade that leads to cell death. Both pathways lead to apoptosis of the target cell and in turn its removal by phagocytic cells of the immune system. In addition to inducing apoptosis, cytotoxic molecules can also directly inhibit viruses by degrading viral DNA and therefore preventing virion formation. Activated T cells also express FasL, which is

a member of the TNF family and can induce apoptosis of target cells expressing Fas. Fas is also expressed by activated T cells and maybe involved in regulating T cell numbers post pathogen clearance (Fuse *et al.*, 1997).

Once a target cell has been eliminated, the $CD8^+$ T cell disengages and can then continue to kill other target cells.

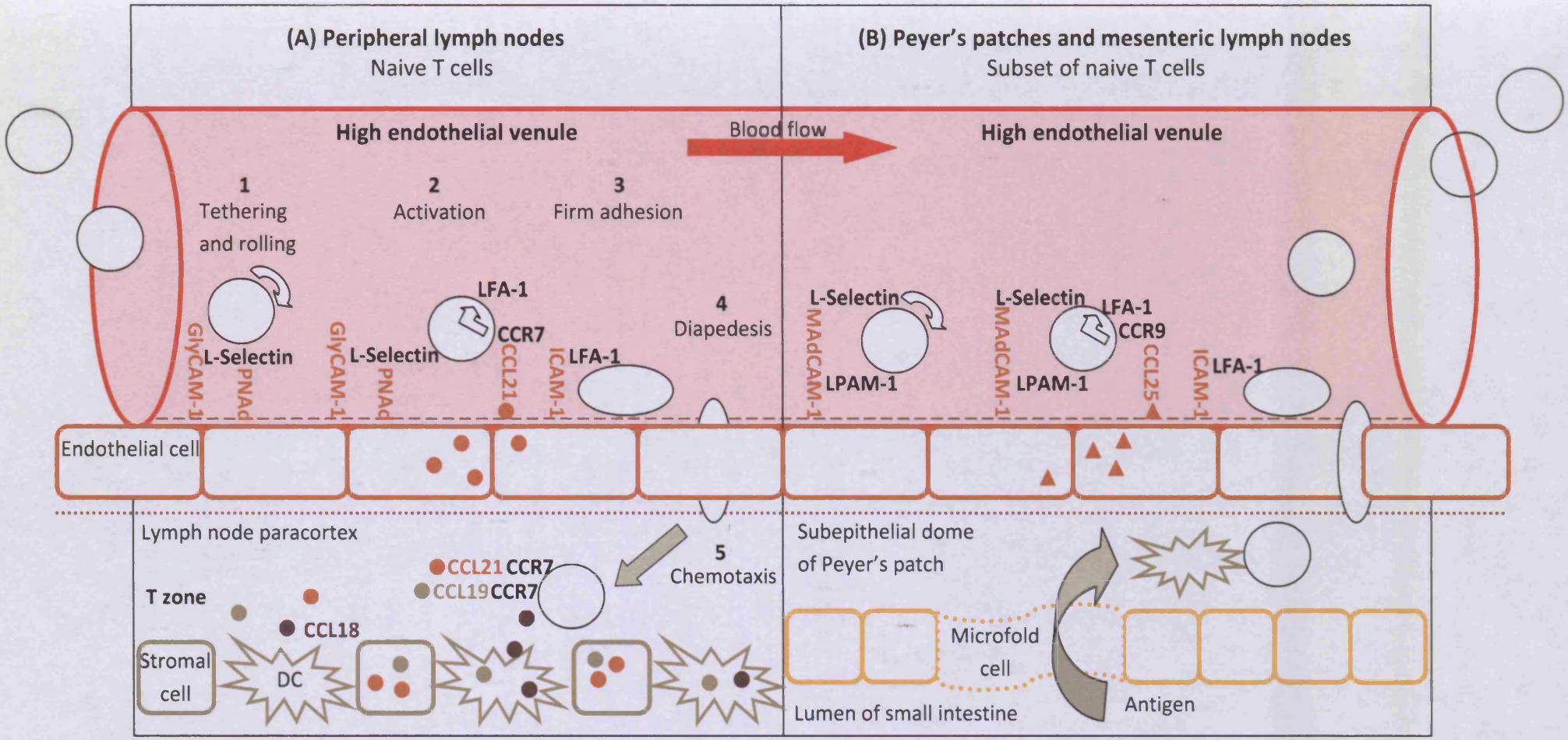


Figure 1.4: Naive T cells home to peripheral lymph nodes (LN), Peyer's patches (PP) and mesenteric (M) LNs in order to screen for cognate antigen. This is achieved by the coordinated action of homing molecules and their ligands, which are expressed by naive T cells and endothelial cells of high endothelial venules (HEVs). For naive T cell entry in to LNs, the binding of L-selectin to glycosylation dependent (Gly) cellular adhesion molecule-1 (CAM-1) or peripheral node addressin (PNAd)(1) brings the T cell into contact with the chemokine, CCL21 (2), which is released by the HEVs and binds to CCR7 on naive T cells. This enhances both the affinity and avidity of binding of lymphocyte function associated antigen-1 (LFA-1) for its ligand, Intercellular (I) CAM-1 (2), thereby leading to firm adhesion of the T cell on the HEV wall (3). The T cell is then able to cross the endothelial cell barrier and enter the lymphoid tissue parenchyma (4). A subset of T cells express the lymphocyte Peyer's patch adhesion molecule (LPAM-1, $\alpha_4\beta_7$), and the chemokine receptor, CCR9. These bind to mucosal vascular addressin (Mad) CAM-1 and the chemokine, CCL25, respectively, which are both expressed by HEVs of PPs. This confers the T cells with preferential homing capabilities to the PPs. Once in a LN, T cells are further directed to T zones, by the release of chemokines from lymph node stromal cells (CCL21 and CCL19) and dendritic cells (CCL19 and CCL18) (A). Microfold cells of the PPs sample antigen from the intestinal lumen, and pass them on to DCs, which process and present the antigen to surveying T cells (B).

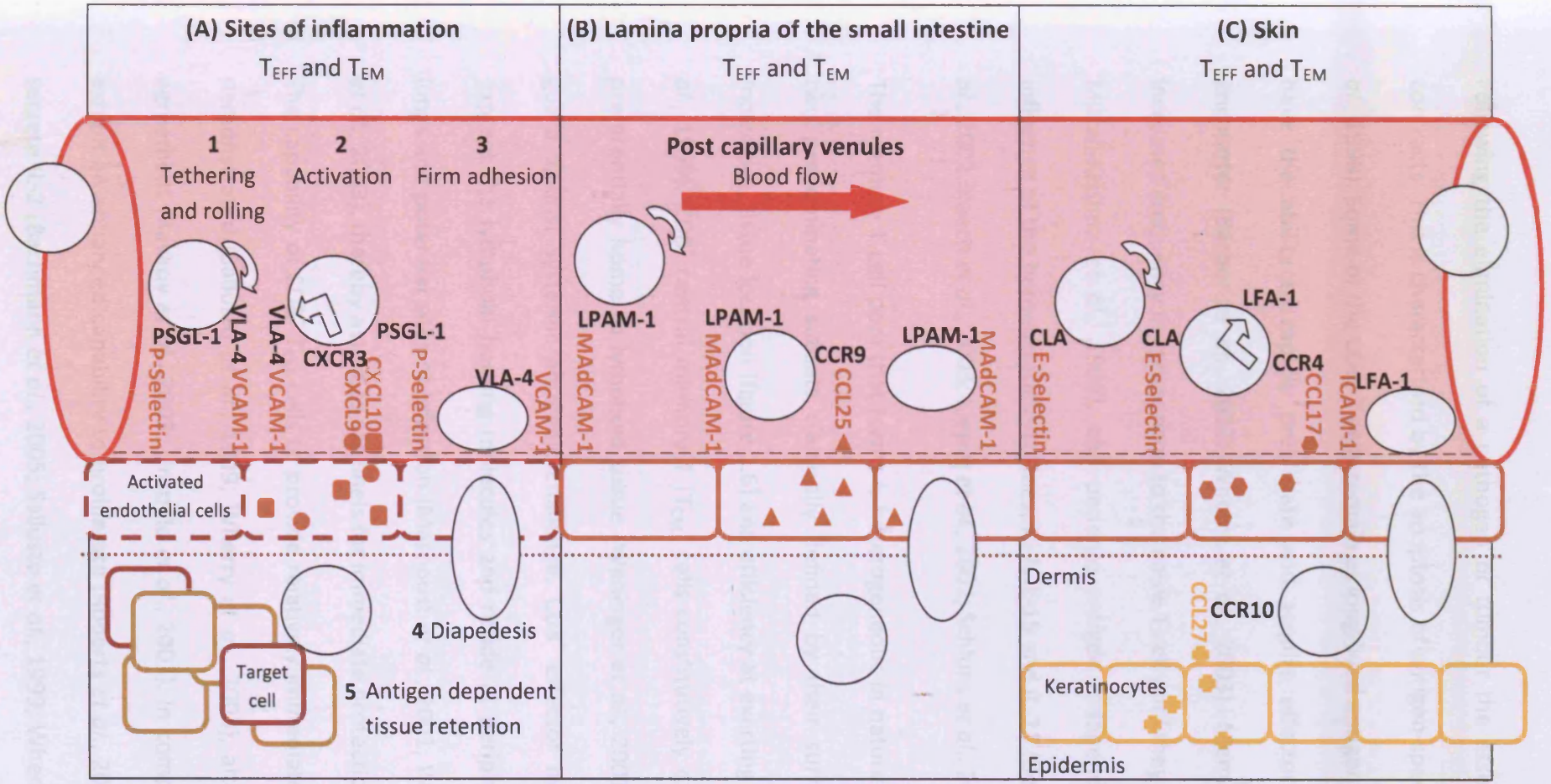


Figure 1.5: Activated effector (T_{EFF}) and effector memory (T_{EM}) T cells home to sites of inflammation (A). Activated T cells preferentially express P-selectin glycoprotein ligand-1 (PSGL-1), the chemokine receptor, CXCR3, and the integrin, very late antigen-4 (VLA-4, $\alpha_4\beta_1$). These bind to P-selectin, chemokines and vascular cell adhesion molecule (VCAM-1) respectively, which are expressed by activated endothelial cells of inflamed tissue. These homing molecules mediate the entry of T cells (4) in to inflamed tissues, beginning with the tethering of T cells to endothelial cells (1). This allows chemokines to bind to T cell expressed chemokine receptors (2), thus inducing T cell integrin activation (2), which leads to firm adhesion between T cells and endothelial cells (3). Once extravasated (4), T cells remain in the inflamed tissue if they detect cognate antigen (5). **T cells that have been conferred tissue specific homing capabilities during their priming preferentially home to either the gut (B) or the skin (C).** This is mediated by T cell expressed molecules that pair with tissue specific molecules expressed by endothelial cells in a non-inflammatory dependent manner. T cells expressing lymphocyte Peyer's patch activation molecule -1 (LPAM-1, $\alpha_4\beta_7$) and the chemokine receptor, CCR9, home to the lamina propria of the small intestine. Those T cells expressing cutaneous lymphocyte antigen (CLA) and the chemokine receptor, CCR4, preferentially home to the skin. Once in the dermis, T cells are further directed, and also retained, by the binding of CCL27, which is expressed by keratinocytes, to CCR10 on T cells. Further abbreviations: lymphocyte function-associated antigen (LFA-1, $\alpha_L\beta_2$), intercellular adhesion molecule-1 (ICAM-1).

1.6 $CD8^+$ T cell memory

Following the elimination of a pathogen or tumour the associated $CD8^+$ T cell response contracts. This is characterised by the apoptosis of antigen-specific T cells (Murali-Krishna *et al.*, 1998). Some of the $CD8^+$ T cells remain as long-lived antigen-specific memory cells, which have the ability to rapidly proliferate and acquire effector function upon antigen re-encounter (Barber *et al.*, 2003; Wherry *et al.*, 2003). Memory T cells are found at an increased frequency in comparison to the naive T cell pool they arose from (Hou *et al.*, 1994; Murali-Krishna *et al.*, 1998), and undergo antigen independent self-renewal under the influence of the homeostatic cytokines, IL-7, IL-15 and IL-21 (Becker *et al.*, 2002; Goldrath *et al.*, 2002; Kaech *et al.*, 2003; Kieper *et al.*, 2002; Schluns *et al.*, 2000; Tan *et al.*, 2002).

The memory T cell pool that forms is heterogeneous in nature but not totally distinct, with two predominating subsets classically defined by their surface expression of adhesion molecules, tissue location (figure 1.6) and efficiency at exerting effector function (Sallusto *et al.*, 1999). $CD8^+$ central memory T (T_{CM}) cells constitutively express CD62L and CCR7 and preferentially home to lymphoid tissue (Weninger *et al.*, 2001; Wherry *et al.*, 2003), thus guard against systemic antigenic challenge. $CD8^+$ effector memory T (T_{EM}) cells do not express the lymphoid homing molecules and reside at peripheral sites, such as the liver, lungs and potential sites of infection (Masopust *et al.*, 2001; Weninger *et al.*, 2001; Wherry *et al.*, 2003), thereby acting as sentinels for immediate protection against pathogen invasion. The capability of $CD8^+$ T_{EM} cells to provide relatively immediate cytolytic function has been demonstrated (Sallusto *et al.*, 1999; Wherry *et al.*, 2003), although not all studies are in agreement (Ravkov *et al.*, 2003; Unsoeld *et al.*, 2002). In comparison to T_{EM} cells, T_{CM} cells exhibit an enhanced capability to proliferate (Roberts *et al.*, 2005; Wherry *et al.*, 2003) and secrete IL-2 (Bachmann *et al.*, 2005; Sallusto *et al.*, 1999; Wherry *et al.*, 2003) upon antigen re-encounter. Mouse studies have also suggested that a stem cell subset of memory $CD8^+$ T

cells may also exists, which can give rise to all central and effector memory and effector $CD8^+$ T cell subsets, but are distinct from naive T cells. Indeed, subsets of memory T cells share transcriptional programs of self-renewal with long term haematopoietic stem cells, highlighting their capacity for long term protection (Luckey *et al.*, 2006).

Models have proposed that $CD8^+$ T_{CM} and T_{EM} T cells arise from separate lineages, based on the distinct nature of TCR repertoires of each subset found in humans (Baron *et al.*, 2003). This model has been challenged by the demonstration that both subsets can be generated from a common naive T cell precursor (Bouneaud *et al.*, 2005). Current research suggests that $CD8^+$ T cells follow a linear differentiation pathway, with memory T cells forming either directly from effector T cells (naive – effector - T_{EM} – T_{CM}) (Marzo *et al.*, 2005), or as intermediates between naive and effector T cells (naive – T_{CM} – T_{EM} –effector). In support of the latter model, $CD8^+$ T_{EM} and effector cells exhibit a shortened telomere length in comparison to naive and T_{CM} cells, suggesting they have undergone multiple rounds of division, and are therefore further along a linear differentiation pathway. Studies of acute and chronic viral infections have also supported the latter model of T cell differentiation (Appay *et al.*, 2002). During an acute viral infection $CD8^+$ T cells are successful in clearing the virus and a memory pool persists consisting of T_{CM} and T_{EM} cells. In the setting of a chronic viral infection, the memory T cell pool is continually exposed to antigen, therefore the T cells undergo repeated rounds of clonal expansion and differentiation. The chronic stimulation of antigen-specific $CD8^+$ T cells is associated with changes in cell surface phenotype. The progressive differentiation is associated with the downregulation of CD62L and CCR7, which are associated with $CD8^+$ TCM cells, and results in the predominance of T_{EM} cells residing at peripheral tissues.

Along with changes in tissue location, chronically stimulated $CD8^+$ T cells lose functional characteristics associated with T_{CM} cells and gain those associated with T_{EM} and effector

cells. Chronically stimulated T cells become replicatively senescent, which is a characteristic of $CD8^+$ T_{EM} and effector cells. This is attributed to their inability to respond to homeostatic signals from IL-7 and IL-15, as they downregulate the α chain of the IL-7 receptor and the β chain of the IL-2/IL-15 receptor (Boutboul *et al.*, 2005; Wherry and Ahmed, 2004). The differentiation of T cells during chronic stimulation is also associated with an increased unresponsiveness to antigen, as they are unable to divide upon stimulation (Champagne *et al.*, 2001; Wherry *et al.*, 2005). This may be attributed to the downregulation of costimulatory molecules, such as CD28 (Appay and Rowland-Jones, 2002), and upregulation of inhibitory receptors (Barber *et al.*, 2006; Thimme *et al.*, 2005). They also become functionally exhausted and exhibit reduced cytolytic potential (Appay *et al.*, 2000; Fuller *et al.*, 2004). Additionally, the potential to release IL-2, which is a characteristic of $CD8^+$ T_{CM} cells is lost as T cells are chronically stimulated. With ongoing stimulation, highly differentiated $CD8^+$ T cells may undergo apoptosis, thus removing them from the memory T cell pool.

In a physiological context, such as with HIV infected individuals, chronic stimulation can leave $CD8^+$ T cells in an exhausted state, as determined by their surface phenotype and inability to both proliferate (Papagno *et al.*, 2004) and control CMV infections (Sacre *et al.*, 2005). Both murine and non-human primate studies have demonstrated that $CD8^+$ T_{CM} cells confer enhanced protection against viral and bacterial challenge, compared to T_{EM} cells (Roberts *et al.*, 2005; Vaccari *et al.*, 2005; Wherry *et al.*, 2003). This is regardless of either a systemic or peripheral site challenge (Wherry *et al.*, 2003).

The factors determining $CD8^+$ T cell differentiation and the generation of memory T cell subsets have not been fully defined. APCs, other immune cells and non-immune cells orchestrate the process of $CD8^+$ T cell differentiation via the actions of membrane-bound and soluble factors. Signals provided from cytokine receptors can influence lineage

commitment by $CD8^+$ T cells. IL-2 promotes the formation of T_{EM} cells, whereas IL-15 preferentially generates T_{CM} cells. $CD8^+$ T cells produced in the presence of IL-21 retain the ability to secrete IL-2 after antigen exposure and have a stable phenotype characterised by CD28 expression (Li *et al.*, 2005; Zeng *et al.*, 2005).

These signals induce epigenetic changes leading to heritable gene expression patterns within $CD8^+$ T cells. The epigenetic changes may include DNA methylation, methyl-CpG-binding proteins and histone modification (Wilson *et al.*, 2002; Wilson *et al.*, 2005), leading to changes in the accessibility of transcription factors that mediate the process of differentiation. For $CD8^+$ T cells, the transcription factors, T-bet, and its paralog, eomesodermin may play a role in memory cell formation (Intlekofer *et al.*, 2005). Furthermore, the process may also require transcriptional repressors, so that the differentiation state of memory cells is maintained. The action of the B cell associated, Bcl-6, its homologue, Bcl-6b (Ichii *et al.*, 2002; Ichii *et al.*, 2004), isoforms of lymphoid enhancer-binding factor 1 (Lef-1), and transcription factor 7 (Tcf7) may be required to arrest differentiation of $CD8^+$ memory T cells (Willinger *et al.*, 2006).

The action of $CD4^+$ T cells on the formation and maintenance of $CD8^+$ memory T cells has been demonstrated to be of critical importance. Helper $CD4^+$ T cells contribute to $CD8^+$ T cell function, persistence and ability to control a secondary challenge by a pathogen (Sun and Bevan, 2003). The exact mechanism of $CD4^+$ help to $CD8^+$ T cells has not been fully defined, and may occur during the priming of $CD8^+$ T cells (Janssen *et al.*, 2003) and/or during the maintenance of a $CD8^+$ T cell pool (Antony *et al.*, 2005; Sun and Bevan, 2003). Interestingly, $CD8^+$ T cells primed in the absence of $CD4^+$ T cells undergo death via TRAIL mediated signalling upon re-challenge (Janssen *et al.*, 2005). Regulatory $CD4^+$ T cells have been demonstrated to negatively influence memory $CD8^+$ T cells in both a quantitative and qualitative manner (Murakami *et al.*, 2002; Suvas *et al.*, 2003).

The ability of the immune system to deal with a pathogen by forming memory cells has been of great clinical importance whereby the introduction of various vaccination regimens has seen the disappearance of many diseases. With this in mind, the role of the immune system in dealing with tumourigenesis could also be of significant importance. In the year 2000, 12% of the 56 million total deaths worldwide were attributable to cancer (World Health Organisation). The World Cancer Report (issued by the International Agency for Research on Cancer, which is part of the World Health Organisation) suggests this may increase by as much as 50% by the year 2020.

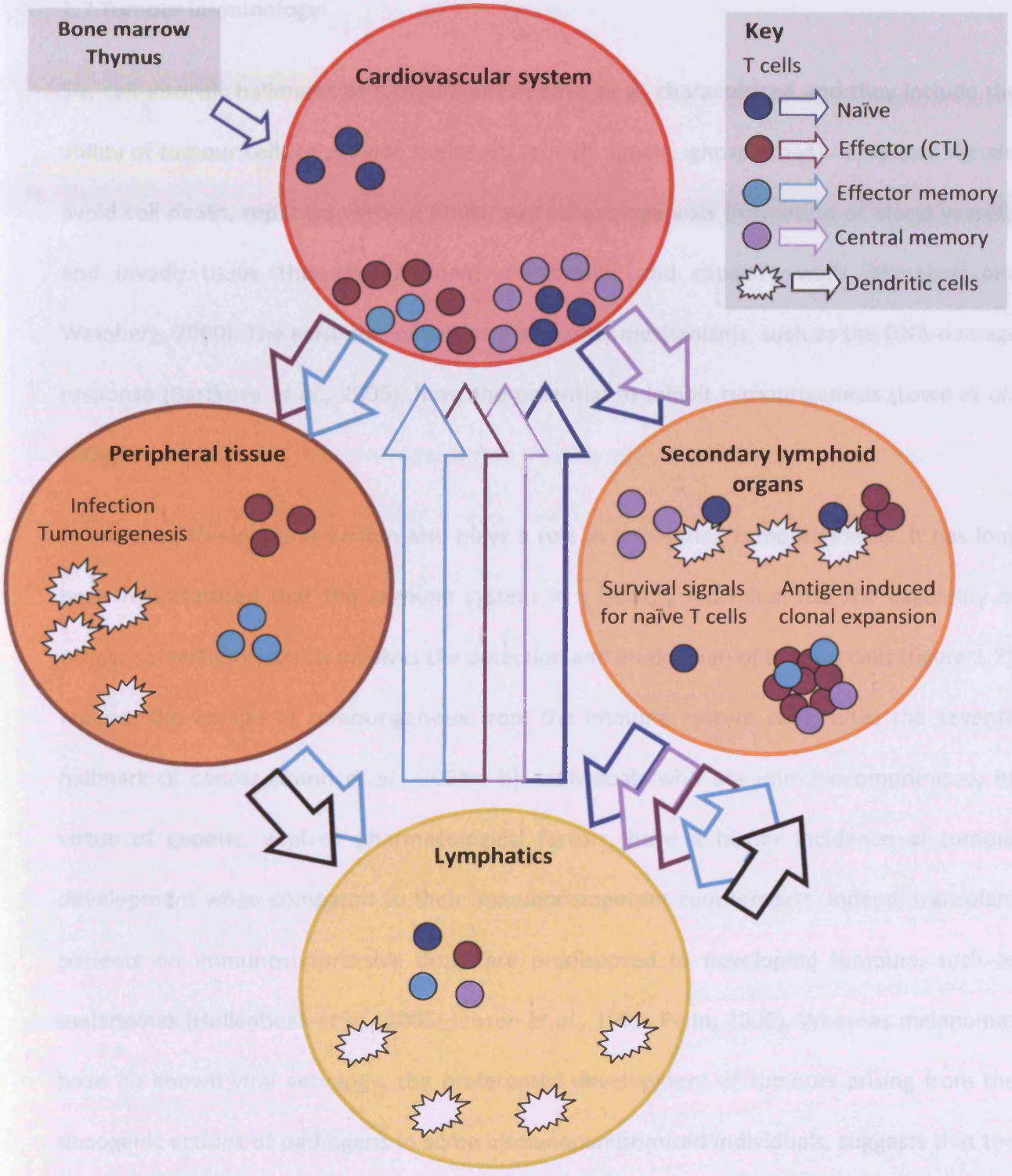


Figure 1.6: CD8$^+$ T cells patrol lymphoid organs and peripheral tissue for cognate antigen

Naïve T cells entering the blood from the thymus traffic to secondary lymphoid organs in search of cognate antigen. T cells that encounter their cognate antigen, which is displayed by dendritic cells, undergo clonal expansion. This involves differentiation into effector (CTL - cytotoxic lymphocytes), central and effector memory T cell subsets. Effector T cells migrate to peripheral tissue in order to provide host protection from infection or tumour development. Naïve T cells that do not encounter antigen receive survival signals thus allowing them to continue immune surveillance. Memory T cell subsets disperse to peripheral tissue (effector memory) and lymphoid organs (central memory), thereby providing long-term protection from the pathogen or tumour that was the source of antigen.

1.7 Tumour immunology

Six, cell-intrinsic hallmarks of tumourigenesis have been characterised and they include the ability of tumour cells to provide their own growth signals, ignore growth-inhibitory signals, avoid cell death, replicate without limits, sustain angiogenesis (formation of blood vessels) and invade tissue through basement membranes and capillary walls (Hanahan and Weinberg, 2000). The existence of cell intrinsic safety mechanisms, such as the DNA-damage response (Bartkova *et al.*, 2005), have the potential to inhibit tumourigenesis (Lowe *et al.*, 2004).

In addition, the immune system also plays a role in preventing tumourigenesis. It has long been hypothesised that the immune system in a healthy individual has the capability of cancer surveillance, which involves the detection and eradication of tumour cells (figure 1.7). Indeed, the escape of tumourigenesis from the immune system constitutes the seventh hallmark of cancer (Dunn *et al.*, 2004a, b). Individuals who are immunocomprimised, by virtue of genetic, viral or pharmacological factors, have a higher incidence of tumour development when compared to their immunocompetent counterparts. Indeed, transplant patients on immunosuppressive drugs are predisposed to developing tumours, such as melanomas (Hollenbeak *et al.*, 2005; Jensen *et al.*, 1999; Penn, 2000). Whereas melanomas have no known viral aetiology, the preferential development of tumours arising from the oncogenic actions of pathogens in some immunocomprimised individuals, suggests that the role of a healthy immune system in this scenario is acting to control pathogens that have the potential to induce malignant conversion. More direct *in vivo* evidence for tumour surveillance in humans comes from colorectal and ovarian cancer patients with data showing that the presence of lymphocytes at the site of tumour development correlates with a positive prognosis (Chiba *et al.*, 2004; Galon *et al.*, 2006; Pages *et al.*, 2005). In addition, it

has been shown that healthy women possessing antibodies against the tumour-associated antigen, MUC-1, have a lower risk of developing ovarian cancer (Cramer *et al.*, 2005).

More extensive evidence for the presence of tumour immunosurveillance has been provided by *in vivo* mouse studies. The generation of inbred congenic mouse strains has facilitated such research, as it specifically allows an anti-tumour immune response to be studied rather than an immune response due to differences in histocompatability. As a result, tumours can be transplanted between congenic mice, and cell lines from defined MHC backgrounds can also be used *in vivo*. Furthermore, genetically modified mice, which lack specific cellular or molecular immune elements allows the role of certain immune components involved in tumour surveillance to be highlighted. Similarly, the availability of monoclonal antibodies that bind to, and inhibit specific immune system components also facilitates the research in this field.

Pioneering *in vivo* tumour studies, which were performed by Ludwig Gross in the mid twentieth century, used congenic mice and the chemical carcinogen, methylcholanthrene (MCA), to demonstrate that mice are able to reject a transplanted tumour if they had previously been exposed to the tumour. These experiments indicated that tumour cells could be recognised by the immune system, leading to their targeted elimination.

1.7.1 Tumour antigens

A significant advance in the field of tumour immunology has been the discovery of tumour antigens, which allow for the identification and elimination of tumour cells by the immune system (Boon *et al.*, 1997; Boon and Old, 1997).

Tumour specific antigens (TSA) are derived from proteins that are unique to the tumour and are encoded by mutated cellular genes or viral oncogenes. The mutation of a gene may lead to the production of altered peptides from the mutated protein. The mutated peptide may

still bind MHC class I molecules, but with a slightly different amino acid sequence than the wild-type peptide, thereby creating a new epitope for T cell binding. Alternatively, the mutated peptide may undergo *de novo* binding to MHC class I molecules and therefore acts as a new antigen for T cell recognition.

Tumour associated antigens (TAA) are expressed by normal cellular genes that have become dysregulated during malignant conversion. The resulting antigen is expressed by a tumour cell at a concentration, location or time that is abnormal when compared to healthy cells and therefore contributes to tumour cell immunogenicity. With regards to T cells, TAAs can be broadly categorised into the following groups: normal cellular antigens, differentiation antigens, tissue-specific antigens and embryonic antigens (Robbins *et al.*, 1996). Normal cellular genes can undergo amplification during malignancy, resulting in a higher level of expression by tumour cells when compared to normal cells. The transmembrane tyrosine kinase receptor, Her-2, is normally expressed by cardiac tissue but is overexpressed by breast cancer cells (Peoples *et al.*, 1995). Differentiation antigens are expressed by a particular cell type at a specific time, but also by tumour cells, such as melanoma cell expression of proteins involved in melanin production (Kawakami *et al.*, 1995). Tissue-specific antigens such as the cancer-testis antigens, which are normally expressed by male germ cells alone, are also expressed by tumour cells of unrelated tissue. An example of which are the melanoma antigen genes (MAGE) proteins which are normally expressed by testicular cells (Chaux *et al.*, 1999a; Chaux *et al.*, 1999b). Cancer-testis antigens can also be classed as TSAs, as male germ cells do not express MHC class I molecules. Therefore the expression of this type of antigen, by a tumour cell, would be the only way the immune system could encounter the antigen. Carcino-embryonic antigen (CEA) is normally expressed in the liver, pancreas and intestines of a human foetus but can also be expressed by tumour cells found in the colon. TRAs can also be non-peptidic in nature and can therefore be

recognised by other cells of the immune system. The antigens can be carbohydrates and lipids, which may be aberrantly produced by the action of a mutated protein. Also, proteins that are normally found located within the interior of a cell can be found at the surface of the cell as a result of malignant conversion, and may therefore act as antigens for certain cell types of the immune system.

1.7.2 The role of the immune system in tumourigenesis

Acute inflammation in response to an invading microbial pathogen plays a pivotal role in alerting the immune system to act in an efficient manner to deal with the assault. In a similar fashion, it has been proposed that innate and adaptive immune cells are able to detect tumour cells and therefore initiate an immune response. The generation and release of metabolites, such as uric acid, and potential ligands for toll like receptors, by tumour cells may provide the danger signals required by the immune system in order to act. Once the immune system had been alerted to the presence of tumour cells, a defining step of the response is the production of IFNγ. The cellular targets of IFNγ include innate and adaptive immune cells, and tumour cells, with the latter being rendered more immunogenic as a result of exposure to IFNγ. IFNγ can also inhibit angiogenesis, which is a process involving the generation of new blood vessels in order to sustain tumour growth. In both humans and mice with malignancies, the lack of IFNγ production leaves the host susceptible to tumour progression (Shankaran *et al.*, 2001; Street *et al.*, 2002). Mice lacking expression of either IFNγ, STAT-1, which is a component of the IFNγ signalling pathway, or the IFNγ receptor have a significantly greater incidence of carcinogen induced, spontaneous and genetically driven tumour progression (Lesinski *et al.*, 2003; Mitra-Kaushik *et al.*, 2004).

In vivo studies have implicated innate immune cells in having an important role in tumour surveillance. The production of IFNγ during an immune response leads to the expression of

TNF related apoptosis inducing ligand (TRAIL) by NK cells and DCs. TRAIL can induce apoptosis of a target cell when it engages with its receptor, TRAIL-R2, which is often upregulated in tumour cells in response to DNA damage. Mice that lack TRAIL expression or receive a TRAIL neutralising antibody exhibit a higher incidence of MCA induced tumour development (Takeda *et al.*, 2002). The *in vivo* immunostimulatory regimen that uses imatinib mesylate (marketed as Gleevec) activates DCs that express TRAIL, resulting in the TRAIL-dependent regression of tumours (Chaput *et al.*, 2006).

NK cells are innate cells that are capable of directly killing tumour cells and also producing cytokines. Their actions are coordinated by the expression of a variety of activatory and inhibitory receptors. NKG2D (Natural-killer group 2, member D) is a lectin-type activating receptor that is expressed at the surface of NK cells. Its ligands are MHC-class-I polypeptide related sequence A (MICA) and MICB in humans, and retinoic acid early transcript 1 (RAE1) and H60 in mice. Such ligands are expressed at the surface of infected, stressed or tumour cells. The inhibitory receptors of NK cells, such as KIRs (killer immunoglobulin-like receptors), bind MHC class I molecules, which means NK cells are capable of killing tumour cells that have downregulated MHC class I molecules. The administration of IL-12, which is a potent stimulator of NK and NKT cells leads to a delay and reduction in the appearance of MCA induced tumours in mice (Noguchi *et al.*, 1996). In addition, mice treated with anti-asialo-GMI (Smyth *et al.*, 2001), which targets NK cells and macrophages have a higher incidence of MCA induced tumour development .

More evidence for the role of innate cells in tumour surveillance has come from a single BALB/c mouse, which is able to reject aggressive sarcomas during routine production of ascites. The resulting strain has been termed "spontaneous regression/complete remission" (SR/CR) and investigations have demonstrated that the tumour protection is germline transmissible and effective against a number of tumour cell lines (Hicks *et al.*, 2006a). The

protective immunity is also conferred to nude mice by back-crossing them with SR/CR mice, suggesting the phenotype is mainly attributable to innate immune cells (Hicks *et al.*, 2006b).

Mice lacking expression of the recombinase activating genes (Rag) 1 and 2 have provided evidence for the role of lymphocytes in tumour surveillance, as they are unable to somatically re-arrange their antigen receptors and therefore produce lymphocytes (Shinkai *et al.*, 1992). These mice have a higher incidence of carcinogen induced tumour formation and also spontaneous tumour development as they age. As the lack of Rag1 and 2 expression leads to an absence of αβ T cells, B cells, NKT cells and γδ T cells, the contributing role of each cell type has been the focus of various studies.

Natural killer T cells are innate-like lymphocytes that are characterised by co-expression of a semi-variant αβTCR together with NK cell associated receptors. The TCRs of NKT cells recognise CD1d molecules displaying glycolipid or non-peptidic ligands. An activated NKT cell can directly kill target cells and also release cytokines such as IFNγ. Mice ($J\alpha28^{-/-}$) that lack NKT cells have an increased incidence of MCA induced tumour development. Furthermore, mice injected with a ligand (a-galactosylceramide) for CD1d have a reduced incidence of tumour metastasis, mediated by the production of IFNγ by NKT cells (Ambrosino *et al.*, 2008).

A second type of innate-like lymphocytes are the γδ T cells. In humans, γδ T cells make up 50% of intraepithelial lymphocytes, whereas in mice they make up the total of this population. They express both the γδTCR, that recognises non-peptidic ligands, and the NK cells associated NKG2D receptor, which is able to recognise the stress proteins, MICA and MICB. Once activated, γδ T cells can exert direct cytolytic action and therefore kill target cells. Mice that are deficient for γδ ($TCR\delta^{-/-}$) T cells have a higher incidence of carcinogen induced tumour formation (Girardi *et al.*, 2001). Apart from the cytolytic capabilities of γδ T

cells, it has been hypothesised that they may also be an important source of IFNγ during the initial stages of tumour surveillance. The creation of bone marrow chimeric mice, which possess either γδ/IFNγ$^{-/-}$ or γδ/IFNγ$^{+/+}$ T cells, has demonstrated that the presence γδ T cells that produce IFNγ is important in preventing tumour progression (Gao *et al.*, 2003b).

Alongside the production of IFNγ during an anti-tumour immune response, the cytolytic capability of the immune system is also crucial. Mice that are deficient for perforin, which is released in cytotoxic granules from CD8$^+$ T cells, NKT, NK and γδ cells, have an increased incidence of carcinogen induced and spontaneous tumours (van den Broek *et al.*, 1996). In concurrence with this observation, mice specifically lacking αβ (TCRβ$^{-/-}$) T cells have a higher incidence or carcinogen induced tumour formation (Girardi *et al.*, 2003). In further support of the role of αβ T cells in tumour surveillance, mice that have been immunised with irradiated tumour cells and depleted of CD8$^+$ T cells are unable to reject subsequent transplants of non-irradiated tumours. In humans, the bone marrow of patients with breast cancer contains CD8$^+$ T cells specific for peptides derived from breast-cancer-associated proteins mucin-1 (MUC1) and Her-2, which can mediate destruction of autologous human tumours when transferred to immunodeficient non-obese diabetic mice (Beckhove *et al.*, 2004). CD8$^+$ T cells also express the activatory receptor, NKG2D, which means they have the potential to become activated through interactions with the stress ligands presented by many human tumour cells. DNA based tumour vaccines that encode NKG2D ligands elicit both NK and CD8$^+$ T cell-mediated anti-tumour immune responses, suggesting a role for NKG2D on CD8$^+$ T cells (Zhou *et al.*, 2006; Zhou *et al.*, 2005a). In reality, a tumour-bearing host may not possess CD8$^+$ T cells within their T cell pool that can recognise a specific TRA. This is due to thymic deletion of CD8$^+$ T cells that have the potential to react to self-antigens expressed by tissue cells, and TAAs expressed by tumour cells in the periphery. Tumour reactive CD8$^+$ T cells that may exist within a T cell pool are endowed with TCRs of varying

avidity for tumour antigen:MHC class I complexes. Those with low avidity TCRs may remain in an antigen ignorant state, due to their inability to respond to antigen, thus making them inept at mediating tumour regression. Tumour reactive $CD8^+$ T cells with high avidity TCRs have the potential to respond to tumour antigen, but may exist in a chronically stimulated state by repeated exposure to the tumour derived antigens. Akin to chronic stimulation of anti-viral $CD8^+$ T cells, the continual presence of tumour antigens can impair a $CD8^+$ T cell response, by eliciting functional exhaustion and replicative senescence of the responding T cells (Anichini *et al.*, 2004; den Boer *et al.*, 2004; Zippelius *et al.*, 2004).

1.7.3 Cancer immunoediting

Tumour surveillance can be viewed as a binary process, which involves either the success or failure of the immune system to protect against tumour development. As research has progressed, it has become apparent that the interplay between the immune system and tumourigenesis is more dynamic, with the immune system having a direct role in shaping tumour development. Indeed, the tumour may exist in a state of equilibrium, where it is chronically maintained by the immune system in a sub-clinically observed state (figure 1.7). In mouse tumour studies, mice that did not develop chemically induced tumours as expected, by comparison to those that did in the same experimental group, went onto develop tumours once their lymphocytes had been depleted (Koebel *et al.*, 2007). This suggests that malignant cells were present within these mice but were kept in check by a functional immune system. Moreover, the existence of tumour equilibrium has been demonstrated in two organ transplant recipients, both of whom developed metastatic melanoma post kidney transplant (MacKie *et al.*, 2003). The kidney donor had been treated for metastatic melanoma sixteen years prior to donation, suggesting the melanoma cells had been kept in a state of equilibrium within the donor.

The genetic instability of a tumour allows it to evolve in such a way as to escape the attention of the immune system, thus advancing from the equilibrium stage to one of escape and clinical detection of the tumour (figure 1.7). Indeed, tumour immunogenicity decreases under the selective pressure of a fully functional immune system. This was demonstrated by studies showing that a greater proportion of tumours transferred from immunodeficient mice, than those from immunocompetent mice, were rejected by immunocompetent recipient mice (Engel *et al.*, 1997; Svane *et al.*, 1997). A large number of epithelial-cell cancers and melanomas are able to evade $CD8^+$ T cell mediated immune rejection by the downregulation, or loss of expression, of MHC class I molecules (So *et al.*, 2005). Furthermore, tumour cells may also lose expression of molecules involved in antigen processing (Atkins *et al.*, 2004a; Atkins *et al.*, 2004b). Tumour cells can also avoid $CD8^+$ T cell mediated cytolysis by overexpressing an inhibitor of the granzyme B and perforin mediated pathway of target cell lysis (Medema *et al.*, 2001).

In addition to the immune system's inadvertent selection of tumour cells that are non-immunogenic, the cell intrinsic characteristics that are involved in the process of tumourigenesis (six hallmarks of tumourigenesis) can also act to subvert tumour immunosurveillance. Tumour cells produce soluble factors such as IL-4, IL-10 and IL-6, which act in an autocrine fashion to directly facilitate tumour growth. These molecules can also alter or inhibit an immune response. IL-4 and IL-10 can polarise a $CD4^+$ T cell response from Th1 to Th2, which is associated with a decline in anti-tumour activity (Stassi *et al.*, 2003).

In order to avoid anti-growth signals, tumour cells are capable of disabling components of the TGFβ signalling pathway, therefore allowing escape from the anti-proliferative influences of TGFβ. They also secrete TGFβ, which allows them to inhibit cells of the immune system, directly, or indirectly by activating Treg cells (Ghiringhelli *et al.*, 2005a; Ghiringhelli *et al.*, 2005b). Tregs are capable of suppressing the actions of anti-tumour $CD8^+$ T cells (Antony *et*

al., 2005; Sakaguchi, 2005; Turk *et al.*, 2004; Viguier *et al.*, 2004; Woo *et al.*, 2001), and their presence at the site of tumour development is associated with poor survival of cancer patients (Curiel *et al.*, 2004; Sato *et al.*, 2005). In aim of avoiding apoptosis, tumour cells express a number of different molecules that are able to prevent cell death. The expression of survivin (Dohi *et al.*, 2004) confers anti-apoptotic properties to the tumour cell, but also leads to the upregulation of FasL by the tumour cells. This can directly affect a T cell response, as FasL engagement of Fas on T cells can induce T cell death (Asanuma *et al.*, 2004).

In conjunction with the immunosuppressive nature of molecules produced by tumour cells that are vital for tumourigenesis, a tumour can further facilitate its own propagation by additional mechanisms. Tumour cells create a tolerogenic environment, by producing molecules that prevent the differentiation, maturation and function of DCs, thus rendering the T cells they engage with anergic. The tumour environment can also facilitate the development and recruitment of immune cells with suppressive capabilities, including subsets of NKT cells, macrophages and plasmacytoid DCs (Guiducci *et al.*, 2005; Terabe *et al.*, 2004). Plasmocytoid DCs have been shown to induce the clonal expansion of IL-10 producing $CD8^+$ regulatory T cells (Wei *et al.*, 2005). Tumour instructed myeloid cells can over produce nitric oxide and arginase-1, which can inhibit T cell function (Bronte and Zanovello, 2005). Tumour cells can also express, or induce tumour-associated cells to express, indoleamine 2,3-dioxygenase (IDO). The IDO mediated metabolism of the essential amino acid tryptophan, to kyneurines, has a two-fold impact on T cells. Firstly, tryptophan is essential for the function of T cells and a reduced availability can impair T cell function (Uyttenhove *et al.*, 2003). Secondly, the metabolites of tryptophan are directly toxic to T cells, leading to their apoptosis (Terness *et al.*, 2002; Terness *et al.*, 2006).

In light of these observations, the understanding of the process involving immune system and tumour interaction has been broadened to one that encompasses tumour surveillance and also tumour equilibrium and escape, which are collectively termed tumour immunoediting (summarised in figure 1.7).

Although the presence of inflammation is important for tumour regression, it can in some cases assist with tumourigenesis. This tends to be in the situation where inflammation is chronic and cytokines are produced in abundance. Plasmacytoid DCs can be recruited to the tumour bed by pro-inflammatory mediators such β-defensins, and can contribute to angiogenesis (Coukos *et al.*, 2005).

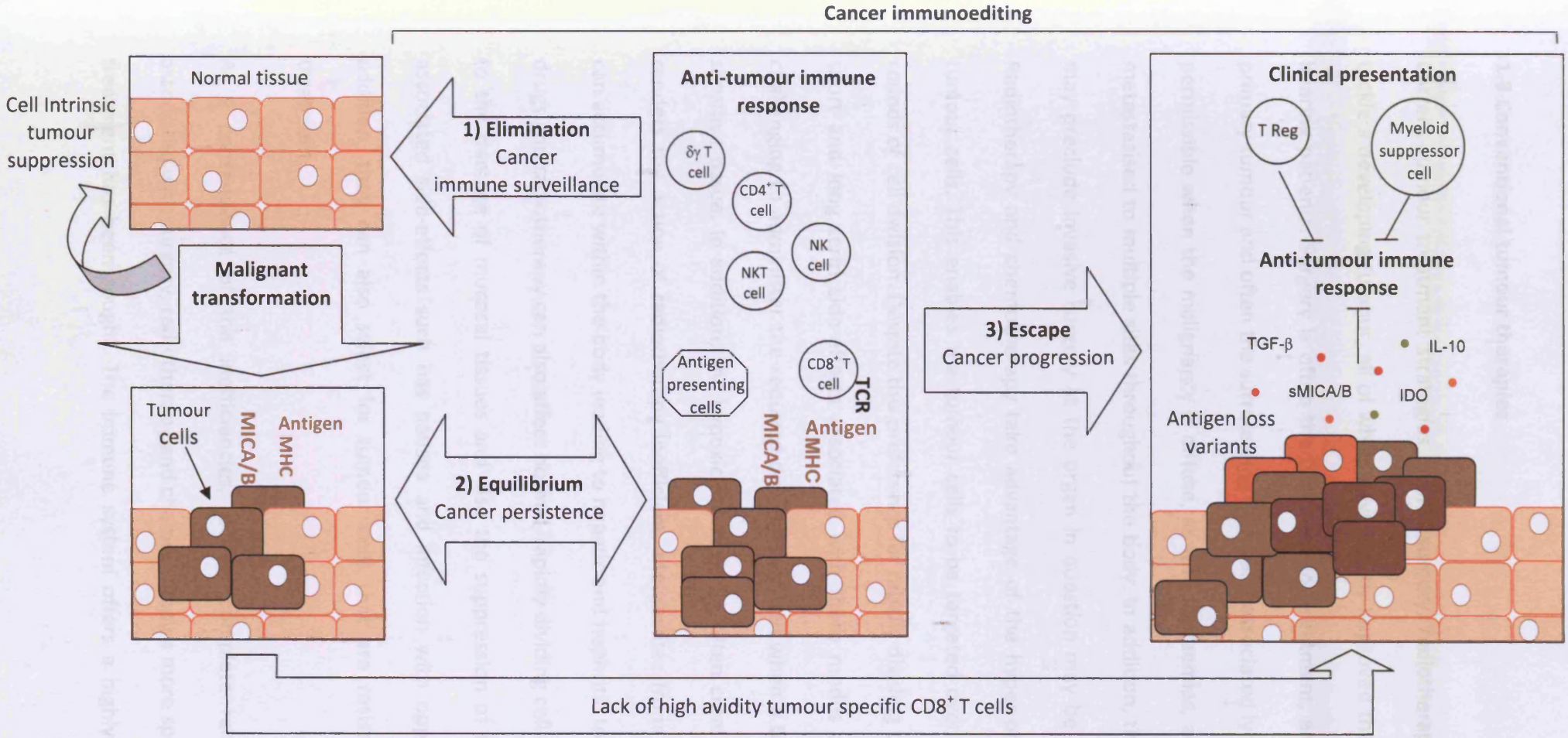


Figure 1.7: Cancer immunoediting is composed of 3 phases: elimination (1), equilibrium (2) and escape (3). Transformation events, which may lead to malignant conversion of normal cells can be reversed by cell intrinsic pathways. Malignant cells can also be effectively detected and removed by cells of the immune system, which is known as cancer immunosurveillance. The immune system may also keep the developing tumour in a state of dormancy, where tumour cells and immunity enter into dynamic equilibrium that keeps tumour expansion in check. The selective pressure of an immune response and/or the genetic instability of the tumour cells allows the tumour cell to escape the attention of the immune system. In addition, tumours cells are able to subvert an anti-tumour response by enlisting regulatory cells and by releasing soluble factors that have inhibitory affects on immune cells. This further facilitates the progression of a malignancy, leading to clinical presentation of a tumour. Indolamine 2,3-dioxygenase (IDO); MHC class I chain-related antigens A and B (MICA/B); soluble (s).

1.8 Conventional tumour therapies

Current tumour treatment strategies involve surgery, radiotherapy and chemotherapy to tackle a developing tumour, all of which have greatly improved the survival rate of tumour-bearing patients. Surgery is often the first mode of treatment, and involves removing the primary tumour and often the surrounding tissue and associated lymph nodes. Surgery is not permissible when the malignancy is diffuse, as with leukaemias, and when the tumour has metastasised to multiple sites throughout the body. In addition, the location of the tumour may preclude invasive surgery as the organ in question may be damaged beyond repair. Radiotherapy and chemotherapy take advantage of the hyper-proliferative phenotype of tumour cells. This enables the tumour cells to be targeted over cells undergoing normal rounds of cell division. Despite this preference for rapidly dividing cells, there can be serious short and long term side-effects associated with these modes of treatment. It is often challenging to administer the required dose of radiation when a tumour is neighboured by sensitive tissue. In addition, the hypoxic environment often created within bulky tumours renders the action of radiotherapy inefficient. Metabolites from chemotherapeutic drugs can accumulate within the body leading to hepatic and nephritic toxicity. Chemotherapeutic drugs and radiotherapy can also affect normal, rapidly dividing cells within the body, leading to the damage of mucosal tissues and also the suppression of bone marrow cells, with associated side-effects such has nausea and infection with opportunistic pathogens. In addition, they can also select for tumour cells that are resistant to these modes of treatment.

As a consequence of the inefficiencies, lack of complete remission and side-effects associated with surgery, radiotherapy and chemotherapy a more specific approach to cancer treatment has been sought. The immune system offers a highly specific alternative and

research in the field of tumour immunotherapy strives to develop strategies that harness the immune system or its components to mediate tumour protection or regression.

1.9 Tumour immunotherapy

1.9.1 General approaches

The ability of cytokines to induce and enhance the actions of immune cells has led to the development of cytokine based tumour therapies. These involve the systemic transfer of purified cytokines to tumour-bearing patients, in order to promote an anti-tumour response. IL-2 has the ability to promote the expansion of tumour-specific T cells and counteract the effects of immunosuppressive cytokines, yet the treatment of melanoma or renal carcinoma patients with IL-2 has only been effective in approximately 10-20% of patients (Dutcher *et al.*, 1989; Legha *et al.*, 1996; Rosenberg *et al.*, 1985; Rosenberg *et al.*, 1994). The efficacy of such therapies can be hindered by the toxic side-effects of administering high systemic concentrations of cytokine that are necessary to induce an anti-tumour response. In attempts to overcome this problem, strategies have been developed to deliver cytokines to the site of tumour development in a sustainable manner (Veelken *et al.*, 1997). This involves the *in vitro* transfection of irradiated autologous tumour cells with the genes of chosen cytokines. Once transferred *in vivo* the manipulated tumour cells home to the site of primary tumour development and secrete the cytokine. Although some clinical success has been obtained with such an approach, the generation of cells expressing cytokines can be time-consuming, which often delays treatment and allows the tumour to advance.

Despite the lack of productive *in vivo* B cell responses to tumours, monoclonal antibodies based immunotherapies have repeatedly been used to combat tumourigenesis. Monoclonal antibodies can be raised against TSAs and TAAs in animals, humanised and used in the clinic. Upon binding to a TAA or TSA on the surface of tumour cells the monoclonal antibodies induce the destruction of the tumour cell by phagocytic cells or the classical complement system. Alternatively, therapeutic monoclonal antibodies work by blocking or sequestering

factors involved in angiogenesis, tumour cell division or by inhibiting delivery of growth signals to the tumour cells. Some monoclonal antibody therapies are based on immunoconjugates, which deliver toxins, radioisotopes, enzymes or cytokines to tumour cells (Bagshawe *et al.*, 1999a). In the case of immunotoxins and immunradioisotopes, the immunoconjugate kills the tumour cells because the toxin or radioisotope is internalised following antibody binding to the tumour cell. The premise of antibody directed enzymes is to deliver an enzyme to a tumour cell that is capable of converting an inert pro-drug into an active cytotoxic drug within the tumour, thereby mediating its demise (Bagshawe *et al.*, 1999b). Immunocytokines may possess direct anti-tumour properties, or act to promote immune cell activity at the site of tumour growth. The efficacy of monoclonal antibody application is reliant upon the presence of a tumour antigen that can be bound successfully by an antibody, the extent to which antibodies distribute once administered, and the expression profile of the target antigen.

Based upon the tremendous impact vaccines have had on diseases with a pathogen aetiology, vaccine administration to combat tumourigenesis offers an appealing aim of tumour immunotherapy. Ideally, prophylactic vaccine regimens would be routinely used to prime individuals in order to prevent tumourigenesis (figure 1.8). To date, the only prophylactic vaccines that prevent tumourigenesis are those directed at pathogens that have the potential to induce malignant conversion. Routine prophylactic vaccine regimens used in some geographic locations that target the hepatitis B virus have been associated with a decline in the incidence of hepatocarcinoma (Vildosola, 2000). Similar success has been seen in trials involving vaccination against human papilloma virus (HPV), which lead to a decreased incidence of pre-cancerous cervical lesions (Garland *et al.*, 2007; Villa *et al.*, 2006). Researchers are also striving to develop vaccines against *Helicobacter pylori* in the aim of reducing the incidence of gastric lymphomas and carcinomas (Roggero *et al.*, 1995). The

development of prophylactic vaccines for tumours with no pathogen aetiology would be desirable but has yet to be realised. In contrast to a prophylactic approach, vaccines can also be applied in a therapeutic setting to combat pre-existing tumour development within a tumour-bearing host.

1.9.2 Therapeutic vaccination involving $CD8^+$ T cells

The definition of MHC complex class I restricted tumour rejection antigens has driven the development of $CD8^+$ T cell based therapeutic cancer vaccines (Gilboa, 1999), which can be active or passive in nature (figure 1.8). The aim of active tumour vaccination is to elicit or augment an anti-tumour T cell response within a tumour-bearing host in order to mediate tumour regression. Passive vaccination involves the adoptive cell transfer (ACT) of tumour reactive T cells, thus conferring anti-tumour immunity to a tumour-bearing host. For both approaches, the desired TRA being targeted would be a TSA, thereby removing the possibility of autoimmune side-effects. When a TAA is the target of vaccination, any potential autoimmunity that arises may be restricted to non-essential tissue or be clinically manageable. Furthermore, the relatively lower expression of a TAA by tissue cells in comparison to tumour cells, may allow tissue to escape the attention of the antigen-reactive T cells (Gao *et al.*, 2003a).

Peptide-based active vaccination involves the transfer of either a peptide or the protein from which the antigenic peptide is derived. A consideration when using a whole protein is the requirement of *in vivo* processing by either the standard or immunoproteasome, which if absent may preclude the generation of the desired peptide(s). The peptide should also be able to bind to HLA molecules within a potential vaccinee, to ensure that it is presented to T cells in order to elicit a response. The direct transfer of purified tumour rejection antigens has been used in trials involving patients with metastatic melanoma, eosophogeal, colon and

prostate cancer. Vaccination of melanoma patients with peptides derived from either tyrosinase, gp100, MAGE or MelanA-MART-1 have induced T cell responses in some patients, with a proportion of these exhibiting tumour regression (Jaeger *et al.*, 1996). An alternative to transferring the tumour rejection antigen alone is to use heat shock proteins (HSPs), DCs or cytokines as adjuvants to increase the likelihood of generating an anti-tumour response. HSPs can elicit an inflammatory response and also act as chaperones for peptides between necrotic cells and APCs, therefore assisting in the process of stimulating T cells. The non-specific nature of peptide binding to HSP allows both known purified peptides or a mixture of peptides from tumour cell lysates to be loaded on to HSPs prior to transfer. Therapeutic vaccination using HSPs has been trialled using patients with pancreatic, breast, colorectal and gastric cancer. A proportion of patients receiving HSPs exhibited expansion of T cell populations and some had favourable clinical outcomes. The superior T cell priming capabilities of DCs makes them an ideal adjuvant for tumour vaccination. Their ex-vivo activation may also overcome the lack of *in vivo* inflammatory signals that can leave endogenous DCs in an immature state. The source of peptides to load DCs may be tumour cell lysates, native peptides or peptides released from MHC class I molecules of tumour cells by acid treatment. Alternatively, researchers have introduced the DNA or RNA of known TRA to DCs, which is then expressed and processed by the DC. Melanoma patients receiving *in vitro* matured DCs that had been loaded with known melanoma peptides induced strong T cell expansion, but negligible tumour regression. Similar observations have been made in trials involving patients with breast, ovarian, colon, small cell lung and prostate cancer. More success has been gained when active vaccination with TAAs was used as an adjunct to the surgical removal of a primary tumour and its metastases. Stage II melanoma patients receiving a post-operative vaccine (called Canvaxin) prepared from irradiated allogeneic

melanoma cells, had an improved long term prognosis compared to patients that did not receive the vaccine (Morton, 2004; Morton *et al.*, 2002).

Unfortunately, the collective outcome of trials involving active vaccination for tumours have so far been disappointing, with objective response rates of only 5% or less according to response evaluation criteria in solid tumours (RECIST) (Rosenberg *et al.*, 2004; Therasse *et al.*, 2000).

The inefficiencies of active vaccination in mediating tumour regression have been attributed to many factors, including the lack of inflammatory signals and the absence of T cells in the periphery that can respond to a given tumour rejection antigen. Furthermore, if tumour specific T cells exist in a tumour-bearing host they may be present at low frequencies or possess low avidity TCRs, due to thymic selection (section 1.4). These factors may prevent an effective anti-tumour T cell response from being stimulated upon vaccination. In attempts to induce a response from low avidity T cells, repetitive administration of a vaccine has often been applied. However, this may act to further preclude an effective anti-tumour response, as the repetitive stimulation of the T cells promotes their differentiation to the point of exhaustion (Powell and Rosenberg, 2004). When high avidity T cells are present, repetitive vaccine administration may lead to their activation-induced apoptosis, as they are present in an already chronically stimulated state (Anichini *et al.*, 2004; Dutoit *et al.*, 2002). Overall, the use of an active vaccination to stimulate T cells may only act to exacerbate a pre-existing defunct anti-tumour T cell response of a tumour-bearing host. Furthermore, when a robust T cell response has been induced by a vaccine regimen it then faces other hurdles, which may avert tumour regression. These include peripheral tolerance and tumour-mediated regulatory mechanisms that suppress anti-tumour T cell responses (as discussed above). Indeed, the generation of large numbers of T cells alone, is not sufficient to consistently

induce objective clinical responses (Ayyoub *et al.*, 2003; Rosenberg *et al.*, 2005; Rosenberg *et al.*, 2003; Rosenberg *et al.*, 1998; Smith *et al.*, 2003; Speiser *et al.*, 2005).

In attempts to overcome the hurdles associated with therapeutic active vaccination, alternative T cell immunotherapy strategies have been sought. One approach with great potential is passive vaccination, which involves adoptive cell transfer (ACT). The premise of such an approach involving T cells is the ex-vivo generation of large numbers of T cells with appropriate specificity and avidity to mediate tumour regression upon re-introduction to the tumour-bearing host (figure 1.8).

In combination with the identification of a wide range of tumour antigens (Gilboa, 1999), the improvement of cell culture and isolation technology (Jotereau *et al.*, 1991) has facilitated ACT approaches involving T cells. Various selection techniques have been applied in order to isolate autologous antigen-specific T cells from tumour-bearing patients. Patient PBMC can be stimulated with APCs displaying TRA(s), thus stimulating antigen specific T cells to expand. Alternatively, T cells can be expanded non-specifically by the use of CD3 and CD28 antibodies. The ex-vivo generation of tumour-reactive T cells is often supported by their supplementation with T cell growth cytokines, such as IL-2. The resulting T cell clones or lines are quality tested, for parameters such as sterility and cytotoxicity before *in vivo* application. The process of acquiring activated T cells for ACT can be enhanced by priming the tumour-bearing patient with a vaccine prior to T cell harvest, thereby increasing the frequency of the antigen specific T cells (Chang *et al.*, 1997; Li *et al.*, 1999; Shu *et al.*, 1989).

Multiple clinical trials have been performed to establish the efficacy of using adoptively transferred T cells to combat malignancies. The adoptive transfer of antigen-specific T cells has been successful in both preventing and treating malignancies with a viral component. More specifically, the transfer of Epstein Barr virus (EBV) specific allogeneic or autologous

PBMC or T cell lines has proven efficacious for the prevention and treatment of EBV-induced diseases. These malignancies can develop in patients who are immunosuppressed due to bone marrow or organ transplantation and included EBV-induced lymphoproliferative disease (Comoli *et al.*, 2002; Heslop *et al.*, 1994; Heslop and Rooney, 1997; Khanna *et al.*, 1999; O'Reilly *et al.*, 1997; Rooney *et al.*, 1995; Rooney *et al.*, 1998), Nasopharyngeal carcinoma (Chua *et al.*, 2001; Comoli *et al.*, 2004; Straathof *et al.*, 2005) and Hodgkin's disease (Bollard *et al.*, 2004; Laport *et al.*, 2003; Lucas *et al.*, 2004; Roskrow *et al.*, 1998). To build on these successes, multiple trials have been performed involving the targeting of tumours with no known viral aetiology, namely metastatic melanoma (see below), renal cell carcinoma (Thompson *et al.*, 2003), breast (Visonneau *et al.*, 2000) and prostate cancer (Ross *et al.*, 1993).

In one such trial, $CD8^+$ T cells specific for MelanA-MART-1 were purified from the PBMC of patients with metastatic melanoma, expanded ex-vivo in the presence of IL-2 and transferred back to patients. Eight out of twenty patients exhibited either minor, mixed or stable anti-tumour responses (Yee *et al.*, 2002). The T cells were encouragingly detected at the site of the tumour development, but there was a selective outgrowth of tumours lacking expression of MelanA-MART-1 (Yee *et al.*, 2000). Similarly, in another trial utilising T cells specific for one tumour antigen, the T cells engrafted successfully, but disappointingly selected for tumours that did not express the antigen (Mackensen *et al.*, 2006). These studies highlight the caveat of transferring monoclonal tumour specific $CD8^+$ T cells, in that tumour cells that either don't express the antigen, or evolve under the selective pressure of the T cells to not express the antigen, are left unchecked and continue to develop (Marincola *et al.*, 2000; Norell *et al.*, 2006).

A second approach of ACT has been to utilise $CD8^+$ T cells of tumour infiltrating lymphocytes (TILs), which are purified from tumour biopsy specimens. The cells are expanded ex-vivo

with antibody and cytokines prior to infusion back to the tumour-bearing patient. This differs to using one clone of $CD8^+$ T cells as the T cell population in this context is most likely to be polyclonal for the antigens expressed by the tumour from which they were purified. In pre-clinical mouse models, this approach has proved to be successful (Alexander and Rosenberg, 1990) but in contrast, human clinical trials involving the transfer of TILs to patients with metastatic melanoma have proven to be unsuccessful in reaching objective clinical responses (Dreno *et al.*, 2002; Figlin *et al.*, 1999; Rosenberg *et al.*, 2004). It was established that the TILs used in these trials did not persist for extended periods of time once transferred *in vivo*, and as a result, the T cell responses were only transient in nature.

In attempts to improve the clinical outcome of ACT trials involving TILs, patients with metastatic melanoma were conditioned prior to the transfer of the expanded lymphocyte population. The conditioning step involved using the chemotherapeutic drugs, cyclophosphamide and fludarabine, which are immunosuppressive by inducing lymphopaenia, but do not have any direct anti-melanoma activity. Promisingly, as a result of this conditioning regimen, six out of thirteen patients in one clinical trial had partial responses, and a further two had mixed responses, which overall represents a 50% objective response (Dudley *et al.*, 2002a; Dudley *et al.*, 2005) (figure 1.8). Incidentally, the patients in this trial had already undergone episodes of conventional cancer therapy and also received IL-2 during TIL treatment. The conditioning regimen may augment the anti-tumour efficacy of TIL therapy by removing Tregs, cytokine sinks and/or improving the immunogenicity of the tumours (Berd and Mastrangelo, 1987a, b; Pages *et al.*, 2005; Sato *et al.*, 2005), thereby allowing the cells to function optimally and mediate tumour regression (Rapoport *et al.*, 2005; Wrzesinski and Restifo, 2005). Indeed, the T cells in this trial exhibited long term engraftment when compared to patients that had not received the chemotherapeutic drugs.

In addition to the lymphodepletion of a tumour-bearing patient prior to T cell transfer, other components may be included as part of an ACT strategy in order to enhance an anti-tumour T cell response. These may include cytokine adjuvants (Cheever *et al.*, 1982; Ku *et al.*, 2000) and the administration of antibodies to either block inhibitory signals (Barber *et al.*, 2006; Kim *et al.*, 2001) or to enhance costimulatory signals to T cells (Sutmuller *et al.*, 2001). *In vivo* mouse studies have demonstrated that the combination of lymphopenia, T cell transfer and administration of an altered peptide vaccine can enhance an anti-tumour response (Wang *et al.*, 2005). During ACT immunotherapy, the co-transfer of $CD4^+$ T cells has been responsible for the long term maintenance of $CD8^+$ T cells (Wang *et al.*, 2007a). An alternative approach to co-transferring tumour reactive $CD4^+$ T cells would be to administer helper $CD4^+$ T cell associated cytokines, such as IL-2, IL-7, IL-15 and IL-21 (Blattman *et al.*, 2003; Klebanoff *et al.*, 2004; Melchionda *et al.*, 2005; Zeng *et al.*, 2005). Current constraints that may preclude the efficacy of using TILs as a standard therapy include their acquisition, which is not always feasible as dictated by the cancer type, and the time it takes to generate sufficient numbers to infuse back to the patient (Dudley *et al.*, 2003).

A common theme gleaned from clinical trials involving ACT of TILs or $CD8^+$ T cells to combat tumour development has been the importance of the differentiation state of the $CD8^+$ T cells that are transferred. In clinical trials using adoptively transferred $CD8^+$ T cells to treat metastatic melanoma, it is evident that the multiple rounds of ex-vivo stimulation result in $CD8^+$ T cells that are unable to persist and therefore mediate tumour regression. The cells have a phenotype of more differentiated late effector T cells, akin to chronically stimulated T cells (Dudley *et al.*, 2002b; Yee *et al.*, 2002). In support of this, the repeated stimulation of mouse MHC class I restricted T cells (Overwijk *et al.*, 2003) in an *in vitro* setting has been associated with a step-wise impairment of effector function and proliferative capacity, thus abrogating an effective anti-tumour response when transferred *in vivo* (den Boer *et al.*,

2004; Gattinoni *et al.*, 2005; Sussman *et al.*, 2004). It has been demonstrated that $CD8^+$ T cells that are able to undergo repeated rounds of proliferation *in vivo* provide superior anti-tumour properties (Dudley *et al.*, 2002a; Gattinoni *et al.*, 2005; Klebanoff *et al.*, 2005). In addition, telomere length positively correlates with long term persistence of tumour reactive adoptively transferred $CD8^+$ T cells, and as a result, tumour regression (Robbins *et al.*, 2004; Zhou *et al.*, 2005b). Overall, the transfer of tumour-reactive $CD8^+$ T_{CM} cells is found to be therapeutically superior in combating an established tumour, compared to $CD8^+$ T_{EM} cells (Klebanoff *et al.*, 2005). The $CD8^+$ T_{CM} cells have a greater proliferative capacity and ability to interact with antigen presenting cells than $CD8^+$ T_{EM} cells, which contributes to tumour regression.

Human clinical trials and mouse models have highlighted areas that need to be addressed in order to achieve objective clinical responses during ACT immunotherapy using $CD8^+$ T cells. In addition to the pre-conditioning of tumour-bearing patients, the ability to acquire and generate tumour-reactive $CD8^+$ T cells is of importance. The $CD8^+$ T cells used for therapy need to be of the correct specificity, possess sufficiently avid TCRs and be at the optimal state of differentiation. Furthermore, $CD4^+$ T cell help (or the associated cytokines) and polyclonal populations of $CD8^+$ T cells may also improve the outcome of ACT therapies. These improvements may be facilitated by the development of T cell gene modification technologies and may allow for the production of tumour reactive $CD8^+$ T cells that meet the desired criteria.

1.9.3 Genetic modification of $CD8^+$ T cells for use in ACT immunotherapy

The genetic modification of T cells used in ACT strategies provides scope to further improve the clinical outcome of such therapies. The use of recombinant retrovirus to genetically modify T cells has proved to be effective in the treatment of patients with congenital and

acquired immunodeficiency (Blaese *et al.*, 1995; Mitsuyasu *et al.*, 2000). The modified T cells have persisted for considerable lengths of time, thus demonstrating the feasibility of using such an approach to combat cancer. Disappointingly, retroviral insertional mutagenesis has led to malignancies in some circumstances (Hacein-Bey-Abina *et al.*, 2003). The preferential use of lentiviruses over more traditionally used retroviruses may preclude such problems when engineering T cells. In comparative studies, lentiviral vectors have been shown to be less prone to insertional mutagenesis than retroviral vector counterparts (Montini *et al.*, 2006). Furthermore, HIV infected individuals do not have an increased incidence of T cell leukaemia, which further indicates lentiviral vectors are possibly safer than retroviral ones.

The genetic engineering of T cells may overcome the limitations associated with a pre-existing T cell repertoire of a tumour-bearing patient, including the absence of $CD8^+$ T cells with the required TCR specificity and avidity for antigen clearance. Furthermore, the type of tumour may preclude the physical acquisition of $CD8^+$ T cells. Therefore, the ex-vivo generation of T cells with required tumour antigen specificity and avidity is a desired aim of ACT therapies.

One approach has been to introduce chimeric antigen receptors (CARs), termed T-bodies, to $CD8^+$ T cells. Early T-bodies consisted of an external antibody-based domain, that confers specificity and the cytosolic domains containing the signal transduction components of the TCR (Ciceri *et al.*, 2007). This endows a T cell with antigen specificity in a non-MHC class I molecule dependent manner, which may be of benefit when a tumour has evolved to not express MHC class I molecules. Indeed T cells possessing T-bodies have proven efficient in mediating tumour rejection in mouse models (Kershaw *et al.*, 1996a; Kershaw *et al.*, 1996b). New generation T-bodies also contain costimulatory molecule signalling domains (Loskog *et al.*, 2006) in order to enhance T cell expansion in response to antigen (Krause *et al.*, 1998). In a clinical setting, this approach seems safe, but requires further optimisation with regards to

the persistence of the transferred T cells (Kershaw *et al.*, 2006; Lamers *et al.*, 2006; Park *et al.*, 2007), expression of the transgene, the correct avidity of the T body to allow serial killing of target cells and the identification of suitable antigens expressed at the surface of tumour cells.

$CD8^+$ T cells have also been engineered to express the α and β chains of TCRs with known avidity and antigen specificity. Clinical trials have been performed using adoptively transferred $CD8^+$ T cells expressing a transgene encoding a TCR recognising the melanoma associated gp100 antigen. Patients were also lymphodepleted and given an infusion IL-2 alongside the transferred T cells (Morgan *et al.*, 2006). The T cells persisted *in vivo*, trafficked to the site of tumour development and mediated tumour regression in some patients. Potential side-effects of TCR gene transfer could include autoimmunity by three different mechanisms. Firstly, the possibility of novel TCR combinations encompassing the transgenic and endogenous α and β chains could generate mixed TCR dimers with new specificities. Secondly, triggering through the exogenous TCR could allow a normally antigen-ignorant endogenous TCR to become auto-reactive, due to the activated status of the T cell. Finally, if the TCR gene is derived from a donor that is not MHC-matched with the recipient it could lead to reactivity towards allogeneic MHC molecules. The development of strategies that could suppress endogenous TCR expression or ensure that the exogenous TCR chains preferentially pair could potentially eliminate these autoimmune concerns. Alternatively, the introduction of suicide genes, such as the herpes simplex virus thymidine kinase, could allow selective destruction of auto-reactive transferred T cells by administering gancyclovir (Bonini *et al.*, 1997).

In addition to conferring specificity and avidity to $CD8^+$ T cells, genetic manipulation may also assist with improving the function of $CD8^+$ T cells used in ACT immunotherapy. Efforts have been made to improve T cell expansion by the introduction of constitutively expressed CD28

(Topp *et al.*, 2003) or chimeric GM-CSF-IL-2 receptors (Evans *et al.*, 1999), thereby enhancing the production and signals provided by IL-2. The long term *in vivo* persistence of transferred T cells has correlated with improved clinical responses. With this in mind, the survival of T cells has been improved *in vitro* by the introduction of the catalytic subunit of telomerase (Rufer *et al.*, 2001) or Bcl-2 (Lin and Wang, 2002).

The introduction of chemokine receptors to T cells has the potential to target their effector function to sites of malignancy. The chemokine receptor CXCR4 may be useful to target CTL to bone marrow for treating leukaemia or tumour metastases of the bone (Peled *et al.*, 1999). T cell function can also be improved by protecting the T cells from extrinsic inhibitory influences, such as that imposed by the cytokine, TGFβ. The introduction of a dominant negative TGFβ receptor to T cells enhanced their tumour reactive activity *in vitro*, when compared to unmodified counterparts (Bollard *et al.*, 2002). Similarly, the removal of intrinsic inhibitory factors may also help improve T cell function. One such candidate is Casitas B cell lymphoma (Cbl-b), which is a member of the mammalian Cbl E3 ubiquitin ligases (Thien and Langdon, 2001). Mice lacking Cbl-b expression developed fewer UVB induced skin malignancies and rejected transplanted tumours (Loeser *et al.*, 2007). The adoptive transfer of Cbl-$b^{-/-}$ T cells conferred tumour protection to the recipient mice. The enhanced anti-tumour activity may be attributed to their resistance to Treg suppression, enhanced expansion, formation of an increased memory T cell pool and rapid tumour infiltration (Loeser *et al.*, 2007).

The transfer of genes encoding particular proteins that enhance T cell activity is one way to improve ACT therapies. A different approach is required when the action of a protein needs to be removed in order to achieve the same end. Pharmacological inhibitors of specific proteins may provide one such avenue but this relies on the development of specific drugs

for each protein concerned. One technology that has wider applications, and could potentially be used for any protein with a known DNA sequence, is RNA interference (RNAi).

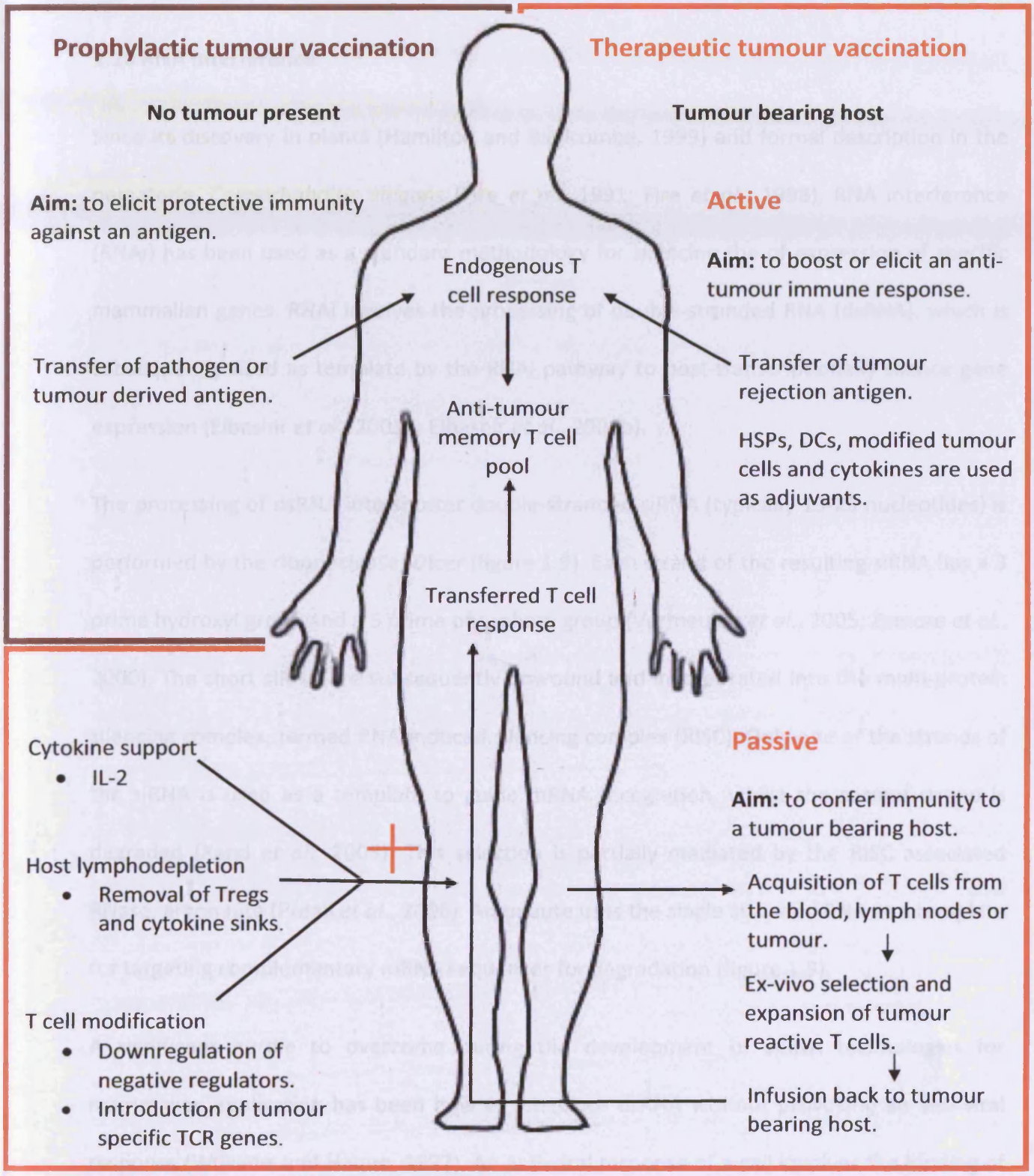


Figure 1.8: Tumour immunotherapy approaches

Both prophylactic and active therapeutic vaccination approaches aim to activate T cells within the host, thereby providing anti-tumour immunity. Prophylactic approaches often target pathogens that have the potential to aid malignant conversion. Passive vaccination approaches do not alter cells within the tumour-bearing host, but involve the adoptive transfer of tumour reactive T cells. The T cells are obtained from a tumour-bearing host and cultured in vitro prior to their reintroduction. This allows the cells to be expanded to sufficient numbers and tested for tumour antigen reactivity. It has been found that depleting the host of endogenous lymphocytes, prior to T cell transfer, greatly improves the efficacy of this type of immunotherapy.

1.10 RNA interference

Since its discovery in plants (Hamilton and Baulcombe, 1999) and formal description in the nematode, *Caenorhabditis elegans* (Fire *et al.*, 1991; Fire *et al.*, 1998), RNA interference (RNAi) has been used as a standard methodology for silencing the of expression of specific mammalian genes. RNAi involves the processing of double-stranded RNA (dsRNA), which is subsequently used as template by the RNAi pathway to post-transcriptionally silence gene expression (Elbashir *et al.*, 2001a; Elbashir *et al.*, 2001b).

The processing of dsRNA into shorter double-stranded siRNA (typically 19-25 nucleotides) is performed by the ribonuclease, Dicer (figure 1.9). Each strand of the resulting siRNA has a 3 prime hydroxyl group and a 5 prime phosphate group (Vermeulen *et al.*, 2005; Zamore *et al.*, 2000). The short siRNA are subsequently unwound and incorporated into the multi-protein silencing complex, termed RNA-induced silencing complex (RISC). Only one of the strands of the siRNA is used as a template to guide mRNA recognition, whilst the second strand is degraded (Rand *et al.*, 2005). This selection is partially mediated by the RISC associated RNase, argonaute (Preall *et al.*, 2006). Argonaute uses the single stranded RNA as a template for targeting complementary mRNA sequences for degradation (figure 1.9).

A significant hurdle to overcome during the development of siRNA technologies for mammalian application has been how to introduce dsRNA without provoking an anti-viral response (Williams and Haque, 1997). An anti-viral response of a cell involves the binding of the enzyme, dsRNA-dependent protein kinase (PKR) to dsRNA, which leads to wide-spread RNAi, in a sequence-independent manner. It was later discovered that the introduction of short dsRNA, of less than 30bp, could initiate the sequence-specific RNAi pathway but avoid an anti-viral response (Elbashir *et al.*, 2001b). A number of standard transfection mechanisms can be used to introduce dsRNA to cells. The efficiency of transfection, the

potency of the siRNA sequence and the amount an individual cell receives all have an impact of the overall efficacy of a siRNA approach. A second approach to introducing dsRNA to cells has been to introduce DNA that encodes short hairpin RNAs (shRNA). They can be introduced to cells as DNA vectors by standard transfection techniques, to give transient or stable expression, and also by viruses. The DNA encodes for the sense and antisense strands of the dsRNA separated by a short nucleotide sequence, termed a spacer. The expression of the RNA can be driven by constitutive or inducible promoter systems (Paddison *et al.*, 2004). Once expressed the complementary RNA sequences pair and form dsRNA, with a hairpin of unpaired nucleotides at one end. The shRNA is then processed by Dicer to form siRNA, which is incorporated into the RISC complex.

The effectiveness of a siRNA or shRNA sequence is based upon the siRNA structure and determined at the point of RISC assembly. Many algorithms are now available for choosing effective sequences for a given gene. The algorithms apply thermodynamic criteria, which can identify sequences that facilitate the incorporation of the antisense strand of the siRNA into RISC. These criteria were based on studies showing that there is an unequal incorporation of the siRNA sequence into RISC (Khvorova *et al.*, 2003; Reynolds *et al.*, 2004; Schwarz *et al.*, 2003; Silva *et al.*, 2003). The algorithms also allow sequences that may have off-target effects to be excluded. With the availability of siRNA technologies it may be feasible to target negative regulators of T cell signalling pathways. One other candidate for such modality is the PTP known as Src homology 2 domain containing PTP-1 (SHP-1).

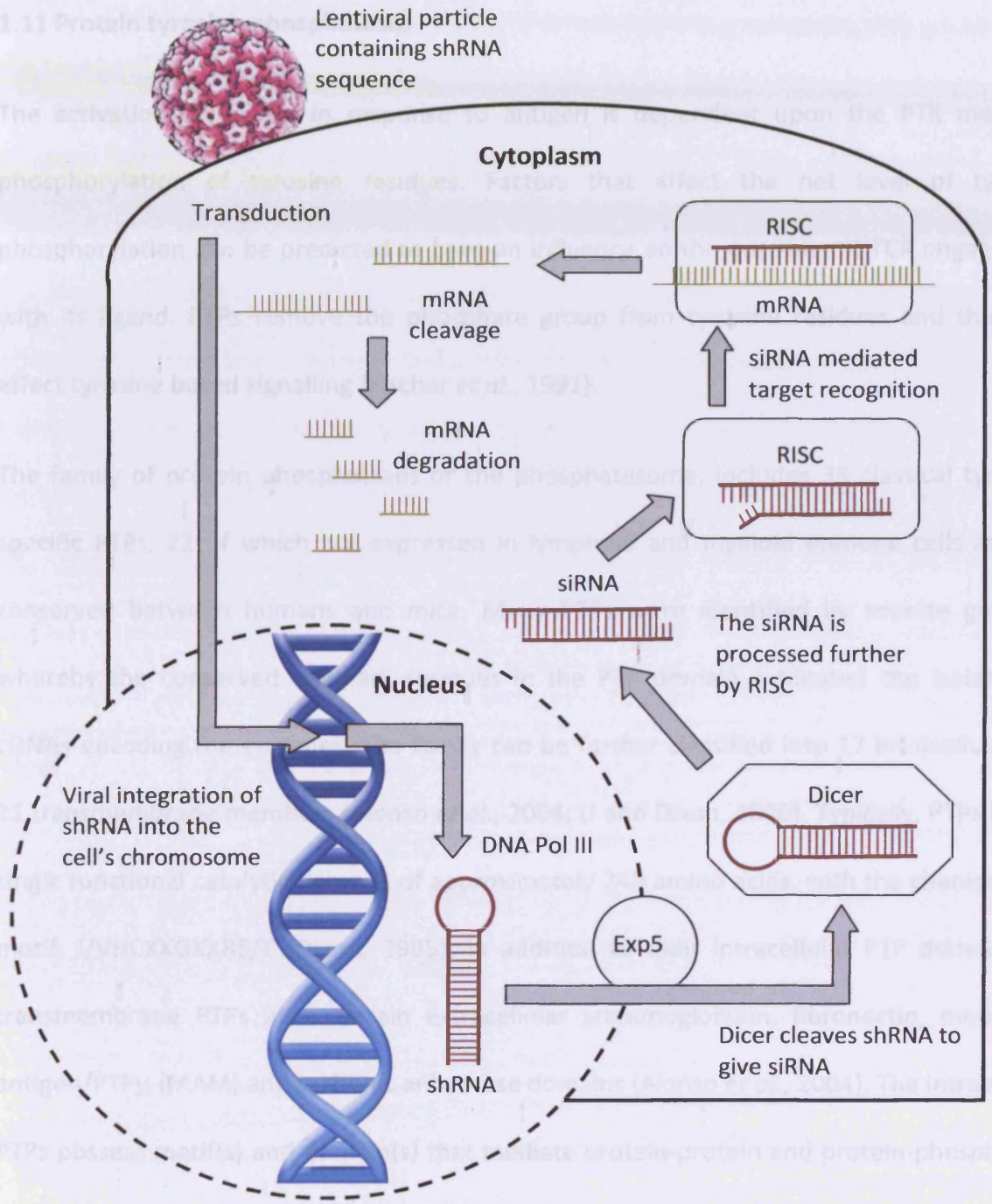


Figure 1.9: The basis of siRNA mediated regulation of gene expression using lentiviral particles containing shRNA sequences

Lentiviral particles can be produced that contain the shRNA sequence for specific downregulation of a chosen protein. Following integration the shRNA is produced and exported from the nucleus into the cytoplasm. The hairpin of the shRNA is cleaved by the enzyme, DICER, thereby yielding a siRNA sequence. The siRNA is then incorporated into RISC, which firstly unwinds the RNA duplex and secondly retains one stand to use as a template to recognise corresponding mRNA transcripts for cleavage. The mRNA fragments are degraded by normal cellular machinery, thus leading to the loss of translation and therefore protein function.

1.11 Protein tyrosine phosphatases

The activation of T cells in response to antigen is dependent upon the PTK mediated phosphorylation of tyrosine residues. Factors that affect the net level of tyrosine phosphorylation can be predicted to have an influence on the outcome of TCR engagement with its ligand. PTPs remove the phosphate group from tyrosine residues and therefore effect tyrosine based signalling (Fischer *et al.*, 1991).

The family of protein phosphatases or the phosphatasome, includes 38 classical tyrosine-specific PTPs, 22 of which are expressed in lymphoid and myeloid immune cells and are conserved between humans and mice. Many PTPs were identified by reverse genetics, whereby the conserved hallmark residues in the PTP domain facilitated the isolation of cDNAs encoding the enzymes. The family can be further classified into 17 intracellular and 21 transmembrane members (Alonso *et al.*, 2004; Li and Dixon, 2000). Typically, PTPs have a single functional catalytic domain, of approximately 240 amino acids, with the characteristic motif, I/VHCXXGXXRS/T (Dixon, 1995). In addition to their intracellular PTP domain, the transmembrane PTPs also contain extracellular immunoglobulin, fibronectin, meprin/A5 antigen/PTPμ (MAM) and carbonic anhydrase domains (Alonso *et al.*, 2004). The intracellular PTPs possess motif(s) and domain(s) that mediate protein-protein and protein-phospholipid interactions. The intracellular PTPs can be further classified based on the possession of distinct non-catalytic domains. SHP-1 and SHP-2, which share 60% overall homology, belong to the same sub-family of PTPs as they possess SH2 domains.

The crystal structures of PTP1B, SHP-1, SHP-2 and a PTP, YopH from the bacterium Yersinia have revealed a common mechanism of catalysis by PTPs. Catalysis proceeds via two steps (Barford *et al.*, 1994a; Hof *et al.*, 1998; Stuckey *et al.*, 1994; Yang *et al.*, 1998); the first being the formation of an enzyme-substrate complex (Denu *et al.*, 1996), involving the transfer of

the phosphate to the enzyme and thus a dephosphorylated substrate; the second step involves hydrolysis of the enzyme thio-phosphate intermediate to yield the enzyme and released phosphate (Denu *et al.*, 1996). The archetypal PTP, PTP1B, accommodates the pY substrate in a catalytic binding pocket at the base of which lies an active site cysteine (Barford *et al.*, 1994a; Barford *et al.*, 1994b). Approximately 30-40 residues distal to the active site cysteine is an aspartate residue involved in catalysis and moved into position as a result of substrate binding (Denu *et al.*, 1996). Hydrogen bonds are formed between the oxygens of the phosphoryl group, and the guanidium group of the active site arginine, and the backbone amide N-H groups of the active site loop. The thiolate anion of the active site cysteine mediates the nucleophillic attack of the P-0 bond of the substrate, leading to the formation of a phosphoryl-cysteine enzyme intermediate and a dephosphorylated substrate (Denu *et al.*, 1996). The aspartate may function as a general base in this instance, by extracting a proton from a water molecule thus allowing hydrolysis of the phosphoenzyme by the hydroxyl group, and therefore completing the reaction by release of a phosphate and rejuvenated enzyme (Li and Dixon, 2000).

1.11.1 SHP-1 (also known as SHP, SH-PTP-1, PTP1C and HCP)

SHP-1 is an intracellular member of the family of protein tyrosine phosphatases, and has been implicated in the negative regulation of a diverse range of signalling pathways in leukocytes.

SHP-1's pattern of expression encompasses all haematopoietic cells, at all stages of their differentiation, certain epithelial cells (Matthews *et al.*, 1992; Plutzky *et al.*, 1992a; Plutzky *et al.*, 1992b; Yi *et al.*, 1992b) and oligodendrocytes of the central nervous system (Horvat *et al.*, 2001; Massa *et al.*, 2000). Two major forms of SHP-1 have been indentified in humans and mice, and differ at the 5'untranslated regions of the initial coding nucleotides due to

two transcription initiation sites, thus giving SHP-1 polypeptides of 595 or 597 amino acids (Banville *et al.*, 1995; Martin *et al.*, 1999; Tsui *et al.*, 2002), with the former being primarily expressed in haematopoietic cells.

The three-dimensional structure of SHP-1 has been revealed by crystallography of an experimentally generated isoform lacking 61 amino acids at the carboxyl terminus (Yang *et al.*, 2003). The images have revealed three main domains; two SH2 domains at the amino terminus followed by a PTP domain (figure 1.10), as previously predicted from the translated sequence of human, rat and mouse SHP-1 (Matthews *et al.*, 1992; Plutzky *et al.*, 1992a; Shen *et al.*, 1991; Yi *et al.*, 1992a). More specifically, residues 1-108 and 116-208 form the amino (N) and carboxyl (C) SH2 domains, and residues 270-532 form the PTP domain. SHP-1 also contains a C-terminal domain rich in basic amino acids (Yang *et al.*, 2003).

The SH2 domains of SHP-1 have two defined roles; allosteric inhibition of the PTP domain and mediation of the binding of SHP-1 to its ligands. Evidence suggesting that the SH2 domains of SHP-1 have an auto-regulatory role have come from *in vitro* studies of SHP-1 lacking the SH2 domains (Pei *et al.*, 1993; Zhao *et al.*, 1993), which unlike full length SHP-1 exhibits catalytic activity. Truncation of each SH2 domain in turn has revealed that the NSH2 domain has an inhibitory influence over SHP-1 activity (Pei *et al.*, 1993; Zhao *et al.*, 1993). The phosphotyrosine binding sites of the SH2 domians are orientated away from the PTP domain, but unlike the CSH2 domain, the NSH2 domain makes extensive interactions with the PTP domain (Yang *et al.*, 2003). This may serve to sterically occlude the PTP active site and prevent any interaction with potential substrates. Whereas the NSH2 of SHP-1 may have a direct regulatory role on the PTP domain, both SH2 domains need to be engaged for full SHP-1 activity. Engagement of individual SH2 domains with phosphotyrosyl peptides is associated with a moderate increase in SHP-1 activity, whereas engagement of both SH2 domains leads to a 100 fold increase in PTP activity (Lechleider *et al.*, 1993; Pluskey *et al.*,

1995; Sugimoto *et al.*, 1994). Moreover, mutation of a critical arginine of both SH2 domains, which is involved in phosphopeptide binding has revealed that both SH2 domains need to be engaged for optimal activity (Pei *et al.*, 1996).

In a physiological setting, the NSH2 and CSH2 domains of SHP-1 bind to tandem (Bruhns *et al.*, 1999; Burshtyn *et al.*, 1999; Kabat *et al.*, 2002), tyrosine phosphorylated ITIM motifs, present on members of the Inhibitory-Receptor Superfamily (IRS), which constitute the major ligands of SHP-1 (Long, 1999; Ravetch and Lanier, 2000) (figure 1.11). Members of the IRS are transmembrane proteins with ITIM motifs present within their cytoplasmic domains. As a result, SHP-1 is located at the plasma membrane when associated with its ligand. The ITIM motif for SHP-1 has been defined as [S/V/I/L]pYXX[L/V] (where X is any amino acid) (Beebe *et al.*, 2000; Burshtyn *et al.*, 1997; Vely *et al.*, 1997) and the spacing between ITIMs can range between 19 and 31 amino acids (Blery and Vivier, 1999). It may also be feasible for the SH2 domains of SHP-1 to bind to ligands expressing a single ITIM, but with the requirement that both SH2 domains must be engaged for SHP-1 activation, such as during ligand dimerisation.

In an inactive configuration, the NSH2 domain of SHP-1 interacts with the PTP domain (figure 1.12). Furthermore, the phosphotyrosine binding site of the NSH2 domain is present in a distorted state and unable to bind to ITIMs. Ligand engagement by the CSH2 domain is predicted to lead to conformational changes in the NSH2 domain, which restores the ligand binding pocket, thus allowing binding to an ITIM. Once both SH2 domains are engaged by ITIMs, the PTP domain is released from auto-inhibition (Pei *et al.*, 1996) and is therefore free to interact with potential substrates (figure 1.11).

By using different biochemical approaches, researchers have endeavoured to identify the substrate(s) of SHP-1, but to date no bona fide substrate(s) of SHP-1 have been formally

identified. *In vitro* studies have demonstrated that SHP-1 is capable of dephosphorylating a number of candidate substrates (Chiang and Sefton, 2001; Raab and Rudd, 1996; Somani *et al.*, 2001), but with the caveat being the physiological relevance of such substrates. Based on the assumption that the substrate(s) of SHP-1 should be hyperphosphorylated in its absence, the phosphotyrosyl state of candidate proteins has been assessed (Johnson *et al.*, 1999; Pani *et al.*, 1996; Pani *et al.*, 1995; Sathish *et al.*, 2001). These included proteins involved in TCR and BCR signalling pathways, such as PTKs (Src-, Syk- and Btk family members), invariant chains of the TCR and BCR (CD3, zeta, Ig α and β chains) and various downstream adaptors and effectors. A second approach has involved examining the molecular consequences of triggering inhibitory receptors, with the premise that the recruitment and activation of SHP-1 will leave the substrate(s) in a dephosphorylated state and facilitate their identification (Binstadt *et al.*, 1998; Binstadt *et al.*, 1996; Dietrich *et al.*, 2001; Valiante *et al.*, 1996). The generation of SHP-1 substrate trapping mutants has provided another potential mode to identifying SHP-1 substrates. PTP mutants maintain their binding capacity for their substrate(s) but are unable to catalyse substrate dephosphorylation, due to specific alterations of key amino acids of the WDP loop (Garton *et al.*, 1996). SHP-1 substrate trapping mutants (C453S or D419A) were unable to directly purify substrates from cell lysates (Timms *et al.*, 1998). An indirect approach using the trapping mutants involved expressing them in cell lines (Berg *et al.*, 1999; Dustin *et al.*, 1999; Mizuno *et al.*, 2000; Timms *et al.*, 1998; Wu *et al.*, 1998). In this context the substrate(s) of SHP-1 would theoretically be left in a hyperphosphorylated state and thus aid their identification. The above studies have indicated certain proteins as potential substrate(s) of SHP-1, but due to their indirect nature the authenticity of the indentified proteins as SHP-1 substrates remains unclear.

The carboxy terminus domain of SHP-1 possesses two tyrosine residues, which mediate interactions with other proteins and may give SHP-1 an adaptor role. When phosphorylated, the tyrosine residues at the carboxy tail of SHP-1 are able to recruit the adaptor protein, Grb-2, which in turn can be complexed with other proteins, such as the inhibitory protein, suppressor of cytokine signalling (SOCS-1) (Minoo *et al.*, 2004). The tyrosine residues of the C terminal domain also interact with the adaptor protein 3BP2 (Yu *et al.*, 2006), which in turn binds ZAP-70, Vav and PLCγ, which further demonstrates the potential role of SHP-1 as an adaptor protein. It has been demonstrated that SHP-1 associates both basally and post TCR triggering to lipid rafts (Fawcett and Lorenz, 2005). The identification of a novel, six amino acid lipid raft-targeting motif, in the C terminal domain of SHP-1 may assist with this localisation to membrane microdomains (Sankarshanan *et al.*, 2007). Furthermore, *in vitro* studies have shown that the binding of anionic phospholipids to SHP-1, via the presence of a high-affinity binding site in the C terminal domain, can lead to activation of the PTP domain (Frank *et al.*, 1999; Zhao *et al.*, 1993). There is also evidence that tyrosine phosphorylation of the C terminal domain may influence the NSH2 mediated inhibition of PTP activity (Zhang *et al.*, 2003).

A great deal of the research into the function of SHP-1 has been facilitated by the availability of the spontaneous mouse mutant strains, termed motheaten and motheaten viable. The mutations were originally reported as recessive single gene mutations, transmitted in a Mendelian manner (Green and Shultz, 1975; Shultz *et al.*, 1984). The mutations were mapped to chromosome six, and subsequently to the gene encoding SHP-1 (Shultz *et al.*, 1993; Yi *et al.*, 1992a). Homozygosity of either mutation causes a lethal autoreactive disease, resulting in a mean lifespan of 3 weeks for motheaten mice and 9 weeks for motheaten viable mice.

The motheaten allele contains a single nucleotide deletion of a cytidine residue, which generates a cryptic 5' splice donor for a 3' acceptor site, and results in a deletion of 101 nucleotides of mRNA encoding the last half of the N-SH2 domain. This creates a frameshift, which results in the generation of an early termination codon. Consequently, the predicted protein of 102 amino acids contains a disrupted N-SH2 domain and no C-SH2 or PTP domain (figure 1.12). Therefore mice homozygous for the motheaten allele lack SHP-1 activity.

The motheaten viable allele has a single base pair substitution leading to the loss of a highly conserved splice donor consensus sequence and consequently produces two aberrant transcripts. The first transcript involves the activation of a downstream splice donor, which results in an insertion of 69 nucleotides. The second transcript is generated by the activation of an upstream cryptic splice donor that results in a deletion of 15 nucleotides. Both alterations maintain the reading frame and therefore an entire SHP-1 protein is produced, but with either a 23 amino acid insertion or 5 amino acid deletion (figure 1.12). The motheaten viable mutations affect the substrate binding pocket of the PTP domain, and reduce SHP-1 activity by 80% in comparison to that of wild-type SHP-1.

Motheaten individuals can be identified several days post partum by the appearance of skin abscesses. These abscesses manifest as patchy alopecia as the mice develop, giving them their characteristic motheaten appearance, from which they take their name (figure 1.13). This distinctive phenotype is attributed to the accumulation of activated neutrophils within the epidermis of the skin. Indeed, motheaten pathology is dominated by over-expansion of myelomonocytic lineage cells. Motheaten mice succumb to an inflammatory pathology that includes haemorrhagic pneumonitis accompanied by the accumulation of expanded myeloid cell populations within the alveoli of the lung (Shultz *et al.*, 1997).

The ex-vivo study of myeloid cells form motheaten mice confirms their hyper-reactivity. Bone marrow granulocytes form motheaten viable mice exhibit enhanced proliferative responses to the growth factor G-CSF (Tapley *et al.*, 1997). The enhanced proliferation is also evident for macrophages from motheaten mice, in response to GM-CSF (Jiao *et al.*, 1997). In addition, macrophages from motheaten mice exhibit an increased adhesion and spreading, which is accompanied by dysregulated detachment (Roach *et al.*, 1998). Similarly, bone marrow motheaten neutrophils are hyperadherent and demonstrate decreased chemotaxis, which may be attributed to a decrease in de-adhesion (Kruger *et al.*, 2000).

In NK cells, SHP-1 plays a role in regulating cytotoxic function and the polarisation of lipid rafts. Inhibitory receptors expressed by NK cells, such as KIRs, contain ITIMs that are capable of recruiting and activating SHP-1 (Binstadt *et al.*, 1996; Burshtyn *et al.*, 1996; Nakamura *et al.*, 1997). KIR engagement appears to disrupt an early adhesion step in the NK killing program, which is mediated primarily by integrins. This precludes the formation of stable conjugates between an NK cell and its target (Burshtyn *et al.*, 2000). Substituting the intracellular domain of KIR with full length SHP-1 also blocks conjugate formation thereby demonstrating a critical role for SHP-1 in the inhibition of adhesion. Under activatory conditions a NK cell undergoes rapid polarisation, which is associated with the accumulation of lipid rafts (Lou *et al.*, 2000), signalling proteins, talin and lysosomes at the immunological synapse that forms between a NK cell and a potential target cell (Vyas *et al.*, 2002; Vyas *et al.*, 2001). KIR engagement is associated with the inhibition of NK cell polarisation towards a target cell. Indeed, the engagement of KIR dramatically inhibits raft polarisation and is dependent on the activity of SHP-1 (Lou *et al.*, 2000).

In B cells, SHP-1 has been implicated in the negative regulation of signals from antigen receptors. B cells from motheaten mice hyperproliferate in response to stimuli through the BCR (Pani *et al.*, 1995). Additionally, SHP-1 deficient B cells possessing a transgenic BCR

undergo antigen induced death when stimulated with cognate peptide, which is an effect not seen in normal B cells (Cyster and Goodnow, 1995). SHP-1 deficient B cells also exhibited an elevated level of intracellular Ca^{2+} (Ono *et al.*, 1997). Studies involving B cells that express a dominant negative form of SHP-1 have similarly indicated elevated levels of Ca^{2+}, and also a marked increase in cell adhesiveness (Dustin *et al.*, 1999). SHP-1 binds to a number of ITIM-containing receptors in B cells, including CD22, CD72 and PIR-B. When each of these inhibitory receptors is separately co-ligated with the BCR, activation induced mobilisation of Ca^{2+} is depressed (Aldachi *et al.*, 1998; Blery *et al.*, 1998; Smith *et al.*, 1998). Furthermore, B cells deficient for either CD22 or CD72 are hyper-responsive to BCR triggering and exhibit enhanced Ca^{2+} and proliferative responses (Nitschke *et al.*, 1997; O'Keefe *et al.*, 1996; Pan *et al.*, 1999).

Although T cells are not involved in the pathology observed in motheaten and motheaten viable mice, it does not preclude a role for SHP-1 in T cells (Yu *et al.*, 1996). Indeed, SHP-1 has been implicated in having a negative regulatory role in T cells, thereby raising TCR signalling thresholds.

SHP-1 has been demonstrated to associate with several receptors in T cells, including LAIR-1, CD22 and CEACAM-1. Cross-linking the human inhibitory receptor, LAIR-1, on peripheral T cells inhibits anti-CD3 induced killing of target cells. Other studies have demonstrated that SHP-1 constitutively associates with LAIR-1 at the cell membrane of the human Jurkat T cell line and human peripheral T cells. This association is independent of TCR triggering, indicating the LAIR-1/SHP-1 complex mediates a basal tonic inhibition of TCR signalling. The introduction of catalytically inactive form of SHP-1 to T cells leads to an increase in TCR triggering, but without the required coengagement of any inhibitory receptors with the TCR. CD22 has also been confirmed as a ligand of SHP-1 in mouse T cells (Sathish *et al.*, 2004). Ligation of CD22 on naive T cells has been reported to inhibit anti-CD3 induced T cell

proliferation. In addition, T cells from $CD22^{-/-}$ mice hyperproliferate upon TCR triggering (Sathish *et al.*, 2004). Engagement of CEACAM-1, which is expressed by T cells following activation, inhibits IL-2 production and proliferation in human T cells by association with SHP-1 (Chen *et al.*, 2008). Engagement of the TCR and crosslinking of the inhibitory receptor, ILT2, inhibits early TCR triggered events via recruitment of SHP-1 and leads to suppression of actin cytoskeletal re-organisation (Saverino *et al.*, 2000). Interestingly, the preferential expression of ILT2 on $CD4^+$ leukaemic, Sezary cells, may assist with their malignancy, as it confers resistance to activation induced apoptosis following CD3/TCR engagement when compared to autologous $CD4^+ILT2^-$ cells (Nikolova *et al.*, 2002). Moreover, evidence suggests that SHP-1 may influence the activities of the cytoskeleton, and associated actin polymerisation in T cells (Dietrich *et al.*, 2001). It has also been demonstrated that motheaten viable T cells have a greater *in vitro* chemotactic response to the chemokine, SDF-1 (Kim *et al.*, 1999).

As discussed earlier, TCR signalling plays an important role during T cell maturation in the thymus. SHP-1 deficiency leads to increased positive selection of thymocytes in motheaten mice expressing MHC class I or II restricted transgenic TCR (Carter *et al.*, 1999; Johnson *et al.*, 1999; Plas *et al.*, 1999; Zhang *et al.*, 1999b), which is consistent with lowered thresholds for TCR activation. Moreover, SHP-1 deficiency leads to an increased TCR signal strength whereby TCR signals too weak to induce survival, are sufficiently strong in the absence of SHP-1 to elicit positive selection. In addition, the introduction of a dominant negative form of SHP-1 in to mice by transgenesis recapitulates the findings obtained from motheaten and motheaten viable mice (Plas *et al.*, 1999; Zhang *et al.*, 1999b).

Ex-vivo functional analysis of thymocytes from motheaten and motheaten viable mice has demonstrated that they proliferate to a greater degree and also secrete increased amounts of IL-2 when stimulated with anti-TCR/CD3 antibodies (Lorenz *et al.*, 1996; Pani *et al.*, 1996;

Sathish *et al.*, 2001; Zhang *et al.*, 1999b). Similarly, SHP-1 deficient peripheral T cells expressing transgenic TCRs also exhibit an enhanced proliferative response when stimulated by cognate peptide/MHC complexes (Carter *et al.*, 1999; Johnson *et al.*, 1999; Zhang *et al.*, 1999b). These data demonstrate that SHP-1 raises the threshold of TCR signalling. The hyper-responsive phenotype has also been observed following the introduction of a dominant negative form of SHP-1 in to T cell hybridomas (Carter *et al.*, 1999; Plas *et al.*, 1996) and the human Jurkat T cell line (Plas *et al.*, 1996).

In addition, SHP-1 deficient peripheral T cells from mice expressing transgenic TCRs proliferate more at all intensities of TCR stimulation with cognate antigen (Carter *et al.*, 1999; Johnson *et al.*, 1999; Zhang *et al.*, 1999a). This indicates that even the strongest of TCR signals is unable to override the effect of SHP-1 activity, suggesting that SHP-1 does not necessarily act on pathways disseminating from the TCR. Costimulatory molecules such as CD28 (Viola and Lanzavecchia, 1996) are involved in lowering thresholds of TCR responsiveness. Indeed, data indicates that increased stimulus from CD28 eliminates the proliferative differences detected between SHP-1 deficient and sufficient thymocytes (Sathish *et al.*, 2001).

By using the intracellular dye, CFSE, it has been demonstrated that a greater proportion of TCR transgenic motheaten T cells from a given population have the ability to enter into cell division following TCR triggering (Sathish *et al.*, 2007). This data was supported by the observation that a greater proportion of SHP-1 deficient T cells downregulate their TCR upon stimulation with cognate peptide loaded APCs, which is a consequence of increased antigen encounter by the SHP-1 deficient T cells. At a cellular level, SHP-1 deficient T cells exhibit the ability to form more stable conjugates with APCs displaying cognate antigen (Sathish *et al.*, 2007), which may contribute to their hyper-proliferative phenotype.

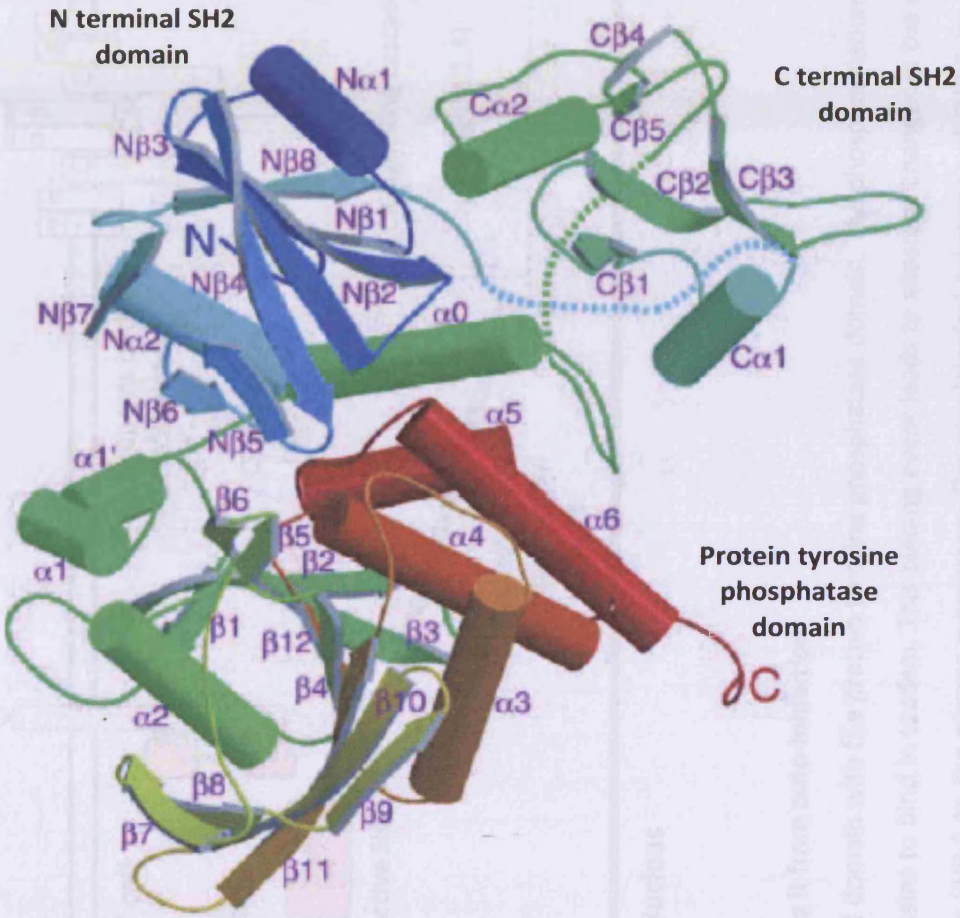


Figure 1.10: Overall structure of SHP-1

A schematic representation of the crystal structure of human SHP-1. The colour graduates from blue (N terminal) to red (C terminal) and the secondary domains are labelled accordingly.

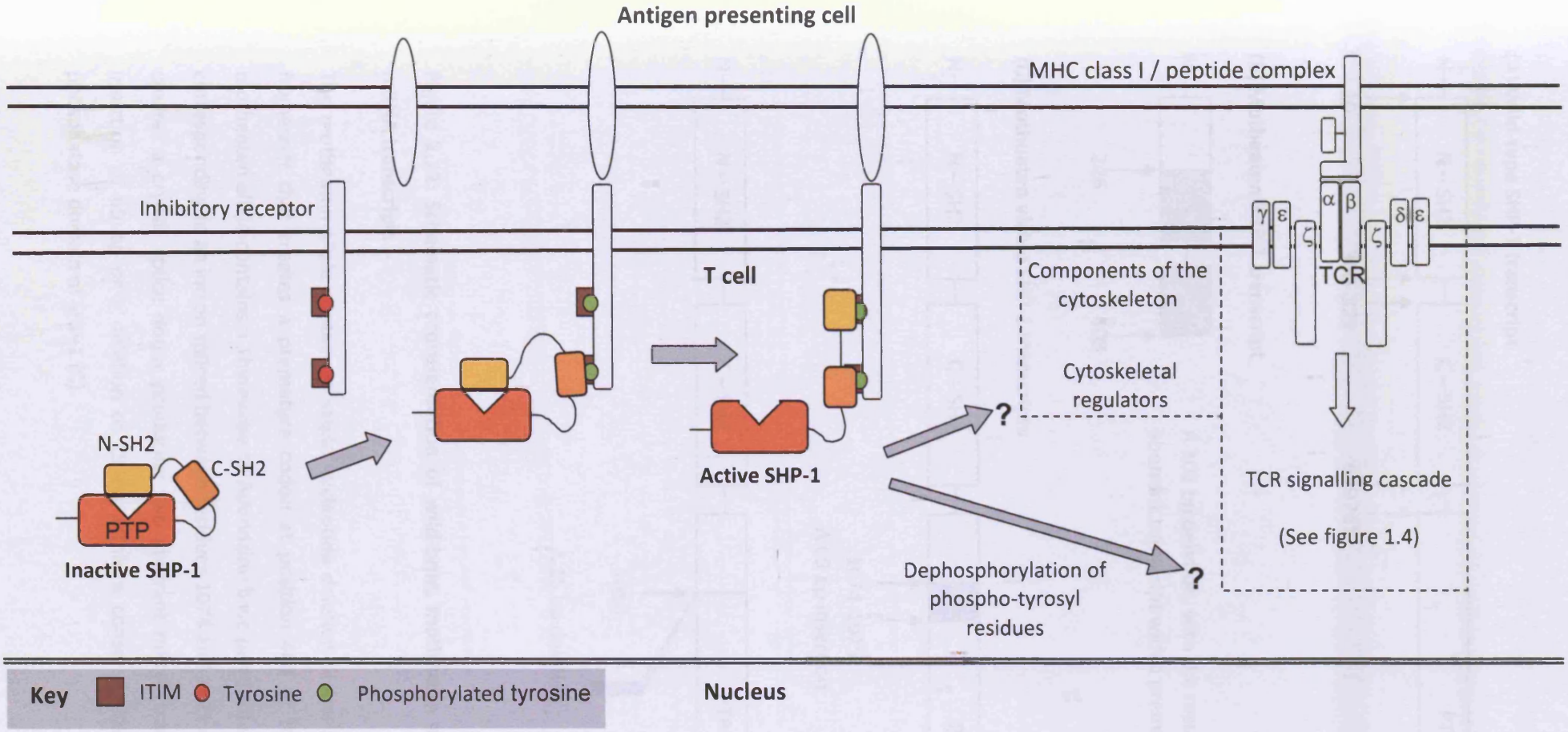


Figure 1.11: The binding of SHP-1 to tandem phosphorylated ITIMs releases it from auto-inhibition.

SHP-1s catalytic activity is regulated by the interaction of its N terminal SH2 domain with the protein tyrosine phosphatase domain. The phosphorylation of tyrosine residue of ITIM's belonging to inhibitory receptors allows SHP-1's SH2 domains to bind in tandem. This binding event leads to allosteric changes in the structure of SHP-1 thus relieving the PTP domain from auto-inhibition and also recruits SHP-1 to the plasma membrane. The physiological substrates of SHP-1 have yet to be elucidated, although it seems that SHP-1 may act upon cytoskeletal components or regulators.

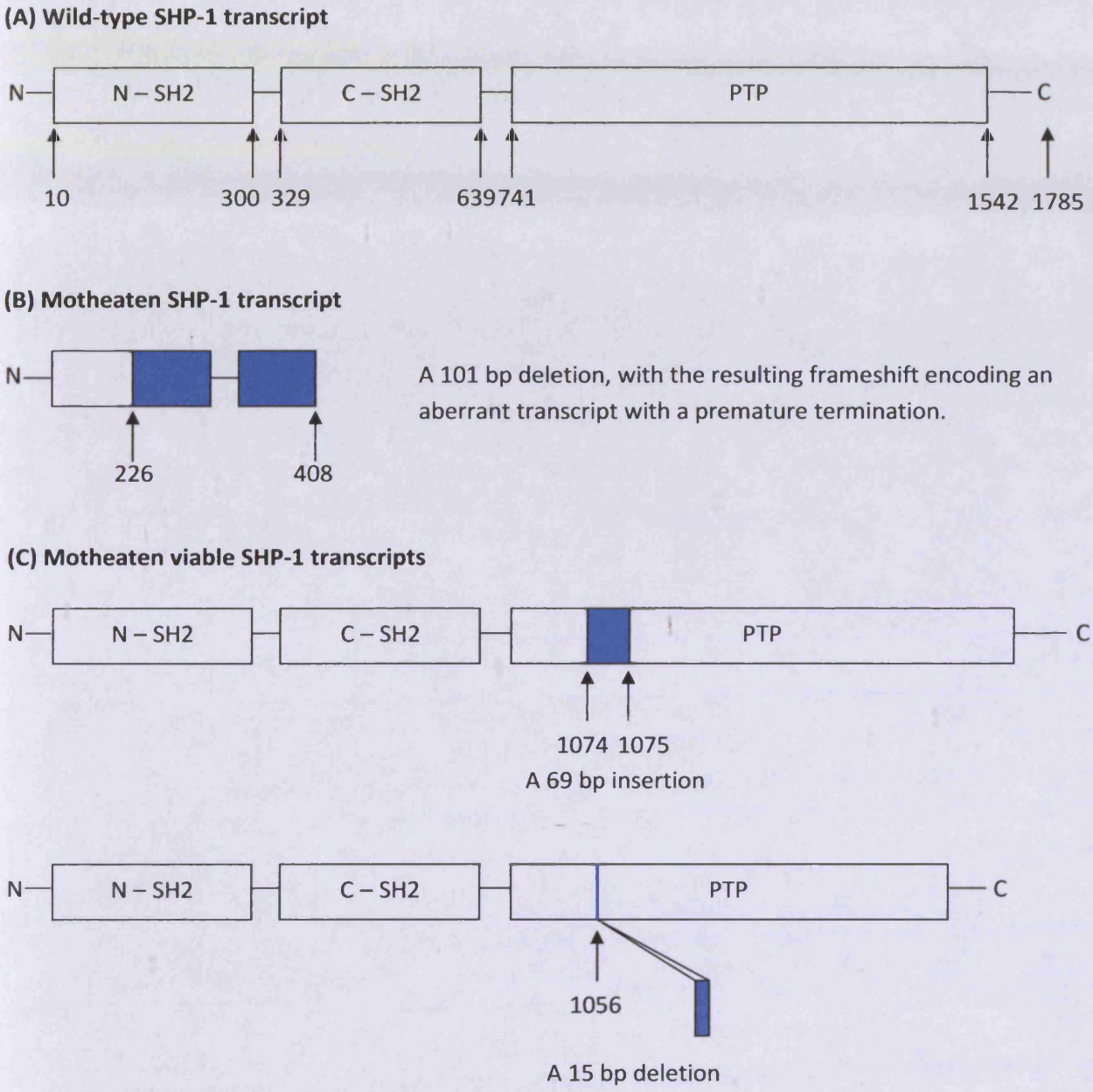


Figure 1.12: Schematic representation of wild-type, motheaten and motheaten viable SHP-1 mRNA transcripts

The motheaten allele contains a single nucleotide deletion of the *Shp-1* gene, which leads to a frameshift that creates a premature codon at position 408 of the mRNA transcript (B). The motheaten allele contains a Thymidine to Adenosine base pair (bp) substitution in the Shp-1 gene corresponding to an intron spliced between residues 1074 and 1075 of the mRNA. The substitution creates a cryptic splice donor producing two aberrant mRNA transcripts containing either an insertion of 69 bp or a deletion of 15 bp within a conserved region of the protein tyrosine phosphatase domain of SHP-1 (C).

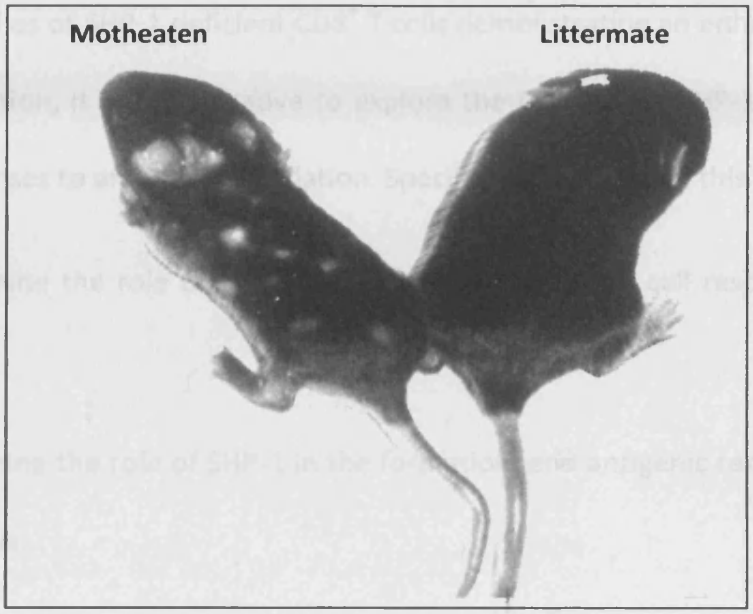


Figure 1.13: A motheaten mouse and a littermate at 10 days old.

Motheaten mice are distinguishable from littermate mice due to the characteristic patchy alopecia and tissue necrosis, which gives them a distinctive appearance, from which they take their name. The typical life expectancy of a motheaten mouse is 21 days, with Home Office stipulations requiring their sacrifice by approximately day 14 post partum. Motheaten viable mice have a similar appearance but have an extended life expectancy of 63 days.

1.12 Aims of the study

With *in vitro* studies of SHP-1 deficient $CD8^+$ T cells demonstrating an enhanced response to antigenic stimulation, it was imperative to explore the *in vivo* role SHP-1 may have during $CD8^+$ T cell responses to antigenic stimulation. Specifically, the aims of this study were:

1) To determine the role of SHP-1 during a primary $CD8^+$ T cell response to antigenic challenge.

2) To determine the role of SHP-1 in the formation, and antigenic response of memory $CD8^+$ T cells.

3) To utilise SHP-1 deficient $CD8^+$ T cells in models of tumourigenesis in order to support its candidature for modulation during ACT therapies.

4) To establish whether SHP-1 expression could be modulated by using siRNA technology.

Chapter 2

Materials and Methods

2.1 Reagents and consumables

2.1.1 Antibiotics

Antibiotic solutions were sterile filtered through a 40μm syringe filter then stored at -20°C, or at 4°C for continuous use.

Ampicillin

Ampicillin was purchased from Sigma Aldrich [Gillingham, Dorset, U.K.] and reconstituted in dH_20 to give a 100mg/ml stock.

Neomycin (G418)

G418 disulphate salt powder was purchased from Sigma Aldrich and reconstituted in PBS to give a stock solution of 200mg/ml.

Puromycin

Puromycin was purchased from Autogen Bioclear [Wiltshire, U.K.] and diluted in serum free DMEM to give a 0.1mg/ml stock.

2.1.2 Antibodies

Immunoblotting antibodies

Rabbit antiserum was raised to the tandem SH2 domains of mouse SHP-1 that had been cleaved and purified from a bacterially expressed GST-fusion protein. The SHP-1 antibody was generated by Dr. R. J. Matthews [Department of Medical Biochemistry and Immunology, Cardiff University, U.K.], in the laboratory of M. L. Thomas [WUMS, St. Louis, MO]. The

rabbit anti-actin polyclonal serum was purchased from Sigma Aldrich. The horseradish peroxidise (HRP) conjugated anti-rabbit secondary monoclonal antibody was purchased from Bio-Rad [Bio-Rad, Hercules, CA].

CD3 activating antibody

The biotin-conjugated anti CD3ε monoclonal antibody, 145-2C11, was purchased from PharMingen [San Diego, CA].

Fluorescent conjugated anti-mouse antibodies for detecting cell surface protein expression

Anti-CD8α(Ly-2)^{PE} antibody was purchased from Serotec [Oxford, U.K.]. Anti-CD11c^{FITC}, anti-CD86^{PE}, anti-TCRαβ^{PE}, B220^{FITC} and anti-CD107a^{FITC} antibodies were purchased from PharMingen.

2.1.3 Cell media and associated reagents

Dulbecco modified Eagle's minimal essential media (DMEM), Roswell Park Memorial Institute medium (RPMI), phosphate buffered saline (PBS), Hank's balanced salt solution (HBSS), L-glutamine, penicillin, streptomycin, sodium pyruvate and 0.5% trypsin in HBSS were purchased from Gibco, Invitrogen [Paisley, U.K.].

2.1.4 Chemicals

All chemicals were of analytical grade and obtained from Fisher Scientific [Leicester, U.K.], unless otherwise stated. Tris was obtained from Amersham Pharmacia Biotech [Buckinghamshire, U.K.]. Tween 20 and Nonidet P-40 (NP-40) were supplied by BDH [Poole, Dorset, U.K.].

2.1.5 Distilled water (dH_2O)

Distilled H_2O was obtained from a Millipore reverse osmosis system followed by filtration through two ion exchange resin columns using a Millipore Milli-Q system.

2.1.6 Foetal calf serum

Foetal calf serum (FCS) was purchased from Sigma Aldrich and PAA Laboratories Limited [Pasching, Austria], and unless done so by the supplier, it was heat inactivated at 56°C for 30 minutes.

2.1.7 Interleukin-2 (IL-2)

Recombinant human IL-2 was purchased as 'Proleukin' from Chiron Limited [Harefield, U.K.] and reconstituted to 1mg/ml under sterile conditions in ddH_20, diluted to 20ng/ml in RPMI and stored in 1ml aliquots at -70°C. For continuous use, aliquots were thawed and stored at 4°C.

2.1.8 Intracellular Dyes

CellTrace™ far red DDAO-SE

7-hydroxy-9*H*(1,3-dichloro-9,9,-dimethylacridin-2-one)-succinimydyl ester (DDAO-SE) was purchased from Invitrogen [Paisley, U.K.] and stored at -20°C in powder form. When required the powder was suspended in tissue culture tested sterile dimethyl sulphoxide (DMSO) to give a 40mM stock solution.

CSFE

Carboxyfluorescein diacetate Succinimydyl Ester (CFSE) powder was purchased from Invitrogen and suspended in ddH_20 to give a 10mM stock solution, which was sterile filtered,

dispensed in to 10µl aliquots and stored at -20°C. Aliquots were used once and not re-frozen.

2.1.9 NP68 peptide

NP68 is derived from the nucleoprotein of the influenza virus A/NT/60/68 (NP366-374) of sequence ASNENMDAM that binds H-2D^b, and is recognised by the cytotoxic TCR clone, F5. The peptide was obtained from Severn Biotech Limited [Kidderminster, U.K.] as a dry powder and reconstituted in dd$H_2$0 to make a 10mM stock, which was aliquoted and stored at -20°C.

2.1.10 Plasmid DNA

pMX expression plasmids containing either the NP68 epitope as a fusion gene with green fluorescent protein (GFP) or firefly luciferase (Luc) with yellow fluorescent protein (YFP) genes (separated by an IRES) were kind gifts from Dr. Ton Schumacher [The Netherlands Cancer Institute, Amsterdam, The Netherlands].

Plasmid for DNA sequencing was purified using a Qiagen [Crawley, U.K.] plasmid mini-prep kit. Plasmid for transfection was prepared using either an Invitrogen PureLink HiPure Plasmid filter Maxiprep kit or a Qiagen plasmid maxi-kit, and then stored at -20°C.

2.1.11 Retinoic acid

All-trans retinoic acid in powder form was purchased from Sigma Aldrich and suspended in PBS to make a 10mM stock, which was sterile filtered and stored at -20°C in black eppendorf tubes.

2.1.12 Tissue culture plastic

All tissue culture flasks (T25, T75 and T180), petri-dishes and tissue culture plates (6, 24 and 96 wells) were supplied by Fisher Scientific.

2.1.13 Viruses

The Influenza A virus and recombinant Vaccinia virus encoding the NP68 epitope were kinds gifts from Dr. A. Gallimore [Department of Biochemistry and Immunology, Cardiff University, U.K.]. Stocks were stored at -70°C.

2.2 Cell based techniques

2.2.1 Counting cells by trypan blue exclusion

An aliquot of cells was mixed with an equal volume of 0.1% trypan blue in PBS (w/v) and loaded on to an improved Neubauer haemocytometer [Weber Scientific International Limited, Lancing, U.K.] and viable cells (clear appearance) counted at 100 times magnification under white light.

2.2.2 Flow Cytometry

A FACSCalibur flow cytometer [BD Biosciences, San Jose, CA] fitted with an argon-ion (488nm) and red diode laser (635nm) and capable of four channels of fluorescent detection was used throughout this study. Acquired data was analysed using CellQuestPro [BD Biosciences, Oxford, U.K.] or FlowJo software [Tree Star Inc, Ashland, OR]. In addition, a DakoCytomation high performance MoFlo cell sorter [Central Biotechnology Service, Henry Wellcome Research Institute, Cardiff University] was used to physically sort cells on a single cell basis.

2.2.2a Labelling cells with fluorescent conjugated antibodies

Cells were counted by trypan blue exclusion and $1x10^6$ transferred to either a 96 well plate or 5ml FACS tube, centrifuged and then the plate flicked or the tube inverted to remove media. Cells were washed with staining buffer (PBS with 2% FCS), by centrifugation at 1500rpm for 5 minutes at 4°C. The cells were incubated for 20 minutes on ice and in the dark with 100µl of staining buffer containing 2µg of the desired antibody. Cells were then washed twice in labelling buffer and finally resuspended in 100-200µl of cell wash [BD Biosciences]. Cells were analysed in FACS tubes containing sheath fluid on a FACSCalibur flow cytometer.

2.2.2b Labelling cells with intracellular dyes

The intracellular dyes CFSE (excitation/emission 492 and 517nm) and DDAO (excitation/emission 600-647 and 656nm) were used throughout this study. The dyes enter the cell by passive diffusion where the succinimydyl ester group reacts with intracellular amines, which occur within proteins and other biomolecules, thereby forming fluorescent conjugates via strong covalent bonds. DDAO was used at a concentration of 10µM, whereas CFSE was used at various concentrations (0.2, 0.5, 2, 3 and 4µM) depending upon the assay requirements. Following the preparation of a single cell suspension, the cells to be labelled were collected by centrifugation and suspended in 10mls of HBSS. A 2X CFSE stock was prepared in 10mls of HBSS then combined with the cells to give a final volume of 20mls. Once the dye had been added to the cells they were immediately mixed by vortexing for 5 seconds. Labelling was carried out in the dark, in a 37°C water-bath for 5 minutes. To quench any excess dye, either 20mls of complete DMEM or 4mls of neat FCS was added to the cells and left at room temperature for 2 minutes. For labelling with DDAO, the cells were treated in the same manner as for CFSE labelling, but 1.5mls of HBSS was used to both resuspend the cells post centrifugation and also to make the 2X DDAO stock, to give a final volume of

3mls. Furthermore, the cells were labelled for 10 minutes and excess dye quenched with either 3mls of complete DMEM or 1ml of neat FCS. Labelled cells were kept on ice and shielded from light until required.

2.2.3 Protein analyses

Immunoblotting techniques were used to detect both endogenous levels of SHP-1 expression in Jurkat cells that had been transiently transfected with shRNA sequences directed against SHP-1 transcripts, and also in Hela cells that had been stably transfected with plasmid DNA encoding mouse or human SHP-1. Actin was used as a control for this analysis.

2.2.3a Detergent lysis of cells

Cells were removed from culture, washed and counted. The cells were then pelleted and the supernatant carefully removed and the cells resuspended in the desired volume of ice cold detergent lysis buffer (150mM NaCl, 50mM Tris-HCl pH 8.0, 25mM NaF, 1mM sodium orthovanadate 0.5% Nonidet P-40) containing protease inhibitors (10μg/ml Aprotinin, 10μg/ml Leupeptin, 10μg/ml Pepstatin A, 1mM EDTA, 1mM Phenylmethylsulfonylfluoride), which were added immediately prior to lysis. Cells were allowed to lyse for 30 minutes on ice. Unlysed cells and nuclear material was removed by centrifugation (Beckham GS15R) at 13000rpm for 10 minutes at 4°C. The post nuclear supernatant was collected and mixed with 6X sample buffer (0.35M Tris pH6.8, 1.65M Dithiothreitol, 33% glycerol (v/v), 10% SDS (w/v), 0.12mg/ml bromophenol blue [Sigma Aldrich]) and, if not immediately required for analysis, stored at -20°C.

2.2.3b SDS-Polyacrylamide Gel Electrophoresis

Proteins were resolved by using NuPAGE Novex 4-12% Bis-Tris pre-cast gels [Invitrogen] mounted in a XCell SureLock Mini-Cell [Invitrogen] which were filled with NuPAGE MOPS SDS running buffer [Invitrogen], according to the manufacturer's instructions. SDS-PAGE samples were boiled for 5 minutes at 100°C and microfuged at 13000rpm for 30 seconds. Samples were loaded into the wells of the gel by careful pipetting using gel tips. For size discrimination of the resolved proteins, 10µl of SeeBlue Plus 2 prestained standard protein ladder [Invitrogen] was loaded in to one well. The gels were resolved at 200 Volts for 1 hour.

2.2.3c Immunoblotting

Following electrophoresis, the gels were removed from the gel cassette and trimmed to remove the wells and gel foot. The gel was then equilibrated in ice cold transfer buffer (48mM Tris, 39mM Glycine, 13mM SDS and 20% Methanol) for 20 minutes. Polyvinylidenedifluoride (PVDF) membranes [Immobilon-P, Millipore, Bedford, MA] were cut to the exact size of the gel, wet with methanol for 10 seconds, rinsed in dH20 and equilibrated in transfer buffer for 20 minutes. Two pieces of blotting pad were also cut to the size of the gel and placed in the transfer buffer to equilibrate for 20 minutes. The PVDF membrane was placed directly beneath the gel while still in the transfer buffer, followed by one piece of blotting pad. The second piece of blotting pad was then placed on top of the gel to form a stack, which was then positioned on the cathode of a semidry transblot system [Bio-Rad]. Trapped air bubbles were removed by gently rolling the stack with a tissue culture pipette. The anode lid was clamped into position and the gels blotted for 16 minutes at 15 Volts.

2.2.2d Immuno-detection by Enhanced Chemiluminesence (ECL)

In order to block non-specific binding sites, the PVDF membranes were placed in blocking buffer (PBS containing 3% non-fat milk) for 1 hour at room temperature. The membranes were then incubated overnight with the primary antibody at a dilution of 1 in 5000 in blocking buffer, by constant rocking at 4°C. The PVDF membrane was then washed for 5 minutes in washing buffer (PBS containing 0.05% Tween 20) followed by two 5 minute washes in PBS, by constant rocking at room temperature. Secondary HRP-conjugated anti-rabbit antibody was added at a dilution of 1µl in 1000µl in blocking buffer and incubated for 1 hour at room temperature by gentle rocking. The membranes were rinsed then washed three times for 10 minutes in washing buffer, followed by one wash in PBS at room temperature by constant rocking. Membranes were covered with a 1:1 mixture of ECL reagents 1 and 2 of [Amersham] and allowed to react for 1 minute. Membranes were subsequently sealed in a polythene sleeve and exposed to photographic film for 10 seconds to 10 minutes. The photographic films were developed automatically with a Compact X2 Processor [X-Ograph Ltd., Wiltshire, U.K.].

2.3 *Escherichia Coli*

2.3.1 Culture media

LB broth (1% Bactotryptone (w/v) [Oxoid, Basingstoke, U.K.], 0.5% Bacto-yeast extract (w/v) [Oxoid] 175mM NaCl, buffered to pH7.0) was autoclaved and allowed to cool at room temperature before the addition of antibiotics (100µg/ml final concentration of ampicillin). LB agar was prepared by the addition of 1.5% Bacto-agar (w/v) to LB broth, autoclaved as before and cooled to 50°C before the addition of the antibiotics (100µg/ml final concentration of ampicillin). The LB agar was dispensed in to petri-dishes and allowed to set at room temperature before being stored at 4°C until required.

2.3.2 Clonal selection

Bacteria collected from 1ml cultures by microfuge centrifugation, following transfection by heat-shock, or directly from frozen stocks, were streaked onto LB-ampicillin (100μg/ml) plates and allowed to grow for 16 hours in an incubator set at 37°C.

2.3.3 Clonal expansion

To obtain a starter culture, single colonies picked from plates were inoculated in 5mls of LB-ampicillin (100μg/ml) broth and incubated overnight at 37°C on an orbital shaker. Subsequently, 1ml of the bacteria starter culture was inoculated in to 500ml litre of LB-ampicillin broth and incubated as before. Bacteria were collected by centrifugation at 6000rpm for 10 minutes at 4°C on a Sorvall Evolution centrifuge.

2.3.4 Storage of bacterial clones

500μl of a 5ml starter culture was added to 500μl of glycerol freezing buffer (65% glycerol, 0.1M $MgSO_4$ and 0.23M Tris, pH 8.0) and stored at -70°C.

2.4 Tissue culture and cell lines

2.4.1 Culture conditions

Cell were cultured in either RPMI or DMEM (4.5g/L glucose and L-Glutamine), with 10% heat-inactivated FCS, 2mM L-glutamine, 100 IU/ml penicillin and 100μg/ml streptomycin, 1 mM sodium pyruvate and 60μM 2Me. Cells were maintained at 37°C in a Heraeus incubator with 5% CO_2. Adherent cells were grown to 50-90% confluence before being divided. When splitting adherent cells, they were removed from tissue culture plastic by incubation with either 0.5% trypsin in HBSS or PBS. Firstly, the media was removed from the cells, and the cells rinsed once with PBS. The cells were then incubated with trypsin for 5 minutes or warm (37°C) PBS for up to 30 minutes. Cells were then removed from the plate, filtered, washed by

centrifugation and finally passed through a 29G needle to create a single cell suspension before being returned to tissue culture plastic. Cells that were grown in tissue culture plates or petri-dishes were placed in a plastic ventilated container with a small reservoir filled with dH_2O.

2.4.2 Human transformed cell lines

The human leukaemic Jurkat cell line was cultured in complete RPMI at a density of 0.5-2x10^6 cells per ml and split at a ratio of 1:10 every 4-5 days. Hela cells, which are an adherent human cervical carcinoma cell line were cultured in complete DMEM.

2.4.2a Production of Hela cells expressing mouse SHP-1

Hela cells were plated in six well plates (1.5x10^5 per well) and left for 24 hours prior to transfection with a plasmid (pSSFV) encoding a full length cDNA for mouse SHP-1. Media (2mls) was replaced 15 minutes prior to transfection. For each well to be transfected, 4μg of DNA was added to 100μl of 150mM NaCl, followed by brief vortexing and centrifugation. Separately, 6μl of Polyplus jetPEI [Autogen Bioclear] was added to 100μl of 150mM NaCl. The jetPEI was added to the DNA and left to stand at room temperature for 30 minutes. The DNA preparation was added drop-wise to the cells and mixed gently and returned to the incubator for 24 hours, after which the media was replaced. Selection for stable transfectants began 48 hours post transfection, with an initial G418 concentration of 1.5mg/ml. Once selected, as assessed by comparison to untransfected cells, the cells were maintained at 0.75-1mg/ml of G418 and grown for 4 weeks and tested for SHP-1 expression by immunoblot analysis.

2.4.2b Production of Hela cells expressing human SHP-1

Hela cell were plated in T75 flasks and left for 24 hours ready for transfection with pSSFV-human SHP-1. The media was replaced prior to transfection. A calcium phosphate and plasmid DNA precipitate was prepared using a calcium phosphate transfection kit [Sigma] according the manufacturer's instructions. Briefly, a 450µl volume of $CaCl_2$/DNA mixture was prepared containing 20µg of DNA, 45µl of 2.5M calcium chloride and the corresponding volume of sterile molecular biology grade water. This was added drop-wise to 450µl of 2X HEPES-buffered saline (HeBs) whilst bubbling with a pipette pump and 5ml strippette fitted with a Gilson pipette tip. The mixture was vortexed for 1-4 seconds and left undisturbed for 20 minutes at room temperature and then added to the cells. Selection of stable transfectants began 48 hours post transfection, with an initial G418 concentration of 1.5mg/ml. Once selected, cells were maintained at 0.75-1mg/ml of G418 and tested for SHP-1 expression by immunoblot analysis.

2.4.2c Mouse GM-CSF production

The cell line, J558L, expressing mouse GM-CSF was a kind a gift from Professor Kim Bottomly [Yale University]. Cells were defrosted and allowed to grow unselected for 2-3 weeks followed by selection in 1mg/ml G418 for a further 1-2 weeks. Cells were then removed from selection and allowed to grow for 7-10 days, until the media had started to turn yellow. The supernatant was harvested and any producer cells removed by centrifugation followed by sterile filtration through a 40µm syringe filter. Supernatant was stored at -20°C until required.

2.4.3 Viral Packaging cell line

A retroviral packaging cell line was used to produce virus from plasmid DNA encoding NP68 with GFP or Luc with YFP.

2.4.3a Phoenix cells

The Phoenix-amphotrophic cell line is based on the 293T cell line, which is a human embryonic kidney (HEK) cell line transformed with adenovirus E1a and carrying a temperature sensitive T antigen co-selected with neomycin. These cells were a kind gift from Dr. Richard Darley [Department of Haematology, Cardiff University, Cardiff, U.K.] and had previously been produced by Dr. G. P. Nolan [Department of Molecular Pharmacology, Stanford University, CA]. The phoenix-ampho cells were generated by stably transfecting HEK293T with a Moloney GagPol-IRES-CD8α construct with an RSV promoter and a pPGK hygromycin selectable marker. In addition, these cells have also been stably transfected with Moloney Amphoteric envelope gene driven by a CMV promoter and co-selected with the Diptheria toxin resistant gene. These cells were grown in complete DMEM in tissue culture flasks that had been batch tested to assess the tissue culture coating, thereby ensuring satisfactory adherence of the cells to the plastic.

2.4.3b Retrovirus production

A total of $7x10^6$ Phoenix cells were cultured in a T75 flask with complete DMEM 24 hours prior to transfection with plasmid DNA. Five minutes prior to transfection the media was replaced with 15ml of fresh media containing 25μM of chloroquine [Sigma Aldrich], which inhibits the degradation of DNA. A calcium phosphate transfection kit [Sigma Aldrich] was used according to the manufacturer's instructions to produce a calcium phosphate precipitate containing the desired DNA (as described for 2.4.2b). The following day the media was aspirated and replaced with 7.5ml of complete DMEM. Cells were then incubated at 33°C for 24 hours, followed by viral harvest. Viral supernatant was snap frozen and stored as 1ml aliquots in cryovials at -70°C. Any transient expression of the fluorescent proteins, GFP and YFP, during the production of virus was assessed by using a fluorescent microscope.

2.4.4 Transformed mouse cell lines

The mouse melanoma cell line, B16, was cultured in complete DMEM. Those cells that were destined for in vivo transfer were removed from tissue culture plastic by incubation with PBS, rather than with trypsin.

2.4.5 Production of mouse B16 melanoma cells expressing the NP68 epitope and luciferase gene

To enable in vivo studies of F5 $CD8^+$ T cell mediated tumour protection and regression, it was necessary to produce B16 melanoma cells that expressed the NP68 epitope. Expression of the luciferase gene by murine tumour cell lines potentially allows tumour development and regression to be monitored in vivo by using an IVIS® imaging system 2000 [Xenogen, Alameda, CA].

2.4.5a Infection of B16 cells with retrovirus

Retrovirus was produced by transfecting Phoenix cells with an expression plasmid encoding the NP68 epitope with GFP (as a fusion protein) or with an expression plasmid encoding the luciferase and YFP genes (separated by an IRES). A total of $2.5x10^5$ wild-type B16 cells were plated in T25 flasks 24 hours prior to infection. The media was removed and the B16 cells incubated at 37°C for 1 hour, in 1ml of complete media containing 10μg/ml of protamine sulphate [Sigma Aldrich], which is a cationic peptide that enhances the transduction of cells. The desired viral supernatant was then added to the flask, making a total of 2mls. Cells were incubated for 16-18 hours after which the media was replaced with fresh media and the cells allowed to rest for 5-6 hours. The process of incubation with protamine sulphate and subsequent viral infection was then repeated for a second time.

To generate B16 cells expressing both the NP68 epitope and luciferase, wild-type B16 cells were first infected with the retrovirus encoding for luciferase and YFP. The infected cells then went through a process of assessment and single cell sorting to produce monoclonal cell lines expressing luciferase. A monoclonal cell line expressing luciferase was then super-infected with a retrovirus encoding the NP68 epitope as a fusion protein with GFP.

2.4.5b Luciferase assay

In order to establish whether B16 cells infected with virus encoding the luciferase gene were indeed expressing the enzyme, the cells were assessed for YFP fluorescence as the luciferase and YFP gene are separated by an IRES. This was done by viewing the cells on a fluorescent microscope and analysing them on a FACSCalibur flow cytometer. In addition, a luciferase assay was performed to check for the expression of functional luciferase. A luciferase reporter assay was used according to the manufacturer's instructions [Promega]. Briefly, $1x10^6$, $5x10^5$, $2.5x10^5$ and $1.25x10^5$ B16 cells infected with the retrovirus encoding the luciferase gene and $1x10^6$ parental wild-type B16 cells were lysed on ice for 10 minutes, in 100µl of passive lysis buffer. Following cell lysis, 50µl of each lysate was transferred to a well of a white 96 well plate. The "stop and glo" reagent was then added to each well at 10 second intervals, with one well left as a blank containing 50µl of water and 50µl of the substrate. Luciferase activity was measured using a luminometer, with the data collected by Fluorostar software.

2.4.5c Single-cell sorting and clonal expansion of B16 cells

To separate cells expressing the luciferase gene a single cell sort was performed using a DakoCytomation high performance MoFlo cell sorter. Cells were separated based upon cell viability, as determined by forward and side scatter, and YFP fluorescence. The cells were sorted directly into the wells of a flat-bottomed 96 well plate and cultured for 4 weeks and

retested for luciferase activity as described above. A monoclonal B16 cell line expressing the luciferase gene was then selected to be infected with the retrovirus encoding the NP68 epitope as a fusion protein with GFP. This involved a process of infection (as described above), single cell sorting and assessment for GFP (flow cytometry) and NP68 expression (in vitro CTL assay).

B16 cells infected with virus encoding the NP68 epitope as a fusion protein with GFP were assessed for GFP expression under a fluorescent microscope at every stage during infection and by a FACSCalibur cell cytometer once the second round of infections was completed. The infected B16 cells were then single cell sorted using a DakoCytomation high performance MoFlo cell sorter. Cells were selected based upon cell viability, as determined by forward and side scatter, and GFP fluorescence. The GFP gate was set above the autofluorescence seen for the parental B16 cells. In addition to the above parameters, wild-type B16 cells infected with the retrovirus encoding the NP68/GFP were also sorted based on pulse-width, to ensure that only single cells were positively sorted. This additional parameter was not applied when sorting the B16 Luc/YFP cells that had been infected with the retrovirus encoding NP68/GFP. Wild-type and the B16 Luc/YFP B16 cells infected with the retrovirus encoding the NP68/GFP were sorted into the wells of flat-bottomed 96 well plate. In addition, $1x10^3$ cells of the wild-type NP68/GFP cells were sorted into the same well to give a polyclonal population. The monoclonal cell lines were transferred from 96 well to 24 well plate when a visible cluster of cells could be seen under the light microscope. As each clone reached 70% to 80% confluency, they were progressively moved from the 24 well plates to 6 well plates, T25 flasks and finally T75 flasks, at which point further analysis was performed and stocks prepared for freezing. The polyclonal population was transferred directly to T75 flasks, and allowed to reach 70% to 80% confluency before further analysis and preparation of stocks for freezing.

2.4.5d Assessing GFP expression of monoclonal B16 cell lines

The next step in the process of generating the transgenic B16 GFP/NP and B16 Luc/YFP/GFP/NP cells was to assess for GFP fluorescence by flow cytometry. The GFP fluorescence was assessed by overlaying histogram plots using FloJo software. For the B16 GFP/NP cells, the autofluorescence from wild-type B16 cells was used as a comparative control. For the B16 Luc/YFP/GFP/NP cells, the autofluorescence from both wild-type B16 cells and fluorescence from B16 Luc/YFP cells were used as a control. As a population of B16 GFP/NP cells was already available prior to the generation of B16 Luc/YFP/GFP/NP cells they were also used as controls. The Luc/YFP/GFP/NP and GFP/NP cells were utilised in an in vitro CTL assays to establish whether the NP68 epitope was being presented at the surface of the cells by MHC class I molecules (as described in 2.8.3). For the B16 Luc/YFP/GFP/NP cells the expression of the luciferase gene was verified for a final time by performing a luciferase reporter assay as described in 2.4.5b, with $6x10^4$ cells used for each reaction. The controls included the parental B16 luc/YFP cells, wild-type B16 cells and also B16 GFP/NP cells.

2.4.6 Primary mouse cell cultures

2.4.6a Generation of dendritic cells

Mouse dendritic cells were produced from bone marrow pre-cursor cells by culturing them with mouse GM-CSF supernatant produced from a cell line (see 2.4.2c) or commercially available GM-CSF [Sigma]. Bone marrow was harvested from adult female C57BL/6J mice and cultured in 10mls of media supplemented with 2% GM-CSF supernatant or 20ng/ml of commercially available GM-CSF. Cells were cultured in bacteria grade petri-dishes with 5-$6x10^6$ cells seeded on each plate. On day 3 or 4 of culture, 10mls of media containing 1% GM-CSF supernatant or 10ng/ml of commercial GM-CSF was added to the cells. On day 6 or 7 of culture, half of the media was removed from the dish and cells collected by

centrifugation at 1500rpm for 4 minutes. Cells were then resuspended in 10mls of fresh media containing 1% GM-CSF supernatant or 10ng/ml of commercial GM-CSF, which was then added back to the dishes. Cells were matured on days 10, 11 or 12 as desired, by the addition of 1μg/ml of lipopolysaccharide (LPS) [Sigma] to the cultures for 24 hours prior to harvest. The process of producing dendritic cells was assessed by various methods; including their ability to present NP68 peptide in both an in vivo and in vitro setting. The proportion of cells expressing the dendritic cell marker, $CD11c^+$, was determined at the start and end points of culture by flow cytometry. In addition, the proportion of cells that expressed the costimulatory molecule, CD86, prior to and after maturation with LPS was also assessed by flow cytometry.

2.4.6b Producing mouse $CD8^+$ F5 T cell blasts and their subsequent culture

The lymph nodes from motheaten and control F5 mice were harvested and a single cell suspension prepared (see 2.6.1a). In order to activate the $CD8^+$ F5 T cells, spleens were taken from adult C57BL/6J mice, irradiated at 1700 centigrays (cGy), homogenised and then pulsed with 5μM NP68 peptide for 1 hour at 37°C. A total of $3x10^6$ lymphocytes were co-cultured in 5mls of complete DMEM with $30x10^6$ NP68 peptide-pulsed splenocytes for 48 hours in six-well plates. The cells were then collected, washed twice and returned to flasks containing 20mls of complete DMEM for each well harvested and supplemented with 360 IU/ml of rIL-2. Cells were then grown for a further 3-4 days before harvesting. In order to remove cellular debris and dead cells, the cells were resuspended in 30mls of ice cold HBSS and 5mls of foetal calf serum layered beneath them. This was followed by centrifugation at 1300rpm for 4 minutes at 4°C and two further washes in ice cold HBSS.

2.4.7 Cryopreservation of cell lines

Cells were removed from tissue culture and washed with HBSS by centrifugation at 1400rpm for 4 minutes at 4°C. Cells were resuspended in freezing buffer (90% FCS and 10% DMSO [Sigma]) to give 0.5-2x10^6 cells per ml, and 1ml aliquots dispensed in to cryo-vials. The cryo-vials were placed in a Nalgene 5100 cryo freezing container [Merc Laboratory Supplies, Dorset, U.K.] for 24 hours at -70°C before being transferred to liquid nitrogen. Cells were removed from cryopreservation by thawing rapidly at 37°C (water-bath) and then washing in HBSS by centrifugation at 1500rpm for 5 minutes at 4°C, before being placed in culture.

2.5 Animals

2.5.1 Husbandry

All mice were generated in house at the Biomedical Services Unit (BSU) located at the School of Medicine, Heath Park, Cardiff University, under project license numbers 30/2266 and 30/2125. Stock mice were kept in groups of between 5-10 animals per cage and breeding animals maintained as harems, with typically 1 male to 3 females. Mice were provided a diet of standard mouse chow and sunflower seeds, with water *ad libitum*. Mice were maintained in rooms with a temperature range of 18-22°C with 12 hour light-dark cycles. Mice were kept under pathogen free conditions in cages contained within an isolator or Scantainer Plus unit [Scanbur, Copenhagen]. Alternatively, mice were housed in cages covered with a filter membrane.

2.5.2 Breeding of Motheaten Mice expressing the MHC class I restricted TCR, F5

Motheaten (me/me) mice lack expression of the SHP-1 protein and due to their early mortality were generated from the breeding of mice heterozygous at the motheaten locus

(me/+). The motheaten mice were used between the ages of 7 and 14 days, depending upon their health status.

In order to perform experiments using $CD8^+$ T cells from both me/me and control mice (me/+ and +/+) in an antigenic context, a H-$2D^b$ restricted αβTCR transgene, named F5, that recognises a nonamer peptide (NP68) from influenza virus A/NT/60/68 nucleoprotein was introduced into the motheaten genetic background. Briefly, C57BL/10 mice expressing the F5 transgene were obtained from Dr. D. Kioussis (NIMR, Mill Hill, London) and bred with C57BL/6J me/+ mice, which were supplied by Dr. L. Shultz [Jackson Laboratory, Bar Harbor, Maine]. Subsequently, mice from the inter alia matings of the resulting F1 offspring, which were homozygous for the F5 transgene, were maintained as a breeding colony heterozygous at the motheaten locus. Male mice produced from this colony, with the genotype $F5^{hom}$me/+ were mated with female C57BL/6J me/+ mice, to produce me/me, me/+ and wild-type (+/+) mice that were hemizygous (hem) for the F5 αβTCR transgene.

2.5.3 Genotyping of motheaten mice

Mice heterozygous at the motheaten locus were genotyped by performing PCR using reverse primers complementary to DNA sequences in intron 3 of the SHP-1 gene. The primers [Invitrogen] were 5'-TCC CTG GGA GCT TCC TGG CTC-3' and 5'-TAG GCA GCA GGA ACC CTG CAG-3', which amplify a genomic fragment of 738bp. Samples of DNA were obtained by digesting small sections of tail tissue in PCR lysis buffer (0.1M Tris, pH8.3, 2.5mM Magnesium Chloride hexahydrate, 50mM Potassium chloride, 0.45% v/v Nonidet P40, 0.45% v/v Tween 20 and 0.1ng/ml Gelatin) containing proteinase K (100μg/ml) at 56°C for 16-24 hours. The proteinase K was then inactivated by heating the samples at 96°C for 10 minutes on a Techne PHC-3 thermal cycler [Techne, Oxford, U.K.]. Samples were microfuged at 13000rpm for 5 minutes to sediment tissue material. The PCR reaction buffer contained

20U/ml DyNAzyme EXT [Finnzymes, Finland], 2.5mM of each dNTP [Invitrogen], 10X DyNAzyme EXT buffer with 1.5mM $MgCl_2$ [Finnzymes] and the primers, with 45µl being used for every 5µl of DNA. The PCR reaction was performed on a Hybaid Omn-E [Hybaid Limited, Basingstoke, U.K.] .

The samples were then digested with 20U/ml of Taq 1 restriction endonuclease [New England Biolab, Hitchin, U.K.], for one hour at 65°C on a Hybaid Omn-E [Hybaid]. This restricts the DNA at a restriction site that is absent at the me/me locus, thereby enabling me/+ and +/+ mice to be identified. After digestion, 20µl of each sample was loaded onto a 1% agarose gel containing ethidium bromide (0.4µg/ml) with 4µl of loading buffer (3.6mM Bromophenol Blue and 1.2M Sucrose), and run at 120 Volts for 45 minutes. In addition, 1µl of 1Kb Plus DNA ladder [Invitrogen] was also loaded onto the gel.

2.5.4 Other genetic backgrounds

Mice lacking expression of the recombinase associated gene -1 (Rag-$1^{-/-}$) were used throughout the study as lymphopenic recipient mice. They were maintained under sterile conditions in cages housed within an isolator.

2.6 In vivo methods

All experiments were performed in strict accordance with the Animals Scientific Procedures Act of 1986. They were performed in the BSU, under project license numbers 30/2266 and 30/2125 and personal license number 30/6944.

2.6.1 Harvesting and preparation of mouse tissue

Typically, mice were killed by asphyxiation in a rising concentration of CO_2, followed by cervical dislocation. Unless otherwise stated, the single cell suspensions prepared from

tissue were filtered and washed twice in ice cold HBSS, by centrifugation at 1500rpm for 4 minutes at 4°C. Viable cells were counted by trypan blue exclusion.

2.6.1a Lymph nodes

Lymph nodes (inguinal, mesenteric, axial, brachial, popliteal, and sub-mandibular) were used as a source of lymphocytes and $CD8^+$ T cells. In addition, adoptively transferred cells were retrieved from the lymph nodes for analysis. After excision, a single cell suspension was created by applying 10 strokes of a Jencons unifrom grade B.24 tissue homogeniser followed by filtering and washing.

2.6.1b Mesenteric lymph nodes

The mesenteric lymph nodes were excised from the gut and placed in the well of a 24 well plate and covered with 2mls of HBSS. The flat end of a plunger from a 2ml syringe was used to gently homogenise the lymph nodes. The suspension was taken up in 10mls of HBSS and filtered into a 50ml falcon tube, with the syringe plunger being used gently to assist the passing of the single cell suspension through the filter. The cells were then washed with ice cold HBSS.

2.6.1c Peyer's patches

Peyer's patches are lymphoid clusters found along the length of the small intestine and were used as a target site for migrating T cells. The small intestine was removed from the mouse and flushed with cold PBS by using a 10ml syringe and a blunted 19G needle. A rigid piece of plastic was placed through the lumen of the small intestine, which was gathered at one end of the plastic to aid dissection. The intestine was then moved back along the plastic rod and the Peyer's patches excised using a pair of curved scissors. The tissue was then processed in the same manner as for lymph nodes.

2.6.1d Spleens

Spleens were used as source of cells to generate target, reference and feeder cells. In addition, adoptively transferred cells were often retrieved from the spleens of recipient mice. Once excised, spleens were homogenised in HBSS with 2-5 gentle strokes of a Jencons tissue homogeniser. The single cell suspensions were filtered and then washed, by centrifugation at 1300rpm for 4 minutes at 4°C. The splenocyte pellet from each spleen was covered in 1ml of red blood cell lysis buffer [Sigma] and left undisturbed for 5 minutes. The splenocyte pellet was then agitated by gentle pipetting to give a single cell suspension followed by a further 2 minutes of lysis. The single cell preparation was made up to 10mls with HBSS and filtered prior to centrifugation at 1300rpm for 4 minutes at 4°C. If the splenocytes were to be used as feeder cells the process of homogenisation was performed in complete media and no subsequent washing or red blood cell lysis was required.

2.6.1e Lungs

The lungs of mice receiving B16 melanoma cells were taken as they represented the site of B16 cell growth following their intravenous transfer. The lungs were removed carefully from the mouse and blotted on tissue to remove excess blood. In order to generate a single cell suspension, the lungs were placed in the well of a 24 well plate and covered with 2mls of HBSS. The flat end of a plunger from a 2ml syringe was used to gently homogenise the lung. The suspension was taken up in 10mls of HBSS and filtered into a 50ml falcon tube, with the syringe plunger being used gently to assist the passing of the single cell suspension through the filter. If red blood cells were evident after the first wash, 1ml of red blood cell lysis buffer was added for 5 minutes whilst pipetting gently, followed by washing.

2.6.1f Blood

Blood was taken to retrieve adoptively transferred cells T cells for analysis. Firstly, the mouse was restrained and the tip of the tail sprayed with ethyl chloride BP [Acorus Therapeutics Limited, Durham, U.K.] and allowed to numb. A small section of the tail was removed at its tip and 30-50µl of blood taken by aspirating with a Gilson P200 pipette fitted with a small pipette tip. The blood was mixed immediately with an approximately equal volume of heparin [CP Pharmaceuticals Ltd, Wrexham]. If blood was required at the end of an experiment, it was taken via a cardiac puncture. The mouse was placed in a chamber, which was subsequently filled with anaesthetic gas (isofluorane) using oxygen as a carrier gas. Once the mouse showed signs of anaesthesia it was transferred to a face mask with a lower concentration of anaesthetic gas. A 28G needle was inserted below the sternum and a cardiac withdrawal of blood performed with a syringe containing 200µl of heparin. The blood was then made up to 5mls with HBSS and washed. The cell pellet was resuspended in red blood cell lysis buffer for 5 minutes, followed by washing and centrifugation. If necessary, the red blood cell lysis was repeated a second time, for 1-2 minutes.

2.6.1g Bone marrow

Bone marrow precursor cells were required for culture in GM-CSF to produce dendritic cells. Bone marrow was taken from the femur and tibia of adult C57BL/6 female mice. A scalpel was used to cut away the majority of skin, muscle and connective tissue from the hind legs of a mouse, followed by the gentle removal of the leg from the hip socket by dissection with a small pair of scissors. Once removed, the soft tissue was further removed by rubbing the leg bones between tissue-paper. The femur was removed from the tibia by gentle manipulation of the knee joint, ensuring the bones remain intact at all times. The bones were dipped in 70% ethanol for 1 minute and then placed in ice cold PBS. The bone marrow

was extracted by cutting both ends of the bone and flushing with ice cold PBS from a syringe fitted with 21G needle. The bone marrow was dispersed by repeated pipetting and then filtered before washing.

2.6.1h Ovaries

Following Vaccinia virus transfer to the peritoneal cavity of mice the ovaries become infected and are therefore a potential site for activated $CD8^+$ T cell migration. To retrieve adoptively transferred T cells from Vaccinia virus infected mice, the ovaries were removed from the abdominal cavity and prepared as described above for lymph nodes.

2.6.1i Gut tissue

The gastrointestinal tract was excised in one piece extending from the stomach (proximal) to the anus (distal) and placed in cold PBS. The gut was then placed on a dampened tissue and kept moist with PBS at all times. Cross sections (approximately 5mm in length) were taken from the caecum, small and large intestines and placed in either formalin ready for transfer in to paraffin wax.

2.6.2 Immunomagnetic separation of $CD8^+$ T cells

Mouse $CD8^+$ T cells were separated from single cell suspensions of lymphocytes using CD8 antibody conjugated magnetic beads and MACS MS+ immunomagentic separation columns [Miltenyi Biotec, Surrey, U.K]. Cells were washed and suspended at a density of $1x10^7$ cells per 90µl of ice cold sorting buffer (PBS supplemented with 2mM EDTA and 0.5% BSA), followed by the addition 10µl of magnetic beads per 1 $x10^7$ cells, and incubation at 4°C for 15 minutes. MACS MS+ separation columns were attached to MiniMACS magnets and placed on a MiniMACS stand and primed once with 1ml of sorting buffer. The magnetically labelled cells were resuspended in sorting buffer and centrifuged at 1100rpm for 10 minutes, and

then placed onto the column in 500µl of sorting buffer. The column was washed three times with 500µl of sorting buffer and the run-through collected as the negative fraction. The columns were then removed from the magnet and the positive fraction eluted by applying 1ml of sorting buffer to the column and flushing the cells out by using a column plunger.

2.6.3 Adoptive cell transfers

A number of different cell types were adoptively transferred to recipient mice; including naive $CD8^+$ F5 T cells directly from donor mice, in vitro activated and expanded $CD8^+$ F5 T cells, B16 melanoma cells, splenocytes and in vitro generated dendritic cells. The route of administration depended upon the role and type of cell being transferred. All procedures involving the transfer of cells and priming of mice were performed under sterile conditions in a class 2 microflow advanced bio-safety cabinet.

2.6.3a Donor mice

Naive $CD8^+$ F5 T cells were purified from me/me, me/+ and +/+ mice by immunomagnetic separation. Splenocytes were prepared from adult C57BL/6 female or male mice.

2.6.3b Recipient mice

Lymphopenic mice were used in order to transfer and preferentially prime $CD8^+$ F5 T cells without priming endogenous $CD8^+$ T cells. Typically, female $Rag1^{-/-}$ mice or sub-lethally irradiated female C57BL/6J mice were used for this purpose. For lymphodepletion by irradiation, mice were exposed to 650cGy of irradiation in a gamma cell irradiator, whilst being held securely within a purpose built restrainer. Once irradiated, mice were moved to scantainer cages, with a double positive pressure operating setting, ensuring mice received a constant supply of filtered air. Mice were usually used within 1-2 days of being irradiated.

2.6.3c Intravenous transfer of cells

Naive $CD8^+$ F5 T Cells and splenocytes were prepared directly from donor mice and adoptively transferred, via a tail vein, to recipient mice in 200µl of HBSS using a sterile 29G insulin ultra comfort syringe. $CD8^+$ T cells and B16 melanoma cells that had been taken from tissue culture were transferred in the same manner, importantly ensuring that the cells had been washed, filtered and kept at 4°C at all times prior to transfer. In order to dilate the blood vessels ready for intravenous transfer, mice were placed in a heating chamber set at 37°C for up to an hour prior to injection. Mice were restrained in a purpose built rodent holder to provide easy access to the tail, and the tail wiped with a steret at the injection site prior to transfer. Once injected, the needle was removed from the vein while applying gentle pressure at the injection site to avoid loss of sample from the vein due to back-pressure, and also to stem any bleeding.

2.6.3d Peritoneal transfer of cells

Dendritic cells were administered to mice via the peritoneal cavity in 100µl of HBSS in a 28G insulin syringe. Mice were manually restrained and held at a 45 degree angle to position the head downwards and away from the handler, thereby reducing the possibility of the needle contacting organs during injection. The abdomen of the mouse was wiped with a steret prior to transfer of the cells and the needle penetrated at a sufficient depth to enter the peritoneal cavity.

2.6.3e Subcutaneous transfer of cells

B16 cells were also transferred subcutaneously in 100µl of HBSS using a 29G insulin ultra comfort syringe. The fur in the inguinal region on the underside of the mice was wiped with a sterile steret. The tip of the needle was used to part the hair and reveal the skin. The

needle was inserted subcutaneously to cover the bevel and the cells transferred, ensuring a bleb appeared beneath the skin with no leakage of cells.

2.6.4 In vivo antigenic stimulation of naive and memory CD8$^+$ F5 T cells

Concomitantly with adoptive transfer of naive CD8$^+$ F5 T cells, mice were primed with the NP68 peptide, which was either presented by adoptively transferred in vitro generated, matured and peptide pulsed dendritic cells, or by endogenous antigen presenting cells, through the subcutaneous administration of NP68 peptide in IFA or intranasal infection with influenza A virus. This process was sometimes repeated in the same mouse to elicit a memory T cell response.

2.6.4a Preparation of in vitro generated dendritic cells

Matured dendritic cells were taken from culture and washed in HBSS. The cells were then pulsed with 5µM NP68 peptide for one hour at 37°C in 5% FCS DMEM. The cells were collected and washed once before being suspended to give the desired number of cells per mouse in 100µl of HBSS. The cells were then transferred into the peritoneal cavity (see 2.6.3d).

2.6.4b Preparation and administration of NP68 peptide in IFA

Mice were primed with 100µg of NP68 peptide in 100µl of incomplete Freund's adjuvant, with a final volume made to 200µl with PBS. The IFA and PBS were mixed and left on ice for an hour to ensure complete mixture. Subsequent to adding the peptide, the mixture was vortexed and 200µl drawn up in to a 1ml syringe via a 19G needle. Once aspirated, the 19G was replaced with a 26G needle and kept on ice until injection. Mice were manually restrained and the site of injection wiped with a sterile steret. The IFA/NP68 was transferred subcutaneously, adjacent to the hind leg on the underside of the mouse. The needle was

inserted to sufficiently cover the bevel, the mixture injected steadily and the needle removed carefully to avoid loss of IFA/NP68 from the bolus that had formed. In some experiments it was necessary to give two doses of IFA/NP68 at different times, therefore the second dose of IFA/peptide was injected on the contra-lateral side of the mouse.

2.6.4c Infection with Influenza A virus

The mice were manually restrained and positioned on their back. The virus was administered drop-wise on to the nasal openings of the mouse via a Gilson pipette boy fitted with a small pipette tip, ensuring each drop had been inhaled. The mice were maintained in scantainer cages with a negative flow of air in order to comply with health and safety regulations.

2.6.5 The provision of target cells

In order to assess the $CD8^+$ T cell response, mice received cell populations that acted as targets for the cytotoxic T lymphocytes. These were either NP68 peptide-pulsed B16 cells or splenocytes cells, or B16 cells that expressed the NP68 epitope.

2.6.5a The generation of splenocyte target and reference cells for in vivo transfer

Spleens were harvested from adult C57BL/6J mice, with typically one spleen providing a sufficient number of cells for two recipient mice. Target cells were generated by pulsing splenocytes with 5μM NP68 peptide for 1 hour in complete DMEM containing 5% FCS, at 37°C. Reference splenocytes were treated in the same manner but left unpulsed. The splenocytes were then washed once with HBSS and the target cells labelled with 0.2μM CFSE and the reference cells labelled with 2μM CFSE (see 2.2.2b). Following labelling, the cells were counted by trypan exclusion and the same number of each cell type combined to give an approximate 1:1 ratio of target to reference cells. Prior to the combination of the bulk of the cells, the 1:1 ratio of targets to reference cells was often confirmed by flow cytometry.

Aliquots containing the same cell number from each cell population were combined and analysed. A histogram displaying the CFSE peaks was gated on viable cells, as determined by forward and side scatter, to reveal the proportion of cells in each CFSE labelled population. If an unsatisfactory ratio was seen, adjusted aliquots were then combined and run through the flow cytometer to confirm the desired 1:1 ratio. If necessary, the adjustment was then applied to the bulk of the cells. Once combined the cells were kept on ice until required.

2.6.5b The generation of B16 cell targets

Target B16 cells that were pulsed with NP68 were generated in the same manner as for splenocytes (see 2.6.5a). The production of B16 cells expressing the NP68 epitope is described in 2.4.5.

2.7 In vivo assays

2.7.1 $CD8^+$ F5 T cell expansion assay

Two protocols were utilised to gauge the in vivo expansion of $CD8^+$ T cells, whereby both involved the transfer of 2-3x10^6 $CD8^+$ F5 T cells from motheaten and control mice to recipient mice. The mice were primed with NP68 in IFA followed by seven days of in vivo expansion, after which the spleens were harvested.

Protocol 1: The recipient mice were irradiated and of the strain C57BL/6J. Splenocytes prepared from the spleens of recipient mice were stained with an anti-$CD8^{PE}$ antibody alone or in combination with anti-$Thy1.2^{FITC}$ antibody. The latter is an allelic marker which is expressed in different forms by the donor (Thy1.2) and recipient mice (Thy1.1), and therefore offered a way of further distinguishing donor from recipient cells during cell cytometry. Dot plots were generated and a lymphocyte gate defined based upon a forward and side scatter profile. The proportion of $CD8^+$ cells was revealed by applying the

lymphocyte gate to a dot plot displaying PE fluorescence (CD8) versus side scatter. Alternatively, PE fluorescence (CD8) was displayed versus FITC (Thy1.2). The CD8 gates were defined using samples from mice that received no T cells and also unstained samples.

Protocol 2: $Rag1^{-/-}$ recipient mice were used. Once the spleens had been harvested, $5x10^5$ CFSE labelled splenocytes were added to the intact spleens prior to processing and cell counting. The splenocytes were then labelled with anti-$CD8^{PE}$ antibody and analysed by flow cytometry. Dot plots were generated displaying CFSE (reference cells) and PE fluorescence (CD8) by gating on a lymphocyte population as determined by forward and side scatter. A defined number of CFSE labelled events was acquired, and the number of $CD8^+CFSE^-$ events were then expressed as a percentage of the $CFSE^+$ reference population.

2.7.2 CTL assays

2.7.2a Primary $CD8^+$ T cell response

Once purified by immunomagnetic separation, $2.5\text{-}3.5x10^6$ naive motheaten and control $CD8^+$ F5 T cells were transferred intravenously to sub-lethally irradiated C57BL/6J mice. Concomitant with T cell transfer, mice were primed by the peritoneal transfer of $3\text{-}4x10^6$ matured and NP68 peptide-pulsed dendritic cells or by the subcutaneous injection of NP68 peptide in IFA. Alternatively, mice were primed with influenza A virus four days prior to T cell transfer. Six days post T cell transfer, $10x10^6$ splenocyte target cells (pulsed with 5μM NP68 peptide) labelled with 0.2μM CFSE and $10x10^6$ splenocyte reference cells labelled with 2μM CFSE (see 2.2.2b) were co-transferred to each mouse, including control mice that did not receive any T cells. Twenty-four hours post transfer, the spleens were harvested, homogenised and the red blood cells lysed ready for analysis by flow cytometry. Histograms were generated by electronically gating on both viable cells, as determined by forward and side scatter, and $CFSE^+$ cells, with the necessary number of events acquired to give a

minimum of 200 cell counts (as displayed on the y-axis of the histogram) of the reference cell peak (CFSE high). Gates were set for each peak to reveal the percentage of cells residing in each peak. The data from the control mice and the equation shown below were used to work out the percent-specific lysis, allowing for any deviation from the anticipated 1:1 ratio of target to reference cells,

Percent-specific lysis = 100 – (((% of target cells with T cells / % of reference cells with T cells) / (% of target cells with no T cells / % of reference cells with no T cells)) x 100).

2.7.2b Memory $CD8^+$ T cell response

Between 1-3x10^6 purified naive control or motheaten $CD8^+$ F5 T cells were transferred to recipient mice, which were primed with either NP68 peptide-pulsed dendritic cells (3-4 x10^6) or NP68 in IFA. Six weeks post transfer, mice were primed for a second time with either NP68 peptide pulse dendritic cells or NP68 in IFA, as described for the initial priming. Seven days post recall, mice received 10x10^6 of CFSE labelled target and reference splenocytes. Mice were then sacrificed and the spleens analysed as described for the primary CTL assay.

In total, four protocols were used to assess the memory $CD8^+$ T cells response. These differed in three aspects of the assay; how the T cells were initially primed, the type of recipient to which the T cells were transferred to, and how the T cells were recalled to elicit a memory T cell response.

Protocol numbers 1, 2 and 3 utilised Rag $1^{-/-}$ mice as the recipient mice, but differed with respect to how the T cells were initially primed and then recalled six weeks later. Protocol 1 utilised IFA/NP68 for both primings, protocol 2 used IFA/NP68 for the initial priming and DCs/NP68 for the recall priming, and protocol 3, which used DCs/NP68 for both.

Protocol 4 utilised irradiated C57BL/6J mice, which were primed with NP68 in IFA. Eight weeks post transfer and priming, mice were primed for a second time with NP68 peptide-pulsed dendritic cells. A two-tailed Mann-Whitney nonparametric test, with 95% confidence intervals was applied to generate p values.

2.7.2c Effector memory responses

To further dissect $CD8^+$ T cell memory responses, refinements were made to the above protocols. Mice received T cells and were primed as for protocol 1 above, with some mice receiving a second dose of peptide to recall the memory response. Other mice were not primed for a second time but did go on to receive the target and reference cell populations in order to specifically look at the effector memory CD8 T cell response.

In other experiments, $3x10^6$ or $5x10^6$ in vitro activated and expanded control or motheaten $CD8^+$ F5 T cells were transferred to irradiated C57BL/6J recipient mice. Six weeks post transfer the mice were primed with NP68 peptide in IFA and the assay continued as described above.

2.7.3 In vivo tumour assays

2.7.3a Detecting adoptively transferred B16 cells by flow cytometry

To study the tumour protective capabilities of control and motheaten $CD8^+$ F5 T cells, experiments were performed that involved transferring B16 cells labelled with intracellular dyes. Two populations of cells that had been labelled with different dyes (DDAO and CFSE) or different concentrations of CFSE were transferred to the same recipient mouse. The cells were partnered as follows with the total number of cells transferred shown in brackets; 0.2/2μM CFSE ($1.2x10^6$), 10μM DDAO/2μM CFSE ($2.5x10^5$), 0.2/3μM CFSE ($8x10^5$) and 0.5/4μM CFSE ($8x10^5$). The mice were sacrificed twenty-four hours post transfer and the

spleens and lungs taken for flow cytometry. Mice that received no B16 cells were used to define the gates for DDAO or CFSE fluorescence, by gating above the autofluorescence present in these mice. Dot plots were generated to show DDAO or CFSE fluorescence against side scatter or DDAO and CFSE on the same plot.

2.7.3b Tumour protection assay

This assay involved transferring control and motheaten $CD8^+$ F5 T cells prior to the transfer of B16 cells expressing the NP68 epitope. Groups of 2 to7 sub-lethally irradiated C57BL/6J mice received either $1x10^4$, $2x10^4$, $3.2x10^4$, $5x10^4$, $1x10^5$, $1x10^6$ or $3x10^6$ purified naive $CD8^+$ F5 T cells intravenously. At the same time mice were primed subcutaneously with NP68 peptide in IFA. Two, four or seven days post T cell transfer, mice received an intravenous infusion of either $1x10^5$ or $2.5x10^5$ B16 cells expressing the NP68 epitope. Two weeks post B16 cell transfer mice were sacrificed and the tumour nodules within the lungs enumerated. In one experiment mice were weighed at various time points over the duration of the assay. In addition, blood was taken at defined time points during the assay, and the lungs processed following sacrifice, in order to study the adoptively transferred $CD8^+$ T cells. In two experiments, the lungs of the mice were fixed in 2% paraformaldehyde (equal volumes of 4% paraformaldehyde and cell wash) prior to being photographed, courtesy of the Medical Illustration Department [School of Medicine, Cardiff University]. When enumerating the nodules of mice, a limit of detection was set at 425 nodules, as nodule numbers above this value could not be enumerated accurately. A two-tailed Mann-Whitney nonparametric test, with a 95% confidence interval was applied to generate p values.

2.7.3c Tumour regression assay

Recipient mice were injected subcutaneously with $1x10^5$ B16 cells expressing the NP68 epitope. The developing tumours were assessed regularly by wetting the tumour with water

and measuring the perpendicular diameters with callipers. Two weeks post tumour implantation, mice with similar sized tumours were irradiated and received an intravenous transfer of $1x10^6$ naive control or motheaten $CD8^+$ F5 T cells. Mice were primed subcutaneously at the same time with NP68 peptide in IFA, on the contra lateral side of the mouse to tumour growth. The tumour was measured for a further 10 days, at which point the mice were sacrificed. Data was expressed as an mean of the perpendicular tumour diameters for each mouse against the time points at which the data was collected.

2.7.3d Tumour protection versus enhancement

These assays utilised either irradiated C57BL/6 mice or C57BL/6 $F5^{Hom}$ mice and were prepared in the same manner as described above, but with some exceptions; the number of T cells transferred was $3x10^6$ or $1.8x10^6$ and the corresponding number of B16 cells transferred was $1x10^5$ or $1.75x10^5$. No adoptive $CD8^+$ T cell transfer was performed when C57BL/6 $F5^{Hom}$ mice were used as recipients. As before, a two-tailed Mann-Whitney nonparametric test, with a 95% confidence interval was applied to generate p values.

2.7.4 T cell migration studies

In order to study T cell migration, differentially labelled motheaten and control activated $CD8^+$ F5 T cells were transferred to the same mouse. This was followed by their retrieval from target tissue 16-24 hours post transfer. Cells were labelled with either 0.5μM CFSE or 10μM DDAO, and between $20x10^6$ and $70x10^6$ total cells were transferred intravenously to irradiated recipient mice. It was important to ensure a single cell suspension was being transferred and that the cells were kept on ice at all times prior to transfer. The dyes used to label the cell population (motheaten or control) were alternated between each cell type to eliminate the possibility of any dye specific effects on the T cells being labelled.

2.7.4a Migration to the Peyer's patches

To induce tissue specific homing of T cells to the small intestine, T cells were activated and expanded in the presence of 10nM retinoic acid for 4-5 days prior to intravenous transfer.

2.7.4b Vaccinia infected ovaries

Mice were irradiated and infected with $2x10^6$ plaque forming units of recombinant vaccinia virus expressing the NP68 epitope by injection into the peritoneal cavity. Mice received the T cell infusions 4 days post Vaccinia infection.

2.7.5 T cell infiltration into the bowel

A total of $1x10^6$ $CD8^+$ T cells from control C57BL/6 $F5^{hem}$ mice were transferred to female $Rag1^{-/-}$ mice. A group of mice that received T cells also received a subcutaneous injection of NP68 peptide in IFA. Control mice did not receive T cells or NP68. The mice were weighed at regular intervals over the duration of the assay on a bench-top balance under sterile conditions. The mice were sacrificed 8 weeks post T cells transfer and their spleens, mesenteric lymph nodes, small and large intestines taken for analysis.

2.7.5a Histological characterisation of gut tissue

Gut sections were fixed in NB formaldehyde solution (NBFS) for 16-24 hours at 4°C. The tissue was then placed in an automated Shandon Tissue Processor and taken through serial dehydration cycles of ethanol and xylene (70% Alcohol (1 hour and 30mins), 90% Alcohol (1hour and 30mins), 100% Alcohol (1 hour), 100% Alcohol (1 hour), 100% Alcohol (1 hour), 100% Alcohol (1 hour), 100% Alcohol (1 hour), Xylene (1hour and 30mins at room temperature), Xylene (2 hours at 37° C), Xylene (2 hours at 45° C)), before being permeated with wax at 60°C (10% Wax (2 hours at 60° C), 50%Wax (1hour and 30mins at 60° C) 70% Wax (1hour and 30mins at 60° C), 100% Wax (1hour and 30mins at 60° C)). Tissue was then embedded in wax blocks using a Shandon Histocentre. Serial sections, of 7μm thickness,

were cut with a microtome and situated on superfrost microscope slides [Menzel-Glaser, Braunschweig, Germany].

2.7.5b Haematoxylin and eosin staining of gut tissue sections

The staining of paraffin sections was carried out in a well ventilated area, with all reagents contained in glass-topped staining dishes. After each stage involving deparaffinisation, haematoxylin staining, eosin staining and dehydration, the sections were washed in running tap water for 5 minutes followed by rinsing in dH_20.

The sections were deparaffinised by immersion in three changes of xylene, for 5 minutes each, followed by descending grades of alcohol (100% x 2, 90% and 70%), for 3 minutes in each. Sections were placed in Mayer's Haematoxylin [BD Laboratories] for 1.5 minutes and the stain intensified by placing the sections in Scott's tap water [Sigma] for 30 seconds. Sections were then stained in 1% eosin [Fisher] for 1 minute. Dehydration was achieved by placing the sections in ascending grades of alcohol (90% and 100% x 3) for 2-3 minutes, followed by 3 washes in xylene, for 5 minutes in each. Finally, sections were mounted in Ralmounts mounting media [BD laboratories] covered with a glass cover-slip and then incubated for 12-24 hours in a 45°C oven to set.

2.8 In vitro assays

2.8.1 CD107a assay

As the name suggest, lysosomal associated membrane protein-1 (LAMP-1, CD107a), is a molecule found on the membranes of lysosomes (Rohrer et al., 1996). CD107a appears at the cell surface when lysosomes of cytotoxic $CD8^+$ T cells fuse with the cell surface membrane in order to deploy their cytotoxic granules. CD107a can therefore be used as a measure of cytotoxic function. A total of $5x10^4$ in vitro activated and expanded $CD8^+$ F5 T

cells were placed in a U-bottomed 96well plate with B16 cells that had either been pulsed with 5μM NP68 or left unpulsed. The ratio of T to B16 cells was titrated (5:8, 5:4 and 5:2 for the first experiment and 1:40, 1:20, 1:10, 1:5, 2:5 and 1:1 for the second experiment) and performed in triplicate. T cells were also cultured without B16 cells. Each well contained 200μl of complete DMEM, 0.2μl of golgi-stop™ [BD Biosciences], which halts export of proteins from the golgi, and also 0.5μg of FITC conjugated anti-CD107a monoclonal antibody. Cells were spun at 1300rpm for 2 minutes at room temperature then incubated at 37°C for 4 hours. Cells were pelleted at 2000rpm for 3 minutes at 4°C followed by staining with anti-$CD8^{PE}$ antibody. Cells were analysed for CD107a expression by flow cytometry. Contour plots were generated by gating on viable $CD8^+$ cells, and the CD107a gate set by using the data from the wells that contained T cells and no B16 cells.

2.8.2 In vitro regulatory T cell assay

An in vitro protocol was used to look at the proliferation of control and motheaten $CD8^+$ F5 T cells in the presence or absence of regulatory T cells (Tregs). For optimisation of assay conditions anti-$CD3^{Bio}$ antibody coated (5μg/ml in PBS overnight at 4°C then 1 hour at 37°C prior to culture) or un-coated U-bottomed 96 well plates and anti-$CD3^{Bio}$ antibody coated flat-bottomed plates were used to culture T cells. Control $CD8^+$ F5 T cells were purified from lymph nodes and labelled with 2μM CFSE and cultured with or without irradiated splenocytes from $Rag1^{-/-}$ mice, with the number of T cells and splenocytes used per well as follows; $5x10^4/2x10^5$, $10x10^4/4x10^5$, $15x10^4/2x10^5$ and $15x10^4/6x10^5$. For the actual assay, $15x10^4$ CFSE labelled T cells were co-cultured with $2x10^5$ $Rag1^{-/-}$ splenocytes on anti-$CD3^{Bio}$ antibody coated U-bottomed plates. The Tregs were purified from the spleens of adult C57BL/6 mice based on CD4 and CD25 expression using immunomagnetic beads [Miltenyi Biotech]. Briefly, CD4 expressing T cells were selected first by depletion of non-$CD4^+$ cells using an anti-biotin antibody cocktail and anti-biotin microbeads. Subsequently, CD25

expressing CD4 cells were selected by labelling the cells with anti-$CD25^{PE}$ and anti-PE microbeads. The ratios of T cell to Tregs were as follows; 0:1, 1:10, 1:5, 1:2, 1:1, 2:1 and 4:1 with each condition performed once apart from the ratio of 0:1, which was performed in triplicate. T cells were also cultured in the absence of antibody, splenocytes and Tregs. For both the optimisation and final assay the cells were cultured for 72h at 37°C and once harvested, stained with anti-$CD8^{PE}$ antibody. During the analysis of flow cytometry data, histograms displaying CFSE were gated on viable $CD8^+$ cells. The T cells that had been cultured alone were used to define the undivided CFSE peak. For the optimisation data the undivided peak was used to give a proliferation gate, with the proportion of cells residing within this gate established for each condition. For the final assay, the undivided peak was used in conjunction with the proliferation tool of FloJo software to establish how many T cells from the original population had entered in to proliferation. This data was then used to work out the percentage inhibition using the equation below:

Percentage inhibition = 100 - ((proportion of T cells entering in to proliferation from the initial population in the presence of Tregs / proportion of T cells entering in to proliferation from the initial population in the absence of Tregs) x 100)

2.8.3 In vitro cytotoxicity assay

Two protocols were utilised to look at the killing of B16 cells. The first protocol was used to assess the degree of target cell killing by activated motheaten and control $CD8^+$ F5 T cells. The second protocol was used to establish whether B16 cells infected with a retrovirus encoding NP68/GFP were displaying NP68:MHC class I complexes.

Protocol 1: Wild-type B16 cells were removed from culture and either pulsed with 5μM NP68 peptide at 37°C, in complete media (5% FCS) for 1 hour, or left unpulsed. The cells were washed once with HBSS by centrifugation at 1400rpm for 4 minutes at 4°C.

Subsequently, the target cells that had been pulsed with NP68 peptide were labelled with 0.2μM CFSE and the reference B16 cells that had not been pulsed were labelled with 2μM CFSE. Following labelling, the cells were counted by trypan blue exclusion and $15x10^3$ of each placed in the wells of U-bottomed 96 well plates. Previously activated and expanded $CD8^+$ F5 T cells were added to each well to give the following T cell to B16 cell ratios: 1:2, 1:1, 3:2 and 2:1. The number of T cells added was based upon the total number of B16 cells present in each well. B16 cells were also cultured without T cells and an aliquot of T cells kept to aid analysis. Each condition was repeated in triplicate. Once the cells had been combined, the plate was spun at 1500rpm for 2 minutes then incubated at 37°C. After 4 hours, the cells were harvested by centrifugation and stained with anti-$CD8^{PE}$ antibody ready for analysis by flow cytometry. Histograms displaying CFSE were generated by gating on a $CFSE^+$, $CD8^-$ and viable cell population. Gates were set for each CFSE peak and the proportion of cells that resided in each gate established. The data from the wells where the B16 cells were cultured without T cells and the equation shown in 2.7.2a was used to calculate the percent-specific lysis for each condition.

Protocol 2: An equal number B16 GFP/NP cells and wild-type B16 cells were placed in the wells of either 96 well flat bottomed plates (total of $2x10^4$ B16 cells) or 24 well plates (total of $8x10^4$ B16 cells) and allowed to adhere to the plastic overnight. The media was removed and replaced with complete DMEM. Previously activated and expanded $CD8^+$ F5 T cells were placed in each well to give a $CD8^+$ T cell to B16 cell ratio of 2:1 ($4x10^4$ T cells for 96 well plates and $1.6x10^5$ T cells for 24 well plates). The B16 cells were also cultured in the absence of T cells. After 16 hours, the media was aspirated to remove dead or dying B16 cells along with the $CD8^+$ T cells, followed by 1 further wash. The remaining cells were incubated with trypsin for 5 minutes and washed ready for staining with anti-$CD8^{PE}$ antibody prior to analysis by flow cytometry. Histograms were generated to display GFP fluorescence by

gating on a viable $CD8^-$ cell population. Gates were set for each peak and proportion of GFP^+ cells (target cells) compared to the autofluorescence from the wild-type B16 cells (reference cells).

2.9 Silencing of SHP-1 expression using shRNA technology

2.9.1 Candidate siRNA sequences for SHP-1

A number of different online algorithms were used by James Hindley [Department of Medical Biochemistry and Immunology, Cardiff University] to identify siRNA target sites within the human SHP-1 transcript. The algorithms were performed with an integrated BLAST search to eliminate the possibility of non-specific targeting. Annotation of a map of the SHP-1 transcript sequence with the ten highest ranked target sites from each algorithm, allowed for the selection of the six most frequently identified potential target sites for cloning and functional testing.

2.9.1a Synthesis and annealing of the oligonucleotides

Oligonucleotides were synthesised for subcloning of the SHP-1 shRNA inserts in to the pTER+ vector. Each shRNA insert consisted of a 19 nucleotide (figure 2.1) and were flanked by overhanging Hind III and Bgl II restriction sites.

Complementary oligonucleotides were annealed in annealing buffer (100mM KAc, 2mM MgAc and 30 mM HEPES-KOH pH 7.4) by boiling for 5 minutes in a water bath, followed by cooling to room temperature.

1) 825

5'-GATCCCGGTGAATGCGGCTGACATTTTCAAGAGAAATGTCAGCCGCATTCACCTTTTTGGAAA-3'

2) 989

5'-GATCCCGCAAGAACCGCTACAAGAATTCAAGAGATTCTTGTAGCGGTTCTTGCTTTTTGGAAA-3'

3) 1112

5'-GATCCCGCCCTGATGAGAACGCTAATTCAAGAGATTAGCGTTCTCATCAGGGCTTTTTGGAAA-3'

4) 1236

5'-GATCCCGGAGAAAGGCCGGAACAAATTCAAGAGATTTGTTCCGGCCTTTCTCCTTTTTGGAAA-3'

5) 1341

5'-GATCCCATACAAACTCCGTACCTTATTCAAGAGATAAGGTACGGAGTTTGTATTTTTTGGAAA-3'

6) 1550

5'-GATCCCGCACAGGCACCATCATTGTTTCAAGAGAACAATGATGGTGCCTGTGCTTTTTGGAAA-3'

Figure 2.1 Synthesised shRNA sequences

Each shRNA consists of a siRNA sense sequence (blue, underlined), a loop sequence (red), a 19 nucleotide siRNA antisense sequence (blue) and five thymidines, which acts as a stop signal for RNA polymerase III. The number assigned to each sequence represents the first base of the 19 nucleotide target sequence.

2.9.1b Cloning annealed oligonucleotides into the pTER+ plasmid

Ligation reactions were used to transform competent *Escherichia Coli* strain, DH5α, using heat shock for 20 seconds at 37°C. Transformed bacteria were then grown without selection in 1 ml of LB medium for 1 hour to allow synthesis of plasmid-encoded antibiotic resistant proteins. An aliquot (100µl) of the culture was streaked on to LB agar plates containing 100µg/ml ampicillin and allowed to grow for 16 hours at 37°C. Untransformed cells were also cultured on ampicillin plates to ensure ideal selection conditions for the colonies that had been chosen. Colonies were picked from the agar plate and grown for 16-18 hours in 5mls of LB broth containing 100µg/ml of ampicillin. The plasmid was purified for each clone and the DNA quantitated using a spectrophotometer followed by sequencing of the shRNA inserts.

2.9.1c Sequencing the oligonucleotide inserts

Between 700-1000ng of plasmid DNA was used for PCR amplification ready sequencing. Up to 11.5µl of the DNA was added to 9.5µl of PCR reaction mixture (4µl of 5X primer, 4µl 5X enzyme and dNTP mixture (containing labelled ddNTPs) and 1.5µl of bovine growth hormone oligonucleotide). The PCR was performed on a Hybaid Omne-E for the following cycles: 96°C for 30 seconds, 50°C for 30 seconds and 60°C for 4 minutes (x25). The DNA was precipitated by the addition of 30µl dH_20, 5µl sodium acetate and 140µl of ethanol to the DNA and incubation for 20 minutes at -20°C. The DNA was washed with 70% ethanol, collected by centrifugation at 13000rpm for 20 minutes, and resuspended in 150µl of ethanol ready for sequencing by the DNA sequencing facility of Cardiff University [Central Biotechnology Services, Henry Wellcome Research Institute, Cardiff University]. Clones with the correct DNA insert were amplified, purified and quantified.

2.9.1d Functional testing of candidate shRNA sequences in Jurkat cells

As Jurkat cells are transformed T cells, they express SHP-1 and were therefore used to test shRNA sequences targeting SHP-1. The Jurkat cells were transferred to fresh media (RPMI with 10% FCS) 24 hours prior to transfection with the plasmid DNA encoding the shRNA sequences. Between 1-2x10^7 cells were used per transfection. The cells were taken from culture, washed twice in HBSS by centrifugation at 1500rpm for 5 minutes at 4°C and then suspended to give the desired number of cells in 400µl of complete RPMI. For each transfection, 15µg of the shRNA expression plasmid and 3µg of a GFP expression plasmid (pAL-190) were combined and sodium acetate (1/10^{th} of the volume) and ethanol (2.5 times the volume) added before precipitating at -20°C for 20 minutes. The DNA was then collected by centrifugation at 13000 rpm for 10 minutes at 4°C, and allowed to dry at room temperature before being suspended in 100µl of transfection buffer (10X HeBs buffer (1.4M NaCl, 249mM HEPES acidic, 3mM $NahPO_4$), 625µg/ml Herring sperm DNA and plain RPMI) with no additives. The DNA was added to the cells in a 4mm mammalian transfection cuvette. Cells were electorporated at 140 volts and 1000 µFar (capacitance) on a GenePulse Xcell electroporator [Bio-Rad]. The cells were left on ice for 10 minutes and then returned to culture for 48 hours before being single cell sorted. The cells were taken from culture and suspended in 500µl of complete RPMI in a FACS tube. Cells that had been electroporated in the absence of DNA were used to define a GFP positive gate. Cells that had been electroporated in the presence of DNA were sorted based on viability and GFP fluorescence. Cells were then analysed for SHP-1 expression by western blot analyses.

2.9.2 MISSION™ siRNA

Four sequence-verified shRNA lentiviral plasmids designed to target human SHP-1 (Accession number NM_002831) expression were purchased from Sigma as bacterial stocks. The parental plasmid background (pLKO.1-puro) contains a puromycin resistant gene, a U6

promoter to drive expression of the shRNA and a 21 nucleotide siRNA sense sequence for human SHP-1 (figure 2.2).

1) 2091

5'-CCGGCCTCTCCCTGACCCTGTATATCTCGAGATATACAGGGTCAGGGAGAGGTTTTT-3'

2) 1712

5'-CCGGCCCAGTTCATTGAAACCACTACTCGAGTAGTGGTTTCAATGAACTGGGTTTTT-3'

3) 1326

5'-CCGGGCATGACACAACCGAATACAACTCGAGTTGTATTCGGTTGTGTCATGCTTTTT-3'

4) 1572

5'-CCGGCGACATGCTCATGGAGAACATCTCGAGATGTTCTCCATGAGCATGTCGTTTTT-3'

5) 444

5'-CCGGCGGCACCATCATCCACCTCAACTCGAGTTGAGGTGGATGATGGTGCCGTTTTT-3'

Figure 2.2 *MISSION™ siRNA* shRNA sequences

Each shRNA sequence consists of a sense siRNA sequence (blue, underlined), a loop sequence (red) and an antisense sequence (blue).

2.9.2a Functional testing of the MISSION™ shRNA sequences in Hela cells

Hela cells expressing human SHP-1 were cultured in a T75 flask and allowed to reach 50% confluence. A calcium phosphate transfection kit [Sigma Aldrich] was used according to the manufacturer's instructions to produce a calcium phosphate precipitate containing 20μg of

the desired DNA, which was added to the cell cultures. The following day the media was aspirated and replaced with 10ml of complete DMEM containing 0.4μg/ml of puromycin, and 1mg/ml of G418. The media was changed every 4 days, and the cells cultured for 4 weeks prior to western blot analysis to evaluate SHP-1 expression.

Chapter 3

Exploring the role of SHP-1 in T cells during *in vivo* antigenic stimulation

3.1 Introduction

In vitro data has demonstrated that motheaten $CD8^+$ T cells hyper-proliferate in response to antigenic stimulation when compared to control $CD8^+$ T cells. This data has revealed that a greater proportion of motheaten T cells from a naive population enter into cell division upon stimulation with APCs loaded with cognate peptide (Sathish *et al.*, 2007). These findings correlate with data showing that a greater proportion of motheaten versus control $CD8^+$ T cells down regulate their TCRs when incubated with APCs presenting cognate peptide, which is a measure of antigen encounter by $CD8^+$ T cells. It was further demonstrated that motheaten $CD8^+$ T cells have the enhanced capability of forming more stable conjugates with APCs loaded with cognate peptide, which underlies, at least in part, the hyper-proliferative phenotype of motheaten $CD8^+$ T cells. In other *in vitro* studies it has been shown that $CD8^+$ T cells with a reduced level of SHP-1 expression exhibit an enhanced chemotactic response to a chemokine gradient (Kim *et al.*, 1999). It is therefore conceivable that T cells lacking SHP-1 expression may exhibit an enhanced response in an *in vivo* setting.

The impact of these *in vitro* observations has not been explored in an *in vivo* setting. Therefore, it was important to make this transition in the study of the role of SHP-1 in $CD8^+$ T cells, as the physical requirements of a $CD8^+$ T cell in a mammalian system during immunosurveillance and response to antigen are very different to that of a T cell that is interacting with APCs in tissue culture. Briefly, naive $CD8^+$ T cells are endowed with receptors that allow them to adhere to and cross cellular barriers, thus leaving the cardiovascular system and entering secondary lymphoid organs. It is here that they may encounter their cognate antigen, and with the necessary requirements met become activated and undergo

clonal expansion. An activated T cell then enters the lymphatics and returns to the cardiovascular system, from which it homes to peripheral sites of infection or tumour development, which also involves the adherence to and crossing of cellular barriers. It is in the periphery that a $CD8^+$ T cell can then exert its effector function by specifically killing target cells. In addition, extrinsic factors to the T cell, such as the action of regulatory T cells and availability of cytokines, may influence the dynamics and magnitude of an antigenic driven $CD8^+$ T cell response in an *in vivo* setting.

In order to study the *in vivo* role of SHP-1 in $CD8^+$ T cells during an antigenic response, $CD8^+$ T cells from motheaten and control mice were purified and adoptively transferred to recipient mice. Alternatively, naive T cells were first activated *in vitro* and expanded in the presence of IL-2 prior to their transfer to recipient mice. The adoptive transfer of T cells overcomes the early mortality associated with motheaten mice, which precludes any *in vivo* T cell studies being performed within these mice. The adoptive transfer also removes the T cells from an abnormal cytokine environment within the motheaten mouse, which could impact upon T cell behaviour. The study of antigenic T cell responses was feasible as the T cells from the motheaten and control mice expressed a transgenic TCR, F5, which can be stimulated with APCs presenting the cognate peptide, NP68. The T cells were either studied directly by recovering them from the recipient mice and using antibodies compatible with flow cytometry or the T cells were labelled prior to their transfer, to allow for their detection at different sites within the recipient mouse. To study T cell responses indirectly, mice that had already received naive $CD8^+$ T cells went on to receive a population of target cells and the magnitude of the response assessed by the extent of target cell killing. An additional *in vitro* assay was also performed to explore the impact regulatory T cells on $CD8^+$ T cell responses to antigenic stimulation.

3.2 Mouse bone marrow cells cultured with GM-CSF are enriched for CD11c$^+$ cells and up-regulate CD86 following maturation with LPS

In order to conduct *in vivo* experiments exploring the role of SHP-1 in CD8$^+$ T cells during antigenic stimulation, it was necessary to prime recipient mice that had received naive CD8$^+$ F5 T cells. To achieve this goal, a protocol for generating dendritic cells *in vitro* from mouse bone marrow precursor cells was initially used.

Firstly, the supernatant from a GM-CSF producer cell line obtained from Professor Kim Bottomly (Yale University) was assessed for its ability to produce DCs, as it offered an economically favourable alternative to commercially available GM-CSF.

Cells harvested from the bone marrow of mice were cultured with either commercially available GM-CSF (10ng/ml or 20ng/ml at different time points) or supernatant from a GM-CSF producer cell line (used at 1% or 2% final volume at different time points). Following 10 days of culture with commercial GM-CSF, the proportion of cells expressing the dendritic cell marker, CD11c, went from 5.6% to 77% (figure 3.1). The proportion of immature cells co-expressing CD11c and the costimulatory molecule, CD86, was 1.79% and 9.44% for those cultured with commercially available GM-CSF and GM-CSF supernatant respectively (figures 3.2A and B). Following maturation for a period of 24 hours with LPS, the proportion of cells co-expressing CD11c and CD86 was 21.9% and 21% for the cells cultured with commercially available GM-CSF and GM-CSF supernatant respectively (figures 3.2A and B).

3.3 *In vitro* generated dendritic cells present NP68 peptide to naive CD8$^+$ F5 T cells

To ensure that the *in vitro* generated dendritic cells were capable of presenting NP68 peptide to naive CD8$^+$ F5 T cells they were utilised in an *in vitro* T cell proliferation assay.

Once matured, the dendritic cells were pulsed with NP68 peptide and co-cultured with CFSE labelled naive $CD8^+$ F5 T cells. Cells were analysed by flow cytometry and histograms generated and analysed using the proliferation tool of FlowJo software. Following four days of culture, 42.4% (figure 3.3A) and 59.7% (figure 3.3B) of the $CD8^+$ T cells from the original population had entered into proliferation when cultured with DCs generated with either commercial GM-CSF or GM-CSF supernatant respectively. No spontaneous division of the T cells was seen in the absence of dendritic cells (data not shown).

3.4 Mice receiving naive $CD8^+$ F5 T cells and *in vitro* generated dendritic cells pulsed with NP68 peptide are capable of killing NP68 loaded target cells

To establish whether *in vitro* generated dendritic cells could both function and present NP68 peptide *in vivo*, they were pulsed with NP68 peptide and co-transferred with CFSE labelled naive $CD8^+$ F5 T cells to recipient mice. Upon transfer, DCs and T cells are required to migrate to secondary lymphoid organs prior to interacting with one another. Labelling the T cells with CFSE allowed T cell division to be tracked, which was used as a measure of how effective the DCs were at functioning *in vivo*.

DCs that had been generated by culturing bone marrow cells with commercially available GM-CSF were transferred intravenously (tail vein), subcutaneously (inguinal region) or into the peritoneal cavity of individual recipient mice. The intravenous cotransfer of dendritic and T cells proved to be detrimental to the mice as it lead to death soon after transfer, therefore the subcutaneous and peritoneal administration sites were explored further. Four days post dendritic cell and T cell transfer, the spleen, axial, brachial and inguinal lymph nodes were harvested and T cell proliferation assessed by flow cytometry. Figure 3.4 shows that the percentage of T cells entering into proliferation in mice receiving DCs either subcutaneously or peritoneally respectively was 23% and 32% in the spleen, 38% and 42% for the pooled

axial and brachial lymph nodes, and 36% and 50% for the inguinal lymph nodes. In light of this data and the fact that the peritoneal transfer of DCs offered the most straightforward means of injecting a mouse all subsequent experiments involving dendritic cells used the peritoneal route of delivery.

To compare the efficiency of matured dendritic cells generated with either commercially available GM-CSF or GM-CSF supernatant to present NP68 peptide *in vivo*, DCs were transferred into the peritoneal cavity of individual sub-lethally irradiated mice that had also received naive $CD8^+$ F5 T cells. Six days post T cell transfer the mice received CFSE labelled target (0.2μM) and reference cells (2μM), to assess the magnitude of the T cell response. The spleens were harvested after a further 24 hours for analysis by flow cytometry. A mouse receiving DCs generated with commercially available GM-CSF killed 47.5% of the target cells, compared to 48% of the target cells killed in the mouse receiving DCs generated with GM-CSF supernatant (figure 3.5).

Overall, it was established that mouse bone marrow cells cultured with supernatant containing GM-CSF produced DCs that could function and present NP68 peptide to adoptively transferred $CD8^+$ F5 T cells as well as those raised with commercial GM-CSF. In addition, the transfer of dendritic cells to the peritoneal cavity of mice provided a convenient and effective way to administer the cells and prime $CD8^+$ F5 T cells.

3.5 Mice receiving naive $CD8^+$ F5 T cells and the influenza A virus are able to kill NP68 labelled target cells

As an alternative to using exogenous DCs to prime mice, the enlistment of endogenous DCs and other APCs to present NP68 peptide to $CD8^+$ F5 T cells was assessed.

As the NP68 peptide is derived from the nucleoprotein of the influenza A virus, it was assessed whether infection with the virus could prime a transferred population of naive

$CD8^+$ F5 T cells. Four mice were sublethally irradiated and three of them infected intranasally with the influenza A virus. Four days post infection, CFSE labelled lymphocytes from control F5 mice were transferred to one infected and one uninfected mouse. Four days later mice that had received T cells were sacrificed and their spleens and submandibular lymph nodes taken for analysis by flow cytometry. Histograms were generated and a gate set for those cells that had entered in to proliferation to reveal the percentage of cells residing within this gate. Figure 3.6 shows that a similar proportion of the transferred cells in the spleen (17%) and submandibular lymph nodes (19%) from the infected mouse and in the spleen (18%) from the uninfected mouse, were in the proliferating population. However, a greater proportion of cells were in the proliferating population (37%) in the submandibular lymph nodes of the mouse that had been infected (figure 3.6B).

Six days post T cell transfer the remaining two mice that received unlabelled T cells received CFSE labelled target and reference cells. Twenty-four hours later the mice were sacrificed and their spleens taken for analysis by flow cytometry. The infected mouse that received the lymphocytes killed 77.4% of the target cells (figure 3.6D).

The use of the influenza A virus to prime adoptively T cells had the potential to allow for the study of motheaten and control $CD8^+$ F5 T cells in a system that is physiologically relevant with regards to the priming of the T cells. However, the necessity to prime mice with the virus prior to T cell transfer did not allow assays to be performed at short notice, which was often the case with motheaten mouse availability.

3.6 Mice receiving naive $CD8^+$ F5 T cells and NP68 in IFA are able to kill NP68 labelled target cells

In order to explore other methods of priming mice receiving CD8+ F5 T cells which were more flexible, IFA was used to deliver NP68 to mice.

Sub-lethally irradiated mice were injected subcutaneously (inguinal region) with NP68 peptide in a mixture of incomplete Freund's adjuvant and PBS. Six days post T cell transfer and priming, mice received a population of CFSE labelled target (0.2μM) and reference cells (2μM). After a further 24 hours the spleens were taken for analysis by flow cytometry. Mice receiving T cells and primed with NP68 peptide in IFA killed 48% of the target cells (Figure 3.7). This offered a more logistically convenient way of priming adoptively transferred $CD8^+$ T cells as the motheaten mice were often available at short notice with the need for immediate use, which did not leave time for dendritic cells to be produced or mice to be primed with influenza virus.

3.7 Mice receiving naive motheaten $CD8^+$ F5 T cells kill more target cells during a primary T cell response than those mice receiving naive control $CD8^+$ F5 T cells

In order to examine the magnitude of the *in vivo* response of both motheaten and control $CD8^+$ F5 T cells to antigenic stimulation, the same number of naive $CD8^+$ T cells from both control and motheaten mice were transferred to individual recipient mice. The T cell response was then measured indirectly by performing an assay that looked at the ultimate role of a $CD8^+$ T cell, which is to directly kill target cells.

Sub-lethally irradiated mice received 3-3.8x10^6 purified naive $CD8^+$ F5 T cells intravenously. Mice were primed by the transfer of matured and NP68 peptide pulsed DCs into the peritoneal cavity. Control mice did not receive any T cells. Six days later, mice received CFSE labelled target (0.2μM) and reference (2μM) cells in order to assess the magnitude of the T cell response.

The data from three independent experiments demonstrated that mice receiving naive motheaten $CD8^+$ F5 T cells killed more target cells than those mice receiving control naive $CD8^+$ F5 T cells. The extent of target cells killed by mice receiving either control or

motheaten T cells was 47% versus 69% (figure 3.8), 56% versus 84% (figure 3.9) and 54% versus 70% (data not shown) respectively.

3.8 Enhanced accumulation of motheaten $CD8^+$ T cells in the spleens of recipient mice compared to the spleens of mice receiving control $CD8^+$ T cells

In order to explore the possible reasons underlying the enhanced killing of peptide labelled target cells seen in mice receiving motheaten T cells, assays were performed that examined the *in vivo* expansion of control and motheaten $CD8^+$ F5 T cells.

Purified naive motheaten and control $CD8^+$ F5 T cell populations ($2\text{-}3x10^6$) were transferred to sub-lethally irradiated mice. Mice were subcutaneously primed at the same time as T cell transfer with NP68 peptide in IFA. Control mice did not receive any T cells. Seven days later spleens were removed and the cells counted by trypan blue exclusion and stained with anti-$CD8^{PE}$ antibody (and for some assays also stained with anti-$Thy1.2^{FITC}$ antibody). The $CD8^+$ T cells were expressed as a proportion of a lymphocyte gate, which was determined by the forward and side scatter profiles of the cells. This data was then used to calculate the absolute $CD8^+$ T cell number (figure 3.10). From four independent experiments those mice receiving naive motheaten T cells had consistently more $CD8^+$ T cells of a lymphocyte gate compared to mice receiving control T cells (summarised in figure 3.10). However, the data seemed to vary considerably between experiments, with the primary concern being the extent to which the total number of splenoctyes and also the percentage of cells residing within a lymphocyte gate varied between mice. To overcome the possibility that the process of red blood lysis was adversely affecting the total cell counts and that the irradiation of mice could have differing affects on the lymphocyte compartment of individual mice a second protocol was developed.

In order to circumvent the need for irradiation, Rag-$1^{-/-}$ mice were selected for use as lymphopaenic recipients. In addition, in order to control for the loss of cells during red blood cell lysis, a reference population of cells was introduced to the protocol to act as an internal control.

Rag-$1^{-/-}$ mice received $3x10^6$ purified $CD8^+$ F5 T cells and a subcutaneous injection of NP68 peptide in IFA. Seven days post T cell transfer, spleens were removed and a defined number of CFSE labelled reference cells added to each sample prior to processing. Single cell suspensions were then prepared, stained with anti-$CD8^{PE}$ antibody and analysed by flow cytometry. A defined number of $CFSE^+$ cell events were acquired and the $CFSE^-/CD8^+$ cells expressed as a comparative percentage of the $CFSE^+$ reference cell population. In the mouse receiving naive motheaten $CD8^+$ T cells the percentage was 31% compared to 16% for the mouse receiving naive control $CD8^+$ T cells (Figure 3.11).

3.9 Mice receiving activated motheaten $CD8^+$ F5 T cells kill more target cells than mice receiving activated control $CD8^+$ F5 T cells

An *in vitro* study had previously shown that motheaten $CD8^+$ F5 T cells they have an equivalent cytotoxic activity on a per cell basis to that of control $CD8^+$ F5 T cells, when the target cells were NP68 peptide pulsed EL4 cells (Johnson *et al.*, 1999). In order to explore the *in vivo* cytotoxic function of motheaten and control T cells on a per cell basis, equal numbers of *in vitro* generated activated T cells were transferred to recipient mice, which then received target cells to kill.

Naive $CD8^+$ F5 T cells were activated *in vitro* for two days with NP68 pulsed splenocytes and then expanded for a further two days in IL-2. Initially, different numbers of activated control or motheaten $CD8^+$ F5 T cells were transferred to establish an optimum T cell number in relation to the number of target and reference cells transferred ($20x10^6$ in total). Therefore,

$10x10^6$, $20x10^6$ and $30x10^6$ of control $CD8^+$ F5 T cells were transferred to individual mice. Twenty-four hours later the mice received CFSE labelled target (2μM) and reference (0.2μM) cells, which were subsequently retrieved from the spleen after a further twenty-four hours. Those mice receiving $10x10^6$ control $CD8^+$ F5 T cells killed 89.3% and 74.8% of the targets (figure 3.12B), compared to 95%, 94.9% and 96.4% of the target cells killed by the mice that received the same number of motheaten $CD8^+$ F5 T cells (figure 3.12E). Mice that received $20x10^6$ control $CD8^+$ F5 T cells killed 95.3% and 95% of the targets (figure 3.12C). Finally, one mouse that received $30x10^6$ control T cells killed 92.9% of the target cells (figure 3.12D).

As the killing within these mice had reached a near maximum, the number of T cells transferred in a subsequent experiment was reduced. Mice received $2x10^6$ control or motheaten T cells. Those receiving the control T cells killed 1.07%, 3.7% and 3.9% of the target cells (figure 3.13B), compared to 16%, 21% and 24% of the target cells killed in mice receiving motheaten T cells (figure 3.13C). This was not statistically significant (p=0.100) according to a non parametric Mann-Whitney test.

In a third independent experiment mice received $5x10^6$ of either control or motheaten T cells. Those mice receiving control T cells killed 32%, 38.6% and 41.1% of the target cells (figure 3.14B), whereas those receiving motheaten T cells killed 42%, 52% and 52.9% of the target cells (figure 3.14C). Again, this was not statistically significant (p=0.100) according to a non parametric Mann-Whitney test.

3.10 Altered ratios of motheaten $CD8^+$ F5 T cells in the blood and Peyer's patches of recipient mice

As the efficiency at which naive and activated $CD8^+$ T cells home to secondary lymphoid organs and peripheral sites may influence the outcome of an antigenic $CD8^+$ T cell response,

a protocol was developed to compare the homing capabilities of control and motheaten $CD8^+$ F5 T cells.

The primary reason for these experiments was to further investigate the underlying basis for the enhanced killing of peptide labelled targets by mice receiving SHP-1 deficient $CD8^+$ T cells when compared to those receiving control $CD8^+$ T cells. In support of a SHP-1 effect on T cell migration, *in vitro* studies have demonstrated that a reduction in SHP-1 expression in T cells leads to an enhanced chemotactic response (Kim *et al.*, 1999). In addition, SHP-1 has been shown to play an important role in myeloid cell adhesion and homing, as demonstrated in the motheaten mouse (Shultz *et al.*, 1997) and by *in vitro* studies (Roach *et al.*, 1998).

Ideally, the homing capacity of both naive and activated $CD8^+$ T cells would be studied but the limited availability and young age of motheaten mice meant that not enough naive T cells would have been available to transfer to recipient mice at any one time. The vast number of secondary lymphoid organs in a recipient mouse would have resulted in a wide distribution of a limited number of transferred naive T cells and therefore precluded detection by flow cytometry. As a result naive T cells were first activated and expanded *in vitro* to generate enough T cells to transfer *in vivo*.

It has been previously reported that T cells primed in the presence of retinoic acid exhibit a preferential homing capacity to gut associated tissue (Stagg *et al.*, 2002). This offered a means of focusing the migratory behaviour of transferred activated T cells to a site that could be harvested and analysed. In order to study the homing capabilities of motheaten and control T cells in parallel within the same mouse, two intracellular dyes were used to differentially label the T cells. When labelling motheaten and control T cells for transfer, both dyes were used for both cell types to eliminate the possibility of any dye induced effects on the T cells.

The intracellular dye CFSE had already been used for labelling T cells destined for various assays; therefore a second intracellular dye was required to label T cells. The first requirement of a prospective partner dye for CFSE was that its emission spectra was different to that of CFSE. The dye also needed to be non-toxic to cells and resistant to excessive bleaching when exposed to light. The intracellular dye, DDAO, met these requirements and was therefore used to label T cells.

Firstly, the Peyer's patches, which are lymphoid clusters found along the length of the small intestine, were excised from C57BL/6 mice to confirm that T cells could be detected in this gut associated lymphoid tissue. Samples were stained in order to examine both T cells and B cells by flow cytometry. Figure 3.15A revealed populations of both lymphocytes residing in the Peyer's patches. This meant that adoptively transferred T cells should potentially migrate to this tissue.

Initial concentrations of retinoic acid (1μM) proved to be toxic to the T cells, so the final concentration used for T cell culture was 10nM. Lymphocytes from control and motheaten mice were co-cultured for 2 days with irradiated splenocytes loaded with NP68 peptide, then expanded for 3 days with IL-2. Initially, a CFSE labelled population of control $CD8^+$ F5 T cells was transferred to non-irradiated recipient mice. Upon harvesting the Peyer's patches, the CFSE labelled cells could not be distinguished from the autofluorescence of this tissue. Therefore, T cells were transferred to either Rag-$1^{-/-}$ mice or sub-lethally irradiated mice, which possess no or limited numbers of lymphocytes at this site respectively. The Peyer's patches in the Rag-$1^{-/-}$ were difficult to detect and therefore excise, but this was not the case for the Peyer's patches in the irradiated mice. Twenty four hours post transfer CFSE labelled cells were present in the blood, spleen and Peyer's patches (figure 3.15C, D and E). A lower proportion of CFSE labelled cells was seen in the mesenteric (figure 3.15G), axial, brachial (figure 3.15H) and inguinal lymph nodes (Figure 3.15F). In an independent experiment, T

cells that had been activated *in vitro* in the absence of retinoic acid did not appear in the Peyer's patches twenty-four hours post transfer, but were present in the blood, spleen and lungs (figure 3.16).

Twenty-four hours following the transfer of $25x10^6$ of both motheaten and the control activated $CD8^+$ F5 T cells that had been labelled with either CFSE or DDAO, the blood and Peyer's patches were taken for analysis by flow cytometry. In two independent experiments, recipient mice had a greater proportion of motheaten compared to control T cells in their blood. Conversely, mice had a greater proportion of control versus motheaten T cells in their Peyer's patches. The ratio of motheaten T cells to control T cells in the blood of mice was 1.66:1 (CFSE:DDAO) and 1.63:1 (DDAO:CFSE) for the first experiment (Figure 3.17B and C), and 2.3:1 (CFSE:DDAO) and 1.56:1 (DDAO:CFSE) for the second experiment (Figure 3.18C and D). The ratio of motheaten T cells to control T cells in Peyer's patches in the first experiment was 0.68:1 (CFSE:DDAO) and 0.65:1 (DDAO:CFSE) (figure 3.17E and F), and for the second experiment it was 0.46:1 (CFSE:DDAO) and 0.78:1 (DDAO:CFSE) (figure 3.18F and G).

Due to the ability of T cells to both enter and exit the Peyer's patches, it was decided that this was not an ideal model for studying T cell migration. Ideally, the tissue to which the T cells migrate would be the final destination for the T cells, thereby leading to their accumulation in the tissue. Consequently, this would allow any differences in the numbers of motheaten or control $CD8^+$ T cells found in the tissue to be attributed to their capacity to migrate.

3.11 *In vitro* activated T cells labelled with intracellular dyes are evident in the ovaries of Vaccinia virus infected and non-infected mice following adoptive transfer

In addition to using the Peyer's patches as a tissue to study T cell homing, virally infected tissue was also evaluated as a possible means to study the homing capabilities of motheaten

and control $CD8^+$ T F5 cells. The vaccinia virus has a tropism for the ovaries when transferred into the peritoneal cavity of mice.

T cells were activated for 2 days with irradiated splenocytes pulsed with NP68 peptide, then expanded for a further two days in IL-2. A total of $20x10^6$ control T cells was labelled with either the intracellular dye, DDAO, or CFSE and transferred intravenously to mice that had been infected four days previously with recombinant vaccinia virus expressing the NP68 peptide. The same number of labelled T cells was also transferred to a mouse that had not been infected with the vaccinia virus. The ratio of CFSE to DDAO labelled cells was checked by flow cytometry prior to adoptive transfer (figure 3.19A), with a ratio of 1.52:1 in favour of CFSE labelled cells. Twenty-four hours following the transfer of the T cells, the blood, spleen and ovaries were taken from each mouse for analysis by flow cytometry. The T cells were present in all tissues taken from both the infected and un-infected mice. The CFSE to DDAO labelled cell ratios for the infected and uninfected mice respectively, were 1.05:1 and 0.88:1 in the blood, 1.02:1 and 1.02:1 in the spleens and 1.43:1 and 1.21:1 in the ovaries (figure 3.19).

In light of these observations it would be necessary to repeat such experiments and establish whether the total number of cells differed between infected and uninfected mice.

3.12 Motheaten $CD8^+$ F5 T cells exhibit a greater resistance to regulatory T cell induced inhibition on T cell proliferation than control $CD8^+$ F5 T cells

The regulatory influence of $CD4^+CD25^+Foxp3^+$ T cells on $CD8^+$ T cells can have profound effects upon the outcome of a T cell response to antigen. *In vitro* assays were performed to establish whether there were any differences in the resistance of control and motheaten $CD8^+$ T cells to the action of regulatory T cells. This assay looked at the proliferation of CFSE

labelled naive control and motheaten $CD8^+$ F5 T cells in the presence or absence of $CD4^+CD25^+$ regulatory T cells.

Firstly, pilot experiments were performed to establish the ideal tissue culture conditions to give optimum T cell proliferation in the absence of regulatory T cells. This was achieved by culturing T cells in U- or flat-bottomed 96 well plates, in the presence or absence of both anti-$CD3^{Bio}$ antibody (coated plates) and irradiated splenocytes (devoid of T cells).

Anti-$CD3^{Bio}$ antibody or splenocytes were used in isolation to stimulate $5x10^4$ $CD8^+$ T cells in U-bottomed 96 well plates. This induced means of 45% and 10% of the respective T cells to appear in a dividing gate (figure 3.20A). Anti-$CD3^{Bio}$ antibody was also used in combination with either $2x10^5$ or $4x10^5$ splenocytes to stimulate $5x10^4$ or $10x10^4$ T cells respectively. This resulted in means of 18% and 32% of the T cells residing in the proliferating gate respectively (figure 3.20A).

In a second control assay, anti-$CD3^{Bio}$ antibody was used in combination with $2x10^5$ or $6x10^5$ splenocytes to stimulate $15x10^4$ T cells in either U- or flat-bottomed 96 well plates. This resulted in means of 70% and 71% of T cells cultured in the U-bottomed plates in the dividing gate compared to means of 60% and 61% for those in flat-bottomed plates (figure 3.20B).

For the final assay, a total of $15x10^4$ motheaten or control T cells labelled with CFSE was cultured in U-bottomed 96 well plates coated with anti-$CD3^{Bio}$ and $2x10^5$ splenocytes. Regulatory T cells were purified by immunomagnetic separation based upon CD4 and CD25 expression and added to each well to give the following Treg to T cell ratios; 0:1, 1:10, 1:5, 1:1, 1:2, 2:1, 4:1. Each condition was performed singly apart from the 0:1 ratio, which was performed in triplicate. The T cells were co-cultured for four days and then harvested and stained with anti-$CD8^{PE}$ antibody and analysed by flow cytometry. Histograms displaying

CFSE fluorescence were gated on viable and $CD8^+$ cells. The histograms were analysed using the proliferation tool of FlowJo software. The undivided peak was set using the data from wells of T cells that had been cultured without Tregs and anti-$CD3^{Bio}$ antibody (figure 3.21). This setting was then applied to each of the histograms to give the percentage of cells that had entered into proliferation from the initial T cell population. From this data, the percentage of inhibition was calculated (figure 3.22) by comparing the proportion of T cells that had entered in to proliferation in the presence of Tregs (ratios 1:10 to 4:1 for figures 3.21A and B) to the proportion of T cells that had entered into proliferation in the absence of Tregs (0:1 ratio for figures 3.21A and B). Figure 3.22 shows this data graphically, with a greater inhibition of control $CD8^+$ F5 T cell proliferation detected than that detected for motheaten $CD8^+$ F5 T cell proliferation at all Treg to T cell ratios. At the Treg to T cell ratios of 1:10 and 1:5, motheaten $CD8^+$ F5 T cells were not inhibited, whereas there was 16.5% and 21.4% inhibition of control $CD8^+$ F5 T cell proliferation. At the four higher Treg to T cell ratios, the percentage inhibition for control $CD8^+$ F5 T cells was 28.5% (0.5:1), 46.8% (1:1), 38.2% (2:1) and 58.8% (4:1), whereas for motheaten $CD8^+$ F5 T cells this was 8.9% (0.5:1), 25.8% (1:1), 21% (2:1) and 36.6% (4:1) (figure 3.22).

3.13 Summary of results

The employment of adoptive cell transfer techniques during this study allowed motheaten and control $CD8^+$ F5 T cells to be studied in an *in vivo* setting. This represented an advance in the study of SHP-1's role in $CD8^+$ T cells.

All methods trialled for the priming of mice (adoptive transfer of *in vitro* generated DCs pulsed with NP68, infection with the influenza A virus and subcutaneous injection of NP68 in IFA) that received $CD8^+$ F5 T cells, proved to be successful. Logistically, the subcutaneous

injection of NP68 in IFA proved to be most convenient when considering the sporadic nature of motheaten mice availability and the age that they had to be used.

It was demonstrated that mice receiving motheaten (SHP-1 deficient) $CD8^+$ F5 T cells and *in vitro* cultured DCs exhibited and enhanced primary T cell response, with regards to the expansion of the motheaten $CD8^+$ T cells and as a result, the proportion of NP68 labelled target cells killed.

To further explore the possible reasons underlying the enhanced killing of peptide labelled targets seen in the absence of SHP-1, attempts were made to investigate other aspects of T cell function *in vivo*. Moreover, in addition to the assays used to study *in vivo* T cell expansion, assays were also developed to explore *in vivo* T cell migration and *in vivo* cytotoxicity on a per cell basis. These assays would require further optimisation in order for conclusive data to be obtained.

Finally, an *in vitro* assay was developed to explore the regulatory action of Tregs on the proliferation of motheaten and control $CD8^+$ F5 T cells. Although the assay worked in principle, with T cell proliferation being inhibited in the presence of the Tregs, the assays would need repeating in order for data to be validated.

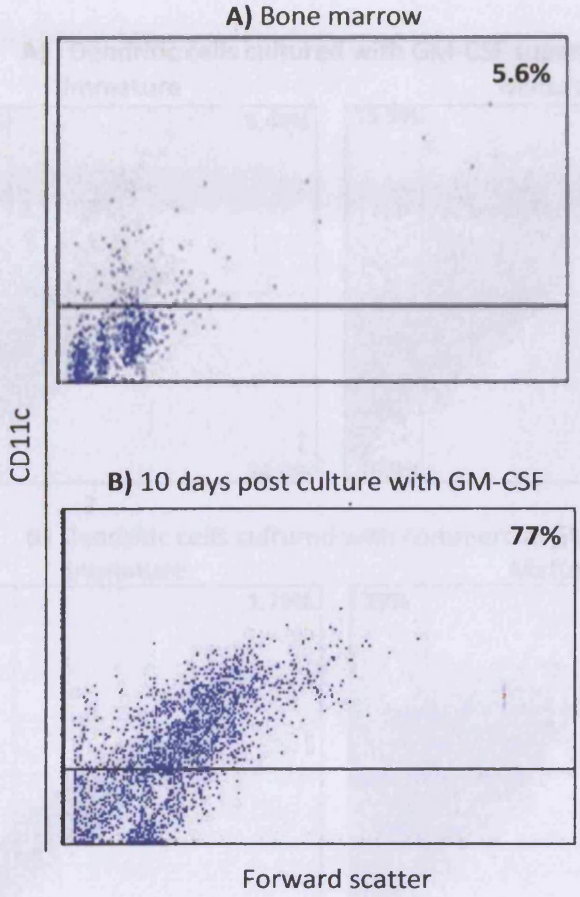


Figure 3.1: Bone marrow cells cultured with GM-CSF are enriched for CD11c^{+} cells

Bone marrow was harvested form C57BL/6 mice and cultured with commercially available GM-CSF for ten days. The cells were then harvested and stained with anti-CD11c^{FITC} antibody and analysed by flow cytometry. Freshly harvested bone marrow was also stained with anti-CD11c^{FITC} antibody. The dot plots generated were gated on viable cells and the gate set according to the autofluorescence seen in an unstained sample (data not shown). The proportion of bone marrow cells expressing CD11c was 5.6% and after ten days of culture this increased to 77%.

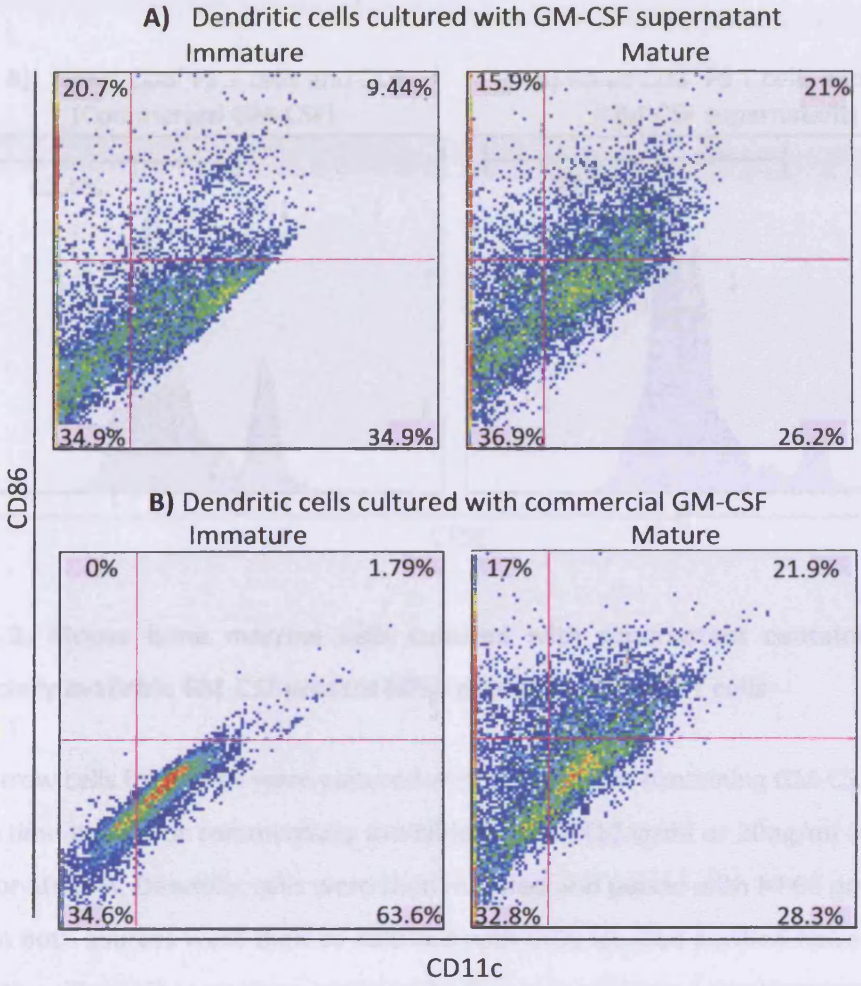


Figure 3.2: Mouse bone marrow cells cultured with supernatant containing GM-CSF or commercially available GM-CSF for 10 days have a similar proportion of $CD11^{+}CD86^{+}$ cells after maturation with LPS

Bone marrow cells from mice were cultured with supernatant containing GM-CSF (1% and 2% at different time points) or commercially available GM-CSF (10ng/ml or 20ng/ml at different time points) for 10 days. Cells were matured for 24 hours in the presence of 20µg/ml of LPS. Cells were taken before and after maturation and stained with anti-$CD11c^{PE}$ and anti-$CD8^{FITC}$ antibodies ready for flow cytometry. Pseudocolour dot plots were gated on a viable cell population to show CD11c and CD86 expression. Unstained cells were used to set the quadrant and the percentages of cells residing in each quarter shown. The proportion of the cells co-expressing CD11c and CD86 went from 9.44% when immature to 21% once matured (A) for the cells that were cultured with GM-CSF supernatant and from 1.79% to 21.9% for the cells cultured with commercially available GM-CSF (B).

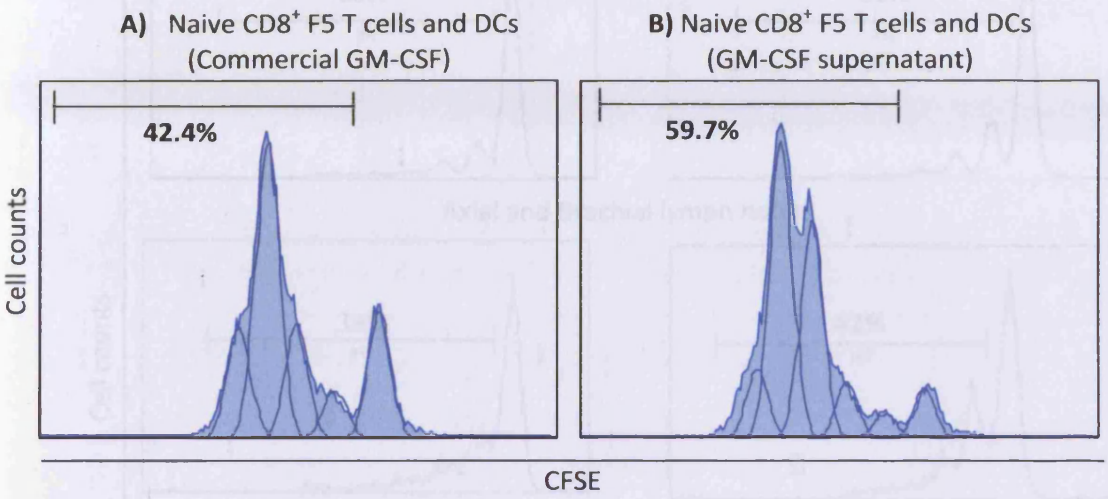


Figure 3.3: Mouse bone marrow cells cultured with supernatant containing GM-CSF or commercially available GM-CSF present NP68 peptide to CD8$^+$ F5 T cells

Bone marrow cells from mice were cultured with supernatant containing GM-CSF (1% and 2% at different time points) or commercially available GM-CSF (10ng/ml or 20ng/ml at different time points) for 10 days. Dendritic cells were then matured and pulsed with NP68 peptide. Dendritic cells from both sources were then co-cultured with CFSE labelled purified naive CD8$^+$ F5 T cells for four days. The cells were then analysed by flow cytometry and the histograms displayed to show CFSE fluorescence. The data was analysed by FlowJo software to reveal the number of cells from the original T cell population that had entered into proliferation, with the percentages shown for each histogram. When naive CD8$^+$ F5 T cells were cultured with dendritic cells that had been generated by culturing with commercially available GM-CSF, 42.4% of them entered into proliferation (A). For the T cells cultured with GM-CSF supernatant, 59.7% of them entered into proliferation (B).

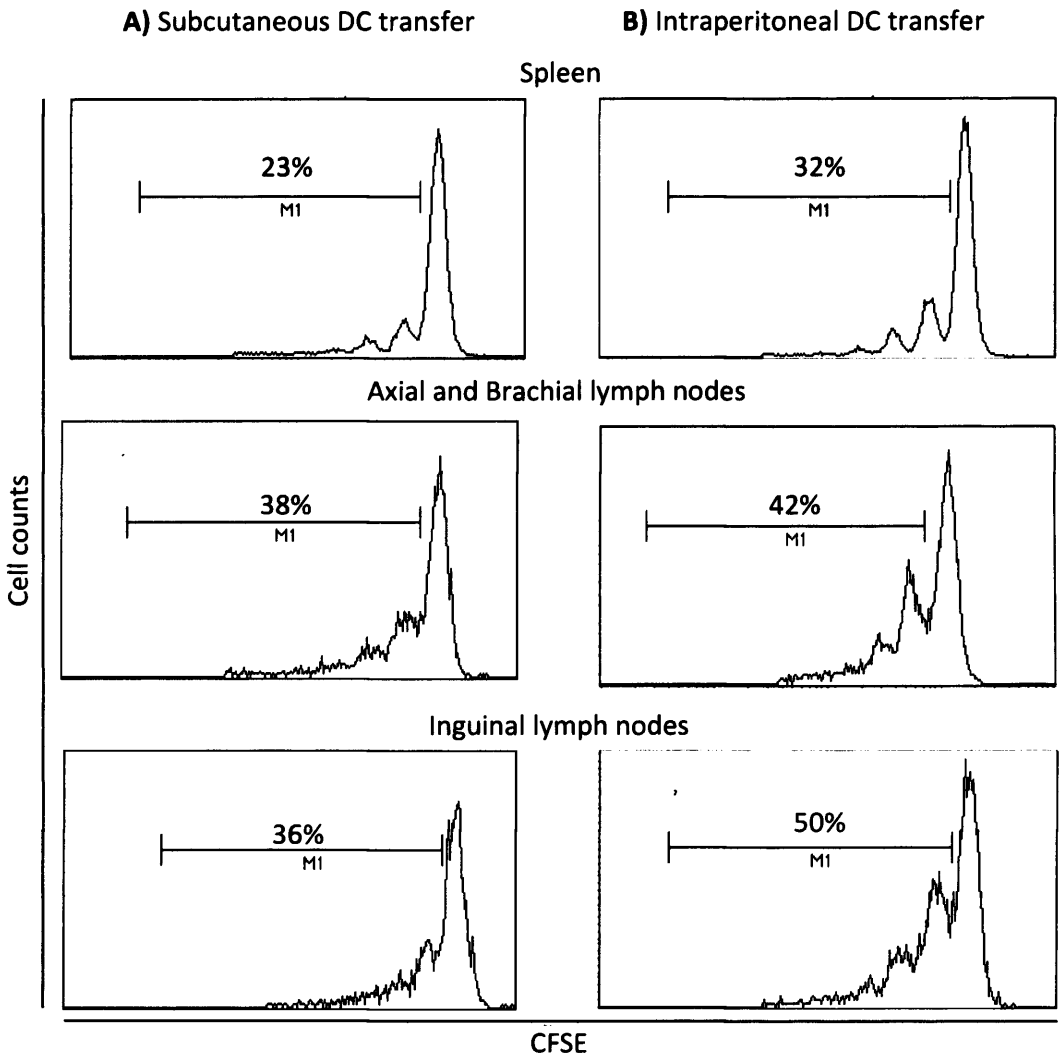


Figure 3.4: Adoptively transferred naive CD8$^+$ F5 T cells proliferate in mice receiving NP68 loaded dendritic cells

Dendritic cells were generated by culturing mouse bone marrow cells with commercially available GM-CSF. They were matured with LPS and pulsed with NP68 peptide prior to being transferred to recipient mice. A total of $1x10^6$ dendritic cells were transferred either subcutaneously (A) or in to the peritoneal cavity (B) of individual mice. Mice also received $4x10^6$ naive control CD8$^+$ F5 T cells labelled with 4μM CFSE. Four days later the mice were sacrificed and the spleens and axial, inguinal and brachial lymph modes taken and prepared for flow cytometry. Histograms displaying CFSE were gated on viable and CFSE$^+$ cells. A gate was set over the T cells that had entered into proliferation and the percentage of cells within this gate displayed for each histogram. T cell proliferation was present in all lymphoid tissues taken from both mice.

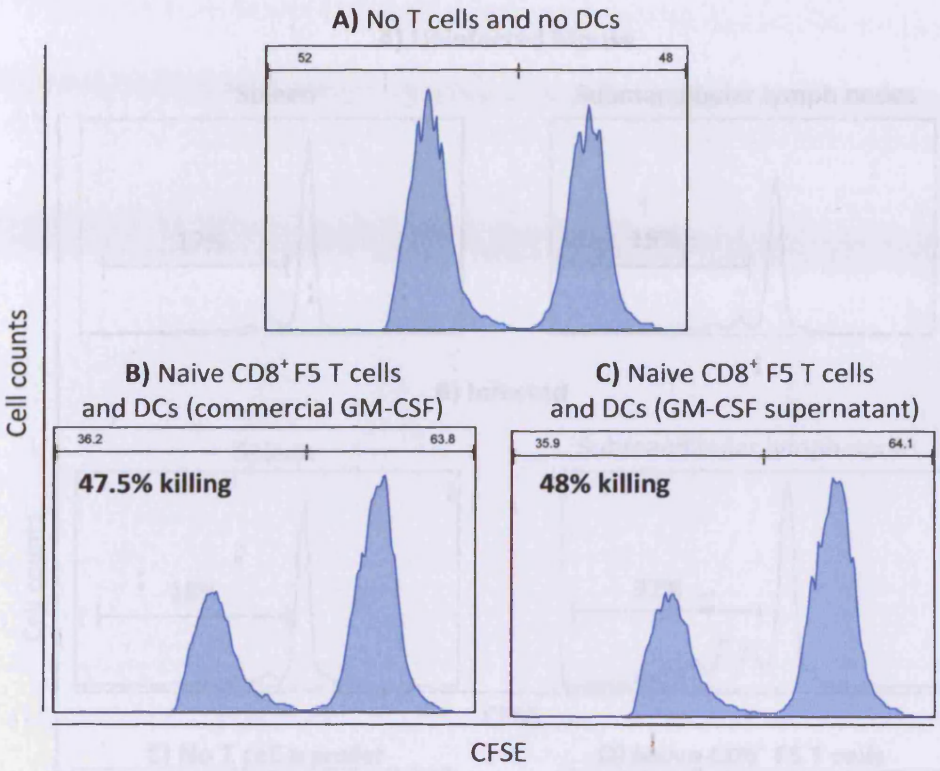


Figure 3.5: Mouse bone marrow cells cultured with supernatant containing GM-CSF or commercially available GM-CSF are able to present NP68 peptide to F5 T cells in an *in vivo* context

Bone marrow cells from mice were cultured with supernatant containing GM-CSF (1% and 2% at different time points) or commercially available GM-CSF (10ng/ml or 20ng/ml at different time points) for 10 days. Dendritic cells were then matured and pulsed with NP68 peptide. A total of $3x10^6$ dendritic cells were transferred into the peritoneal cavity of irradiated mice at the same time as the intravenous transfer of $2x10^6$ purified naive control $CD8^+$ F5 T cells. Six days later, mice received $10x10^6$ target (0.2µM CFSE and pulsed with NP68) and $10x10^6$ reference splenocytes (2µM CFSE) intravenously. Twenty-four hours post transfer, mice were sacrificed and their spleens taken for analysis by flow cytometry. The percentage of target cells killed is shown for each histogram. Any deviation from the anticipated 1:1 ratio of target to reference cells in the mice not receiving T cells (A) was used to adjust the percentage killing in the mice receiving T cells. The mouse that received naive T cells and dendritic cells that had been cultured with commercially available GM-CSF killed 47.5% of the target cells (B) and the mouse that received the dendritic cells that had been cultured with GM-CSF supernatant killed 48% of the target cells (C).

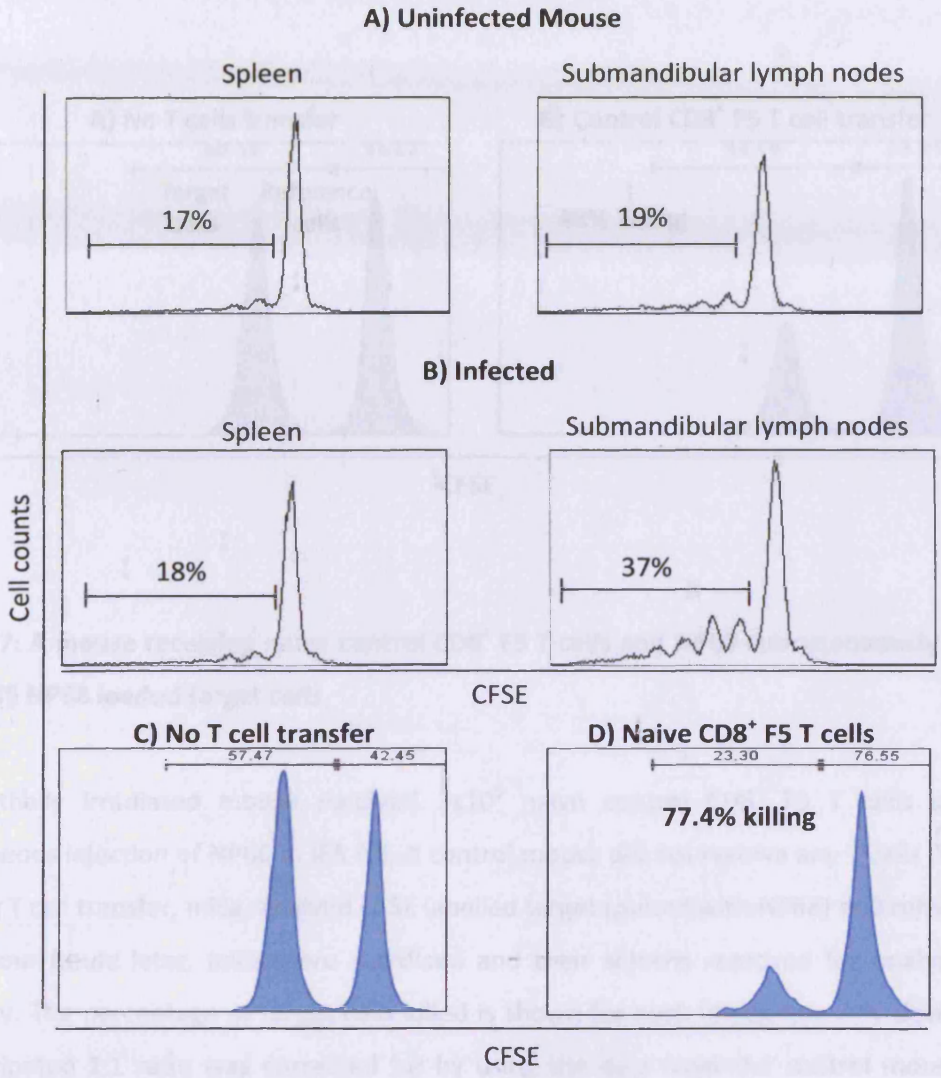


Figure 3.6: Mice receiving naive CD8$^+$ F5 T cells and the influenza A virus were able to mount a T cell response

Four mice were sub-lethally irradiated and three of them were infected intranasally with the influenza A virus (B, C and D). Four days later one mouse that had been infected (B) and one that was uninfected (A) received CFSE labelled lymphocytes from control F5 mice. The two remaining infected mice received unlabelled lymphocytes from control F5 mice (C and D). Four days post transfer the mice that received CFSE labelled lymphocytes were sacrificed and their spleens and submandibular lymph nodes taken for analysis by flow cytometry. Histograms were gated on viable and CFSE$^+$ cells with a gate showing cells that had entered into proliferation. A similar proportion of cells was found in the proliferating gate in the spleens from both mice (A and B) and in the submandibular lymph nodes of the uninfected mouse (A). A greater proportion of cells in the submandibular lymph nodes was seen in the proliferating gate from the infected mouse (B). Six days post T cell transfer the mice that received unlabelled lymphocytes received CFSE labelled target and reference cells. Twenty-four hours later the spleens were taken for analysis by flow cytometry. Any deviation from the anticipated 1:1 ratio of target to reference cells was adjusted for by using the data from the infected mouse that did not receive any T cells (C). The infected mouse that did receive naive CD8$^+$ F5 T cells killed 77.4% of the target cells (D).

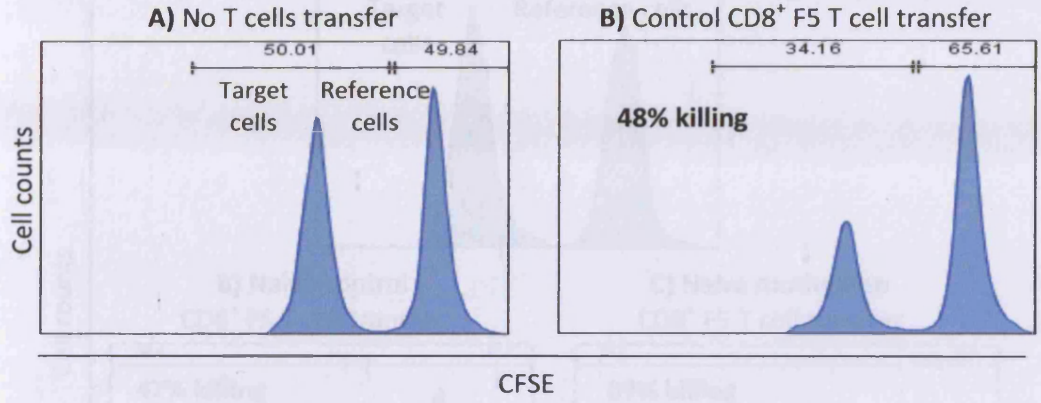


Figure 3.7: A mouse receiving naive control CD8$^+$ F5 T cells and NP68 subcutaneously in IFA was able to kill NP68 loaded target cells

A sub-lethally irradiated mouse received 3x10^6 naive control CD8$^+$ F5 T cells and also a subcutaneous injection of NP68 in IFA (B). A control mouse did not receive any T cells (A). Six days following T cell transfer, mice received CFSE labelled target (pulsed with NP68) and reference cells. Twenty-four hours later, mice were sacrificed and their spleens removed for analysis by flow cytometry. The percentage of target cells killed is shown for each histogram. Any deviation from the anticipated 1:1 ratio was corrected for by using the data from the control mouse (A). The mouse that received naive CD8$^+$ F5 T cells killed 48% of the target cells (B).

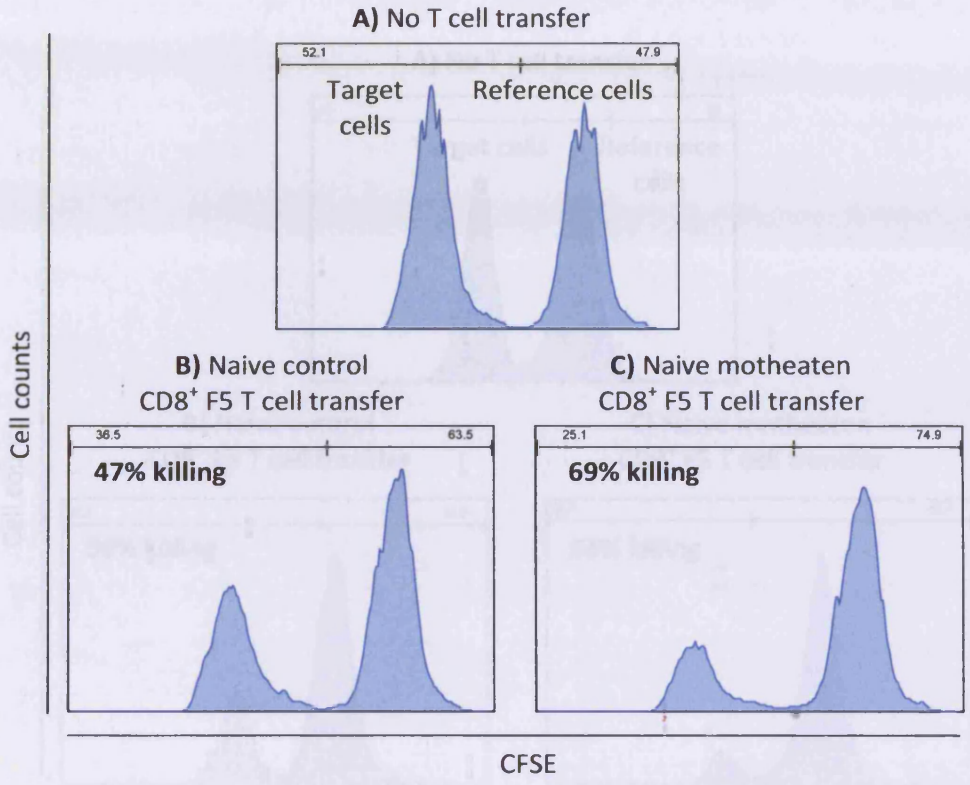


Figure 3.8: A mouse receiving naive motheaten CD8$^+$ F5 T cells kills more target cells during a primary T cell response than a mouse receiving naive control CD8$^+$ F5 T cells

Sub-lethally irradiated mice received 3.8x10^6 naive control (B) or motheaten (C) CD8$^+$ F5 T cells intravenously and a peritoneal transfer of 3x10^6 in vitro matured and NP68 pulsed dendritic cells. A control mouse (A) did not receive any T cells. Six days post T cell transfer, mice received 10x10^6 target (0.2µM CFSE and pulsed with NP68) and 10x10^6 reference splenocytes (2µM CFSE) intravenously. Twenty-four hours post transfer, mice were sacrificed and their spleens taken for analysis by flow cytometry. Histograms were gated on viable and CFSE$^+$ cells. The percentage of target cells killed is shown for each histogram. Any deviation from the anticipated 1:1 ratio of target to reference cells in the mice not receiving T cells (A and D) was used to adjust the percentage killing in the mice receiving T cells. Those mice receiving naive motheaten CD8$^+$ F5 T cells (C) killed more target cells than those receiving control CD8$^+$ F5 T cells (B).

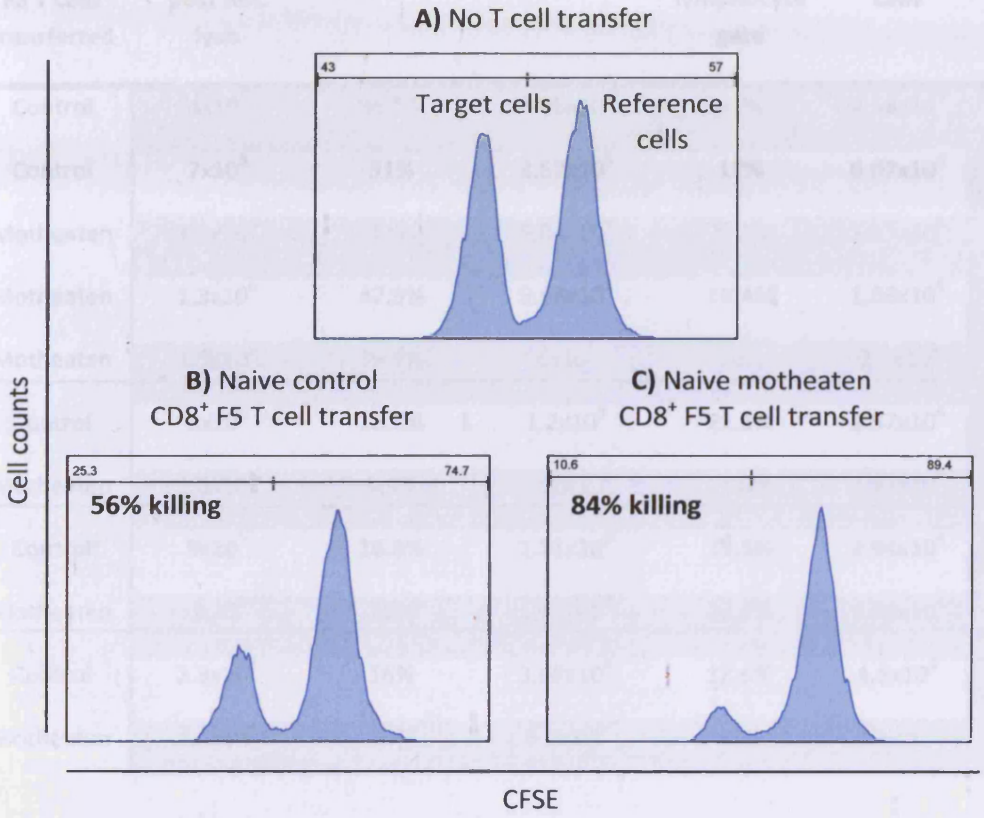


Figure 3.9: A mouse receiving naive motheaten CD8$^+$ F5 T cells kills more target cells during a primary T cell response than a mouse receiving naive control CD8$^+$ F5 T cells

Sub-lethally irradiated mice received 3x10^6 naive control (B) or motheaten (C) CD8$^+$ F5 T cells intravenously and a peritoneal transfer of 3x10^6 in vitro matured and NP68 pulsed dendritic cells. A control mouse (A) did not receive any T cells. Six days post T cell transfer mice received 10x10^6 target (0.2µM CFSE) and 10x10^6 reference splenocytes (2µM CFSE) intravenously. Twenty-four hours post transfer mice were sacrificed and their spleens taken for analysis by flow cytometry. Histograms were gated on viable and CFSE$^+$ cells. The percentage of target cells killed is shown for each histogram. Any deviation from the anticipated 1:1 ratio of target to reference cells in the mice not receiving T cells (A and D) was used to adjust the percentage killing in the mice receiving T cells. The mouse that received naive motheaten CD8$^+$ F5 T cells (C) killed more target cells than the mouse that received control CD8$^+$ F5 T cells (B).

	Type of naive $CD8^+$ F5 T cells transferred	Number of splenocytes post RBC lysis	Lymphocytes of total cells	Number of lymphocytes	$CD8^+$ cells of the lymphocyte gate	Number of $CD8^+$ T cells	Motheaten versus control
A	Control	$4x10^5$	36.6%	$1.46x10^5$	32%	$4.68x10^4$	
	Control	$7x10^5$	51%	$3.57x10^5$	17%	$6.07x10^4$	
	Motheaten	$1.2x10^6$	42%	$5.04x10^5$	22.5%	$1.13x10^5$	x2.92
	Motheaten	$1.3x10^6$	42.9%	$5.58x10^5$	18.4%	$1.03x10^5$	
	Motheaten	$1.5x10^6$	39.9%	$6x10^5$	16%	$9.6x10^4$	
B	Control	$1x10^6$	12.2%	$1.2x10^5$	21.1%	$2.57x10^4$	x1.33
	Motheaten	$1.6x10^6$	9.9%	$1.58x10^5$	21.6%	$3.42x10^4$	
C	Control	$9x10^5$	16.8%	$1.51x10^5$	19.5%	$2.94x10^4$	x1.31
	Motheaten	$6x10^5$	29%	$1.74x10^5$	22.2%	$3.86x10^4$	
D	Control	$2.3x10^6$	16%	$3.68x10^6$	12.6%	$4.6x10^4$	x3.47
	Motheaten	$2.6x10^6$	20%	$5.2x10^5$	31%	$1.6x10^5$	

Figure 3.10: Mice receiving naive motheaten $CD8^+$ F5 T cells have more $CD8^+$ cells in their spleens than mice receiving control $CD8^+$ F5 T cells

Naive $CD8^+$ F5 T cells were purified from control and motheaten mice. Either $3x10^6$ (A) or $2x10^6$ (B, C and D) of each population were transferred intravenously to recipient mice. Each mouse was primed subcutaneously with NP68 peptide in IFA. Seven days post T cell transfer each mouse was sacrificed and the spleen removed for analysis. following red blood cell lysis the splenoctyes were counted by trypan blue exclusion. The cells were then stained with anti-$CD8^{PE}$ (A and B) and anti-$Thy1.2^{FITC}$ (C and D) antibodies and analysed by flow cytometry. A lymphocyte gate was defined as determined by forward and side scatter and the percentage of $CD8^+$ or $CD8^+Thy1.2^+$ of this gate established for each mouse. In turn the absolute number of $CD8^+$ T cells was determined by using the initial cell counts. For each independent experiment the mice that received naive motheaten $CD8^+$ F5 T cells had consistently more $CD8^+$ cells in their spleens than mice that received control $CD8^+$ F5 T cells.

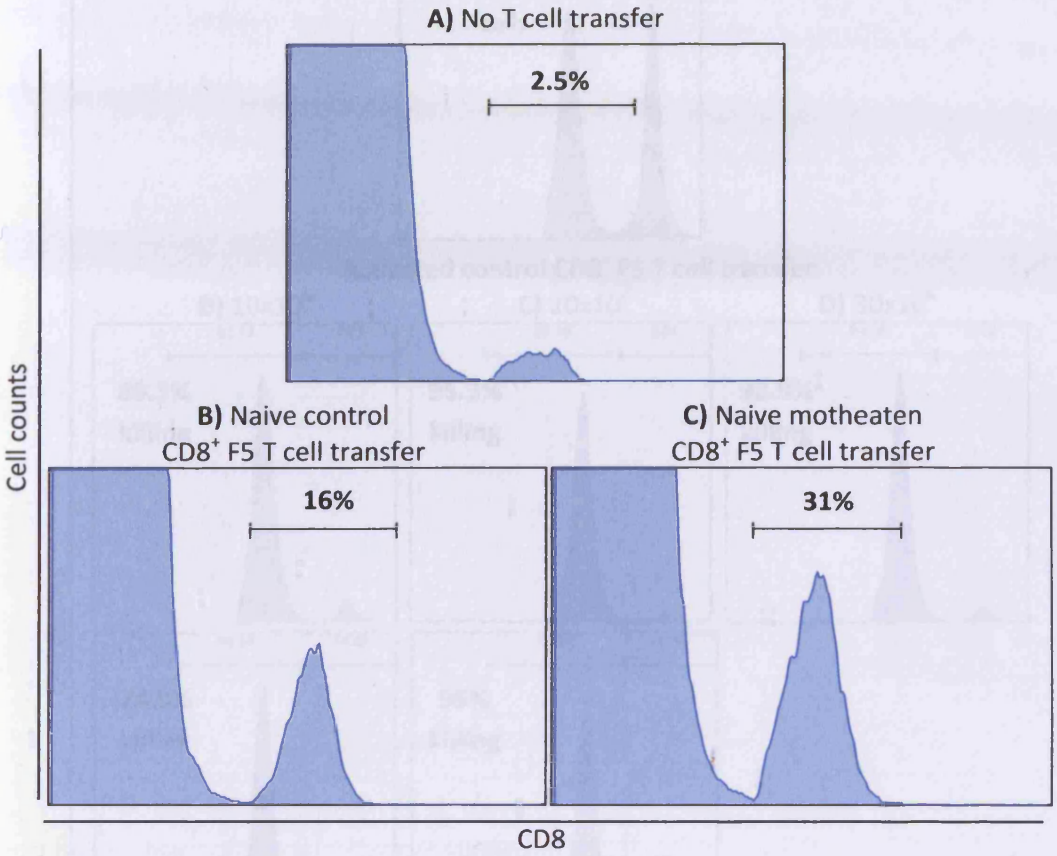


Figure 3.11: A mouse receiving naive motheaten $CD8^+$ F5 T have a greater proportion of $CD8^+$ cells in their spleen after seven days, when compared to a mouse receiving naive control $CD8^+$ F5 T cells

Rag-$1^{-/-}$ mice received $3x10^6$ naive control (B) or motheaten (C) $CD8^+$ F5 T cells intravenously and a subcutaneous injection of NP68 peptide in IFA. A control mouse (A) did not receive any T cells. Seven days post transfer the mice were sacrificed and their spleens taken. Prior to homogenisation a defined number of CFSE labelled splenocytes was added to each sample before labelling with anti-$CD8^{PE}$ antibody. The cells were then analysed by flow cytometry, during which a defined number of $CFSE^+$ cell events was acquired. Histograms were gated on a lymphocyte population to display the $CD8^+$ cells. The percentages represent the proportion of $CD8^+$ cells in comparison to the CFSE labelled reference cells. For the mouse that received naive control $CD8^+$ F5 T cells this was 16% (B), in comparison to 31% for the mouse that received naive motheaten $CD8^+$ F5 T cells (C).

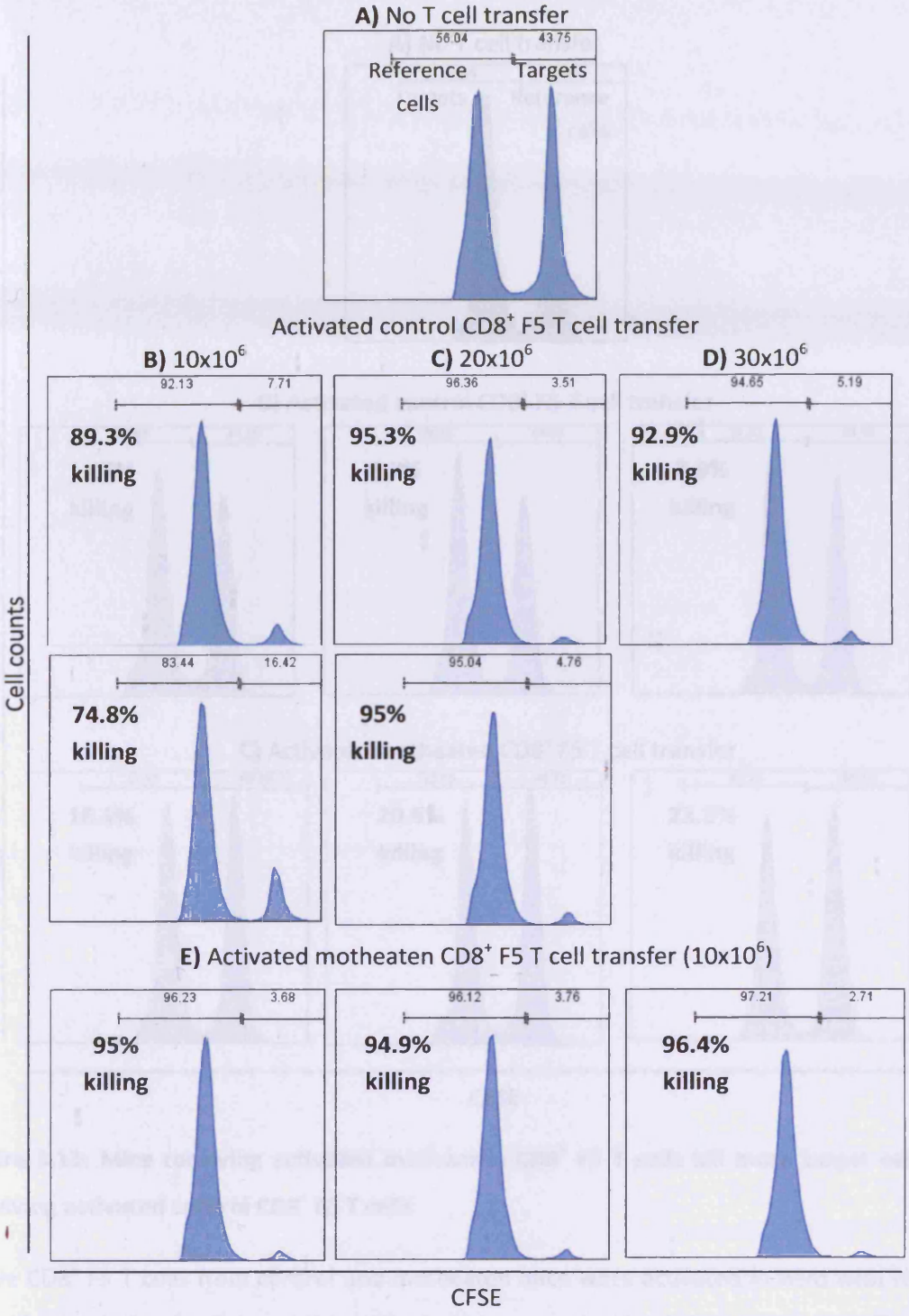


Figure 3.12: Mice receiving *in vitro* activated control or motheaten CD8$^+$ F5 T cells were able to kill target cells

Naive CD8$^+$ F5 T cells from control and motheaten mice were activated *in vitro* with NP68 peptide-pulsed splenocytes for 2 days and expanded for a further 2 days with IL-2. Cells were washed and prepared for intravenous transfer to recipient mice. Mice received either10x10^6 (B), 20x10^6 (C) or 30x10^6 (D) of control CD8$^+$ F5 T cells or 10x10^6 motheaten CD8$^+$ F5 T cells (E). A control mouse did not receive any T cells. Twenty-four hours later all mice received target and reference cell populations via an intravenous injection. Twenty-four hours later the mice were sacrificed and the spleens taken and prepared for analysis by flow cytometry. Histograms were generated by gating on viable and CFSE$^+$ cells, with the percentage of target cells killed displayed for each histogram. Any deviation from the anticipated 1:1 ratio of target to reference cells was adjusted for by using data from the mouse that did not receive any T cells (A).

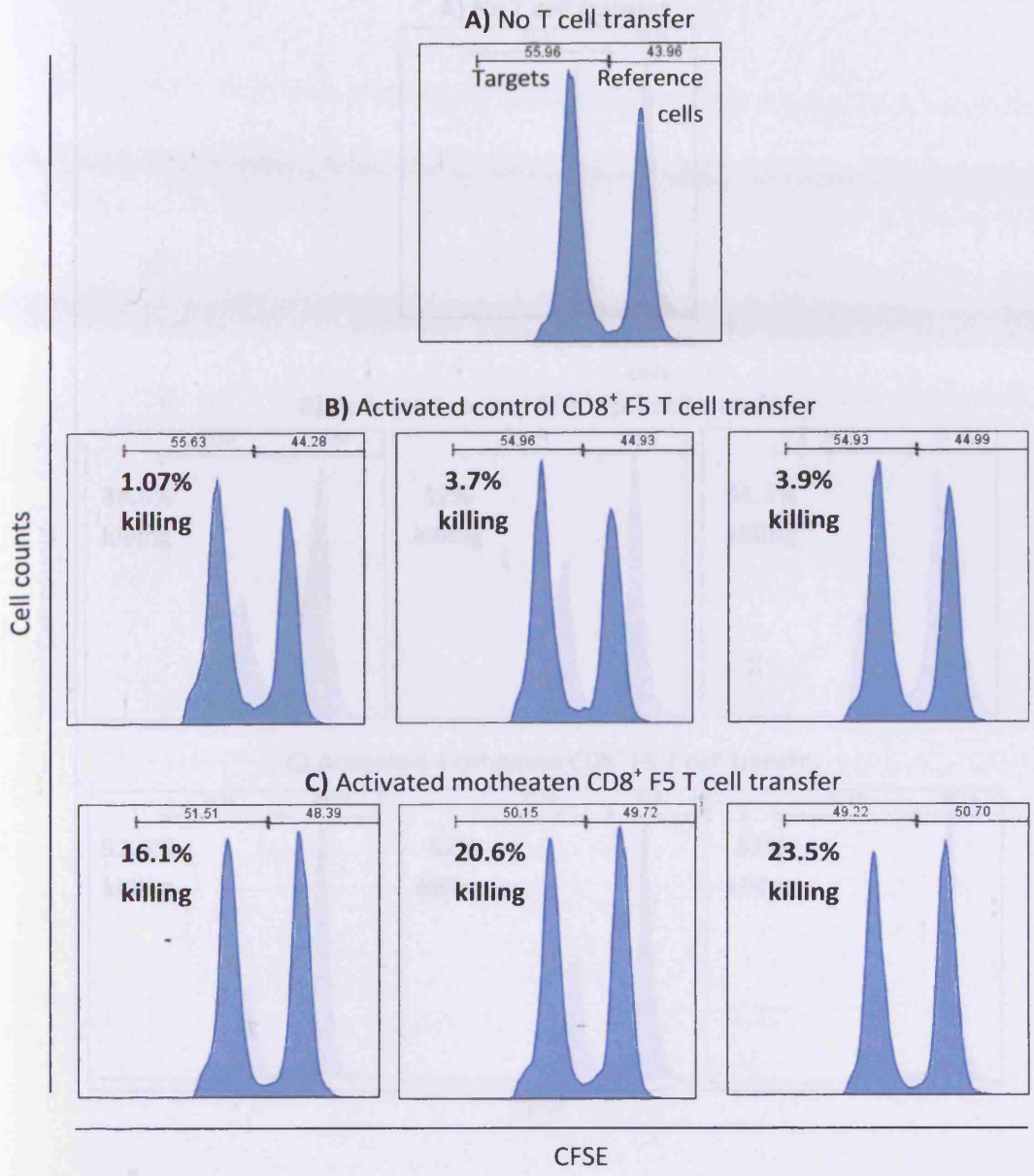


Figure 3.13: Mice receiving activated motheaten CD8$^+$ F5 T cells kill more target cells than mice receiving activated control CD8$^+$ F5 T cells

Naive CD8$^+$ F5 T cells from control and motheaten mice were activated *in vitro* with NP68 peptide-pulsed splenocytes for 2 days followed by further expansion for 2 days with IL-2. Cells were washed and prepared for intravenous transfer to recipient mice. A total of 2x10^6 of control or motheaten CD8$^+$ F5 T cells were transferred to each mouse. A control mouse did not receive any T cells. Twenty-four hours later all mice received target and reference cell populations via an intravenous injection. Twenty-four hours later the mice were sacrificed and the spleens taken and prepared for analysis by flow cytometry. Histograms were generated by gating on viable and CFSE$^+$ cells, with the percentage of target cells killed displayed for each histogram. Any deviation from the anticipated 1:1 ratio of target to reference cells was adjusted for by using data from the mouse that did not receive any T cells (A). All three mice that received activated motheaten CD8$^+$ F5 T cells (B) killed more of the target cells than the mice that received activated control CD8$^+$ F5 T cells (C).

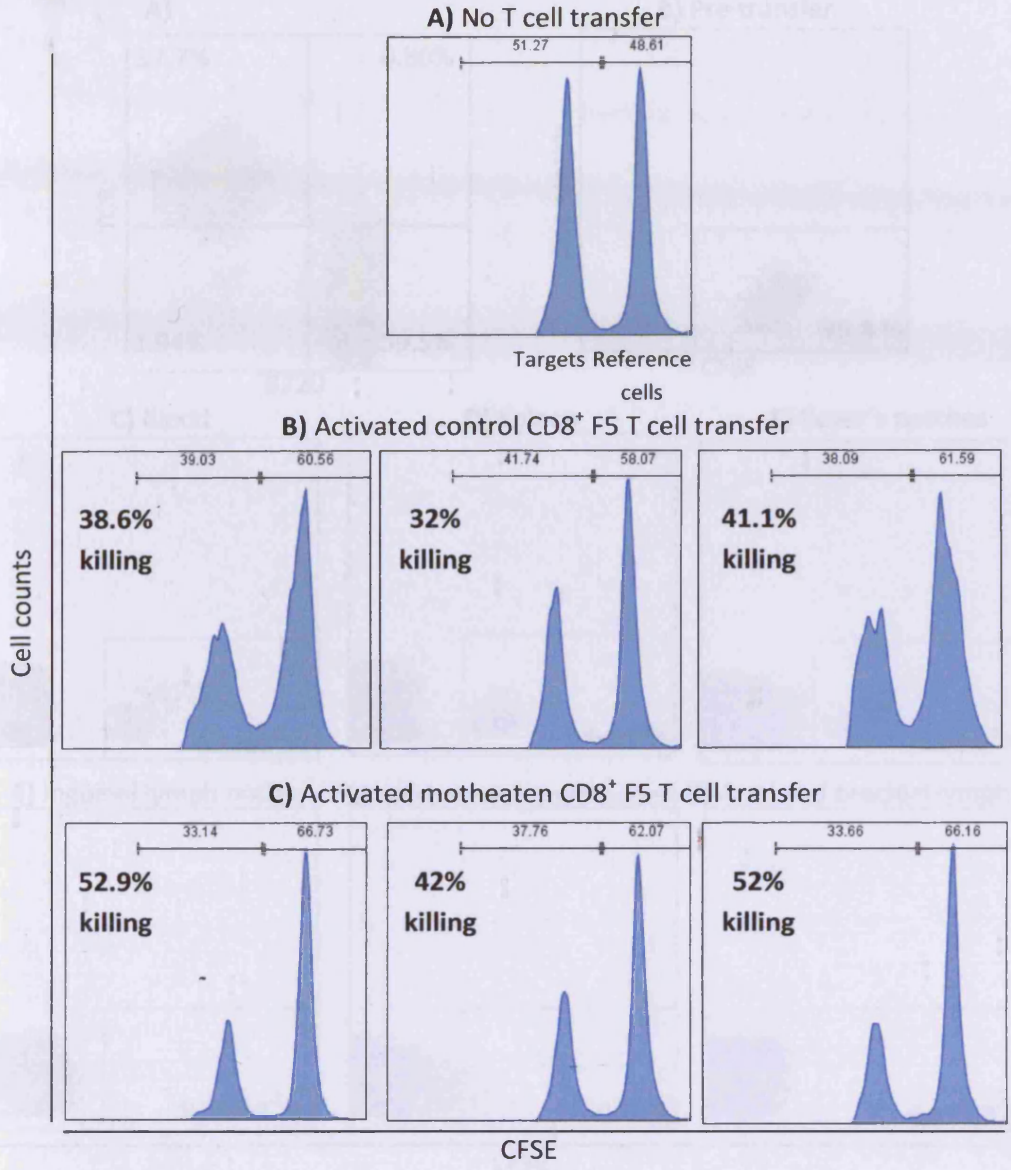


Figure 3.14: Mice receiving activated motheaten CD8$^+$ F5 T cells kill more target cells than mice receiving activated control CD8$^+$ F5 T cells

Naive CD8$^+$ F5 T cells from control and motheaten mice were activated *in vitro* with NP68 peptide-pulsed splenocytes for 2 days and further expanded for 2 days with IL-2. Cells were washed and prepared for intravenous transfer to recipient mice. A total of 5x10^6 of control or motheaten CD8$^+$ F5 T cells were transferred to each mouse. A control mouse did not receive any T cells. Twenty-four hours later all mice received target and reference cell populations via an intravenous injection. Twenty-four hours later the mice were sacrificed and the spleens taken and prepared for analysis by flow cytometry. Histograms were generated by gating on viable and CFSE$^+$ cells, with the percentage of target cells killed displayed for each histogram. Any deviation from the anticipated 1:1 ratio of target to reference cells was adjusted for by using data from the mouse that did not receive any T cells (A). All three mice that received activated motheaten CD8$^+$ F5 T cells (B) killed more of the target cells than the mice that received activated control CD8$^+$ F5 T cells (C).

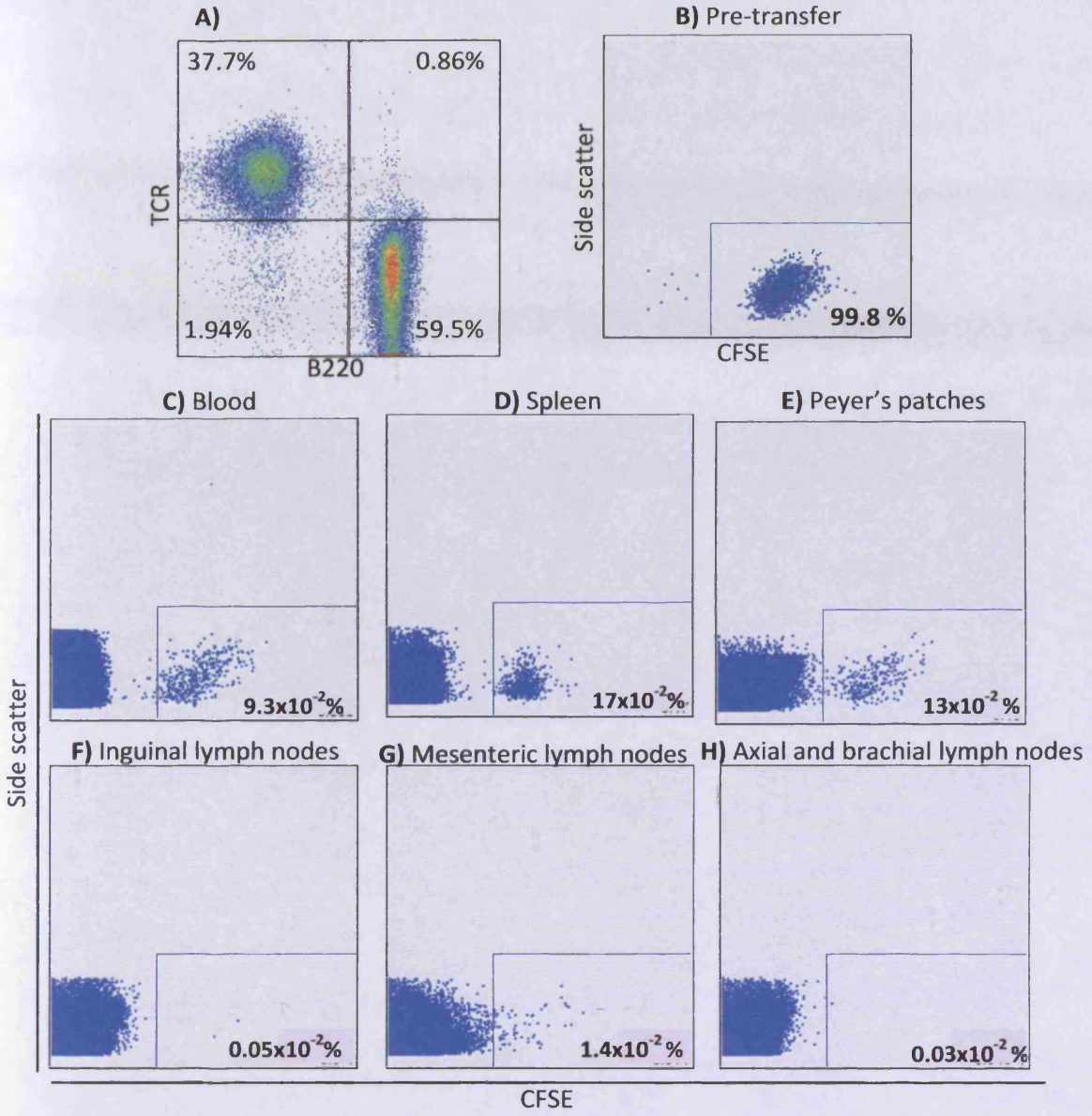


Figure 3.15: CD8$^+$ F5 T cells activated and expanded in vitro in the presence of retinoic acid are found in the Peyer's patches of a recipient mouse

The Peyer's patches from C57BL/6 mice contained both T cells and B cells (A), suggesting transferred T cells would migrate to this tissue. Naive control CD8$^+$ F5 T cells were activated in vitro and expanded in IL-2 for 5 days in total. This was done in the presence of 10nM retinoic acid. A mouse was sub-lethally irradiated twenty-four hours prior to the intravenous transfer of $25x10^6$ T cells labelled with 2μM CFSE. The blood, spleen, Peyer's patches, inguinal lymph nodes, brachial lymph nodes and axial lymph nodes were taken twenty-four hours post T cell transfer and prepared for flow cytometry. Dots plots were gated on a lymphocyte gate, as determined by forward and side scatter. The pre-transfer CFSE labelled cells (B) were used to define the CFSE$^+$ gate with the percentage of cells residing within this gate shown for each plot. The labelled cells were present in the blood (C), spleen (D) and Peyer's patches (E), with less in the mesenteric lymph nodes (G). Small numbers were present in the inguinal (F), axial and brachial lymph nodes (H).

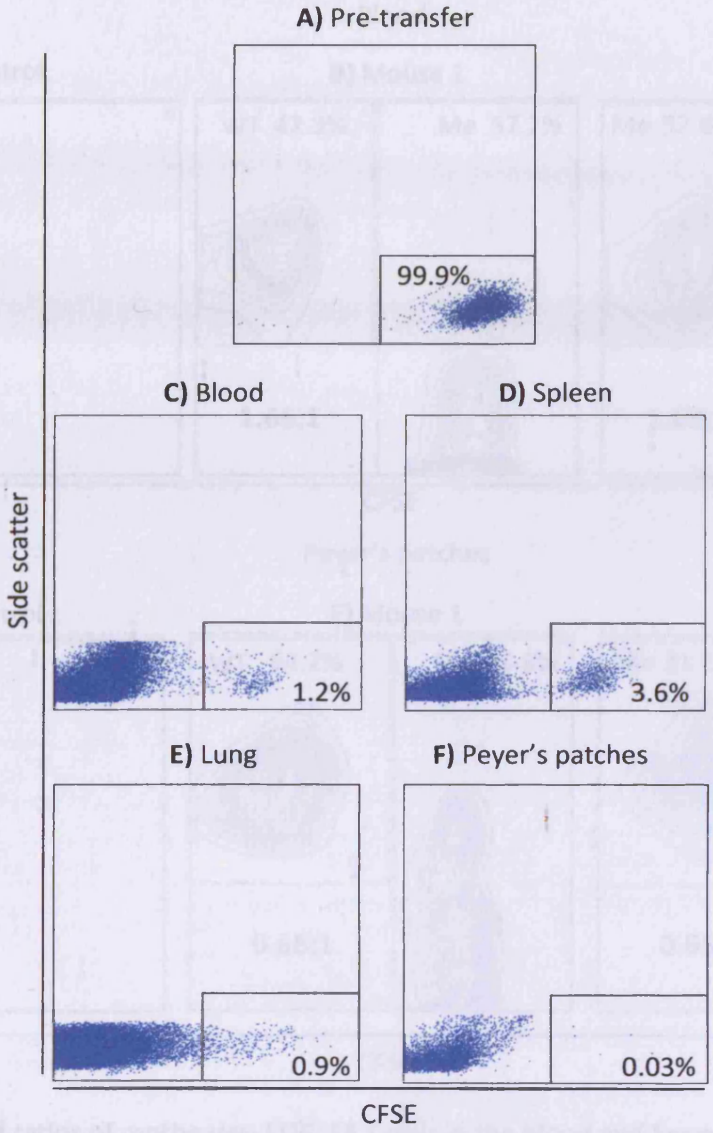


Figure 3.16: CD8$^+$ F5 T cells activated *in vitro* in the absence of retinoic acid are found in the blood, spleen and lungs but not the Peyer's patches of recipient mice

CD8$^+$ F5 T cells were activated *in vitro* and expanded in IL-2 for 5 days in total. This was done in the absence of retinoic acid. Mice were sub-lethally irradiated twenty-four hours prior to the intravenous transfer of 25x10^6 T cells labelled with 2μM CFSE. The blood, spleen, Peyer's patches, and lungs were taken 24 hours post T cell transfer and prepared for analysis by flow cytometry. The dots plots were gated on a lymphocyte gate as determined by forward and side scatter. The pre-transfer CFSE labelled cells (A) were used to define the CFSE$^+$ gate with the percentage of cells residing within this gate shown for each plot. The labelled cells were present in the blood (B), spleen (C) and lungs (D) but not in the Peyer's patches (E).

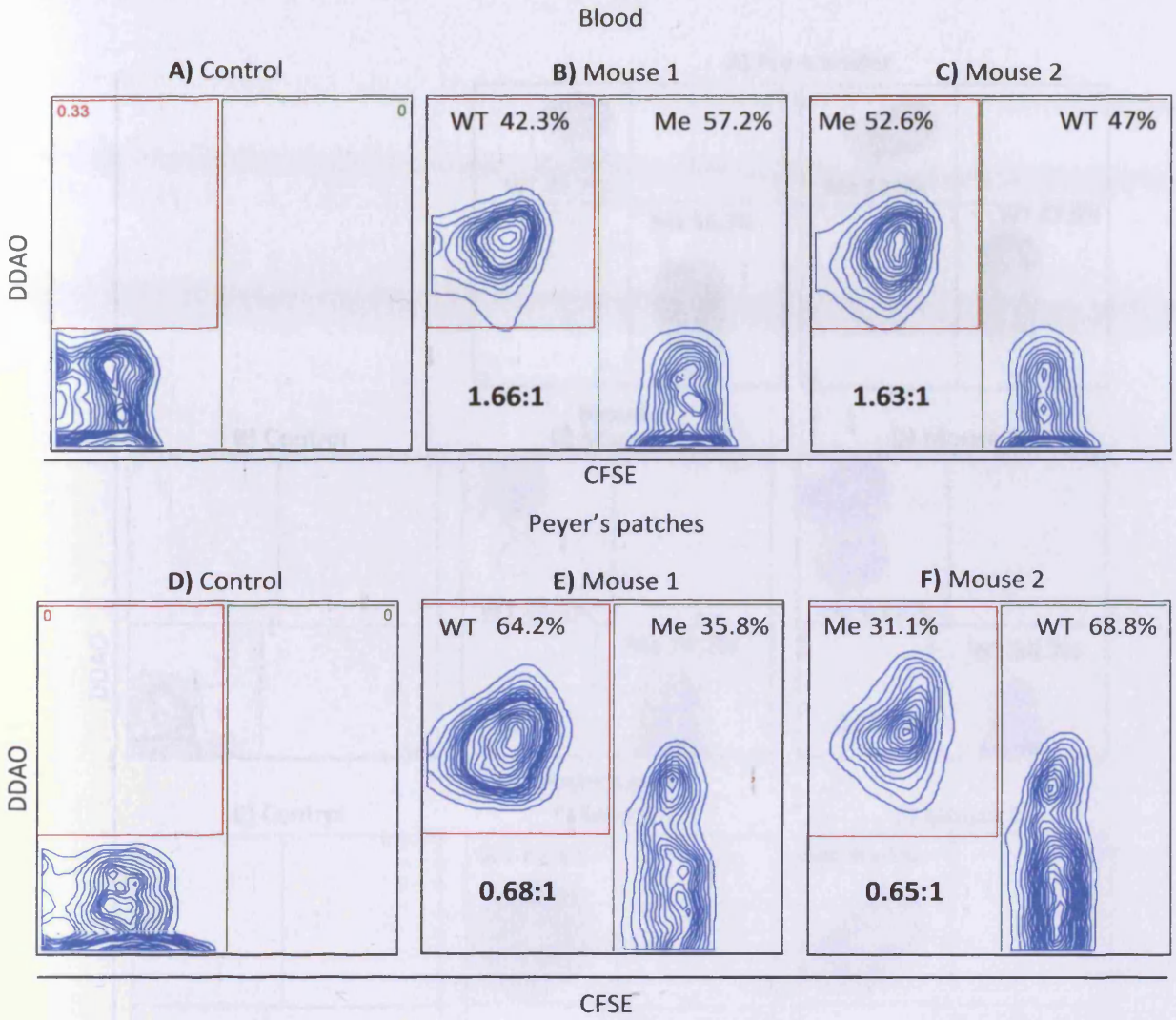


Figure 3.17: Altered ratios of motheaten CD8$^+$ F5 T cells in the blood and Peyer's patches of recipient mice

CD8$^+$ F5 T cells from motheaten and control mice were activated in vitro and expanded in IL-2 in the presence of retinoic acid. Mice were sub-lethally irradiated twenty-four hours prior to the intravenous transfer of 25x10^6 motheaten and 25x10^6 control T cells to the same mouse. The T cells were labelled with either 2μM CFSE or 10μM DDAO, and the dyes reversed for each T cell type to eliminate the possibility of any dye induced effects on the T cells. Two mice received T cells; the first had CFSE labelled motheaten T cells and DDAO labelled control T cells (B and E). The second mouse received DDAO labelled motheaten T cells and CFSE labelled control T cells (C and F). A third mouse did not receive any T cells (A and D). The pre-transfer ratio of motheaten to control T cells was established by flow cytometry (data not shown) and any deviation from the anticipated 1:1 ratio was later used to adjust the ratios of the cells harvested from mice. The contour plots are gated on a lymphocyte gate as determined by forward and side scatter, with the two gates shown set above the background from the mouse that did not receive any T cells (A and D). The percentage of cells residing in each gate is shown, and the ratio of motheaten to control T cells is shown in the lower left of each plot. For both mice, a greater proportion of motheaten T cells was found in the blood compared to control T cells (B and C). In the Peyer's patches a greater proportion of control T cells was found in comparison to motheaten T cells (E and F).

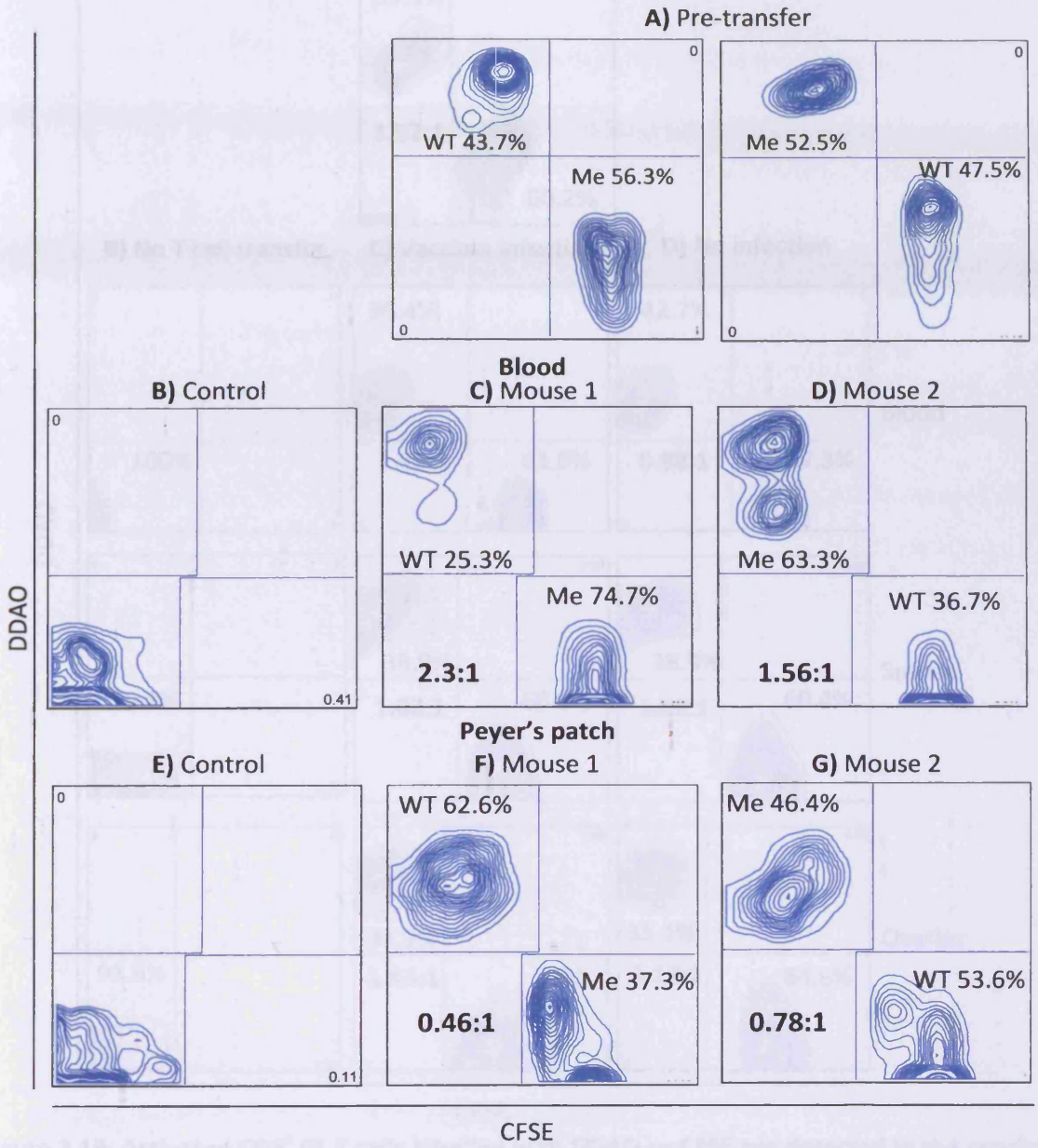


Figure 3.18: Altered ratios of motheaten CD8$^+$ F5 T cells in the blood and Peyer's patches of recipient mice

Motheaten and control CD8$^+$ F5 T cells were activated in vitro and expanded in IL-2 in the presence of retinoic acid. Sub-lethally irradiated mice received 25x10^6 motheaten and 25x10^6 control T cells. One mouse received motheaten T cells labelled with CFSE and control T cells labelled with DDAO (C and F). The second mouse received CFSE labelled motheaten T cells and DDAO labelled control T cells (D and G). A third mouse did not receive any T cells (B and E). The contour plots were gated on a lymphocyte gate with the two fluorescent gates set above the background from the mouse that did not receive any T cells (B and E). The percentage of cells is shown for each gate and the ratio of motheaten to control T cells is shown in the lower left of each plot. The ratio was adjusted for any deviation from the anticipated 1:1 ratio of DDAO labelled to CFSE labelled cell by using the pre-transfer plots. For both mice, a greater proportion of motheaten T cells was found in the blood compared to control T cells (C and D). In the Peyer's patches a greater proportion of control T cells was found in comparison to motheaten T cells (F and G).

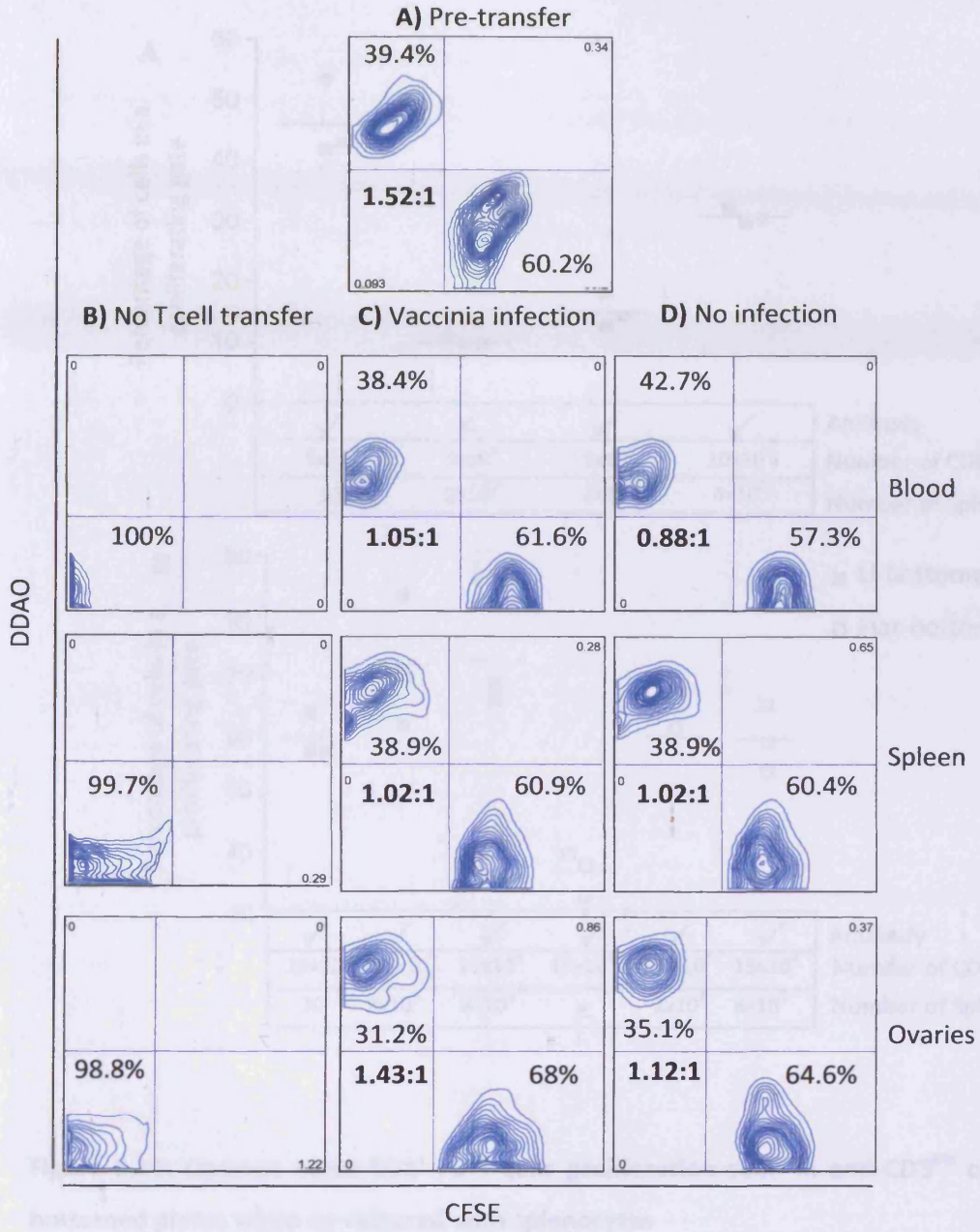


Figure 3.19: Activated CD8$^+$ F5 T cells labelled with DDAO or CFSE are detected in the ovaries of recipient mice

Mice were sub-lethally irradiated twenty-four hours prior to peritoneal injection of 1x10^6 P.F.U. of recombinant Vaccinia virus encoding the NP68 epitope. Four days post Vaccinia infection mice received at total of 20x10^6 CD8$^+$ F5 T cells that were labelled with either CFSE or DDAO. The T cells had been activated in vitro and expanded for four days with IL-2. Immediately prior to intravenous transfer of the T cells the ratio of DDAO labelled to CFSE labelled cells was confirmed by flow cytometry (A). Twenty-four hours post adoptive transfer of T cells the mice were sacrificed and the blood, spleen and ovaries taken and prepared for flow cytometry. Contour plots displaying fluorescence were gated on a viable cells and the autofluorescence seen in the mouse that did not receive T cells was gated out. The percentage of cells residing in each quadrant is shown for each plot. Labelled cells were detected in the blood, spleen and ovaries of both the infected and un-infected mice (C and D). The proportion of DDAO and CFSE labelled T cells in the tissues of the mice was similar to the proportion that was initially transferred (A).

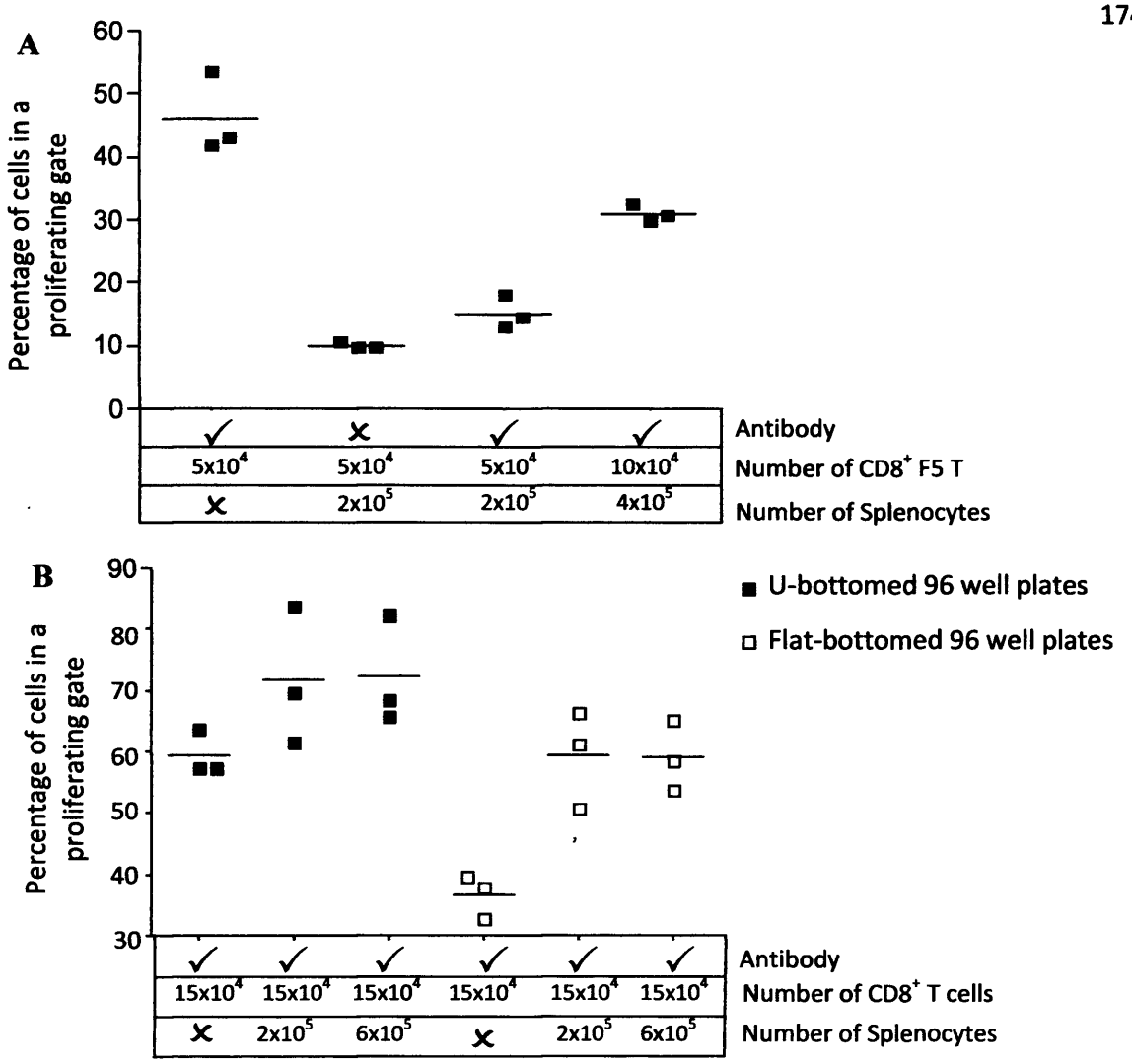


Figure 3.20: Optimal naive CD8$^+$ F5 T cells proliferation seen in anti-CD3^{Bio} coated U-bottomed plates when co-cultured with splenocytes

Flat-bottomed and U-bottomed plates were coated with 5μg/ml of anti-CD3^{Bio} antibody overnight at 4°C and then incubated at 37°C for an hour. Either 5x10^4 (a), 10x10^4 (a) or 15x10^4 (b) purified CD8$^+$ CFSE (2μM) labelled T cells were plated out with antibody alone (a and b), splenocytes alone (a) or with antibody and different numbers (in brackets) of splenocytes from Rag1$^{-/-}$ mice. Three days later cells were harvested and labelled with CD8^{PE}. Cells were then analysed by flow cytometry and the percentage of cells in the proliferating gate plotted for comparison.

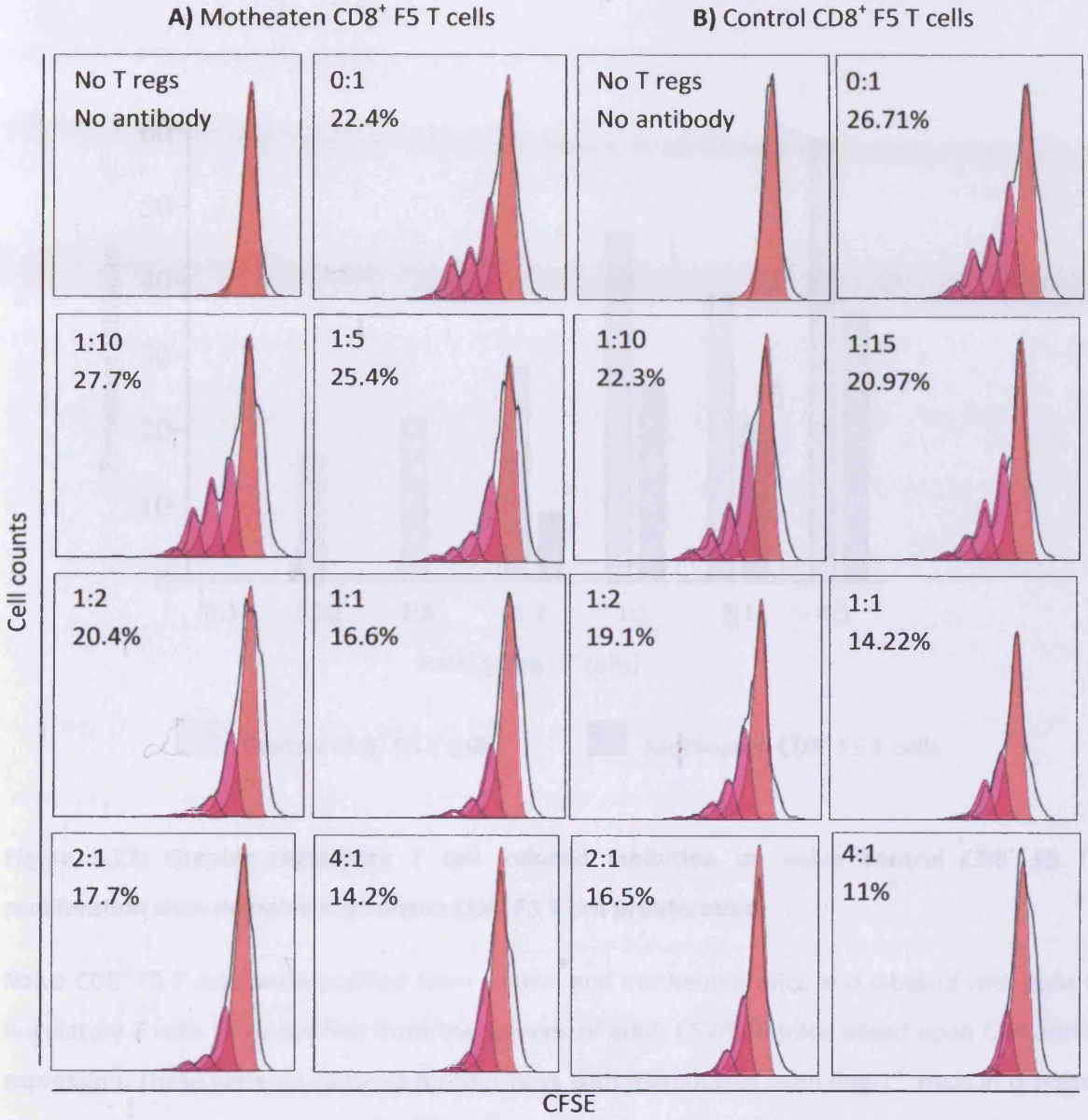


Figure 3.21: Regulatory T cells inhibited both naive control and motheaten CD8^{+} F5 T cells proliferation

Naive CD8^{+} F5 T cells were purified from control and motheaten mice and labelled with 2μM CFSE. Regulatory T cells were purified form the spleens of adult C57BL/6 mice based upon CD4 and CD25 expression. These were co-cultured for four days with splenocytes from Rag-1$^{-/-}$ mice in U-bottomed 96 well plates coated with anti-CD3^{Bio} antibody. This was done at seven Treg to T cell ratios, as shown for each histogram. T cells were also cultured alone in un-coated plates. Each condition was performed once apart from the 0:1 ratio, which was performed in triplicate. Cells were harvested and stained with anti-CD8^{PE} antibody and analysed by flow cytometry. Histograms displaying CFSE fluorescence were gated on CD8^{+} cells. Data was analysed using the proliferation tool of FlowJo software. The undivided population (in red) was defined using the data from wells were T cells were cultured without Tregs and anti-CD3^{Bio} antibody. This was set for each histogram plot to reveal the percentage of cells from the original population that had entered in to proliferation (shown for each histogram, with the mean displayed for the 0:1 ratio). From this data the percentage inhibition was calculated (Figure 3.22).

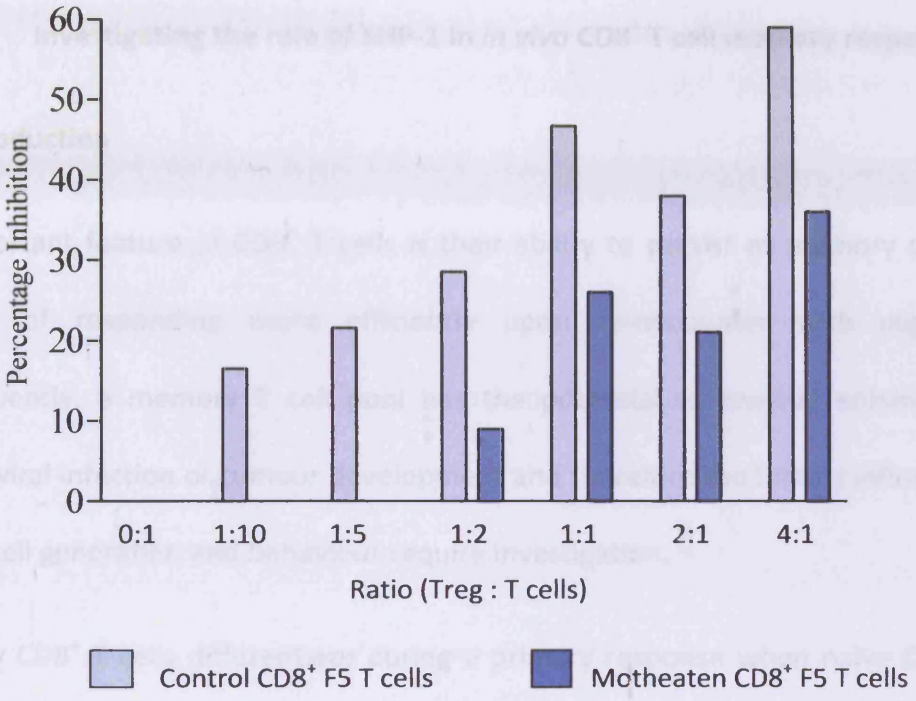


Figure 3.22: Greater regulatory T cell induced inhibition on naive control CD8$^+$ F5 T cell proliferation than on naive motheaten CD8$^+$ F5 T cell proliferation

Naive CD8$^+$ F5 T cells were purified from control and motheaten mice and labelled with 2μM CFSE. Regulatory T cells were purified form the spleens of adult C57BL/6 mice based upon CD4 and CD25 expression. These were co-cultured for four days with splenocytes from Rag-1$^{-/-}$ mice in U-bottomed 96 well plates coated with anti-CD3^{Bio} antibody. This was done for seven Treg to T cell ratios. Each condition was performed once apart from the ratio of 0:1, which was performed in triplicate. Cells were harvested and stained with anti-CD8^{PE} antibody and analysed by flow cytometry. Histogram displaying CFSE fluorescence were gated on CD8$^+$ cells and analysed using the proliferation tool of FlowJo software (figure 3.21). The percentage inhibition was then calculated by comparing the proportion of naive T cells that had entered into proliferation for each condition with the proliferation seen when the T cells had been cultured without Tregs (this figure). At each ratio a greater degree of Treg induced inhibition of T cell proliferation was seen for control CD8$^+$ F5 T cells than motheaten CD8$^+$ F5 T cells.

Chapter 4

Investigating the role of SHP-1 in *in vivo* $CD8^+$ T cell memory responses

4.1 Introduction

An important feature of $CD8^+$ T cells is their ability to persist as memory cells, which are capable of responding more efficiently upon re-encounter with cognate antigen. Consequently, a memory T cell pool has the potential to provide enhanced protection against viral infection or tumour development and therefore the factors influencing memory $CD8^+$ T cell generation and behaviour require investigation.

Memory $CD8^+$ T cells differentiate during a primary response when naive $CD8^+$ T cells are stimulated by cognate antigen. In humans, there are two main memory $CD8^+$ T cell subtypes, known as central and effector. The subtypes are distinguished based upon their role and tissue location (Sallusto *et al.*, 1999), as determined by their expression of key genes. Central memory $CD8^+$ T cells act as stem cells for the memory T cell pool, as they maintain the ability to divide. They are predominantly found in secondary lymphoid organs as they express cell surface molecules that allow them to home to these sites. Effector memory $CD8^+$ T cells are mainly found in peripheral tissue and have the potential to exert immediate cytotoxic function as they produce molecules that are able to directly kill target cells.

Thus far, the potential role of SHP-1 in memory $CD8^+$ T cell has not been explored, in either an in ex-vivo or *in vivo* context. However, the adaptation of protocols and assays developed during this study to look at primary *in vivo* $CD8^+$ T cell responses to antigen has additionally allowed SHP-1 deficient $CD8^+$ F5 T cells to be studied in *in vivo* memory responses.

Briefly, naive $CD8^+$ F5 T cells were purified from both control and motheaten mice and transferred to individual recipient mice, which were primed with NP68 peptide. Mice were

left for a defined period to allow a memory T cell pool to form, which was then recalled with a second dose of NP68 peptide. The memory $CD8^+$ T cell response mounted by the recipient mice was assessed by providing CFSE labelled target (0.2μM) and reference (2μM) cells, as described above in chapter three. Control mice for each experiment did not receive any T cells but subsequently received the target and reference cells. Data from the control mice was used to adjust for any deviation from the anticipated 1:1 ratio of target to reference cells in recipient mice. During analysis, histograms were generated by gating on a viable and $CFSE^+$ cell population.

During this study, experiments were performed that utilised different modes of priming the naive and memory $CD8^+$ T cells within recipient mice, with the aim of defining a protocol to study memory $CD8^+$ F5 T cells. In addition, a number of pilot experiments were performed, which had the potential to further dissect the role of SHP-1 in memory $CD8^+$ T cell formation and function.

4.2 Mice receiving naive control $CD8^+$ F5 T cells killed more target cells during a memory T cell response than mice receiving naive motheaten $CD8^+$ F5 T cells, when the memory T cells are recalled by priming with NP68 peptide in IFA

Initially Rag-$1^{-/-}$ were used as recipient mice for the study of memory $CD8^+$ F5 T cell responses. This ensured that it was exclusively the adoptively transferred T cells being studied over the duration of the assay.

In three independent experiments, Rag-$1^{-/-}$ recipient mice received an intravenous transfer of naive control or motheaten $CD8^+$ F5 T cells and a subcutaneous injection of NP68 peptide in IFA. Control mice did not receive any T cells. In each of the successive experiments the number of $CD8^+$ F5 T cells transferred was $3x10^6$, $2x10^6$ and $2.2x10^6$ respectively, as dictated by the availability of motheaten mice. Six weeks following T cell transfer, all mice received

NP68 peptide in IFA as a subcutaneous injection. Seven days later, all mice received CFSE labelled target and reference cells intravenously. Twenty-four hours later, mice were sacrificed and their spleens taken for analysis by flow cytometry. Histograms were generated by gating on a viable and $CFSE^+$ cell population.

The data from three independent experiments showed that the mice that received naive control $CD8^+$ F5 T cells killed 81% (figure 4.1B), 74% (figure 4.2B) and 72% (figure 4.3B) of the target cells during a memory response in comparison to 47% (figure 4.1C), 55% (figure 4.2C) and 37% (figure 4.3C) of the target cells killed in the corresponding mice that received naive motheaten $CD8^+$ F5 T cells.

The spleens from the mice in the second experiment (74% and 55% of target cells killed by control and motheaten T cells respectively) were stained with anti-$CD8^{PE}$ antibody prior to flow cytometry. The proportion of $CD8^+/CFSE^-$ cells of a lymphocyte gate in the spleen of the mouse that received naive control $CD8^+$ F5 T cells was 26% (figure 4.2B) compared to 15.4% in the mouse that received naive motheaten $CD8^+$ F5 T cells (figure 4.2C). For the mouse that did not receive any T cells the proportion of $CD8^+/CFSE^-$ cells of a lymphocyte gate within the spleen was 8.97% (figure 4.2A). Therefore the enhanced killing seen in the mouse that received naive control $CD8^+$ F5 T cells correlated with a greater proportion of adoptively transferred $CD8^+$ cells at the site of killing.

4.3 The mode of priming memory control and motheaten $CD8^+$ F5 T cells impacts upon the memory $CD8^+$ F5 T cell response

During the early stages of the memory T cell studies it became an increasing concern that when NP68 peptide is administered in IFA it may bind to MHC class I molecules belonging to adoptively transferred T cells. This would potentially lead to fratricide within the adoptively transferred $CD8^+$ memory T cell pool, which could in turn influence the memory T cell

response. Therefore, it seemed logical to explore a different mode of priming the memory T cells to see whether in made a difference to the memory response being detected.

Rag-$1^{-/-}$ recipient mice received an intravenous transfer of $2.2x10^6$ naive control or motheaten $CD8^+$ F5 T cells and a subcutaneous injection of NP68 peptide in IFA. Control mice did not receive any T cells. Six weeks following T cell transfer, mice were primed with either NP68 peptide in IFA as a subcutaneous injection, or by the peritoneal transfer of $3x10^6$ matured and NP68 peptide-pulsed dendritic cells. Seven days later, all mice received CFSE labelled target and reference cells intravenously. Twenty-four hours later, mice were sacrificed and their spleens taken for analysis by flow cytometry. Histograms were gated on viable and $CFSE^+$ cells to reveal the target and reference cells.

When mice were primed with NP68 peptide in IFA, for both the initial and recall priming, the mouse that received naive control $CD8^+$ F5 T cells killed 72% of the target cells (figure 4.3B) compared to 37% of the target cells being killed in the mouse that received naive motheaten $CD8^+$ F5 T cells (figure 4.3C). However, when mice were primed with NP68 peptide in IFA for the initial priming and matured NP68 peptide-pulsed DCs for the recall priming, the mouse that received naive control $CD8^+$ F5 T cells killed 52% of the target cells (figure 4.3D) whereas the mouse that received naive motheaten $CD8^+$ F5 T cells killed 80% of the targets (figure 4.3E).

4.4 Mice receiving naive motheaten $CD8^+$ T cells killed more target cells during a memory T cell response than mice receiving naive control $CD8^+$ T cells, when memory T cells are recalled by priming with NP68 peptide-pulsed DCs

Previous data demonstrated that when memory T cells were primed with NP68 peptide in IFA, mice that received control $CD8^+$ F5 T cells killed more targets than mice that received motheaten $CD8^+$ F5 T cells (three experiments; figures 4.1, 4.2 and 4.3B and C), whereas

when DCs pulsed with NP68 peptide were used to re-challenge mice for a second time the converse was seen (Figure 4.3C and 4.3D). In light of this, two further independent experiments were performed that used NP68 peptide-pulsed DCs to prime memory $CD8^+$ F5 T cells.

For each experiment Rag-$1^{-/-}$ recipient mice received an intravenous transfer of naive control or motheaten $CD8^+$ F5 T cells and a subcutaneous injection of NP68 peptide in IFA. Control mice did not receive any T cells. For the first experiment, mice received $2x10^6$ T cells (figure 4.4), whereas $2.8x10^6$ were transferred in the second experiment (figure 4.5). Six weeks following T cell transfer, all mice including the control mouse, received $3x10^6$ matured and NP68 peptide-pulsed dendritic cells by peritoneal transfer. Seven days later, all mice received CFSE labelled target and reference cells intravenously. Twenty-four hours later mice were sacrificed and their spleens taken for analysis by flow cytometry. Histograms displaying CFSE fluorescence were gated on viable and $CFSE^+$ cells.

The data from two independent experiments demonstrated that the mice that received naive control $CD8^+$ F5 T cells killed 68% (figure 4.4B) and 72% (figure 4.5B) of the target cells during a memory response in comparison to 78% (figure 4.4C) and 84% (figure 4.5C) of the target cells killed in the corresponding mice receiving naive motheaten $CD8^+$ F5 T cells. This tallied with an earlier experiment where 52% of the target cells were killed by a mouse that received naive control $CD8^+$ F5 T cells (figure 4.3D) compared to 80% of target cells killed by a mouse that received naive motheaten $CD8^+$ F5 T cells (figure 4.3E).

4.5 Mice receiving naive motheaten $CD8^+$ T cells killed more target cells during a memory T cell response than mice receiving naive control $CD8^+$ T cells, when both naive and memory T cells are primed with NP68 peptide pulsed DCs

Previous data showed that the mode of priming memory T cells seemed to have an impact upon the memory response of control and motheaten $CD8^+$ F5 T cells. To further explore this observation, an experiment was performed that utilised matured and NP68 peptide-pulsed dendritic cells to prime both naive and memory $CD8^+$ F5 T cells.

Rag-$1^{-/-}$ recipient mice received an intravenous transfer of $1x10^6$ naive control or motheaten $CD8^+$ F5 T cells and a peritoneal transfer of $3.8x10^6$ matured and NP68 peptide-pulsed DCs. Control mice did not receive any T cells. Six weeks following T cell transfer, all mice received $3x10^6$ matured and NP68 peptide-pulsed dendritic cells by peritoneal transfer. Seven days later all mice received CFSE labelled target and reference cells intravenously. Twenty-four hours later, mice were sacrificed and their spleens taken for analysis by flow cytometry.

The mice that received naive control $CD8^+$ F5 T cells killed 61% and 62% of the target cells (figure 4.6B) during a memory response in comparison to 89% and 78% of the target cells killed in the mice that received naive motheaten $CD8^+$ F5 T cells (figure 4.6C).

4.6 Mice receiving *in vitro* activated control $CD8^+$ T cells kill target cells during a memory response seven weeks post transfer

The data in chapter three demonstrated that after one week of antigen driven T cell expansion mice that received naive motheaten $CD8^+$ F5 T cells had a greater proportion of $CD8^+$ cells in their spleens compared to mice that received naive control $CD8^+$ F5 T cells. It is a possibility that the enhanced expansion of motheaten $CD8^+$ F5 T cells during a primary response may lead to the accumulation of more memory motheaten $CD8^+$ F5 T cells, when compared to control $CD8^+$ F5 T cells. This may explain the data shown earlier in this chapter demonstrating the enhanced killing of target cells by memory motheaten $CD8^+$ F5 T cells following DC priming. To explore this hypothesis further an experiment was planned that involved transferring the same number of *in vitro* activated and expanded control and

motheaten $CD8^+$ F5 T cells to recipient mice. The mice would then be primed six weeks later followed by the administration of target and reference cells to assess the magnitude of the memory response. Although the lack of availability of motheaten mice did not allow this experiment to be conducted, a pilot experiment was nevertheless performed using control $CD8^+$ F5 T cells to establish whether *in vitro* activated $CD8^+$ F5 T cells could differentiate into memory cells and mount a response following their *in vivo* transfer.

Naive control $CD8^+$ F5 T cells were activated *in vitro* for 2 days with NP68 loaded splenocytes followed by two days of expansion in IL-2. Cells were washed thoroughly and either $3x10^6$ or $5x10^6$ transferred to Rag-$1^{-/-}$ recipient mice. A control mouse did not receive any T cells. Six weeks post T cell transfer the mice were primed with $3x10^6$ matured and NP68 peptide-pulsed DCs that were transferred into the peritoneal cavity. Six weeks later all mice received CFSE labelled target and reference cells intravenously. Twenty-four hours later the spleens were taken and prepared for flow cytometry.

The mouse that received $3x10^6$ activated T cells killed 64% of the targets (figure 4.7B) and the mouse that received $5x10^6$ T cells killed 85% of the targets (figure 4.7C) thus demonstrating the feasibility of the proposed assay.

4.7 A mouse kills target cells during a memory T cell response without being primed for a second time

Memory $CD8^+$ T cells are found in two main subsets, those that can provide immediate effector action (effector memory) and those that expand upon antigenic stimulation (central memory). In order to potentially distinguish the contributions of central and effector memory T cells to a memory response in mice receiving control or motheaten $CD8^+$ F5 T cells, a further pilot experiment was performed that looked at both the effector and central memory response.

Two Rag-$1^{-/-}$ recipient mice received $2.5x10^6$ control $CD8^+$ F5 T cells and a subcutaneous injection of NP68 peptide in IFA. Control mice did not receive any T cells. Six weeks following T cell transfer, one mouse received $3x10^6$ matured and NP68 peptide-pulsed DCs by peritoneal transfer in order to look at the total memory $CD8^+$ T cell response. The second mouse did not receive a re-challenge with DCs in order to examine the effector memory $CD8^+$ T cell response. Seven days later all mice received CFSE labelled target and reference cells intravenously. Twenty-four hours later, mice were sacrificed and their spleens taken for analysis by flow cytometry.

The mouse that received naive $CD8^+$ F5 T cells and two challenges with NP68 peptide killed 59.1% of the target cells (figure 4.8C). The mouse that received naive $CD8^+$ F5 T cells and a single challenge with NP68 peptide killed 41.8% of the target cells (figure 4.8B), which can be attributed to the action of effector memory $CD8^+$ F5 T cells. The difference in the number of targets killed between the two mice can be attributed to the action of the central memory $CD8^+$ F5 T cells.

4.8 Mice receiving naive motheaten $CD8^+$ F5 T cells kill more target cells during a memory T cell response than mice receiving naive control $CD8^+$ F5 T cells

As the memory T cell studies progressed it became increasingly apparent that the transfer of naive $CD8^+$ F5 T cells was having a negative effect on the health of the Rag-$1^{-/-}$ recipient mice. Towards the end of the assay (at 6-7 weeks) those mice that had received T cells started to lose condition; their fur became dull, they exhibited weight loss and had diarrhoea. Due to both ethical reasons and the concern that this may affect the memory T cell response an alternative protocol was sought.

As Rag-$1^{-/-}$ mice lack any regulatory T cells it was proposed that the decline in health maybe due to the unchecked activity of the transferred $CD8^+$ F5 T cells in the tissue of the

gastrointestinal tract. Therefore sub-lethally irradiated mice were used instead of Rag-$1^{-/-}$ mice as their T cell compartments (including Tregs) would recover over the duration of the assay.

A group of three mice received either $1x10^6$ naive control or motheaten $CD8^+$ F5 T cells. A group of four mice did not receive any T cells. All mice were primed subcutaneously with NP68 peptide in IFA. The mice remained healthy throughout the assay, with the only evident side effect of the irradiation (650cGy) being the greying of the fur. Six weeks post-transfer, each mouse received $3x10^6$ matured and NP68 peptide-pulse DCs via the peritoneal cavity. Seven days later all mice received CFSE labelled target and reference cells intravenously. At this point a control mouse was irradiated and received the CFSE labelled target and reference cells. Twenty-four hours later all mice were sacrificed and their spleens prepared for analysis by flow cytometry.

No target cells were killed by the mice that did not receive any T cells but were primed in the same manner as those that did (figures 4.9B and 4.10), indicating that the recipient mice were unable to mount an endogenous $CD8^+$ F5 T cell response under these conditions. The mice that received naive control $CD8^+$ F5 T cells killed 3.6%, 10.7% and 22% of the target cells (figures 4.9C and 4.10), whereas the mice that received naive motheaten $CD8^+$ F5 T cells killed 32%, 53% and 56% of the target cells (figures 4.9D and 4.10). The difference in the number of target cells killed between the two sets of mice was not statistically significant (p=0.1).

4.9 Rag-$1^{-/-}$ mice receiving naive $CD8^+$ F5 T cells develop colitis

An experiment was performed to further investigate the progressive wasting exhibited by Rag-$1^{-/-}$ mice involved in the study of memory T cell responses. A group of three Rag-$1^{-/-}$ mice received naive $CD8^+$ F5 T cells and NP68 in IFA (mice 4, 5 and 6). Two Rag-$1^{-/-}$ mice received

naive $CD8^+$ F5 T cells but no NP68 (mice 7 and 8). A control group of mice did not receive $CD8^+$ F5 T cells or NP68 (mice 1, 2 and 3). Each group of mice was kept in separate cages in order to monitor for symptoms of colitis.

Mice that received $CD8^+$ F5 T cells and NP68 produced loose stools from 2 weeks onwards, whereas those that received T cells alone produced loose stools from weeks 6-7 onwards. The control group remained healthy throughout the experiment. The body weight of the mice was monitored weekly for the duration of the assay. The controls, mice 1, 2 and 3 (no T cells and no NP68) gained 26.4% (mean) of their initial body weight over the duration of the assay (8 weeks) (figure 4.11). Mice that received T cells but no NP68 (numbers 7 and 8) initially gained 5.3% (mean) of their initial body weight but subsequently lost 7.44% (mean) of their maximum body weight (weeks 3 and 4 for individual mice) (figure 4.11). Finally, mice that received both T cells and NP68 (numbers 4, 5 and 6) lost 3.4% (mean) of their initial body weight, and 18.3% (mean) of their maximum body weight (weeks 3 and 5 for individual mice) over the duration of the assay (figure 4.11). As mice had lost a considerable percentage of their body weight by week 8 the assay was terminated and tissues harvested for further analysis.

4.10 Mice receiving naive $CD8^+$ F5 T cells exhibit splenomegaly, lymphomegaly and a cellular infiltrate into their large intestine

Eight weeks post T cell transfer (as described for 4.9) mice were sacrificed and tissues taken for analyses. Upon dissection, it was immediately apparent that all mice that had received T cells and NP68 (numbers 4, 5 and 6) had splenomegaly, lymphomegaly (mesenteric lymph nodes) and an enlarged large intestine, when compared to control mice. One mouse that had received T cells but no NP68 peptide (number 8) also exhibited a similar gross pathology to that of the mice that also received NP68 peptide. The second mouse that received T cells

but no NP68 (number 7) did not exhibit splenomegaly but did exhibit lymphomegaly (mesenteric lymph nodes) and a slight enlargement of the large intestine.

The spleen and mesenteric lymph nodes were harvested and homogenised and the total cell number counted by trypan blue exclusion (figure 4.12). Control mice that did not receive T cells or NP68 peptide (numbers 1, 2 and 3) had $2.02x10^6$, $4x10^6$ and $4.8x10^6$ (mean of $3.6x10^6$) total cells in their spleen, whereas mice that had received T cells and NP68 (number 4, 5 and 6) had on average, 17 times more T cells in their spleen (mean of $6.4x10^7$). For the two mice that had received T cells but no NP68 (numbers 7 and 8), one (number 7) had similar numbers of cells in its spleen ($2.96x10^6$) to that of the control mice, whereas the second mouse (number 8) had 27 times more cells ($9.7x10^7$) than the control mice (figure 4.12). The cells from the mesenteric lymph nodes were also counted by trypan blue exclusion (figure 4.12). Control mice that did not receive T cells (numbers 1, 2 and 3) had $3.2x10^5$, $4.75x10^5$ and $3x10^5$ (mean of $3.65x10^5$) in their mesenteric lymph nodes. Compared to control mice those that had received T cells with NP68 (numbers 4,5 and 6), or T cells alone (numbers 7 and 8), had 3.6 and 3.8 times the number of cells in their mesenteric lymph nodes respectively.

In order for histological analysis to be performed on tissue from the gastrointestinal tract, proximal, medial and distal sections were taken from the small and large intestine, set in paraffin wax and stained with haematoxylin (H) and eosin (E).

The small intestines from mouse 3 (no T cells and no NP68), 4 (recipient of T cells and NP68) and 7 (recipient of T cells) were stained with H and E and viewed under a light microscope at 10x magnification. Mouse 3 and 4 had no cellular infiltrate in the small intestine, whereas 4 had discreet clusters of cells at the base of the villi adjacent to the muscle surrounding the gut (figure 4.13). Sections from the large intestines were analysed (10x magnification) for

mouse 3 (no T cells and no NP68), mice 4 and 5 (recipients of T cells and NP68), and mice 7 and 8 (recipients of T cells). No cellular infiltrate was present in the sections of the large intestine from mice 3 and 7. Mouse 4 had a significant influx of cells at the bass of the villi throughout the section viewed (figure 4.13). The infiltrate also extended into the villi itself, between the crypts and when compared to mice 3 and 7 an elongation of the villi was evident. Mouse 5 also exhibited a cellular infiltrate between the crypts of the villi and also within the muscle tissue surrounding the gut tissue. A section of the large intestine from mouse 8 was also analysed, but unfortunately the muscle tissue surrounding the gut and the base of the villi was not present. Despite this, a cellular infiltrate was evident between the crypts of the villi (figure 4.13.2).

Upon greater magnification (20x) there was evidence of cryptitis in mice 4, 5 (recipients of T cells and NP68) and 8 (recipient of T cells) (figure 4.14). Cryptitis involves the movement of cells of the immune system across the epithelia of the crypts, thus entering the crypts themselves.

4.11 Summary of results

Assays that were initially developed to look at the role of SHP-1 in primary *in vivo* T cell responses were adapted to enable the role of SHP-1 in memory T cells to be studied.

To begin, NP68 peptide in IFA was used to prime both naive and memory $CD8^+$ F5 T cells in recipient mice. With this approach, mice receiving naive control $CD8^+$ F5 T cells killed more target cells during a memory T cell response than mice receiving motheaten $CD8^+$ F5 T cells. However, when DCs were used to prime the memory T cells the converse was seen, with the mice that received motheaten $CD8^+$ F5 T cells killing more target cells than the mice receiving control $CD8^+$ F5 T cells. Mice receiving motheaten $CD8^+$ F5 T cells also killed more target cell when naive and memory $CD8^+$ F5 T cells were stimulated with DCs.

As Rag-$1^{-/-}$ mice developed colitis when receiving $CD8^+$ F5 T cells a new protocol to study memory T cell responses was developed, which involved using sublethally irradiated mice. The revised protocol also demonstrated that mice receiving motheaten $CD8^+$ F5 T cells killed more target cells than mice receiving control $CD8^+$ F5 T cells.

Rag-$1^{-/-}$ that developed colitis as a result of $CD8^+$ F5 T cell transfer and exhibited a cellular infiltrate into their large intestine, as shown by histological analysis.

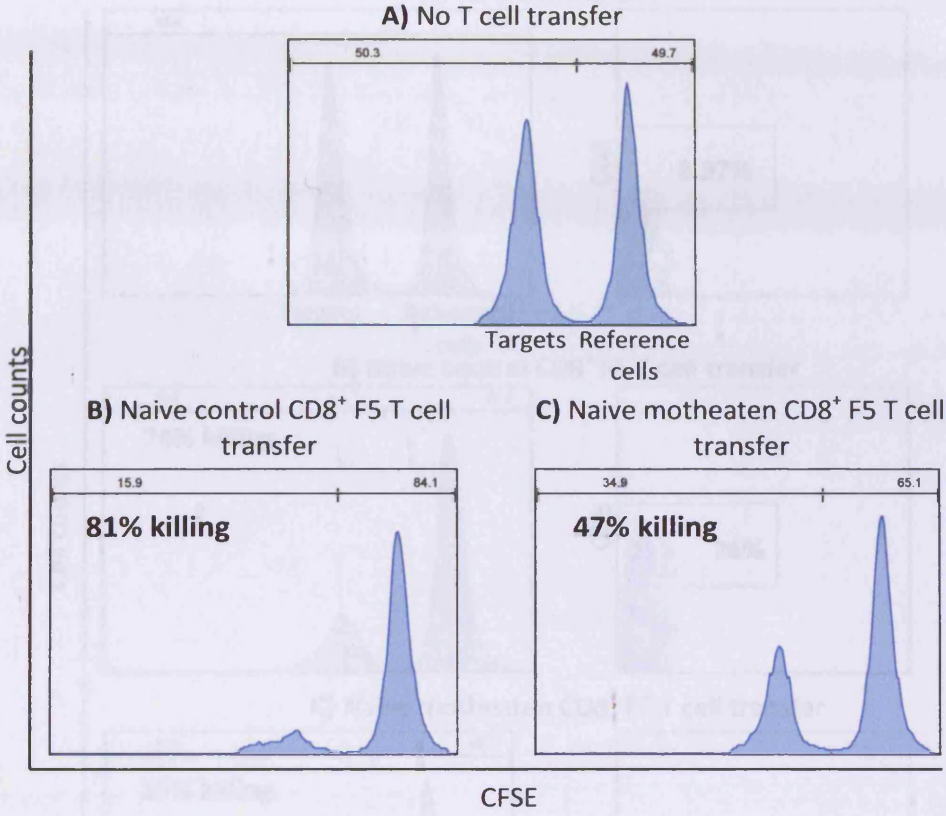


Figure 4.1: A mouse receiving control CD8$^+$ F5 T cells kills more target cells during a memory T cell response than a mouse receiving motheaten CD8$^+$ F5 T cells, when memory T cells were primed with NP68 in IFA

Rag-1$^{-/-}$ mice received either 3x10^6 control (B) or motheaten (C) CD8$^+$ F5 T cells intravenously and also a subcutaneous injection of NP68 in IFA. A control mouse did not receive any T cells (A). Six weeks following T cell transfer, mice received NP68 peptide in IFA as a subcutaneous injection. Seven days later, mice received CFSE labelled target and reference cells. Twenty-four hours later, mice were sacrificed and their spleens taken for analysis by flow cytometry. The percentage of target cells killed is shown for each histogram. Any deviation from the anticipated 1:1 ratio of target to reference cells in the control mouse (A) was used to adjust the data from mice that received T cells. The mice that received control CD8$^+$ T cells killed more targets (B) when compared to the mice that received motheaten T cells (C).

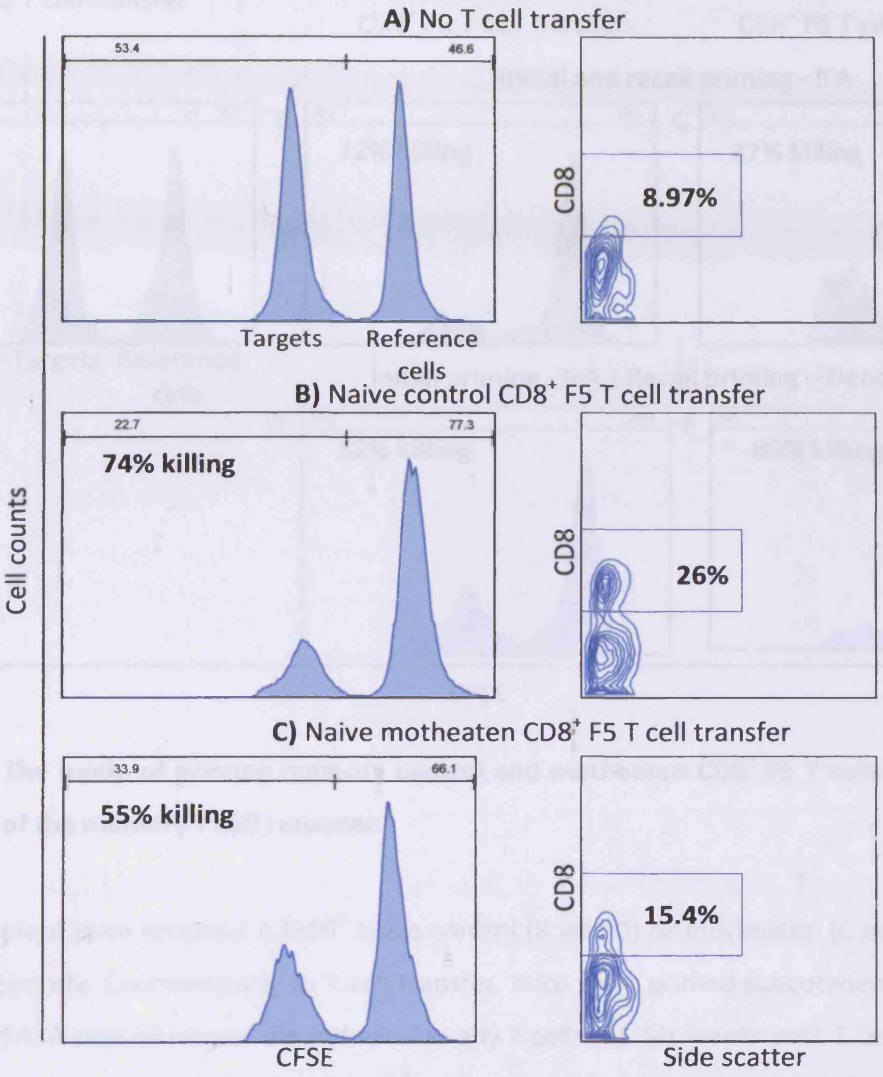


Figure 4.2: A mouse receiving control CD8$^+$ F5 T cells kills more target cells during a memory T cell response than a mouse receiving motheaten CD8$^+$ F5 T cells, when memory T cells are primed with NP68 in IFA

Rag-1$^{-/-}$ mice received either 2x10^6 control (B) or motheaten (C) CD8$^+$ F5 T cells intravenously and NP68 in IFA subcutaneously. A control mouse did not receive any T cells (A). Six weeks following T cell transfer, mice received NP68 peptide in IFA as a subcutaneous injection. Seven days later, mice received CFSE labelled target (pulsed with NP68) and reference cells. Twenty-four hours later, mice were sacrificed and their spleens taken and stained with anti-CD8^{PE} antibody, ready for analysis by flow cytomerty. The percentage of target cells killed is shown for each histogram. Any deviation from the anticipated 1:1 ratio of target to reference cells was corrected for by using the data from the control mouse (A). The contour plots show the proportion of CFSE$^-$/CD8$^+$ cells residing in a lymphocyte gate, as determined by forward and side scatter. The mice that received control CD8$^+$ T cells killed more targets (B) when compared to the mice that received motheaten T cells (C). In addition, the mouse that received control T cells had a greater proportion of CD8$^+$ cells in its spleen (B) compared to the mouse that received motheaten T cells (C).

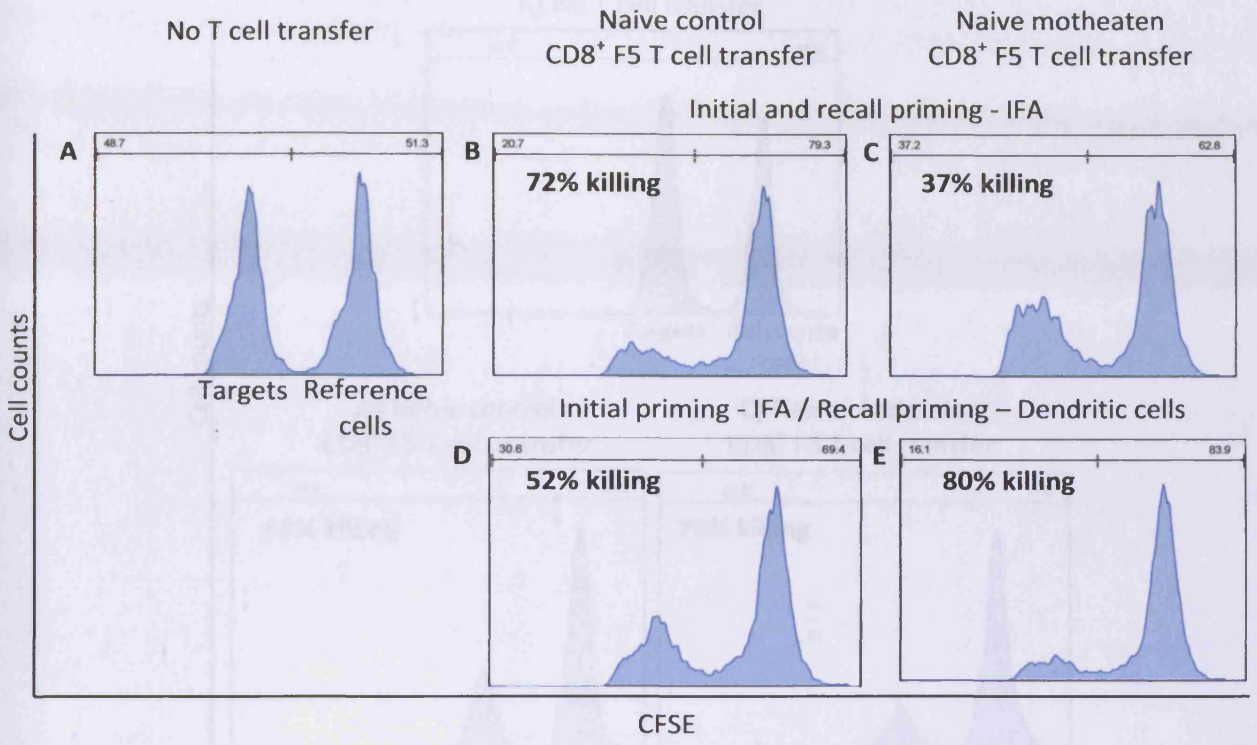


Figure 4.3: The mode of priming memory control and motheaten CD8$^+$ F5 T cells influences the magnitude of the memory T cell response

Rag-1$^{-/-}$ recipient mice received 2.2x10^6 naive control (B and D) or motheaten (C and E) CD8$^+$ F5 T cells intravenously. Concomitantly to T cell transfer, mice were primed subcutaneously with NP68 peptide in IFA. A control mouse did not receive any T cells (A). Six weeks post T cell transfer mice received either a peritoneal transfer of 3x10^6 matured and NP68 peptide pulsed DCs (D and E) or a subcutaneous injection of NP68 in IFA (B and C). Six days later mice received an intravenous infusion of CFSE labelled target and reference cells. Twenty-four hours post transfer, mice were sacrificed and their spleens taken for analysis by flow cytometry. The percentage of target cells killed is shown for each histogram. Any deviation from the anticipated 1:1 ratio of target to reference cells in the mouse that received no T cells (A) was used to adjust the percentage killing in the mice receiving T cells. The mouse that received control T cells (B) killed more target cells than the mouse that received motheaten T cells (C), when primed for a second time with NP68 in IFA. However, when DCs were used for priming memory T cells the mouse that received motheaten T cells (E) killed more target cells compared to the mouse that received control T cells (D).

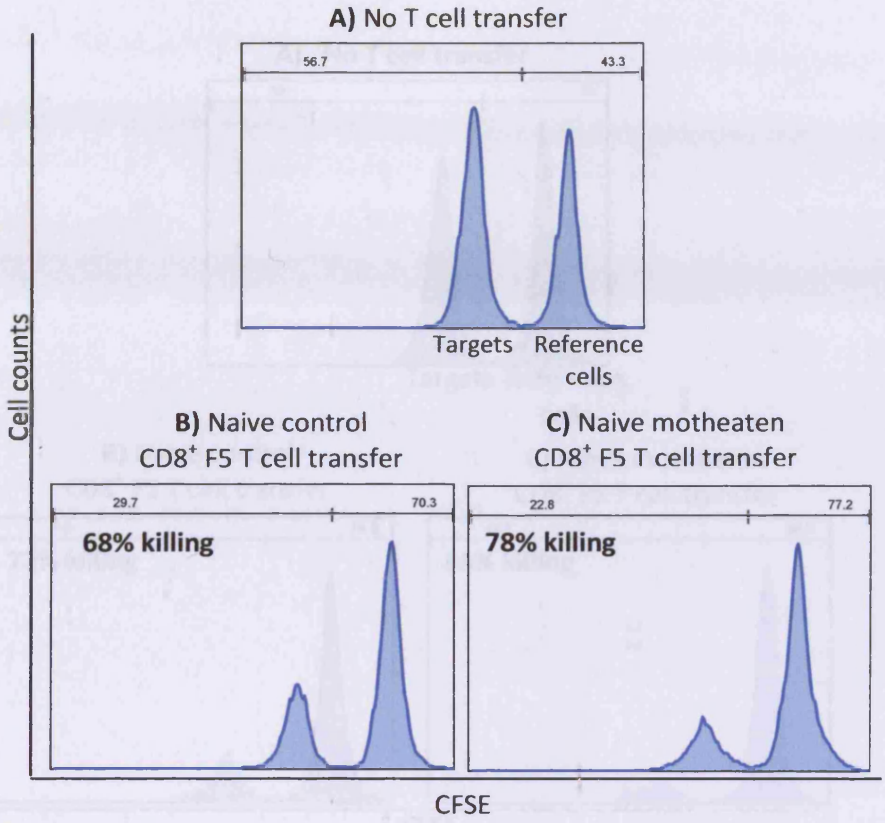


Figure 4.4: A mouse receiving naive motheaten CD8$^+$ F5 T cells killed more target cells during a memory T cell response than a mouse receiving naive control CD8$^+$ F5 T cells, when memory T cells were primed with NP68 loaded dendritic cells

Rag-1$^{-/-}$ mice received either 2x10^6 naive control (B) or motheaten (C) CD8$^+$ F5 T cells intravenously and also a subcutaneous injection of NP68 in IFA. A control mouse did not receive any T cells (A). Six weeks following T cell transfer, mice received a peritoneal transfer of 3x10^6 matured and NP68 peptide-pulsed dendritic cells. Seven days later mice received CFSE labelled target (pulsed with NP68) and reference cells. Twenty-four hours later mice were sacrificed and their spleens taken ready for analysis by flow cytometry. The percentage of target cells killed is shown for each histogram. Any deviation from the anticipated 1:1 ratio of target to reference cells was corrected for, by using the data from the control mouse (A). The mouse that received naive motheaten CD8$^+$ F5 T cells killed more targets (C) when compared to the mouse that received naive control CD8$^+$ F5 T cells (B).

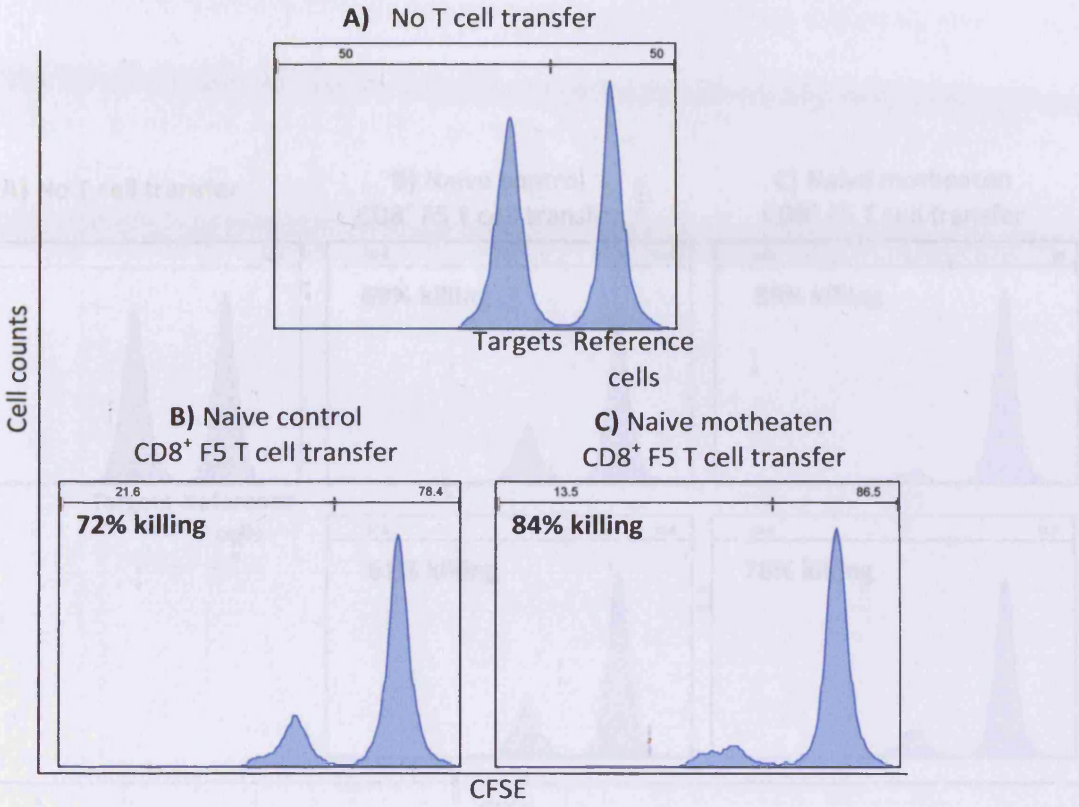


Figure 4.5: A mouse receiving naive motheaten CD8$^+$ F5 T cells kills more target cells during a memory T cell response than mice receiving naive control CD8$^+$ F5 T cells, when memory T cells are primed with NP68 loaded dendritic cells

Rag-1$^{-/-}$ mice received either 2.8x10^6 naive control (B) or motheaten (C) CD8$^+$ F5 T cells intravenously and also a subcutaneous injection of NP68 in IFA. A control mouse did not receive any T cells (A). Six weeks following T cell transfer mice received a peritoneal transfer of matured and NP68 peptide-pulsed DCs. Seven days later mice received CFSE labelled target and reference cells. Twenty-four hours later, mice were sacrificed and their spleens taken ready for analysis by flow cytometry. The percentage of target cells killed is shown for each histogram. The mouse that received naive motheaten CD8$^+$ F5 T cells killed more targets (C) when compared to the mouse that received naive control CD8$^+$ F5 T cells (B).

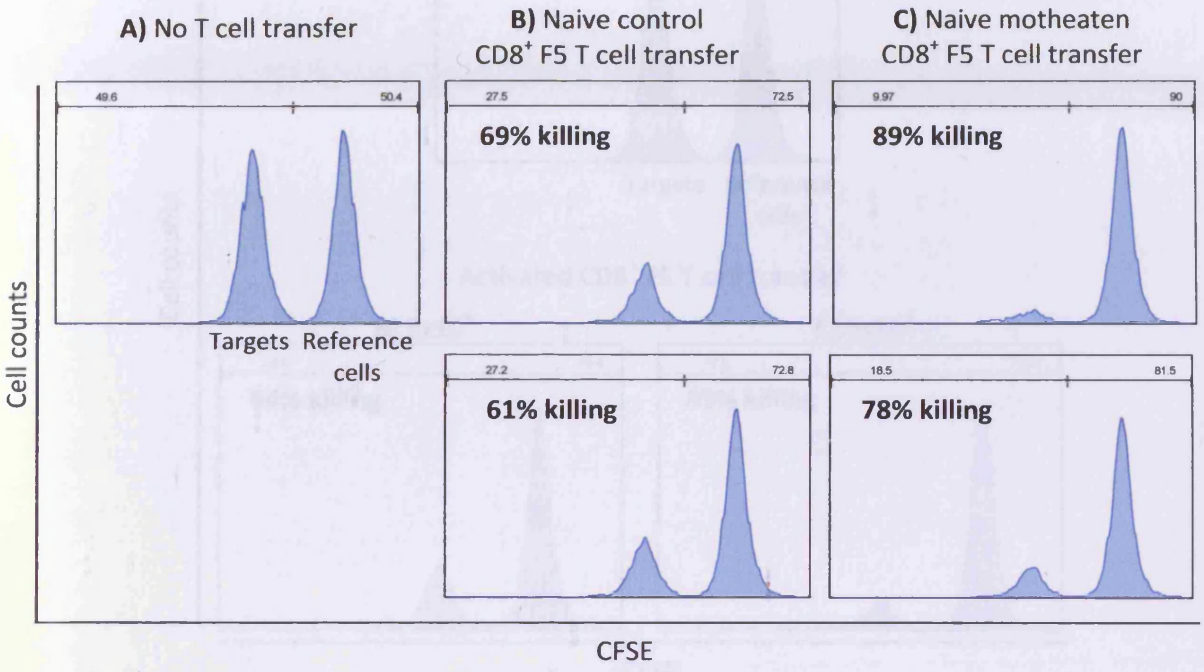


Figure 4.6: Mice receiving naive motheaten CD8$^+$ F5 T cells kill more target cells during a memory T cell response than mice receiving naive control CD8$^+$ F5 T cells, when naive and memory T cells are primed with NP68 loaded dendritic cells

Rag-1$^{-/-}$ mice received either 1.5x10^6 naive control (B) or motheaten (C) CD8$^+$ F5 T cells intravenously and also 2.5x10^6 in vitro matured and NP68 peptide-pulsed DCs. A control mouse did not receive any T cells (A). Six weeks following T cell transfer, mice received 3x10^6 matured and NP68 peptide-pulsed DCs. Seven days later, mice received CFSE labelled target (pulsed with NP68 peptide) and reference cells. Twenty-four hours later, mice were sacrificed and their spleens taken ready for analysis by flow cytometry. The percentage of target cells killed is shown for each histogram. Any deviation from the anticipated 1:1 ratio of target to reference cells in the control mouse (A) was used to adjust the data from mice that received T cells. The mice receiving naive motheaten CD8$^+$ F5 T cells killed more target cells (B) when compared to the mice that received naive control CD8$^+$ F5 T cells (C).

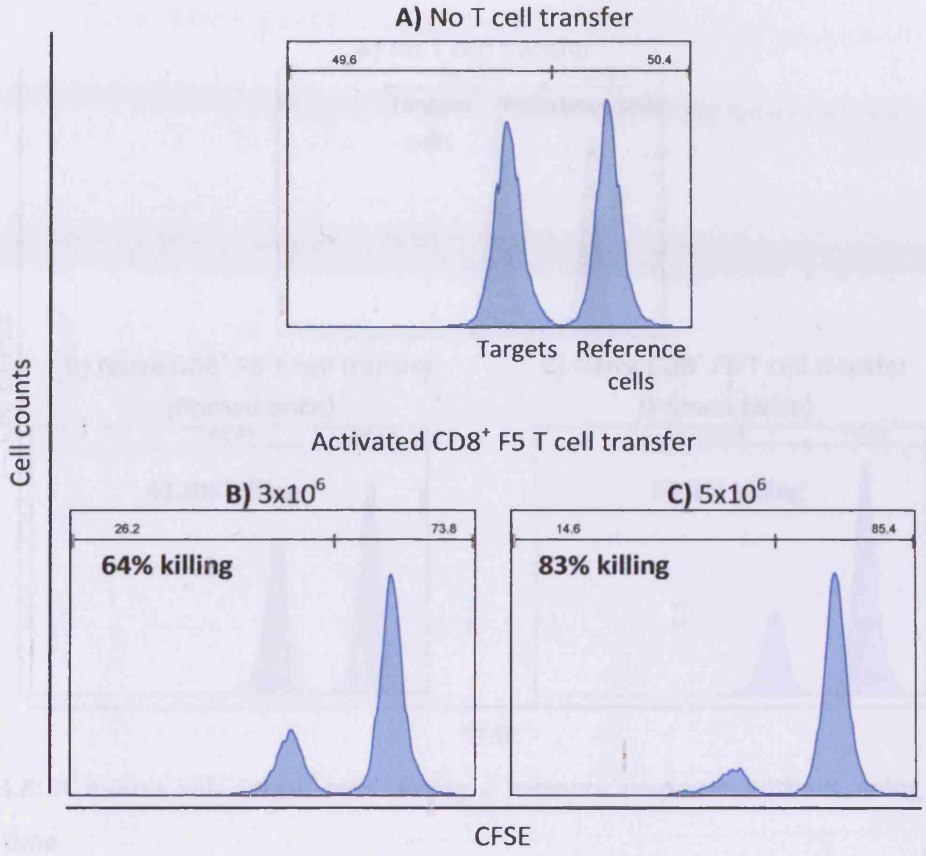


Figure 4.7: Mice receiving in vitro activated and expanded $CD8^+$ F5 T cells mount a memory T cell response

Naive $CD8^+$ F5 T cells were activated and expanded in vitro for four days. Rag-$1^{-/-}$ recipient mice received an intravenous transfer of either $3x10^6$ (B) or $5x10^6$ (C) activated T cells. A control mouse did not receive any T cells (A). Six weeks post T cell transfer, mice were primed subcutaneously with NP68 peptide in IFA. Six days later, all mice received CFSE labelled target (pulsed with NP68 peptide) and reference cells intravenously. Twenty-four hours post transfer mice were sacrificed and their spleens taken for analysis by flow cytometry. The percentage of target cells killed is shown for each histogram. Any deviation from the anticipated 1:1 ratio of target to reference cells in the mice not receiving T cells (A) was used to adjust the percentage killing in the mice receiving T cells. Those mice that received the activated T cells were able to mount a memory T cell response (B and C), with the mouse that received $5x10^6$ T cells (C) killing more targets than the mouse that received $3x10^6$ T cells (B).

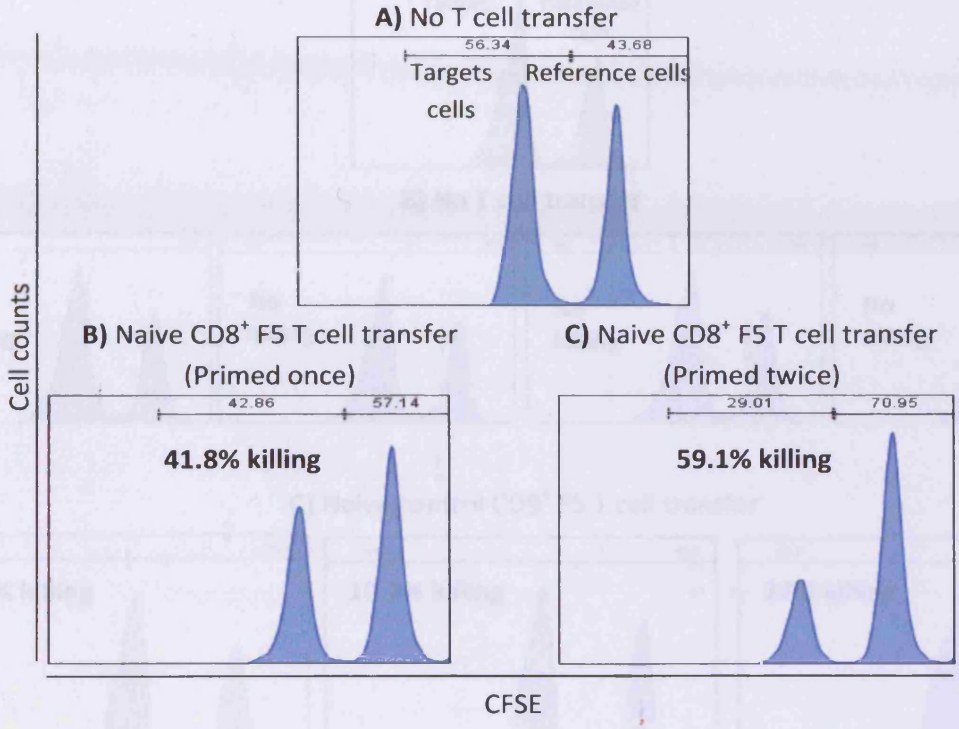


Figure 4.8: A mouse kills target cells during a memory response without being primed for a second time

Rag-1$^{-/-}$ mice received 2.5x10^{6} naive control CD8^{+} F5 T cells intravenously and also a subcutaneous injection of NP68 in IFA (B and C). A control mouse did not receive any T cells (A). Six weeks following T cell transfer one mouse that received T cells was primed subcutaneously with NP68 peptide in IFA (C). The second mouse was not primed (B). Seven days later all mice received CFSE labelled target and reference cells. Twenty-four hours later mice were sacrificed and their spleens taken ready for analysis by flow cytomerty. The percentage of target cells killed is shown for each histogram. Any deviation from the anticipated 1:1 ratio was corrected for, by using the data from the control mouse (A). The mouse that received T cells and was primed for a second time killed 59.1% of the target cells (B). The mouse that received T cells but was not primed for a second time killed 41.8% of the target cells (C).

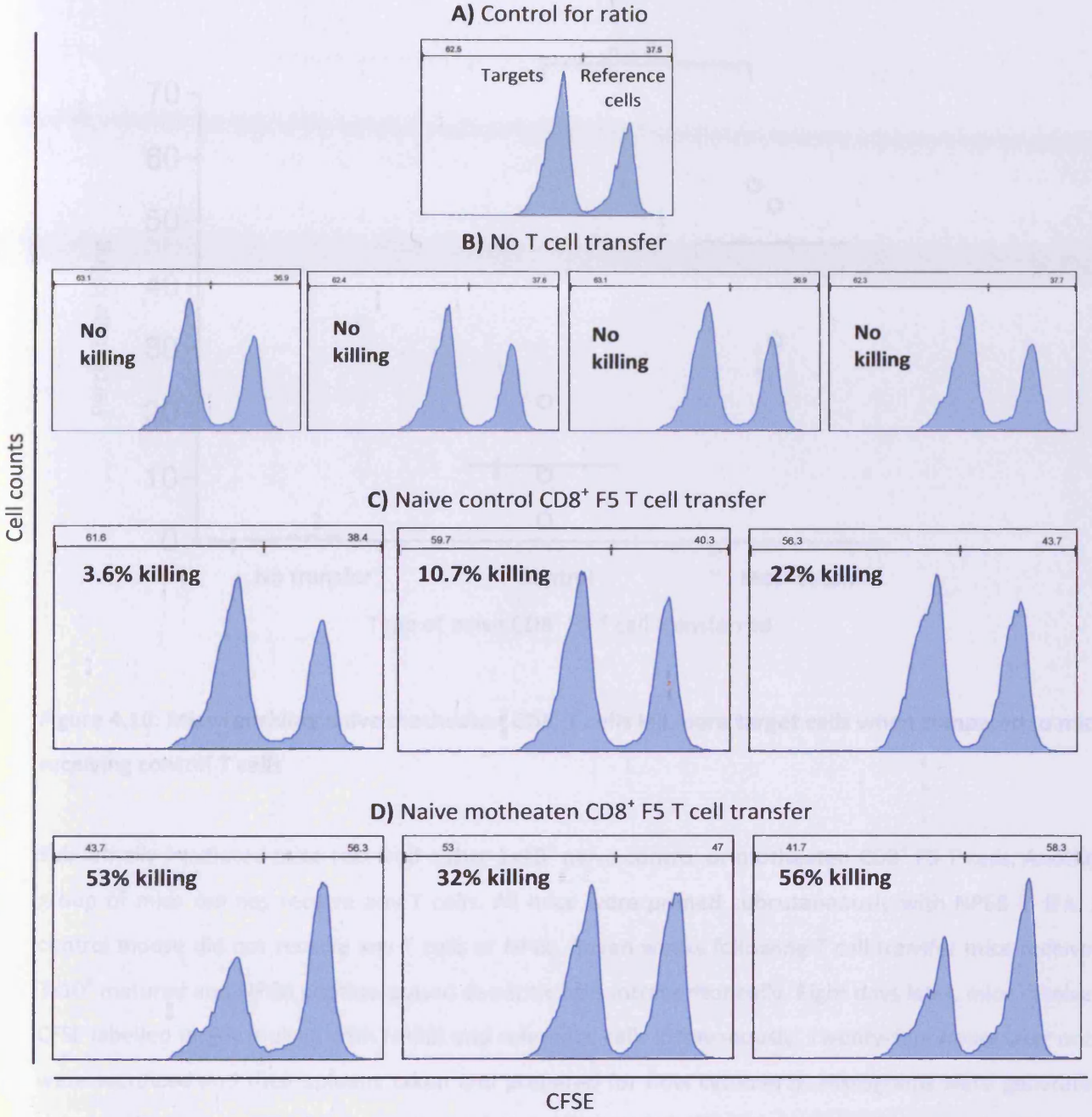


Figure 4.9: Mice receiving naive motheaten CD8$^+$ F5 T cells kill more target cells when compared to mice receiving naive control CD8$^+$ F5 T cells

Sublethally irradiated mice received either 1x10^6 naive control (C) or motheaten (D) CD8$^+$ F5 T cells. Another group of mice did not receive any T cells (B). All mice were primed subcutaneously with NP68 in IFA. A control mouse did not receive any T cells or NP68 (A). Seven weeks following T cell transfer mice received 3.8x10^6 matured and NP68 peptide-pulsed dendritic cells intraperitoneally. Eight days later mice received CFSE labelled target and reference cells intravenously. Twenty-four hours later, mice were sacrificed and their spleens taken and prepared for flow cytometry. The percentage killing is shown for each histogram and was also plotted to enable statistical analysis to be performed (Figure 4.10).Any deviation from the anticipated 1:1 ratio of target to reference cells was corrected for by using the data from the control mouse (A). The mice receiving no T cells did not kill any target cells (B). All mice that originally received naive motheaten CD8$^+$ F5 T cells (B) killed more target cells than mice that received naive control CD8$^+$ F5 T cells (C).

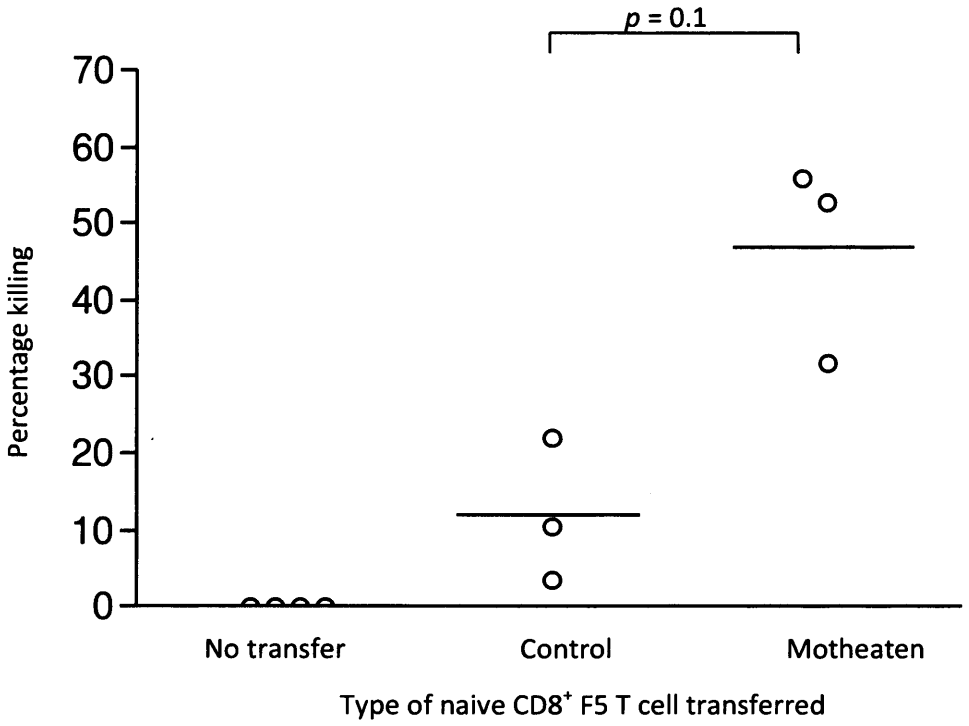


Figure 4.10: Mice receiving naive motheaten CD8$^+$ T cells kill more target cells when compared to mice receiving control T cells

Sub-lethally irradiated mice received either 1x10^6 naive control or motheaten CD8$^+$ F5 T cells. Another group of mice did not receive any T cells. All mice were primed subcutaneously with NP68 in IFA. A control mouse did not receive any T cells or NP68. Seven weeks following T cell transfer mice received 3x10^6 matured and NP68 peptide-pulsed dendritic cells intraperitoneally. Eight days later, mice received CFSE labelled target (pulsed with NP68) and reference cells intravenously. Twenty-four hours later mice were sacrificed and their spleens taken and prepared for flow cytomerty. Histograms were generated showing the target and reference cell populations (Figure 4.9). The percentage of target cells killed was calculated for each mouse (this figure). The mice that received no T cells did not kill any target cells (B). All mice that received naive motheaten CD8$^+$ F5 T cells (B) killed more target cells than mice that received naive control CD8$^+$ F5 T cells (C). The difference in the percentage of target cells killed between the mice that received either naive control or motheaten CD8$^+$ F5 T cells was not statistically significant (p=0.1).

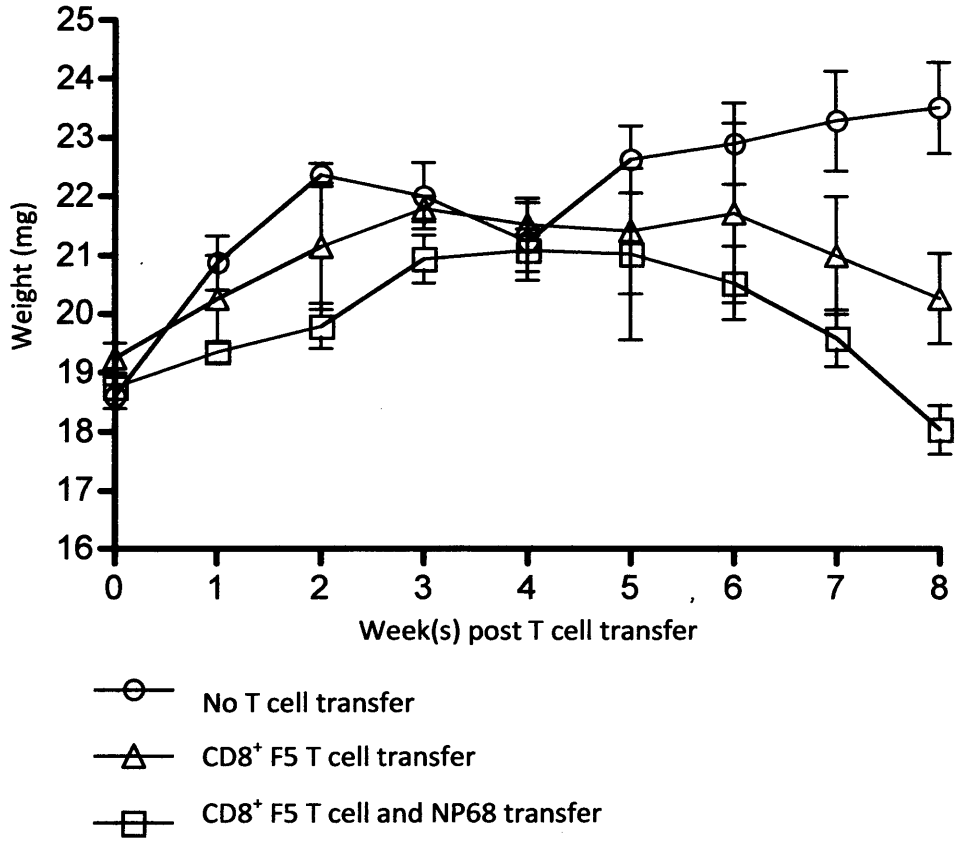


Figure 4.11: Mice receiving $CD8^+$ F5 T cells lose body weight

Mice received $1x10^6$ $CD8^+$ F5 T cells and NP68 in IFA (□) or $CD8^+$ F5 T cells alone (Δ). Control mice did not receive T cells or NP68 (○). The weight of the mice was monitored weekly for the duration of the assay.

A

Mouse number	Treatment		Cell counts	
	Naive $CD8^+$ F5 T cell transfer	Primed with NP68	Spleen	Mesenteric lymph nodes
1	×	×	$2.02x10^6$	$3.2x10^5$
2	×	×	$4x10^6$	$4.75x10^5$
3	×	×	$4.8x10^6$	$3x10^5$
4	✓	✓	$6x10^7$	$1.65x10^6$
5	✓	✓	$7.1x10^7$	$1.12x10^6$
6	✓	✓	$6.3x10^7$	$1.15x10^6$
7	✓	×	$2.95x10^6$	$1.32x10^6$
8	✓	×	$9.7x10^7$	$1.47x10^6$

B

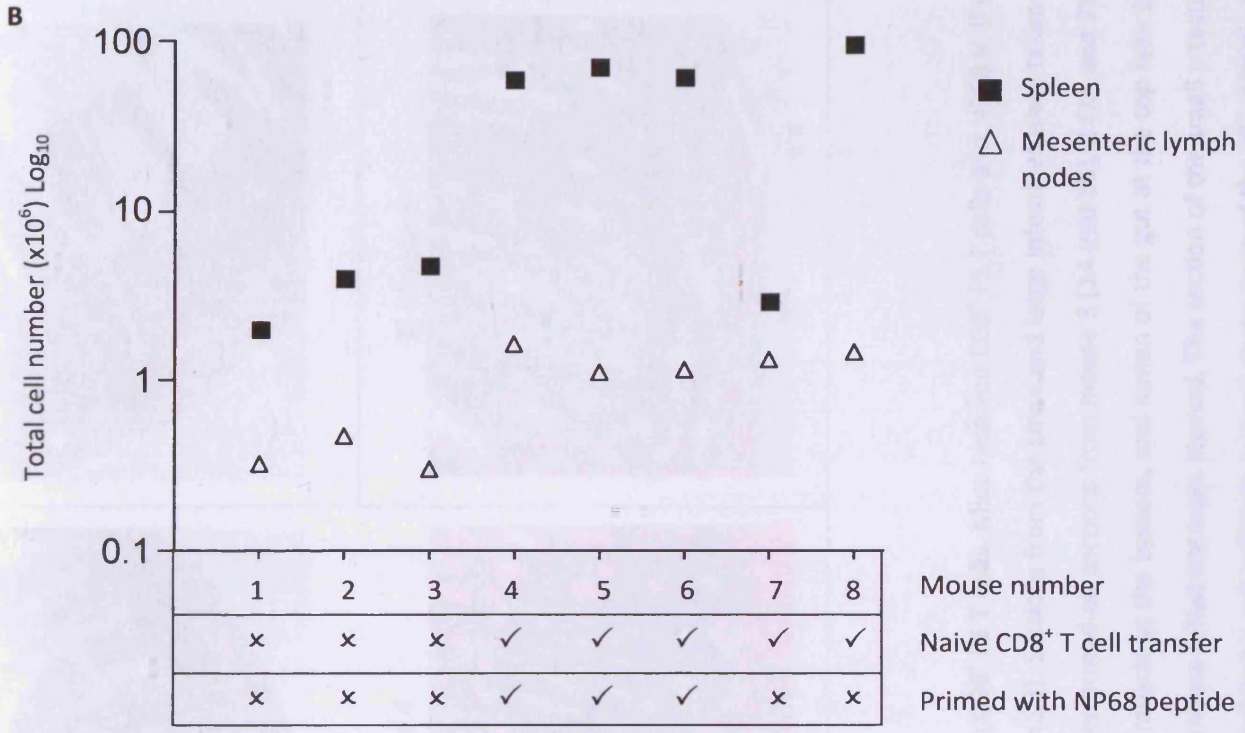


Figure 4.12: Mice receiving NP68 and naive $CD8^+$ F5 T cells have a greater number of cells in their spleens and mesenteric lymph nodes than mice receiving no T cells

Five Rag-$1^{-/-}$ recipient mice received $1x10^6$ naive $CD8^+$ F5 T cells intravenously (A). Three other mice did not receive any T cells (A). Mice 4, 5 and 6 were primed subcutaneously with NP68 peptide in IFA, with all other mice not being primed (A). Seven weeks post T cell transfer, mice were sacrificed and the spleens, mesenteric lymph nodes and both the small and large intestines taken for analysis. A single cell preparation of the spleens and mesenteric lymph nodes was prepared and counted by trypan blue exclusion. All mice receiving T cells had similar total cell numbers in their mesenteric lymph nodes (A and B). All three mice that received T cells and were primed, and one mouse that received T cells but was not primed, had similar total cell counts in their spleens (A and B). The mice that did not receive any T cells had the lowest number of cells in their spleens and mesenteric lymph nodes (A and B).

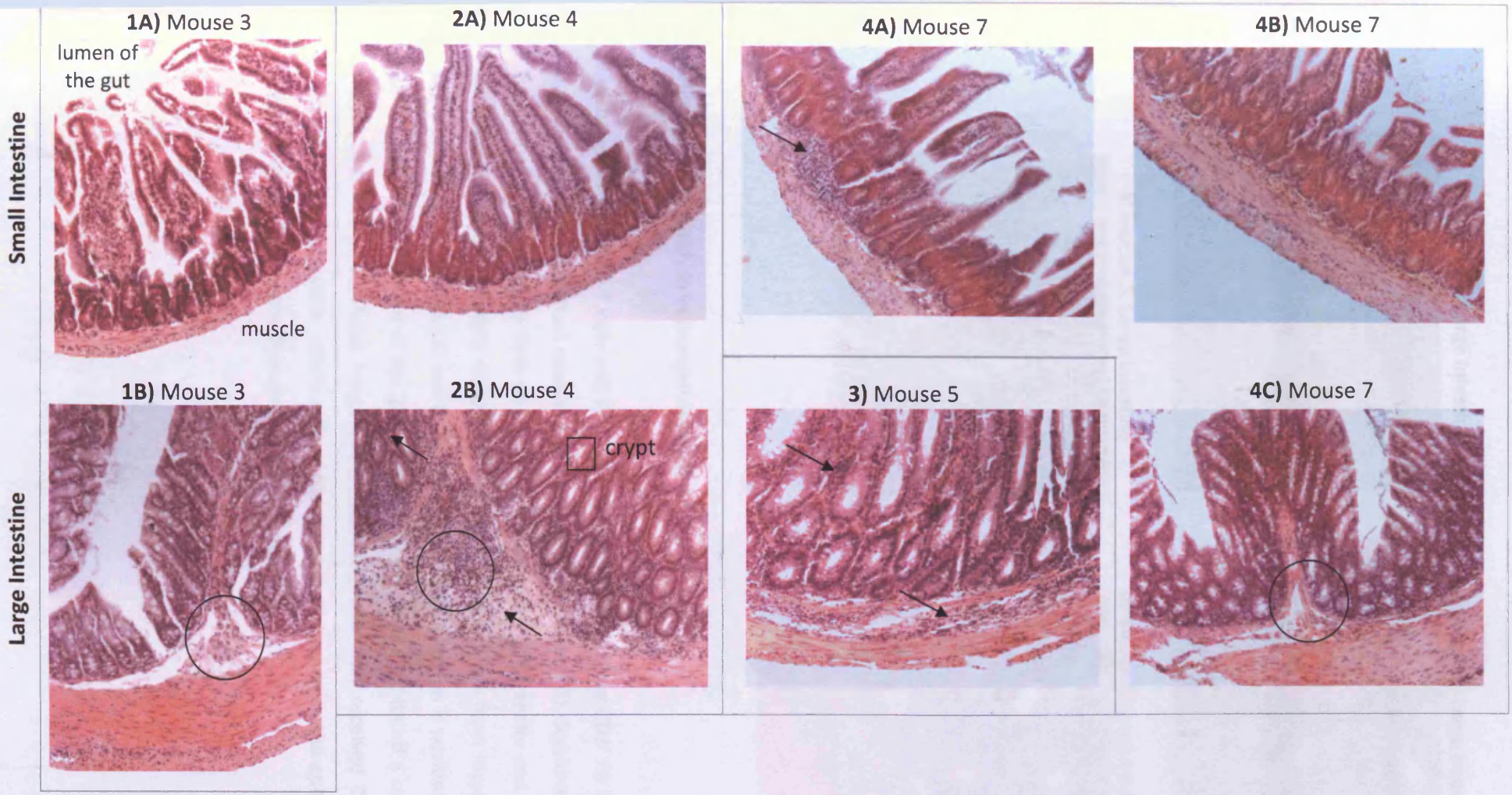


Figure 4.13: Cell infiltrate in the large intestine of mice receiving CD8$^+$ F5 T cells. Mice received CD8$^+$ F5 T cells and NP68 in IFA (mice 4, 5 and 6) or CD8$^+$ F5 T cells alone (mice 7 and 8). Control mice did not receive T cells or NP68 (Mice 1, 2 and 3). Sections from the small and large intestines were taken from all mice eight weeks post T cell transfer and mounted in paraffin wax. Haemotoxylin and eosin staining was performed on sections from mouse 3 (1A and 1B), 2 (2A and 2B), 5 (3), 7 (4A, 4B and 4C) and 8 (figure 4.13). The image of each section (10x magnification) is positioned with the muscle at the bottom, and lumen of the gut at the top (see 1A). No infiltrate was seen in the small intestine of mouse 3 (1A) and 4 (2A). The section of the small intestine from mouse 5 had not been stained. The section of the small intestine from mouse 7 had clusters of cells (arrow, 4A), which were not present throughout the section (4B). Mouse 4 exhibited a cell infiltrate (arrow) at the base of the villi (circle), which extended into the villi towards the lumen of the gut (arrow, 2B). This was not evident in mouse 3 (1B) and 7 (4B). Mouse 5 had a cell infiltrate in the muscle surrounding the section and also between the crypts (3).

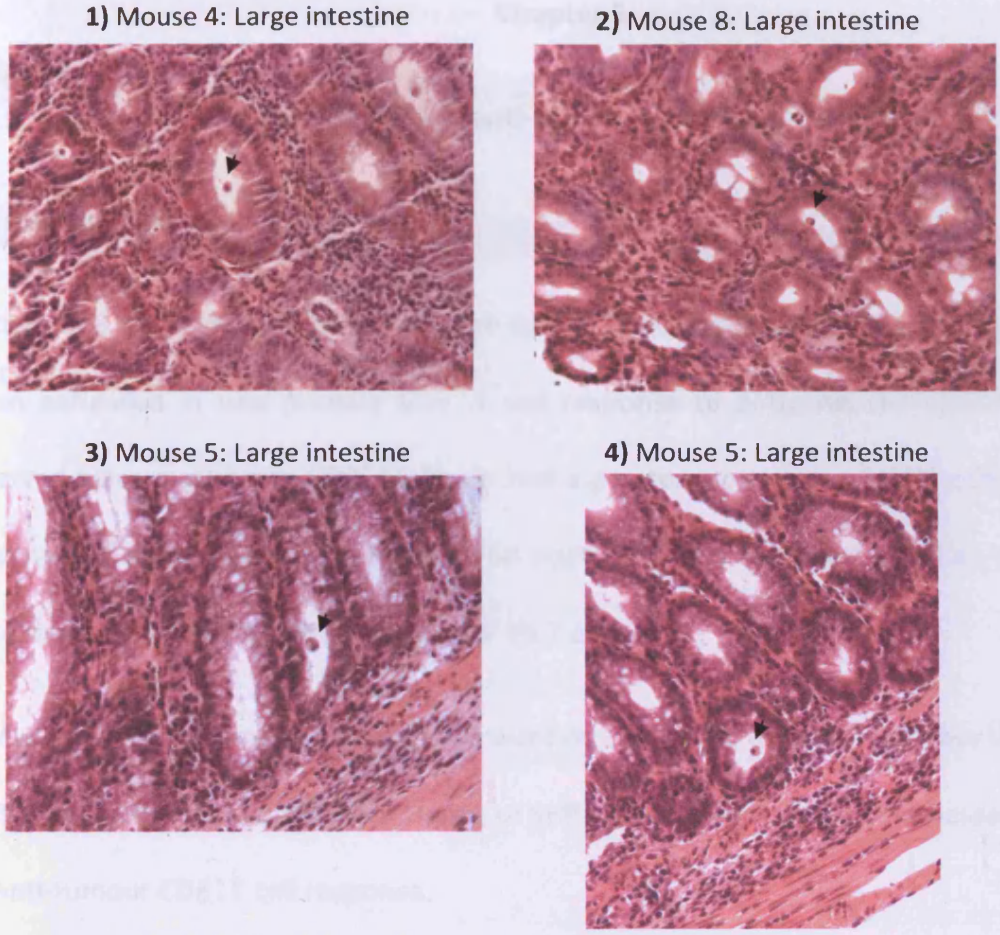


Figure 4.14: Cryptitis in mice receiving $CD8^+$ F5 T cells

Mice received $CD8^+$ F5 T cells and NP68 in IFA (mice 4, 5 and 6) or $CD8^+$ F5 T cells alone (mice 7 and 8). Control mice did not receive T cells or NP68 (mice 1 and 2). Sections from the small and large intestines were taken from all mice eight weeks post T cell transfer and mounted in paraffin wax. Haemotoxylin and eosin staining was performed on sections from mouse 3 (figure 4.12), 4 (1), 5 (4 and 5), 7 (figure 4.12) and 8 (2). The image of each section is positioned with the muscle at the bottom, and lumen of the gut at the top. Each mouse exhibited a cell infiltrate into the muscle and villi of the large intestines. In addition, mice that received $CD8^+$ F5 T cells also displayed signs of cryptitis, where cells of the immune system cross the epithelia and enter the crypts (arrowhead). Images displayed at 20x magnification.

Chapter 5

The role of SHP-1 in anti-tumour $CD8^+$ T cell responses

5.1 Introduction

In chapter 3 it was demonstrated that the lack of SHP-1 expression in $CD8^+$ F5 T cells resulted in an enhanced *in vivo* primary $CD8^+$ T cell response to antigenic stimulation. Mice that received naive motheaten $CD8^+$ F5 T cells had a greater proportion of $CD8^+$ cells within their spleens and killed more target cells (NP68 peptide pulsed splenocytes) when compared to mice that had received naive control $CD8^+$ F5 T cells.

To explore these findings further, assays were performed to establish whether the enhanced $CD8^+$ T cell response seen in the absence of SHP-1 expression could be harnessed to improve an anti-tumour $CD8^+$ T cell response.

A mouse model of tumour development was combined with protocols and techniques that had previously been developed during this study. The mouse melanoma cell line known as B16 has been used extensively to study both tumour development and treatment. The B16 cells can be transferred either intravenously or subcutaneously to recipient mice. When transferred intravenously, the B16 cells home to the lungs where they develop into pulmonary tumours. After a period of fourteen days the tumours appear as small pigmented nodules and can therefore be enumerated. This mode of transfer is used as a model of tumour metastases. When transferred subcutaneously, the B16 melanoma cells form a solid tumour mass, which is can be monitored by measuring with callipers.

In order to use the B16 melanoma cells in conjunction with purified $CD8^+$ TCR transgenic F5 T cells from both motheaten and control mice, the tumour cells were either pulsed with the NP68 peptide or transfected to constitutively express the NP68 epitope. In this context the

NP68 peptide was being used as a model for either a tumour-specific or tumour-associated antigen.

5.2 *In vitro* activated control $CD8^+$ F5 T cells kill NP68 peptide pulsed B16 melanoma cells in an *in vitro* setting

An *in vitro* cytotoxic T lymphocyte (CTL) assay was performed to establish whether $CD8^+$ F5 T cells were capable of killing NP68 peptide-pulsed B16 cells. Naive $CD8^+$ F5 T cells from control mice were activated *in vitro* for two days with NP68 peptide-pulsed splenocytes followed by two days of expansion with IL-2. Three components were combined to establish whether the $CD8^+$ F5 T cells could kill the NP68 peptide labelled B16s. These were activated $CD8^+$ F5 T cells, NP68 peptide-pulsed B16 cells labelled with 0.2μM CFSE and un-pulsed B16 cells labelled with 2μM CFSE. The NP68 peptide-pulsed B16 cells acted as a target cell population whereas the un-pulsed cells acted as a reference cell population to establish the proportion of target cells that were killed. The ratio of $CD8^+$ T cells to the total number of B16 cells was titrated, with the number of T cell added being determined by the total number of B16 cells. The target and reference B16 cells were used at a 1:1 ratio.

After four hours of co-culture, the cells were harvested and labelled with anti-$CD8^{PE}$ antibody ready for analysis by flow cytometry. Histogram plots were gated on CD8 negative cells and a viable cell population (Representative plots are shown in figures 5.1A to 5.1E). B16 cells were also cultured without T cells and the data shows that the target to reference B16 cell ratio remained at 1:1 (figure 5.1A).

At a T to B16 cell ratio of 1:2 the proportion of target B16 cells killed was 4%, 5% and 8% (figures 5.1B and 5.1F). At a ratio of 1:1, 19%, 21% and 24% of the target B16 cells were killed (figures 5.1C and 5.1F). At a ratio of 3:2, 23%, 24% and 28% of the target B16 cells were killed (figures 5.1D and 5.1F) and at a ratio of 2:1, 29%, 34% and 37% of the target B16

cells were killed (figures 1E and 1F). This demonstrated that activated $CD8^+$ F5 T cells were capable at killing B16 cells.

5.3 Sub-lethally irradiated mice have fewer lung tumour nodules compared to non-irradiated mice fourteen days post intravenous transfer of wild-type B16 cells

As a preliminary step to the *in vivo* studies which involved the intravenous transfer of B16 cells to recipient mice, a control experiment was performed to establish how many B16 cells could be transferred to mice that had been sub-lethally irradiated. Irradiating mice was a necessary aspect of the *in vivo* studies that involved the adoptive transfer of $CD8^+$ F5 T cells as it removed any endogenous T cells that may have responded to the NP68 peptide.

Mice were sub-lethally irradiated twenty-four hours prior to the intravenous transfer of either $1x10^5$, $5x10^4$ or $2.5x10^4$ wild-type B16 cells. Three non-irradiated mice received $1x10^5$ wild-type B16 cells. Fourteen days post transfer the mice were sacrificed and the tumour nodules in their lungs enumerated.

The non-irradiated mice that received $1x10^5$ B16 cells had 108, 112 and 150 tumour nodules in their lungs compared to 55, 65 and 77 in the lungs of the irradiated mice receiving the same number of B16 cells (figure 5.2). The difference in the number of nodules between the two sets of mice was not statistically significant (p=0.1). Irradiated mice that received $5x10^4$ B16 cells had 40 and 50 tumour nodules in their lungs and a mouse that received $2.5x10^4$ B16 cells had 18 tumour nodules in its lung (figure 5.2). This intriguing result was pursued later in this chapter.

Overall, this data suggested that an equivalent number of B16 cells that are normally transferred to non-irradiated recipient mice can be transferred to irradiated mice.

5.4 B16 cells labelled with intracellular dyes are detected in the lungs of mice twenty-four hours following intravenous transfer

The next step in the tumour studies was to develop an *in vivo* assay that allowed the killing of B16 cells by control and motheaten $CD8^+$ F5 T cells to be studied. An assay that involved the transfer of differentially labelled target (NP68 peptide-pulsed) and reference B16 cells to mice that had previously received naive $CD8^+$ F5 T cells was initially trialled. This involved performing pilot assays to establish whether fluorescently labelled B16 cells could be detected in the lungs of sub-lethally irradiated recipient mice following their intravenous transfer.

To begin, a total of $1.2x10^6$ B16 cells labelled with either 0.2μM or 2μM CFSE were transferred intravenously to the same recipient mice. A control mouse did not receive any B16 cells. A total of three mice received CFSE labelled B16 cells, but the cells proved to be toxic to one mouse, which died soon after B16 cell transfer. After twenty-four hours the remaining mice were sacrificed and the spleens and lungs taken for analysis by flow cytometry. The gates were set above the autofluorescence found in the spleen and lungs of the mouse that did not receive any B16 cells (figures 5.3A and B). There were no CFSE labelled cells detected in the spleens of recipient mice (figures 5.3C and E). However, the two mice receiving B16 cells had CFSE labelled cells within their lungs but the differentially CFSE labelled B16 cell populations could not be distinguished (figures 5.3D and F).

In a subsequent pilot assay the number of B16 cells transferred was reduced to potentially avoid any toxic side-effects to recipient mice. Also, a different combination of fluorescent dyes was used to label the B16 cells to assist with their detection in the lungs of recipient mice. Therefore, a total of $5x10^5$ B16 cells labelled with either 2μM CFSE or 10μM DDAO were transferred to a recipient mouse. A control mouse did not receive any T cells. Twenty

four hours later the mice were sacrificed and their lungs taken for analysis by flow cytometry. Dots plots were gated on viable cells and the fluorescence from CFSE and DDAO displayed as single plots, versus side scatter (figures 5.4A, B, C and D), or on the same dot plot (figures 5.4E and F). The gates defining fluorescent cells were set above the autofluorescence found in the lungs of the mouse did not receive any B16 cells (figures 5.4A, C and E). The differentially labelled B16 cells were apparent in the lungs of the recipient mouse but in low numbers (figures 5.4B, D and F).

In an attempt to address the problems associated with detecting fluorescently labelled B16 cells in sufficient numbers and distinguishable from the background fluorescence in the lungs of recipient mice a third pilot assay was performed. A recipient mouse received a total of $8x10^5$ B16 cells that had been labelled with either 0.2μM or 3μM CFSE. A second mouse received $8x10^5$ B16 cells labelled with either 0.5μM or 4μM CFSE. A control mouse did not receive any B16 cells. Even though the number of B16 cells transferred was not immediately toxic to the recipient mice they appeared to go in to a state of mild shock (lethargic and not responsive to surrounding stimulus) following B16 cell transfer, but recovered after 30 minutes. Mice were sacrificed twenty-four hours post B16 cell transfer and their lungs taken for analysis by flow cytometry. The gates defining fluorescent cells were set above the auto-fluorescence found in the lungs of the mouse not receiving any B16 cells (figure 5.5A). The mouse that received B16 cells labelled with 0.2μM and 3μM CFSE had fluorescent cells within its lung but the differentially labelled populations were not distinguishable (figure 5.5B). The mouse that received B16 cells labelled with 0.3μM and 4μM CFSE had two evident populations of fluorescently labelled cells within its lung (figure 5.5C).

The approach of labelling B16 cells with fluorescent dyes in order to study the killing of tumour cells was not pursued any further, as cells were not always detectable upon

retrieval, and the number required for transfer to allow detection had adverse side-effects on the recipient mice.

5.5 A similar number of B16 nodules are present in mice receiving $CD8^+$ F5 T cells and either B16 cells pulsed with NP68 peptide or unpulsed B16 cells

An alternative method was sought to that using fluorescently labelled B16 cells to look at the *in vivo* killing of NP68 peptide-pulsed B16 cells by $CD8^+$ F5 T cells. The proposed alternative protocol involved transferring NP68 peptide labelled B16 cells to mice that had already been primed NP68 in IFA and were recipients of either naive control or motheaten $CD8^+$ F5 T cells. The enumeration of the nodules in the lungs of the mice fourteen days post B16 cell transfer was predicted to be an indirect readout of the number of B16 cells initially killed upon their intravenous transfer.

To assess the feasibility of the alternative protocol, sub-lethally irradiated mice received $3x10^6$ naive control $CD8^+$ F5 T cells intravenously and a subcutaneous injection of NP68 peptide in IFA. Seven days post T cell transfer mice received either $1x10^5$ B16 cells that had been pulsed with NP68 peptide or $1x10^5$ B16 cells that had not been pulsed. Fourteen days post B16 cell transfer the mice were sacrificed and the B16 nodules in the lungs enumerated. Mice that received un-pulsed B16 cells had 345, 233, 261 and 200 tumour nodules in their lungs compared to 215, 305, 267 and 199 tumour nodules in the lungs of mice that received B16 cells pulsed with NP68 peptide (figure 5.6). Any difference in the number of lung tumour nodules between the two groups of mice was not statistically significant (p=0.8857). Presumably, the NP68 peptide is lost from the surface of the B16 cells once transferred *in vivo*. As attempts to develop a protocol using B16 cells pulsed with NP68 peptide were unsuccessful it was necessary to produce B16 cells that constitutively expressed the NP68 eptiope.

5.6 Successful infection of B16 cells with a retrovirus encoding the NP68 epitope as a fusion protein with GFP

One approach to producing B16 cells expressing the NP68 was to use a cDNA construct that encodes the NP68 epitope as a fusion protein with GFP.

Retrovirus encoding the NP68 epitope as a fusion protein with GFP was produced by transfecting a packaging cell line, known as Phoenix, with the corresponding cDNA. At the point of viral harvest, between 80-90% of the Phoenix cells were fluorescent when viewed under a fluorescent microscope (data not shown).

Wild-type B16 cells were infected twice with the retrovirus on subsequent days. As a control for the infection protocol, a previously verified control retrovirus encoding GFP (named Pinco) was also used to infect B16 cells. Seven days post-infection, the cells were analysed for GFP expression by flow cytometry. Histograms displaying GFP fluorescence were gated on viable cells as determined by forward and side scatter. The B16 cells infected with the control retrovirus encoding GFP were 35% GFP positive (figure 5.7B). Those B16 cells infected with the retrovirus encoding GFP as a fusion protein with the NP68 epitope were 19.1% GFP positive (figure 5.7C). Subsequently, B16 cells infected with the virus encoding the NP68 peptide as a fusion protein with GFP were single cell sorted based upon viability, pulse width and GFP fluorescence. A polyclonal B16 cell population (originally $1x10^4$ cells) was GFP positive two weeks post cell sorting (figure 5.8A). A total of twenty-four wells of a 96-well plate received individual B16 cells and from these, two monoclonal cells lines were grown successfully. Both monoclonal cell lines were GFP positive five weeks following single cell sorting (figures 5.8B and C).

5.7 B16 cells infected with a retrovirus encoding the NP68 epitope are killed *in vitro* by $CD8^+$ F5 T cells

An *in vitro* CTL assay was performed to test for the constitutive expression and the presentation by MHC class I of the NP68 epitope by B16 cells that had been infected with a retrovirus encoding the NP68 epitope as a fusion protein with GFP.

Naive $CD8^+$ F5 T cells were activated *in vitro* with NP68 peptide-pulsed splenocytes for two days followed by their expansion for a further two days with IL-2. Both monoclonal B16 cell lines expressing GFP were tested for the surface presentation of the NP68 epitope. Parental B16 cells and the GFP positive B16 cells were plated-out at a 1:1 ratio twenty-four hours prior to the addition of the activated T cells (figures 5.9A and C). The B16 cells were then incubated with the activated T cells for sixteen hours, followed by staining with anti-$CD8^{PE}$ antibody prior to analysis by flow cytometry. Histograms displaying CFSE fluorescence were generated on viable and $CD8^-$ cells. Over 99% of the GFP positive cells of both monoclonal cell lines were killed by the activated $CD8^+$ F5 T cells (figures 5.9B and D).

5.8 Mice receiving $3x10^6$ naive control $CD8^+$ F5 T cells and $1.5x10^5$ B16 cells expressing the NP68 epitope are clear of lung tumours

To establish whether the B16 cells that express the NP68 epitope could both grow and be killed in an *in vivo* setting, B16 cells were transferred to irradiated recipient mice, that had previously received naive control $CD8^+$ F5 T cells, or to mice that had received no T cells.

Sub-lethally irradiated mice received $3x10^6$ naive control $CD8^+$ F5 T cells intravenously. These were activated by the subcutaneous injection of NP68 peptide in IFA. Control mice did not receive any T cells. Seven days post T cell transfer, all mice received $1x10^5$ B16 cells that expressed the NP68 epitope. Fourteen days later the mice were sacrificed and the pigmented tumour nodules in their lungs enumerated. Those mice that did not receive any T cells had 101, 89, 90 and 79 tumour nodules within their lungs (figure 5.10). The mice that

were primed and the recipients of $CD8^+$ F5 T cells had no tumour nodules within their lungs (figure 5.10).

5.9 Complete protection from tumour development in the lungs of mice receiving either naive control or motheaten $CD8^+$ F5 T cells

The B16 cells expressing the NP68 epitope were utilised to establish whether there was any difference in protection from tumour development in the lungs of mice that received either naive control or naive motheaten $CD8^+$ F5 T cells. Sub-lethally irradiated mice received purified naive $CD8^+$ F5 T cells intravenously and NP68 peptide subcutaneously in IFA. After a defined number of days, the mice then received a population of B16 cells expressing the NP68 epitope. Fourteen days post B16 cell transfer, the mice were sacrificed and the pigmented nodules in their lungs enumerated. Control mice for each experiment did not receive any T cells but did receive the B16 cells. Four independent experiments were performed to help establish how many $CD8^+$ T cells and B16 cells to transfer to recipient mice, and also the duration between T cell and B16 cell transfer to give an acceptable level of tumour development.

Initially, $3x10^6$ naive control or motheaten $CD8^+$ F5 T cells were transferred to individual mice. Four days later, mice received $1x10^5$ B16 cells expressing the NP68 epitope. Those mice that did not receive any T cells had 50, 80 and 110 tumour nodules in their lungs whereas the mice receiving naive control or naive motheaten $CD8^+$ F5 T cells had no tumour nodules within their lungs (figure 5.11A).

In three subsequent experiments the number of B16 cells transferred was increased to $2.5x10^5$ and the duration between T cell and B16 cell transfer was reduced to two days. In addition, for each subsequent experiment the number of naive control or naive motheaten $CD8^+$ F5 T cells transferred was $1x10^6$, $1x10^5$ and $5x10^4$. The number of tumour nodules in

the lungs of the control mice that did not receive T cells, were as follows: 240, 262 and 320 for the experiment where mice received $1x10^6$ T cells (figure 5.11B); 200, 260 and 340 for the experiment where mice received $1x10^5$ T cells (figure 5.11D) and 144, 258 and 288 for the experiment where mice received $5x10^4$ T cells. For each experiment the mice that received either naive control or motheaten $CD8^+$ F5 T cells had no tumour development in their lungs after fourteen days (figure 5.11B, C and D).

5.10 Similar tumour nodule formation in mice receiving either $1x10^4$ control or motheaten $CD8^+$ F5 T cells or no T cells

As no tumour development was seen in the lungs of mice that received $5x10^4$ naive control or motheaten $CD8^+$ F5 T cells, and $2.5x10^5$ B16 cells expressing the NP68 epitope, the number of T cells transferred was reduced further.

Sub-lethally irradiated mice received $1x10^4$ control or motheaten naive $CD8^+$ F5 T cells and NP68 peptide subcutaneously in IFA. One day post T cell transfer, all mice had an intravenous transfer of $2.5x10^5$ B16 cells expressing the NP68 peptide. Fourteen days later the mice were sacrificed and the pigmented nodules in their lungs enumerated. Those mice receiving no T cells had 302, 288 and 345 tumour nodules in their lungs (figure 5.12). Those mice receiving naive control $CD8^+$ F5 T cells had 275, 345 and 280 tumour nodules in their lungs (Figure 5.12) compared to 325, 299 and 269 tumour nodules in the lungs of mice that received naive motheaten $CD8^+$ F5 T cells (figure 5.12). There was no significant difference in the number of tumour nodules between the three groups of mice (No T cell transfer versus control $CD8^+$ F5 T cell transfer: $p = 0.7$. No T cell transfer versus motheaten $CD8^+$ F5 T cell transfer: $p = 0.4$. Control $CD8^+$ F5 T cell transfer versus motheaten $CD8^+$ F5 T cell transfer: $p = 0.7$)(figure 5.12).

5.11 Reduced tumour nodule formation in mice receiving $2x10^4$ naive motheaten $CD8^+$ F5 T cells compared to mice that receiving no T cells

As a result of the equivalent lung tumour nodule formation seen in mice that received no T cells and mice that received either $1x10^4$ naive control or naive motheaten $CD8^+$ F5 T cells the number of adoptively transferred T cells was increased for subsequent assays.

Sub-lethally irradiated mice received $2x10^4$ control or motheaten naive $CD8^+$ F5 T cells and NP68 peptide subcutaneously in IFA. Twenty-four hours post T cell transfer all mice had an intravenous transfer of $2.5x10^5$ B16 cells expressing the NP68 peptide. Fourteen days later the mice were sacrificed and the pigmented nodules in their lungs enumerated. Those mice receiving no T cells had 299, 345, 380 and 398 tumour nodules in their lungs (figure 5.13). Those mice receiving naive control $CD8^+$ F5 T cells had 240, 255 and 301 tumour nodules in their lungs (figure 5.13). Finally, the mice that received motheaten naive $CD8^+$ F5 T cells had 169, 210 and 258 nodules in their lungs (figure 5.13), which was a statistically significant reduction ($p = 0.05$) when compared to mice that did not receive any T cells. Any difference in the number lung tumour nodules between mice that received naive control or naive motheaten $CD8^+$ F5 T cells was not statistically significant (p=0.4).

5.12 Reduced tumour nodules formation in the lungs of mice receiving $3.2x10^4$ motheaten naive $CD8^+$ F5 T cells, when compared to mice receiving $3.2x10^4$ control naive $CD8^+$ F5 T cells

With $1x10^4$ T cells giving no protection to mice receiving B16 cells and with $2x10^4$ naive motheaten $CD8^+$ F5 T cells giving some protection from lung tumour development the number of T cells transferred was increased further. Two pairs of sub-lethally irradiated mice received either $3.2x10^4$ naive control or motheaten $CD8^+$ F5 T cells concomitantly with the subcutaneous injection of NP68 peptide in IFA. A third pair of sub-lethally irradiated mice did

not receive any T cells. After one day all mice had an intravenous transfer of $2.5x10^5$ B16 cells expressing the NP68 peptide. Fourteen days later the mice were sacrificed and the lungs photographed (figure 5.14) from one set of mice and the pigmented lung nodules enumerated for all mice (figure 5.15). Figure 14 illustrates the degree of tumour load in the lungs of the mice, with highly pigmented lungs having a greater tumour load. The lungs from the mouse not receiving any T cells and the mouse that received control naive $CD8^+$ F5 T cells had many pigmented tumour nodules. In contrast the lungs of the mouse that received motheaten $CD8^+$ F5 T cells appeared normal. The enumeration data revealed that the mice receiving no T cells had 254 and 289 tumour nodules in their lungs (figure 5.15). Those mice receiving naive control $CD8^+$ F5 T cells had 168 and 125 tumour nodules in their lungs compared to 0 and 2 tumour nodules in the lungs of mice that received naive motheaten $CD8^+$ F5 T cells (figure 5.15).

As only two mice for each group were used for this experiment no statistical analysis was performed, therefore the experiment was repeated with more mice in each group.

5.13 Significantly enhanced protection against lung tumour formation in mice receiving $3.2x10^4$ naive motheaten versus control $CD8^+$ F5 T cells

A group of six sub-lethally irradiated mice received either $3.2x10^4$ naive control or motheaten $CD8^+$ F5 T cells. Another group of six mice did not receive any T cells. All mice that received T cells were primed subcutaneously with NP68 peptide in IFA. One day following T cell transfer, all mice received an intravenous infusion of $2.5x10^5$ B16 cells expressing the NP68 peptide. Fourteen days post B16 cell transfer mice were sacrificed and the lungs photographed (figure 5.16) prior to the enumeration of the pigmented lung tumour nodules (figure 5.17). Those mice that did not receive any T cells and those that received naive control $CD8^+$ T cells had highly pigmented lungs when compared to the mice

that received motheaten $CD8^+$ F5 T cells (figure 5.16). Mice that received motheaten naive $CD8^+$ F5 T cells had significantly (p=0.0022) fewer tumour nodules (12, 14, 91, 98, 116 and 170) in their lungs compared to mice receiving control naive $CD8^+$ F5 T cells (225, 239, 251, 281, 305 and 315) (figure 5.17). Two of the mice that did not receive T cells died before the end of the assay and the remaining four mice had over 425 nodules in their lungs (figure 5.17).

In a further independent experiment, all conditions were kept the same as the previous tumour protection assay (as described above). Briefly, sub-lethally irradiated mice were primed subcutaneously and received either $3.2x10^4$ naive control or motheaten $CD8^+$ F5 T cells followed by $2.5x10^5$ B16 cells a day later. Only a sufficient number of motheaten $CD8^+$ F5 T cells were available for three recipient mice during this experiment. Fourteen days post B16 cell transfer the three mice that were recipients of motheaten naive $CD8^+$ F5 T cells had significantly (p=0.023) fewer tumour nodules in their lungs (0, 0 and 53) compared to six mice that received control $CD8^+$ F5 T cells (98, 122, 200, 226, 283 and 296) (figure 5.18). Four of the mice that did not receive any T cells had over 425 nodules in their lungs with the remaining two mice having 159 and 315 lung tumour nodules (figure 5.18).

5.14 Activated motheaten $CD8^+$ F5 T cells exhibit an enhanced effector function on a per cell basis when compared to activated control $CD8^+$ F5 T cells

In order to explore the potential factors that may contribute to the enhanced protection from lung tumour development seen in mice that received naive motheaten $CD8^+$ F5 T cells, *in vitro* assays were performed that looked at the effector function of activated control and motheaten $CD8^+$ F5 T cells on a per cell basis.

Previous experimental work (Johnson *et al.*, 1999) had demonstrated that there was no difference in the degree of direct target cell killing by control and motheaten $CD8^+$ F5 T cells

on a per cell basis, when the target cells were NP68 peptide-pulsed mouse EL4 cells. The aim here was to explore the effector capabilities of activated control and motheaten $CD8^+$ F5 T cells when the targets were B16 cells.

In vitro assays were performed to look at the surface expression of CD107a on activated control and motheaten $CD8^+$ F5 T cells upon encounter with target B16 cells. In addition, the direct killing of target B16 cells by control and motheaten $CD8^+$ F5 T cells was also studied.

5.14a A greater proportion of activated motheaten $CD8^+$ F5 T cells upregulate CD107a upon encounter with B16 cells expressing the NP68 epitope in comparison to activated control $CD8^+$ F5 T cells

When a $CD8^+$ T cell encounters a target cell, it releases cytotoxic granules that are capable of directly killing the target cell. These granules are released from intracellular vesicles which fuse with the cell surface membrane. As a result of this fusion, CD107a molecules, which line the inside of the vesicle's membrane, are displayed on the surface of the cell. Therefore, the appearance of CD107a on the surface of the $CD8^+$ T cells is an indicator of its direct encounter with an appropriate target cell.

In an initial experiment *in vitro* activated control and motheaten $CD8^+$ F5 T cells were incubated with either B16 cells that had been pulsed with NP68 peptide or left un-pulsed. This was done in triplicate and at three B16 to T cell ratios (5:8, 5:4 and 5:2). The assay media contained both an anti-$CD107a^{FITC}$ antibody and golgi-stop. After four hours of incubation, the cells were harvested and stained with an anti-$CD8^{PE}$ antibody and analysed by flow cytometry. Contour plots were gated on a viable $CD8^+$ cell population and displayed as CD8 versus CD107a (representative plots shown in figure 5.19). The CD107a positive gate was set above the fluorescence seen in the absence of B16 cells (figures 5.19A and D). There was minimal up-regulation of surface CD107a in the presence of un-pulsed B16 cells for both

control (figure 5.19B and figure 5.20) and motheaten (figure 5.19E and figure 5.20) $CD8^+$ F5 T cells. In the presence of NP68 peptide pulsed B16 cells, a greater proportion of motheaten $CD8^+$ F5 T cells up-regulated CD107a on their cell surface (figure 5.19F and figure 5.20) in comparison to control $CD8^+$ F5 T cells (figure 5.19C and figure 5.20). This was not statistically significant according to a non-parametric Mann-Whitney test.

In a subsequent assay, all conditions were kept the same but with six B16 to T cell ratios (1:40, 1:20, 1:10, 1:5, 2:5 and 1:1) being used in an attempt to titrate the degree of CD107a upregulation detected on the surface of the T cells. The data was generated in the same manner as the previous assay (as described above). At each ratio, a greater proportion of activated motheaten $CD8^+$ F5 T cells up-regulated CD107a expression on their cell surface (Figure 5.21D and figure 5.22) in comparison to activated control $CD8^+$ F5 T cells (Figure 5.21B and figure 5.22). This was not statistically significant according to a non-parametric Mann-Whitney test.

5.14b Activated motheaten versus control $CD8^+$ F5 T cells kill a greater proportion of NP68 peptide-pulsed B16 cells

In order to look at the direct killing of target B16 cells by activated control and motheaten $CD8^+$ F5 T cells an *in vitro* CTL assay was performed.

Naive $CD8^+$ F5 T cells from control and motheaten mice were activated and expanded *in vitro* for four days prior to use. Wild-type and B16/NP cells were plated out at a 1:1 ratio twenty-four hours prior to the start of the assay. The activated T cells were added to the B16 cells to give five different T cell to B16 cell ratios (1:10, 1:5, 1:1, 5;1 and 10:1), with the number of T cells added determined by the total number of B16 cells used in each well. Each condition was performed in triplicate and cells were harvested after 4 hours and stained with anti-$CD8^{PE}$ antibody followed by analysis by flow cytometry. Histograms displaying GFP

fluorescence were generated by gating on a viable $CD8^-$ cell population (Figure 23 shows representative histogram plots). The percentage killing was calculated by comparing the GFP^+ B16 cells to the GFP^- cells and adjustments made for any deviation from the anticipated 1:1 ratio of target to reference B16 cells by using data from wells where B16 cells were cultured in the absence of T cells (figure 5.23A). No B16 cells were killed by activated control $CD8^+$ F5 T cells at the ratios of 1:10, 1:5 and 1:1 (figure 5.23B and figure 5.24), whereas B16 cells were killed by the motheaten $CD8^+$ F5 T cells at the ratio of 1:1 (figure 5.23C and figure 5.24). At the ratios of 5:1 and 10:1 more B16 cells were killed by the motheaten $CD8^+$ F5 T cells than the control $CD8^+$ F5 T cells (figure 5.24). This was not statistically significant according to a non-parametric Mann-Whitney test.

5.15 Development of *in vivo* assays to examine other aspects associated with the enhanced tumour protection seen with motheaten $CD8^+$ F5 T cells

To further compare the antigen induced response of naive control and naive motheaten $CD8^+$ F5 T cells in mice with developing tumours in their lungs, a control experiment was performed to assess the feasibility of measuring other parameters alongside the enumeration of the tumour lung nodules.

The ultimate aim of such experiments would be to further define the underlying reason(s) for the enhanced protection from lung tumour development seen in mice that received naive motheaten $CD8^+$ F5 T cells. As motheaten mice were no longer available at this point of the study, the feasibility of the assays was assessed using $CD8^+$ F5 T cells from control mice.

A group of seven sub-lethally irradiated mice received $3.2x10^4$ control naive $CD8^+$ F5 T cells. A group of six mice did not receive any T cells. All mice were subcutaneously primed with NP68 peptide in IFA. One day following T cell transfer, all mice received an intravenous

infusion of $2.5x10^5$ B16 cells expressing the NP68 peptide. Fourteen days post B16 cell transfer, mice were sacrificed and the tumour lung nodules enumerated. Mice that received control naive $CD8^+$ F5 T cells had significantly (p=0.0022) fewer tumour nodules (0, 0, 5, 10, 22, 57 and 78) in their lungs compared to mice that received no T cells (116, 124, 198, 201, 215 and 235) (figure 5.25). This result was consistent with earlier assays with regards to the reduced tumour formation in mice receiving T cells but, the overall number of tumour nodules forming in the lungs of mice was reduced.

The $CD8^+$ T cells were monitored directly throughout the assay by taking blood from mice (figure 5.26) and also looking at the $CD8^+$ T cells present in the lungs of the mice at the end of the assay (figure 5.27).

5.15a A greater proportion of $CD8^+$ T cells are present in the blood of irradiated mice receiving naive control $CD8^+$ F5 T cells when compared to irradiated mice receiving no T cells

Peripheral blood was taken from one mouse that received T cells (Figure 5.26D) and one that did not receive T cells (figure 5.26C) on days 1, 4, 7, 11 and 15 following T cell transfer. The blood was processed and stained with anti-$CD8^{PE}$ antibody ready for analysis by flow cytometry. Dot plots were gated on a lymphocyte gate as determined by forward and side scatter. Aliquots of blood from each mouse were pooled and left unstained in order to define the $CD8^+$ gate above any autofluorescence (figure 5.26A). Blood was also taken from a non-irradiated mouse to assist with analysis by revealing the location of the $CD8^+$ cells on the dot plots (figure 5.26B).

A greater proportion of $CD8^+$ cells were seen in the mouse that had received an adoptive transfer of $CD8^+$ F5 T cells, which was above the recovering endogenous $CD8^+$ T pool following sub-lethal irradiation. On days 1, 4, 7, 11 and 15 the respective proportions of cells

in the $CD8^+$ gate for the mouse that received T cells and the mouse that did not receive T cells were 3.36% versus 2.44%, 11% versus 5.07%, 7.07% versus 3.62% (data acquired on a different flow cytometer to that used on other days), 7.49% versus 3.01% and 6.12% versus 1.92% (figure 5.26).

5.15b A greater proportion of $CD8^+$ cells were present in the lungs of mice receiving control naive $CD8^+$ F5 T cells when compared to mice receiving no T cells

Fourteen days following B16 cell transfer, mice were sacrificed and the tumour nodules in the lungs enumerated. The lungs were then homogenised from three mice that had received T cells and three mice that received no T cells. The cell preparations were stained with anti-$CD8^{PE}$ antibody to enable analyses by flow cytometry. Aliquots of blood from each mouse were pooled and left unstained in order to define the CD8 positive gate above the auto-fluorescence (figure 5.27A). Dot plots were gated on a lymphocyte gate as determined by forward and side scatter.

As shown in figures 5.27B and 5.27C, the mice that received T cells had 19.4%, 14.2% and 14.9% CD8 positive cells in the lymphocyte gate compared to 4.21%, 3.42% and 5.54% CD8 positive cells in the lymphocyte gate of the mice that received no T cells. Therefore, the adoptively transferred $CD8^+$ T cells could be detected above the endogenous $CD8^+$ cells present in the lungs of sub-lethally irradiated mice.

5.15c Mice receiving B16 cells lost weight over the duration of the tumour protection assay, regardless of T cell transfer, whereas those that did not receive any B16 cells gained weight

In addition to monitoring the $CD8^+$ T cells during the control assay, the impact of differing tumour loads on the physical health of the mice was also monitored. It had been observed in

previous tumour protection assays that mice with lower tumour loads maintained a better state of general health; therefore the mice were weighed over the duration of the assay.

Mice were initially weighed prior to sub-lethal irradiation (-1) and then again on day(s) 1, 3, 7, 9, 11, 13 and 15 following T cell transfer. All mice that were irradiated lost weight from the point of irradiation (Day -1) to the transfer of T cells (Day 0) (figure 5.28A). Mice that had not been irradiated gained weight over the same time period (figure 5.28A). From the point of B16 cell transfer (Day 1) those mice that had received T cells lost 4.44% of their initial body weight between days 2 and 15 (figures 5.28A and 5.28B). Over the same time period mice that received B16 cells but no T cells lost 6.74% of their initial body weight (figures 5.28A and 5.28B). Mice that had been irradiated but were not the recipients of T cells or B16 cells gained weight over the same time period, with an overall gain of 6.01% of their initial body weight (figures 5.28A and 5.28B). Those mice that were left untreated also gained weight, with a growth of 6.20% of their initial body weight (figures 5.28A and 5.28B).

5.16 Partial regression and delayed growth of a subcutaneous B16 melanoma in a mouse receiving motheaten naive $CD8^+$ F5 T cells

In order to study the relative efficiency of motheaten and control $CD8^+$ F5 T cells in a model of T cell induced tumour regression, ten mice received a subcutaneous injection of $1x10^5$ B16 cells expressing the NP68 epitope. The tumours were monitored by measuring their perpendicular diameters with a set of callipers (figure 5.29). Two mice did not develop tumours at the site of transfer. The remaining tumours grew at different rates and reached differing sizes by day fourteen (figure 5.29).

Three of the mice with similar sized tumours were chosen to study tumour regression. They were sub-lethally irradiated twenty-four hours prior to the transfer of either $1x10^6$ motheaten or $1x10^6$ control naive $CD8^+$ F5 T cells. A third mouse did not receive any T cells.

The tumour in the mouse that received no T cells continued to grow over the duration of the assay. It grew from an average diameter of 2.2mm on day 1, to 8mm on day 17, which represented a 3.6 fold increase in size (figure 5.30). After an initial period of size reduction between day(s) 1 and 5 following T cell transfer, the tumour in the mouse that received naive control $CD8^+$ F5 T cells grew from 3.1mm on day 5 to 7.9mm on day 15, representing a 2.5 fold increase in size (figure 5.30). The tumour in the mouse that received naive motheaten $CD8^+$ F5 T cells grew from 2.5mm, on day 1 following T cells transfer, to a maximum size of 6.3mm on day 8. From this point the tumour reduced in size to 3.6mm on day 11, representing a 2.2 fold reduction in size (figure 5.30). The tumour then continued to grow and reached a size of 4mm on day 18, which was 2 fold less than the size of the tumour in the mouse receiving no T cells and 1.98 fold less than the size of the tumour in the mouse receiving naive control $CD8^+$ T cells.

5.17 Successful co-infection of B16 cells with a retrovirus encoding the Luciferase gene and a retrovirus encoding the NP68 epitope

To enable the tumour regression studies to progress, a more accurate method of monitoring the size of a developing tumour is necessary. One possibility is the use of a whole body imaging unit that can detect bioluminescence. However, to detect luminescence from genetically engineered tumour cells required the production of B16 cells expressing the luciferase gene. Once mice have been injected with luciferin, which is the substrate for the luciferase enzyme, the imaging unit allows the mice to be maintained under anaesthetic whilst it captures bioluminescent images of the tumour. This ultimately allows for the accurate imaging and quantification of both pulmonary and subcutaneous tumours during development and potential regression.

A recombinant retrovirus encoding the luciferase gene and the YFP gene (separated by an IRES) was produced by transfecting the packaging cell line, Phoenix, with the corresponding cDNA. At the point of viral harvest no YFP fluorescence was detected when viewing the cells under a fluorescent microscope (data not shown).

Wild-type B16 cells were infected twice with the retrovirus on subsequent days. At each stage of infection the cells were viewed under the fluorescent microscope, but no YFP fluorescence could be detected (data not shown). The infected B16 cells were also assessed for luciferase activity by performing an *in vitro* luciferase assay. The cells exhibited luciferase activity, with the parental B16 cells being used as a negative control (figure 5.31A).

In view of this result, it was decided to perform a single cell sort based upon viability. However, when cells were analysed using a MoFlo cell sorter it revealed a weak YFP signal. Therefore, cells were sorted based upon cell viability and YFP fluorescence (figure 5.31B). Twelve monoclonal cells grew from a total of 84 sorted cells, one of which (number 8) had a poor growth profile and was therefore not used for further analysis. After an expansion of five weeks the cells were re-tested for luciferase activity. Four of the monoclonal cell lines exhibited low luciferase activity (numbers 1, 4, 10 and 12), with the remaining eight having higher levels of luciferase activity (figure 5.31C). The monoclonal cell line designated number 11 was chosen for further manipulation due to its high luciferase activity and similar growth profile to the parental B16 cell line. This cell line also exhibited low YFP expression when analysed by a FACScalibur flow cytometer (Figure 5.32A).

The luciferase expressing monoclonal B16 cell line (number 11) was then infected twice on subsequent days, with a retrovirus encoding the NP68 epitope as a fusion protein with GFP. Seven days post infection the cells were single cell sorted based upon viability and GFP

expression. At this point 56.4% of the cells were expressing GFP (figure 5.32B). The cells were single cell sorted based upon cell viability and GFP fluorescence (figure 5.32C).

From a total of one hundred and sixty-eight sorted single cells, eighteen of them grew to a stage that allowed for further analysis. Whilst in culture it became evident that clones 1, 8, 14 and 18 had very slow growth and as a result were not used any further. After three weeks of expansion the remaining cell lines were assessed for GFP expression by flow cytometry. The level of GFP expression was compared to that of a previously generated B16 cell line that expressed GFP as a fusion protein with the NP68 epitope and the autofluorescence from wild-type B16 cells. The parental cell line that expressed YFP was also used as a control during analysis. Clones six and seven both expressed GFP (figure 5.33A) but had an abnormal appearance (granular cytoplasm and multiple dendrites) under the light microscope when compared to the parental cell line. Clone three expressed no GFP but appeared to still express some YFP (figure 5.33B). Clones two and nine had a bi-fluorescent GFP profile, with both GFP^+ and GFP^- cells being present (figure 5.33B). In light of this data, clones 6, 7, 3, 2 and 9 were not used for further analysis. The remaining nine clones (4, 5, 10, 11, 12, 13, 15, 16 and 17) all expressed GFP (Figure 4A), with a distribution of expression comparable to the GFP fluorescence from a cell line previously generated during this study. In addition, all nine clones exhibited luciferase activity (figure 5.34B).

The nine B16 Luciferase/YFP/GFP/NP monoclonal cell lines were then tested for the surface presentation of NP68 peptide by MHC class I molecules. Each clone was plated out with an equal number of wild-type B16 cells and allowed to adhere to the plastic for 24 hours. Previously activated $CD8^+$ F5 T cells were then added to the B16 cells at a 2:1 ratio of T cells to B16 cells. As a control, B16 cells were also cultured without T cells. In addition a previously generated B16 cell line that had already been tested for NP68 peptide

presentation at their cell surface was used as a positive control for the killing assay (figure 5.35J). Twenty-four hours later, the $CD8^+$ T cells and dead B16 cells were washed from the wells and the remaining B16 cells removed by incubation with trypsin. Cell were then analysed by flow cytometry, with histograms being generated showing GFP fluorescence by gating on a viable B16 cell population as determined by forward and side scatter. The majority of each clone was killed by the $CD8^+$ F5 T cells as seen by the disappearance of the GFP^+ peak (figure 5.35).

5.18 Significantly enhanced tumour formation in the lungs of irradiated mice receiving control $CD8^+$ F5 T cells, when compared to irradiated mice receiving no T cells

To further explore the intriguing observation that sub-lethally irradiated mice had fewer lung tumour nodules when compared to non-irradiated mice (figure 5.2) an additional experiment was performed. Mice were irradiated six days prior to the intravenous transfer of $1x10^5$ wild-type B16 cells. A second group of mice were not irradiated but received the same number of B16 cells. Fourteen days post transfer, the mice were sacrificed and the tumour nodules in their lungs enumerated.

As shown in figure 5.36 the non-irradiated mice had 40, 41, 58 and 62 tumour nodules in their lungs compared to 8, 9, 15 and 18 tumour nodules in the lungs of the irradiated mice receiving the same number of B16 cells. The difference in the number of tumour nodules between the two sets of mice was statistically significant (p=0.01).

A second group of four irradiated mice received $3x10^6$ purified control naive $CD8^+$ F5 T cells intravenously five days prior to the transfer of $1x10^5$ B16 cells. The mice were also primed subcutaneously at the same time as T cell transfer with NP68 peptide in IFA. The mice had 99, 111, 154 and 168 tumour nodules in their lungs, which was significantly more than irradiated mice that had not received any T cells (p = 0.01) (figure 5.36).

5.19 A tumour specific $CD8^+$ T cell response protects against lung tumour development, whereas a non-specific $CD8^+$ T cell response promotes lung tumour formation

With the availability of both wild-type B16 cells and B16 cells expressing the NP68 epitope an experiment was performed to look at the impact of both a tumour-specific and non-specific $CD8^+$ T cells response on tumour development in the lungs of mice.

A group of twelve sub-lethally irradiated mice received $1.8x10^6$ purified control naive $CD8^+$ F5 T cells intravenously. A second group of twelve sub-lethally irradiated mice did not receive any T cells. A third group of twelve mice were not irradiated and did not receive any T cells. All mice that were recipients of T cells were primed subcutaneously with NP68 peptide in IFA at the same time as T cell transfer.

Three days post T cell transfer six of the irradiated mice that received T cells, six of the irradiated mice that did not receive T cells and six of the mice that were not irradiated or recipients of T cells then received an intravenous infusion of either $1.75x10^5$ B16 cells expressing the NP68 epitope or $1.75x10^5$ wild-type B16 cells. Fourteen days post B16 cell transfer, all mice were sacrificed and the lung tumour nodules enumerated.

The mice that were irradiated and not recipients of T cells had significantly fewer tumour nodules when compared to non-irradiated mice. This was regardless of the type of B16 cells transferred; the non irradiated mice that received the wild-type B16 cells had 199, 210, 244, 299, 301 and 325 tumour nodules in their lungs (figure 5.37A) compared to 59, 73, 94, 148, 202 and 247 tumour nodules in the lungs of irradiated mice that also received wild-type B16 cells (figure 5.37B). The number of lung tumour nodules developing was statistically significant between the two groups (p = 0.026). The non irradiated mice that received the B16 cells expressing the NP68 epitope had 159, 225, 245, 261, 288 and 330 tumour nodules in their lungs (figure 5.37D) compared to 65, 81, 99, 128, 166 and 268 tumour nodules in the

lungs of irradiated mice that also received B16 cells expressing the NP68 epitope (figure 5.37E). This number of lung tumour nodules developing was again statistically significant between the two groups ($p = 0.041$).

The mice that were irradiated and recipients of both $CD8^+$ F5 T cells and wild-type B16 cells had 284, 348, 365, 385, 420 and 450 tumour nodules in their lungs (figure 5.37C), which was significantly more ($p = 0.0022$) than mice that had not received T cells but had received wild-type B16 cells (figure 5.37B). There were no tumour nodules in five of the six mice that had been irradiated and recipients of both $CD8^+$ F5 T cells and B16 cells expressing the NP68 epitope, with the sixth mouse having two tumour nodules in its lungs (figure 5.37F). This was significantly less (p=0.022) than the mice that had not received T cells but had received the B16 cells expressing the NP68 epitope (figure 5.37E).

5.20 Tumour specific $CD8^+$ T cells protect from tumour developments, whereas non-specific CD8+ T cells promote tumour growth

A group of eleven F5 TCR transgenic mice were primed subcutaneously with NP68 peptide in IFA. A second group of 12 F5 TCR transgenic mice were left un-primed. Three days post priming five primed and six un-primed mice received $2x10^5$ wild-type B16 cells. At the same time six primed and six un-primed mice received $2x10^5$ B16 cells expressing the NP68 epitope. Fourteen days post B16 cell transfer the mice were sacrificed and the tumour nodules in their lungs enumerated.

As shown in figure 38 those mice that were primed with NP68 peptide and recipients of wild-type B16 cells had significantly more ($p = 0.0043$) tumour nodule in their lungs (290, 330, 338, 425 and 450) (figure 5.38A) than mice that were not primed (130, 167, 186, 197, 210 and 285) (figure 5.38B) and recipients of wild-type B16 cells. Those mice that were primed with NP68 peptide and recipients of B16 cells expressing the NP68 epitope had virtually no

tumour formation in their lungs (figure 5.38C). This was also the case for the mice that had not been primed and were recipients of the B16 cells expressing the NP68 epitope (figure 5.38D).

In order for SHP-1 to be targeted to improve human T cell function, means are required to modulate its expression. In aim of this, siRNA sequences that target human SHP-1 were tested *in vitro* for their efficacy at downregulating SHP-1.

5.21 Partial downregulation of SHP-1 expression in Jurkat cells using siRNA sequences identified by online algorithms

Online algorithms were utilised to identify candidate siRNA sequences to target SHP-1 expression. The algorithms were performed with an integrated BLAST search in order to remove siRNA sequences with the potential to mediate downregulation of other proteins. The first nucleotide of each 19 nucleotide siRNA sequence was used to annotate a map of the SHP-1 transcript (figure 5.39). The six most frequently identified siRNA sequences (figure 5.39) were synthesised as DNA that encoded for the corresponding shRNA. Each shRNA sequence was cloned into expression vector, ready for functional testing (see materials and methods: 2.9).

Jurkat cells were used for the functional testing of the siRNA sequences, as they express SHP-1. Due to the cost of sorting cells by flow cytometry is was important to establish the minimum number of cells that could be used to give an interpretable SHP-1 signal during western blot analysis. A titration was performed using $4x10^7$, $2x10^7$, $1x10^7$ and $5x10^6$ cells per ml of lysis buffer. SHP-1 protein could be detected at all cell densities, but with an ideal number of cells being $1x10^7$ or above (figure 5.40).

Electroporation was used as the method for introducing plasmid DNA to the Jurkat cells. As electroporation is not 100% efficient with regards to transfection, means were required to identify those cells that had taken up the DNA. In order to achieve this goal, shRNA plasmid was used in conjunction with a GFP expression plasmid at a 5:1 ratio respectively. At this ratio, the likelihood of a GFP expressing cell to also express the shRNA was high. Typically, $1x10^7$ cells were electroporated in the presence of the DNA, with up to 50% of the cells surviving the process. Approximately 2-4% of the surviving cells expressed GFP and were subsequently sorted by flow cytometry. Jurkat cells that had not been transfected with DNA were used to define a GFP positive gate. In addition, Jurkat cells that had been transfected with plasmid DNA containing no shRNA sequence, and the GFP plasmid were also sorted in the same manner. Each sample took approximately one hour to sort and gave $3x10^5$ cells for immunoblot analysis.

Following immunoblotting, densitometry was used to adjust for any differences between each sample, as determined by the actin band for each sample. The actin band with the highest density was identified, and the necessary adjustments required to normalise the other actin bands was then applied to the SHP-1 bands. The adjusted densities of the SHP-1 bands were then compared to the density of the SHP-1 bands from the cells that had been transfected with plasmid containing no shRNA sequence. Sequences 1341 and 1550 mediated no SHP-1 knockdown, whereas 1236, 825, 989 and 1112 mediated 25%, 10%, 23% and 22% SHP-1 knockdown respectively (figure 5.41).

In order to repeat the functional testing of candidate siRNA sequences it was necessary to develop a revised siRNA screening protocol, which allowed for more efficient transfection of cells and a more economically favourable method of isolating cells.

5.22 Successful production of Hela cells expressing mouse and human SHP-1

Due to their non-adherent nature, Jurkat cells proved challenging to transfect, as seen with the 2-4% success rate above. Adherent cell lines are recognised to be more readily transfected, and also by methods that are not as harsh as electroporation. In light of this, Hela cells, which are a transformed adherent cell line, were chosen to genetically modify in order to express either mouse of human SHP-1. Mouse SHP-1 was introduced using a transfection reagent called jetPEI, whereas human SHP-1 was introduced using calcium phosphate. This was due to the availability of the reagents at the time of cell line generation. In addition, calcium phosphate proves more cost effective than jetPEI, and therefore allows greater numbers of cells to be transfected at any one time. The use of plasmids containing the neomycin resistance gene allowed cells to be selected without the need for flow cytometry. This proved advantageous when taking into consideration the cost of sorting cells. Furthermore, the periodic blocking of the flow cytometer during cell sorting often meant low numbers of cells were obtained, which precluded analysis by immunoblotting techniques. Transfected cells were selected by G418 treatment, and between 30% and 50% of the transfected Hela cells survived by the time all untransfected cells had died. Four weeks post antibiotic selection both cells lines were expressing the corresponding SHP-1 (Figure 5.42A and B). Interestingly, the parental Hela cells used for the generation of human SHP-1 expressing cells were also expressing some SHP-1 (Figure 5.42B).

5.23 Successful reduction of human SHP-1 expression in Hela cells receiving *MISSION*™ shRNA sequences

Concomitant with the production of Hela cells expressing human SHP-1, commercially produced shRNA sequences for targeting SHP-1 were becoming available. Specific algorithms are used by companies to identify groups of siRNA sequences for each protein, which should

yield at least one shRNA capable of mediating downregulation of the protein being targeted. Sigma-Aldrich produced four such sequences for human SHP-1, which were subsequently tested for their efficacy at downregulating SHP-1 in Hela cells.

Plasmid DNA was prepared for transfection using calcium phosphate and the cells transfected. The cells were selected with puromycin and G418 for a total of six weeks. Immunoblotting and densitometry analysis revealed that sequence 444 did not mediate SHP-1 knockdown, but sequences 1712, 1572 and 1376 gave 56%, 61% and 53% SHP-1 downregulation respectively (figure 5.43).

5.24 Summary of results

It was previously demonstrated during this study that SHP-1 deficient $CD8^+$ F5 T cells exhibit an enhanced *in vivo* expansion and cytotoxic capacity. In order to explore the possibility of harnessing these findings to improve adoptive cell transfer immunotherapy strategies, a mouse model (B16 melanoma) of tumourigenesis was used. In pursuit of this aim, B16 tumour cells were produced that constitutively express the NP68 epitope and could therefore be used in conjunction with F5 $CD8^+$ T cells from transgenic motheaten and littermate mice.

It was conclusively demonstrated that SHP-1 deficient T cells provide superior protection against tumour development in a lung model of tumourigenesis. In addition, preliminary data indicates that SHP-1 deficient $CD8^+$ T cells may also mediate enhanced regression of established solid tumours. In light of these observations, B16 cells were produced that express the luciferase gene, and would therefore allow future tumour studies to be performed in a non-invasive and quantitative manner, by using a whole body imaging unit that detects bioluminescence.

In order for $CD8^+$ T cells lacking SHP-1 expression to be used in a therapeutic setting, it would be necessary to induce SHP-1 downregualtion in human T cells. In light of this, candidate siRNA sequences were screened for their efficacy at mediating SHP-1 expression. At best, a commercially available shRNA sequence mediated 61% reduction in SHP-1 expression. This was achieved in Hela cells that had been generated to express the human SHP-1 gene.

Finally, it was demonstrated that tumour non-specific $CD8^+$ T cells have a pro-tumoural role in a mouse model of lung tumour development, whereas a tumour specific $CD8^+$ T cell response was completely protective.

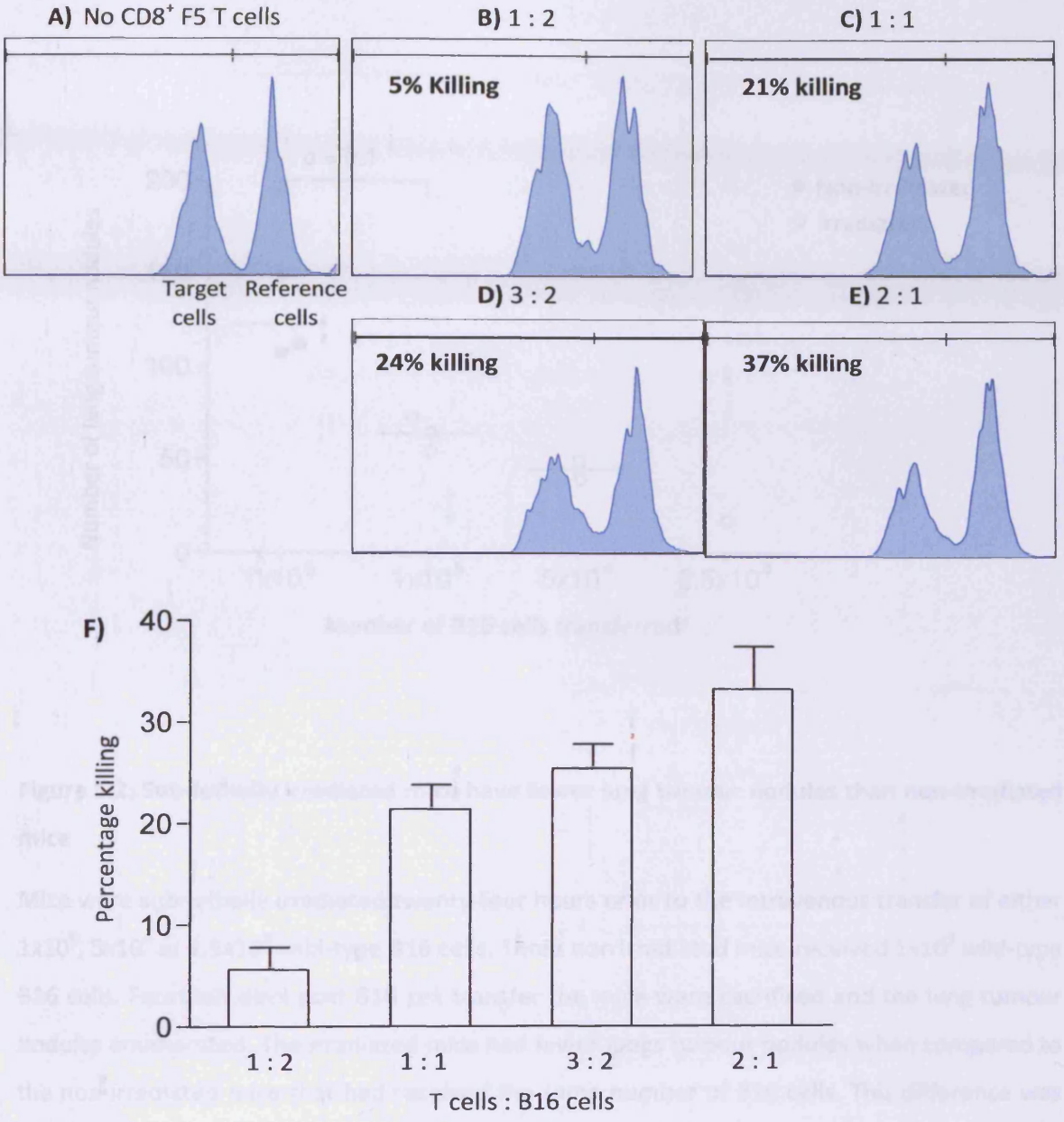


Figure 5.1: Activated CD8$^+$ F5 T cells kill NP68 peptide pulsed B16 cells

CD8$^+$ F5 T cells were activated in vitro for two days and expanded for a further 3 days in IL-2. B16 cells were either pulsed with NP68 peptide (target cells) or left unpulsed (reference cells). Those B16 cells pulsed with NP68 peptide were labelled with 0.2µM CFSE, whereas those that had not been pulsed were labelled with 2µM CFSE (A). Equal numbers of target and reference B16 cells were then co-cultured, in U-bottomed 96 well plates, with the corresponding number of activated CD8$^+$ F5 T cells. The ratio of CD8$^+$ F5 T cells to B16 cells was based upon the total number of B16 cells in each well, with each condition being performed in triplicate (F). After 4 hours the cells were removed from the wells and stained with anti-CD8^{PE} antibody. Cells were analysed by flow cytometry and the histograms (A to E, representative histograms) electronically gated on CD8$^-$ and CFSE$^+$ cells. The percentage killing (F) was assessed by comparing the target cell population to the reference cells. B16 cells were killed at all ratios by the activated CD8$^+$ F5 T cells.

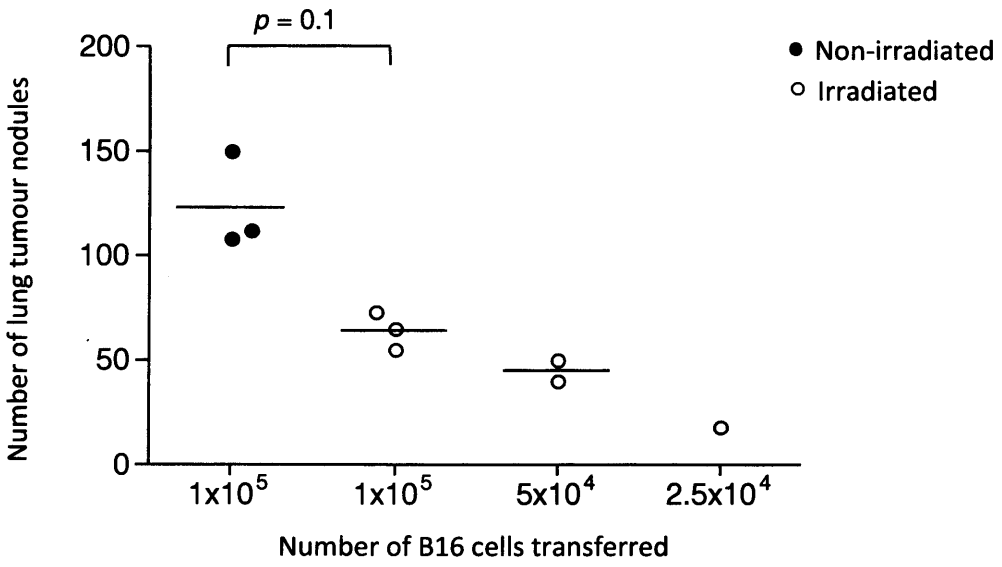


Figure 5.2: Sub-lethally irradiated mice have fewer lung tumour nodules than non-irradiated mice

Mice were sub-lethally irradiated twenty-four hours prior to the intravenous transfer of either $1x10^5$, $5x10^4$ or $2.5x10^4$ wild-type B16 cells. Three non irradiated mice received $1x10^5$ wild-type B16 cells. Fourteen days post B16 cell transfer the mice were sacrificed and the lung tumour nodules enumerated. The irradiated mice had fewer lungs tumour nodules when compared to the non-irradiated mice that had received the same number of B16 cells. This difference was not statistically significant ($p = 0.1$).

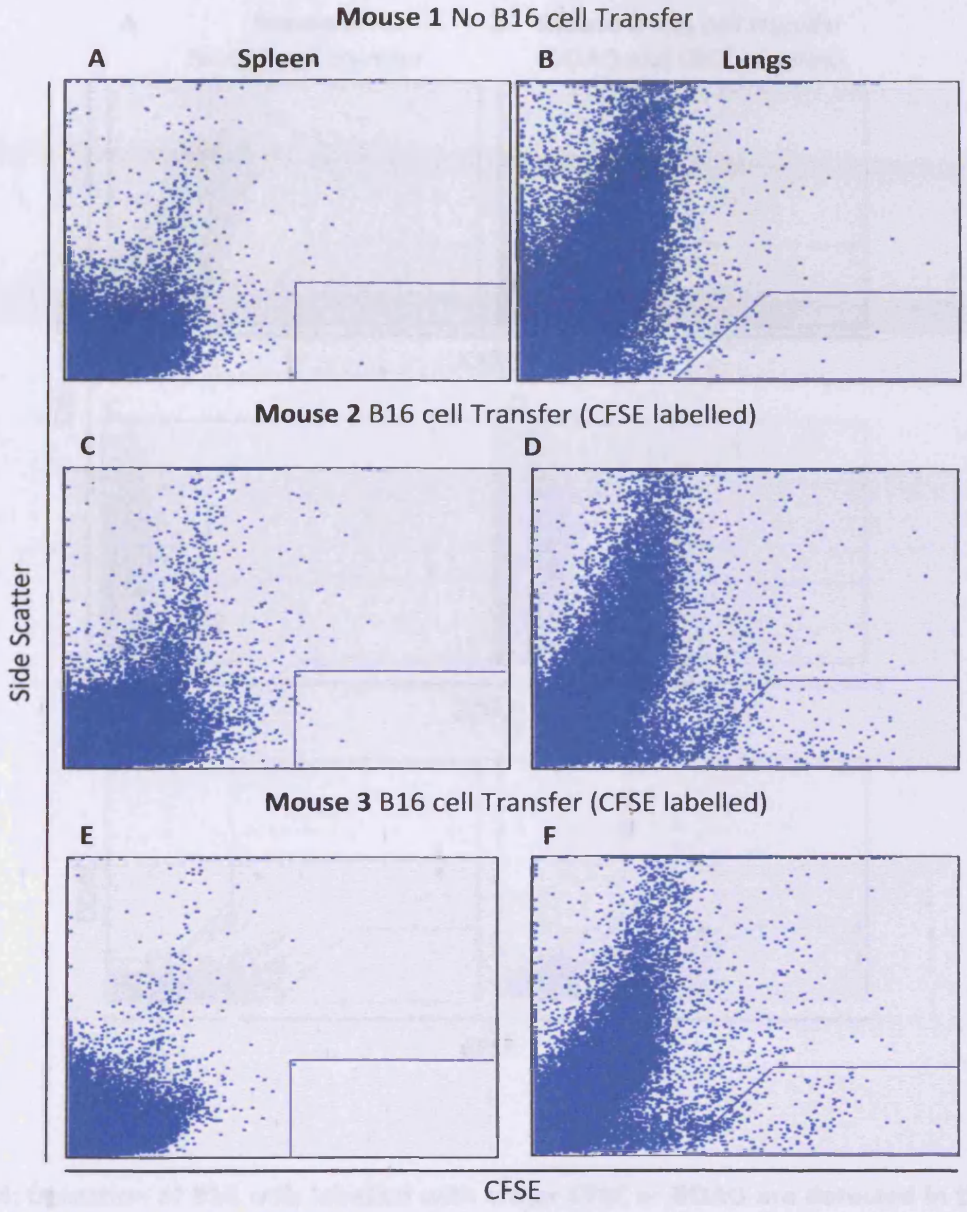


Figure 5.3: CFSE labelled B16 melanoma cells are present in the lungs of mice twenty-four hours post intravenous transfer

Mice were sub-lethally irradiated twenty-four hours prior to cell transfer. B16 cells were labelled with either 0.2μM or 2μM CFSE, and $6x10^5$ of each population was transferred intravenously to the same recipient mouse (C,D and E,F). One mouse did not receive any B16 cells (A and B). Twenty-four hours post transfer the mice were sacrificed and the spleens and lungs taken and prepared for flow cytometry. The CFSE positive gates were set by using the data from the mouse that did not receive any T cells (A and B). CFSE labelled cells were not detected in the spleens of recipient mice (C and E) but CFSE positive cells were evident in the lungs (D and F), although the two populations of CFSE labelled B16 cells could not be distinguished.

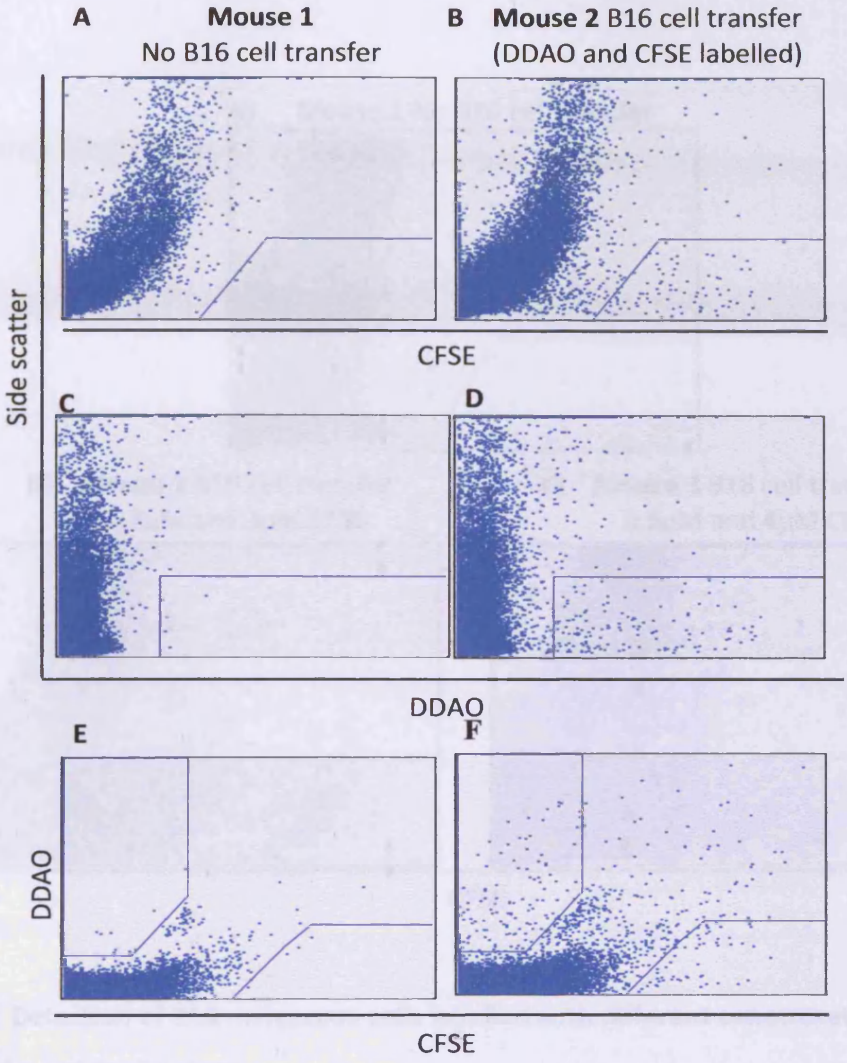


Figure 5.4: Detection of B16 cells labelled with either CFSE or DDAO are detected in the lungs of a mouse twenty-four hours post intravenous transfer

Recipient mice were sub-lethally irradiated twenty-four hours prior to the transfer of B16 melanoma cells. B16 cells were labelled with either 2μM CFSE or 10μM DDAO and $2.5x10^5$ of each population was transferred intravenously to a recipient mouse (B, D and F). A second mouse did not receive any B16 cells (A, C and E). Twenty-four hours post transfer, the mice were sacrificed and the lungs homogenised and analysed by flow cytometry. The dot plots show the cells obtained from the lungs, with the gates set above the autofluorescence found in the control mouse (A, C and E). Dot plots are displayed to show the labelled cells individually, for CFSE (B) and DDAO (D) against side scatter, or on the same plot (F). Cells labelled with either DDAO or CFSE were detected in the lungs of the recipient mouse (B, D and F).

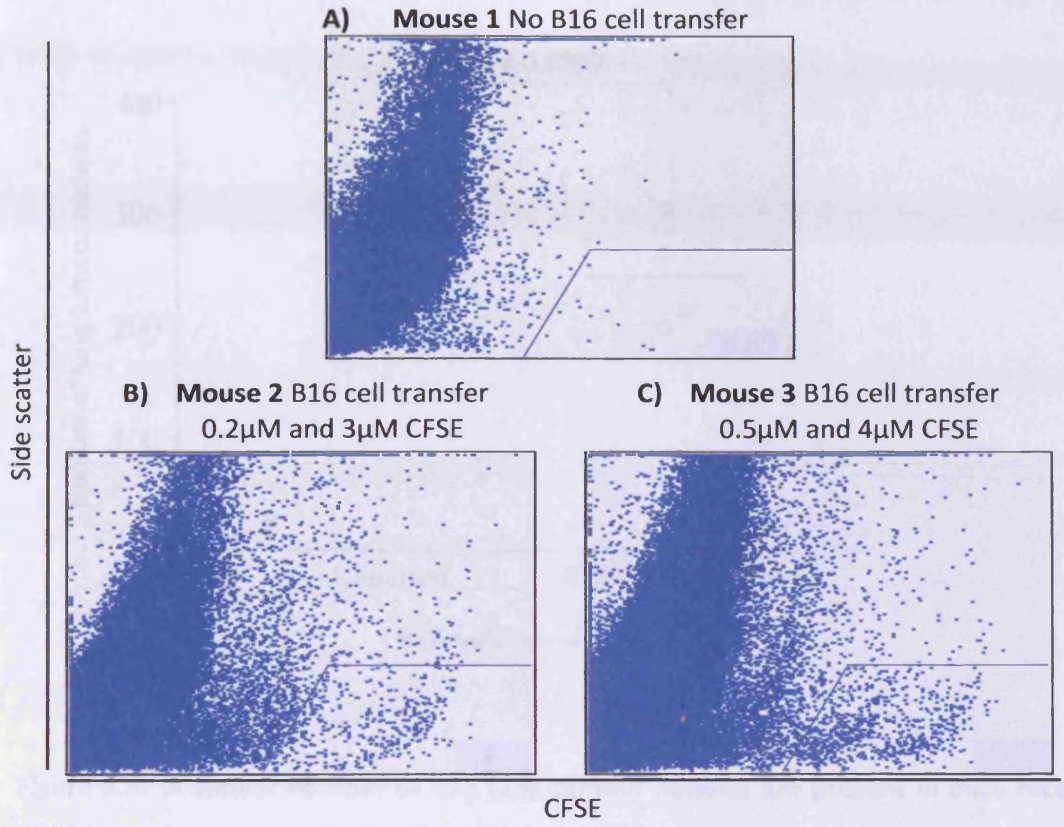


Figure 5.5: Detection of B16 melanoma cells labelled with different concentrations of CFSE cells in the lungs of a recipient mouse

Recipient mice were sub-lethally irradiated twenty-four hours prior to transfer of B16 melanoma cells. B16 cells were labelled with either 0.2μM, 0.5μM, 3μM and 4μM CFSE and paired as shown above (B and C). A total of $8x10^5$ B16 cells were transferred intravenously to each recipient mouse. A third mouse did not receive any B16 cells (A). Twenty-four hours post transfer the mice were sacrificed and the lungs homogenised and analysed by flow cytometry. The dot plots show the cells obtained from the lungs, with the gates set above the autofluorescence found in the mouse that did not receive any B16 cells (A). CFSE labelled cells were detected in the lungs of the mouse that received B16 cells labelled with 0.2μM or 3μM CFSE (B), although the two populations could not be detected. CFSE labelled cells were also detected in the lungs of the mouse that received B16 cells labelled with 0.5μM or 4μM CFSE (C), with both populations being evident.

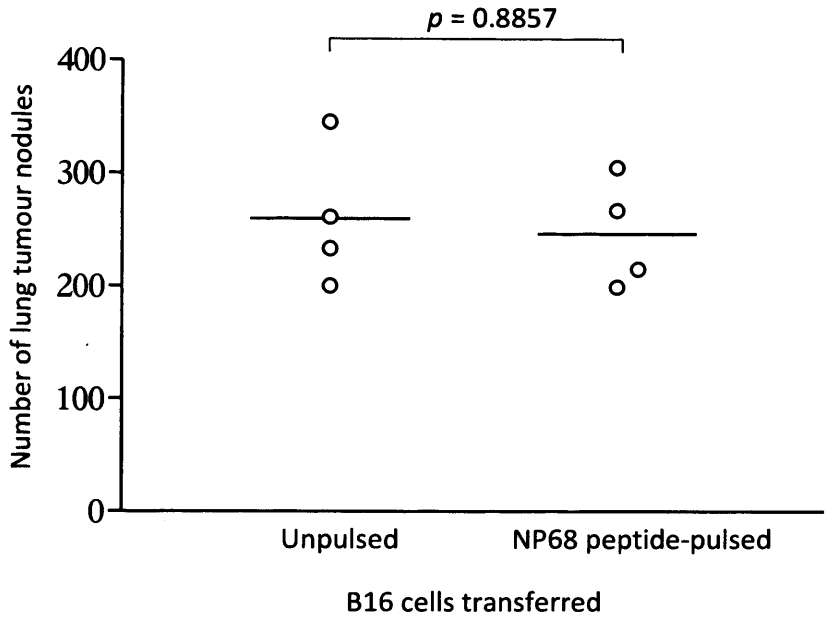


Figure 5.6: A similar number of B16 lung tumour nodules are present in mice receiving $CD8^+$ F5 T cells and either B16 cells pulsed with NP68 peptide or unpulsed B16 cells

Sub-lethally irradiated mice received $3x10^6$ naive control $CD8^+$ F5 T cells and a subcutaneous injection of NP68 peptide in IFA. Seven days post T cell transfer, mice received either $2x10^5$ wild-type B16 cells that had been pulsed with 5μM NP68 peptide or $2x10^5$ wild-type B16 cells that were left unpulsed. Fourteen days post transfer the mice were sacrificed and the lung tumour nodules enumerated. There was no significant difference between the number of tumour nodules in the lungs of mice from each group ($p = 0.8857$).

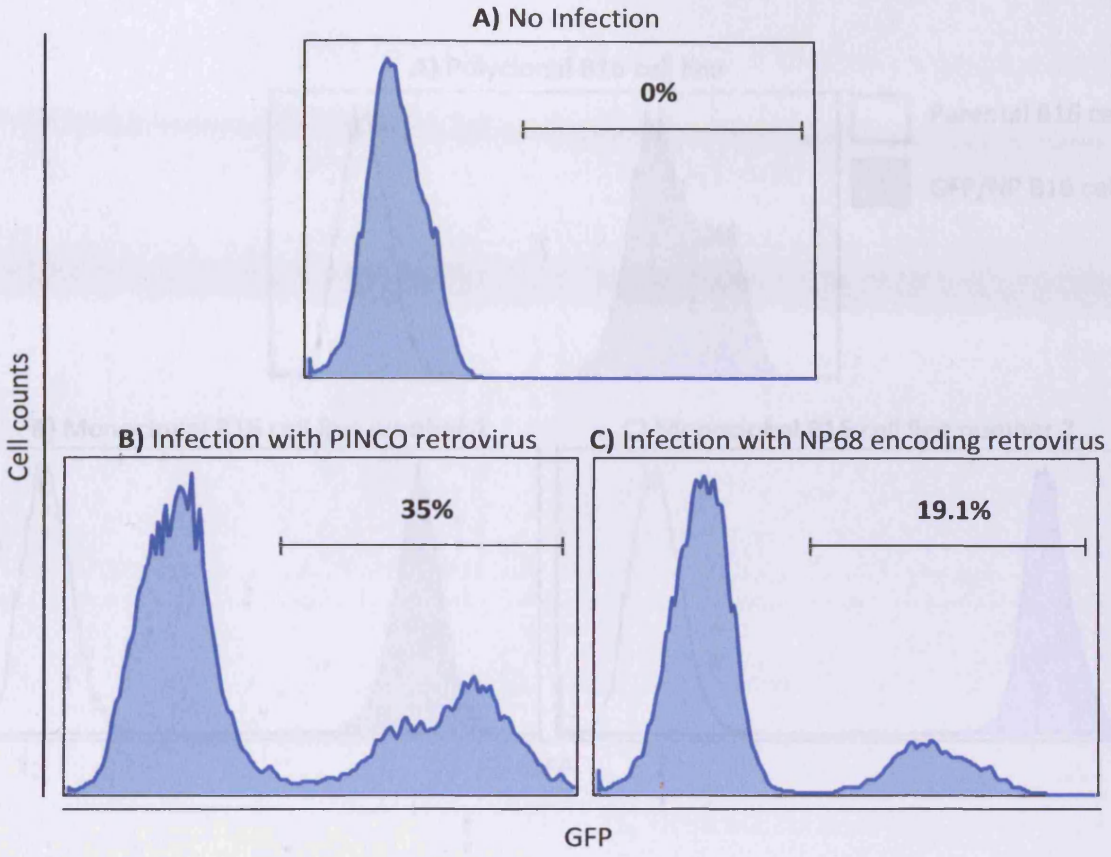


Figure 5.7: Successful infection of B16 cells with a retrovirus encoding the NP68 epitope as a fusion protein with GFP

B16 melanoma cells were plated out twenty-four hours prior to infection. Cells were then incubated with protamine sulphate for 1 hour prior to the addition of an equal volume of supernatant containing either a control retrovirus, encoding GFP (B), or a retrovirus encoding GFP as a fusion protein with the NP68 epitope (C). After a further 24 hours the process was repeated for a second round of infection. The degree of GFP expression was assessed by flow cytometry 7 days post infection. Gates were defined based upon the autofluorescence from the parental B16 cell line (A), with the percentage of cells residing in each gate displayed for each histogram. The B16 cells infected with the control retrovirus were 35% GFP positive (B) whereas the cells infected with the retrovirus encoding the NP68 epitope were 19.1% GFP positive (C).

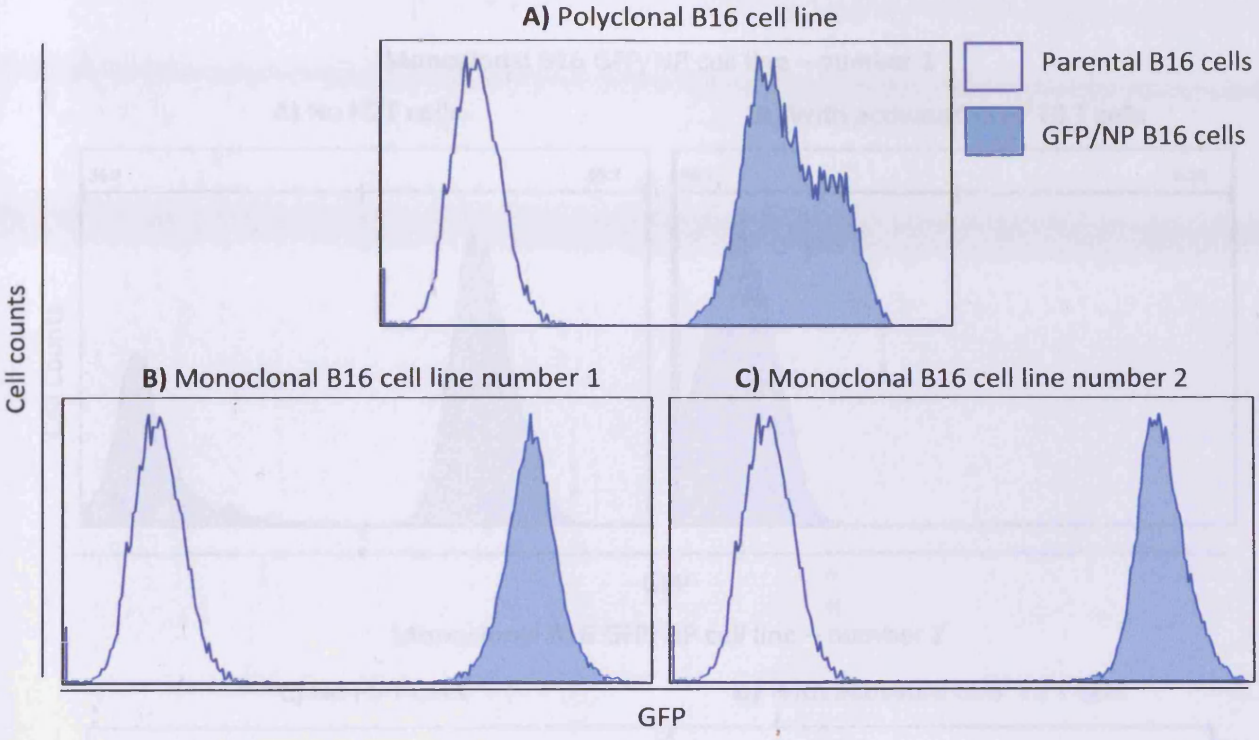


Figure 5.8: Successful cloning of B16 melanoma cell expressing the NP epitope as a fusion protein with GFP

B16 cells that had been infected with a retrovirus encoding the NP68 epitope as a fusion protein with GFP were single cell sorted based upon cell viability, GFP expression and pulse width. The overlay histogram plots were gated on a viable cell population as determined by forward and side scatter. A polyclonal cell line (originally $1x10^4$ cells) was GFP positive 2 weeks following single cell sorting (A). Two monoclonal B16 cell lines were GFP positive 5 weeks post single cell sorting (B and C).

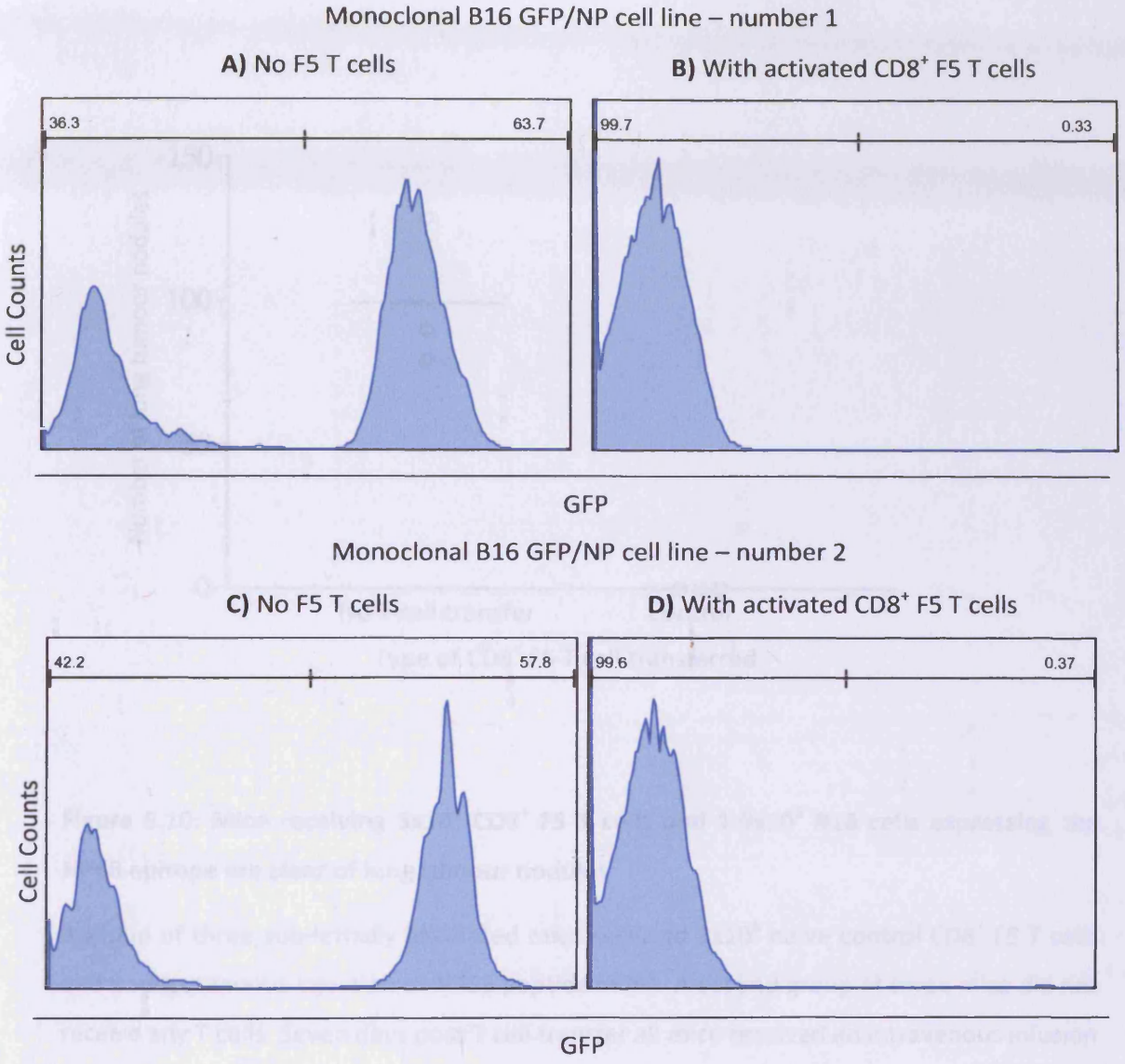


Figure 5.9: B16 cells infected with a retrovirus encoding the NP68 epitope are successfully killed by activated CD8$^+$ F5 T cells

Wild-type B16 cells were plated out at an approximate 1:1 ratio with monoclonal B16 cells expressing the NP68 peptide as a fusion protein with GFP (A and C). After twenty-four hours activated control CD8$^+$ F5 T cells were added to the B16 cells and incubated for a further 16 hours (B and D). B16 cells were also incubated without activated CD8$^+$ F5 T cells (A and C). Cell were harvested and stained with anti-CD8^{PE} and analysed by flow cytometry. Over 99% of the B16 cells were killed by the CD8$^+$ F5 T cells (B and D).

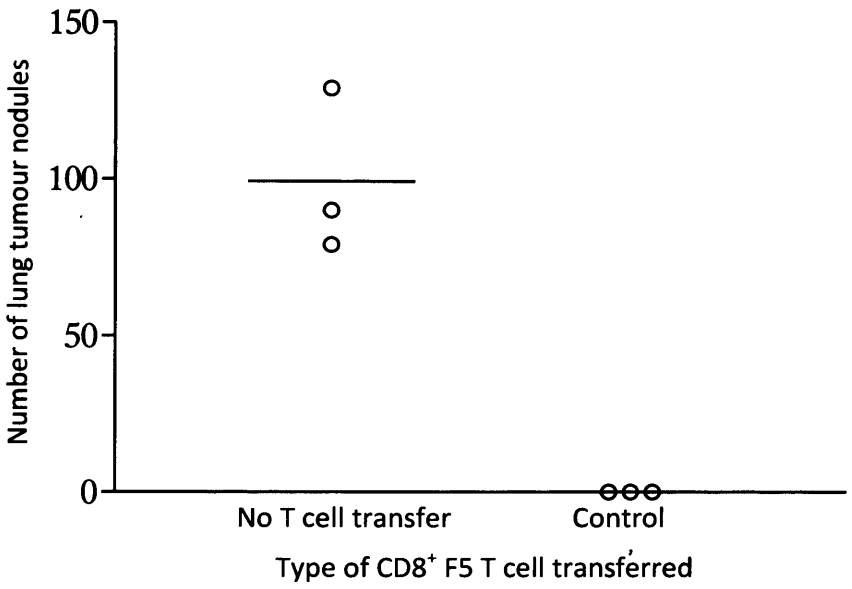


Figure 5.10: Mice receiving $3x10^6$ $CD8^+$ F5 T cells and $1.5x10^5$ B16 cells expressing the NP68 epitope are clear of lung tumour nodules

A group of three sub-lethally irradiated mice received $3x10^6$ naive control $CD8^+$ F5 T cells and a subcutaneous injection of NP68 peptide in IFA. A second group of three mice did not receive any T cells. Seven days post T cell transfer all mice received an intravenous infusion of $1.5x10^5$ B16 expressing the NP68 epitope. Fourteen days post transfer the mice were sacrificed and the lung tumour nodules enumerated. There were no lung tumour nodules in the mice that received an adoptive transfer of naive $CD8^+$ F5 T cells seven days prior to B16 cell transfer. Mice that did not receive $CD8^+$ F5 T cells had 129, 90 and 79 tumour nodules in their lungs. The solid line represents the mean tumour nodule number.

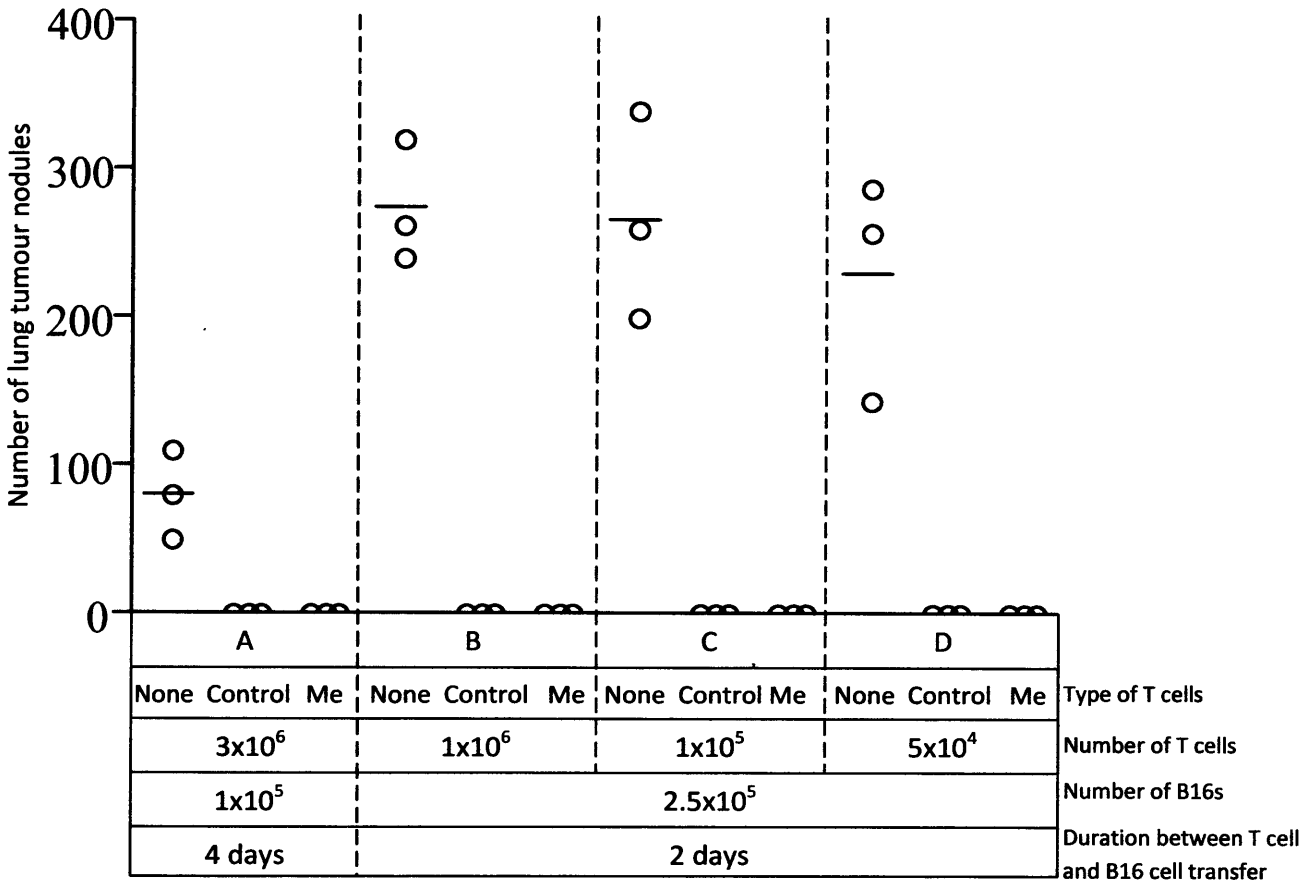


Figure 5.11: Complete protection from B16 tumour formation in the lungs of mice receiving naive control or motheaten CD8$^+$ F5 T cells

In four independent experiments sub-lethally irradiated mice received either naive control or motheaten (Me) CD8$^+$ F5 T cells and also a subcutaneous injection of NP68 in IFA. For each subsequent experiment mice received $3x10^6$ (A), $1x10^6$ (B), $1x10^5$ (C) or $5x10^4$ (D) naive CD8$^+$ F5 T cells. The number of B16 cells expressing the NP68 epitope transferred to each mice was either $1x10^5$ (A) or $2.5x10^5$ (B, C and D) and the time between T cell and B16 cell transfer was either 4 (A) or 2 days (B, C and D). Mice were sacrificed fourteen days post tumour cell transfer and the tumour nodules in their lungs enumerated. Mice that did not receive any T cells all developed lung tumour nodules, with a greater number seen in mice that received $2.5x10^5$ B16 cells (B, C and D) than those that received $1x10^5$ B16 cells (A). Mice that received either control or motheaten CD8$^+$ F5 T cells had no tumour formation within their lungs after fourteen days.

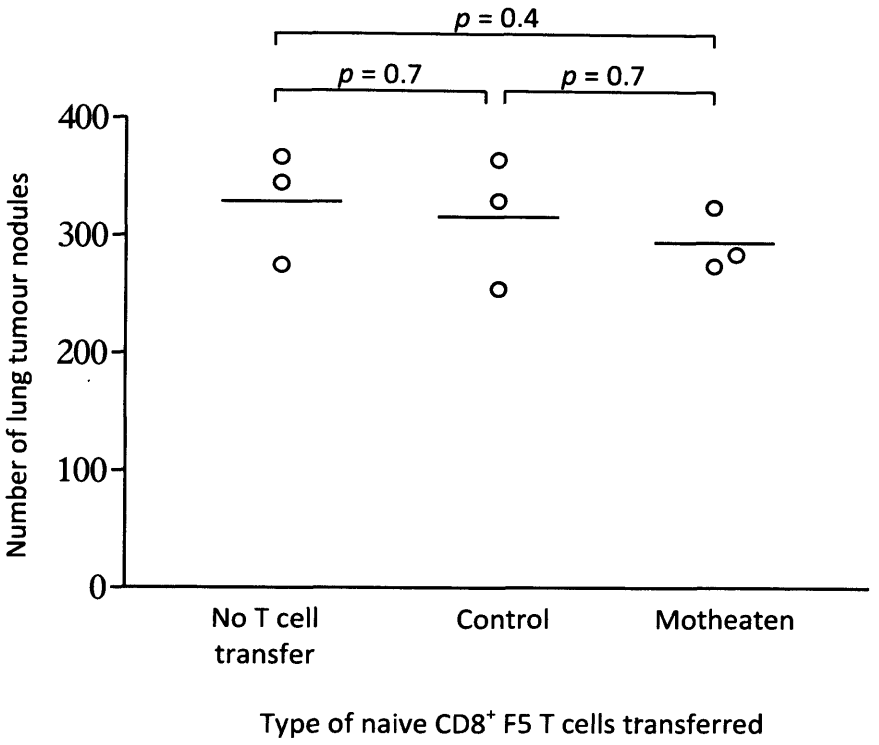


Figure 5.12: Similar lung tumour formation in mice receiving no $CD8^+$ F5 T cells and mice receiving either $1x10^4$ naive control or motheaten $CD8^+$ F5 T cells

Recipient mice were sub-lethally irradiated twenty-four hours prior to adoptive cell transfer. Two groups of mice received either $1x10^4$ naïve control or motheaten $CD8^+$ F5 T cells intravenously. A third group of mice received no T cells. Concomitantly to T cell transfer, each mouse was primed subcutaneously with NP68 peptide in IFA. The following day $2.5x10^5$ B16 melanoma cells expressing the NP68 epitope were transferred intravenously. Fourteen days post tumour cell transfer mice were sacrificed and the tumour nodules in their lungs enumerated. The solid line shows the mean for each pair of mice. All mice had similar tumour nodule formation in their lungs, regardless of T cell transfer or the type of T cells transferred.

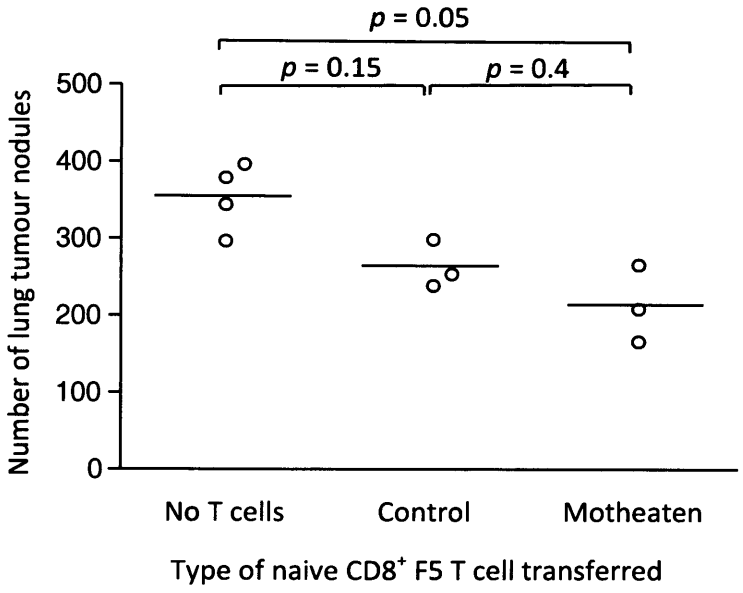


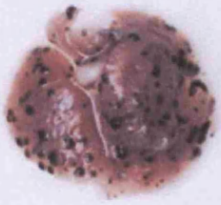
Figure 5.13: Statistically significant reduced lung tumour formation in mice receiving $2x10^4$ naive motheaten $CD8^+$ F5 T cells in comparison to mice that did not receive any T cells

Recipient mice were sub-lethally irradiated twenty-four hours prior to adoptive cell transfer. A group of three mice received either $2x10^4$ naive control or motheaten $CD8^+$ F5 T cells intravenously. A third group containing four mice did not receive any T cells. Concomitantly with T cell transfer, each mouse was primed subcutaneously with NP68 peptide in IFA. The following day, $2.5x10^5$ B16 melanoma cells expressing the NP68 epitope were transferred intravenously. Fourteen days post tumour cell transfer, mice were sacrificed and the pigmented tumour nodules in the lungs enumerated. The mice that received naive motheaten $CD8^+$ F5 T cells had significantly fewer ($p = 0.05$) lung tumour nodules than mice that did not receive any T cells. Any difference between the number of lung tumour nodules in mice that received either control or motheaten $CD8^+$ F5 T cells were not statistically significant ($p = 0.4$). The solid line represents the mean for each group.

A) No T cells transferred



B) Naive Control $CD8^+$ F5 T cell transfer



C) Naive motheaten $CD8^+$ F5 T cell transfer



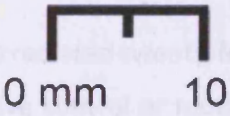


Figure 5.14: A reduced tumour load in the lungs of a mouse receiving naive motheaten $CD8^+$ F5 T cells

Recipient mice were sub-lethally irradiated twenty-four hours prior to adoptive cell transfer. Pairs of mice received either $3.2x10^4$ naive motheaten or control $CD8^+$ F5 T cells intravenously. A third pair of mice received no T cells. Concomitantly with T cell transfer, each mouse was primed subcutaneously with NP68 peptide in IFA. The following day $2.5x10^5$ B16 melanoma cells expressing the NP68 epitope were transferred intravenously. Fourteen days post tumour cell transfer mice were sacrificed and the lungs from one mouse from each pair of mice was photographed (this figure) and the number of lung tumour nodules enumerated for all mice (Figure 5.15). The B16 melanoma nodules appear as pigmented nodules. The mouse that did not receive any T cells had highly pigmented lungs (A). The mouse that received naive control $CD8^+$ F5 T cells had a greater tumour load (B) than the mouse that received naive motheaten $CD8^+$ F5 T cells (C).

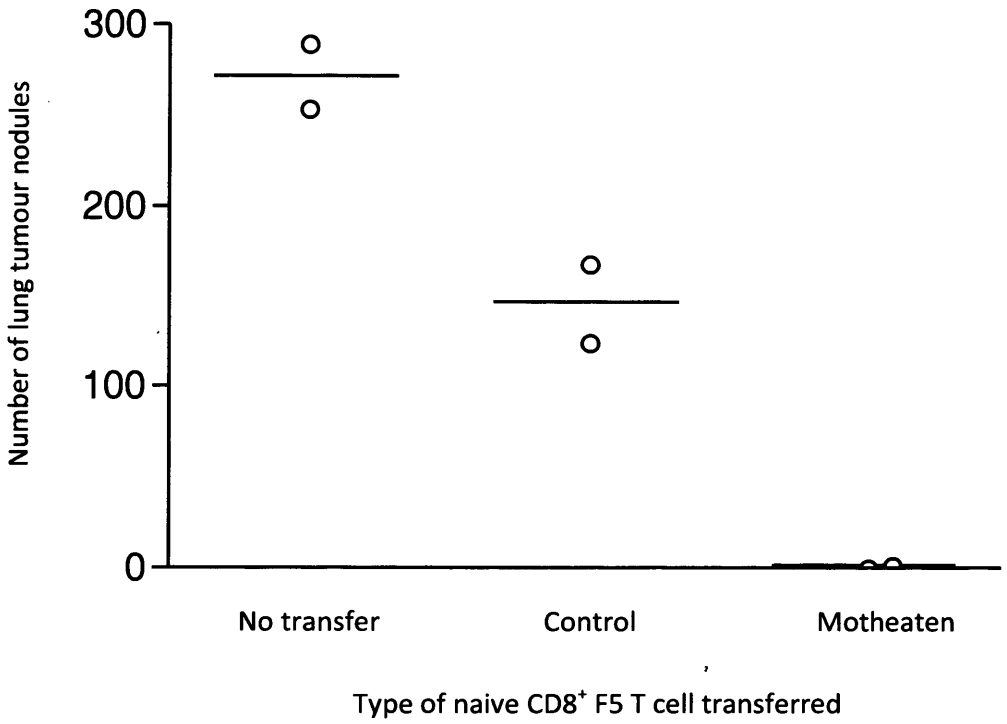


Figure 5.15: A reduced number of tumour nodules in the lungs of mice receiving naive motheaten $CD8^+$ F5 T cells, when compared to those mice receiving naive control $CD8^+$ F5 T cells

Recipient mice were sub-lethally irradiated twenty-four hours prior to adoptive cell transfer. Two pairs of mice received $3.2x10^4$ naïve control or motheaten $CD8^+$ F5 T cells intravenously. A third pair of mice received no T cells. Concomitantly to T cell transfer, each mouse was primed subcutaneously with NP68 peptide in IFA. The following day, $2.5x10^5$ B16 melanoma cells expressing the NP68 epitope were transferred intravenously. Fourteen days post tumour cell transfer, mice were sacrificed and their lungs photographed (figure 5.14) prior to the enumeration of the tumour nodules (this figure). The mice that recevied naive motheaten $CD8^+$ F5 T cells had less lung tumour nodules than the mice that received naive control $CD8^+$ F5 T cells. The solid line shows the mean for each pair of mice.

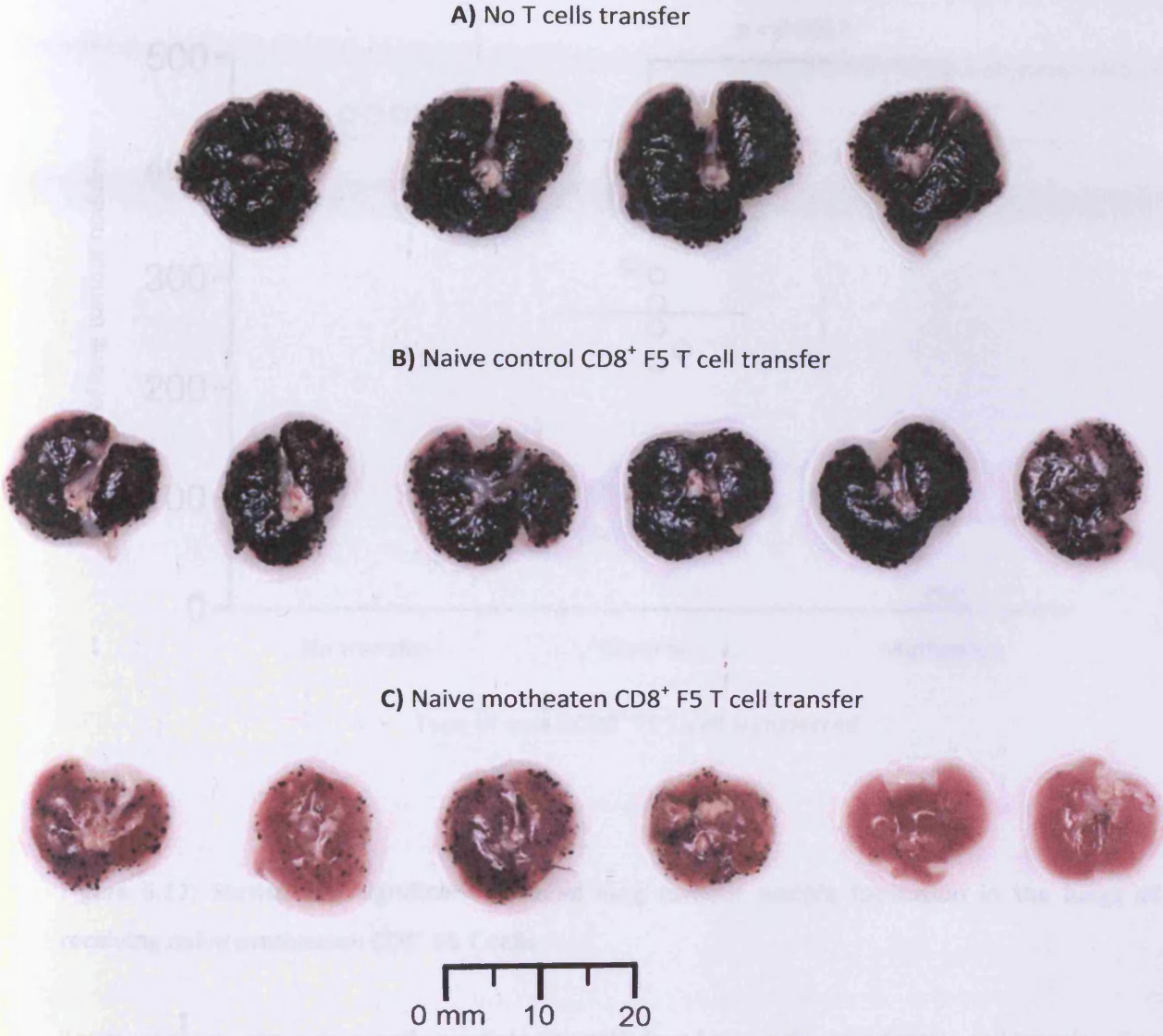


Figure 5.16: A reduced tumour load in the lungs of mice receiving naive motheaten $CD8^+$ F5 T cells

Recipient mice were sub-lethally irradiated twenty-four hours prior to adoptive $CD8^+$ T cell transfer. Groups of six mice received either $3.2x10^4$ naive control or motheaten $CD8^+$ F5 T cells intravenously. A third group of six mice did not receive any T cells. Concomitantly with T cell transfer, each mouse was primed subcutaneously with NP68 peptide in IFA. The following day, $2.5x10^5$ B16 melanoma cells expressing the NP68 epitope were transferred intravenously. Fourteen days post tumour cell transfer, mice were sacrificed and their lungs removed and photographed (this figure) prior to the enumeration of the tumour nodules (Figure 5.17). Two mice from the group that did not receive T cells died on days 11 and 12 post tumour cell transfer. The mice that did not receive any T cells (A) and the mice that received naive control $CD8^+$ F5 T cells (B) had highly pigmented lungs, indicating a high tumour load in comparison to mice that received naive motheaten $CD8^+$ F5 T cells (C).

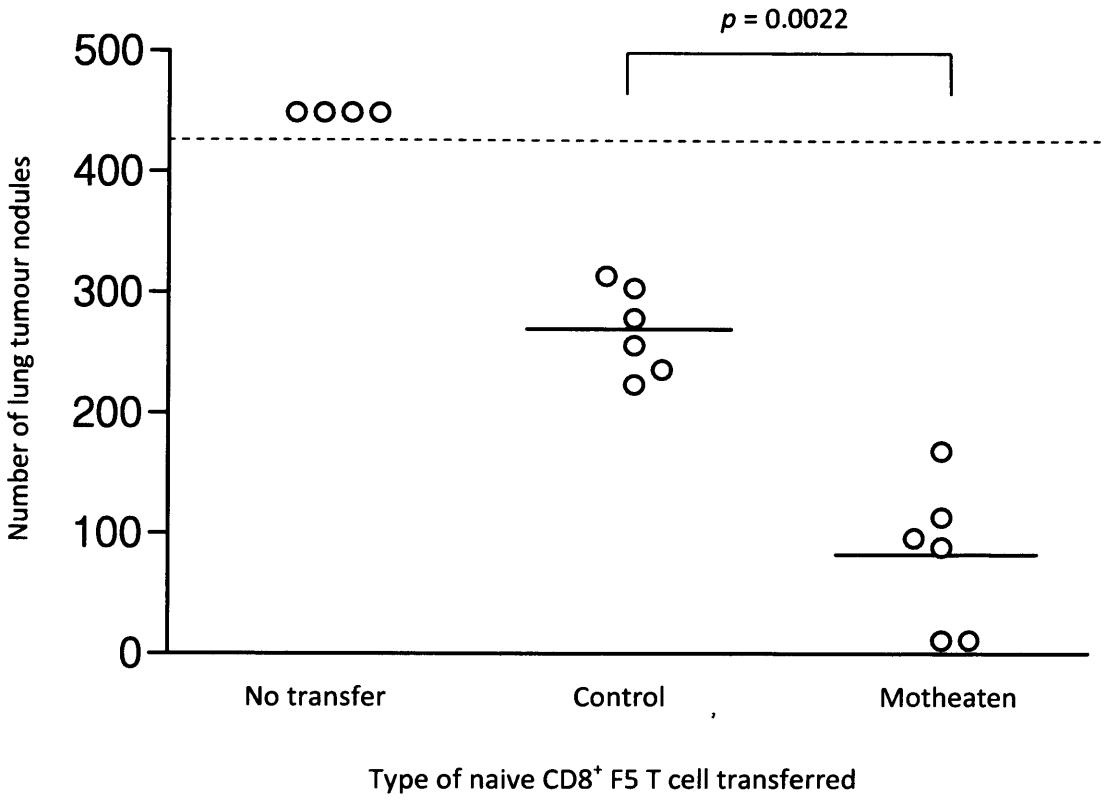


Figure 5.17: Statistically significant reduced lung tumour nodule formation in the lungs of mice receiving naïve motheaten $CD8^+$ F5 T cells

Recipient mice were sub-lethally irradiated twenty-four hours prior to adoptive cell transfer. Groups of six mice received either $3.2x10^4$ naïve motheaten or control $CD8^+$ F5 T cells intravenously. A third group of six mice did not receive any T cells. Concomitantly with T cell transfer, each mouse was primed subcutaneously with NP68 peptide in IFA. The following day $2.5x10^5$ B16 melanoma cells expressing the NP68 epitope were transferred intravenously. Fourteen days post tumour cell transfer, mice were sacrificed and the lungs photographed (Figure 5.16) prior to the enumeration of the pigmented tumour nodules (this figure). There were significantly less tumour nodules in the lungs of mice receiving naive motheaten $CD8^+$ F5 T cells, compared to those mice receiving naive control $CD8^+$ F5 T cells ($p = 0.0022$). Two mice from the group that did not receive T cells died on days 11 and 12 post tumour cell transfer and therefore were not included in the analysis. The dashed line represents the upper limit at which the tumour nodules can be enumerated and the solid lines show the mean for each group.

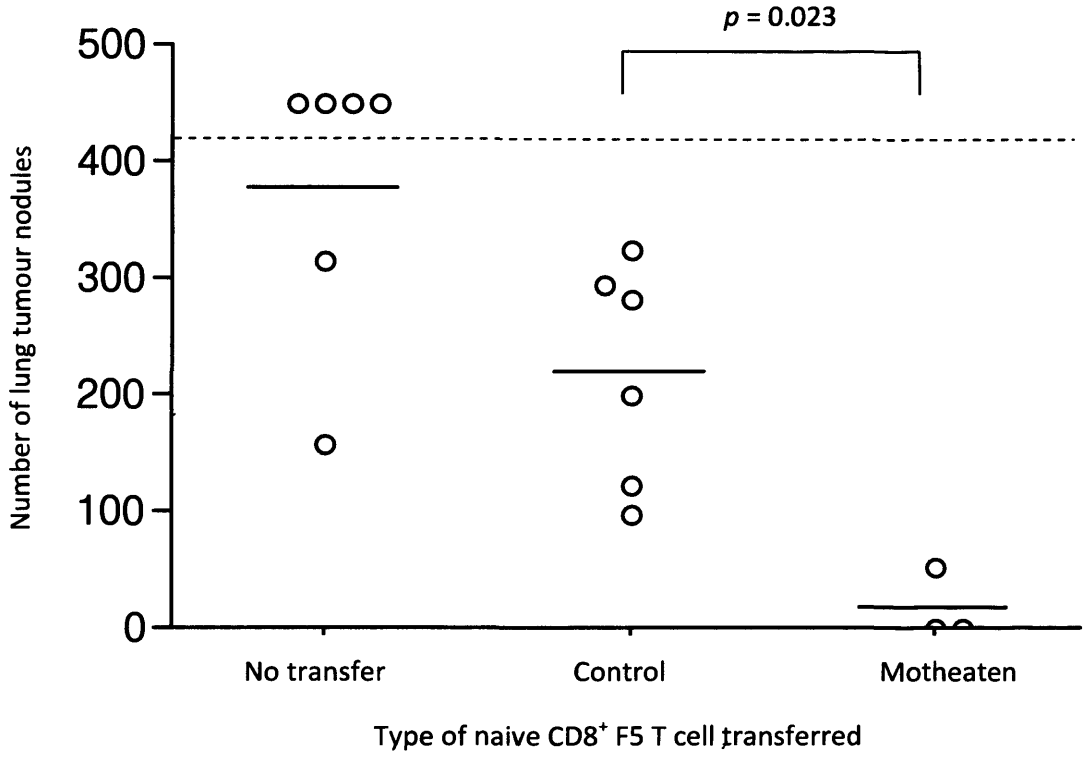


Figure 5.18: Statistically significant reduced lung tumour nodule formation in mice receiving naïve motheaten $CD8^+$ F5 T cells in comparison to mice receiving naïve control $CD8^+$ F5 T cells

Recipient mice were sub-lethally irradiated twenty-four hours prior to adoptive cell transfer. A group of three mice received $3.2x10^4$ naive motheaten $CD8^+$ F5 T cells intravenously. A second group containing six mice received an equivalent number of naive control $CD8^+$ F5 T cells intravenously. A further six mice did not receive any T cells. Concomitantly with T cell transfer, each mouse was primed subcutaneously with NP68 peptide in IFA. The following day $2.5x10^5$ B16 melanoma cells expressing the NP68 epitope were transferred intravenously. Fourteen days post tumour cell transfer mice were sacrificed and the pigmented tumour nodules in the lungs enumerated. There were significantly fewer tumour nodules in the lungs of the mice receiving naive motheaten $CD8^+$ F5 T cells, compared to mice receiving naive control $CD8^+$ F5 T cells ($p = 0.023$). The dashed line represents the upper limit at which the tumour nodules can be enumerated and the solid line represents the mean for each group.

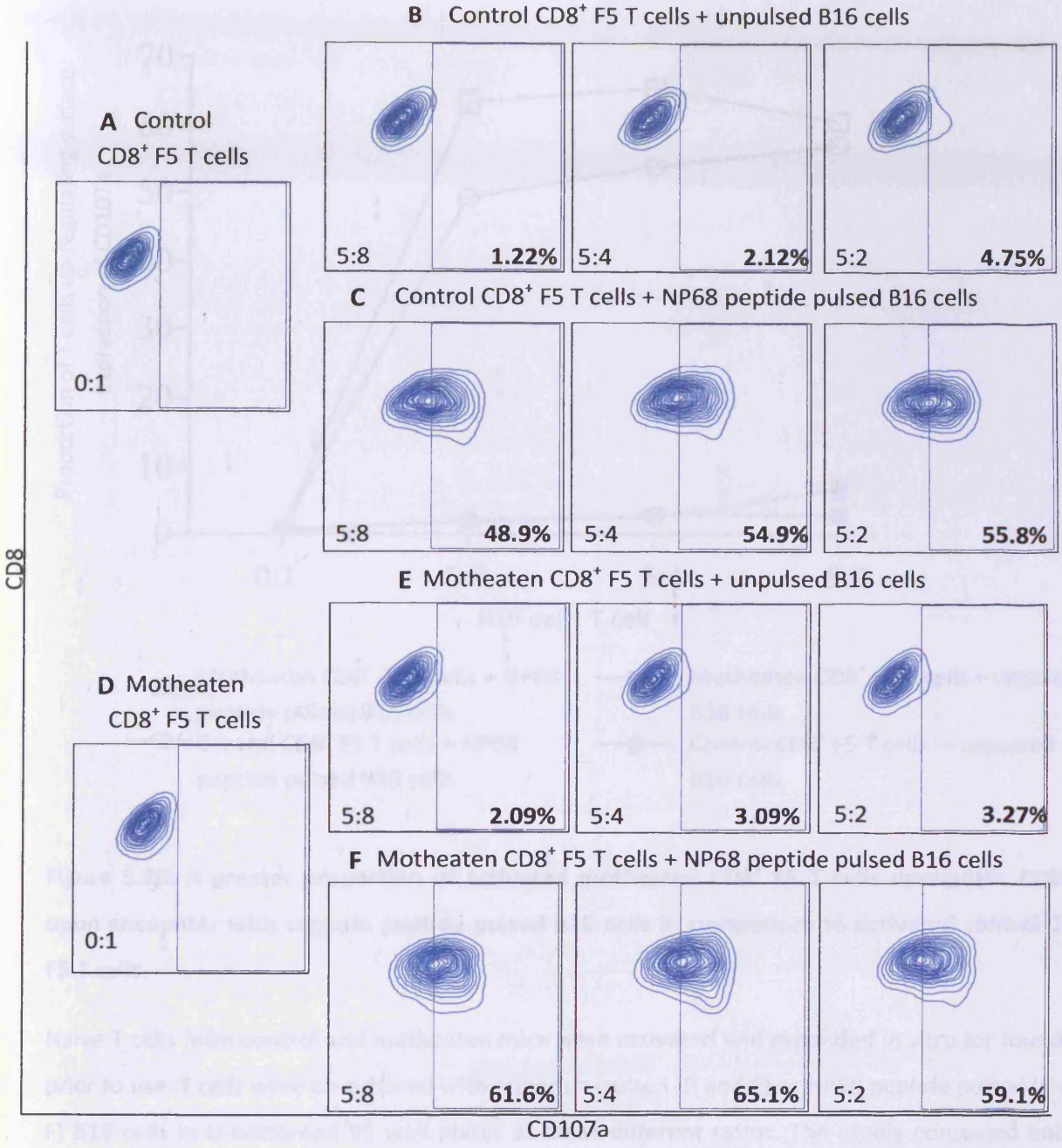


Figure 5.19: Activated control and motheaten CD8$^+$ F5 T cells upregulate CD107a upon encounter with NP68 peptide-pulsed B16 cells

In vitro activated T cells were co-cultured with either un-pulsed (B and E) or NP68 peptide pulsed (C and F) B16 cells at three different ratios (shown in bottom left hand corner of each plot). Each condition was performed in triplicate (Figure 5.20), with representative data shown here. The media contained both FITC-conjugated CD107a antibody and golgi-stop™. Cells were harvested after four hours and stained with anti-CD8^{PE} antibody prior to analysis by flow cytometry. Contour plots were electronically gated on a viable and CD8 positive cell population. The CD107a gate was set above the fluorescence seen in the absence of B16 cells (A and D), with the percentages of cells residing in the gate shown for each plot. Both control and motheaten CD8$^+$ F5 T cells upregulated CD107a in the presence of B16 cells pulsed with NP68 peptide (C and F).

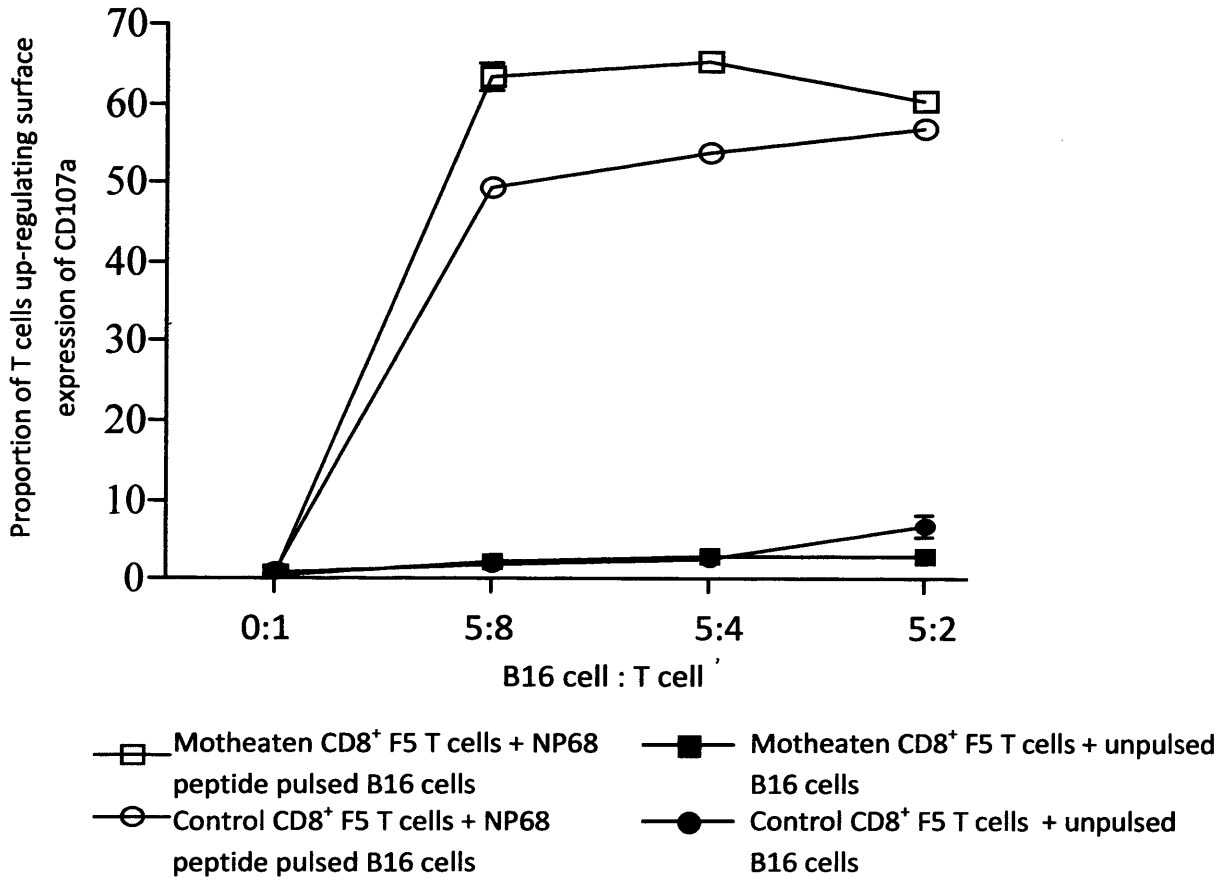


Figure 5.20: A greater proportion of activated motheaten CD8$^+$ F5 T cells upregulate CD107a upon encounter with cognate peptide pulsed B16 cells in comparison to activated control CD8$^+$ F5 T cells

Naive T cells form control and motheaten mice were activated and expanded in vitro for four days prior to use. T cells were co-cultured with either un-pulsed (B and E) or NP68 peptide pulsed (C and F) B16 cells in U-bottomed 96 well plates at three different ratios. The media contained both a FITC-conjugated CD107a antibody and golgi-stop™. After four hours the cells were labelled with anti-CD8^{PE} antibody and analysed by flow cytometry. Contour plots were generated and gated to show the proportion of T cells that had up-regulated their surface expression of CD107a (Figure 5.19). The data from figure 5.19 was plotted to show the percentage up-regulation versus ratio of B16 to T cells (this figure). Both activated control and motheaten CD8$^+$ F5 T cells showed minimal spontaneous up-regulation of CD107a upon encounter with un-pulsed B16 cells (■ and ●). A greater proportion of activated motheaten CD8$^+$ F5 T cells (□) up-regulated the surface expression of CD107a in comparison to activated control CD8$^+$ F5 T cells (○). For each condition, the difference in CD107a expression between motheaten and control T cells was not statistically significant, according to a Mann-Whitney test.

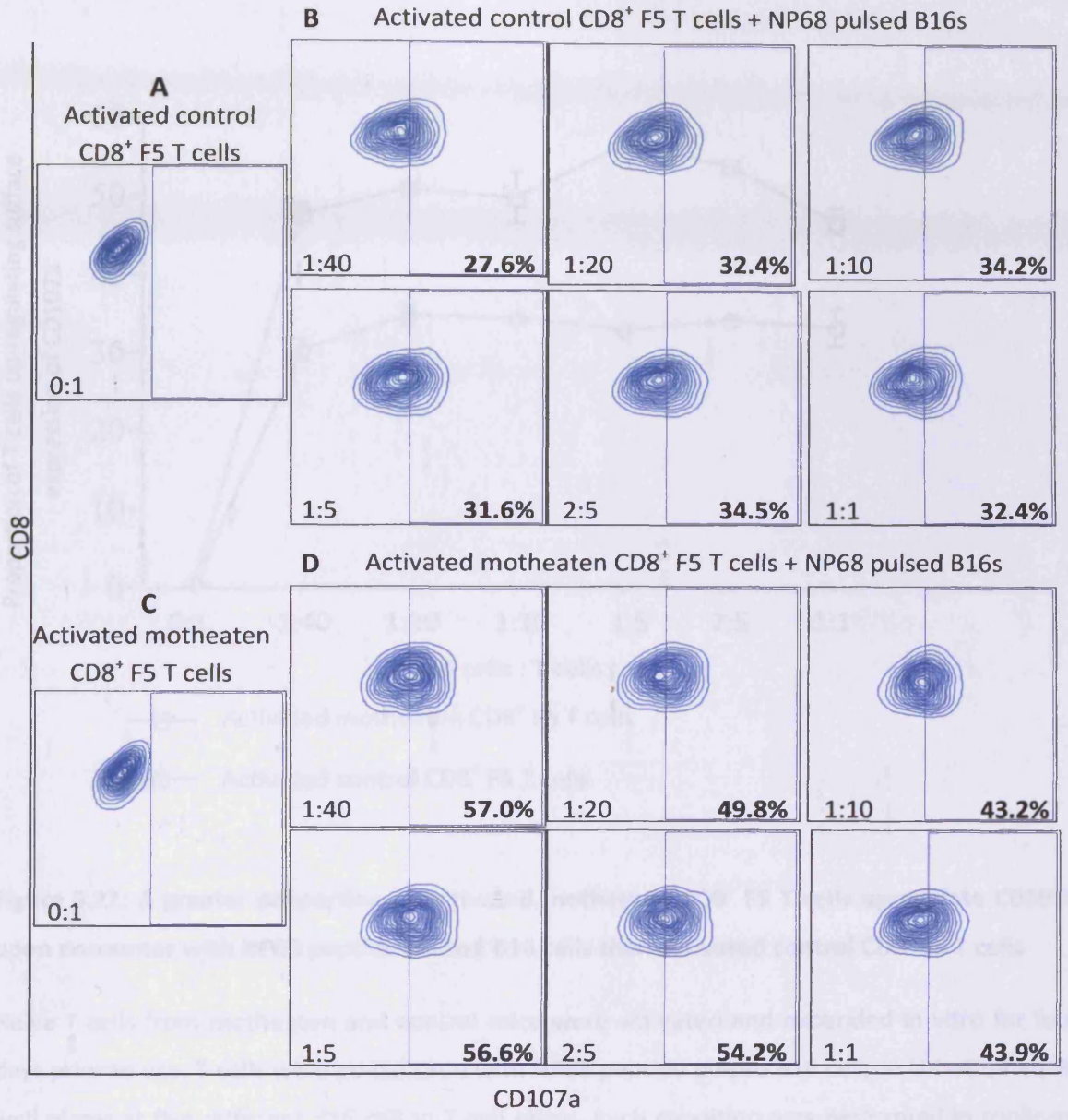


Figure 5.21: A greater proportion of activated control and motheaten CD8$^+$ F5 T cells upregulate CD107a upon encounter with NP68 peptide-pulsed B16 cells

Naive T cells form motheaten and control mice were activated and expanded in vitro for four days prior to use. T cells were co-cultured with NP68 peptide pulsed B16 cells in U-bottomed 96 well plates at five different B16 cell to T cell ratios (shown in bottom left hand corner of each plot). Each condition was performed in triplicate (Figure 5.22), with representative data shown here. The assay media contained both FITC-conjugated CD107a antibody and golgi-stop™. Cells were harvested after four hours and stained with anti-CD8^{PE} antibody prior to analysis by flow cytometry. Contour plots were electronically gated on a viable and CD8 positive cell population. The CD107a gate was set above the fluorescence seen in the absence of B16 cells (A and C), with the percentages of cells residing in the gate shown for each plot. At each ratio a greater proportion of activated motheaten CD8$^+$ F5 T cells (D) upregulated CD107a in the presence of B16 cells pulsed with NP68 peptide (C and F) when compared to activated control CD8$^+$ F5 T cells (B).

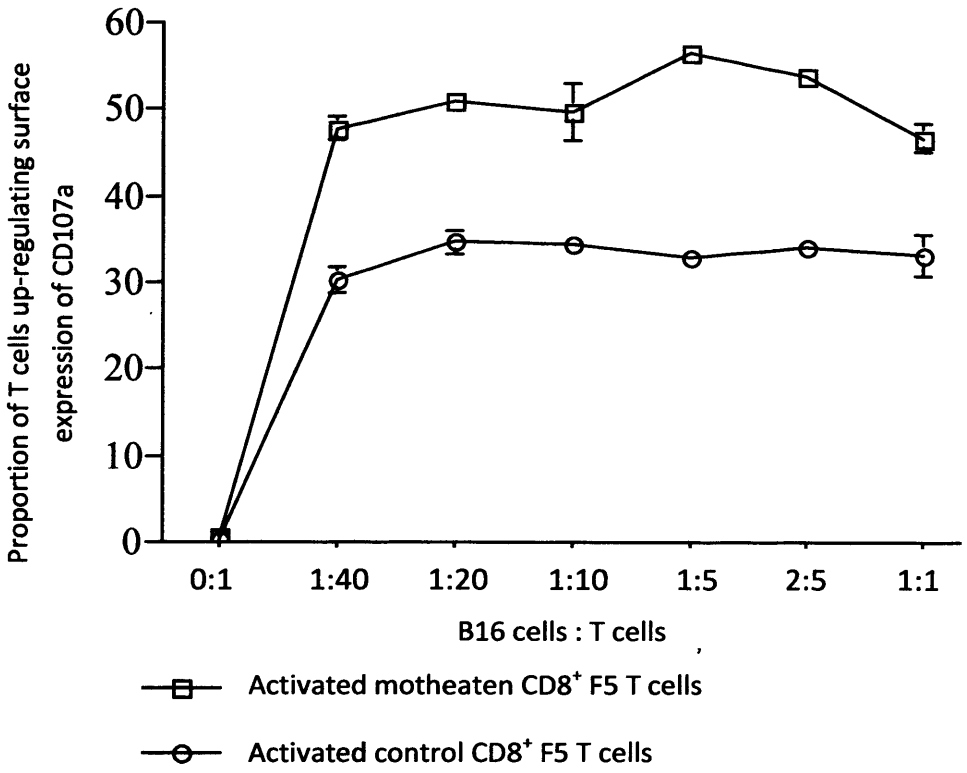


Figure 5.22: A greater proportion of activated motheaten CD8$^+$ F5 T cells upregulate CD107a upon encounter with NP68 peptide-pulsed B16 cells than activated control CD8$^+$ F5 T cells

Naive T cells from motheaten and control mice were activated and expanded in vitro for four days prior to use. T cells were co-cultured with NP68 peptide pulsed B16 cells in U-bottomed 96 well plates at five different B16 cell to T cell ratios. Each condition was performed in triplicate (this figure). The assay media contained both a FITC-conjugated CD107a antibody and golgi-stop™. Cells were harvested after 4h and stained with anti-CD8^{PE} antibody prior to analysis by flow cytometry. Contour plots were electronically gated on viable and CD8 positive cell populations (figure 5.21), and the CD107a gate set above the fluorescence seen in the absence of B16 cells. At each ratio a greater proportion of activated motheaten CD8$^+$ F5 T cells (□) up-regulated CD107a in the presence of B16 cells pulsed with NP68 peptide when compared to activated control CD8$^+$ F5 T cells (○). For each condition, the difference in CD107a expression between motheaten and control T cells was not statistically significant according to a Mann-Whitney test.

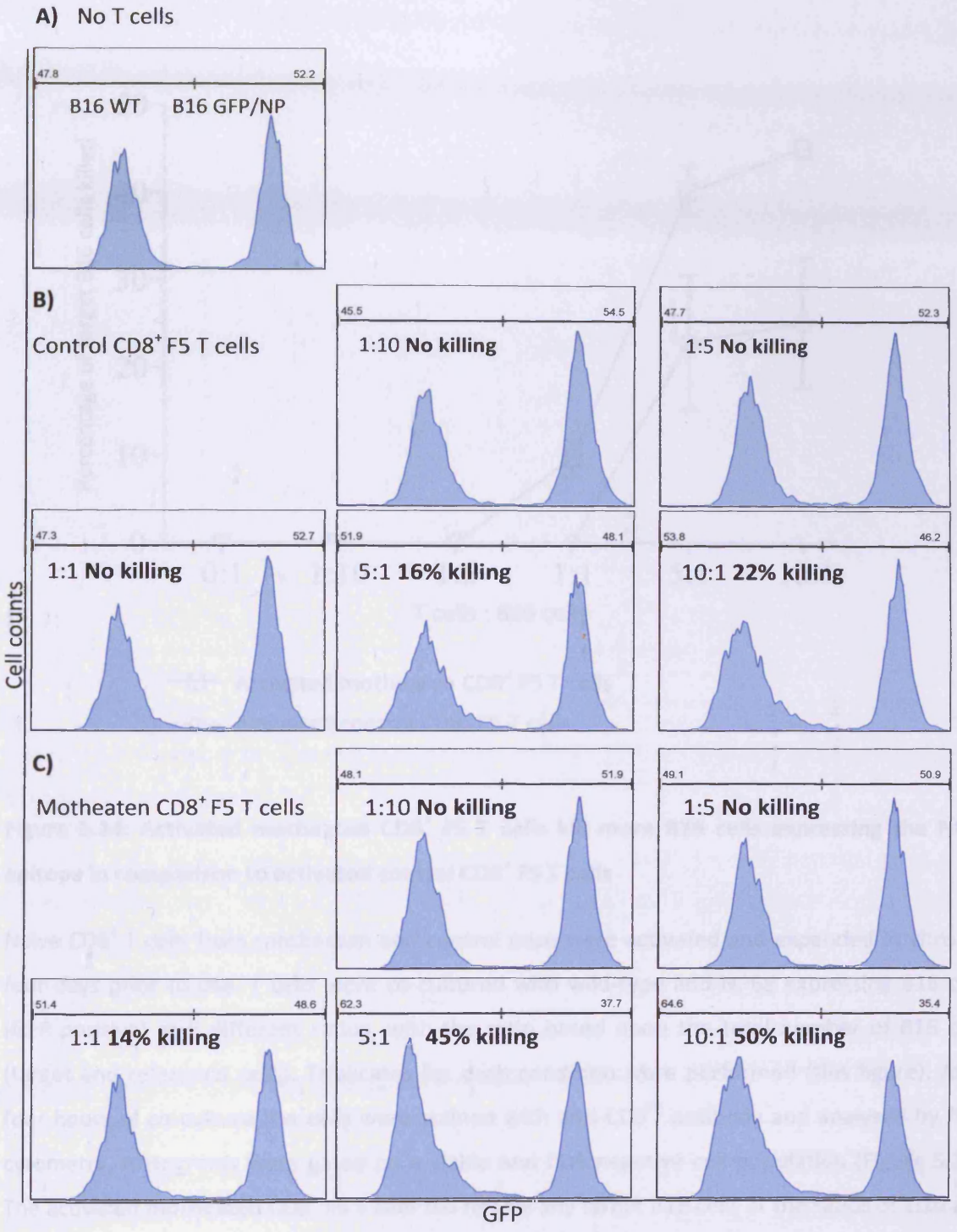


Figure 5.23: Activated motheaten CD8$^+$ F5 T cells kill more B16 cells expressing the NP68 epitope than activated control CD8$^+$ F5 T cells

Naive CD8$^+$ T cells from control and motheaten mice were activated and expanded in vitro for four days prior to use. T cells were co-cultured with wild-type and NP68 expressing B16 cells (GFP positive) at 5 different ratios (shown for each histogram). Triplicates for each condition were performed (Figure 5.24) with representative data shown here. After four hours of co-culture the cells were stained with anti-CD8^{PE} antibody and analysed by flow cytometry. Histograms were gated on viable and CD8 negative cell populations. Activated motheaten CD8$^+$ F5 T cells killed more target B16 cells (C - ratio of 1:1, 5:1 and 10:1) than activated control CD8$^+$ F5 T cells (B).

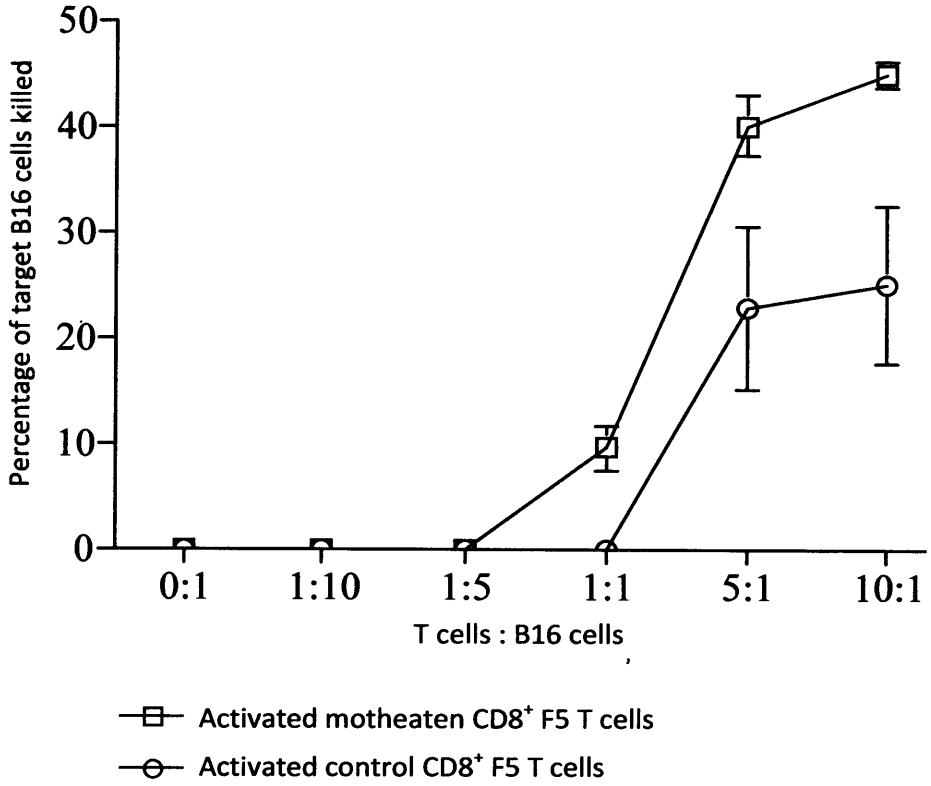


Figure 5.24: Activated motheaten CD8$^+$ F5 T cells kill more B16 cells expressing the NP68 epitope in comparison to activated control CD8$^+$ F5 T cells

Naive CD8$^+$ T cells from motheaten and control mice were activated and expanded in vitro for four days prior to use. T cells were co-cultured with wild-type and NP68 expressing B16 cells (GFP positive) at 5 different ratios, with the ratio based upon the total number of B16 cells (target and reference cells). Triplicates for each condition were performed (this figure). After four hours of co-culture the cells were stained with anti-CD8^{PE} antibody and analysed by flow cytometry. Histograms were gated on a viable and CD8 negative cell population (Figure 5.23). The activated motheaten CD8$^+$ F5 T cells did not kill any target B16 cells at the ratios of 1:10 and 1:5 (□). Control CD8$^+$ F5 T cells did not kill B16 cells at the ratios of 1:10, 1:5 and 1:1 (○). Activated motheaten CD8$^+$ F5 T cells killed more target B16 cells (□) than activated control CD8$^+$ F5 T cells (○) at the T cell to B16 cell ratios of 1:1, 5:1 and 10:1. For each condition, the difference in B16 cells killed by motheaten and control T cells was not statistically significant, according to a Mann-Whitney test.

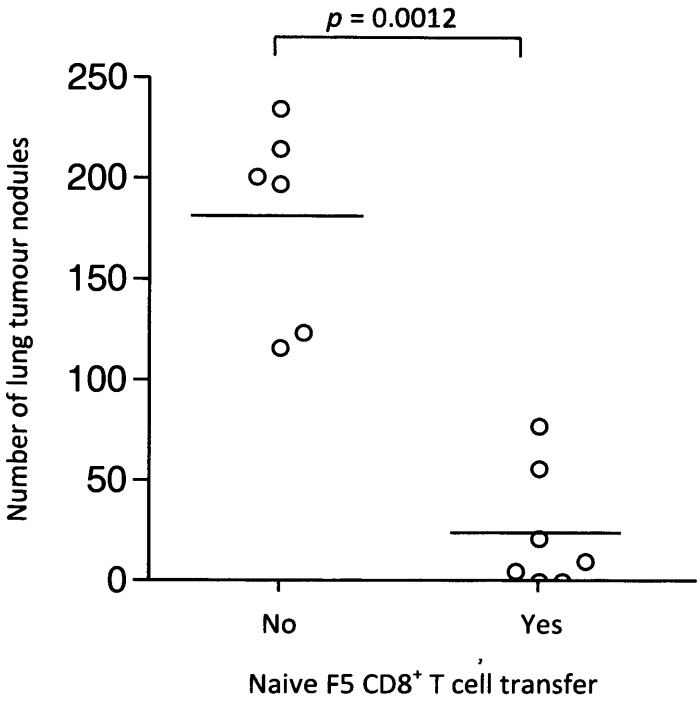


Figure 5.25: Significantly reduced tumour nodule formation in the lungs of mice receiving naive control CD8$^+$ F5 T cells

Recipient mice were sub-lethally irradiated twenty-four hours prior to adoptive cell transfer. A group of seven mice received $3.2x10^4$ naive control CD8$^+$ F5 T cells. A further six mice did not receive any T cells. Concomitantly with T cell transfer, each mouse was primed subcutaneously with NP68 peptide in IFA. The following day, $2.5x10^5$ B16 cells expressing the NP68 epitope were transferred intravenously to all mice. Fourteen days post B16 cells transfer, the mice were sacrificed and the tumour nodules in their lungs enumerated. Significantly fewer (p=0.0012) tumour nodules were present in mice that received control CD8$^+$ F5 T cells, when compared to mice that did not receive any T cells. The solid line shows the mean for each group. The physical condition of the mice during the assay was monitored by weighing them at regular intervals (figure 5.28). In order to monitor transferred T cells, blood was taken at various time points from one mouse that did not receive any T cells and one mouse that received T cells (figure 5.26). Once the lungs had been harvested the proportion of CD8$^+$ cells within the lungs of three mice from each group was also examined (figure 5.27).

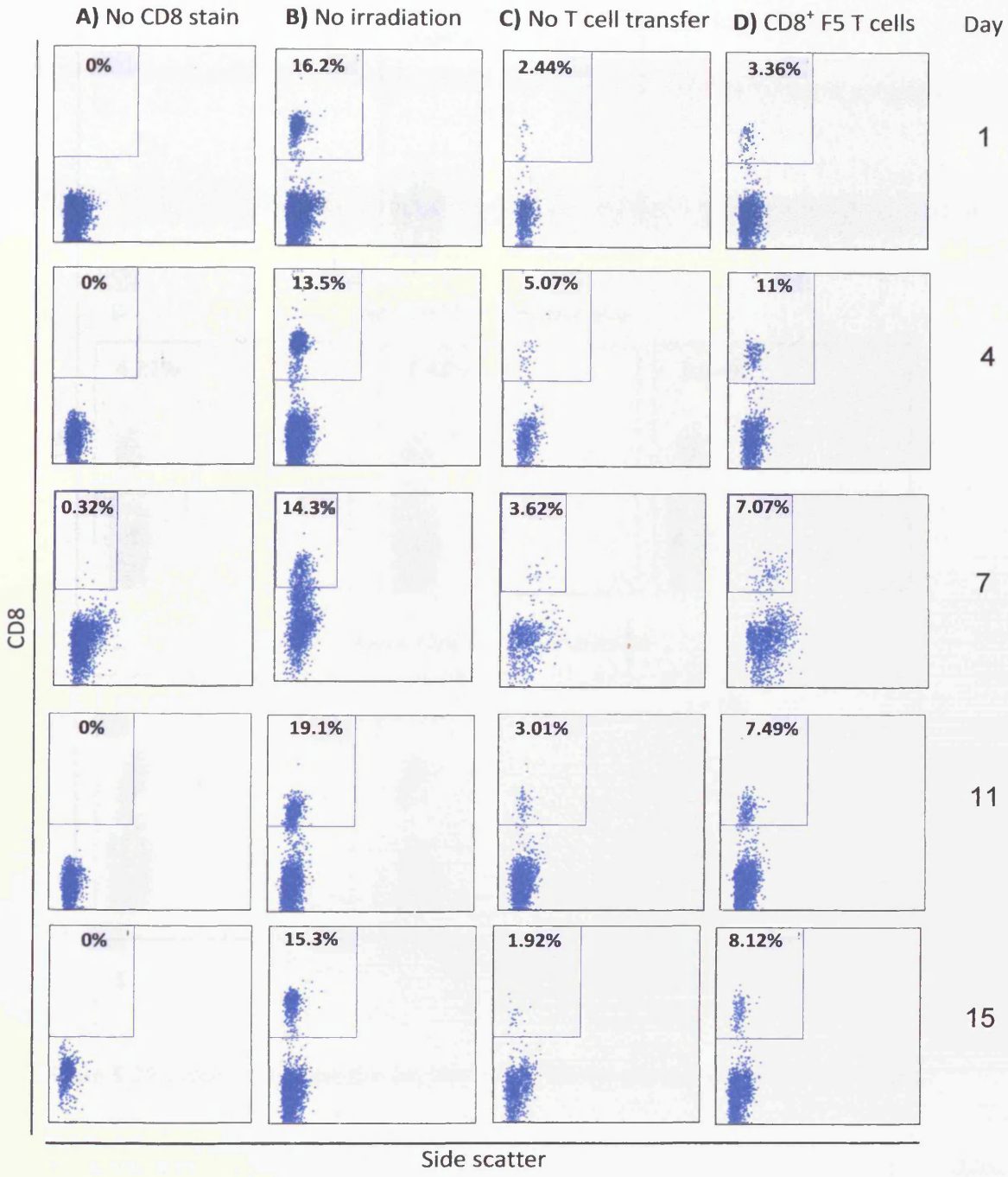


Figure 5.26: Adoptively transferred CD8$^+$ F5 T cells are detected in the blood of mice

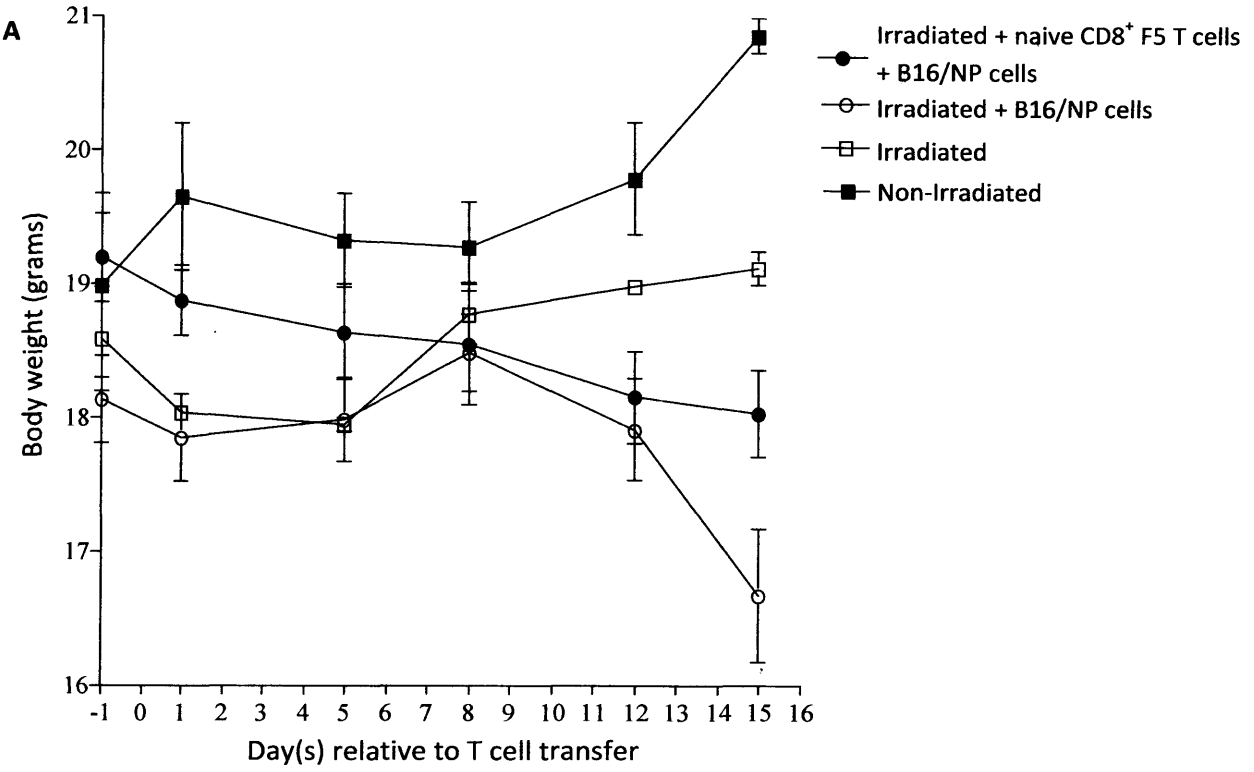
This assay was conducted as an adjunct to the experiment described in figure 5.25. Peripheral blood was taken from a tail vein on day(s) 1, 4, 7, 10 and 15 following adoptive transfer of naive CD8$^+$ F5 T cell. One mouse that received no T cells (C) and one mouse that received naive control CD8$^+$ F5 T cells (D) were used over the duration of the assay for blood analysis. In addition, blood was also taken from a non-irradiated mouse (B) and aliquots of blood from each mouse were pooled and left unstained (A) to enable the CD8 positive gate to be set. The blood was depleted of red blood cells and stained with anti-CD8^{PE} antibody and analysed by flow cytometry. The blood taken on day 7 was analysed using a different FACSCalibur to that on the other days. Dot plots were gated on a lymphocyte gate as determined by forward and side scatter and the number shown in the gate is the percentage of CD8$^+$ cells residing within that gate. A greater proportion of CD8$^+$ cells were seen in the mouse that received T cells compared to the mouse that did not receive T cells.



Figure 5.27: Adoptively transferred $CD8^+$ F5 T cells are detected in the lungs of mice

The assay was a component of the tumour protection experiment described in figure 5.25. Fourteen days post tumour cell transfer, mice were sacrificed and the lung tumour nodules enumerated (figure 5.25). The lungs of three mice from each group were homogenised and stained with anti-$CD8^{PE}$ antibody and analysed by flow cytometry. Dot plots were gated on a lymphocyte gate and the CD8 positive gate set above the autofluorescence of an unstained lung cell preparation (A). The number in each gate shows the percentage of $CD8^+$ cells of the lymphocyte gate. There was an accumulation of $CD8^+$ T cells in the lungs of mice that had received T cells (C), which was above that found in the mice that received no T cells (B).

A



B

Treatment	Change in body weight by day 15	
	Relative to weight on day -1 (Pre-irradiation)	Relative to weight on day 1 (B16/NP cell transfer)
Irradiated + T cells + B16/NP cells	- 6.02%	- 4.44%
Irradiated + B16/NP cells	- 8.10%	- 6.74%
Irradiated	+ 2.88%	+ 6.01%
No Irradiation	+ 9.98%	+ 6.20%

Figure 5.28: Mice receiving B16/NP cells lost weight over the duration of a tumour protection experiment

This experiment was a component of the experiment described in figure 5.25. Mice were weighed prior to sub-lethal irradiation (day -1) and again on day(s) 1, 3, 7, 9, 11, 13 and 15 following T cell transfer (A). Mice received naive $CD8^+$ F5 T cells on day 0 and B16/NP cells on day 1. Mice that were not recipients of either T cells or B16 cells gained weight over the duration of the assay, with irradiated mice gaining 2.88% of their initial body weight and non-irradiated mice gaining 9.98% (B). From the point of B16 cell transfer (day 1) those mice that received B16 but no T cells lost 6.74% of their initial body weight in comparison to a loss of 4.44% seen for the mice that received B16 and naive $CD8^+$ F5 T cells (B).

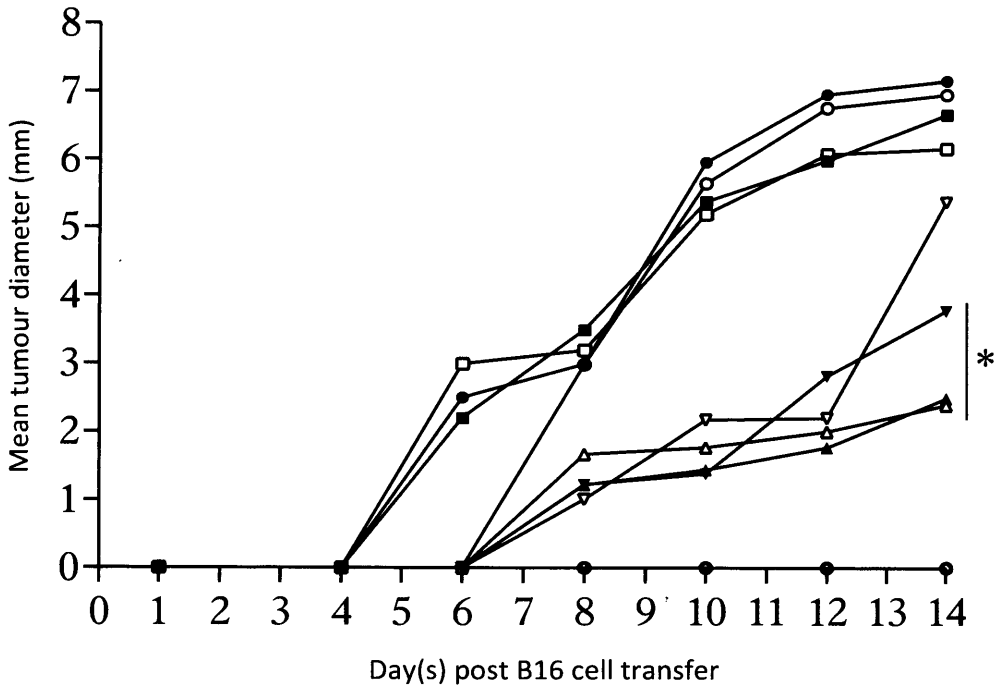


Figure 5.29: Subcutaneous B16 tumour growth over 14 days

Ten recipient mice received a subcutaneous injection of $1x10^5$ B16 cells expressing the NP68 epitope. The perpendicular diameter of each tumour was measured with callipers on day(s) 1, 4, 6, 8, 10, 12 and 14 post tumour cell transfer. The average diameter of each developing tumour was plotted against the day that it was measured. Two of the mice did not develop a tumour at the site of transfer. Tumours grew in all other mice at different rates and with a range of sizes seen at day fourteen. Three mice with similar sized tumours (*) were used to study tumour regression (Figure 5.30).

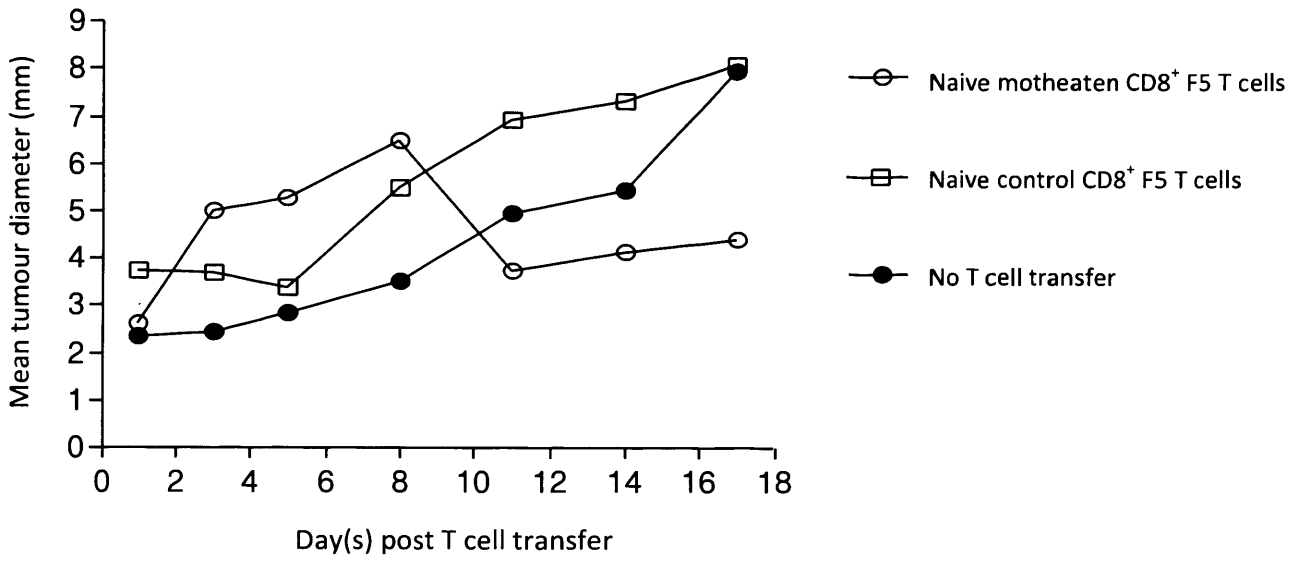


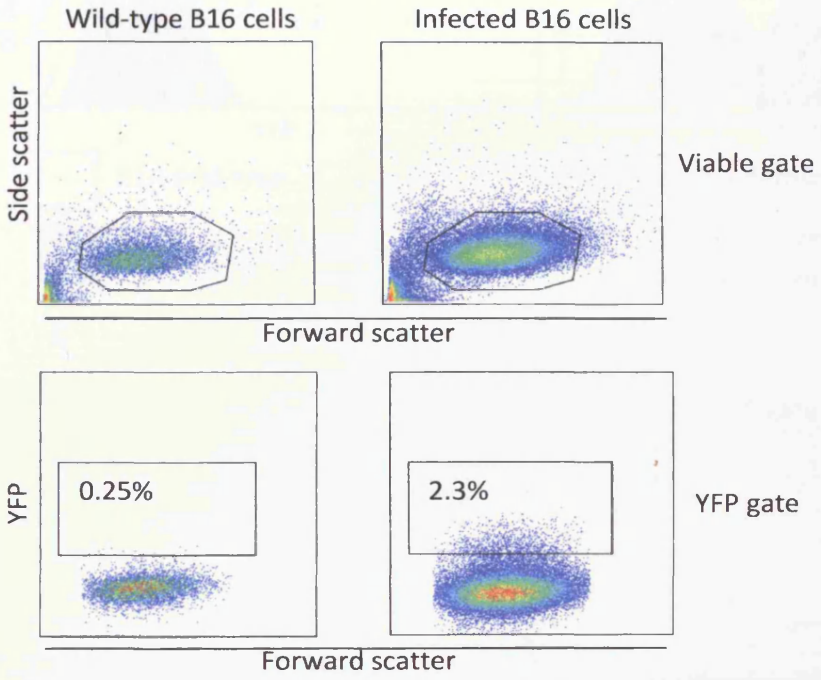
Figure 5.30: Partial regression and delayed growth of a subcutaneous B16 melanoma in a mouse receiving naïve motheaten $CD8^+$ F5 T cells

Mice received $1x10^6$ B16 melanoma cells expressing the NP68 epitope subcutaneously. Thirteen days post tumour challenge mice were sub-lethally irradiated. After a further twenty-four hours, mice received either $1x10^6$ naive control or motheaten $CD8^+$ F5 T cells. A third mouse received no T cells. Mice were subsequently primed subcutaneously with NP68 peptide in IFA. The perpendicular diameters of each tumour were measured with callipers and the mean of the diameters plotted against the number of days post T cell transfer. The tumour in the mouse that received naive control $CD8^+$ F5 T cells reduced in size between days 1 and 5, then grew to the same size of the tumour in the mouse that did not receive any T cells. The tumour in the mouse receiving naive motheaten $CD8^+$ F5 T cells exhibited regression between days 8 and 11, followed by delayed growth until the end of the assay.

A

Cell line	Number of cells	Luciferase readout
B16 wild-type	$2.5x10^5$	124
B16 cells	$2.5x10^5$	$2.97x10^6$
infected with a	$1.25x10^5$	$1.8x10^6$
Luc/YFP	$6.1x10^4$	$1.14x10^6$
retrovirus	$3x10^4$	$2.06x10^5$

B



C

Cell line	Luciferase readout	Cell line	Luciferase readout
B16 wild-type	785	6	$7x10^6$
1	$1.2x10^3$	7	$1.23x10^6$
2	$1.98x10^6$	9	$7.71x10^6$
3	$1.32x10^7$	10	$1x10^4$
4	$6.2x10^3$	**11**	$\mathbf{1.55x10^7}$
5	$1.48x10^6$	12	$5.11x10^5$

Figure 5.31: Production of monoclonal B16 cell lines expressing the luciferase gene

Wild-type B16 cells were infected twice on subsequent days with a retrovirus encoding the luciferase and YFP. Eight days post infection the cells were assayed for luciferase activity, which revealed enhanced luciferase activity when compared to the background activity seen with wild-type B16 cells (A). The cells were then single cell sorted based on cell viability and YFP fluorescence by using wild-type B16 cells to set the sorting gates (B). Twelve monoclonal cell lines were successfully grown but one (number 8) had a poor growth habit and was not included in further analysis. After five weeks of expansion the remaining cell lines were assayed for luciferase activity. All eleven monoclonal cell lines exhibited luciferase activity but to varying degrees (C). The cell line designated number 11, which had the highest luciferase activity, was chosen for further manipulation.

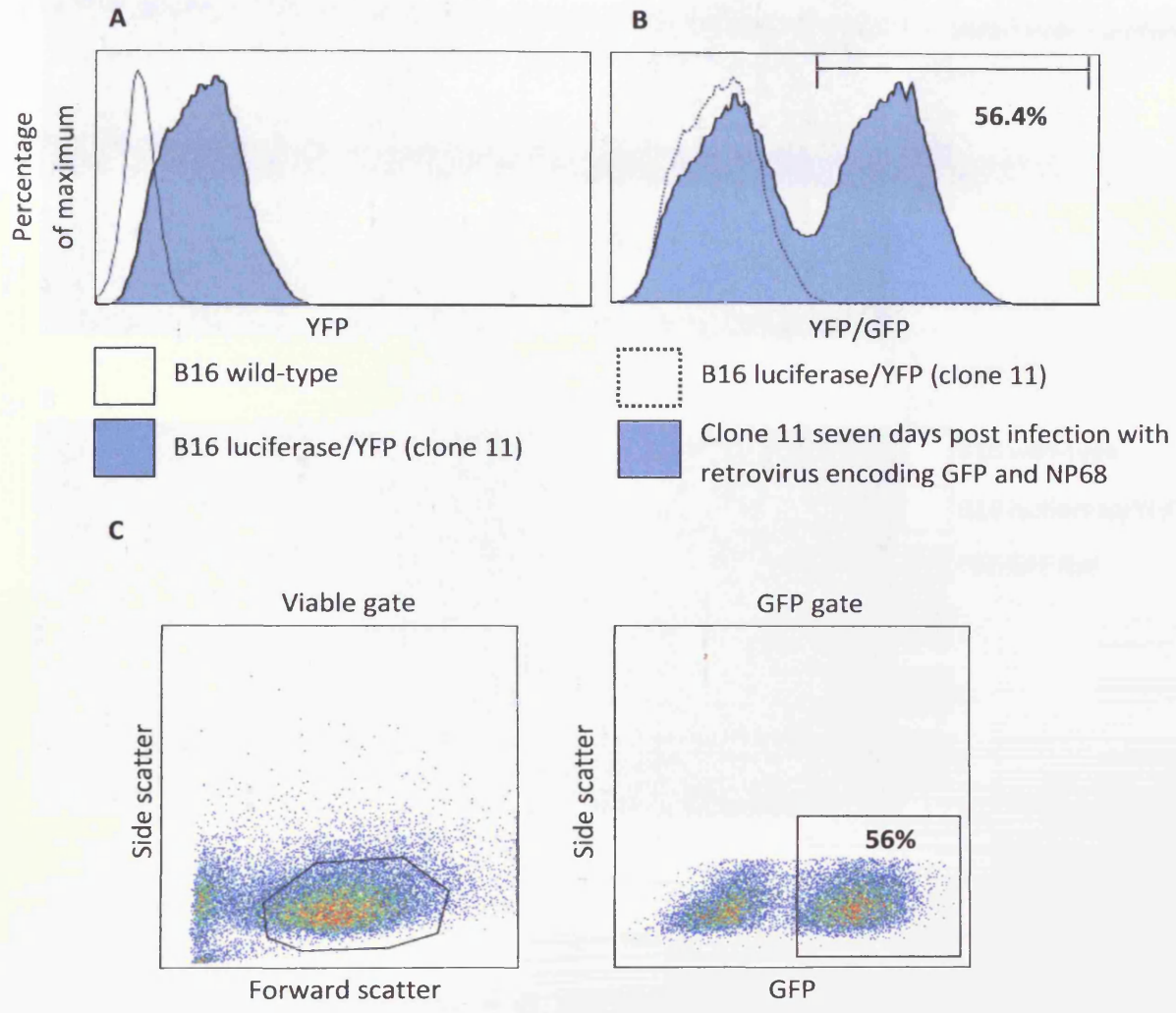


Figure 5.32: Infection of B16 luciferase/YFP cells with a retrovirus encoding the NP68 epitope as a fusion protein with GFP

B16 cells that were infected with a retrovirus encoding luciferase and YFP were sorted based on cell viability and YFP fluorescence (figure 5.31). Five weeks post single cell sorting the monoclonal cell lines were assessed for luciferase activity (Figure 5.31). One of the luciferase positive B16 cell clones (number 11) was chosen for further manipulation. Firstly, the cells were analysed by flow cytometry for YFP expression (A). Histograms were gated on viable cells as determined by forward and side scatter, revealing YFP expression (A). This cell line was then infected twice on subsequent days with a retrovirus encoding the NP68 epitope as a fusion protein with GFP. Six days later, 56.4% of the cells were positive for GFP fluorescence (B). The infected cells were then single cell sorted based on cell viability and GFP fluorescence (C).

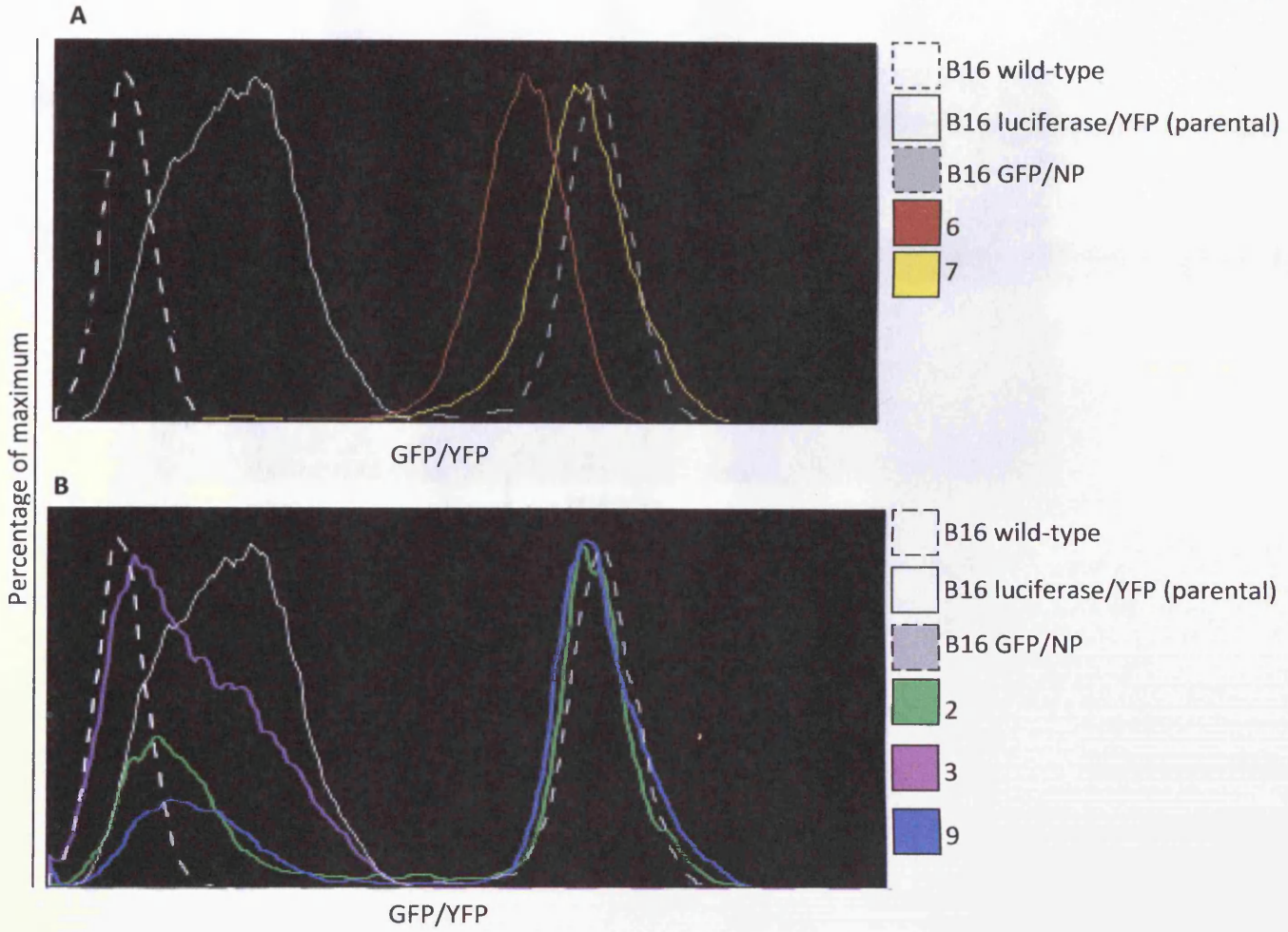
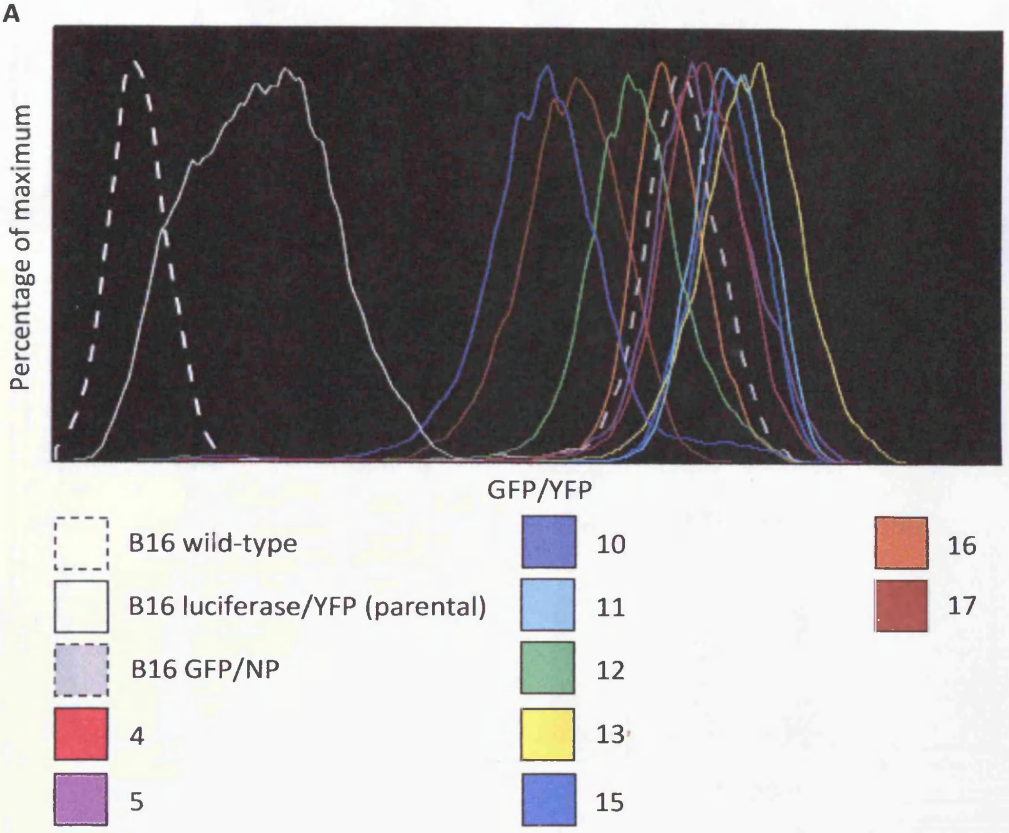


Figure 5.33: Differential GFP expression by B16 luciferase/YFP cells infected with a retrovirus encoding the NP68 epitope as a fusion protein with GFP

B16 cells expressing the luciferase gene (Clone 11, figure 5.31) were infected twice on subsequent days with a retrovirus encoding the NP68 epitope as a fusion protein with GFP. Three weeks post single cell sorting, fourteen monoclonal cell lines were assessed for GFP expression by flow cytometry. The overlay histograms were gated on a viable cell population as determined by forward and side scatter. Their fluorescence was compared to wild-type B16 cells (white dashed line), parental B16 cells that expresses the luciferase gene with YFP (white line) and also a previously generated B16 cell line that expresses GFP as a fusion protein with the NP68 epitope (grey dashed line). Nine of the fourteen monoclonal cell lines generated expressed GFP (Figure 5.34). Cell lines 6 and 7 also expressed GFP (A) but their growing profile was inferior to that of the parental cell line. Cell lines 2 and 9 had a bi-fluorescent profile, with GFP^+ and GFP^- cells evident on the histogram (B). Cell line 3 did not express GFP but appeared to express some YFP (B).

A



B

Cell line	Luciferase readout	Cell line	Luciferase readout
B16 wild-type	175	11	1.84×10^7
B16 Luc/YFP (11)	1.85×10^7	12	9.09×10^6
B16 GFP/NP	202	13	1.44×10^7
4	1.02×10^7	15	1.45×10^7
5	1.34×10^7	16	1.71×10^7
10	1.99×10^7	17	1.60×10^7

Figure 5.34: GFP expression and luciferase activity of B16 luciferase/YFP cells infected with a retrovirus encoding GFP and NP68

B16 cells expressing the luciferase gene (clone 11, figure 5.31) were infected twice on subsequent days with a retrovirus encoding the NP68 epitope as a fusion protein with GFP. Three weeks post single cell sorting each monoclonal cell line was assessed for GFP expression by flow cytometry. The overlay histogram was gated on a viable cell population as determined by forward and side scatter. The fluorescence from GFP was compared to both wild-type B16 cells (dashed white line) and the parental B16 cell line that expresses the luciferase gene with the YFP gene (white line). Nine (Numbers shown in key) of the fourteen monoclonal cell lines had a similar growing habit to the parental cell line and all nine expressed GFP (A). The level of GFP expression was greater than, similar to or less than that of a previously generated B16 cell line that expresses GFP as a fusion protein with the NP68 epitope (Grey dashed line) (A). All nine cell lines were then tested for luciferase activity (B).

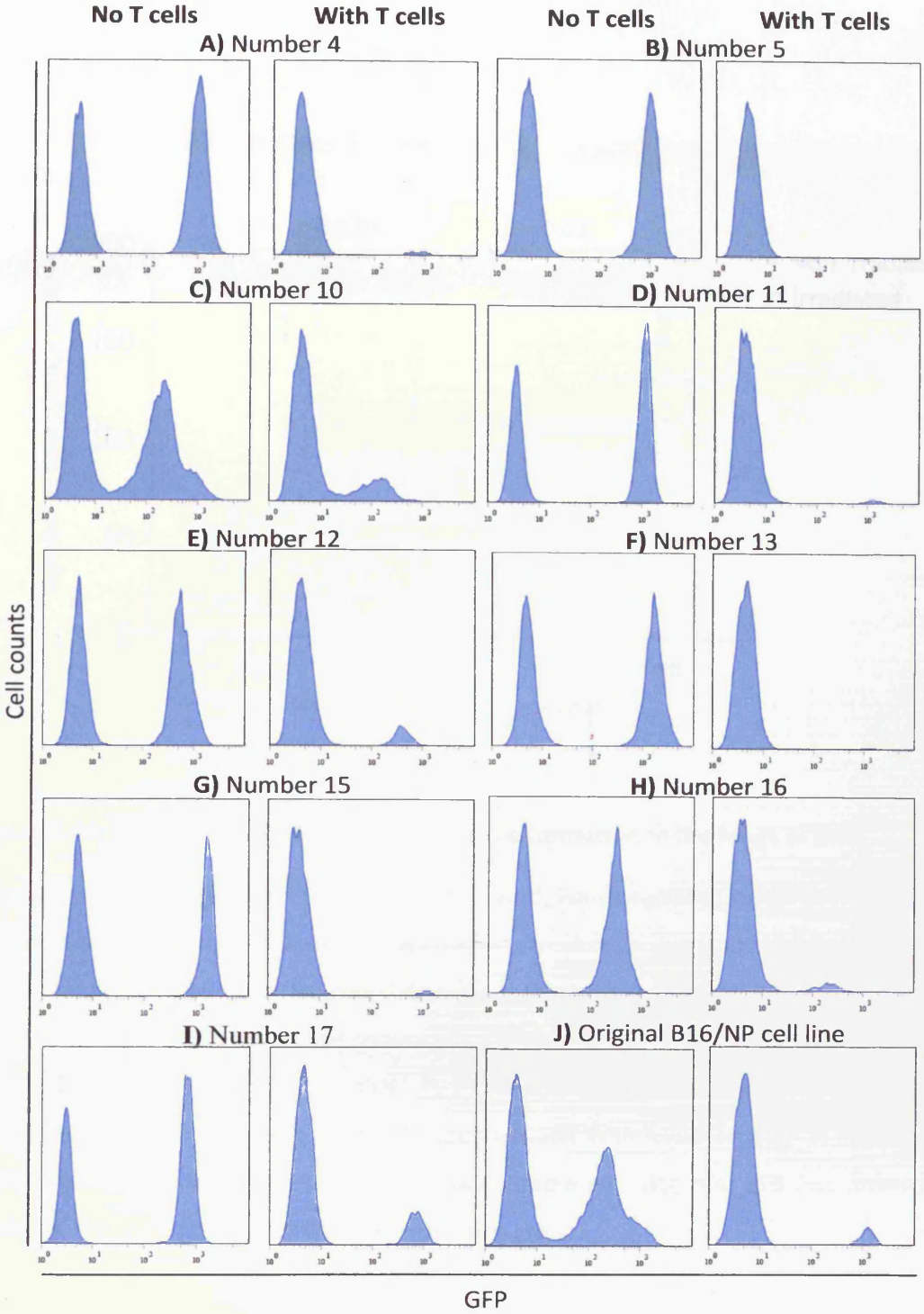


Figure 5.35: B16 luciferase/YFP cells infected with a retrovirus encoding the NP68 epitope as a fusion protein with GFP are killed by activated CD8$^+$ F5 T cells

B16 cells expressing the luciferase gene were infected on subsequent days with a retrovirus encoding the NP68 epitope as a fusion protein with GFP. Four weeks post single cell sorting, the cells were assessed for NP68 presentation at their surface. Each cell line was plated out at a 1:1 ratio with wild-type B16 cells twenty-four hours prior to the addition of in vitro activated CD8$^+$ F5 T cells. B16 cells were also cultured without T cells. Previously generated B16/NP cells were used as a positive control for the killing (J). Twenty-four hours later the wells were washed to remove the T cells and then the B16 cells removed with trypsin. Cells were analysed by flow cytometry and histograms gated on a viable B16 cell population as determined by forward and side scatter. The vast majority of each cell line were killed over the duration of the assay, with all of cell line number 5 being killed (B).

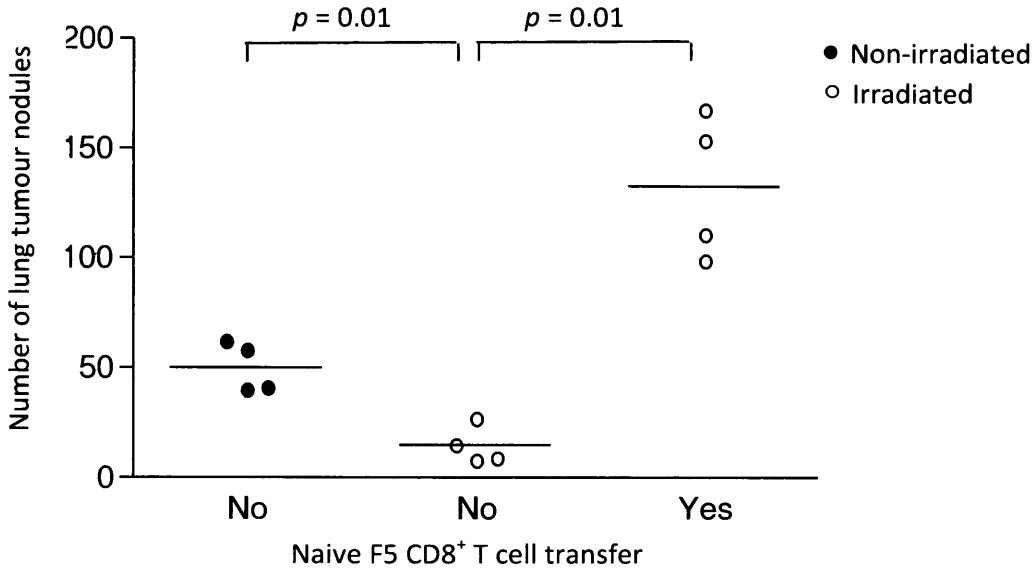


Figure 5.36: CD8$^+$ T cells enhance tumour nodule formation in the lungs of mice

Mice were sub-lethally irradiated or left untreated. Four irradiated mice received 1x10^5 wild-type B16 cells six days after irradiation. A second group of mice were not irradiated but received the same number of B16 cells. Fourteen days later the irradiated mice had significantly fewer lung tumour nodules compared to the non-irradiated mice (p = 0.01). A second group of four irradiated mice received 3x10^6 naive control CD8$^+$ F5 T cells five days prior to the transfer of 1x10^5 wild-type B16 cells. The mice were also primed subcutaneously with NP68 peptide in IFA. These mice had significantly more lung tumour nodules than irradiated mice that did not receive any T cells (p=0.01). The solid lines show the mean for each group.

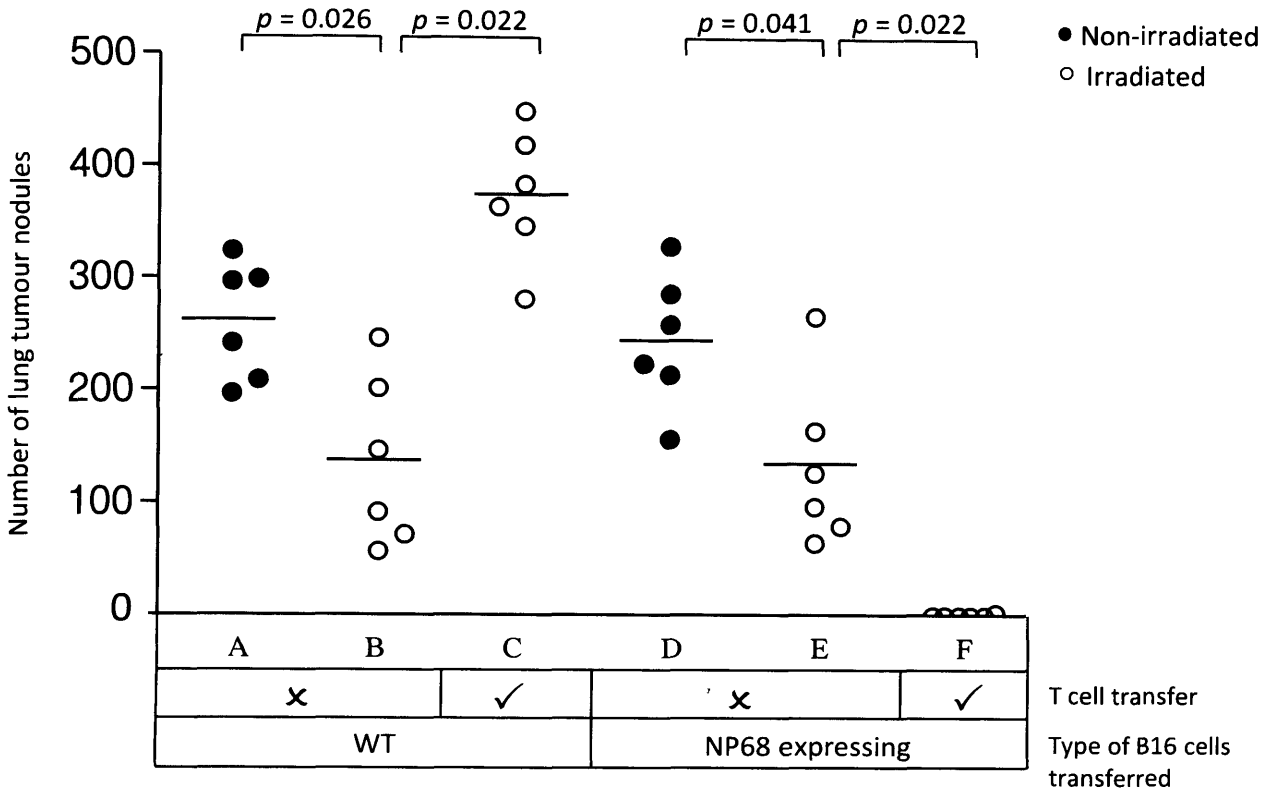


Figure 5.37: A tumour-specific CD8$^+$ T cell response protects mice from tumour formation, whereas a non-specific CD8$^+$ T cell response promotes tumour formation

A group of twelve sub-lethally irradiated mice received $1.8x10^6$ purified naïve CD8$^+$ F5 T cells and subcutaneous injection of NP68 peptide in IFA (C and F). A second group of twelve irradiated mice and also a group of twelve non-irradiated mice did not receive any T cells (A, B, D and E). Three days post T cell transfer, mice received intravenous infusions of either $1.75x10^5$ wild-type B16 cells (A, B and C) or $1.75x10^5$ B16 cells expressing the NP68 epitope (D, E and F). Fourteen days post B16 cell transfer, mice were sacrificed and the nodules in their lungs enumerated. As previously demonstrated mice that were sub-lethally irradiated had significantly fewer nodules in their lungs compared to non-irradiated mice (figure 5.36). This applied to mice that received either wild-type B16 cells (A versus B, $p = 0.026$) or B16 cells expressing the NP68 epitope (D versus E, $p = 0.041$). Furthermore, mice receiving CD8$^+$ F5 T cells and wild-type B16 cells exhibited an enhanced number of nodules in their lungs in comparison to mice that did not receive T cells (B versus C, $p = 0.0022$). In contrast, those mice that received CD8$^+$ F5 T cells and the NP68 expressing B16 cells were clear from tumour nodules in the lungs in comparison to mice that received the NP68 expressing B16 cells and no T cells (E versus F, $p = 0.0022$). The solid line shows the mean for each group of mice.

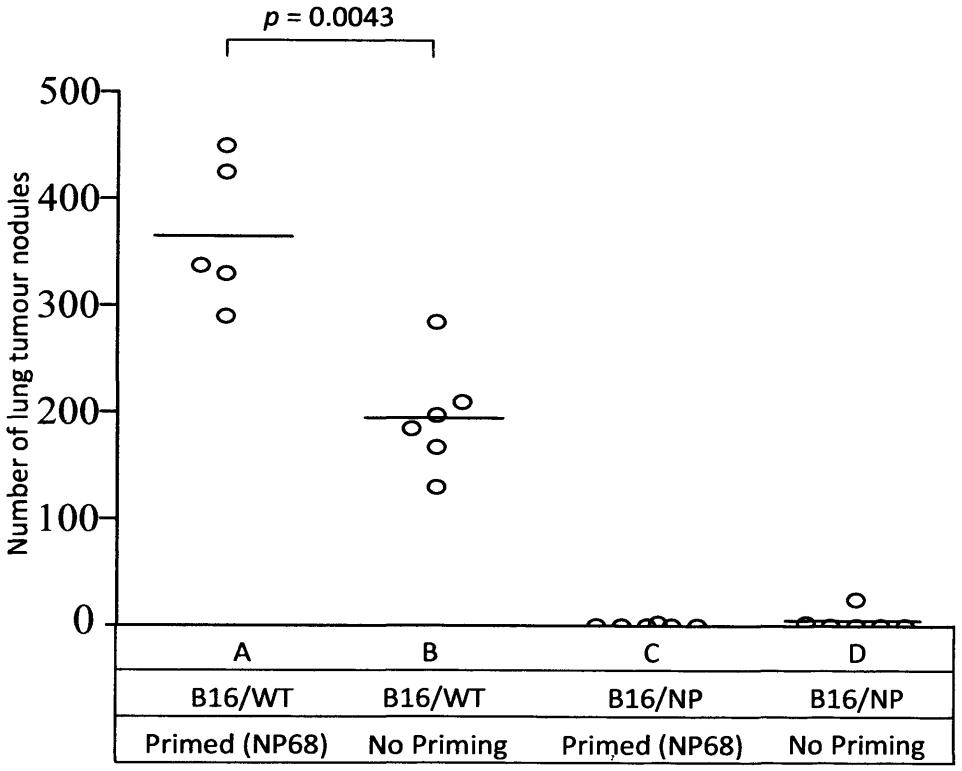


Figure 5.38: Mice primed with NP68 peptide in IFA have significantly more lung tumour nodules than mice that are not primed

Groups of F5 TCR transgenic mice were either primed subcutaneously with NP68 peptide (A and C) or left un-primed (B and D). Three days post priming mice received either wild-type (WT) B16 cells (A and B) or B16 cells expressing the NP68 (NP) epitope (C and D). Fourteen days post B16 cell transfer, mice were sacrificed and the tumour nodules in their lungs enumerated. Mice that were either primed or left un-primed and the recipients of B16 cells expressing the NP68 epitope were virtually tumour free (C and D). The mice that were primed and recipients of wild-type B16 cells (A) had significantly more (p=0.0043) tumour nodules in their lungs in comparison to mice that were not primed (B).

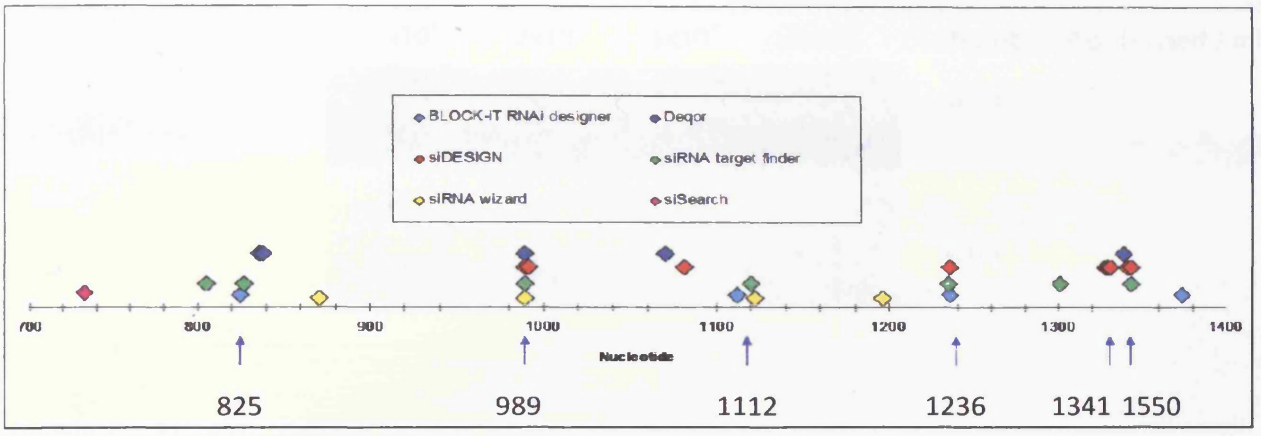


Figure 5.39: Algorithm-identified candidate sequences within the SHP-1 transcript for siRNA targeting

Online algorithms were utilised to identify suitable sequences within the SHP-1 transcript for targeting with siRNA. The algorithms utilised an integrated BLAST search to eliminate sequences that could have potential off-target effects. The SHP-1 transcript was annotated according to the first nucleotide of the sequences (19 nucleotides) deemed suitable for siRNA targeting (blue arrow). These were subsequently synthesised into shRNA sequences and cloned into plasmid vectors ready for functional testing in Jurkat cells (figure 5.41).

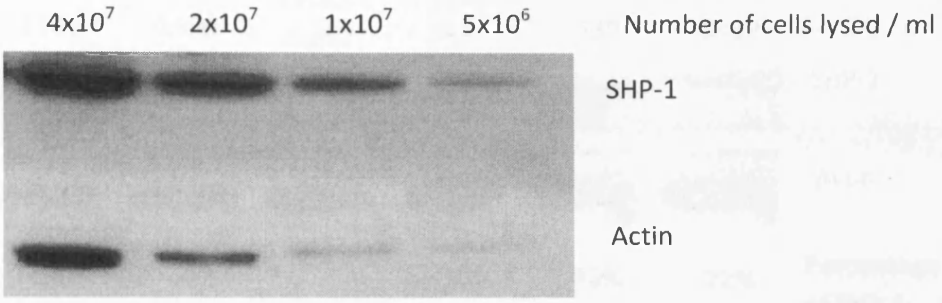


Figure 5.40: SHP-1 protein detection in Jurkat cells by immunoblot analysis

In preparation for shRNA screening, a titration was performed to establish the minimum number of cells that could be used to allow SHP-1 detection. Jurkat cells were taken from culture and lysed to give $1x10^6$, $5x10^5$, $2.5x10^5$ and $1.25x10^5$ cells per 25µl of lysis buffer. Six times loading buffer was added to each lysate and 20µl of each sample loaded onto SDS-PAGE gels ready for immunoblot analysis.

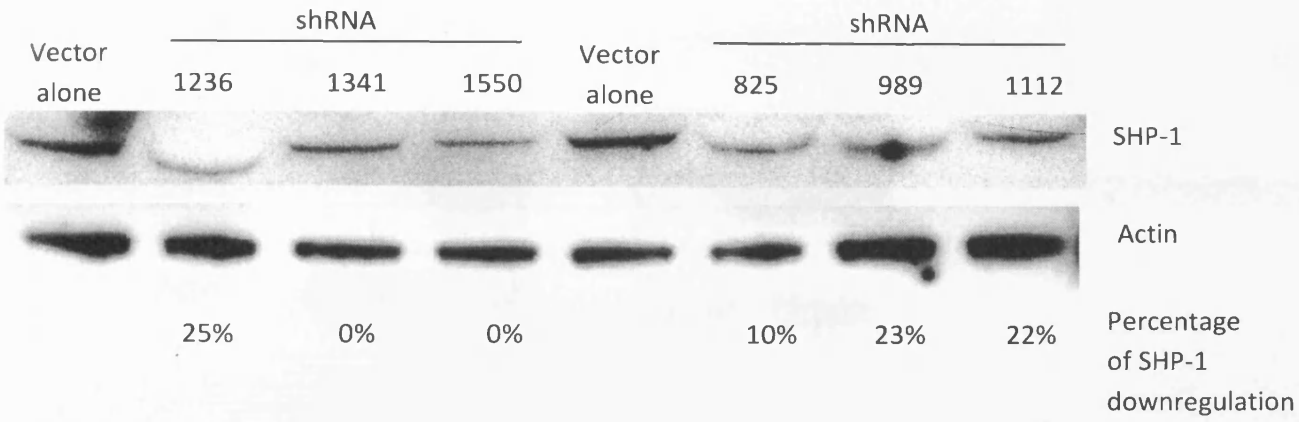


Figure 5.41: Reduced SHP-1 expression in Jurkat cells receiving shRNA expression plasmids

Jurkat cells were electroporated in the presence of plasmid DNA encoding six individual shRNA sequences, and also a GFP expression plasmid, at a 5:1 ratio respectively. To act as a control, Jurkat cells were also electroporated in the presence of the plasmid DNA that did not contain a shRNA encoding sequence (vector alone). The cells were cultured for 48 hours post electroporation before being sorted on a single cell basis by flow cytometry. Cells were sorted based on GFP expression, with untransfected cells being used as a control to define a GFP positive gate. Cells were then prepared for immunoblot analysis to detect SHP-1 levels. ImageJ software was used for densitometry analysis, with the level of SHP-1 protein being normalised according to the level of actin detected. The percentage downregulation was then calculated by comparison to untransfected parental Jurkat cells expressing SHP-1 (control). Two of the shRNA sequences (2 and 3) did not mediate any reduction of SHP-1, whereas four sequences were successful at knocking down SHP-1 expression to some degree (1, 4, 5 and 6).

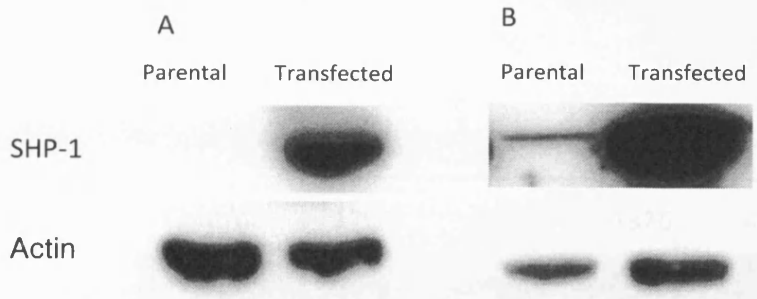


Figure 5.42: Successful introduction of mouse and human SHP-1 genes to Hela cells

Cells were transfected with plasmid DNA encoding a neomycin resistance gene and either mouse (A) or human SHP-1 (B) genes. DNA was prepared by using either JetPEI reagent (A) or calcium phosphate (B) and subsequently delivered to the Hela cells. Forty-eight hours post transfection the cells were cultured with 1.5mg/ml of G418. Four weeks post antibiotic treatment cells were assessed for SHP-1 expression by western blot analysis, with SHP-1 being detected in both cell lines.

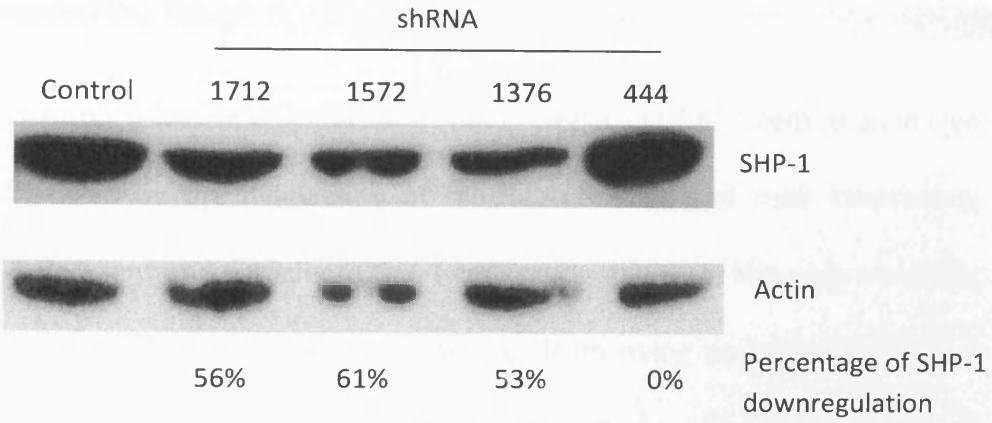


Figure 5.43: Reduced SHP-1 expression in Hela cells receiving *MISSION*™ shRNA plasmids

Hela cells expressing the human SHP-1 gene were transfected with a plasmid expressing the puromycin resistance gene, and one of four different shRNA sequences targeting SHP-1 expression. The cells were selected in 0.4μg/ml of puromycin for six weeks prior to immunoblot analysis for SHP-1 protein. ImageJ software was used for densitometry analysis, with the level of SHP-1 protein being normalised according to the level of actin detected. The percentage downregulation was then calculated by comparison to untransfected parental Hela cells expressing SHP-1 (control). Three of the shRNA sequences were successful at mediating partial knockdown of SHP-1 expression.

Chapter 6

Discussion

6.1 Aims and challenges of the study

The ultimate aim of this study was to elucidate the role of SHP-1 in $CD8^+$ T cells in an *in vivo* setting. This was facilitated by the availability of motheaten mice and their littermates, which provided SHP-1 deficient and sufficient $CD8^+$ T cells respectively. As the early mortality of motheaten mice precluded direct *in vivo* T cell studies from being performed, adoptive cell transfer techniques were used throughout this study. The availability of immunomagnetic separation techniques allowed $CD8^+$ T cells to be purified from donor motheaten and littermate mice and subsequently transferred to recipient mice, where they could be studied. In addition, the expression of the transgenic TCR, F5, by the donor mice allowed $CD8^+$ T cells to be studied in an antigenic context by using the peptide, NP68.

A practical consideration that was echoed throughout this study was the number of motheaten mice available at any given time. Although the motheaten allele is inherited in a Mendelian manner, the number of motheaten mice actually produced is below that expected, when considering the total number of mice born. Homozygosity at the motheaten allele may hinder the development of motheaten embryos, thereby precluding successful gestation. The motheaten pups may also not compete as well as littermates during weaning. In addition, the financial constraints of supporting very large mouse colonies to produce more motheaten mice also influenced the number of motheaten mice produced. Overall, these factors had a direct impact upon the availability of naive motheaten $CD8^+$ F5 T cells for experimentation. On average, $1x10^6$ $CD8^+$ T cells were purified from a single motheaten mouse, and approximately 2-5 motheaten mice were available at the same time. Therefore, assays were designed in such a way as to be compatible with numbers of motheaten $CD8^+$ T

cells available. Wherever possible, experimental conditions were performed in multiples and experiments repeated on separate occasions. T cell numbers sometimes precluded multiple repeats of a condition within an experiment, and in these circumstances, assays were repeated in order to validate the data being acquired.

6.2 Priming $CD8^+$ F5 T cells *in vivo*

Several methods of priming adoptively transferred $CD8^+$ F5 T cells were initially trialled, and all proved to be successful at eliciting an *in vivo* $CD8^+$ F5 T cell response. The first method involved the *in vitro* generation of DCs by culturing bone marrow precursor cells with the cytokine, GM-CSF. Commercially available GM-CSF and supernatant from a GM-CSF producer cell line were tested for their ability to yield DCs for *in vivo* use. Both sources of GM-CSF were able to enrich bone marrow cultures for DCs, as assessed by CD11c expression, and also DCs that upregulated costimulatory molecule ligands upon LPS treatment. As a result, the DCs were functionally viable and able to present NP68 peptide to $CD8^+$ F5 T cells, in both an *in vitro* and *in vivo* setting. As the GM-CSF supernatant was readily available, more economically favourable, and capable of producing DCs of the same quality as those produced with commercially available GM-CSF, it was the preferred choice for routine use during this study. DCs were administered into the peritoneal cavity of recipient mice, as it not only provided the most straightforward mode of transfer, but also gave equivalent $CD8^+$ F5 T cell responses as the subcutaneous route. An ongoing logistical challenge of this study was the coordination of DC cultures with the availability of motheaten mice. Both the early mortality of the motheaten mice and Home Office regulations meant the appearance of a motheaten mouse within a litter gave a window of approximately 5-7 days, in which the mice had to be used. This often did not give sufficient time to produce DCs, which required 10-14 days of culture. One approach would have been to routinely set-up DC cultures so that DCs were available at all times. Although feasible, this would have meant the routine

sacrifice of mice for their bone marrow, with no guarantee that the resulting DCs would have been used. Therefore, in accordance with the 'three Rs' (reduction, refinement and replacement) outlined by the Home Office, other modes of priming $CD8^+$ F5 T cells were explored. The second mode of priming T cells utilised the Influenza A virus. As the NP68 peptide is derived from the nucleoprotein of Influenza A, mice infected with the virus generate the peptide and present it to adoptively transferred T cells. Although this represents a more physiological relevant mode of priming T cells, it still required forward planning as mice needed to be infected several days prior to T cell transfer. Finally, the subcutaneous administration of NP68 in IFA utilised endogenous DCs to present the peptide to transferred $CD8^+$ F5 T cells. This proved to be convenient, straightforward and efficacious at eliciting a T cell response in recipient mice and was therefore used routinely to prime mice, unless deemed unsuitable for a particular assay (discussed later for memory cell assays). The amount of NP68 peptide required for priming mice with IFA was far greater than that required for pulsing DCs ready for *in vivo* transfer. Despite this, the ethical costs and cost of consumables and media required for producing DCs on a regular basis offset some of the financial cost of using more NP68 peptide.

6.3 The role SHP-1 in primary $CD8^+$ T cell responses

The ultimate role of a $CD8^+$ T cell is to clear cognate antigen, and in doing so eliminate malignant cells or cells that harbour pathogens. *In vitro* studies of SHP-1 deficient T cells have demonstrated that they possess an enhanced capability at forming cellular conjugates with APCs (Sathish *et al.*, 2007). Consequently, a greater proportion of SHP-1 deficient naive $CD8^+$ T cells from a given population enter into cellular division (Sathish *et al.*, 2007). The *in vivo* relevance of these observations was undetermined until this study, which successfully demonstrated that mice that received a naive population of motheaten $CD8^+$ F5 T cells were capable of killing more target cells (NP68 pulsed splenocytes) than mice that received

control $CD8^+$ F5 T cells. These data represent a significant advance in SHP-1 related research. The transition from studying T cells *in vitro* to an *in vivo* setting is an important one to take, as the physical requirements of $CD8^+$ T cells during the detection and response to cognate antigen *in vivo* are very different to those found in an *in vitro* setting. $CD8^+$ T cells are required to traffic to secondary lymphoid organs in search of antigen, and following activation and clonal expansion, migrate to peripheral sites of inflammation or infection.

As the above protocol looked at the killing of target cells in the spleen of recipient mice it cannot be said whether effector cells generated in the spleen were solely responsible for the killing, or T cells primed in other lymphoid organs also contributed to target cell clearance. The latter would involve two migratory steps for the T cells, firstly to the lymphoid organ in which they would be primed and then to the spleen via the lymph and blood. As SHP-1 has been implicated in having a role in immune cell migration (Kim *et al.*, 1999) it would be reasonable to assume that SHP-1 deficient T cells may exhibit an enhanced ability to migrate to both lymphoid organs and peripheral sites harbouring target cells. In light of this, assays were performed to explore this hypothesis (discussed later). In addition, the above protocol could be developed further to ensure both migratory events are involved in the killing of target cells in the spleen. By infecting mice with Influenza A virus the adoptively transferred $CD8^+$ F5 T cells would be primed in lung-associated lymph nodes. Therefore, the priming would take place at sites that are distant from the site of target cell killing (spleen), thereby ensuring the T cells are required to migrate from the lymph nodes to the spleen. This approach may reveal further differences in the number of target cells killed between mice receiving either motheaten or control $CD8^+$ F5 T cells.

The observation that more targets cells were killed by motheaten CD8+ F5 T cells raised the question, why does SHP-1 deficiency in $CD8^+$ T cells lead to enhanced *in vivo* CTL activity? One possibility is that the enhanced killing of target cells could be attributed to the presence

of more CTLs. This would be a plausible explanation given the hyperproliferative phenotype of naive motheaten $CD8^+$ T cells seen *in vitro*. A protocol that was initially used during this study to measure *in vivo* $CD8^+$ T cell expansion suggested that SHP-1 deficient $CD8^+$ T cells do undergo an enhanced *in vivo* expansion. Despite this general trend, components of the protocol did not allow for the production of concise and reproducible data. The protocol gauged $CD8^+$ T cell expansion by either looking at the absolute number of cells seen in the spleens of recipient mice, or by comparison of $CD8^+$ T cells to a lymphocyte population of cells during analysis of flow cytometry data. The necessary step of lysing red blood cells prior to enumeration of splenocytes was associated with the formation of cell clumps, which meant cells were lost from the samples. Although efforts were made to minimise the occurrence of clumping their continued presence meant cells were lost from samples in a non-uniform manner, thereby giving data that was unreliable with regards to the absolute number of cells present in each spleen. It also became apparent that sub-lethally irradiating recipient mice altered their lymphocytes in a manner unique to each mouse. This resulted in a different proportion of cells residing in the lymphocyte population for each individual mouse. Therefore, expressing $CD8^+$ T cells as a proportion of a lymphocyte gate also precluded the generation of accurate data. In light of this, a second protocol was developed to study *in vivo* $CD8^+$ T cell expansion. In order to overcome the issue of cells clumping prior to analysis, a fluorescently labelled (CFSE) reference population of cells was added to each sample prior to its preparation for flow cytometry. As the clumping does not discriminate between the splenocytes and the CFSE labelled population the latter acted as an internal control. This allowed the $CD8^+$ T cells to be compared to the reference cell population rather than cells within a lymphocyte gate. This approach proved successful and it was demonstrated that motheaten $CD8^+$ T cells exhibit an enhanced *in vivo* expansion. Although Rag-$1^{-/-}$ mice were used at this stage of study, the use of a CFSE labelled reference

population of cells would also have been compatible with using irradiated mice as recipients. To further explore the expansion data the intracellular dye, CFSE, could potentially be used to track T cell proliferation *in vivo*. This would be informative with regards to establishing the proportion of adoptively transferred $CD8^+$ F5 T cells that actually enter into proliferation, and also the number of subsequent cell divisions. Control experiments (data not shown) indicated that approximately $6x10^6$ naive $CD8^+$ T cells would be required to perform this type of assay, as this number would allow for loss of cells during the labelling process, and also for their detection *in vivo*.

Prior to this study, *in vitro* CTL data have demonstrated that there are no differences between the cytotoxic function of motheaten and control $CD8^+$ F5 T cells on a per cell basis (Johnson *et al.*, 1999). In contrast to this observation, *in vivo* data from this study seem to suggest that SHP-1 deficient $CD8^+$ T cells kill more target cells on a per cell basis. The optimisation of these experiments proved to be challenging with regards to the number of *in vitro* activated and expanded $CD8^+$ F5 T cells to transfer in relation to the number of target cells that were subsequently administered. As the extent of target cell killing varied greatly between assays it would be necessary to repeat this assay to ensure reliable data were being acquired. In addition, a number of control experiments would also need to be performed to ensure the enhanced CTL activity seen when transferring equal numbers of activated $CD8^+$ F5 T cells was only attributable to enhanced CTL function on a per cell basis. Firstly, the cells could be labelled with different intracellular dyes and transferred in equal numbers to the same mouse. This would reveal whether or not motheaten and control $CD8^+$ F5 T cells have the same homing capabilities to the spleen, as any difference in migration could influence the number of target cells killed. Naive motheaten and control $CD8^+$ F5 T cells exhibit the same *in vitro* division index, which is the number of cell divisions cells undergo once cells have entered into proliferation. It would be necessary to confirm the same was true for *in*

vitro activated $CD8^+$ F5 T cells once they have been transferred *in vivo*. This could be achieved by using CFSE to label the T cells prior to *in vivo* transfer, followed by analysing cells from the spleen by flow cytometry. Any differences in the division index between activated motheaten and control $CD8^+$ F5 T cells would indicate that different numbers of CTL had been generated and therefore this could influence the extent of target cell killing.

As indicated above, it has previously been demonstrated that $CD8^+$ T cells expressing reduced levels of SHP-1 exhibit an enhanced *in vitro* chemotactic response. The implication of this finding is that an enhanced *in vivo* trafficking ability of SHP-1 deficient $CD8^+$ T cells could contribute to the enhanced CTL response discussed earlier. Enhanced migration could potentially affect the efficiency at which antigen is detected in secondary lymphoid tissues and also the speed at which antigen is cleared in the periphery. Ideally, this study would have looked at the trafficking behaviour of naive motheaten and control $CD8^+$ F5 T cells mice to lymph node. However, due to the limited number of motheaten T cells available at any one time and the large number of lymph nodes present within a mouse, it seemed unfeasible that naive T cells could be detected in lymph nodes following their *in vivo* transfer. As naive $CD8^+$ F5 T cells could be activated and expanded *in vitro*, thus generating decent numbers of T cells for experimentation, assays were developed that examined the *in vivo* migration of adoptively transferred activated T cells. The fluorescent dye, DDAO, proved to be a good partner dye for CFSE when labelling different populations of T cells ready for transfer to the same recipient mouse. DDAO was non-toxic at the concentration used during this study and did not bleach excessively, therefore allowing cells to be distinguished from the autofluorescence of endogenous cells during flow cytometry analysis. In order to retrieve cells from a mouse post adoptive transfer, a method of directing the T cells to a specific tissue or organ was required. The culture of $CD8^+$ F5 T cells with NP68 peptide loaded APCs in the presence of retinoic acid confers a preferential homing ability to the T

cells. Once transferred *in vivo*, the conditioned $CD8^+$ T cells migrate to the Peyer's patches. This system was used to study the homing capabilities of motheaten and control $CD8^+$ F5 T cells within the same recipient mouse. These assays revealed a difference with regards the distribution of the adoptively transferred cells, with more motheaten T cells present in the blood than the Peyer's patches, when compared to control T cells. Although the retinoic acid system worked with regards to conferring specific tissue homing capabilities to the T cells it was not an ideal tissue to use for T cell migration studies. The reasoning for this is that T cells not only enter Peyer's patches but also exit freely to return to the blood. For data acquired from this type of approach to be interpreted correctly, the tissue or organ used needs to be the end point for T cell migration, thereby leading to an accumulation of T cells at that site. These experiments could be repeated, but with the Lamina propria also been taken for analysis, as this represents the tissue to which the T cells would ultimately migrate to. Alternatively, S1P receptor inhibitors (Chiba *et al.*, 1998) could be used to block the egress of the adoptively transferred T cells from the Peyer's patches, which would lead to their accumulation at this tissue site. With the Peyer's patches deemed unsuitable as a tissue to study T cell migration, a second protocol was explored for its feasibility to study T cell migration. The peritoneal transfer of recombinant Vaccinia virus to mice leads to infection of the ovaries, thereby providing a site for T cell migration. Indeed, fluorescently labelled T cells did appear in the ovaries post adoptive transfer, although this seemed to be independent of infection, and would therefore require further investigation to optimise this approach for future studies of T cell migration.

Ultimately, any T cell migration studies would need to be performed in conjunction with other experiments in order to interpret the data correctly. The expression level of chemokine receptors and adhesion molecules that are involved in the migration would need to be established for both naive and activated motheaten and control $CD8^+$ T cells, as any

differences could influence the migratory capabilities of the T cells. In previous studies it was shown that equivalent levels of LFA-1 (Sathish *et al.*, 1999) are expressed by motheaten and control $CD8^+$ F5 T cells. In addition, cells could be screened for expression of L-selectin and other molecules involved in T cell homing. Furthermore, if studies did reveal a difference between the migratory behaviours of motheaten and control T cells, their locality within the tissue being studied would need to be confirmed. This could be achieved by fixing and taking sections of the tissue and viewing them under a fluorescent microscope. This would establish whether T cells have extravasated and entered the tissue or remain associated with the lumen wall of the blood vessel. Ideally, real-time imaging would be used to observe the behaviour of motheaten and control $CD8^+$ F5 T cells in the blood vessels that supply lymphoid or peripheral tissue.

Regulatory T cells play an important role in shaping the magnitude and quality of *in vivo* T cell responses. An *in vitro* assay was performed to establish the extent of Treg suppression on the proliferation of naive motheaten and control $CD8^+$ F5 T cells. Although the majority of the *in vivo* assays performed during this study were carried out in lymphopaenic mice, which do not possess any Tregs, it was still considered an important assay to perform given the *in vivo* role of Tregs during T cell responses to antigen (Zou, 2006). Tregs were successfully purified from the spleens of mice based upon CD4 and CD25 expression, which was confirmed by flow cytomertry (data not shown, analysis perfomed by Dr. Gareth Betts, Department of Medical Biochemistry and Immunology, Cardiff University). Although the data from the Treg assay suggested that motheaten $CD8^+$ T cells were more resilient to the inhibitory effects of Tregs, the data needs to be viewed with caution. Firstly, conditions were not performed in triplicate due to the limited availability of motheaten $CD8^+$ T cells. Furthermore, the enhanced proliferation of control versus motheaten T cells in response to anti-CD3 antibody stimulation is contradictory to previously published data (Lorenz *et al.*,

1996; Pani *et al.*, 1996; Sathish *et al.*, 2001), which have demonstrated a hyperproliferative phenotype of motheaten $CD8^+$ T cells upon anti-CD3 antibody stimulation. As the extent of suppression was calculated by using this data, it could be misleading and would therefore need to be repeated, and with T cell numbers permitting the different conditions performed in triplicate. Overall, the assay was successful with regards to the T cell proliferation being susceptible to Treg suppression and could be repeated and also developed further to look at other aspects of Treg activity. In addition to Tregs mediating T cell suppression via release of soluble factors (Turk *et al.*, 2004) Tregs are also capable of conditioning APCs so the APCs are rendered less efficient at priming $CD8^+$ T cells (Zou, 2006). In light of this, *in vitro* generated DCs loaded with NP68 could be used to prime naive $CD8^+$ F5 T cells instead of using anti-CD3 antibody. This approach to a Treg assay may be particularly relevant when considering the ability of SHP-1 deficient $CD8^+$ T cells to form more stable conjugates with APCs.

6.4 The role of SHP-1 in memory $CD8^+$ T cell responses

The ability of T and B cells to persist as long lived memory cells is a hallmark of the adaptive immune response. Immunological memory provides superior protection against re-encounter with cognate antigen and is the basis of many successful vaccination regimens. It is also evident that the long term persistence of memory cells during ACT immunotherapy strategies correlates with an improved anti-tumour activity. Therefore, the factors that may influence the generation and function of memory T cells require ongoing investigation. This study provided the opportunity to explore the *in vivo* role of SHP-1 in memory $CD8^+$ T cells.

Previous to the study, the early mortality of motheaten mice precluded direct *in vivo* studies from being performed within these mice, but with the development of adoptive T cell transfer techniques during this study, motheaten T cells could be studied for extended periods in recipient mice. Protocols that were developed to look at primary $CD8^+$ F5 T cells

responses were adapted to study memory T cells. Mice were primed twice, firstly to elicit a primary response of adoptively transferred $CD8^+$ T cells, and secondly to activate memory $CD8^+$ T cells. Initially, irradiated mice were not used as recipients to study T cell memory, as their recovering T cell pool post irradiation meant endogenous T cells capable of responding to NP68 would have been present by the time of the second priming. As an alternative, Rag-$1^{-/-}$ mice were used as recipients as they are genetically lymphopaenic and therefore allowing the adoptively transferred cells to be preferentially studied. In the early stages of the study of memory $CD8^+$ T cell responses, IFA was used to deliver NP68 peptide to mice for both the initial and recall priming, as it was convenient to use and also efficient at priming T cells *in vivo*. Using this form of priming, mice that received naive control $CD8^+$ F5 T cells had an enhanced memory response compared to mice that received motheaten $CD8^+$ F5 T cells. Based on this data, it appeared that the enhanced *in vivo* primary response seen with motheaten $CD8^+$ F5 T cells did not necessarily translate to an enhanced memory response. Although an intriguing result, it was considered that the administration of NP68 in IFA may lead to the peptide binding to MHC class I molecules expressed by cell types other than APCs. This may include the memory $CD8^+$ F5 T cells, thereby making them targets for direct cytolysis by other $CD8^+$ F5 T cells. The extent of T cell fratricide may have been greater in mice that received motheaten T cells as more T cells would have been present due to enhanced *in vivo* expansion. This would increase the likelihood of T cells encountering one another, leading to more T cells being killed, thus leaving a reduced number to clear target cells. Although no data was generated to support this hypothesis it seemed a plausible explanation.

To establish whether the mode of priming did indeed influence the extent of target cells killed, subsequent experiments used *in vitro* generated DCs loaded with NP68 to prime memory $CD8^+$ F5 T cells. Interestingly, with this approach, mice that received naive

motheaten $CD8^+$ F5 T cells killed more target cells during a memory response than mice that received control $CD8^+$ F5 T cells. This was also the observation for mice primed with DCs for both the initial and recall priming.

As the study of memory T cell responses progressed it became increasingly evident that the health of mice was declining towards the end of the experiment, and only in mice that received $CD8^+$ F5 T cells. Symptoms included diarrhoea and weight loss, which are characteristic of colitis. In order to establish the underlying reason for the decline in the health of the Rag-$1^{-/-}$ recipient mice an independent experiment was performed. Mice receiving NP68 in IFA and naive $CD8^+$ F5 T cells were the first to develop diarrhoea and lost the greatest amount of their original body weight. Mice that received T cells alone went on to develop diarrhoea and also lost a considerable amount of body weight. Upon dissection, mice that received $CD8^+$ F5 T cells had an enlarged colon, spleen and mesenteric lymph nodes. Histopathological analysis revealed a striking infiltrate of cells into the muscle and mucosa of the colon. The cells were later shown to be predominantly $CD8^+$ T cells by fluorescent antibody staining (Performed by Dr. Jason Twohig from the Department of Biochemistry and Immunology, Cardiff University). The inflammation would have been anticipated to have had a significant impact on the absorptive function of the affected GI tract and therefore explains the wasting seen with the mice. Although an interesting observation (discussed later), it was imperative to develop an assay that examined memory T cell responses *in vivo* without the above complications, as these could have an impact upon the memory T cell pool being studied. During the development of a new assay it was found that the initial reservations about using irradiated mice to study memory T cell responses were not justified. Mice that were concomitantly irradiated and primed with NP68 in IFA did not exhibit a T cell response when primed for a second time. The lack of an endogenous T cell response could be due to the presence of the NP68 peptide and tolerance

mechanisms, which may influence the developing T cell pool as it recovers from irradiation. This indicated that the responses in mice that received adoptively transferred cells could be solely attributed to the exogenous cells. Using the new protocol it was demonstrated that mice that received naive motheaten $CD8^+$ F5 T cells exhibited an enhanced memory response, although repeats would be necessary to validate this finding, and sufficient numbers of mice included to ensure statistical data could be generated.

Overall, by using three different protocols it was demonstrated that the transfer of a naive population of motheaten $CD8^+$ F5 T cells allowed recipient mice to mount an enhanced memory response in comparison to the transfer of control T cells. The underlying reasons for this observation would need further investigation. During a primary T cell response it was shown that there was an enhanced expansion of T cells in the absence of SHP-1. Therefore, it would seem reasonable to hypothesise that the generation of more T cells during a primary response would translate to the formation of more memory T cells, resulting in the killing of more target cells. This interpretation would be independent of which linear model of memory T cell formation is accepted. The entry of more naive motheaten $CD8^+$ T cells into cell division during a primary response could give rise to more memory T cell intermediates during differentiation to effector cells (naive - TCM – TEM - effector). Alternatively, the generation of more effector cells from naive T cells in the absence of SHP-1 could then differentiate into more memory T cells (naive – effector – TEM – TCM). The number of memory T cells could be assessed to establish whether greater numbers of memory motheaten T cells exist, both before and after antigenic stimulation. The protocol developed to look at T cell expansion during a primary response could also be used to study memory T cell expansion. In addition, assays involving the transfer of the same number of effector cells, rather than naive cells, would reveal whether the enhanced expansion of SHP-1 deficient naive T cells is responsible for the generation of an enhanced memory response.

Pilot experiments performed during this study demonstrated that this approach is feasible, as *in vitro* generated effector cells mounted a memory response after an extended period post *in vivo* transfer. Ideally, cells would be generated in mice, purified by immunomagnetic separation, and then transferred to recipient mice. It would also be necessary to ensure that T cells of exactly the same differentiation state were being transferred, as more naive T cells may remain in mice receiving control $CD8^+$ F5 T cells than in mice receiving motheaten $CD8^+$ F5 T cells. This could be achieved by using the fluorescent dye CFSE, which is diluted during cell division. This would allow motheaten and control $CD8^+$ F5 T cells to be purified by flow cytometry based upon the division peak in which they reside. In addition to studying the numbers of memory T cells it would also be informative to investigate other potential reasons for the enhanced memory response seen in the absence of SHP-1. It is also possible that the enhanced ability of naive motheaten $CD8^+$ F5 T cells to form conjugates may also apply to motheaten memory T cells and this may contribute to the hyperproliferative phenotype. Memory cells could be generated *in vivo*, purified using immunomagnetic techniques and used in ex-vivo or *in vivo* studies. By transferring the same number of memory motheaten and control $CD8^+$ F5 T cells to individual recipient mice and stimulating them, it would provide valuable information concerning the latter stages of a T memory response. Similarly, *in vivo* generated memory cells could be utilised in *in vitro* assays, such as those which are routinely used to study T cell proliferation and CTL function. It would also be informative to explore whether SHP-1 influences the relative proportion of TCM and TEM $CD8^+$ T cell subsets. Given the *in vitro* observation that SHP-1 deficient $CD8^+$ T cells have the enhanced capability of forming conjugates with APCs, this may influence the type of memory T cell pool formed. This hypothesis is supported by *in vivo* models, which suggest that the dynamic interaction of T cells with APCs influences the differentiation of memory T cells. A pilot assay confirmed that it was possible to delineate an effector memory response from a

total memory response. This assay is based on the contentious observation that TEM cells have the ability to provide immediate protection when compared to TCM cells. Despite this contention, the assay may nevertheless provide further information about the role of SHP-1 in $CD8^+$ T cell memory. Furthermore, *in vivo* generated memory T cells could be further characterised ex-vivo by looking at various surface markers. During the initial stages of T cell differentiation the IL-7 receptor has been shown to demarcate memory T cell precursors during clonal expansion (Huster *et al.*, 2004) and could therefore be used to establish what proportion of activated motheaten and control T cells express this marker. Additionally, the expression of CD62L and CD28 could be assessed as their expression is associated with distinct memory T cell subsets.

6.5 The role of $CD8^+$ T cells in inflammatory bowel disease (IBD)

As discussed earlier, Rag-$1^{-/-}$ mice that received $CD8^+$ F5 T cells developed colitis due to an influx of $CD8^+$ F5 T cells. Curiously, this only occurs when the transferred $CD8^+$ F5 T cells are taken from donor mice that are transgenic for the F5 TCR and on a Rag-$1^{+/+}$ background. Experiments performed by Dr. Jean G. Sathish, from our group, have demonstrated that disease does not develop when monoclonal $CD8^+$ F5 T cells are transferred from mice of a Rag-$1^{-/-}$ background.

The F5 TCR uses the Vα4 and Vβ11 gene segments of the α and β chain variable-region gene families respectively (Palmer *et al.*, 1989), and recognises the NP68 peptide in the context of the mouse MHC class I molecules H-$2D^b$. On a Rag-$1^{+/+}$ background the F5 transgenic TCRβ chain is able to pair with endogenous TCRα chains, thereby creating novel TCRs at the surface of the $CD8^+$ T cells (Simpson *et al.*, 1995a). Therefore, the T cells have the ability to recognise peptide antigens other than NP68. Interestingly, the colitis inducing $CD8^+$ F5 T cells do not cause disease in the donor mice from which they were purified, which may be attributed to the suppressive actions of Tregs within these mice. The histological analysis of

the bowels from the mice during this study highlights similarities to the bowels of patients with IBD.

In humans, IBD constitutes a group of chronic inflammatory conditions of the gastrointestinal (GI) tract that affects a significant fraction of the population (Russel and Stockbrugger 1996; Shivananda *et al.*, 1996). The two main forms of IBD are Crohn's disease (CD) and Ulcerative Colitis (UC), with differences between them attributed to the location and nature of the inflammation. Whereas UC is restricted to the colon and rectum, CD can affect any part of the GI tract from the mouth to the anus. Microscopically, UC is restricted to the musocsal layer of the gut whereas CD can affect the entire bowel wall. Both CD and UC can also have extra-intestinal manifestations (Hendrickson *et al.*, 2002). Although considerable progress has been made in the understanding of IBD, research has yet to fully define its aetiology. Studies have indicated that the inflammation associated with IBD may be caused by the complex interaction of various factors: including genotype (Bouma at al., 2003; Taylor *et al.*, 2003), the immune system (Podolsky 2002), and environmental components (Podolsky 2002). More specifically, animal models have demonstrated that $CD4^+$ T cells are the main mediators of the inflammation seen in IBD (Strober *et al.*, 2002; Powrie *et al.*, 1993). The most favoured hypothesis involves the activation of $CD4^+$ T cells by antigens derived from enteric bacteria. Alongside the role of $CD4^+$ T cells in the pathogenesis, other immune cells, namely APCs, have been implicated in the induction of IBD (Malmstrom *et al.*, 2001). Despite $CD8^+$ T cells exhibiting an activated phenotype in IBD patients (Senju *et al.*, 1991a; Senju *et al.*, 1991b; Senju *et al.*, 1991c; Muller *et al.*, 1998), their role in the pathophysiology of IBD has not been fully investigated. Conflicting data have been acquired from a limited number of studies that have looked at the role of $CD8^+$ T cells in models of intestinal inflammation. In a study of colitis performed in IL-2 deficient mice, $CD8^+$ T cells did not appear to have a role in disease progression (Simpson *et al.*, 1995b). In

contrast, a Crohn's-like model (Kontoyiannis et al., 2002) and a study involving the adoptive transfer of auto-antigen specific $CD8^+$ T cells (Steinhoff *et al.*, 1999) both supported a role for $CD8^+$ T cells in intestinal inflammation. In light of this, further investigations could potentially lead to the development of a mouse model that allows for an increased understanding of the role of $CD8^+$ T cells in the pathogenesis of IBD.

Adoptive transfer experiments could be repeated with different numbers of naive $CD8^+$ F5 T cell, in order to establish a minimum number of $CD8^+$ F5 T cells required to mediate disease. In addition, a scoring system could be used to determine the extent of disease and may include parameters such as the severity of inflammation, hyperplasia of mucosal epithelium and mucosal ulceration.

It would be imperative to ensure the pathophysiology seen in the Rag-$1^{-/-}$ mice was indeed attributable to the adoptively transferred $CD8^+$ F5 T cells and not $CD4^+$ T cells, which may contaminate the immunomagnetic cell preparations (95% pure for $CD8^+$ T cells). This could be addressed by using anti-CD4 antibodies to deplete transferred $CD4^+$ T cells, or by performing experiments in Rag-$1^{-/-}$ mice that lack expression of MHC class II molecules. Alternatively, experiments performed in Rag-$1^{-/-}$ mice that lack expression of B_2M would also provide means of demonstrating that $CD8^+$ are the primary force behind the pathophysiology seen in these mice. This approach would also confirm that the $CD8^+$ T cells were expanding as a result of antigenic peptide presentation rather than due to the action of homeostatic cytokines, although this seems unlikely given the observation that $CD8^+$ F5 T cells from a $Rag1^{-/-}$ background do not induce disease.

It was also be informative to delineate whether the $CD8^+$ F5 T cells are reacting to foreign antigens from bacteria in the gut or to autoantigens expressed by the GI tract. The administration of antibiotics and the housing of mice under sterile conditions would ensure

mice were free of gut bacteria. If disease developed under these conditions it would be likely that the transferred T cells were responding to auto-antigens expressed in the GI tract.

6.6 *In vivo* tumour studies

In light of the data demonstrating that primary $CD8^+$ T cell response are enhanced in the absence of SHP-1, studies were carried out to explore whether this could be exploited in a therapeutic setting. With the availability of the C57BL/6 mouse melanoma cell line, B16, assays were developed to study the properties of SHP-1 deficient $CD8^+$ T cells at combating tumourigenesis. The premise of such experiments was to explore the possibility of eventually downregulating SHP-1 expression in tumour-specific human T cells in order to improve T cell adoptive immunotherapy strategies. Although encouraging clinical outcomes have been achieved from the adoptive transfer of $CD8^+$ T cells during clinical trials, there is still a need for further optimisation in order for such approaches to be used in the clinic on a routine basis.

As the B16 melanoma cells metastasise to the lungs upon intravenous transfer, assays were initially trialled that involved the detection of fluorescently labelled B16 cells in the lungs of mice by flow cytometry. This approach proved to be unsuccessful due to side-effects exhibited by the mice when transferring the number of B16 cells that were required to allow detection of the cells in the lungs. A second approach involved transferring B16 cells that had been labelled with NP68 peptide to mice that had previously received naive $CD8^+$ F5 T cells. The measurable parameter of this assay would have been the number of tumour nodules in the lungs of the mice fourteen days post B16 cell transfer, allowing comparisons to be made between mice receiving either naive motheaten or control $CD8^+$ F5 T cells. However, this approach was not feasible, as an equivalent number of nodules formed in the lungs of mice that received naive control $CD8^+$ F5 T cells followed one week later by either

NP68 labelled or unlabelled B16 cells. This implied that the NP68 peptide is either lost from the surface of the cells or diluted between cells during cell division, thereby allowing the B16 cells to escape cytolysis by the T cells.

In order for the tumour studies to proceed, B16 cells were engineered to constitutively express the NP68 peptide. This process involved producing virus using the retroviral packaging cell line, Phoenix, and the cloning of B16 cells expressing the NP68 peptide. This was facilitated by the expression of GFP as a fusion protein with the NP68 epitope. The NP68 expressing B16 cells were successfully killed by activated $CD8^+$ F5 T cells, in both an *in vitro* and *in vivo* setting, and were therefore used extensively during this study. The $CD8^+$ F5 T cells were very efficient at preventing tumour development within the lungs of recipient mice. As a consequence, a number of optimisation experiments were necessarily performed in order to optimise tumour development and clearance. These assays established the number of T cells and B16 cells to transfer, the duration between transfer, and the order of cells transferred with the T cells being transferred first. As a result of defining the conditions for a tumour protection assay, it was demonstrated that the transfer of naive motheaten $CD8^+$ F5 T cells conferred mice with enhanced protection against tumour growth. Mice that received naive motheaten $CD8^+$ F5 T cells had significantly fewer tumour nodules in their lungs than mice that received control $CD8^+$ F5 T cells.

It would be informative to establish the underlying reason for the enhanced anti-tumour response seen in the absence of SHP-1, and pilot experiments demonstrated that tracking the adoptively transferred T cells in the blood and lungs was a feasible approach. *In vitro* experiments were also performed to explore the underlying reasons for the enhanced anti-tumour response seen in the absence of SHP-1. From one *in vitro* experiment it was established that motheaten $CD8^+$ F5 T cells killed more B16 target cells on a per cell basis than control $CD8^+$ F5 T cells. This apparent enhanced cytolysis is contradictory to previously

published data showing equal killing by motheaten and control $CD8^+$ F5 T cells on a per cell basis, when the target cells were EL4s. In light of this, experiments would ideally be performed again with both B16 and EL4 cells being used as targets. It may also be of interest to establish the expression of costimulatory molecule ligands by the target cells as it has been demonstrated that costimulation can enhance the effector function of T cells (Bai *et al.*, 2001). A study of naive $CD8^+$ T cells has shown that costimulation can override the proliferative differences detected between motheaten and control $CD8^+$ F5 T cells, when using anti-CD3 antibody to stimulate the cells (Sathish *et al.*, 2001). Therefore, it may be plausible that this differential requirement for costimulation may also be true for activated control and motheaten $CD8^+$ F5 T cells. It was also established during *in vitro* investigations that a greater proportion of activated $CD8^+$ F5 T cells express CD107a upon encounter with B16 target cells, which correlates with the enhanced killing seen on a per cell basis. This assay needed further optimisation as the T cells were extremely sensitive to antigen recognition, which resulted in maximal CD107a expression. This could be addressed by further increasing T cell to target cell ratios, or by titrating the concentration of NP68 peptide that was used to label the B16 target cells. Again, it would be informative to repeat such an assay with EL4 cells, to establish if differences in cytolysis between the two T cell populations are dependent upon the cells being targeted. With repeated experiments and further improvements to the assays being used it would be possible to validate the results that examined the cytolytic function of motheaten and control $CD8^+$ F5 T cells on a per cell basis. It would also be informative to look at other facets associated with effector function, such as the expression levels of molecules associated with cytotoxicity, including perforin and the granzymes.

Although an important milestone of this study, the demonstration that SHP-1 deficient $CD8^+$ T cells provide an enhanced anti-tumour response in a prophylactic context does not

translate to what happens in a clinical situation, where patients present with established tumours. In order to address this and acquire proof-of-principle data it would be imperative to progress to using mouse models of tumour regression rather than tumour protection. Due to time constraints of this study, this aim was not met, although some important ground-work was carried out to enable such experiments to be performed in the future.

The B16 cells expressing the NP68 epitope were used to establish subcutaneous tumours, which grew in a non-uniform manner within a group of mice. This pattern of growth may be attributed to the injection technique, as ensuring the cells are administered sub-cutaneously rather than intra-dermally may impact on the growth kinetics of the tumour. Despite this disparity, mice with similar sized tumours were used for adoptive $CD8^+$ T cell transfer experiments. Although this assay was limited by the number of recipient mice, it did reveal an encouraging result. The mouse that received naive motheaten $CD8^+$ F5 T cells exhibited enhanced regression of the tumour and at the end point of the assay had a tumour that was smaller in size than the mouse that received either no T cells or naive control $CD8^+$ F5 T cells. During this assay, it also became apparent that measuring the developing tumour with callipers may not be the most precise way to monitor tumour growth and regression. This was not a shortfall in the accuracy of the callipers to measure distances, but the nature of the subcutaneous tumours. Firstly, the tumours were not always uniform in shape, which could potentially lead to an over estimation of the size of the tumour mass. Additionally, the small size of tumour masses at certain times during the assays meant it was practically challenging to measure them accurately. Finally, the tumour masses being measured were not totally solid and therefore had the potential to be compressed during measurement, which could alter the readout from the callipers. Therefore, B16 cells were engineered to constitutively express the NP68 epitope and the enzyme, luciferase. The generation of these cells will enable an *in vivo* imaging unit that is capable of detecting bio-luminescence to be

used to monitor tumour growth in an non-invasive and quantitative manner. This would allow tumour regression studies to be performed in an accurate manner. Potentially, either the subcutaneous or pulmonary B16 model could be used, with B16 tumours established prior to T cell transfer. For the lung model, the tumours could be monitored at regular intervals throughout the assay without the need to sacrifice the mice. Despite the presence of an IRES between the genes for luciferase and YFP it was hard to detect any fluorescence from transfected cells until they had been cloned. Both a fluorescent microscope and a FACScalibur flow cytometer were unable to detect YFP fluorescence from polyclonal cells, even though the cells were positive for luciferase activity. A weak fluorescent signal was detected from polyclonal cells when using a Moflo flow cytometer, which aided the cloning of the B16 cells. Monoclonal cell lines were found to be weakly fluorescent when analysed by a FACScalibur flow cytometer. The low level of fluorescence may be attributed to the inefficiency of the IRES at initiating transcript translation.

The tumour models established also have the potential to be adapted to continue the studies of T cell migration, as developing tumours would be a target tissue for T cell migration.

6.7 siRNA studies

In order to exploit the findings of this study in a therapeutic setting it would be necessary to modulate SHP-1 expression in human $CD8^+$ T cells. The introduction of siRNA into $CD8^+$ T cells may offer a vital tool in regulating SHP-1 expression. During this study, several methods were used to screen candidate siRNA sequences for effective targeting of SHP-1 expression. Jurkat T cells constitute a suitable cell to test the candidate shRNA sequences as they express SHP-1. Electroporating the Jurkat cells in order to introduce DNA results in a dramatic loss of cells and therefore had an impact on the number of cells available for

immunoblotting. This limitation is further compounded by low transfection efficiencies, which means the time it takes to sort a sufficient number of cells by flow cytometry has financial implications. Overall this mode of testing candidate shRNA sequences is not very efficient. Hence, in attempting to overcome this issue, Hela cells were engineered to express mouse and human SHP-1, as they are more readily transfected by methods other than electroporation, such as DNA-containing calcium phosphate precipitates. Hela cells are also more selectable by antibiotic treatment when compared to Jurkat cells, which meant flow cytometry was not required for selecting transfected cells.

Overall, it was demonstrated that SHP-1 protein levels can be downregulated in either Jurkat cells or Hela cells expressing human SHP-1 by using shRNA, with a maximum reduction of 53% seen during this study. Although it would be imperative to identify a siRNA sequence to give a more robust knockdown of human SHP-1 in $CD8^+$ T cells it would also be advantageous to pursue a viable sequence that gave knockdown of SHP-1 in mouse $CD8^+$ T cells. This would allow SHP-1 manipulated primary mouse T cells to be utilised in the types of assays developed during this study. Additionally, it was also allow comparisons to be made between manipulated T cells and motheaten T cells, and would give an indication of the degree of downregulation required to achieve the functional properties of T cells that are totally deficient of SHP-1 activity.

The recent optimisation of lentiviral production and infection techniques within our laboratory may further assist with the progress of the siRNA studies. Lentivirus can be produced that encode specific shRNA sequences and subsequently be used to infect desired cells. Indeed, data from our research group has shown that lentivirus can be used to transfer genes at high efficiency to Jurkat cells, and more importantly human PBMCs. Therefore, this area of research is poised ready for the testing of candidate shRNA sequences in human cells, in order to downregulate SHP-1 expression. The use of lentivirus offers the means of

transferring genetic material to cells that are not actively dividing, which is normally a pre-requisite of other retroviruses for successful transduction. This could assist with the improvement of adoptive T cell tumour immunotherapy strategies, as SHP-1 expression could be ablated in naive human $CD8^+$ T cells without the need for excessive ex-vivo activation. This would be favourable as it has been repeatable demonstrated that less differentiated T cell populations have the greatest *in vivo* impact on tumourigenesis (Klebanoff *et al.*, 2005).

Ultimately, it would be desirable to use manipulated human $CD8^+$ T cells in various assays to explore their functional properties. Human tumour specific T cell lines could be manipulated using identified SHP-1 specific shRNA sequences for targeting SHP-1 and then used in *in vitro* proliferation assays. Hopefully, this type of experiment would be able to recapture what has been previously observed with motheaten mouse $CD8^+$ T cells, in terms of enhanced proliferation and cytolysis. Furthermore, the NOD SCID mouse model could also be utilised to study manipulated human T cells. As this mouse does not reject transferred human cells it would be possible to examine the CTL function of manipulated human $CD8^+$ T cells in an *in vivo* model. Human PBMCs could be harvested and the $CD8^+$ T cells purified and infected with lentiviruses that encode for both a tumour specific TCR, such as for Wilm's tumour antigen, and also a shRNA sequence to target SHP-1 expression. The T cells could be transferred *in vivo*, along with human leukaemia cells that express the Wilm's tumour antigen, and the extent of tumour cell engraftment assessed.

6.8 Pro-tumoural role of $CD8^+$ T cells in a lung tumour model

During the optimisation of the tumour protection assay it was found that mice rendered lymphopaenic by irradiation developed significantly fewer pulmonary tumours when compared to mice that were not irradiated. Concomitant with this observation, Dr. Simone

Cuff (Department of Medical Biochemistry and Immunology, Cardiff University) also observed reduced pulmonary tumour nodule formation when B16 cells were transferred intravenously to Rag-$1^{-/-}$ mice and also in mice that had been depleted of $CD8^+$ T cells using an anti-CD8 antibody. Thus, the pro-tumoural phenomenon was demonstrated in three separate systems by using the pulmonary B16 model. The use of Rag-$1^{-/-}$ mice confirmed that the pro-tumoural observation in anti-CD8 antibody depleted mice was due to $CD8^+$ T cell depletion rather than other $CD8^+$ cell subsets, such as DCs (Iyoda *et al.*, 2002., McLellan *et al.*, 2002). Interestingly, the pro-tumoural observation was not mirrored for subcutaneous B16 tumours, in both Rag-$1^{-/-}$ and $CD8^+$ T cell depleted mice. The pro-tumoural pulmonary observation seems counter-intuitive when considering the premise of tumour vaccine strategies, which enlist $CD8^+$ T cells to combat tumourigenesis, and also the positive correlation seen between $CD8^+$ T cell tumour filtration and tumour patient prognosis (Chiba *et al.*, 2004; Galon *et al.*, 2006; Pages *et al.*, 2005). In addition, the transfer of naive $CD8^+$ F5 T cells to recipient mice during this study provided complete protection from pulmonary tumour development when B16 cells expressing NP68. Whereas tumour-specific adaptive immune responses have the capacity for anti-tumoural activity the actions of non-specific adaptive immune responses on tumourigenesis have not been fully explored. Indeed, innate immune responses rather than adaptive immune responses have been associated with augmentation of tumour growth. Some studies have implicated $CD8^+$ T cells with a regulatory role in a number of human tumours (Filaci *et al.*, 2007). In addition, pro-tumoural $CD8^+$ T cells have been described in a chemically induced tumour mouse model (Roberts *et al.*, 2007), although the antigen specificity of the T cells was not defined.

In light of these findings, collaborative work was undertaken during this study to explore the pro-tumoural role of antigen specific $CD8^+$ F5 T cells in the B16 pulmonary tumour model. This aim was facilitated by the availability of B16 cells generated during this study that

expressed the NP68 epitope and also wild-type B16 cells that do not express the cognate antigen. The experimental findings demonstrated that an antigen specific $CD8^+$ T cell response was potently anti-tumoural, whereas an antigen non-specific $CD8^+$ T cell response was pro-tumoural in nature. The $CD8^+$ F5 T cells could either have a pro-tumoural or anti-tumoural role depending upon the presence of absence of expression of the cognate antigen by the tumour cells being targetted. It can therefore be concluded that the T cells do not belong to a regulatory subset of T cells. Dr. Simone Cuff has further demonstrated that the absence of $CD8^+$ T cells correlated with an increased number of NK cells in the lungs of mice with developing tumours. NK cells play an important anti-tumoural role in the B16 pulmonary model as demonstrated by the extreme susceptibility of NK1.1 depleted mice to sub-tumoural doses of B16 tumour cells, and also by the increased anti-tumour response seen when NK cell activity is enhanced. These findings may have implications for tumour development when non-specific inflammatory conditions are present, such as during infection of the lungs or during therapeutic vaccination, which may elicit a $CD8^+$ T cell response that is not specific for the tumour.

6.9 Overall summary and conclusions

During this study it has been conclusively demonstrated that the absence of SHP-1 in $CD8^+$ T cells results in an enhanced *in vivo* response to antigenic stimulation. This is characterised by an enhanced *in vivo* expansion and an increase in cytotoxicity. Importantly, the enhanced *in vivo* activity of SHP-1 deficient $CD8^+$ T cells provided superior protection against tumour formation in a lung model of tumour development.

In addition to an enhanced primary response in the absence of SHP-1, preliminary data from this study has indicated that SHP-1 deficient T cells exhibit an enhanced memory response.

These data support the notion that SHP-1 expression could be targeted for downregulation in $CD8^+$ T cells in order to improve the efficacy of adoptive T cell transfer immunotherapy strategies. Current strategies involve the ex-vivo generation of large number of T cells for in vivo transfer. Often, the *in vivo* function of the T cells is impaired due to their repeated ex-vivo stimulation, which leads to a terminally differentiated T cell phenotype. The downregulation of SHP-1 in T cells used for ACT immunotherapy may potentially overcome this problem. In the absence of SHP-1 expression, T cells could be transferred in a less differentiated state, without precluding the generation of sufficient T cell numbers to mediate tumour regression.

References

Agrawal, A., and Schatz, D.G. (1997). RAG1 and RAG2 form a stable postcleavage synaptic complex with DNA containing signal ends in V(D)J recombination. Cell *89*, 43-53.

Albert, M.L., Pearce, S.F., Francisco, L.M., Sauter, B., Roy, P., Silverstein, R.L., and Bhardwaj, N. (1998a). Immature dendritic cells phagocytose apoptotic cells via alphavbeta5 and CD36, and cross-present antigens to cytotoxic T lymphocytes. J Exp Med *188*, 1359-1368.

Albert, M.L., Sauter, B., and Bhardwaj, N. (1998b). Dendritic cells acquire antigen from apoptotic cells and induce class I-restricted CTLs. Nature *392*, 86-89.

Alexander, R.B., and Rosenberg, S.A. (1990). Long-term survival of adoptively transferred tumor-infiltrating lymphocytes in mice. J Immunol *145*, 1615-1620.

Alonso, A., Sasin, J., Bottini, N., Friedberg, I., Osterman, A., Godzik, A., Hunter, T., Dixon, J., and Mustelin, T. (2004). Protein tyrosine phosphatases in the human genome. Cell *117*, 699-711.

Ambrosino, E., Berzofsky, J.A., and Terabe, M. (2008). Regulation of tumor immunity: the role of NKT cells. Expert Opin Biol Ther *8*, 725-734.

Anderson, G., Moore, N.C., Owen, J.J., and Jenkinson, E.J. (1996). Cellular interactions in thymocyte development. Annu Rev Immunol *14*, 73-99.

Anichini, A., Vegetti, C., and Mortarini, R. (2004). The paradox of T-cell-mediated antitumor immunity in spite of poor clinical outcome in human melanoma. Cancer Immunol Immunother *53*, 855-864.

Antony, P.A., Piccirillo, C.A., Akpinarli, A., Finkelstein, S.E., Speiss, P.J., Surman, D.R., Palmer, D.C., Chan, C.C., Klebanoff, C.A., Overwijk, W.W., *et al.* (2005). CD8+ T cell immunity against a tumor/self-antigen is augmented by CD4+ T helper cells and hindered by naturally occurring T regulatory cells. J Immunol *174*, 2591-2601.

Appay, V., Dunbar, P.R., Callan, M., Klenerman, P., Gillespie, G.M., Papagno, L., Ogg, G.S., King, A., Lechner, F., Spina, C.A., *et al.* (2002). Memory CD8+ T cells vary in differentiation phenotype in different persistent virus infections. Nat Med *8*, 379-385.

Appay, V., Nixon, D.F., Donahoe, S.M., Gillespie, G.M., Dong, T., King, A., Ogg, G.S., Spiegel, H.M., Conlon, C., Spina, C.A., *et al.* (2000). HIV-specific CD8(+) T cells produce antiviral cytokines but are impaired in cytolytic function. J Exp Med *192*, 63-75.

Appay, V., and Rowland-Jones, S.L. (2002). The assessment of antigen-specific CD8+ T cells through the combination of MHC class I tetramer and intracellular staining. J Immunol Methods *268*, 9-19.

Arbones, M.L., Ord, D.C., Ley, K., Ratech, H., Maynard-Curry, C., Otten, G., Capon, D.J., and Tedder, T.F. (1994). Lymphocyte homing and leukocyte rolling and migration are impaired in L-selectin-deficient mice. Immunity *1*, 247-260.

Arstila, T.P., Casrouge, A., Baron, V., Even, J., Kanellopoulos, J., and Kourilsky, P. (1999). A direct estimate of the human alphabeta T cell receptor diversity. Science *286*, 958-961.

Asada, H., Ishii, N., Sasaki, Y., Endo, K., Kasai, H., Tanaka, N., Takeshita, T., Tsuchiya, S., Konno, T., and Sugamura, K. (1999). Grf40, A novel Grb2 family member, is involved in T cell signaling through interaction with SLP-76 and LAT. J Exp Med *189*, 1383-1390.

Asanuma, K., Tsuji, N., Endoh, T., Yagihashi, A., and Watanabe, N. (2004). Survivin enhances Fas ligand expression via up-regulation of specificity protein 1-mediated gene transcription in colon cancer cells. J Immunol *172*, 3922-3929.

Ashwell, J.D., and D'Oro, U. (1999). CD45 and Src-family kinases: and now for something completely different. Immunol Today *20*, 412-416.

Atkins, D., Breuckmann, A., Schmahl, G.E., Binner, P., Ferrone, S., Krummenauer, F., Storkel, S., and Seliger, B. (2004a). MHC class I antigen processing pathway defects, ras mutations and disease stage in colorectal carcinoma. Int J Cancer *109*, 265-273.

Atkins, D., Ferrone, S., Schmahl, G.E., Storkel, S., and Seliger, B. (2004b). Down-regulation of HLA class I antigen processing molecules: an immune escape mechanism of renal cell carcinoma? J Urol *171*, 885-889.

Ayyoub, M., Zippelius, A., Pittet, M.J., Rimoldi, D., Valmori, D., Cerottini, J.C., Romero, P., Lejeune, F., Lienard, D., and Speiser, D.E. (2003). Activation of human melanoma reactive CD8+ T cells by vaccination with an immunogenic peptide analog derived from Melan-A/melanoma antigen recognized by T cells-1. Clin Cancer Res *9*, 669-677.

Bachmann, M.F., Wolint, P., Schwarz, K., and Oxenius, A. (2005). Recall proliferation potential of memory CD8+ T cells and antiviral protection. J Immunol *175*, 4677-4685.

Bagshawe, K.D., Burke, P.J., Knox, R.J., Melton, R.G., and Sharma, S.K. (1999a). Targeting enzymes to cancers--new developments. Expert Opin Investig Drugs *8*, 161-172.

Bagshawe, K.D., Sharma, S.K., Burke, P.J., Melton, R.G., and Knox, R.J. (1999b). Developments with targeted enzymes in cancer therapy. Curr Opin Immunol *11*, 579-583.

Bai, X.F., Bender, J., Liu, J., Zhang, H., Wang, Y., Li, O., Du, P., Zheng, P., and Liu, Y. (2001). Local costimulation reinvigorates tumor-specific cytolytic T lymphocytes for experimental therapy in mice with large tumor burdens. J Immunol *167*, 3936-3943.

Banville, D., Stocco, R., and Shen, S.H. (1995). Human protein tyrosine phosphatase 1C (PTPN6) gene structure: alternate promoter usage and exon skipping generate multiple transcripts. Genomics *27*, 165-173.

Barber, D.L., Wherry, E.J., and Ahmed, R. (2003). Cutting edge: rapid in vivo killing by memory CD8 T cells. J Immunol *171*, 27-31.

Barber, D.L., Wherry, E.J., Masopust, D., Zhu, B., Allison, J.P., Sharpe, A.H., Freeman, G.J., and Ahmed, R. (2006). Restoring function in exhausted CD8 T cells during chronic viral infection. Nature *439*, 682-687.

Barford, D., Flint, A.J., and Tonks, N.K. (1994a). Crystal structure of human protein tyrosine phosphatase 1B. Science *263*, 1397-1404.

Barford, D., Keller, J.C., Flint, A.J., and Tonks, N.K. (1994b). Purification and crystallization of the catalytic domain of human protein tyrosine phosphatase 1B expressed in Escherichia coli. J Mol Biol *239*, 726-730.

Bartkova, J., Horejsi, Z., Koed, K., Kramer, A., Tort, F., Zieger, K., Guldberg, P., Sehested, M., Nesland, J.M., Lukas, C., *et al.* (2005). DNA damage response as a candidate anti-cancer barrier in early human tumorigenesis. Nature *434*, 864-870.

Becker, T.C., Wherry, E.J., Boone, D., Murali-Krishna, K., Antia, R., Ma, A., and Ahmed, R. (2002). Interleukin 15 is required for proliferative renewal of virus-specific memory CD8 T cells. J Exp Med *195*, 1541-1548.

Beckhove, P., Feuerer, M., Dolenc, M., Schuetz, F., Choi, C., Sommerfeldt, N., Schwendemann, J., Ehlert, K., Altevogt, P., Bastert, G., *et al.* (2004). Specifically activated memory T cell subsets from cancer patients recognize and reject xenotransplanted autologous tumors. J Clin Invest *114*, 67-76.

Beebe, K.D., Wang, P., Arabaci, G., and Pei, D. (2000). Determination of the binding specificity of the SH2 domains of protein tyrosine phosphatase SHP-1 through the screening of a combinatorial phosphotyrosyl peptide library. Biochemistry *39*, 13251-13260.

Berd, D., and Mastrangelo, M.J. (1987a). Depletion of suppressor-cytotoxic T-lymphocytes by administration of a murine monoclonal antibody. Cancer Res *47*, 2727-2732.

Berd, D., and Mastrangelo, M.J. (1987b). Effect of low dose cyclophosphamide on the immune system of cancer patients: reduction of T-suppressor function without depletion of the CD8+ subset. Cancer Res *47*, 3317-3321.

Berg, K.L., Siminovitch, K.A., and Stanley, E.R. (1999). SHP-1 regulation of p62(DOK) tyrosine phosphorylation in macrophages. J Biol Chem *274*, 35855-35865.

Berlin, C., Berg, E.L., Briskin, M.J., Andrew, D.P., Kilshaw, P.J., Holzmann, B., Weissman, I.L., Hamann, A., and Butcher, E.C. (1993). Alpha 4 beta 7 integrin mediates lymphocyte binding to the mucosal vascular addressin MAdCAM-1. Cell *74*, 185-195.

Berridge, M.J. (1993). Inositol trisphosphate and calcium signalling. Nature *361*, 315-325.
Bi, K., and Altman, A. (2001). Membrane lipid microdomains and the role of PKCtheta in T cell activation. Semin Immunol *13*, 139-146.

Binstadt, B.A., Billadeau, D.D., Jevremovic, D., Williams, B.L., Fang, N., Yi, T., Koretzky, G.A., Abraham, R.T., and Leibson, P.J. (1998). SLP-76 is a direct substrate of SHP-1 recruited to killer cell inhibitory receptors. J Biol Chem *273*, 27518-27523.

Binstadt, B.A., Brumbaugh, K.M., Dick, C.J., Scharenberg, A.M., Williams, B.L., Colonna, M., Lanier, L.L., Kinet, J.P., Abraham, R.T., and Leibson, P.J. (1996). Sequential involvement of Lck and SHP-1 with MHC-recognizing receptors on NK cells inhibits FcR-initiated tyrosine kinase activation. Immunity *5*, 629-638.

Bjorkman, P.J., Saper, M.A., Samraoui, B., Bennett, W.S., Strominger, J.L., and Wiley, D.C. (1987). Structure of the human class I histocompatibility antigen, HLA-A2. Nature *329*, 506-512.

Blaese, R.M., Culver, K.W., Miller, A.D., Carter, C.S., Fleisher, T., Clerici, M., Shearer, G., Chang, L., Chiang, Y., Tolstoshev, P., *et al.* (1995). T lymphocyte-directed gene therapy for ADA- SCID: initial trial results after 4 years. Science *270*, 475-480.

Blattman, J.N., Grayson, J.M., Wherry, E.J., Kaech, S.M., Smith, K.A., and Ahmed, R. (2003). Therapeutic use of IL-2 to enhance antiviral T-cell responses in vivo. Nat Med *9*, 540-547.

Blery, M., and Vivier, E. (1999). How to extinguish lymphocyte activation, immunotyrosine-based inhibition motif (ITIM)-bearing molecules a solution? Clin Chem Lab Med *37*, 187-191.

Boise, L.H., Minn, A.J., Noel, P.J., June, C.H., Accavitti, M.A., Lindsten, T., and Thompson, C.B. (1995). CD28 costimulation can promote T cell survival by enhancing the expression of Bcl-XL. Immunity *3*, 87-98.

Bollard, C.M., Rossig, C., Calonge, M.J., Huls, M.H., Wagner, H.J., Massague, J., Brenner, M.K., Heslop, H.E., and Rooney, C.M. (2002). Adapting a transforming growth factor beta-related tumor protection strategy to enhance antitumor immunity. Blood *99*, 3179-3187.

Bollard, C.M., Straathof, K.C., Huls, M.H., Leen, A., Lacuesta, K., Davis, A., Gottschalk, S., Brenner, M.K., Heslop, H.E., and Rooney, C.M. (2004). The generation and characterization of LMP2-specific CTLs for use as adoptive transfer from patients with relapsed EBV-positive Hodgkin disease. J Immunother *27*, 317-327.

Bonini, C., Ferrari, G., Verzeletti, S., Servida, P., Zappone, E., Ruggieri, L., Ponzoni, M., Rossini, S., Mavilio, F., Traversari, C., *et al.* (1997). HSV-TK gene transfer into donor lymphocytes for control of allogeneic graft-versus-leukemia. Science *276*, 1719-1724.

Boon, T., Coulie, P.G., and Van den Eynde, B. (1997). Tumor antigens recognized by T cells. Immunol Today *18*, 267-268.

Boon, T., and Old, L.J. (1997). Cancer Tumor antigens. Curr Opin Immunol *9*, 681-683.

Bouma, G., and Strober, W. (2003). The immunological and genetic basis of inflammatory bowel disease. Nat Rev Immunol *3*, 521-533.

Bouneaud, C., Garcia, Z., Kourilsky, P., and Pannetier, C. (2005). Lineage relationships, homeostasis, and recall capacities of central- and effector-memory CD8 T cells in vivo. J Exp Med *201*, 579-590.

Boutboul, F., Puthier, D., Appay, V., Pelle, O., Ait-Mohand, H., Combadiere, B., Carcelain, G., Katlama, C., Rowland-Jones, S.L., Debre, P., *et al.* (2005). Modulation of interleukin-7 receptor expression characterizes differentiation of CD8 T cells specific for HIV, EBV and CMV. AIDS *19*, 1981-1986.

Bronte, V., and Zanovello, P. (2005). Regulation of immune responses by L-arginine metabolism. Nat Rev Immunol *5*, 641-654.

Bruhns, P., Marchetti, P., Fridman, W.H., Vivier, E., and Daeron, M. (1999). Differential roles of N- and C-terminal immunoreceptor tyrosine-based inhibition motifs during inhibition of cell activation by killer cell inhibitory receptors. J Immunol *162*, 3168-3175.

Bunnell, S.C., Diehn, M., Yaffe, M.B., Findell, P.R., Cantley, L.C., and Berg, L.J. (2000). Biochemical interactions integrating Itk with the T cell receptor-initiated signaling cascade. J Biol Chem *275*, 2219-2230.

Burshtyn, D.N., Lam, A.S., Weston, M., Gupta, N., Warmerdam, P.A., and Long, E.O. (1999). Conserved residues amino-terminal of cytoplasmic tyrosines contribute to the SHP-1-mediated inhibitory function of killer cell Ig-like receptors. J Immunol *162*, 897-902.

Burshtyn, D.N., Scharenberg, A.M., Wagtmann, N., Rajagopalan, S., Berrada, K., Yi, T., Kinet, J.P., and Long, E.O. (1996). Recruitment of tyrosine phosphatase HCP by the killer cell inhibitor receptor. Immunity *4*, 77-85.

Burshtyn, D.N., Shin, J., Stebbins, C., and Long, E.O. (2000). Adhesion to target cells is disrupted by the killer cell inhibitory receptor. Curr Biol *10*, 777-780.

Burshtyn, D.N., Yang, W., Yi, T., and Long, E.O. (1997). A novel phosphotyrosine motif with a critical amino acid at position -2 for the SH2 domain-mediated activation of the tyrosine phosphatase SHP-1. J Biol Chem *272*, 13066-13072.

Cambier, J.C. (1995). Antigen and Fc receptor signaling. The awesome power of the immunoreceptor tyrosine-based activation motif (ITAM). J Immunol *155*, 3281-3285.

Campbell, J.J., Haraldsen, G., Pan, J., Rottman, J., Qin, S., Ponath, P., Andrew, D.P., Warnke, R., Ruffing, N., Kassam, N., *et al.* (1999). The chemokine receptor CCR4 in vascular recognition by cutaneous but not intestinal memory T cells. Nature *400*, 776-780.

Cantrell, D.A., and Smith, K.A. (1984). The interleukin-2 T-cell system: a new cell growth model. Science *224*, 1312-1316.

Carbone, F.R., Belz, G.T., and Heath, W.R. (2004). Transfer of antigen between migrating and lymph node-resident DCs in peripheral T-cell tolerance and immunity. Trends Immunol *25*, 655-658.

Carter, J.D., Neel, B.G., and Lorenz, U. (1999). The tyrosine phosphatase SHP-1 influences thymocyte selection by setting TCR signaling thresholds. Int Immunol *11*, 1999-2014.

Chambers, C.A. (2001). The expanding world of co-stimulation: the two-signal model revisited. Trends Immunol *22*, 217-223.

Champagne, P., Ogg, G.S., King, A.S., Knabenhans, C., Ellefsen, K., Nobile, M., Appay, V., Rizzardi, G.P., Fleury, S., Lipp, M., *et al.* (2001). Skewed maturation of memory HIV-specific CD8 T lymphocytes. Nature *410*, 106-111.

Chan, A.C., Dalton, M., Johnson, R., Kong, G.H., Wang, T., Thoma, R., and Kurosaki, T. (1995). Activation of ZAP-70 kinase activity by phosphorylation of tyrosine 493 is required for lymphocyte antigen receptor function. EMBO J *14*, 2499-2508.

Chan, A.C., Desai, D.M., and Weiss, A. (1994). The role of protein tyrosine kinases and protein tyrosine phosphatases in T cell antigen receptor signal transduction. Annu Rev Immunol *12*, 555-592.

Chan, W.L., Pejnovic, N., Liew, T.V., Lee, C.A., Groves, R., and Hamilton, H. (2003). NKT cell subsets in infection and inflammation. Immunol Lett *85*, 159-163.

Chang, A.E., Aruga, A., Cameron, M.J., Sondak, V.K., Normolle, D.P., Fox, B.A., and Shu, S. (1997). Adoptive immunotherapy with vaccine-primed lymph node cells secondarily activated with anti-CD3 and interleukin-2. J Clin Oncol *15*, 796-807.

Chaput, N., Taieb, J., and Zitvogel, L. (2006). [Innate defence against tumor cells: the killer cell IKDC]. Bull Cancer *93*, 449-451.

Chaux, P., Luiten, R., Demotte, N., Vantomme, V., Stroobant, V., Traversari, C., Russo, V., Schultz, E., Cornelis, G.R., Boon, T., *et al.* (1999a). Identification of five MAGE-A1 epitopes recognized by cytolytic T lymphocytes obtained by in vitro stimulation with dendritic cells transduced with MAGE-A1. J Immunol *163*, 2928-2936.

Chaux, P., Vantomme, V., Stroobant, V., Thielemans, K., Corthals, J., Luiten, R., Eggermont, A.M., Boon, T., and van der Bruggen, P. (1999b). Identification of MAGE-3 epitopes presented by HLA-DR molecules to CD4(+) T lymphocytes. J Exp Med *189*, 767-778.

Cheever, M.A., Greenberg, P.D., Fefer, A., and Gillis, S. (1982). Augmentation of the anti-tumor therapeutic efficacy of long-term cultured T lymphocytes by in vivo administration of purified interleukin 2. J Exp Med *155*, 968-980.

Chen, L. (2004). Co-inhibitory molecules of the B7-CD28 family in the control of T-cell immunity. Nat Rev Immunol *4*, 336-347.

Chen, Z., Chen, L., Qiao, S.W., Nagaishi, T., and Blumberg, R.S. (2008). Carcinoembryonic antigen-related cell adhesion molecule 1 inhibits proximal TCR signaling by targeting ZAP-70. J Immunol *180*, 6085-6093.

Chiang, G.G., and Sefton, B.M. (2001). Specific dephosphorylation of the Lck tyrosine protein kinase at Tyr-394 by the SHP-1 protein-tyrosine phosphatase. J Biol Chem *276*, 23173-23178.

Chiba, T., Ohtani, H., Mizoi, T., Naito, Y., Sato, E., Nagura, H., Ohuchi, A., Ohuchi, K., Shiiba, K., Kurokawa, Y., *et al.* (2004). Intraepithelial CD8+ T-cell-count becomes a prognostic factor after a longer follow-up period in human colorectal carcinoma: possible association with suppression of micrometastasis. Br J Cancer *91*, 1711-1717.

Chiba, K., Yanagawa, Y., Masubuchi, Y., Kataoka, H., Kawaguchi, T., Ohtsuki, M., and Hoshino, Y. (1998). FTY720, a novel immunosuppressant, induces sequestration of circulating mature lymphocytes by acceleration of lymphocyte homing in rats. I. FTY720 selectively decreases the number of circulating mature lymphocytes by acceleration of lymphocyte homing. J Immunol *160*, 5037-5044.

Chothia, C., Boswell, D.R., and Lesk, A.M. (1988). The outline structure of the T-cell alpha beta receptor. EMBO J *7*, 3745-3755.

Chu, D.H., Morita, C.T., and Weiss, A. (1998). The Syk family of protein tyrosine kinases in T-cell activation and development. Immunol Rev *165*, 167-180.

Chua, D., Huang, J., Zheng, B., Lau, S.Y., Luk, W., Kwong, D.L., Sham, J.S., Moss, D., Yuen, K.Y., Im, S.W., *et al.* (2001). Adoptive transfer of autologous Epstein-Barr virus-specific cytotoxic T cells for nasopharyngeal carcinoma. Int J Cancer *94*, 73-80.

Ciceri, F., Bonini, C., Marktel, S., Zappone, E., Servida, P., Bernardi, M., Pescarollo, A., Bondanza, A., Peccatori, J., Rossini, S., *et al.* (2007). Antitumor effects of HSV-TK-engineered donor lymphocytes after allogeneic stem-cell transplantation. Blood *109*, 4698-4707.

Cinamon, G., Grabovsky, V., Winter, E., Franitza, S., Feigelson, S., Shamri, R., Dwir, O., and Alon, R. (2001a). Novel chemokine functions in lymphocyte migration through vascular endothelium under shear flow. J Leukoc Biol *69*, 860-866.

Cinamon, G., Shinder, V., and Alon, R. (2001b). Shear forces promote lymphocyte migration across vascular endothelium bearing apical chemokines. Nat Immunol *2*, 515-522.

Comoli, P., De Palma, R., Siena, S., Nocera, A., Basso, S., Del Galdo, F., Schiavo, R., Carminati, O., Tagliamacco, A., Abbate, G.F., *et al.* (2004). Adoptive transfer of allogeneic Epstein-Barr virus (EBV)-specific cytotoxic T cells with in vitro antitumor activity boosts LMP2-specific immune response in a patient with EBV-related nasopharyngeal carcinoma. Ann Oncol *15*, 113-117.

Comoli, P., Labirio, M., Basso, S., Baldanti, F., Grossi, P., Furione, M., Vigano, M., Fiocchi, R., Rossi, G., Ginevri, F., *et al.* (2002). Infusion of autologous Epstein-Barr virus (EBV)-specific cytotoxic T cells for prevention of EBV-related lymphoproliferative disorder in solid organ transplant recipients with evidence of active virus replication. Blood *99*, 2592-2598.

Coudronniere, N., Villalba, M., Englund, N., and Altman, A. (2000). NF-kappa B activation induced by T cell receptor/CD28 costimulation is mediated by protein kinase C-theta. Proc Natl Acad Sci U S A *97*, 3394-3399.

Coukos, G., Benencia, F., Buckanovich, R.J., and Conejo-Garcia, J.R. (2005). The role of dendritic cell precursors in tumour vasculogenesis. Br J Cancer *92*, 1182-1187.

Crabtree, G.R., and Clipstone, N.A. (1994). Signal transmission between the plasma membrane and nucleus of T lymphocytes. Annu Rev Biochem *63*, 1045-1083.

Cramer, D.W., Titus-Ernstoff, L., McKolanis, J.R., Welch, W.R., Vitonis, A.F., Berkowitz, R.S., and Finn, O.J. (2005). Conditions associated with antibodies against the tumor-associated antigen MUC1 and their relationship to risk for ovarian cancer. Cancer Epidemiol Biomarkers Prev *14*, 1125-1131.

Curiel, T.J., Coukos, G., Zou, L., Alvarez, X., Cheng, P., Mottram, P., Evdemon-Hogan, M., Conejo-Garcia, J.R., Zhang, L., Burow, M., *et al.* (2004). Specific recruitment of regulatory T cells in ovarian carcinoma fosters immune privilege and predicts reduced survival. Nat Med *10*, 942-949.

Cyster, J.G., and Goodnow, C.C. (1995). Protein tyrosine phosphatase 1C negatively regulates antigen receptor signaling in B lymphocytes and determines thresholds for negative selection. Immunity *2*, 13-24.

Davis, M.M., and Bjorkman, P.J. (1988). T-cell antigen receptor genes and T-cell recognition. Nature *334*, 395-402.

del Pozo, M.A., Sanchez-Mateos, P., Nieto, M., and Sanchez-Madrid, F. (1995). Chemokines regulate cellular polarization and adhesion receptor redistribution during lymphocyte interaction with endothelium and extracellular matrix. Involvement of cAMP signaling pathway. J Cell Biol *131*, 495-508.

den Boer, A.T., van Mierlo, G.J., Fransen, M.F., Melief, C.J., Offringa, R., and Toes, R.E. (2004). The tumoricidal activity of memory CD8+ T cells is hampered by persistent systemic antigen, but full functional capacity is regained in an antigen-free environment. J Immunol *172*, 6074-6079.

Denu, J.M., Lohse, D.L., Vijayalakshmi, J., Saper, M.A., and Dixon, J.E. (1996). Visualization of intermediate and transition-state structures in protein-tyrosine phosphatase catalysis. Proc Natl Acad Sci U S A *93*, 2493-2498.

Dienz, O., Hehner, S.P., Droge, W., and Schmitz, M.L. (2000). Synergistic activation of NF-kappa B by functional cooperation between vav and PKCtheta in T lymphocytes. J Biol Chem *275*, 24547-24551.

Dietrich, J., Cella, M., and Colonna, M. (2001). Ig-like transcript 2 (ILT2)/leukocyte Ig-like receptor 1 (LIR1) inhibits TCR signaling and actin cytoskeleton reorganization. J Immunol *166*, 2514-2521.

Dixon, J.E. (1995). Structure and catalytic properties of protein tyrosine phosphatases. Ann N Y Acad Sci *766*, 18-22.

Dohi, T., Beltrami, E., Wall, N.R., Plescia, J., and Altieri, D.C. (2004). Mitochondrial survivin inhibits apoptosis and promotes tumorigenesis. J Clin Invest *114*, 1117-1127.

Dornan, S., Sebestyen, Z., Gamble, J., Nagy, P., Bodnar, A., Alldridge, L., Doe, S., Holmes, N., Goff, L.K., Beverley, P., *et al.* (2002). Differential association of CD45 isoforms with CD4 and CD8 regulates the actions of specific pools of p56lck tyrosine kinase in T cell antigen receptor signal transduction. J Biol Chem *277*, 1912-1918.

Dreno, B., Nguyen, J.M., Khammari, A., Pandolfino, M.C., Tessier, M.H., Bercegeay, S., Cassidanius, A., Lemarre, P., Billaudel, S., Labarriere, N., *et al.* (2002). Randomized trial of adoptive transfer of melanoma tumor-infiltrating lymphocytes as adjuvant therapy for stage III melanoma. Cancer Immunol Immunother *51*, 539-546.

Dudley, M.E., Wunderlich, J.R., Robbins, P.F., Yang, J.C., Hwu, P., Schwartzentruber, D.J., Topalian, S.L., Sherry, R., Restifo, N.P., Hubicki, A.M., *et al.* (2002a). Cancer regression and autoimmunity in patients after clonal repopulation with antitumor lymphocytes. Science *298*, 850-854.

Dudley, M.E., Wunderlich, J.R., Shelton, T.E., Even, J., and Rosenberg, S.A. (2003). Generation of tumor-infiltrating lymphocyte cultures for use in adoptive transfer therapy for melanoma patients. J Immunother *26*, 332-342.

Dudley, M.E., Wunderlich, J.R., Yang, J.C., Hwu, P., Schwartzentruber, D.J., Topalian, S.L., Sherry, R.M., Marincola, F.M., Leitman, S.F., Seipp, C.A., *et al.* (2002b). A phase I study of nonmyeloablative chemotherapy and adoptive transfer of autologous tumor antigen-specific T lymphocytes in patients with metastatic melanoma. J Immunother *25*, 243-251.

Dudley, M.E., Wunderlich, J.R., Yang, J.C., Sherry, R.M., Topalian, S.L., Restifo, N.P., Royal, R.E., Kammula, U., White, D.E., Mavroukakis, S.A., *et al.* (2005). Adoptive cell transfer therapy following non-myeloablative but lymphodepleting chemotherapy for the treatment of patients with refractory metastatic melanoma. J Clin Oncol *23*, 2346-2357.

Dunn, G.P., Old, L.J., and Schreiber, R.D. (2004a). The immunobiology of cancer immunosurveillance and immunoediting. Immunity *21*, 137-148.

Dunn, G.P., Old, L.J., and Schreiber, R.D. (2004b). The three Es of cancer immunoediting. Annu Rev Immunol *22*, 329-360.

Dustin, L.B., Plas, D.R., Wong, J., Hu, Y.T., Soto, C., Chan, A.C., and Thomas, M.L. (1999). Expression of dominant-negative src-homology domain 2-containing protein tyrosine phosphatase-1 results in increased Syk tyrosine kinase activity and B cell activation. J Immunol *162*, 2717-2724.

Dustin, M.L., Bromley, S.K., Kan, Z., Peterson, D.A., and Unanue, E.R. (1997). Antigen receptor engagement delivers a stop signal to migrating T lymphocytes. Proc Natl Acad Sci U S A *94*, 3909-3913.

Dustin, M.L., and Chan, A.C. (2000). Signaling takes shape in the immune system. Cell *103*, 283-294.

Dustin, M.L., and Cooper, J.A. (2000). The immunological synapse and the actin cytoskeleton: molecular hardware for T cell signaling. Nat Immunol *1*, 23-29.

Dutcher, J.P., Creekmore, S., Weiss, G.R., Margolin, K., Markowitz, A.B., Roper, M., Parkinson, D., Ciobanu, N., Fisher, R.I., Boldt, D.H., *et al.* (1989). A phase II study of interleukin-2 and lymphokine-activated killer cells in patients with metastatic malignant melanoma. J Clin Oncol *7*, 477-485.

Dutoit, V., Guillaume, P., Romero, P., Cerottini, J.C., and Valmori, D. (2002). Functional analysis of HLA-A*0201/Melan-A peptide multimer+ CD8+ T cells isolated from an HLA-A*0201- donor: exploring tumor antigen allorestricted recognition. Cancer Immun *2*, 7.

Ebinu, J.O., Bottorff, D.A., Chan, E.Y., Stang, S.L., Dunn, R.J., and Stone, J.C. (1998). RasGRP, a Ras guanyl nucleotide- releasing protein with calcium- and diacylglycerol-binding motifs. Science *280*, 1082-1086.

Elbashir, S.M., Harborth, J., Lendeckel, W., Yalcin, A., Weber, K., and Tuschl, T. (2001a). Duplexes of 21-nucleotide RNAs mediate RNA interference in cultured mammalian cells. Nature *411*, 494-498.

Elbashir, S.M., Lendeckel, W., and Tuschl, T. (2001b). RNA interference is mediated by 21- and 22-nucleotide RNAs. Genes Dev *15*, 188-200.

Engel, A.M., Svane, I.M., Rygaard, J., and Werdelin, O. (1997). MCA sarcomas induced in scid mice are more immunogenic than MCA sarcomas induced in congenic, immunocompetent mice. Scand J Immunol *45*, 463-470.

Evans, L.S., Witte, P.R., Feldhaus, A.L., Nelson, B.H., Riddell, S.R., Greenberg, P.D., Lupton, S.D., and Jones, L.A. (1999). Expression of chimeric granulocyte-macrophage colony-stimulating factor/interleukin 2 receptors in human cytotoxic T lymphocyte clones results in granulocyte-macrophage colony-stimulating factor-dependent growth. Hum Gene Ther *10*, 1941-1951.

Fawcett, V.C., and Lorenz, U. (2005). Localization of Src homology 2 domain-containing phosphatase 1 (SHP-1) to lipid rafts in T lymphocytes: functional implications and a role for the SHP-1 carboxyl terminus. J Immunol *174*, 2849-2859.

Fields, B.A., Ober, B., Malchiodi, E.L., Lebedeva, M.I., Braden, B.C., Ysern, X., Kim, J.K., Shao, X., Ward, E.S., and Mariuzza, R.A. (1995). Crystal structure of the V alpha domain of a T cell antigen receptor. Science *270*, 1821-1824.

Figlin, R.A., Thompson, J.A., Bukowski, R.M., Vogelzang, N.J., Novick, A.C., Lange, P., Steinberg, G.D., and Belldegrun, A.S. (1999). Multicenter, randomized, phase III trial of CD8(+) tumor-infiltrating lymphocytes in combination with recombinant interleukin-2 in metastatic renal cell carcinoma. J Clin Oncol *17*, 2521-2529.

Filaci, G., Fenoglio, D., Fravega, M., Ansaldo, G., Borgonovo, G., Traverso, P., Villaggio, B., Ferrera, A., Kunkl, A., Rizzi, M., *et al.* (2007). CD8+ CD28- T regulatory lymphocytes inhibiting T cell proliferative and cytotoxic functions infiltrate human cancers. J Immunol *179*, 4323-4334.

Fire, A., Albertson, D., Harrison, S.W., and Moerman, D.G. (1991). Production of antisense RNA leads to effective and specific inhibition of gene expression in C. elegans muscle. Development *113*, 503-514.

Fire, A., Xu, S., Montgomery, M.K., Kostas, S.A., Driver, S.E., and Mello, C.C. (1998). Potent and specific genetic interference by double-stranded RNA in Caenorhabditis elegans. Nature *391*, 806-811.

Fischer, E.H., Charbonneau, H., and Tonks, N.K. (1991). Protein tyrosine phosphatases: a diverse family of intracellular and transmembrane enzymes. Science *253*, 401-406.

Frank, C., Keilhack, H., Opitz, F., Zschornig, O., and Bohmer, F.D. (1999). Binding of phosphatidic acid to the protein-tyrosine phosphatase SHP-1 as a basis for activity modulation. Biochemistry *38*, 11993-12002.

Fraser, J.D., Straus, D., and Weiss, A. (1993). Signal transduction events leading to T-cell lymphokine gene expression. Immunol Today *14*, 357-362.

Fuller, M.J., Khanolkar, A., Tebo, A.E., and Zajac, A.J. (2004). Maintenance, loss, and resurgence of T cell responses during acute, protracted, and chronic viral infections. J Immunol *172*, 4204-4214.

Fuse, Y., Nishimura, H., Maeda, K., and Yoshikai, Y. (1997). CD95 (Fas) may control the expansion of activated T cells after elimination of bacteria in murine listeriosis. Infect Immun *65*, 1883-1891.

Galon, J., Costes, A., Sanchez-Cabo, F., Kirilovsky, A., Mlecnik, B., Lagorce-Pages, C., Tosolini, M., Camus, M., Berger, A., Wind, P., *et al.* (2006). Type, density, and location of immune cells within human colorectal tumors predict clinical outcome. Science *313*, 1960-1964.

Gao, L., Xue, S.A., Hasserjian, R., Cotter, F., Kaeda, J., Goldman, J.M., Dazzi, F., and Stauss, H.J. (2003a). Human cytotoxic T lymphocytes specific for Wilms' tumor antigen-1 inhibit engraftment of leukemia-initiating stem cells in non-obese diabetic-severe combined immunodeficient recipients. Transplantation *75*, 1429-1436.

Gao, Y., Yang, W., Pan, M., Scully, E., Girardi, M., Augenlicht, L.H., Craft, J., and Yin, Z. (2003b). Gamma delta T cells provide an early source of interferon gamma in tumor immunity. J Exp Med *198*, 433-442.

Garboczi, D.N., Ghosh, P., Utz, U., Fan, Q.R., Biddison, W.E., and Wiley, D.C. (1996). Structure of the complex between human T-cell receptor, viral peptide and HLA-A2. Nature *384*, 134-141.

Garcia, K.C., Degano, M., Speir, J.A., and Wilson, I.A. (1999). Emerging principles for T cell receptor recognition of antigen in cellular immunity. Rev Immunogenet *1*, 75-90.

Garcia, K.C., Degano, M., Stanfield, R.L., Brunmark, A., Jackson, M.R., Peterson, P.A., Teyton, L., and Wilson, I.A. (1996). An alphabeta T cell receptor structure at 2.5 A and its orientation in the TCR-MHC complex. Science *274*, 209-219.

Garland, S.M., Hernandez-Avila, M., Wheeler, C.M., Perez, G., Harper, D.M., Leodolter, S., Tang, G.W., Ferris, D.G., Steben, M., Bryan, J., *et al.* (2007). Quadrivalent vaccine against human papillomavirus to prevent anogenital diseases. N Engl J Med *356*, 1928-1943.

Garton, A.J., Flint, A.J., and Tonks, N.K. (1996). Identification of p130(cas) as a substrate for the cytosolic protein tyrosine phosphatase PTP-PEST. Mol Cell Biol *16*, 6408-6418.

Gattinoni, L., Klebanoff, C.A., Palmer, D.C., Wrzesinski, C., Kerstann, K., Yu, Z., Finkelstein, S.E., Theoret, M.R., Rosenberg, S.A., and Restifo, N.P. (2005). Acquisition of full effector function in vitro paradoxically impairs the in vivo antitumor efficacy of adoptively transferred CD8+ T cells. J Clin Invest *115*, 1616-1626.

Gauss, G.H., and Lieber, M.R. (1996). Mechanistic constraints on diversity in human V(D)J recombination. Mol Cell Biol *16*, 258-269.

Gebert, A., Goke, M., Rothkotter, H.J., and Dietrich, C.F. (2000). [The mechanisms of antigen uptake in the small and large intestines: the roll of the M cells for the initiation of immune responses]. Z Gastroenterol *38*, 855-872.

Ghiringhelli, F., Menard, C., Terme, M., Flament, C., Taieb, J., Chaput, N., Puig, P.E., Novault, S., Escudier, B., Vivier, E., *et al.* (2005a). CD4+CD25+ regulatory T cells inhibit natural killer cell functions in a transforming growth factor-beta-dependent manner. J Exp Med *202*, 1075-1085.

Ghiringhelli, F., Puig, P.E., Roux, S., Parcellier, A., Schmitt, E., Solary, E., Kroemer, G., Martin, F., Chauffert, B., and Zitvogel, L. (2005b). Tumor cells convert immature myeloid dendritic cells into TGF-beta-secreting cells inducing CD4+CD25+ regulatory T cell proliferation. J Exp Med *202*, 919-929.

Gilboa, E. (1999). The makings of a tumor rejection antigen. Immunity *11*, 263-270.

Girard, J.P., and Springer, T.A. (1995). High endothelial venules (HEVs): specialized endothelium for lymphocyte migration. Immunol Today *16*, 449-457.

Girardi, M., Glusac, E., Filler, R.B., Roberts, S.J., Propperova, I., Lewis, J., Tigelaar, R.E., and Hayday, A.C. (2003). The distinct contributions of murine T cell receptor (TCR)gammadelta+ and TCRalphabeta+ T cells to different stages of chemically induced skin cancer. J Exp Med *198*, 747-755.

Girardi, M., Oppenheim, D.E., Steele, C.R., Lewis, J.M., Glusac, E., Filler, R., Hobby, P., Sutton, B., Tigelaar, R.E., and Hayday, A.C. (2001). Regulation of cutaneous malignancy by gammadelta T cells. Science *294*, 605-609.

Goldrath, A.W., Sivakumar, P.V., Glaccum, M., Kennedy, M.K., Bevan, M.J., Benoist, C., Mathis, D., and Butz, E.A. (2002). Cytokine requirements for acute and Basal homeostatic proliferation of naive and memory CD8+ T cells. J Exp Med *195*, 1515-1522.

Gowans, J.L., and Knight, E.J. (1964). The Route of Re-Circulation of Lymphocytes in the Rat. Proc R Soc Lond B Biol Sci *159*, 257-282.

Grawunder, U., West, R.B., and Lieber, M.R. (1998). Antigen receptor gene rearrangement. Curr Opin Immunol *10*, 172-180.

Green, M.C., and Shultz, L.D. (1975). Motheaten, an immunodeficient mutant of the mouse. I. Genetics and pathology. J Hered *66*, 250-258.

Guiducci, C., Vicari, A.P., Sangaletti, S., Trinchieri, G., and Colombo, M.P. (2005). Redirecting in vivo elicited tumor infiltrating macrophages and dendritic cells towards tumor rejection. Cancer Res *65*, 3437-3446.

Gunn, M.D., Tangemann, K., Tam, C., Cyster, J.G., Rosen, S.D., and Williams, L.T. (1998). A chemokine expressed in lymphoid high endothelial venules promotes the adhesion and chemotaxis of naive T lymphocytes. Proc Natl Acad Sci U S A *95*, 258-263.

Hacein-Bey-Abina, S., von Kalle, C., Schmidt, M., Le Deist, F., Wulffraat, N., McIntyre, E., Radford, I., Villeval, J.L., Fraser, C.C., Cavazzana-Calvo, M., *et al.* (2003). A serious adverse event after successful gene therapy for X-linked severe combined immunodeficiency. N Engl J Med *348*, 255-256.

Hamilton, A.J., and Baulcombe, D.C. (1999). A species of small antisense RNA in posttranscriptional gene silencing in plants. Science *286*, 950-952.

Han, J., Das, B., Wei, W., Van Aelst, L., Mosteller, R.D., Khosravi-Far, R., Westwick, J.K., Der, C.J., and Broek, D. (1997). Lck regulates Vav activation of members of the Rho family of GTPases. Mol Cell Biol *17*, 1346-1353.

Hanahan, D., and Weinberg, R.A. (2000). The hallmarks of cancer. Cell *100*, 57-70.
Heath, W.R., and Carbone, F.R. (1999). Cytotoxic T lymphocyte activation by cross-priming. Curr Opin Immunol *11*, 314-318.

Hendrickson, B.A., Gokhale, R., and Cho, J.H. (2002). Clinical aspects and pathophysiology of inflammatory bowel disease. Clin Microbiol Rev *15*, 79-94.

Hernandez, M.G., Shen, L., and Rock, K.L. (2007). CD40-CD40 ligand interaction between dendritic cells and CD8+ T cells is needed to stimulate maximal T cell responses in the absence of CD4+ T cell help. J Immunol *178*, 2844-2852.

Heslop, H.E., Brenner, M.K., and Rooney, C.M. (1994). Donor T cells to treat EBV-associated lymphoma. N Engl J Med *331*, 679-680.

Heslop, H.E., and Rooney, C.M. (1997). Adoptive cellular immunotherapy for EBV lymphoproliferative disease. Immunol Rev *157*, 217-222.

Hicks, A.M., Riedlinger, G., Willingham, M.C., Alexander-Miller, M.A., Von Kap-Herr, C., Pettenati, M.J., Sanders, A.M., Weir, H.M., Du, W., Kim, J., *et al.* (2006a). Transferable anticancer innate immunity in spontaneous regression/complete resistance mice. Proc Natl Acad Sci U S A *103*, 7753-7758.

Hicks, A.M., Willingham, M.C., Du, W., Pang, C.S., Old, L.J., and Cui, Z. (2006b). Effector mechanisms of the anti-cancer immune responses of macrophages in SR/CR mice. Cancer Immun *6*, 11.

Hieshima, K., Ohtani, H., Shibano, M., Izawa, D., Nakayama, T., Kawasaki, Y., Shiba, F., Shiota, M., Katou, F., Saito, T., *et al.* (2003). CCL28 has dual roles in mucosal immunity as a chemokine with broad-spectrum antimicrobial activity. J Immunol *170*, 1452-1461.

Hiltbold, E.M., and Roche, P.A. (2002). Trafficking of MHC class II molecules in the late secretory pathway. Curr Opin Immunol *14*, 30-35.

Hof, P., Pluskey, S., Dhe-Paganon, S., Eck, M.J., and Shoelson, S.E. (1998). Crystal structure of the tyrosine phosphatase SHP-2. Cell *92*, 441-450.

Hogquist, K.A., Tomlinson, A.J., Kieper, W.C., McGargill, M.A., Hart, M.C., Naylor, S., and Jameson, S.C. (1997). Identification of a naturally occurring ligand for thymic positive selection. Immunity *6*, 389-399.

Hollenbeak, C.S., Todd, M.M., Billingsley, E.M., Harper, G., Dyer, A.M., and Lengerich, E.J. (2005). Increased incidence of melanoma in renal transplantation recipients. Cancer *104*, 1962-1967.

Homey, B., Alenius, H., Muller, A., Soto, H., Bowman, E.P., Yuan, W., McEvoy, L., Lauerma, A.I., Assmann, T., Bunemann, E., *et al.* (2002). CCL27-CCR10 interactions regulate T cell-mediated skin inflammation. Nat Med *8*, 157-165.

Horvat, A., Schwaiger, F., Hager, G., Brocker, F., Streif, R., Knyazev, P., Ullrich, A., and Kreutzberg, G.W. (2001). A novel role for protein tyrosine phosphatase shp1 in controlling glial activation in the normal and injured nervous system. J Neurosci *21*, 865-874.

Hou, S., Hyland, L., Ryan, K.W., Portner, A., and Doherty, P.C. (1994). Virus-specific CD8+ T-cell memory determined by clonal burst size. Nature *369*, 652-654.

Hsi, E.D., Siegel, J.N., Minami, Y., Luong, E.T., Klausner, R.D., and Samelson, L.E. (1989). T cell activation induces rapid tyrosine phosphorylation of a limited number of cellular substrates. J Biol Chem *264*, 10836-10842.

Huster, K.M., Busch, V., Schiemann, M., Linkemann, K., Kerksiek, K.M., Wagner, H., and Busch, D.H. (2004). Selective expression of IL-7 receptor on memory T cells identifies early CD40L-dependent generation of distinct CD8+ memory T cell subsets. Proc Natl Acad Sci U S A *101*, 5610-5615.

Ichii, H., Sakamoto, A., Hatano, M., Okada, S., Toyama, H., Taki, S., Arima, M., Kuroda, Y., and Tokuhisa, T. (2002). Role for Bcl-6 in the generation and maintenance of memory CD8+ T cells. Nat Immunol *3*, 558-563.

Ichii, H., Sakamoto, A., Kuroda, Y., and Tokuhisa, T. (2004). Bcl6 acts as an amplifier for the generation and proliferative capacity of central memory CD8+ T cells. J Immunol *173*, 883-891.

Intlekofer, A.M., Takemoto, N., Wherry, E.J., Longworth, S.A., Northrup, J.T., Palanivel, V.R., Mullen, A.C., Gasink, C.R., Kaech, S.M., Miller, J.D., *et al.* (2005). Effector and memory CD8+ T cell fate coupled by T-bet and eomesodermin. Nat Immunol *6*, 1236-1244.

Itano, A., Kioussis, D., and Robey, E. (1994). Stochastic component to development of class I major histocompatibility complex-specific T cells. Proc Natl Acad Sci U S A *91*, 220-224.

Iyoda, T., Shimoyama, S., Liu, K., Omatsu, Y., Akiyama, Y., Maeda, Y., Takahara, K., Steinman, R.M., and Inaba, K. (2002). The CD8+ dendritic cell subset selectively endocytoses dying cells in culture and in vivo. J Exp Med *195*, 1289-1302.

Jaeger, E., Bernhard, H., Romero, P., Ringhoffer, M., Arand, M., Karbach, J., Ilsemann, C., Hagedorn, M., and Knuth, A. (1996). Generation of cytotoxic T-cell responses with synthetic melanoma-associated peptides in vivo: implications for tumor vaccines with melanoma-associated antigens. Int J Cancer *66*, 162-169.

Janssen, E.M., Droin, N.M., Lemmens, E.E., Pinkoski, M.J., Bensinger, S.J., Ehst, B.D., Griffith, T.S., Green, D.R., and Schoenberger, S.P. (2005). CD4+ T-cell help controls CD8+ T-cell memory via TRAIL-mediated activation-induced cell death. Nature *434*, 88-93.

Janssen, E.M., Lemmens, E.E., Wolfe, T., Christen, U., von Herrath, M.G., and Schoenberger, S.P. (2003). CD4+ T cells are required for secondary expansion and memory in CD8+ T lymphocytes. Nature *421*, 852-856.

Jensen, P., Hansen, S., Moller, B., Leivestad, T., Pfeffer, P., Geiran, O., Fauchald, P., and Simonsen, S. (1999). Skin cancer in kidney and heart transplant recipients and different long-term immunosuppressive therapy regimens. J Am Acad Dermatol *40*, 177-186.

Jiao, H., Yang, W., Berrada, K., Tabrizi, M., Shultz, L., and Yi, T. (1997). Macrophages from motheaten and viable motheaten mutant mice show increased proliferative responses to GM-CSF: detection of potential HCP substrates in GM-CSF signal transduction. Exp Hematol *25*, 592-600.

Johnson, K.G., LeRoy, F.G., Borysiewicz, L.K., and Matthews, R.J. (1999). TCR signaling thresholds regulating T cell development and activation are dependent upon SHP-1. J Immunol *162*, 3802-3813.

Jotereau, F., Pandolfino, M.C., Boudart, D., Diez, E., Dreno, B., Douillard, J.Y., Muller, J.Y., and LeMevel, B. (1991). High-fold expansion of human cytotoxic T-lymphocytes specific for autologous melanoma cells for use in immunotherapy. J Immunother (1991) *10*, 405-411.

Kabat, J., Borrego, F., Brooks, A., and Coligan, J.E. (2002). Role that each NKG2A immunoreceptor tyrosine-based inhibitory motif plays in mediating the human CD94/NKG2A inhibitory signal. J Immunol *169*, 1948-1958.

Kaech, S.M., Tan, J.T., Wherry, E.J., Konieczny, B.T., Surh, C.D., and Ahmed, R. (2003). Selective expression of the interleukin 7 receptor identifies effector CD8 T cells that give rise to long-lived memory cells. Nat Immunol *4*, 1191-1198.

Kane, L.P., Andres, P.G., Howland, K.C., Abbas, A.K., and Weiss, A. (2001). Akt provides the CD28 costimulatory signal for up-regulation of IL-2 and IFN-gamma but not TH2 cytokines. Nat Immunol *2*, 37-44.

Karin, M., and Ben-Neriah, Y. (2000). Phosphorylation meets ubiquitination: the control of NF-[kappa]B activity. Annu Rev Immunol *18*, 621-663.

Kavanaugh, W.M., Turck, C.W., and Williams, L.T. (1995). PTB domain binding to signaling proteins through a sequence motif containing phosphotyrosine. Science *268*, 1177-1179.

Kawakami, Y., Eliyahu, S., Jennings, C., Sakaguchi, K., Kang, X., Southwood, S., Robbins, P.F., Sette, A., Appella, E., and Rosenberg, S.A. (1995). Recognition of multiple epitopes in the human melanoma antigen gp100 by tumor-infiltrating T lymphocytes associated with in vivo tumor regression. J Immunol *154*, 3961-3968.

Keir, M.E., Butte, M.J., Freeman, G.J., and Sharpe, A.H. (2008). PD-1 and its ligands in tolerance and immunity. Annu Rev Immunol *26*, 677-704.

Kershaw, M.H., Darcy, P.K., Hulett, M.D., Hogarth, P.M., Trapani, J.A., and Smyth, M.J. (1996a). Redirected cytotoxic effector function. Requirements for expression of chimeric single chain high affinity immunoglobulin e receptors. J Biol Chem *271*, 21214-21220.

Kershaw, M.H., Darcy, P.K., Trapani, J.A., and Smyth, M.J. (1996b). The use of chimeric human Fc(epsilon) receptor I to redirect cytotoxic T lymphocytes to tumors. J Leukoc Biol *60*, 721-728.

Kershaw, M.H., Westwood, J.A., Parker, L.L., Wang, G., Eshhar, Z., Mavroukakis, S.A., White, D.E., Wunderlich, J.R., Canevari, S., Rogers-Freezer, L., *et al.* (2006). A phase I study on adoptive immunotherapy using gene-modified T cells for ovarian cancer. Clin Cancer Res *12*, 6106-6115.

Khanna, R., Bell, S., Sherritt, M., Galbraith, A., Burrows, S.R., Rafter, L., Clarke, B., Slaughter, R., Falk, M.C., Douglass, J., *et al.* (1999). Activation and adoptive transfer of Epstein-Barr virus-specific cytotoxic T cells in solid organ transplant patients with posttransplant lymphoproliferative disease. Proc Natl Acad Sci U S A *96*, 10391-10396.

Khvorova, A., Reynolds, A., and Jayasena, S.D. (2003). Functional siRNAs and miRNAs exhibit strand bias. Cell *115*, 209-216.

Kieper, W.C., Tan, J.T., Bondi-Boyd, B., Gapin, L., Sprent, J., Ceredig, R., and Surh, C.D. (2002). Overexpression of interleukin (IL)-7 leads to IL-15-independent generation of memory phenotype CD8+ T cells. J Exp Med *195*, 1533-1539.

Kim, C.H., Qu, C.K., Hangoc, G., Cooper, S., Anzai, N., Feng, G.S., and Broxmeyer, H.E. (1999). Abnormal chemokine-induced responses of immature and mature hematopoietic cells from motheaten mice implicate the protein tyrosine phosphatase SHP-1 in chemokine responses. J Exp Med *190*, 681-690.

Kim, J.A., Averbook, B.J., Chambers, K., Rothchild, K., Kjaergaard, J., Papay, R., and Shu, S. (2001). Divergent effects of 4-1BB antibodies on antitumor immunity and on tumor-reactive T-cell generation. Cancer Res *61*, 2031-2037.

Kishimoto, H., and Sprent, J. (1997). Negative selection in the thymus includes semimature T cells. J Exp Med *185*, 263-271.

Klebanoff, C.A., Finkelstein, S.E., Surman, D.R., Lichtman, M.K., Gattinoni, L., Theoret, M.R., Grewal, N., Spiess, P.J., Antony, P.A., Palmer, D.C., *et al.* (2004). IL-15 enhances the in vivo antitumor activity of tumor-reactive CD8+ T cells. Proc Natl Acad Sci U S A *101*, 1969-1974.

Klebanoff, C.A., Gattinoni, L., Torabi-Parizi, P., Kerstann, K., Cardones, A.R., Finkelstein, S.E., Palmer, D.C., Antony, P.A., Hwang, S.T., Rosenberg, S.A., *et al.* (2005). Central memory self/tumor-reactive CD8+ T cells confer superior antitumor immunity compared with effector memory T cells. Proc Natl Acad Sci U S A *102*, 9571-9576.

Koebel, C.M., Vermi, W., Swann, J.B., Zerafa, N., Rodig, S.J., Old, L.J., Smyth, M.J., and Schreiber, R.D. (2007). Adaptive immunity maintains occult cancer in an equilibrium state. Nature *450*, 903-907.

Koegl, M., Zlatkine, P., Ley, S.C., Courtneidge, S.A., and Magee, A.I. (1994). Palmitoylation of multiple Src-family kinases at a homologous N-terminal motif. Biochem J *303 (Pt 3)*, 749-753.

Konig, R. (2002). Interactions between MHC molecules and co-receptors of the TCR. Curr Opin Immunol *14*, 75-83.

Kontoyiannis, D., Boulougouris, G., Manoloukos, M., Armaka, M., Apostolaki, M., Pizarro, T., Kotlyarov, A., Forster, I., Flavell, R., Gaestel, M., *et al.* (2002). Genetic dissection of the cellular pathways and signaling mechanisms in modeled tumor necrosis factor-induced Crohn's-like inflammatory bowel disease. J Exp Med *196*, 1563-1574.

Krause, A., Guo, H.F., Latouche, J.B., Tan, C., Cheung, N.K., and Sadelain, M. (1998). Antigen-dependent CD28 signaling selectively enhances survival and proliferation in genetically modified activated human primary T lymphocytes. J Exp Med *188*, 619-626.

Kruger, J., Butler, J.R., Cherapanov, V., Dong, Q., Ginzberg, H., Govindarajan, A., Grinstein, S., Siminovitch, K.A., and Downey, G.P. (2000). Deficiency of Src homology 2-containing phosphatase 1 results in abnormalities in murine neutrophil function: studies in motheaten mice. J Immunol *165*, 5847-5859.

Kruisbeek, A.M. (1993). Development of alpha beta T cells. Curr Opin Immunol *5*, 227-234.

Ku, C.C., Murakami, M., Sakamoto, A., Kappler, J., and Marrack, P. (2000). Control of homeostasis of CD8+ memory T cells by opposing cytokines. Science *288*, 675-678.

Kucik, D.F., Dustin, M.L., Miller, J.M., and Brown, E.J. (1996). Adhesion-activating phorbol ester increases the mobility of leukocyte integrin LFA-1 in cultured lymphocytes. J Clin Invest *97*, 2139-2144.

Kyriakis, J.M., App, H., Zhang, X.F., Banerjee, P., Brautigan, D.L., Rapp, U.R., and Avruch, J. (1992). Raf-1 activates MAP kinase-kinase. Nature *358*, 417-421.

Lamers, C.H., van Elzakker, P., Langeveld, S.C., Sleijfer, S., and Gratama, J.W. (2006). Process validation and clinical evaluation of a protocol to generate gene-modified T lymphocytes for imunogene therapy for metastatic renal cell carcinoma: GMP-controlled transduction and expansion of patient's T lymphocytes using a carboxy anhydrase IX-specific scFv transgene. Cytotherapy *8*, 542-553.

Lankat-Buttgereit, B., and Tampe, R. (2002). The transporter associated with antigen processing: function and implications in human diseases. Physiol Rev *82*, 187-204.

Laport, G.G., Levine, B.L., Stadtmauer, E.A., Schuster, S.J., Luger, S.M., Grupp, S., Bunin, N., Strobl, F.J., Cotte, J., Zheng, Z., *et al.* (2003). Adoptive transfer of costimulated T cells induces lymphocytosis in patients with relapsed/refractory non-Hodgkin lymphoma following CD34+-selected hematopoietic cell transplantation. Blood *102*, 2004-2013.

Lechleider, R.J., Sugimoto, S., Bennett, A.M., Kashishian, A.S., Cooper, J.A., Shoelson, S.E., Walsh, C.T., and Neel, B.G. (1993). Activation of the SH2-containing phosphotyrosine phosphatase SH-PTP2 by its binding site, phosphotyrosine 1009, on the human platelet-derived growth factor receptor. J Biol Chem *268*, 21478-21481.

Legha, S.S., Gianan, M.A., Plager, C., Eton, O.E., and Papadopoulous, N.E. (1996). Evaluation of interleukin-2 administered by continuous infusion in patients with metastatic melanoma. Cancer *77*, 89-96.

Lenschow, D.J., Walunas, T.L., and Bluestone, J.A. (1996). CD28/B7 system of T cell costimulation. Annu Rev Immunol *14*, 233-258.

Leppert, D., Waubant, E., Galardy, R., Bunnett, N.W., and Hauser, S.L. (1995). T cell gelatinases mediate basement membrane transmigration in vitro. J Immunol *154*, 4379-4389.

Lesinski, G.B., Anghelina, M., Zimmerer, J., Bakalakos, T., Badgwell, B., Parihar, R., Hu, Y., Becknell, B., Abood, G., Chaudhury, A.R., *et al.* (2003). The antitumor effects of IFN-alpha are abrogated in a STAT1-deficient mouse. J Clin Invest *112*, 170-180.

Li, B., Ding, J., Larson, A., and Song, S. (1999). Tumor tissue recycling--a new combination treatment for solid tumors: experimental and preliminary clinical research. In Vivo *13*, 433-438.

Li, L., and Dixon, J.E. (2000). Form, function, and regulation of protein tyrosine phosphatases and their involvement in human diseases. Semin Immunol *12*, 75-84.

Li, Y., Bleakley, M., and Yee, C. (2005). IL-21 influences the frequency, phenotype, and affinity of the antigen-specific CD8 T cell response. J Immunol *175*, 2261-2269.

Li, Z., Menoret, A., and Srivastava, P. (2002). Roles of heat-shock proteins in antigen presentation and cross-presentation. Curr Opin Immunol *14*, 45-51.

Lin, C.L., Suri, R.M., Rahdon, R.A., Austyn, J.M., and Roake, J.A. (1998). Dendritic cell chemotaxis and transendothelial migration are induced by distinct chemokines and are regulated on maturation. Eur J Immunol *28*, 4114-4122.

Lin, C.M., and Wang, F.H. (2002). Selective modification of antigen-specific CD4(+) T cells by retroviral-mediated gene transfer and in vitro sensitization with dendritic cells. Clin Immunol *104*, 58-66.

Loeser, S., Loser, K., Bijker, M.S., Rangachari, M., van der Burg, S.H., Wada, T., Beissert, S., Melief, C.J., and Penninger, J.M. (2007). Spontaneous tumor rejection by cbl-b-deficient CD8+ T cells. J Exp Med *204*, 879-891.

Long, E.O. (1999). Regulation of immune responses through inhibitory receptors. Annu Rev Immunol *17*, 875-904.

Lorenz, U., Ravichandran, K.S., Burakoff, S.J., and Neel, B.G. (1996). Lack of SHPTP1 results in src-family kinase hyperactivation and thymocyte hyperresponsiveness. Proc Natl Acad Sci U S A *93*, 9624-9629.

Loskog, A., Giandomenico, V., Rossig, C., Pule, M., Dotti, G., and Brenner, M.K. (2006). Addition of the CD28 signaling domain to chimeric T-cell receptors enhances chimeric T-cell resistance to T regulatory cells. Leukemia *20*, 1819-1828.

Lou, Z., Jevremovic, D., Billadeau, D.D., and Leibson, P.J. (2000). A balance between positive and negative signals in cytotoxic lymphocytes regulates the polarization of lipid rafts during the development of cell-mediated killing. J Exp Med *191*, 347-354.

Lowe, S.W., Cepero, E., and Evan, G. (2004). Intrinsic tumour suppression. Nature *432*, 307-315.

Lucas, K.G., Salzman, D., Garcia, A., and Sun, Q. (2004). Adoptive immunotherapy with allogeneic Epstein-Barr virus (EBV)-specific cytotoxic T-lymphocytes for recurrent, EBV-positive Hodgkin disease. Cancer *100*, 1892-1901.

Luckey, C.J., Bhattacharya, D., Goldrath, A.W., Weissman, I.L., Benoist, C., and Mathis, D. (2006). Memory T and memory B cells share a transcriptional program of self-renewal with long-term hematopoietic stem cells. Proc Natl Acad Sci U S A *103*, 3304-3309.

Luther, S.A., Bidgol, A., Hargreaves, D.C., Schmidt, A., Xu, Y., Paniyadi, J., Matloubian, M., and Cyster, J.G. (2002). Differing activities of homeostatic chemokines CCL19, CCL21, and CXCL12 in lymphocyte and dendritic cell recruitment and lymphoid neogenesis. J Immunol *169*, 424-433.

Lutz, M.B., Kukutsch, N.A., Menges, M., Rossner, S., and Schuler, G. (2000). Culture of bone marrow cells in GM-CSF plus high doses of lipopolysaccharide generates exclusively immature dendritic cells which induce alloantigen-specific CD4 T cell anergy in vitro. Eur J Immunol *30*, 1048-1052.

Mackensen, A., Meidenbauer, N., Vogl, S., Laumer, M., Berger, J., and Andreesen, R. (2006). Phase I study of adoptive T-cell therapy using antigen-specific CD8+ T cells for the treatment of patients with metastatic melanoma. J Clin Oncol *24*, 5060-5069.

MacKie, R.M., Reid, R., and Junor, B. (2003). Fatal melanoma transferred in a donated kidney 16 years after melanoma surgery. N Engl J Med *348*, 567-568.

Madden, D.R., Garboczi, D.N., and Wiley, D.C. (1993). The antigenic identity of peptide-MHC complexes: a comparison of the conformations of five viral peptides presented by HLA-A2. Cell *75*, 693-708.

Malmstrom, V., Shipton, D., Singh, B., Al-Shamkhani, A., Puklavec, M.J., Barclay, A.N., and Powrie, F. (2001). CD134L expression on dendritic cells in the mesenteric lymph nodes drives colitis in T cell-restored SCID mice. J Immunol *166*, 6972-6981.

Manolios, N., Kemp, O., and Li, Z.G. (1994). The T cell antigen receptor alpha and beta chains interact via distinct regions with CD3 chains. Eur J Immunol *24*, 84-92.

Marincola, F.M., Jaffee, E.M., Hicklin, D.J., and Ferrone, S. (2000). Escape of human solid tumors from T-cell recognition: molecular mechanisms and functional significance. Adv Immunol *74*, 181-273.

Marrack, P., and Kappler, J. (1997). Positive selection of thymocytes bearing alpha beta T cell receptors. Curr Opin Immunol *9*, 250-255.

Martin, A., Tsui, H.W., and Tsui, F.W. (1999). SHP-1 variant proteins are absent in motheaten mice despite presence of splice variant transcripts with open reading frames. Mol Immunol *36*, 1029-1041.

Martin, G.A., Bollag, G., McCormick, F., and Abo, A. (1995). A novel serine kinase activated by rac1/CDC42Hs-dependent autophosphorylation is related to PAK65 and STE20. EMBO J *14*, 4385.

Marzo, A.L., Klonowski, K.D., Le Bon, A., Borrow, P., Tough, D.F., and Lefrancois, L. (2005). Initial T cell frequency dictates memory CD8+ T cell lineage commitment. Nat Immunol *6*, 793-799.

Masopust, D., Vezys, V., Marzo, A.L., and Lefrancois, L. (2001). Preferential localization of effector memory cells in nonlymphoid tissue. Science *291*, 2413-2417.

Massa, P.T., Saha, S., Wu, C., and Jarosinski, K.W. (2000). Expression and function of the protein tyrosine phosphatase SHP-1 in oligodendrocytes. Glia *29*, 376-385.

Matloubian, M., Lo, C.G., Cinamon, G., Lesneski, M.J., Xu, Y., Brinkmann, V., Allende, M.L., Proia, R.L., and Cyster, J.G. (2004). Lymphocyte egress from thymus and peripheral lymphoid organs is dependent on S1P receptor 1. Nature *427*, 355-360.

Matthews, R.J., Bowne, D.B., Flores, E., and Thomas, M.L. (1992). Characterization of hematopoietic intracellular protein tyrosine phosphatases: description of a phosphatase containing an SH2 domain and another enriched in proline-, glutamic acid-, serine-, and threonine-rich sequences. Mol Cell Biol *12*, 2396-2405.

May, M.J., and Ghosh, S. (1998). Signal transduction through NF-kappa B. Immunol Today *19*, 80-88.

McLellan, A.D., Kapp, M., Eggert, A., Linden, C., Bommhardt, U., Brocker, E.B., Kammerer, U., and Kampgen, E. (2002). Anatomic location and T-cell stimulatory functions of mouse dendritic cell subsets defined by CD4 and CD8 expression. Blood *99*, 2084-2093.

Medema, J.P., de Jong, J., Peltenburg, L.T., Verdegaal, E.M., Gorter, A., Bres, S.A., Franken, K.L., Hahne, M., Albar, J.P., Melief, C.J., *et al.* (2001). Blockade of the granzyme B/perforin pathway through overexpression of the serine protease inhibitor PI-9/SPI-6 constitutes a mechanism for immune escape by tumors. Proc Natl Acad Sci U S A *98*, 11515-11520.

Melchionda, F., Fry, T.J., Milliron, M.J., McKirdy, M.A., Tagaya, Y., and Mackall, C.L. (2005). Adjuvant IL-7 or IL-15 overcomes immunodominance and improves survival of the CD8+ memory cell pool. J Clin Invest *115*, 1177-1187.

Metkar, S.S., Wang, B., Aguilar-Santelises, M., Raja, S.M., Uhlin-Hansen, L., Podack, E., Trapani, J.A., and Froelich, C.J. (2002). Cytotoxic cell granule-mediated apoptosis: perforin delivers granzyme B-serglycin complexes into target cells without plasma membrane pore formation. Immunity *16*, 417-428.

Miller, J.F., Kurts, C., Allison, J., Kosaka, H., Carbone, F., and Heath, W.R. (1998). Induction of peripheral CD8+ T-cell tolerance by cross-presentation of self antigens. Immunol Rev *165*, 267-277.

Minoo, P., Zadeh, M.M., Rottapel, R., Lebrun, J.J., and Ali, S. (2004). A novel SHP-1/Grb2-dependent mechanism of negative regulation of cytokine-receptor signaling: contribution of SHP-1 C-terminal tyrosines in cytokine signaling. Blood *103*, 1398-1407.

Mitra-Kaushik, S., Harding, J., Hess, J., Schreiber, R., and Ratner, L. (2004). Enhanced tumorigenesis in HTLV-1 tax-transgenic mice deficient in interferon-gamma. Blood *104*, 3305-3311.

Mitsuyasu, R.T., Anton, P.A., Deeks, S.G., Scadden, D.T., Connick, E., Downs, M.T., Bakker, A., Roberts, M.R., June, C.H., Jalali, S., *et al.* (2000). Prolonged survival and tissue trafficking following adoptive transfer of CD4zeta gene-modified autologous CD4(+) and CD8(+) T cells in human immunodeficiency virus-infected subjects. Blood *96*, 785-793.

Mizuno, K., Tagawa, Y., Mitomo, K., Arimura, Y., Hatano, N., Katagiri, T., Ogimoto, M., and Yakura, H. (2000). Src homology region 2 (SH2) domain-containing phosphatase-1 dephosphorylates B cell linker protein/SH2 domain leukocyte protein of 65 kDa and selectively regulates c-Jun NH2-terminal kinase activation in B cells. J Immunol *165*, 1344-1351.

Monks, C.R., Freiberg, B.A., Kupfer, H., Sciaky, N., and Kupfer, A. (1998). Three-dimensional segregation of supramolecular activation clusters in T cells. Nature *395*, 82-86.

Montini, E., Cesana, D., Schmidt, M., Sanvito, F., Ponzoni, M., Bartholomae, C., Sergi Sergi, L., Benedicenti, F., Ambrosi, A., Di Serio, C., *et al.* (2006). Hematopoietic stem cell gene transfer in a tumor-prone mouse model uncovers low genotoxicity of lentiviral vector integration. Nat Biotechnol *24*, 687-696.

Mora, J.R., Bono, M.R., Manjunath, N., Weninger, W., Cavanagh, L.L., Rosemblatt, M., and Von Andrian, U.H. (2003). Selective imprinting of gut-homing T cells by Peyer's patch dendritic cells. Nature *424*, 88-93.

Morgan, R.A., Dudley, M.E., Wunderlich, J.R., Hughes, M.S., Yang, J.C., Sherry, R.M., Royal, R.E., Topalian, S.L., Kammula, U.S., Restifo, N.P., *et al.* (2006). Cancer regression in patients after transfer of genetically engineered lymphocytes. Science *314*, 126-129.

Morton, D.L. (2004). Immune response to postsurgical adjuvant active immunotherapy with Canvaxin polyvalent cancer vaccine: correlations with clinical course of patients with metastatic melanoma. Dev Biol (Basel) *116*, 209-217; discussion 229-236.

Morton, D.L., Hsueh, E.C., Essner, R., Foshag, L.J., O'Day, S.J., Bilchik, A., Gupta, R.K., Hoon, D.S., Ravindranath, M., Nizze, J.A., *et al.* (2002). Prolonged survival of patients receiving active immunotherapy with Canvaxin therapeutic polyvalent vaccine after complete resection of melanoma metastatic to regional lymph nodes. Ann Surg *236*, 438-448; discussion 448-439.

Muller, S., Lory, J., Corazza, N., Griffiths, G.M., Z'Graggen, K., Mazzucchelli, L., Kappeler, A., and Mueller, C. (1998). Activated CD4+ and CD8+ cytotoxic cells are present in increased numbers in the intestinal mucosa from patients with active inflammatory bowel disease. Am J Pathol *152*, 261-268.

Murakami, M., Sakamoto, A., Bender, J., Kappler, J., and Marrack, P. (2002). CD25+CD4+ T cells contribute to the control of memory CD8+ T cells. Proc Natl Acad Sci U S A *99*, 8832-8837.

Murali-Krishna, K., Altman, J.D., Suresh, M., Sourdive, D.J., Zajac, A.J., Miller, J.D., Slansky, J., and Ahmed, R. (1998). Counting antigen-specific CD8 T cells: a reevaluation of bystander activation during viral infection. Immunity *8*, 177-187.

Nakamura, M.C., Niemi, E.C., Fisher, M.J., Shultz, L.D., Seaman, W.E., and Ryan, J.C. (1997). Mouse Ly-49A interrupts early signaling events in natural killer cell cytotoxicity and functionally associates with the SHP-1 tyrosine phosphatase. J Exp Med *185*, 673-684.

Neel, B.G., and Tonks, N.K. (1997). Protein tyrosine phosphatases in signal transduction. Curr Opin Cell Biol *9*, 193-204.

Neumeister, E.N., Zhu, Y., Richard, S., Terhorst, C., Chan, A.C., and Shaw, A.S. (1995). Binding of ZAP-70 to phosphorylated T-cell receptor zeta and eta enhances its autophosphorylation and generates specific binding sites for SH2 domain-containing proteins. Mol Cell Biol *15*, 3171-3178.

Nikolova, M., Musette, P., Bagot, M., Boumsell, L., and Bensussan, A. (2002). Engagement of ILT2/CD85j in Sezary syndrome cells inhibits their CD3/TCR signaling. Blood *100*, 1019-1025.

Noguchi, Y., Jungbluth, A., Richards, E.C., and Old, L.J. (1996). Effect of interleukin 12 on tumor induction by 3-methylcholanthrene. Proc Natl Acad Sci U S A *93*, 11798-11801.

Norell, H., Carlsten, M., Ohlum, T., Malmberg, K.J., Masucci, G., Schedvins, K., Altermann, W., Handke, D., Atkins, D., Seliger, B., *et al.* (2006). Frequent loss of HLA-A2 expression in metastasizing ovarian carcinomas associated with genomic haplotype loss and HLA-A2-restricted HER-2/neu-specific immunity. Cancer Res *66*, 6387-6394.

Norian, L.A., and Koretzky, G.A. (2000). Intracellular adapter molecules. Semin Immunol *12*, 43-54.

Okazaki, T., and Honjo, T. (2006). The PD-1-PD-L pathway in immunological tolerance. Trends Immunol *27*, 195-201.

Ono, M., Okada, H., Bolland, S., Yanagi, S., Kurosaki, T., and Ravetch, J.V. (1997). Deletion of SHIP or SHP-1 reveals two distinct pathways for inhibitory signaling. Cell *90*, 293-301.

O'Reilly, R.J., Small, T.N., Papadopoulos, E., Lucas, K., Lacerda, J., and Koulova, L. (1997). Biology and adoptive cell therapy of Epstein-Barr virus-associated lymphoproliferative disorders in recipients of marrow allografts. Immunol Rev *157*, 195-216.

Overwijk, W.W., Theoret, M.R., Finkelstein, S.E., Surman, D.R., de Jong, L.A., Vyth-Dreese, F.A., Dellemijn, T.A., Antony, P.A., Spiess, P.J., Palmer, D.C., *et al.* (2003). Tumor regression and autoimmunity after reversal of a functionally tolerant state of self-reactive CD8+ T cells. J Exp Med *198*, 569-580.

Palmer, M.S., Bentley, A., Gould, K., and Townsend, A.R. (1989). The T cell receptor from an influenza-A specific murine CTL clone. Nucleic Acids Res *17*, 2353.

Pabst, R. (1988). The spleen in lymphocyte migration. Immunol Today *9*, 43-45.

Paddison, P.J., Caudy, A.A., Sachidanandam, R., and Hannon, G.J. (2004). Short hairpin activated gene silencing in mammalian cells. Methods Mol Biol *265*, 85-100.

Pages, F., Berger, A., Camus, M., Sanchez-Cabo, F., Costes, A., Molidor, R., Mlecnik, B., Kirilovsky, A., Nilsson, M., Damotte, D., *et al.* (2005). Effector memory T cells, early metastasis, and survival in colorectal cancer. N Engl J Med *353*, 2654-2666.

Pani, G., Fischer, K.D., Mlinaric-Rascan, I., and Siminovitch, K.A. (1996). Signaling capacity of the T cell antigen receptor is negatively regulated by the PTP1C tyrosine phosphatase. J Exp Med *184*, 839-852.

Pani, G., Kozlowski, M., Cambier, J.C., Mills, G.B., and Siminovitch, K.A. (1995). Identification of the tyrosine phosphatase PTP1C as a B cell antigen receptor-associated protein involved in the regulation of B cell signaling. J Exp Med *181*, 2077-2084.

Papagno, L., Spina, C.A., Marchant, A., Salio, M., Rufer, N., Little, S., Dong, T., Chesney, G., Waters, A., Easterbrook, P., *et al.* (2004). Immune activation and CD8+ T-cell differentiation towards senescence in HIV-1 infection. PLoS Biol *2*, E20.

Park, J.R., Digiusto, D.L., Slovak, M., Wright, C., Naranjo, A., Wagner, J., Meechoovet, H.B., Bautista, C., Chang, W.C., Ostberg, J.R., *et al.* (2007). Adoptive transfer of chimeric antigen receptor re-directed cytolytic T lymphocyte clones in patients with neuroblastoma. Mol Ther *15*, 825-833.

Pawson, T. (1995). Protein modules and signalling networks. Nature *373*, 573-580.
Pawson, T., and Scott, J.D. (1997). Signaling through scaffold, anchoring, and adaptor proteins. Science *278*, 2075-2080.

Paz, P.E., Wang, S., Clarke, H., Lu, X., Stokoe, D., and Abo, A. (2001). Mapping the Zap-70 phosphorylation sites on LAT (linker for activation of T cells) required for recruitment and activation of signalling proteins in T cells. Biochem J *356*, 461-471.

Pei, D., Neel, B.G., and Walsh, C.T. (1993). Overexpression, purification, and characterization of SHPTP1, a Src homology 2-containing protein-tyrosine-phosphatase. Proc Natl Acad Sci U S A *90*, 1092-1096.

Pei, D., Wang, J., and Walsh, C.T. (1996). Differential functions of the two Src homology 2 domains in protein tyrosine phosphatase SH-PTP1. Proc Natl Acad Sci U S A *93*, 1141-1145.

Peled, A., Petit, I., Kollet, O., Magid, M., Ponomaryov, T., Byk, T., Nagler, A., Ben-Hur, H., Many, A., Shultz, L., *et al.* (1999). Dependence of human stem cell engraftment and repopulation of NOD/SCID mice on CXCR4. Science *283*, 845-848.

Penn, I. (2000). Post-transplant malignancy: the role of immunosuppression. Drug Saf *23*, 101-113.

Peoples, G.E., Goedegebuure, P.S., Smith, R., Linehan, D.C., Yoshino, I., and Eberlein, T.J. (1995). Breast and ovarian cancer-specific cytotoxic T lymphocytes recognize the same HER2/neu-derived peptide. Proc Natl Acad Sci U S A *92*, 432-436.

Pfeifer, J.D., Wick, M.J., Roberts, R.L., Findlay, K., Normark, S.J., and Harding, C.V. (1993). Phagocytic processing of bacterial antigens for class I MHC presentation to T cells. Nature *361*, 359-362.

Plas, D.R., Johnson, R., Pingel, J.T., Matthews, R.J., Dalton, M., Roy, G., Chan, A.C., and Thomas, M.L. (1996). Direct regulation of ZAP-70 by SHP-1 in T cell antigen receptor signaling. Science *272*, 1173-1176.

Plas, D.R., Williams, C.B., Kersh, G.J., White, L.S., White, J.M., Paust, S., Ulyanova, T., Allen, P.M., and Thomas, M.L. (1999). Cutting edge: the tyrosine phosphatase SHP-1 regulates thymocyte positive selection. J Immunol *162*, 5680-5684.

Pluskey, S., Wandless, T.J., Walsh, C.T., and Shoelson, S.E. (1995). Potent stimulation of SH-PTP2 phosphatase activity by simultaneous occupancy of both SH2 domains. J Biol Chem *270*, 2897-2900.

Plutzky, J., Neel, B.G., and Rosenberg, R.D. (1992a). Isolation of a src homology 2-containing tyrosine phosphatase. Proc Natl Acad Sci U S A *89*, 1123-1127.

Plutzky, J., Neel, B.G., Rosenberg, R.D., Eddy, R.L., Byers, M.G., Jani-Sait, S., and Shows, T.B. (1992b). Chromosomal localization of an SH2-containing tyrosine phosphatase (PTPN6). Genomics *13*, 869-872.

Podolsky, D.K. (2002b). Inflammatory bowel disease. N Engl J Med *347*, 417-429.

Powell, D.J., Jr., and Rosenberg, S.A. (2004). Phenotypic and functional maturation of tumor antigen-reactive CD8+ T lymphocytes in patients undergoing multiple course peptide vaccination. J Immunother *27*, 36-47.

Preall, J.B., He, Z., Gorra, J.M., and Sontheimer, E.J. (2006). Short interfering RNA strand selection is independent of dsRNA processing polarity during RNAi in Drosophila. Curr Biol *16*, 530-535.

Probst, H.C., McCoy, K., Okazaki, T., Honjo, T., and van den Broek, M. (2005). Resting dendritic cells induce peripheral CD8+ T cell tolerance through PD-1 and CTLA-4. Nat Immunol *6*, 280-286.

Putney, J.W., Jr., and Bird, G.S. (1993). The signal for capacitative calcium entry. Cell *75*, 199-201.

Raab, M., and Rudd, C.E. (1996). Hematopoietic cell phosphatase (HCP) regulates p56LCK phosphorylation and ZAP-70 binding to T cell receptor zeta chain. Biochem Biophys Res Commun *222*, 50-57.

Raja, S.M., Wang, B., Dantuluri, M., Desai, U.R., Demeler, B., Spiegel, K., Metkar, S.S., and Froelich, C.J. (2002). Cytotoxic cell granule-mediated apoptosis. Characterization of the macromolecular complex of granzyme B with serglycin. J Biol Chem *277*, 49523-49530.

Rand, T.A., Petersen, S., Du, F., and Wang, X. (2005). Argonaute2 cleaves the anti-guide strand of siRNA during RISC activation. Cell *123*, 621-629.

Rapoport, A.P., Stadtmauer, E.A., Aqui, N., Badros, A., Cotte, J., Chrisley, L., Veloso, E., Zheng, Z., Westphal, S., Mair, R., *et al.* (2005). Restoration of immunity in lymphopenic individuals with cancer by vaccination and adoptive T-cell transfer. Nat Med *11*, 1230-1237.

Raue, H.P., Brien, J.D., Hammarlund, E., and Slifka, M.K. (2004). Activation of virus-specific CD8+ T cells by lipopolysaccharide-induced IL-12 and IL-18. J Immunol *173*, 6873-6881.

Ravetch, J.V., and Lanier, L.L. (2000). Immune inhibitory receptors. Science *290*, 84-89.

Ravkov, E.V., Myrick, C.M., and Altman, J.D. (2003). Immediate early effector functions of virus-specific CD8+CCR7+ memory cells in humans defined by HLA and CC chemokine ligand 19 tetramers. J Immunol *170*, 2461-2468.

Reynolds, A., Leake, D., Boese, Q., Scaringe, S., Marshall, W.S., and Khvorova, A. (2004). Rational siRNA design for RNA interference. Nat Biotechnol *22*, 326-330.

Roach, T.I., Slater, S.E., White, L.S., Zhang, X., Majerus, P.W., Brown, E.J., and Thomas, M.L. (1998). The protein tyrosine phosphatase SHP-1 regulates integrin-mediated adhesion of macrophages. Curr Biol *8*, 1035-1038.

Robbins, P.F., Dudley, M.E., Wunderlich, J., El-Gamil, M., Li, Y.F., Zhou, J., Huang, J., Powell, D.J., Jr., and Rosenberg, S.A. (2004). Cutting edge: persistence of transferred lymphocyte clonotypes correlates with cancer regression in patients receiving cell transfer therapy. J Immunol *173*, 7125-7130.

Robbins, P.F., El-Gamil, M., Li, Y.F., Kawakami, Y., Loftus, D., Appella, E., and Rosenberg, S.A. (1996). A mutated beta-catenin gene encodes a melanoma-specific antigen recognized by tumor infiltrating lymphocytes. J Exp Med *183*, 1185-1192.

Roberts, A.D., Ely, K.H., and Woodland, D.L. (2005). Differential contributions of central and effector memory T cells to recall responses. J Exp Med *202*, 123-133.

Roberts, S.J., Ng, B.Y., Filler, R.B., Lewis, J., Glusac, E.J., Hayday, A.C., Tigelaar, R.E., and Girardi, M. (2007). Characterizing tumor-promoting T cells in chemically induced cutaneous carcinogenesis. Proc Natl Acad Sci U S A *104*, 6770-6775.

Rock, K.L., York, I.A., Saric, T., and Goldberg, A.L. (2002). Protein degradation and the generation of MHC class I-presented peptides. Adv Immunol *80*, 1-70.

Rodriguez, A., Regnault, A., Kleijmeer, M., Ricciardi-Castagnoli, P., and Amigorena, S. (1999). Selective transport of internalized antigens to the cytosol for MHC class I presentation in dendritic cells. Nat Cell Biol *1*, 362-368.

Roggero, E., Zucca, E., Pinotti, G., Pascarella, A., Capella, C., Savio, A., Pedrinis, E., Paterlini, A., Venco, A., and Cavalli, F. (1995). Eradication of Helicobacter pylori infection in primary low-grade gastric lymphoma of mucosa-associated lymphoid tissue. Ann Intern Med *122*, 767-769.

Rohrer, J., Schweizer, A., Russell, D., and Kornfeld, S. (1996). The targeting of Lamp1 to lysosomes is dependent on the spacing of its cytoplasmic tail tyrosine sorting motif relative to the membrane. J Cell Biol *132*, 565-576.

Rooney, C.M., Smith, C.A., Ng, C.Y., Loftin, S., Li, C., Krance, R.A., Brenner, M.K., and Heslop, H.E. (1995). Use of gene-modified virus-specific T lymphocytes to control Epstein-Barr-virus-related lymphoproliferation. Lancet *345*, 9-13.

Rooney, C.M., Smith, C.A., Ng, C.Y., Loftin, S.K., Sixbey, J.W., Gan, Y., Srivastava, D.K., Bowman, L.C., Krance, R.A., Brenner, M.K., *et al.* (1998). Infusion of cytotoxic T cells for the prevention and treatment of Epstein-Barr virus-induced lymphoma in allogeneic transplant recipients. Blood *92*, 1549-1555.

Rosenberg, S.A., Mule, J.J., Spiess, P.J., Reichert, C.M., and Schwarz, S.L. (1985). Regression of established pulmonary metastases and subcutaneous tumor mediated by the systemic administration of high-dose recombinant interleukin 2. J Exp Med *161*, 1169-1188.

Rosenberg, S.A., Sherry, R.M., Morton, K.E., Scharfman, W.J., Yang, J.C., Topalian, S.L., Royal, R.E., Kammula, U., Restifo, N.P., Hughes, M.S., *et al.* (2005). Tumor progression can occur despite the induction of very high levels of self/tumor antigen-specific CD8+ T cells in patients with melanoma. J Immunol *175*, 6169-6176.

Rosenberg, S.A., Yang, J.C., and Restifo, N.P. (2004). Cancer immunotherapy: moving beyond current vaccines. Nat Med *10*, 909-915.

Rosenberg, S.A., Yang, J.C., Schwartzentruber, D.J., Hwu, P., Topalian, S.L., Sherry, R.M., Restifo, N.P., Wunderlich, J.R., Seipp, C.A., Rogers-Freezer, L., *et al.* (2003). Recombinant fowlpox viruses encoding the anchor-modified gp100 melanoma antigen can generate antitumor immune responses in patients with metastatic melanoma. Clin Cancer Res *9*, 2973-2980.

Rosenberg, S.A., Yang, J.C., Topalian, S.L., Schwartzentruber, D.J., Weber, J.S., Parkinson, D.R., Seipp, C.A., Einhorn, J.H., and White, D.E. (1994). Treatment of 283 consecutive patients with metastatic melanoma or renal cell cancer using high-dose bolus interleukin 2. JAMA *271*, 907-913.

Rosenberg, S.A., Zhai, Y., Yang, J.C., Schwartzentruber, D.J., Hwu, P., Marincola, F.M., Topalian, S.L., Restifo, N.P., Seipp, C.A., Einhorn, J.H., *et al.* (1998). Immunizing patients with metastatic melanoma using recombinant adenoviruses encoding MART-1 or gp100 melanoma antigens. J Natl Cancer Inst *90*, 1894-1900.

Roskrow, M.A., Suzuki, N., Gan, Y., Sixbey, J.W., Ng, C.Y., Kimbrough, S., Hudson, M., Brenner, M.K., Heslop, H.E., and Rooney, C.M. (1998). Epstein-Barr virus (EBV)-specific cytotoxic T lymphocytes for the treatment of patients with EBV-positive relapsed Hodgkin's disease. Blood *91*, 2925-2934.

Ross, S., Liu, V., Abulafia, R., Hogan, C., and Osband, M. (1993). Adoptive immunotherapy of hormone-refractory, stage D2 prostate cancer using ex vivo activated autologous T cells (autolymphocyte therapy): results from a pilot study. Biotechnol Ther *4*, 197-211.

Rufer, N., Migliaccio, M., Antonchuk, J., Humphries, R.K., Roosnek, E., and Lansdorp, P.M. (2001). Transfer of the human telomerase reverse transcriptase (TERT) gene into T lymphocytes results in extension of replicative potential. Blood *98*, 597-603.

Russel, M.G., and Stockbrugger, R.W. (1996). Epidemiology of inflammatory bowel disease: an update. Scand J Gastroenterol *31*, 417-427.

Ryser, J.E., Rungger-Brandle, E., Chaponnier, C., Gabbiani, G., and Vassalli, P. (1982). The area of attachment of cytotoxic T lymphocytes to their target cells shows high motility and polarization of actin, but not myosin. J Immunol *128*, 1159-1162.

Sacre, K., Carcelain, G., Cassoux, N., Fillet, A.M., Costagliola, D., Vittecoq, D., Salmon, D., Amoura, Z., Katlama, C., and Autran, B. (2005). Repertoire, diversity, and differentiation of specific CD8 T cells are associated with immune protection against human cytomegalovirus disease. J Exp Med *201*, 1999-2010.

Sakaguchi, S. (2005). Naturally arising Foxp3-expressing CD25+CD4+ regulatory T cells in immunological tolerance to self and non-self. Nat Immunol *6*, 345-352.

Sallusto, F., Cella, M., Danieli, C., and Lanzavecchia, A. (1995). Dendritic cells use macropinocytosis and the mannose receptor to concentrate macromolecules in the major histocompatibility complex class II compartment: downregulation by cytokines and bacterial products. J Exp Med *182*, 389-400.

Sallusto, F., Lenig, D., Forster, R., Lipp, M., and Lanzavecchia, A. (1999). Two subsets of memory T lymphocytes with distinct homing potentials and effector functions. Nature *401*, 708-712.

Sankarshanan, M., Ma, Z., Iype, T., and Lorenz, U. (2007). Identification of a novel lipid raft-targeting motif in Src homology 2-containing phosphatase 1. J Immunol *179*, 483-490.

Sathish, J.G., Dolton, G., Leroy, F.G., and Matthews, R.J. (2007). Loss of Src homology region 2 domain-containing protein tyrosine phosphatase-1 increases CD8+ T cell-APC conjugate formation and is associated with enhanced in vivo CTL function. J Immunol *178*, 330-337.

Sathish, J.G., Johnson, K.G., LeRoy, F.G., Fuller, K.J., Hallett, M.B., Brennan, P., Borysiewicz, L.K., Sims, M.J., and Matthews, R.J. (2001). Requirement for CD28 co-stimulation is lower in SHP-1-deficient T cells. Eur J Immunol *31*, 3649-3658.

Sathish, J.G., Walters, J., Luo, J.C., Johnson, K.G., Leroy, F.G., Brennan, P., Kim, K.P., Gygi, S.P., Neel, B.G., and Matthews, R.J. (2004). CD22 is a functional ligand for SH2 domain-containing protein-tyrosine phosphatase-1 in primary T cells. J Biol Chem *279*, 47783-47791.

Sato, E., Olson, S.H., Ahn, J., Bundy, B., Nishikawa, H., Qian, F., Jungbluth, A.A., Frosina, D., Gnjatic, S., Ambrosone, C., *et al.* (2005). Intraepithelial CD8+ tumor-infiltrating lymphocytes and a high CD8+/regulatory T cell ratio are associated with favorable prognosis in ovarian cancer. Proc Natl Acad Sci U S A *102*, 18538-18543.

Saverino, D., Fabbi, M., Ghiotto, F., Merlo, A., Bruno, S., Zarcone, D., Tenca, C., Tiso, M., Santoro, G., Anastasi, G., *et al.* (2000). The CD85/LIR-1/ILT2 inhibitory receptor is expressed by all human T lymphocytes and down-regulates their functions. J Immunol *165*, 3742-3755.

Scalapino, K.J., and Daikh, D.I. (2008). CTLA-4: a key regulatory point in the control of autoimmune disease. Immunol Rev *223*, 143-155.

Schirmbeck, R., Bohm, W., Melber, K., and Reimann, J. (1995). Processing of exogenous heat-aggregated (denatured) and particulate (native) hepatitis B surface antigen for class I-restricted epitope presentation. J Immunol *155*, 4676-4684.

Schluns, K.S., Kieper, W.C., Jameson, S.C., and Lefrancois, L. (2000). Interleukin-7 mediates the homeostasis of naive and memory CD8 T cells in vivo. Nat Immunol *1*, 426-432.

Scholer, A., Hugues, S., Boissonnas, A., Fetler, L., and Amigorena, S. (2008). Intercellular adhesion molecule-1-dependent stable interactions between T cells and dendritic cells determine CD8+ T cell memory. Immunity *28*, 258-270.

Schwarz, D.S., Hutvagner, G., Du, T., Xu, Z., Aronin, N., and Zamore, P.D. (2003). Asymmetry in the assembly of the RNAi enzyme complex. Cell *115*, 199-208.

Senju, M., Hulstaert, F., Lowder, J., and Jewell, D.P. (1991a). Flow cytometric analysis of peripheral blood lymphocytes in ulcerative colitis and Crohn's disease. Gut *32*, 779-783.

Senju, M., Makiyama, K., Hara, K., Hulstaert, F., Lowder, J.N., and Jewell, D.P. (1991b). Two-color immunofluorescence and flow cytometric analysis of peripheral blood lymphocyte subsets in Caucasian and Japanese healthy subjects. Jpn J Med *30*, 509-515.

Senju, M., Wu, K.C., Mahida, Y.R., and Jewell, D.P. (1991d). Two-color immunofluorescence and flow cytometric analysis of lamina propria lymphocyte subsets in ulcerative colitis and Crohn's disease. Dig Dis Sci *36*, 1453-1458.

Shankaran, V., Ikeda, H., Bruce, A.T., White, J.M., Swanson, P.E., Old, L.J., and Schreiber, R.D. (2001). IFNgamma and lymphocytes prevent primary tumour development and shape tumour immunogenicity. Nature *410*, 1107-1111.

Shaw, A.S., Chalupny, J., Whitney, J.A., Hammond, C., Amrein, K.E., Kavathas, P., Sefton, B.M., and Rose, J.K. (1990). Short related sequences in the cytoplasmic domains of CD4 and CD8 mediate binding to the amino-terminal domain of the p56lck tyrosine protein kinase. Mol Cell Biol *10*, 1853-1862.

Shen, S.H., Bastien, L., Posner, B.I., and Chretien, P. (1991). A protein-tyrosine phosphatase with sequence similarity to the SH2 domain of the protein-tyrosine kinases. Nature *352*, 736-739.

Shinkai, Y., Rathbun, G., Lam, K.P., Oltz, E.M., Stewart, V., Mendelsohn, M., Charron, J., Datta, M., Young, F., Stall, A.M., *et al.* (1992). RAG-2-deficient mice lack mature lymphocytes owing to inability to initiate V(D)J rearrangement. Cell *68*, 855-867.

Shivananda, S., Lennard-Jones, J., Logan, R., Fear, N., Price, A., Carpenter, L., and van Blankenstein, M. (1996). Incidence of inflammatory bowel disease across Europe: is there a difference between north and south? Results of the European Collaborative Study on Inflammatory Bowel Disease (EC-IBD). Gut *39*, 690-697.

Shu, S.Y., Chou, T., and Sakai, K. (1989). Lymphocytes generated by in vivo priming and in vitro sensitization demonstrate therapeutic efficacy against a murine tumor that lacks apparent immunogenicity. J Immunol *143*, 740-748.

Shultz, L.D., Coman, D.R., Bailey, C.L., Beamer, W.G., and Sidman, C.L. (1984). "Viable motheaten," a new allele at the motheaten locus. I. Pathology. Am J Pathol *116*, 179-192.
Shultz, L.D., Rajan, T.V., and Greiner, D.L. (1997). Severe defects in immunity and hematopoiesis caused by SHP-1 protein-tyrosine-phosphatase deficiency. Trends Biotechnol *15*, 302-307.

Shultz, L.D., Schweitzer, P.A., Rajan, T.V., Yi, T., Ihle, J.N., Matthews, R.J., Thomas, M.L., and Beier, D.R. (1993). Mutations at the murine motheaten locus are within the hematopoietic cell protein-tyrosine phosphatase (Hcph) gene. Cell *73*, 1445-1454.

Sigmundsdottir, H., Pan, J., Debes, G.F., Alt, C., Habtezion, A., Soler, D., and Butcher, E.C. (2007). DCs metabolize sunlight-induced vitamin D3 to 'program' T cell attraction to the epidermal chemokine CCL27. Nat Immunol *8*, 285-293.

Silva, J.M., Sachidanandam, R., and Hannon, G.J. (2003). Free energy lights the path toward more effective RNAi. Nat Genet *35*, 303-305.

Simpson, E., Chandler, P., Sponaas, A., Millrain, M., and Dyson, P.J. (1995a). T cells with dual antigen specificity in T cell receptor transgenic mice rejecting allografts. Eur J Immunol *25*, 2813-2817.

Simpson, S.J., Mizoguchi, E., Allen, D., Bhan, A.K., and Terhorst, C. (1995b). Evidence that CD4+, but not CD8+ T cells are responsible for murine interleukin-2-deficient colitis. Eur J Immunol *25*, 2618-2625.

Smith, J.D., Lie, W.R., Gorka, J., Myers, N.B., and Hansen, T.H. (1992). Extensive peptide ligand exchange by surface class I major histocompatibility complex molecules independent of exogenous beta 2-microglobulin. Proc Natl Acad Sci U S A *89*, 7767-7771.

Smith, J.W., 2nd, Walker, E.B., Fox, B.A., Haley, D., Wisner, K.P., Doran, T., Fisher, B., Justice, L., Wood, W., Vetto, J., *et al.* (2003). Adjuvant immunization of HLA-A2-positive melanoma patients with a modified gp100 peptide induces peptide-specific CD8+ T-cell responses. J Clin Oncol *21*, 1562-1573.

Smyth, M.J., Crowe, N.Y., and Godfrey, D.I. (2001). NK cells and NKT cells collaborate in host protection from methylcholanthrene-induced fibrosarcoma. Int Immunol *13*, 459-463.

So, T., Takenoyama, M., Mizukami, M., Ichiki, Y., Sugaya, M., Hanagiri, T., Sugio, K., and Yasumoto, K. (2005). Haplotype loss of HLA class I antigen as an escape mechanism from immune attack in lung cancer. Cancer Res *65*, 5945-5952.

Somani, A.K., Yuen, K., Xu, F., Zhang, J., Branch, D.R., and Siminovitch, K.A. (2001). The SH2 domain containing tyrosine phosphatase-1 down-regulates activation of Lyn and Lyn-induced tyrosine phosphorylation of the CD19 receptor in B cells. J Biol Chem *276*, 1938-1944.

Speiser, D.E., Lienard, D., Rufer, N., Rubio-Godoy, V., Rimoldi, D., Lejeune, F., Krieg, A.M., Cerottini, J.C., and Romero, P. (2005). Rapid and strong human CD8+ T cell responses to vaccination with peptide, IFA, and CpG oligodeoxynucleotide 7909. J Clin Invest *115*, 739-746.

Stagg, A.J., Kamm, M.A., and Knight, S.C. (2002). Intestinal dendritic cells increase T cell expression of alpha4beta7 integrin. Eur J Immunol *32*, 1445-1454.

Stassi, G., Todaro, M., Zerilli, M., Ricci-Vitiani, L., Di Liberto, D., Patti, M., Florena, A., Di Gaudio, F., Di Gesu, G., and De Maria, R. (2003). Thyroid cancer resistance to chemotherapeutic drugs via autocrine production of interleukin-4 and interleukin-10. Cancer Res *63*, 6784-6790.

Stein, J.V., Rot, A., Luo, Y., Narasimhaswamy, M., Nakano, H., Gunn, M.D., Matsuzawa, A., Quackenbush, E.J., Dorf, M.E., and von Andrian, U.H. (2000). The CC chemokine thymus-derived chemotactic agent 4 (TCA-4, secondary lymphoid tissue chemokine, 6Ckine, exodus-2) triggers lymphocyte function-associated antigen 1-mediated arrest of rolling T lymphocytes in peripheral lymph node high endothelial venules. J Exp Med *191*, 61-76.

Stein, P.H., Fraser, J.D., and Weiss, A. (1994). The cytoplasmic domain of CD28 is both necessary and sufficient for costimulation of interleukin-2 secretion and association with phosphatidylinositol 3'-kinase. Mol Cell Biol *14*, 3392-3402.

Steinhoff, U., Brinkmann, V., Klemm, U., Aichele, P., Seiler, P., Brandt, U., Bland, P.W., Prinz, I., Zugel, U., and Kaufmann, S.H. (1999). Autoimmune intestinal pathology induced by hsp60-specific CD8 T cells. Immunity *11*, 349-358.

Stern, L.J., Brown, J.H., Jardetzky, T.S., Gorga, J.C., Urban, R.G., Strominger, J.L., and Wiley, D.C. (1994). Crystal structure of the human class II MHC protein HLA-DR1 complexed with an influenza virus peptide. Nature *368*, 215-221.

Stinchcombe, J.C., Bossi, G., Booth, S., and Griffiths, G.M. (2001). The immunological synapse of CTL contains a secretory domain and membrane bridges. Immunity *15*, 751-761.

Straathof, K.C., Leen, A.M., Buza, E.L., Taylor, G., Huls, M.H., Heslop, H.E., Rooney, C.M., and Bollard, C.M. (2005). Characterization of latent membrane protein 2 specificity in CTL lines from patients with EBV-positive nasopharyngeal carcinoma and lymphoma. J Immunol *175*, 4137-4147.

Street, S.E., Trapani, J.A., MacGregor, D., and Smyth, M.J. (2002). Suppression of lymphoma and epithelial malignancies effected by interferon gamma. J Exp Med *196*, 129-134.

Stuckey, J.A., Schubert, H.L., Fauman, E.B., Zhang, Z.Y., Dixon, J.E., and Saper, M.A. (1994). Crystal structure of Yersinia protein tyrosine phosphatase at 2.5 A and the complex with tungstate. Nature *370*, 571-575.

Subklewe, M., Paludan, C., Tsang, M.L., Mahnke, K., Steinman, R.M., and Munz, C. (2001). Dendritic cells cross-present latency gene products from Epstein-Barr virus-transformed B cells and expand tumor-reactive CD8(+) killer T cells. J Exp Med *193*, 405-411.

Sugimoto, S., Wandless, T.J., Shoelson, S.E., Neel, B.G., and Walsh, C.T. (1994). Activation of the SH2-containing protein tyrosine phosphatase, SH-PTP2, by phosphotyrosine-containing peptides derived from insulin receptor substrate-1. J Biol Chem *269*, 13614-13622.

Sun, J.C., and Bevan, M.J. (2003). Defective CD8 T cell memory following acute infection without CD4 T cell help. Science *300*, 339-342.

Sussman, J.J., Parihar, R., Winstead, K., and Finkelman, F.D. (2004). Prolonged culture of vaccine-primed lymphocytes results in decreased antitumor killing and change in cytokine secretion. Cancer Res *64*, 9124-9130.

Sutmuller, R.P., van Duivenvoorde, L.M., van Elsas, A., Schumacher, T.N., Wildenberg, M.E., Allison, J.P., Toes, R.E., Offringa, R., and Melief, C.J. (2001). Synergism of cytotoxic T lymphocyte-associated antigen 4 blockade and depletion of CD25(+) regulatory T cells in antitumor therapy reveals alternative pathways for suppression of autoreactive cytotoxic T lymphocyte responses. J Exp Med *194*, 823-832.

Suvas, S., Kumaraguru, U., Pack, C.D., Lee, S., and Rouse, B.T. (2003). CD4+CD25+ T cells regulate virus-specific primary and memory CD8+ T cell responses. J Exp Med *198*, 889-901.

Svane, I.M., Engel, A.M., Thomsen, A.R., and Werdelin, O. (1997). The susceptibility to cytotoxic T lymphocyte mediated lysis of chemically induced sarcomas from immunodeficient and normal mice. Scand J Immunol *45*, 28-35.

Takeda, K., Smyth, M.J., Cretney, E., Hayakawa, Y., Kayagaki, N., Yagita, H., and Okumura, K. (2002). Critical role for tumor necrosis factor-related apoptosis-inducing ligand in immune surveillance against tumor development. J Exp Med *195*, 161-169.

Tan, J.T., Ernst, B., Kieper, W.C., LeRoy, E., Sprent, J., and Surh, C.D. (2002). Interleukin (IL)-15 and IL-7 jointly regulate homeostatic proliferation of memory phenotype CD8+ cells but are not required for memory phenotype CD4+ cells. J Exp Med *195*, 1523-1532.

Tanabe, M., Karaki, S., Takiguchi, M., and Nakauchi, H. (1992). Antigen recognition by the T cell receptor is enhanced by CD8 alpha-chain binding to the alpha 3 domain of MHC class I molecules, not by signaling via the cytoplasmic domain of CD8 alpha. Int Immunol *4*, 147-152.

Tapley, P., Shevde, N.K., Schweitzer, P.A., Gallina, M., Christianson, S.W., Lin, I.L., Stein, R.B., Shultz, L.D., Rosen, J., and Lamb, P. (1997). Increased G-CSF responsiveness of bone marrow cells from hematopoietic cell phosphatase deficient viable motheaten mice. Exp Hematol *25*, 122-131.

Taylor, L., Casson, D., and Platt, M.J. (2003). Issues and experience around the Paediatric Register of Inflammatory Bowel Disease. Arch Dis Child *88*, 891-893.

Teague, R.M., Greenberg, P.D., Fowler, C., Huang, M.Z., Tan, X., Morimoto, J., Dossett, M.L., Huseby, E.S., and Ohlen, C. (2008). Peripheral CD8+ T cell tolerance to self-proteins is regulated proximally at the T cell receptor. Immunity *28*, 662-674.

Terabe, M., Park, J.M., and Berzofsky, J.A. (2004). Role of IL-13 in regulation of anti-tumor immunity and tumor growth. Cancer Immunol Immunother *53*, 79-85.

Terness, P., Bauer, T.M., Rose, L., Dufter, C., Watzlik, A., Simon, H., and Opelz, G. (2002). Inhibition of allogeneic T cell proliferation by indoleamine 2,3-dioxygenase-expressing dendritic cells: mediation of suppression by tryptophan metabolites. J Exp Med *196*, 447-457.

Terness, P., Chuang, J.J., and Opelz, G. (2006). The immunoregulatory role of IDO-producing human dendritic cells revisited. Trends Immunol *27*, 68-73.

Therasse, P., Arbuck, S.G., Eisenhauer, E.A., Wanders, J., Kaplan, R.S., Rubinstein, L., Verweij, J., Van Glabbeke, M., van Oosterom, A.T., Christian, M.C., *et al.* (2000). New guidelines to evaluate the response to treatment in solid tumors. European Organization for Research and Treatment of Cancer, National Cancer Institute of the United States, National Cancer Institute of Canada. J Natl Cancer Inst *92*, 205-216.

Thien, C.B., and Langdon, W.Y. (2001). Cbl: many adaptations to regulate protein tyrosine kinases. Nat Rev Mol Cell Biol *2*, 294-307.

Thimme, R., Appay, V., Koschella, M., Panther, E., Roth, E., Hislop, A.D., Rickinson, A.B., Rowland-Jones, S.L., Blum, H.E., and Pircher, H. (2005). Increased expression of the NK cell receptor KLRG1 by virus-specific CD8 T cells during persistent antigen stimulation. J Virol *79*, 12112-12116.

Thompson, J.A., Figlin, R.A., Sifri-Steele, C., Berenson, R.J., and Frohlich, M.W. (2003). A phase I trial of CD3/CD28-activated T cells (Xcellerated T cells) and interleukin-2 in patients with metastatic renal cell carcinoma. Clin Cancer Res *9*, 3562-3570.

Timms, J.F., Carlberg, K., Gu, H., Chen, H., Kamatkar, S., Nadler, M.J., Rohrschneider, L.R., and Neel, B.G. (1998). Identification of major binding proteins and substrates for the SH2-containing protein tyrosine phosphatase SHP-1 in macrophages. Mol Cell Biol *18*, 3838-3850.

Topp, M.S., Riddell, S.R., Akatsuka, Y., Jensen, M.C., Blattman, J.N., and Greenberg, P.D. (2003). Restoration of CD28 expression in CD28- CD8+ memory effector T cells reconstitutes antigen-induced IL-2 production. J Exp Med *198*, 947-955.

Tsui, H.W., Hasselblatt, K., Martin, A., Mok, S.C., and Tsui, F.W. (2002). Molecular mechanisms underlying SHP-1 gene expression. Eur J Biochem *269*, 3057-3064.

Turk, M.J., Guevara-Patino, J.A., Rizzuto, G.A., Engelhorn, M.E., Sakaguchi, S., and Houghton, A.N. (2004). Concomitant tumor immunity to a poorly immunogenic melanoma is prevented by regulatory T cells. J Exp Med *200*, 771-782.

Turner, J.M., Brodsky, M.H., Irving, B.A., Levin, S.D., Perlmutter, R.M., and Littman, D.R. (1990). Interaction of the unique N-terminal region of tyrosine kinase p56lck with cytoplasmic domains of CD4 and CD8 is mediated by cysteine motifs. Cell *60*, 755-765.

Uematsu, Y., Ryser, S., Dembic, Z., Borgulya, P., Krimpenfort, P., Berns, A., von Boehmer, H., and Steinmetz, M. (1988). In transgenic mice the introduced functional T cell receptor beta gene prevents expression of endogenous beta genes. Cell *52*, 831-841.

Unsoeld, H., Krautwald, S., Voehringer, D., Kunzendorf, U., and Pircher, H. (2002). Cutting edge: CCR7+ and CCR7- memory T cells do not differ in immediate effector cell function. J Immunol *169*, 638-641.

Uyttenhove, C., Pilotte, L., Theate, I., Stroobant, V., Colau, D., Parmentier, N., Boon, T., and Van den Eynde, B.J. (2003). Evidence for a tumoral immune resistance mechanism based on tryptophan degradation by indoleamine 2,3-dioxygenase. Nat Med *9*, 1269-1274.

Vaccari, M., Trindade, C.J., Venzon, D., Zanetti, M., and Franchini, G. (2005). Vaccine-induced CD8+ central memory T cells in protection from simian AIDS. J Immunol *175*, 3502-3507.

Valiante, N.M., Phillips, J.H., Lanier, L.L., and Parham, P. (1996). Killer cell inhibitory receptor recognition of human leukocyte antigen (HLA) class I blocks formation of a pp36/PLC-gamma signaling complex in human natural killer (NK) cells. J Exp Med *184*, 2243-2250.

van den Broek, M.E., Kagi, D., Ossendorp, F., Toes, R., Vamvakas, S., Lutz, W.K., Melief, C.J., Zinkernagel, R.M., and Hengartner, H. (1996). Decreased tumor surveillance in perforin-deficient mice. J Exp Med *184*, 1781-1790.

Van den Eynde, B.J., and Morel, S. (2001). Differential processing of class-I-restricted epitopes by the standard proteasome and the immunoproteasome. Curr Opin Immunol *13*, 147-153.

van Dinther-Janssen, A.C., Horst, E., Koopman, G., Newmann, W., Scheper, R.J., Meijer, C.J., and Pals, S.T. (1991). The VLA-4/VCAM-1 pathway is involved in lymphocyte adhesion to endothelium in rheumatoid synovium. J Immunol *147*, 4207-4210.

Veelken, H., Mackensen, A., Lahn, M., Kohler, G., Becker, D., Franke, B., Brennscheidt, U., Kulmburg, P., Rosenthal, F.M., Keller, H., *et al.* (1997). A phase-I clinical study of autologous tumor cells plus interleukin-2-gene-transfected allogeneic fibroblasts as a vaccine in patients with cancer. Int J Cancer *70*, 269-277.

Vely, F., Olivero, S., Olcese, L., Moretta, A., Damen, J.E., Liu, L., Krystal, G., Cambier, J.C., Daeron, M., and Vivier, E. (1997). Differential association of phosphatases with hematopoietic co-receptors bearing immunoreceptor tyrosine-based inhibition motifs. Eur J Immunol *27*, 1994-2000.

Vermeulen, A., Behlen, L., Reynolds, A., Wolfson, A., Marshall, W.S., Karpilow, J., and Khvorova, A. (2005). The contributions of dsRNA structure to Dicer specificity and efficiency. RNA *11*, 674-682.

Viguier, M., Lemaitre, F., Verola, O., Cho, M.S., Gorochov, G., Dubertret, L., Bachelez, H., Kourilsky, P., and Ferradini, L. (2004). Foxp3 expressing CD4+CD25(high) regulatory T cells are overrepresented in human metastatic melanoma lymph nodes and inhibit the function of infiltrating T cells. J Immunol *173*, 1444-1453.

Vildosola, G.H. (2000). [Hepatitis B.Vaccination Impact on Acute Disease,Chronic Carriers and Hepatocarcinoma Incidence]. Rev Gastroenterol Peru *20*, 414-421.

Villa, L.L., Costa, R.L., Petta, C.A., Andrade, R.P., Paavonen, J., Iversen, O.E., Olsson, S.E., Hoye, J., Steinwall, M., Riis-Johannessen, G., *et al.* (2006). High sustained efficacy of a prophylactic quadrivalent human papillomavirus types 6/11/16/18 L1 virus-like particle vaccine through 5 years of follow-up. Br J Cancer *95*, 1459-1466.

Viola, A., and Lanzavecchia, A. (1996). T cell activation determined by T cell receptor number and tunable thresholds. Science *273*, 104-106.

Visonneau, S., Cesano, A., Porter, D.L., Luger, S.L., Schuchter, L., Kamoun, M., Torosian, M.H., Duffy, K., Sickles, C., Stadtmauer, E.A., *et al.* (2000). Phase I trial of TALL-104 cells in patients with refractory metastatic breast cancer. Clin Cancer Res *6*, 1744-1754.

Vogelzang, A., McGuire, H.M., Yu, D., Sprent, J., Mackay, C.R., and King, C. (2008). A fundamental role for interleukin-21 in the generation of T follicular helper cells. Immunity *29*, 127-137.

Vyas, Y.M., Maniar, H., and Dupont, B. (2002). Cutting edge: differential segregation of the SRC homology 2-containing protein tyrosine phosphatase-1 within the early NK cell immune synapse distinguishes noncytolytic from cytolytic interactions. J Immunol *168*, 3150-3154.

Vyas, Y.M., Mehta, K.M., Morgan, M., Maniar, H., Butros, L., Jung, S., Burkhardt, J.K., and Dupont, B. (2001). Spatial organization of signal transduction molecules in the NK cell immune synapses during MHC class I-regulated noncytolytic and cytolytic interactions. J Immunol *167*, 4358-4367.

Wang, L.X., Shu, S., Disis, M.L., and Plautz, G.E. (2007a). Adoptive transfer of tumor-primed, in vitro-activated, CD4+ T effector cells (TEs) combined with CD8+ TEs provides intratumoral TE proliferation and synergistic antitumor response. Blood *109*, 4865-4876.

Wang, X., Michie, S.A., Xu, B., and Suzuki, Y. (2007b). Importance of IFN-gamma-mediated expression of endothelial VCAM-1 on recruitment of CD8+ T cells into the brain during chronic infection with Toxoplasma gondii. J Interferon Cytokine Res *27*, 329-338.

Wang, X., Wang, J.P., Rao, X.M., Price, J.E., Zhou, H.S., and Lachman, L.B. (2005). Prime-boost vaccination with plasmid and adenovirus gene vaccines control HER2/neu+ metastatic breast cancer in mice. Breast Cancer Res *7*, R580-588.

Wei, S., Kryczek, I., Zou, L., Daniel, B., Cheng, P., Mottram, P., Curiel, T., Lange, A., and Zou, W. (2005). Plasmacytoid dendritic cells induce CD8+ regulatory T cells in human ovarian carcinoma. Cancer Res *65*, 5020-5026.

Weninger, W., Crowley, M.A., Manjunath, N., and von Andrian, U.H. (2001). Migratory properties of naive, effector, and memory CD8(+) T cells. J Exp Med *194*, 953-966.

Wherry, E.J., and Ahmed, R. (2004). Memory CD8 T-cell differentiation during viral infection. J Virol *78*, 5535-5545.

Wherry, E.J., Blattman, J.N., and Ahmed, R. (2005). Low CD8 T-cell proliferative potential and high viral load limit the effectiveness of therapeutic vaccination. J Virol *79*, 8960-8968.

Wherry, E.J., Teichgraber, V., Becker, T.C., Masopust, D., Kaech, S.M., Antia, R., von Andrian, U.H., and Ahmed, R. (2003). Lineage relationship and protective immunity of memory CD8 T cell subsets. Nat Immunol *4*, 225-234.

Whitmarsh, A.J., and Davis, R.J. (1996). Transcription factor AP-1 regulation by mitogen-activated protein kinase signal transduction pathways. J Mol Med *74*, 589-607.

Wiedle, G., Dunon, D., and Imhof, B.A. (2001). Current concepts in lymphocyte homing and recirculation. Crit Rev Clin Lab Sci *38*, 1-31.

Wild, M.K., Cambiaggi, A., Brown, M.H., Davies, E.A., Ohno, H., Saito, T., and van der Merwe, P.A. (1999). Dependence of T cell antigen recognition on the dimensions of an accessory receptor-ligand complex. J Exp Med *190*, 31-41.

Williams, B.L., Irvin, B.J., Sutor, S.L., Chini, C.C., Yacyshyn, E., Bubeck Wardenburg, J., Dalton, M., Chan, A.C., and Abraham, R.T. (1999). Phosphorylation of Tyr319 in ZAP-70 is required for T-cell antigen receptor-dependent phospholipase C-gamma1 and Ras activation. EMBO J *18*, 1832-1844.

Williams, B.R., and Haque, S.J. (1997). Interacting pathways of interferon signaling. Semin Oncol *24*, S9-70-S79-77.

Willinger, T., Freeman, T., Herbert, M., Hasegawa, H., McMichael, A.J., and Callan, M.F. (2006). Human naive CD8 T cells down-regulate expression of the WNT pathway transcription factors lymphoid enhancer binding factor 1 and transcription factor 7 (T cell factor-1) following antigen encounter in vitro and in vivo. J Immunol *176*, 1439-1446.

Wilson, C.B., Makar, K.W., and Perez-Melgosa, M. (2002). Epigenetic regulation of T cell fate and function. J Infect Dis *185 Suppl 1*, S37-45.

Wilson, C.B., Makar, K.W., Shnyreva, M., and Fitzpatrick, D.R. (2005). DNA methylation and the expanding epigenetics of T cell lineage commitment. Semin Immunol *17*, 105-119.

Woo, E.Y., Chu, C.S., Goletz, T.J., Schlienger, K., Yeh, H., Coukos, G., Rubin, S.C., Kaiser, L.R., and June, C.H. (2001). Regulatory CD4(+)CD25(+) T cells in tumors from patients with early-stage non-small cell lung cancer and late-stage ovarian cancer. Cancer Res *61*, 4766-4772.

Wrzesinski, C., and Restifo, N.P. (2005). Less is more: lymphodepletion followed by hematopoietic stem cell transplant augments adoptive T-cell-based anti-tumor immunotherapy. Curr Opin Immunol *17*, 195-201.

Wu, Y., Nadler, M.J., Brennan, L.A., Gish, G.D., Timms, J.F., Fusaki, N., Jongstra-Bilen, J., Tada, N., Pawson, T., Wither, J., *et al.* (1998). The B-cell transmembrane protein CD72 binds to and is an in vivo substrate of the protein tyrosine phosphatase SHP-1. Curr Biol *8*, 1009-1017.

Wulfing, C., and Davis, M.M. (1998). A receptor/cytoskeletal movement triggered by costimulation during T cell activation. Science *282*, 2266-2269.

Yang, J., Liang, X., Niu, T., Meng, W., Zhao, Z., and Zhou, G.W. (1998). Crystal structure of the catalytic domain of protein-tyrosine phosphatase SHP-1. J Biol Chem *273*, 28199-28207.

Yang, J., Liu, L., He, D., Song, X., Liang, X., Zhao, Z.J., and Zhou, G.W. (2003). Crystal structure of human protein-tyrosine phosphatase SHP-1. J Biol Chem *278*, 6516-6520.

Yee, C., Thompson, J.A., Byrd, D., Riddell, S.R., Roche, P., Celis, E., and Greenberg, P.D. (2002). Adoptive T cell therapy using antigen-specific CD8+ T cell clones for the treatment of patients with metastatic melanoma: in vivo persistence, migration, and antitumor effect of transferred T cells. Proc Natl Acad Sci U S A *99*, 16168-16173.

Yee, C., Thompson, J.A., Roche, P., Byrd, D.R., Lee, P.P., Piepkorn, M., Kenyon, K., Davis, M.M., Riddell, S.R., and Greenberg, P.D. (2000). Melanocyte destruction after antigen-specific immunotherapy of melanoma: direct evidence of t cell-mediated vitiligo. J Exp Med *192*, 1637-1644.

Yi, T., Gilbert, D.J., Jenkins, N.A., Copeland, N.G., and Ihle, J.N. (1992a). Assignment of a novel protein tyrosine phosphatase gene (Hcph) to mouse chromosome 6. Genomics *14*, 793-795.

Yi, T.L., Cleveland, J.L., and Ihle, J.N. (1992b). Protein tyrosine phosphatase containing SH2 domains: characterization, preferential expression in hematopoietic cells, and localization to human chromosome 12p12-p13. Mol Cell Biol *12*, 836-846.

Yu, Z., Maoui, M., Zhao, Z.J., Li, Y., and Shen, S.H. (2006). SHP-1 dephosphorylates 3BP2 and potentially downregulates 3BP2-mediated T cell antigen receptor signaling. FEBS J *273*, 2195-2205.

Zabel, B.A., Agace, W.W., Campbell, J.J., Heath, H.M., Parent, D., Roberts, A.I., Ebert, E.C., Kassam, N., Qin, S., Zovko, M., *et al.* (1999). Human G protein-coupled receptor GPR-9-6/CC chemokine receptor 9 is selectively expressed on intestinal homing T lymphocytes, mucosal lymphocytes, and thymocytes and is required for thymus-expressed chemokine-mediated chemotaxis. J Exp Med *190*, 1241-1256.

Zamore, P.D., Tuschl, T., Sharp, P.A., and Bartel, D.P. (2000). RNAi: double-stranded RNA directs the ATP-dependent cleavage of mRNA at 21 to 23 nucleotide intervals. Cell *101*, 25-33.

Zeng, R., Spolski, R., Finkelstein, S.E., Oh, S., Kovanen, P.E., Hinrichs, C.S., Pise-Masison, C.A., Radonovich, M.F., Brady, J.N., Restifo, N.P., *et al.* (2005). Synergy of IL-21 and IL-15 in regulating CD8+ T cell expansion and function. J Exp Med *201*, 139-148.

Zerrahn, J., Held, W., and Raulet, D.H. (1997). The MHC reactivity of the T cell repertoire prior to positive and negative selection. Cell *88*, 627-636.

Zhang, J., Somani, A.K., Watt, S., Mills, G.B., and Siminovitch, K.A. (1999a). The Src-homology domain 2-bearing protein tyrosine phosphatase-1 inhibits antigen receptor-induced apoptosis of activated peripheral T cells. J Immunol *162*, 6359-6367.

Zhang, J., Somani, A.K., Yuen, D., Yang, Y., Love, P.E., and Siminovitch, K.A. (1999b). Involvement of the SHP-1 tyrosine phosphatase in regulation of T cell selection. J Immunol *163*, 3012-3021.

Zhang, W., and Samelson, L.E. (2000). The role of membrane-associated adaptors in T cell receptor signalling. Semin Immunol *12*, 35-41.

Zhang, W., Trible, R.P., Zhu, M., Liu, S.K., McGlade, C.J., and Samelson, L.E. (2000). Association of Grb2, Gads, and phospholipase C-gamma 1 with phosphorylated LAT tyrosine residues. Effect of LAT tyrosine mutations on T cell angigen receptor-mediated signaling. J Biol Chem *275*, 23355-23361.

Zhang, Z., Shen, K., Lu, W., and Cole, P.A. (2003). The role of C-terminal tyrosine phosphorylation in the regulation of SHP-1 explored via expressed protein ligation. J Biol Chem *278*, 4668-4674.

Zhao, Z., Bouchard, P., Diltz, C.D., Shen, S.H., and Fischer, E.H. (1993). Purification and characterization of a protein tyrosine phosphatase containing SH2 domains. J Biol Chem *268*, 2816-2820.

Zhou, H., Luo, Y., Kaplan, C.D., Kruger, J.A., Lee, S.H., Xiang, R., and Reisfeld, R.A. (2006). A DNA-based cancer vaccine enhances lymphocyte cross talk by engaging the NKG2D receptor. Blood *107*, 3251-3257.

Zhou, H., Luo, Y., Lo, J.F., Kaplan, C.D., Mizutani, M., Mizutani, N., Lee, J.D., Primus, F.J., Becker, J.C., Xiang, R., *et al.* (2005a). DNA-based vaccines activate innate and adaptive antitumor immunity by engaging the NKG2D receptor. Proc Natl Acad Sci U S A *102*, 10846-10851.

Zhou, J., Shen, X., Huang, J., Hodes, R.J., Rosenberg, S.A., and Robbins, P.F. (2005b). Telomere length of transferred lymphocytes correlates with in vivo persistence and tumor regression in melanoma patients receiving cell transfer therapy. J Immunol *175*, 7046-7052.

Zinkernagel, R.M., Callahan, G.N., Klein, J., and Dennert, G. (1978). Cytotoxic T cells learn specificity for self H-2 during differentiation in the thymus. Nature *271*, 251-253.

Zippelius, A., Batard, P., Rubio-Godoy, V., Bioley, G., Lienard, D., Lejeune, F., Rimoldi, D., Guillaume, P., Meidenbauer, N., Mackensen, A., *et al.* (2004). Effector function of human tumor-specific CD8 T cells in melanoma lesions: a state of local functional tolerance. Cancer Res *64*, 2865-2873.

Zou, W. (2006). Regulatory T cells, tumour immunity and immunotherapy. Nat Rev Immunol *6*, 295-307.

Appendix

Sathish, J.G., Dolton, G., Leroy, F.G., and Matthews, R.J. (2007). Loss of Src homology region 2 domain-containing protein tyrosine phosphatase-1 increases CD8+ T cell-APC conjugate formation and is associated with enhanced in vivo CTL function. J Immunol *178*, 330-337.

Loss of Src Homology Region 2 Domain-Containing Protein Tyrosine Phosphatase-1 Increases CD8$^+$ T Cell-APC Conjugate Formation and Is Associated with Enhanced In Vivo CTL Function[1]

Jean G. Sathish,[2] Garry Dolton, Frances G. LeRoy, and R. James Matthews[3]

Extensive evidence has been accumulated to implicate the intracellular protein tyrosine phosphatase, Src homology region 2 domain-containing protein tyrosine phosphatase-1 (SHP-1), as a negative regulator of TCR-signaling thresholds. Specifically, T cells from the SHP-1-deficient mouse, motheaten, exhibit a hyperproliferative phenotype when activated by cognate peptide-pulsed APCs. However, the cellular basis for this phenotype has not been fully explained. Using the intracellular fluorescent dye, CFSE, we show that a greater proportion of motheaten vs control naive CD8$^+$ T cells undergo cell division when activated by peptide-pulsed APCs. Furthermore, there is a greater likelihood of TCRs on SHP-1-deficient vs control T cells binding to peptide/MHC ligands on APCs when using TCR down-regulation as an indirect measure of TCR engagement. In addition, T cell-APC conjugate assays provide direct evidence that a greater proportion of SHP-1-deficient T cells are capable of forming stable conjugates with APCs and this may explain, at least in part, their hyperproliferative response to TCR-triggered stimulation. The physiological relevance of the combined in vitro observations is demonstrated by the significantly enhanced in vivo expansion and CTL capacity generated in mice receiving adoptively transferred SHP-1-deficient naive CD8$^+$ T cells when compared with control T cells. ***The Journal of Immunology,*** **2007, 178: 330–337.**

A necessary prelude to T cell activation is the physical encounter and sustained contact with an APC. A prolonged contact of the T cell with the APC is essential to sustain TCR signaling and up to 20 h of such conjugation may be necessary for a naive T cell to commit to a program of full activation (1). Furthermore, the duration of stimulus received by the T cell when in contact with the APC determines its capacity to subsequently respond to homeostatic and proliferative cytokines (2). In vivo-imaging studies (3–7) also point to lengthy interactions of T cells and dendritic cells (DCs)[4] occurring within lymph nodes (LNs) and these interactions are thought to be a prerequisite for T cell activation.

The major physical mechanism by which T cells adhere to APCs is by the binding of lymphocyte integrins on the T cell to their counterligands on the APC. Foremost among the adhesion molecules required for supporting T cell-APC conjugates is the β_2 integrin, LFA-1, on T cells that binds to ICAM-1 on the APCs. T cells deficient in LFA-1 are impaired in their ability to form conjugates with APCs (8) and likewise, Abs directed against LFA-1 can block conjugate formation (9). T cell integrins normally display a state of low-binding activity toward their ligands. However, engagement of TCRs by peptide-MHC complexes on the APCs initiates signals that lead to shape changes and reorganization of the T cell actin cytoskeleton (10–13), ultimately resulting in the activation of integrins, primarily LFA-1 (14). The binding of T cell integrins to their ligands on the APC supports a stable and physical cell-cell conjugate that provides the platform for sustained signaling thus resulting in gene transcription, cytokine production, blasting, and T cell proliferation (15).

It is clear that the cellular and molecular factors influencing T cell-APC conjugate formation need to be fully understood as they are predicted to have a significant impact on T cell responsiveness and the eventual immune response. In addition to adhesion receptors, several signaling molecules including adhesion and degranulation-promoting adaptor protein (16, 17), Vav1 (18), inducible T cell kinase (19) and Src kinase-associated phosphoprotein of 55 kDa (20), and an intact actin cytoskeleton (21, 22) have been shown to be required or to assist in conjugate formation. However, negative regulators of conjugate formation have hitherto not been reported. The Src homology 2 domain containing protein tyrosine phosphatase-1 (SHP-1)-deficient motheaten mouse has been instrumental in demonstrating that SHP-1 functions to raise the signaling thresholds required for triggering through the TCR in both T cell development and in peripheral T cell activation (23, 24). To dissect the role of SHP-1 in T cells in an Ag-specific context, we have introduced the MHC class I-restricted transgenic TCR, F5 (25), into the motheaten genetic background (26). The F5 TCR recognizes a peptide derived from the influenza A virus nucleoprotein, in the context of the MHC molecule H2-D^b (27). When motheaten LN T cells bearing the F5 TCR are stimulated with cognate peptide-pulsed APCs, they exhibit a greater degree of proliferation as measured by tritiated thymidine incorporation (26)

Section of Infection and Immunity, Department of Medical Biochemistry and Immunology, School of Medicine, Cardiff University, Heath Park, Cardiff, United Kingdom

Received for publication July 10, 2006. Accepted for publication October 17, 2006.

The costs of publication of this article were defrayed in part by the payment of page charges. This article must therefore be hereby marked *advertisement* in accordance with 18 U.S.C. Section 1734 solely to indicate this fact.

[1] This work was supported by Project Grant 065556 from the Wellcome Trust and Project Grant G0100191 from the Medical Research Council (to R.J.M.) and a PhD Studentship from the Tenovus Charity (to G.D.).

[2] Current address: Division of Pharmacology and Therapeutics, School of Biomedical Sciences, Sherrington Buildings, University of Liverpool, Liverpool, U.K.

[3] Address correspondence and reprint requests to Dr. R. James Matthews, Section of Infection and Immunity, Department of Medical Biochemistry and Immunology, School of Medicine, Cardiff University, Heath Park, Cardiff CF14 4XX, U.K.

[4] Abbreviations used in this paper: DC, dendritic cell; LN, lymph node; SHP-1, Src homology region 2 domain-containing protein tyrosine phosphatase.

when compared with LN T cells derived from littermate controls. This finding is consistent with similar studies using different transgenic TCRs on the motheaten genetic background (23, 24). However, the cellular basis and in vivo significance of this hyperproliferative phenotype has not been fully established.

In this study, population analyses of motheaten and control T cells were performed to examine whether SHP-1 influences the frequency with which individual T cells are able to enter into cell division. We found that SHP-1 activity has a striking impact on the ability of TCR-stimulated naive $CD8^+$ T cells to enter into cell division. In the absence of SHP-1, the likelihood of a T cell dividing following incubation with Ag-pulsed APCs was significantly increased as demonstrated by a 2-fold increase in the proportion of motheaten vs control T cells that participate in clonal expansion. Further investigations demonstrated that the percentage of SHP-1-deficient vs control T cells that had engaged TCRs was increased substantially and this correlated with an enhanced capacity of SHP-1-deficient T cells to form T cell-APC conjugates. Importantly, the increased in vitro responses of SHP-1-deficient T cells could be replicated in an in vivo context whereby the adoptive transfer and in vivo activation of naive motheaten vs control $CD8^+$ T cells resulted in an increased expansion of effectors and an elevated cytolysis of target cells.

Materials and Methods

Mice

C57BL/6J mice heterozygous at the motheaten locus (C57BL/6J *me/+*) were originally obtained from Dr. L. Shultz at The Jackson Laboratory. The F5-transgenic TCR was introduced into the motheaten genetic background as described in Ref. 26 and motheaten and littermate control mice for experimentation were obtained from litters arising from pairings between C57BL/6J *me/+* and $F5^{homozygous}$ *me/+* mice. The F5 TCR uses the *Vα4* and *Vβ11* gene segments of the TCR α- and β-chain genes, respectively. Motheaten and control mice were sacrificed between 9 and 13 days postpartum and LNs (inguinal, axial, brachial, and submandibular) harvested. C57BL/6J mice purchased from The Jackson Laboratory and C57BL/6J. Rag-$1^{-/-}$ mice provided by Dr. F. Powrie (Sir William Dunn School of Pathology, Oxford University, Oxford, U.K.) were maintained as breeding colonies in our animal facility. All animal experimentation was conducted in accordance with the U.K. Animal (Scientific Procedures) Act 1986 under Project Licenses PPL 30/1715 and 30/2266.

Cells and cell cultures

The mouse B cell line, AB, was generated from H-2^{kxb} bone marrow-derived B cells transformed with Abelson leukemia virus and was a gift from Prof. E. Simpson (Imperial College, London, U.K.; Ref. 28). This cell line was maintained in complete DMEM supplemented with 50 μM 2-ME. Bone marrow-derived DCs were grown as described in Ref. 29. Briefly, bone marrow was flushed from the tibia of C57BL/6J mice and cultured on bacteriological plates in complete RPMI 1640 supplemented with 200 U/ml recombinant mouse GM-CSF (Sigma-Aldrich). At days 5 and 8, half the medium was replaced and 100 U/ml recombinant mouse GM-CSF was added. At day 10, 1 μg/ml LPS was added and 24 h later, mature DCs were pulsed with 5 μM NP68 and used experimentally. Purified $CD8^+$ T cells were obtained by negative depletion of $CD4^+$ T cells, B cells, and myeloid cells with CD4, CD11b, and B220 microbeads (Miltenyi Biotec) or where indicated by positive purification with CD8 microbeads (Miltenyi Biotec) and used in the experiments.

T cell proliferation assay

For cell division measured by CFSE dilution, purified $CD8^+$ T cells were labeled with 2 μM CFSE (Molecular Probes) for 10 min in HBSS at 37°C. Labeling was stopped by addition of FCS and cells were washed and resuspended in complete DMEM. A total of 1×10^6 CFSE-labeled T cells were incubated with 1×10^6 irradiated, peptide-pulsed AB cells for 48 h. At the end of the stimulation, T cells were stained with anti-$CD8a^{TC}$ and acquired by flow cytometry. T cell proliferation was measured by CFSE fluorescence dilution of the electronically gated $CD8^+$ T cell population. CFSE profiles were analyzed using the proliferation platform of the FlowJo software program (Tree Star). The division index indicates the average number of divisions that a T cell in the starting population underwent and the proliferation index is defined as the average number of divisions undergone by those T cells in the starting population that did divide.

Flow cytometry

Cells were washed and incubated with the indicated conjugated Abs in stain buffer (Cell Wash, 2% BSA, and 2 mM EDTA) for 30 min on ice. Conjugated Abs were obtained as follows; anti-$CD8a^{TC}$ was from Caltag Laboratories, anti-$TCR\alpha\beta^{PE}$, anti-$CD8a^{PE}$, anti-$CD11^{FITC}$, anti-$CD49d^{FITC}$ and anti$CD49e^{FITC}$ were purchased from BD Pharmingen while anti-$V\beta11^{FITC}$ was a gift of Dr. D. Kioussis, National Institute for Medical Research (Mill Hill, London, U.K.). Following incubation, cells were washed and acquired on a flow cytometer (FACSCalibur; BD Biosciences) and analyzed by CellQuest Software.

TCR down-regulation assay

Purified $CD8^+$ T cells were incubated with AB cells pulsed with a saturating (10 μM) concentration of NP68 peptide in FACS tubes for 4 h. At the end of the incubation, the cells were washed with Cell Wash (BD Biosciences) and stained with anti-$V\beta11^{FITC}$ (KT-11) and anti-$CD8a^{TC}$ in stain buffer for 30 min on ice followed by washing. The cells were acquired on the flow cytometer and TCR down-regulation assessed on the electronically gated $CD8^+$ T cell population. For anti-CD3-induced down-regulation, T cells were incubated with a titration of anti-$CD3^{Bio}$ ranging from 1.25 to 20 μg/ml on ice for 30 min followed by cross-linking with streptavidin (Pierce Biotechnology) for an additional 30 min on ice. The cells were then incubated at 37°C for 45 min and TCR down-regulation stopped by addition of ice-cold Cell Wash (containing NaN_3). Cells were then stained with anti-$CD8a^{TC}$ and anti-$TCR\alpha\beta^{PE}$, acquired on the flow cytometer and TCR down-regulation was measured as indicated above.

Conjugate assay

A total of 1×10^6 AB cells that express H-$2D^b$ were labeled with 0.1 μM CFSE, pulsed with peptide and incubated with 1×10^6 purified $CD8^+$ T cells in FACS tubes. The tubes were vortexed and conjugates allowed to form by incubation at 37°C for 90 min. Nonspecific conjugates were dispersed by vortexing and cells fixed with 4% paraformaldehyde. Cells were washed, stained with anti-$CD8a^{TC}$, acquired by flow cytometry and analyzed on the electronically gated $CD8^+$ T cell population for conjugate formation. Blocking experiments were conducted by incubating T cells with anti-CD18 integrin Ab (GAME-46; BD Pharmingen) before performing the conjugate assay.

Adhesion assay

Flat-bottom 96-well plates were coated overnight with 10 μg/ml rICAM-1 Fc chimera (Chemicon International) or 30 μg/ml fibronectin (Sigma-Aldrich) in PBS with or without 10 μg/ml anti-CD3. The plates were washed and blocked with 2.5% BSA for 2 h. Purified $CD8^+$ T cells were labeled with 1 μM of the fluorescent dye, 2′,7′-bis(2-carboxyethyl)-5-(and-6)-carboxyfluorescein, acetoxymethyl ester (Calbiochem), resuspended in 2.5% BSA in PBS and seeded at a density of 5×10^5/well. Cell adhesion was allowed to proceed for 30 min at 37°C followed by gently washing of the wells with warmed PBS, 2.5% BSA. Adhesion was quantified by recording fluorescence emission using a Fluostar Optima fluorescence microplate reader (BMG Labtech).

In vivo T cell expansion and cytotoxicity assays

To gauge T cell expansion in vivo, 3.5×10^6 positively purified $CD8^+$ T cells were injected i.v. into C57BL/6J. Rag-$1^{-/-}$ recipient female mice. The recipient mice were subsequently challenged with 100 μg of NP68 peptide in IFA. Six days later, the mice were killed and spleens were harvested and homogenized. Before RBC lysis, the homogenized splenocytes were mixed with an additional reference splenocyte population to facilitate accurate quantitation of the expanded $CD8^+$ T cells in the recipient mice. The reference population consisted of 0.5×10^6 reference splenocytes that had been labeled with 0.2 μM CFSE following their isolation from a C57BL/6J mouse. The mixed splenocyte populations were stained with anti-$CD8^{PE}$ and analyzed by flow cytometry. The percentage of adoptively transferred and expanded $CD8^+$ T cells was assessed by comparison with a defined number of the CFSE-labeled reference splenocytes. To measure in vivo cytotoxicity, $2–3 \times 10^6$ positively purified CD8 T cells were injected i.v. into sublethally (650 cGy) irradiated C57BL/6J recipient female mice. Reference recipient mice received no T cells. In parallel, 4×10^6 mature DCs, pulsed with 5 μM NP68 peptide, were injected i.p. into recipient mice. Six days later, splenocyte targets from naive mice were labeled with either 2 or 0.2 μM CFSE. Splenocyte targets labeled with 0.2 μM CFSE were pulsed for 1 h with 5 μM NP68 while

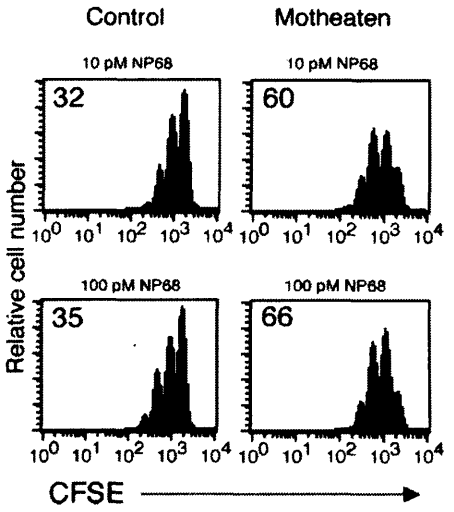


FIGURE 1. An increased proportion of motheaten F5 TCR T cells are capable of proliferating following TCR stimulation. LN T cells from motheaten and littermate control mice expressing the F5 TCR were labeled with 2 μm of CFSE and incubated for 48 h with irradiated AB cells pulsed with 10 or 100 pM NP68 peptide. The cells were stained with anti-CD8a^{TC}, acquired by flow cytometry, and the electronically gated CD8$^+$ T cell population analyzed for CFSE fluorescence. The percentage of naive T cells from the initial starting population that have entered into division is indicated in each histogram. Results are representative of three independent experiments.

the targets labeled with 2 μM CFSE were left unpulsed. Equal numbers (10×10^6) of the two target populations were mixed and injected i.v. into the recipient mice. After an additional 24 h, recipient mice were killed, spleens harvested, single-cell suspensions prepared and the proportions of differentially CFSE-labeled target cells were assessed by flow cytometry. The percent-specific lysis was calculated using the equation: percent-specific lysis = 100 − (((% survival in peptide-pulsed + T cells/% survival in unpulsed + T cells)/(% survival in peptide pulsed + no T cells/% survival in unpulsed and no T cells)) × 100) (30).

Results

A higher frequency of motheaten T cells undergo cell division upon stimulation

Previous studies have demonstrated that SHP-1-deficient motheaten T cells hyperproliferate when stimulated by peptide-bearing APCs (23, 24, 26). In each of these studies, a consistent finding was that motheaten T cells exhibited a higher proliferative capacity at all the doses of peptide tested. Although [^{3}H]thymidine incorporation is a sensitive measure of proliferative activity, it does not distinguish between the possibility that a limited number of motheaten T cells underwent multiple rounds of cell division or that a larger proportion of the initial SHP-1-deficient T cell population entered into cell division. Both these processes could account for the increased [^{3}H]thymidine incorporation by motheaten T cells when compared with control T cells. Labeling T cells with the intracellular fluorescent dye, CFSE, allows one to address this particular question. Therefore, we used CFSE labeling to track cell division in motheaten and control T cells. As shown in Fig. 1, when control T cells were stimulated by APCs pulsed with 10 pM NP68, 32% of the initial CD8$^+$ T cell population underwent cell division. However, the same stimulus elicited an ~2-fold increase (62%) in the proportion of motheaten T cells that entered into cell division. An increase in the concentration of cognate peptide used to stimulate the T cells did not significantly alter the relative proportions of motheaten and control T cells induced to divide. A comparison of the proliferation indices for motheaten and control T cells suggested that once entered into cell cycle, the differences between motheaten and control T cells in terms of number of subsequent divisions are less pronounced (Table I). Finally, neither motheaten nor control T cells underwent spontaneous cell division when incubated with unpulsed APCs (result not shown).

Table I. *Quantitative analysis of motheaten and control CD8$^+$ T cell proliferation in vitro*

Culture	NP68 (pM)	Division Index[a]	Proliferation Index[b]
Control	10	0.4	1.2
	100	0.5	1.3
Motheaten	10	0.9	1.4
	100	1.4	1.4

[a] Measure of the average number of divisions that a T cell in the starting population underwent.
[b] Measure of the average number of divisions undergone by a T cell that did divide.

Higher proportion of motheaten T cells down-regulate TCRs in response to APCs

The increased entry into cell division (Fig. 1) was consistent with a lowered TCR-signaling threshold in the absence of SHP-1 but assumed equivalent engagement of TCR on motheaten and control T cells. It was therefore necessary to explore whether there was an altered likelihood of motheaten vs control T cells encountering Ag presented by MHC class I on the APCs. It has been observed previously that in vitro TCR engagement by MHC/peptide complexes or cross-linking with Abs triggers down-regulation of the TCR from the T cell surface (31). Accordingly, TCR down-regulation can be used as a valid indicator of Ag encounter by a T cell (21, 32). Therefore, we measured TCR down-regulation to ascertain whether motheaten T cells experienced an altered frequency of Ag encounter. It is important to note that equal proportions of motheaten and control CD8$^+$ T cells purified from the LNs expressed the F5 TCR as assessed by staining with KT11, a mAb

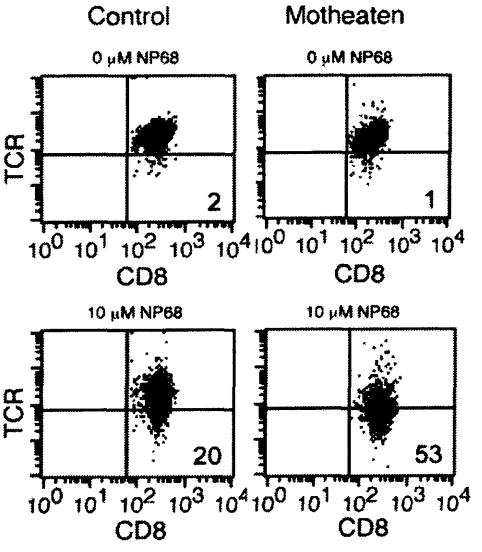


FIGURE 2. A higher proportion of motheaten vs control F5 TCR T cells down-regulate TCRs following incubation with peptide-pulsed APCs. Purified motheaten and control CD8$^+$ T cells expressing the F5 TCR were incubated for 4 h with AB cells left unpulsed or pulsed with 10 μM NP68 peptide. Following incubation cells were stained with anti-vβ11-FITC and anti-CD8a^{TC} and TCR down-regulation assessed by flow cytometry on the electronically gated CD8$^+$ T cell population. The percentage of naive T cells that have down-regulated TCR is indicated in each dot plot. Results are representative of three independent experiments.

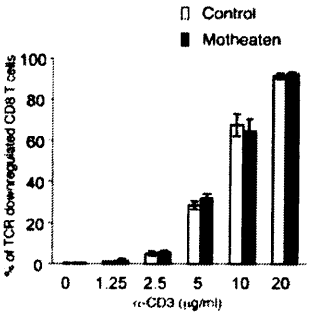


FIGURE 3. Equivalent down-regulation of F5 TCR on motheaten and control T cells following triggering with cross-linked soluble anti-CD3 Ab. Purified motheaten and control $CD8^+$ T cells expressing the F5 TCR were left unstimulated or incubated with a titration of anti-$CD3^{Bio}$ ranging from 1.25 to 20 μg/ml for 30 min on ice followed by cross-linking with streptavidin for an additional 30 min. T cells were incubated for an additional 45 min at 37°C before staining with anti-$CD8^{TC}$ and anti-$TCR\alpha\beta^{PE}$ and assessed by flow cytometry for TCR down-regulation. The graph shows the mean percentage of triplicate samples of naive T cells that have down-regulated TCR. Error bars represent SDs. Results are representative of three independent experiments.

specific for TCRs using the *Vβ11* gene segment. As shown in Fig. 2, when motheaten and control T cells were incubated with unpulsed APCs, a small proportion (1–2%) of each T cell population demonstrated a basal, low-level down-modulation of TCR. However, when control T cells were exposed to APCs pulsed with saturating concentration of cognate peptide, ~20% of the total T cell population exhibited a down-regulation of cell surface TCRs. Furthermore, the same stimulus given to motheaten T cells resulted in a >2-fold increase in the proportion (53%) of T cells with down-regulated TCRs. The important inference from this result is that motheaten T cells are endowed with an increased capacity to engage Ag-bearing APCs. It is possible, however, that the increased TCR down-regulation of motheaten T cells was due to an enhanced intrinsic capacity of these T cells to down-regulate TCR rather than an increased frequency in engaging Ag-bearing APCs. To distinguish between these two possibilities, we measured TCR down-regulation following cross-linking with soluble anti-CD3 Ab. This approach eliminates any contribution made to TCR down-regulation by the interaction of the APC with the T cell. The anti-CD3 Ab is expected to cross-link TCRs on motheaten and control T cells to an equal degree. As demonstrated in Fig. 3, both motheaten and control T cells revealed equivalent TCR down-regulation after 45 min of cross-linking the TCR/CD3 complex with a range of concentrations of anti-CD3 Ab. This indicates that, following direct CD3 cross-linking at least, the intrinsic process of TCR internalization proceeds to a similar degree in motheaten and control T cells.

Increased APC-T cell conjugate formation by motheaten T cells that is LFA-1 dependent

The enhanced down-regulation of TCR detected on motheaten vs control T cells when presented with APC-bearing peptide but not with soluble anti-CD3 Ab was suggestive of an increased ability of motheaten F_5 T cells to engage APCs. Therefore, we predicted that motheaten T cells may have an altered capacity to form conjugates with peptide-pulsed APCs and performed conjugate assays to test this hypothesis. The AB cells were labeled with CFSE to facilitate identification of the T-B cell conjugates. Fig. 4 shows that when control $CD8^+$ T cells were incubated with AB cells pulsed with NP68 peptide at a concentration of 10 pM, the percentage of T cells that formed stable conjugates increased from a baseline of ~6% to that of 28%. However, motheaten T cells showed a significantly higher frequency (57%) of conjugate formation when presented with the same concentration of peptide. The result of this experiment demonstrated that the lack of SHP-1 in the motheaten T cells confers an enhanced capacity to engage and form stable conjugates with the APC and this is manifested as an increased frequency of T cell-APC conjugates.

Conjugate formation is supported by the binding of T cell integrins to counterligands on the APC. LFA-1 is the critical integrin that mediates T-B cell conjugation (8) and it was therefore important to investigate whether the motheaten T cells retained a similar dependence on LFA-1 engagement for conjugate formation. Conjugate formation was therefore examined following blocking of LFA-1-ICAM-1 interaction using an anti-LFA-1 Ab. Fig. 4 shows that when motheaten and control T cells were incubated with unpulsed APCs and anti-LFA-1 Ab, the basal level of conjugate formation was reduced from 6 to 2% for both populations of T cells.

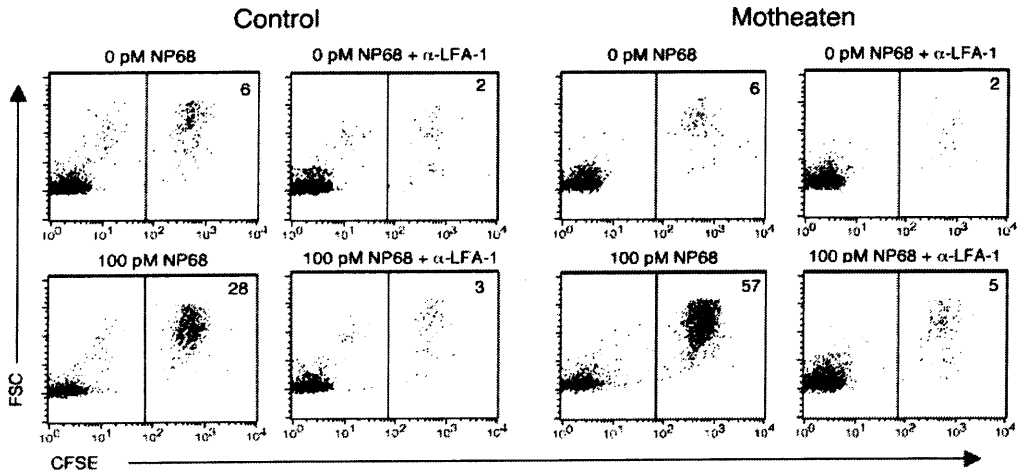


FIGURE 4. Increased number of LFA-1-dependent APC-T cell conjugates formed by motheaten F5 T cells. Purified motheaten and control $CD8^+$ T cells expressing the F5 TCR were incubated with or without anti-CD18 Ab before incubation for 90 min at 37°C with AB cells labeled with 0.1 μM CFSE and left unpulsed or pulsed with 100 pM NP68 peptide. Nonspecific conjugates were dispersed by vortexing and conjugates stained with anti-$CD8^{TC}$. APC-T cell conjugates were identified by flow cytometry on the electronically gated $CD8^+$ T cell population based upon increased FSC and CFSE fluorescence of conjugated cells. The percentage of naive $CD8^+$ T cells that have formed conjugates with the APCs is indicated in each dot plot. Results are representative of three independent experiments.

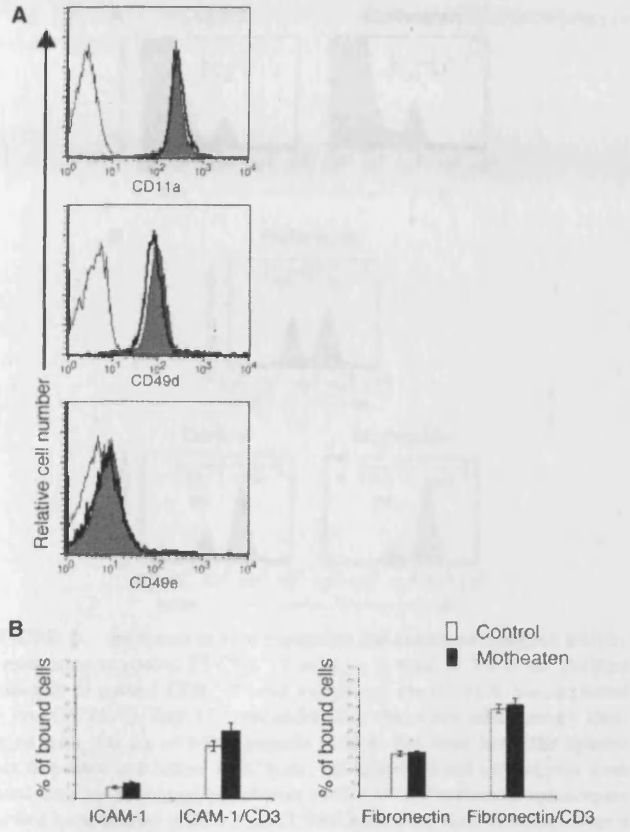


FIGURE 5. Equivalent integrin expression and adhesion of motheaten and control T cells to plate-bound ICAM-1 and fibronectin. *A*, LN cells from motheaten and control were stained with anti-$CD8^{TC}$ and one of three FITC conjugates, anti-CD11a, anti-CD49d, and anti-CD49e. Integrin α-chain expression was assessed by flow cytometry on electronically gated populations $CD8^+$ T cell populations. Histograms depicting integrin expression for motheaten and control T cells are shown and are representative of three independent experiments. Filled and bold-line histograms represent control and motheaten T cell, respectively. Staining with isotype-matched controls is indicated by the open histograms. *B*, Purified motheaten and control $CD8^+$ T cells expressing the F5 TCR were labeled with 1 μM BCECF/AM and seeded at a density of 5×10^5/well precoated with 10 μg/ml rICAM-1 Fc chimera or 30 μg/ml fibronectin with or without 10 μg/ml anti-CD3. Cells were incubated for 30 min at 37°C followed by gentle washing and adhesion assessed as recorded fluorescence. Bar graphs show the mean percentages of bound T cells in each of the four experimental conditions. Error bars represent SDs. Results are representative of five independent experiments.

Furthermore, blocking LFA-1 binding resulted in a similar complete inhibition of conjugate formation for both the motheaten and control T cells following activation with B cells pulsed with 10 pM NP68 peptide. It is therefore apparent from this result that motheaten T cells retain an equivalent dependence on LFA-1 for conjugate formation when compared with control T cells.

Equivalent adhesion of motheaten and control T cells to ICAM-1 and fibronectin

Given the dependence upon LFA-1 for motheaten and control T cells to form conjugates, it is possible that the increased numbers of motheaten T cells forming conjugates could be due to a higher expression of LFA-1 on the surface of motheaten T cells. To test this possibility, the expression of the α-chain of LFA-1 and related T cell integrins, VLA-4 and VLA-5, was examined by flow cytometry. As shown in Fig. 5*A*, both the motheaten and control T cells displayed an equivalent expression of LFA-1, VLA-4, and VLA-5. We conclude from these results that the differences in conjugate formation between motheaten and control T cells cannot be attributed to differential integrin expression. Under resting conditions, T cell integrins do not exhibit a significant level of binding activity to their ligands. However, upon activating the T cell through TCR engagement, integrin binding to ligand is up-regulated by a modulation of integrin affinity and avidity (14). Although the expression levels of surface integrins are similar in the motheaten and control T cells, it is possible that TCR-induced activation might result in enhanced integrin activation in the motheaten T cells. This may then lead to increased conjugate formation. To examine this possibility, we fluorescently labeled motheaten and control T cells and performed adhesion assays. T cells were allowed to adhere onto wells coated with the LFA-1 ligand, ICAM-1, either alone or in conjunction with anti-CD3 (Fig. 5*B*). Alternatively, T cell adhesion to wells coated with the VLA-4 and 5 ligand, fibronectin, either singly or in conjunction with anti-CD3, was analyzed (Fig. 5*B*). The combined results of these experiments indicated that motheaten and control T cells adhere to plate-bound integrin ligands to an equal degree, both basally and following anti-CD3 stimulation.

Enhanced in vivo expansion and cytolysis by motheaten T cells

The increased conjugation of motheaten $CD8^+$ T cells to APCs is likely to provide the basis for the enhanced proliferative capacity of these T cells that is observed in vitro. However, the physiological requirements placed upon a naive $CD8^+$ T cell for expansion in vivo are more complex and include entry into peripheral LNs leading to encounter with Ag-presenting DCs. Hence, it was important to explore whether loss of SHP-1 in $CD8^+$ T cells also translates into enhanced expansion in vivo. The severe autoreactivity and early morbidity associated with the motheaten phenotype (33) precludes any direct in vivo experimentation. Therefore, to address the issue of in vivo relevance, equivalent numbers of naive F5 $CD8^+$ T cells purified from either motheaten or littermate control mice were adoptively transferred into irradiated recipient mice that were then subjected to Ag challenge. Significantly increased percentages of motheaten vs control $CD8^+$ T cells were detected in the spleens of recipient mice 6-day posttransfer and following in vivo TCR stimulation (Fig. 6*A*).

We also examined whether the increased in vivo generation of SHP-1-deficient T cell effectors following adoptive transfer and antigenic challenge correlated with an enhanced killing capacity. To address this question, equivalent numbers of naive F5 $CD8^+$ T cells from either motheaten or littermate control mice were adoptively transferred into irradiated recipient mice subsequently administered with mature DCs pulsed with NP68 peptide. Six days later, after the generation of mature effector $CD8^+$ T cells, the mice were injected with equal numbers of splenocyte targets that had been pulsed or not with NP68 peptide and differentially labeled with CFSE. An additional 24 h later, the proportions of differentially CFSE-labeled cells were assessed as a measure of in vivo CTL activity. Fig. 6*B* reveals that in vivo CTL activity was readily detected in recipient mice receiving wild-type T cells but the level of killing was significantly increased (84 vs 56%) in mice receiving motheaten T cells. In reference recipient mice that received no adoptively transferred T cells, equivalent numbers of each population of target splenocytes were detected. Importantly, these results demonstrate that the increased in vivo expansion of motheaten $CD8^+$ T cells also extends to an elevated cytolysis of target cells.

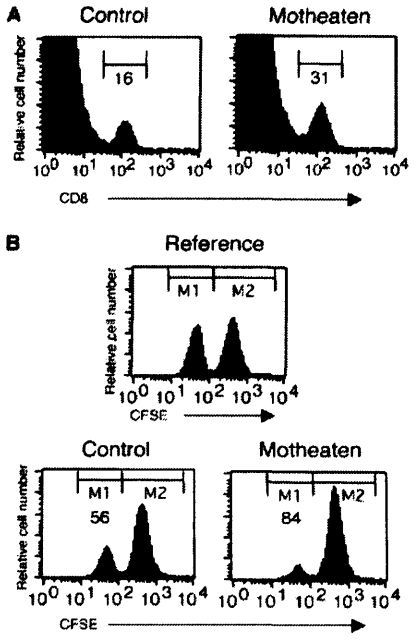


FIGURE 6. Increased in vivo expansion and enhanced cytolytic activity of motheaten vs control F5 $CD8^+$ T cells. *A*, A total of 3.5×10^6 purified motheaten or control $CD8^+$ T cells expressing the F5 TCR were injected i.v. into C57BL/6J. Rag-$1^{-/-}$ recipient mice that were subsequently challenged with 100 μg of NP68 peptide in IFA. Six days later, the spleens were harvested and before RBC lysis, the homogenized splenocytes were mixed with an additional population of 0.5×10^6 reference splenocytes that had been labeled with 0.2 μM CFSE following their isolation from a C57BL/6J mouse. The mixed splenocyte populations were stained with anti-$CD8^{PE}$ and analyzed by flow cytometry. The relative percentage of adoptively transferred and expanded $CD8^+$ T cells was assessed by comparison with a defined number of the CFSE-labeled reference splenocytes and this is indicated in each histogram. Results are representative of three independent experiments. *B*, A total of $2–3 \times 10^6$ purified motheaten or control $CD8^+$ T cells expressing the F5 TCR were injected i.v. into irradiated C57BL/6J recipient mice. A reference recipient mouse group received no T cells. In parallel, 4×10^6 mature DCs pulsed with 5 μM NP68 peptide were injected i.p. into the recipients. Six days later, splenocyte targets were differentially labeled with either 2 or 0.2 μM CFSE. The population of T cells labeled with the lower concentration of CFSE was pulsed for 1 h with 5 μM NP68 before equal numbers of both populations were injected i.v. into the recipient mice. Spleens were harvested after an additional 24 h and the proportions of differentially CFSE-labeled cells assessed by flow cytometry. The marker regions, M1 and M2, on the histograms represent the NP68-pulsed and unpulsed splenocyte target populations respectively. The percentage of NP68-pulsed splenocyte targets killed is indicated in each histogram. Results are representative of three independent experiments.

Discussion

In this study, we have addressed the cellular mechanism that underlies the hyperproliferative phenotype of SHP-1-deficient motheaten T cells and examined its in vivo relevance. The increased proliferation, as measured by thymidine incorporation, of SHP-1-deficient T cells upon Ag receptor stimulation could have resulted from an increase in the proportion of T cells entered into cell division, an increase in the number of divisions, or a combination of these possibilities. To distinguish between the different possibilities, the labeling of motheaten and control T cells with the intracellular fluorescent dye, CFSE (34), has allowed us to analyze the proportion of each population entered into cell division following in vitro antigenic stimulation. The major conclusion from these experiments is that loss of SHP-1 results in an ~2-fold increase in the percentage of naive $CD8^+$ T cells entering into cell division when exposed to APCs bearing the appropriate MHC/peptide complex. Once committed to the first cell division, the subsequent number of cell divisions undertaken by motheaten and control T cells appears similar.

The question therefore shifts as to why the probability of entry into cell cycle is significantly enhanced for individual SHP-1-deficient T cells following exposure to Ag-bearing APCs. Previous studies have suggested that TCR-signaling thresholds are lowered in the absence of SHP-1 (26). However, these conclusions have assumed an equivalent engagement of TCR on motheaten and control T cells by appropriate MHC complexes on the surface of the APC. Using TCR down-regulation to interrogate the history of F_5 TCR engagement by H-$2D^b$/NP68 ligand complexes on B cells, we noted a significantly increased likelihood of TCR engagement on motheaten vs control T cells. Hence, the heightened proliferative responses of motheaten T cells in response to stimulation with cognate peptide-pulsed APCs most likely derive in part from the increased probability of TCR engagement. As a control, cross-linking with soluble anti-CD3 Ab demonstrated that there was no intrinsic difference between motheaten and control T cells for TCR internalization. However, previous data from others (35, 36) and our own group (37) has demonstrated that SHP-1-deficient T cells hyperproliferate in response to anti-CD3 cross-linking. The implication from these combined results is that while SHP-1 can influence the degree of engagement of TCR with its counterligand on the surface of the APC, the effects of SHP-1 on T cell responsiveness cannot be limited solely to the enhanced engagement of TCR but must also influence TCR-signaling thresholds.

When a T cell physically encounters an Ag-bearing APC, a concomitant shape change is induced in the T cell that causes the T cell to spread on the APC surface thus increasing the surface area of contact (38). In addition, relaxation of T cell rigidity, a process regulated by ezrin-radixin-moesin proteins, facilitates efficient T cell-APC conjugate formation (39). Both the initial degree of rigidity and capacity for spreading of the T cell membrane over the surface of the APC are dependent upon the cortical actin cytoskeleton and intriguingly a connection between SHP-1 and the regulation of cytoskeletal processes has begun to emerge (40, 41). It is therefore plausible that an effect of SHP-1 activity on actin polymerization and cytoskeleton remodeling may underlie its ability to affect T cell adhesion to APCs. One possibility is that loss of SHP-1 induces changes in the lymphocyte actin cytoskeleton that enhances the capacity of motheaten T cells to scan the surface of neighboring APCs. This would increase the likelihood of TCRs on the surface of motheaten T cells engaging with MHC/peptide ligands on the APCs.

The enhanced probability of TCR engagement observed for SHP-1-deficient T cells is subsequently manifested in the increased capacity of these T cells to form stable cellular conjugates with the APC. Stable T cell-APC conjugate formation results from TCR triggered increases in the binding activity of LFA-1. We therefore examined whether increases in LFA-1-binding activity, as measured by T cell adhesion to the plate-bound LFA-1 ligand, ICAM-1, could be detected on motheaten T cells following anti-CD3 stimulation. Interestingly, while conjugate formation by SHP-1-deficient and control T cells could be shown to be critically dependent upon LFA-1, no significant differences in the level of expression or binding capacity of LFA-1 to ICAM-1 were detectable when comparing motheaten and control T cells following anti-CD3 stimulation. Therefore, it is possible that the SHP-1 effect on T cell-APC conjugation does not influence the signals that link TCR triggering to LFA-1 activity.

An effect of SHP-1 on cell-cell adhesion has also been demonstrated for NK cells whereby SHP-1 activity can induce a remarkable suppression of NK cell cytolysis of targets. When SHP-1 is recruited and activated by an inhibitory killer Ig-like receptor, on the NK cell line, YTS, conjugates formed between the NK cell and target cells are dramatically reduced (42). Similar to our T cell-APC conjugate system, NK cell-target cell conjugate formation is inhibited by the blocking of LFA-1 binding (42). The inhibition of NK cell killing also appears to be mediated via disruption of actin cytoskeleton remodeling whereby the guanine nucleotide exchange factor, Vav1, has been implicated as a direct substrate of SHP-1 (43, 44). Vav1 is also a candidate substrate for SHP-1 in T cells although the results presented in this study imply that there may be at least one other substrate of SHP-1 that influences the ability of individual TCRs on the T cell surface to engage MHC/peptide complexes on the APC.

The overall significance of T cell-APC conjugate formation is underscored by a number of in vivo imaging studies (3–6) that have revealed a correlation between T cell activation leading to proliferation and the ability of T cells to establish long-lasting stable contact with DCs. Further evidence for the critical relevance of T cell-APC conjugate formation also derives from recent observations (45, 46) indicating that T reg cells may affect the immune response by reducing the capacity for contact formation between DCs and effector T cells. Clearly, a more comprehensive understanding of the cellular and molecular requirements for T cell-APC conjugate formation is needed. The increased percentage of conjugates formed with motheaten $CD8^+$ T cells would be predicted to result in increases in the number of T cells capable of IL-2 synthesis and secretion as stable interactions between T cells and APCs appear to be a prerequisite for IL-2 synthesis to proceed. In an elegant in vitro imaging study, whereby transgenic $CD4^+$ T cells expressing an IL-2 promoter GFP reporter construct were allowed to engage Ag-pulsed DCs, it was demonstrated that only a subset of those T cells that had prolonged and stable interactions with the DCs expressed IL-2 (47). Transient interactions between T cells and DCs were only sufficient for the expression of T cell activation markers such as the α-chain of the IL-2R. We envisage that the greater number of stable conjugates formed with motheaten $CD8^+$ T cells results in a higher proportion of T cells becoming IL-2 producers thereby increasing the recruitment of T cells into the proliferating population. Indeed, we have shown previously that a population of motheaten vs control T cells secreted more IL-2 when stimulated with peptide-pulsed APCs (26). The results reported here have established that motheaten T cells can more readily form conjugates with the APC. However, once conjugates have been allowed to form, it remains to be established whether motheaten T cells retain a further increased capacity for synthesizing IL-2 when compared with control T cells.

The enhanced capacity for conjugate formation leading to increased in vitro proliferative expansion displayed by SHP-1-deficient $CD8^+$ T cells is noteworthy. However, demonstrating effects in vitro does not necessarily equate to how T cells might respond in vivo whereby additional constraints are imposed. Indeed, a naive $CD8^+$ T cell must have the capacity to expand in peripheral LNs, differentiate into a mature CTL, and traffic from the Ag-draining LN to peripheral tissues before eventually lysing the appropriate target cell. Hence, our observations demonstrating enhanced in vivo killing by a population of SHP-1-deficient naive $CD8^+$ T cells following their adoptive transfer and in vivo expansion are especially significant because they establish for the first time that loss of SHP-1 increases the proliferative capacity of T cells in an in vivo context extending to an elevation of CTL killing, the ultimate physiological challenge for a $CD8^+$ T cell.

In conclusion, we provide evidence that SHP-1 negatively regulates the formation of conjugates between $CD8^+$ T cells and APCs. This effect of SHP-1 activity must account, at least in part, for the hyperresponsive phenotype of motheaten T cells observed in the different parameters of T cell function that have been measured (26). Importantly, the enhanced in vivo cytotoxicity of naive SHP-1-deficient T cells highlights the validity of targeting SHP-1 expression by small interfering RNA and pharmacological approaches to potentially boost human $CD8^+$T cell function.

Acknowledgments

We thank Prof. Elizabeth Simpson, Imperial College, for provision of the B cell line AB and K. Davies and staff of the Biomedical Services Unit, School of Medicine, Cardiff University for expert animal husbandry. We also thank S. Llewellyn-Lacey in the Medical Research Council Cooperative Group Tissue Culture Facility for expert maintenance of cells and colleagues, M. Labéta, S. Man, J. Boulter, and P. Brennan for advice and critical comments on the manuscript.

Disclosures

The authors have no financial conflict of interest.

References

1. Iezzi, G., K. Karjalainen, and A. Lanzavecchia. 1998. The duration of antigenic stimulation determines the fate of naive and effector T cells. *Immunity* 8: 89–95.
2. Gett, A. V., F. Sallusto, A. Lanzavecchia, and J. Geginat. 2003. T cell fitness determined by signal strength. *Nat. Immunol.* 4: 355–360.
3. Stoll, S., J. Delon, T. M. Brotz, and R. N. Germain. 2002. Dynamic imaging of T cell-dendritic cell interactions in lymph nodes. *Science* 296: 1873–1876.
4. Mempel, T. R., S. E. Henrickson, and U. H. Von Andrian. 2004. T-cell priming by dendritic cells in lymph nodes occurs in three distinct phases. *Nature* 427: 154–159.
5. Bousso, P., and E. Robey. 2003. Dynamics of $CD8^+$ T cell priming by dendritic cells in intact lymph nodes. *Nat. Immunol.* 4: 579–585.
6. Shakhar, G., R. L. Lindquist, D. Skokos, D. Dudziak, J. H. Huang, M. C. Nussenzweig, and M. L. Dustin. 2005. Stable T cell-dendritic cell interactions precede the development of both tolerance and immunity in vivo. *Nat. Immunol.* 6: 707–714.
7. Miller, M. J., O. Safrina, I. Parker, and M. D. Cahalan. 2004. Imaging the single cell dynamics of $CD4^+$ T cell activation by dendritic cells in lymph nodes. *J. Exp. Med.* 200: 847–856.
8. Bachmann, M. F., K. McKall-Faienza, R. Schmits, D. Bouchard, J. Beach, D. E. Speiser, T. W. Mak, and P. S. Ohashi. 1997. Distinct roles for LFA-1 and CD28 during activation of naive T cells: adhesion versus costimulation. *Immunity* 7: 549–557.
9. Krensky, A. M., E. Robbins, T. A. Springer, and S. J. Burakoff. 1984. LFA-1, LFA-2, and LFA-3 antigens are involved in CTL-target conjugation. *J. Immunol.* 132: 2180–2182.
10. Parsey, M. V., and G. K. Lewis. 1993. Actin polymerization and pseudopod reorganization accompany anti-CD3-induced growth arrest in Jurkat T cells. *J. Immunol.* 151: 1881–1893.
11. Donnadieu, E., G. Bismuth, and A. Trautmann. 1994. Antigen recognition by helper T cells elicits a sequence of distinct changes of their shape and intracellular calcium. *Curr. Biol.* 4: 584–595.
12. Delon, J., N. Bercovici, R. Liblau, and A. Trautmann. 1998. Imaging antigen recognition by naive $CD4^+$ T cells: compulsory cytoskeletal alterations for the triggering of an intracellular calcium response. *Eur. J. Immunol.* 28: 716–729.
13. Lowin-Kropf, B., V. S. Shapiro, and A. Weiss. 1998. Cytoskeletal polarization of T cells is regulated by an immunoreceptor tyrosine-based activation motif-dependent mechanism. *J. Cell Biol.* 140: 861–871.
14. Stewart, M., and N. Hogg. 1996. Regulation of leukocyte integrin function: affinity vs. avidity. *J. Cell. Biochem.* 61: 554–561.
15. Bromley, S. K., W. R. Burack, K. G. Johnson, K. Somersalo, T. N. Sims, C. Sumen, M. M. Davis, A. S. Shaw, P. M. Allen, and M. L. Dustin. 2001. The immunological synapse. *Annu. Rev. Immunol.* 19: 375–396.
16. Griffiths, E. K., C. Krawczyk, Y. Y. Kong, M. Raab, S. J. Hyduk, D. Bouchard, V. S. Chan, I. Kozieradzki, A. J. Oliveira-Dos-Santos, A. Wakeham, et al. 2001. Positive regulation of T cell activation and integrin adhesion by the adapter Fyb/Slap. *Science* 293: 2260–2263.
17. Peterson, E. J., M. L. Woods, S. A. Dmowski, G. Derimanov, M. S. Jordan, J. N. Wu, P. S. Myung, Q. H. Liu, J. T. Pribila, B. D. Freedman, et al. 2001. Coupling of the TCR to integrin activation by Slap-130/Fyb. *Science* 293: 2263–2265.
18. Krawczyk, C., A. Oliveira-dos-Santos, T. Sasaki, E. Griffiths, P. S. Ohashi, S. Snapper, F. Alt, and J. M. Penninger. 2002. Vav1 controls integrin clustering and MHC/peptide-specific cell adhesion to antigen-presenting cells. *Immunity* 16: 331–343.
19. Labno, C. M., C. M. Lewis, D. You, D. W. Leung, A. Takesono, N. Kamberos, A. Seth, L. D. Finkelstein, M. K. Rosen, P. L. Schwartzberg, and J. K. Burkhardt.

2003. Itk functions to control actin polymerization at the immune synapse through localized activation of Cdc42 and WASP. *Curr. Biol.* 13: 1619–1624.
20. Wang, H., E. Y. Moon, A. Azouz, X. Wu, A. Smith, H. Schneider, N. Hogg, and C. E. Rudd. 2003. SKAP-55 regulates integrin adhesion and formation of T cell-APC conjugates. *Nat. Immunol* 4: 366–374.
21. Valitutti, S., M. Dessing, K. Aktories, H. Gallati, and A. Lanzavecchia. 1995. Sustained signaling leading to T cell activation results from prolonged T cell receptor occupancy: role of T cell actin cytoskeleton. *J. Exp. Med.* 181: 577–584.
22. Cannon, J. L., and J. K. Burkhardt. 2002. The regulation of actin remodeling during T-cell-APC conjugate formation. *Immunol. Rev.* 186: 90–99.
23. Carter, J. D., B. G. Neel, and U. Lorenz. 1999. The tyrosine phosphatase SHP-1 influences thymocyte selection by setting TCR signaling thresholds. *Int. Immunol.* 11: 1999–2014.
24. Zhang, J., A. K. Somani, D. Yuen, Y. Yang, P. E. Love, and K. A. Siminovitch. 1999. Involvement of the SHP-1 tyrosine phosphatase in regulation of T cell selection. *J. Immunol.* 163: 3012–3021.
25. Mamalaki, C., J. Elliott, T. Norton, N. Yannoutsos, A. R. Townsend, P. Chandler, E. Simpson, and D. Kioussis. 1993. Positive and negative selection in transgenic mice expressing a T-cell receptor specific for influenza nucleoprotein and endogenous superantigen. *Dev. Immunol.* 3: 159–174.
26. Johnson, K. G., F. G. LeRoy, L. K. Borysiewicz, and R. J. Matthews. 1999. TCR signaling thresholds regulating T cell development and activation are dependent upon SHP-1. *J. Immunol.* 162: 3802–3813.
27. Townsend, A. R., J. Rothbard, F. M. Gotch, G. Bahadur, D. Wraith, and A. J. McMichael. 1986. The epitopes of influenza nucleoprotein recognized by cytotoxic T lymphocytes can be defined with short synthetic peptides. *Cell* 44: 959–968.
28. Scott, D., A. McLaren, J. Dyson, and E. Simpson. 1991. Variable spread of X inactivation affecting the expression of different epitopes of the Hya gene product in mouse B-cell clones. *Immunogenetics* 33: 54–61.
29. Lutz, M. B., N. Kukutsch, A. L. Ogilvie, S. Rossner, F. Koch, N. Romani, and G. Schuler. 1999. An advanced culture method for generating large quantities of highly pure dendritic cells from mouse bone marrow. *J. Immunol. Methods* 223: 77–92.
30. Barber, D. L., E. J. Wherry, and R. Ahmed. 2003. Cutting edge: rapid in vivo killing by memory CD8 T cells. *J. Immunol.* 171: 27–31.
31. Krangel, M. S. 1987. Endocytosis and recycling of the T3-T cell receptor complex: the role of T3 phosphorylation. *J. Exp. Med.* 165: 1141–1159.
32. Viola, A., and A. Lanzavecchia. 1996. T cell activation determined by T cell receptor number and tunable thresholds. *Science* 273: 104–106.
33. Shultz, L. D., P. A. Schweitzer, T. V. Rajan, T. Yi, J. N. Ihle, R. J. Matthews, M. L. Thomas, and D. R. Beier. 1993. Mutations at the murine motheaten locus are within the hematopoietic cell protein-tyrosine phosphatase (Hcph) gene. *Cell* 73: 1445–1454.
34. Lyons, A. B. 1999. Divided we stand: tracking cell proliferation with carboxyfluorescein diacetate succinimidyl ester. *Immunol. Cell Biol.* 77: 509–515.
35. Pani, G., K. D. Fischer, I. Mlinaric-Rascan, and K. A. Siminovitch. 1996. Signaling capacity of the T cell antigen receptor is negatively regulated by the PTP1C tyrosine phosphatase. *J. Exp. Med.* 184: 839–852.
36. Lorenz, U., K. S. Ravichandran, S. J. Burakoff, and B. G. Neel. 1996. Lack of SHPTP1 results in src-family kinase hyperactivation and thymocyte hyperresponsiveness. *Proc. Natl. Acad. Sci. USA* 93: 9624–9629.
37. Sathish, J. G., K. G. Johnson, F. G. LeRoy, K. J. Fuller, M. B. Hallett, P. Brennan, L. K. Borysiewicz, M. J. Sims, and R. J. Matthews. 2001. Requirement for CD28 co-stimulation is lower in SHP-1-deficient T cells. *Eur. J. Immunol.* 31: 3649–3658.
38. Negulescu, P. A., T. B. Krasieva, A. Khan, H. H. Kerschbaum, and M. D. Cahalan. 1996. Polarity of T cell shape, motility, and sensitivity to antigen. *Immunity* 4: 421–430.
39. Faure, S., L. I. Salazar-Fontana, M. Semichon, V. L. Tybulewicz, G. Bismuth, A. Trautmann, R. N. Germain, and J. Delon. 2004. ERM proteins regulate cytoskeleton relaxation promoting T cell-APC conjugation. *Nat. Immunol.* 5: 272–279.
40. Kim, C. H., C. K. Qu, G. Hangoc, S. Cooper, N. Anzai, G. S. Feng, and H. E. Broxmeyer. 1999. Abnormal chemokine-induced responses of immature and mature hematopoietic cells from motheaten mice implicate the protein tyrosine phosphatase SHP-1 in chemokine responses. *J. Exp. Med.* 190: 681–690.
41. Baba, T., N. Fusaki, N. Shinya, A. Iwamatsu, and N. Hozumi. 2003. Actin tyrosine dephosphorylation by the Src homology 1-containing protein tyrosine phosphatase is essential for actin depolymerization after membrane IgM cross-linking. *J. Immunol.* 170: 3762–3768.
42. Burshtyn, D. N., J. Shin, C. Stebbins, and E. O. Long. 2000. Adhesion to target cells is disrupted by the killer cell inhibitory receptor. *Curr. Biol.* 10: 777–780.
43. Stebbins, C. C., C. Watzl, D. D. Billadeau, P. J. Leibson, D. N. Burshtyn, and E. O. Long. 2003. Vav1 dephosphorylation by the tyrosine phosphatase SHP-1 as a mechanism for inhibition of cellular cytotoxicity. *Mol. Cell. Biol.* 23: 6291–6299.
44. Watzl, C., and E. O. Long. 2003. Natural killer cell inhibitory receptors block actin cytoskeleton-dependent recruitment of 2B4 (CD244) to lipid rafts. *J. Exp. Med.* 197: 77–85.
45. Tadokoro, C. E., G. Shakhar, S. Shen, Y. Ding, A. C. Lino, A. Maraver, J. J. Lafaille, and M. L. Dustin. 2006. Regulatory T cells inhibit stable contacts between $CD4^+$ T cells and dendritic cells in vivo. *J. Exp. Med.* 203: 505–511.
46. Tang, Q., J. Y. Adams, A. J. Tooley, M. Bi, B. T. Fife, P. Serra, P. Santamaria, R. M. Locksley, M. F. Krummel, and J. A. Bluestone. 2006. Visualizing regulatory T cell control of autoimmune responses in nonobese diabetic mice. *Nat. Immunol.* 7: 83–92.
47. Hurez, V., A. Saparov, A. Tousson, M. J. Fuller, T. Kubo, J. Oliver, B. T. Weaver, and C. T. Weaver. 2003. Restricted clonal expression of IL-2 by naive T cells reflects differential dynamic interactions with dendritic cells. *J. Exp. Med.* 198: 123–132.